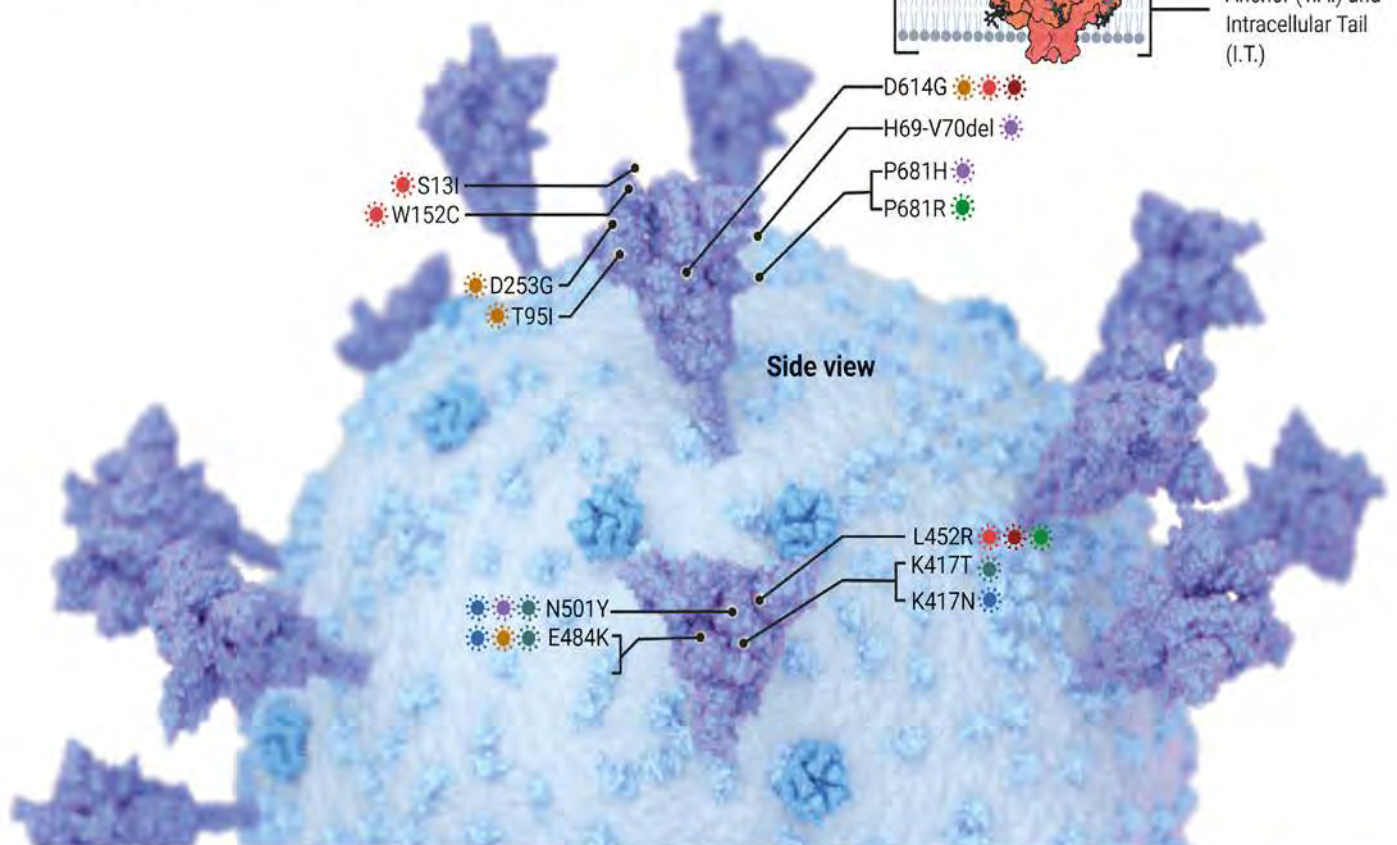
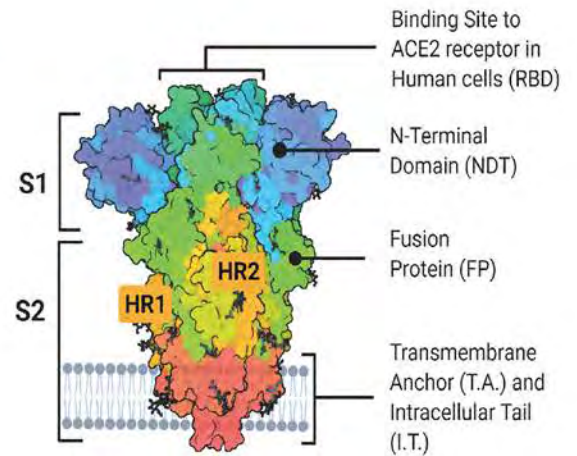


Bionatura

Latin American journal of Biotechnology and Life Sciences

SARS-COV-2

- | | | | |
|---|---|--|--|
|  B.1.526
Discovered:
Nov. 2020 |  B.1.427
Discovered:
Dec. 2020 |  B.1.429
Discovered:
Nov. 2020 |  B.1.617
Discovered:
Oct. 2020 |
|  B.1.1.7
Discovered:
Dec. 14 2020 |  B.1.351
Discovered:
Dec. 18 2020 |  P.1
Discovered:
Dec. 4 2020 | |



Predicting mortality in critically ill patients with COVID-19 in the ICU from a secondary-level hospital in Ecuador
 A16974C polymorphism of the IL-12 p40 gene in Cuban patients having recovered from COVID-19



Es el momento de los que se atreven a
soñar y luchan por alcanzar sus metas.
En la UCO te acompañamos



Vigilada Mineducación

Pregrados

› Tecnología en Operaciones Financieras

SNIES 104841 Registro Calificado - Res. 12903 del 21-09-2015 M.E.N.
96 créditos - A distancia tradicional - Rionegro Ant.

› Contaduría Pública

SNIES 13018 Registro Calificado - Res. 9256 del 07-06-2018
Acreditación de Alta Calidad 4610 del 21-03-2018 M.E.N.
166 créditos Presencial - Rionegro

› Comercio Exterior

SNIES 1854 Registro Calificado - Res. 14314 del 11-12-2019 M.E.N.
159 créditos - Presencial - Rionegro Ant.

› Administración de Empresas

SNIES 55096 Registro Calificado - Res. 7658 del 18-04-2017 M.E.N.
152 créditos - Presencial - Rionegro Ant.

› Tecnología Agropecuaria

SNIES 1850 Registro Calificado - Res. 8884 del 10-07-2013 M.E.N.
113 créditos - Presencial - Rionegro Ant.

› Agronomía

SNIES 4443 Registro Calificado - Res. 8067 del 17-05-2018
Acreditación de Alta Calidad N° 29149 del 26-12-2017
157 créditos - Presencial - Rionegro Ant.

› Zootecnia

SNIES 53037 Registro Calificado - Res. 14468 del 04-09-2014 M.E.N.
156 créditos - Presencial - Rionegro Ant.

› Psicología

SNIES 8562 Registro Calificado - Res. 9902 del 31-07-2013 M.E.N.
Acreditación de Alta Calidad N° 17227 del 24-10-2018
175 créditos - Presencial - Rionegro Ant.

› Comunicación Social

SNIES 53045 Registro Calificado - Res. 14892 del 11-09-2014 M.E.N.
146 créditos - Presencial - Rionegro Ant.

› Trabajo Social

SNIES 106586 Registro Calificado - Res. 26741 del 29-11-2017 M.E.N.
141 créditos - Presencial - Rionegro Ant.

› Derecho

SNIES 53539 Registro Calificado - Res. 10542 del 14-07-2015 M.E.N.
168 créditos - Presencial - Rionegro Ant.

› Nutrición y Dietética

SNIES 104801 Registro Calificado - Res. 7823 del 01-06-2015 M.E.N.
166 créditos - Presencial - Rionegro Ant.

› Gerontología

SNIES 1853 Registro Calificado - Res. 14838 del 22-10-2013 M.E.N.
138 créditos - A distancia con apoyo Virtual - Rionegro Ant.

› Enfermería

SNIES 91027 Registro Calificado - Res. 12600 del 03-06-2018 M.E.N.
166 créditos - Presencial - Rionegro Ant.

› Licenciatura en Filosofía

SNIES 105542 Registro Calificado - Res. 22108 del 24-10-2017 M.E.N.
164 créditos - Presencial - Rionegro Ant.

› Licenciatura en Lenguas Extranjeras con énfasis en Inglés

SNIES 106647 Registro Calificado - Res. 29529 del 29-12-2017 M.E.N.
164 créditos - Presencial - Rionegro Ant.

› Licenciatura en Educación Física, Recreación y Deportes

SNIES 106436 Registro Calificado - Res. 17481 del 31-08-2017 M.E.N.
164 créditos - Presencial - Rionegro Ant.

› Licenciatura en Educación para la Primera Infancia

SNIES 105359 Registro Calificado - Res. 02848 del 16-02-2016 M.E.N.
164 créditos - Presencial - Rionegro Ant.

› Licenciatura en Ciencias Naturales

SNIES 106896 Registro Calificado - Res. 19869 del 18-10-2016 M.E.N.
164 créditos - Presencial - Rionegro Ant.

› Licenciatura en Educación Religiosa

SNIES 106705 Registro Calificado - Res. 2084 del 13-02-2018 M.E.N.
164 créditos - Presencial - Rionegro Ant.

› Técnico Profesional en Programación Web

SNIES 103704 Registro Calificado - Res. 14454 del 04-09-2014 M.E.N.
67 créditos - Presencial - Rionegro Ant.

› Ingeniería Ambiental

SNIES 4361 Registro Calificado - Res. 3654 del 02-03-2018 M.E.N.
Acreditación de Alta Calidad No. 6543 del 18-04-2018
173 créditos - Presencial - Rionegro Ant.

› Ingeniería de Sistemas

SNIES 1855 Registro Calificado - Res. 0178 del 05-01-2019 M.E.N.
164 créditos - Presencial - Rionegro Ant.

› Ingeniería Industrial

SNIES 1856 Registro Calificado - Res. 1293 del 04-02-2019 M.E.N.
160 créditos - Presencial - Rionegro Ant.

› Ingeniería Electrónica

SNIES 20271 Registro Calificado - Res. 24646 del 14-11-2017 M.E.N.
178 créditos - Presencial - Rionegro Ant.

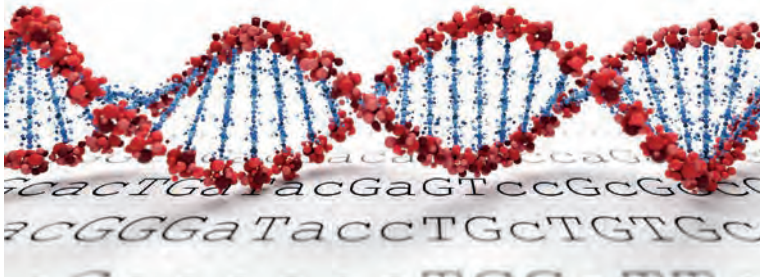
› Teología

SNIES 103450 Registro Calificado - Res. 10638 del 09-07-2014 M.E.N.
130 créditos - A distancia - Rionegro Ant.

¡HAGAMOS QUE PASE!



Bionatura



La Revista Bionatura publica trimestral en español o inglés trabajos inéditos de investigaciones básicas y aplicadas en el campo de la Biotecnología, la Inmunología, la Bioquímica, Ensayos Clínicos y otras disciplinas afines a las ciencias biológicas, dirigidas a la obtención de nuevos conocimientos, evaluación y desarrollo de nuevas tecnologías, productos y procedimientos de trabajo con un impacto a nivel mundial.

Equipo editorial

Editor Jefe / Chief Editor

Dr. Nelson Santiago Vispo, Ph.D. Research / Full Professor. Yachay Tech University, Ecuador. Member of the European Association of Science Editors (EASE) and Council of Science Editors (USA).

Principal Editorial Board / Consejo Editorial Principal

Dr. Fernando Albericio, Ph.D. Full Professor. University of KwaZulu-Natal, Durban, South Africa.

Dr. Spiros N. Agathos, Ph.D. Full Professor. Université Catholique de Louvain - UCLouvain, Louvain-la-Neuve, Belgium.

Dra. Hortensia María Rodríguez Cabrera, Ph.D. Full Professor and Dean, School of Chemical Sciences and Engineering Yachay Tech University, Ecuador.

Dr. Frank Alexis, Research / Full Professor. Vice Chancellor Of Research and Innovation. Yachay Tech University, Ecuador.

Consejo Editorial / Editorial Board

Dr. Gerardo Ferbeyre, Full Professor. Département de biochimie. Faculté de Médecine. Université de Montréal, Canadá.

Dr. Frank Camacho Casanova, Ph.D., Facultad de Ciencias Biológicas. Universidad de Concepción, Chile.

Dr. Eduardo López Collazo, Director IdiPAZ Institute of Biomedical Research, La Paz Hospital, España.

Dr. Yovani Marrero-Ponce, Ph.D. Full Professor. Universidad San Francisco de Quito (USFQ), Quito, Ecuador.

Dr. Manuel Limonta, Prof. PhD. Director: Regional Office for Latin American and the Caribbean International Council for Science (ICSU). Doctor honoris causa Autonomous Metropolitan University of México City (UAM), Dr. Honoris Causa - Universidad Central Ecuador.

Dr. Dagoberto Castro - Restrepo, Prof. PhD. Research and Development Director. Universidad Católica del Oriente, Rio Negro, Colombia

Dr. Michael Szardenings, Ph.D. Ligand Development Unit. Fraunhofer Institute for Cell Therapy and Immunology, Germany.

Dra. Luciana Dente, Research Professor University of Pisa, Italy.

Dr. Costantino Vetriani, Research / Full Professor. Rutgers, The State University of New Jersey, USA.

Dr. Si Amar Dahoumane, Ph.D. Research / Professor. Yachay Tech University, Ecuador.

Dr. Amit Chandra, MD, MSc, FACEP Global Health Specialist, Emergency Physician Millennium Challenge Corporation, London School of Economics and Political Science.

Dr. Silvio e. Perea, Ph.D. Head of the Molecular Oncology Laboratory, Centro de Ingeniería Genética y Biotecnología, Cuba.

Dra. Daynet Sosa del Castillo, Ph.D. Directora del Centro de Investigaciones Biotecnológicas del Ecuador. CIBE-ESPOL.

Dra. Consuelo Macías Abraham, Especialista de II Grado en Inmunología, Investigadora y Profesora Titular, Doctora en Ciencias Médicas y Miembro Titular de la Academia de Ciencias de Cuba. Directora del Instituto de Hematología e Inmunología (IHI), de La Habana, Cuba.

Dr. René Delgado, Ph.D. IFAL / Presidente Sociedad Cubana de Farmacología, Cuba.

Dr. Ramón Guimil, Senior Director. Oligonucleotide Chemistry bei Synthetic Genomics, Estados Unidos.

Dr. Eduardo Penton, MD, PhD, Investigador Titular. Centro de Ingeniería Genética y Biotecnología, Cuba.

Dr. Julio Raúl Fernández Massó, PhD, Investigador Titular. Centro de Ingeniería Genética y Biotecnología, Cuba

Dra. Lisset Hermida, Investigadora Titular. Centro de Ingeniería Genética y Biotecnología, Cuba.

Dr. Tirso Pons, Staff Scientist. Structural Biology and Biocomputing Programme (CNIO), España.

Dr. Che Serguera, French Institute of Health and Medical Research, MIRCen, CEA, Fontenay-aux-Roses Paris, France.

Dr. Jorge Roberto Toledo, Profesor Asociado. Universidad de Concepción, Chile.

Dr. Oliberto Sánchez, Profesor Asociado. Universidad de Concepción, Chile.
Dr. Aminael Sánchez Rodríguez, Ph.D. Director del departamento de Ciencias Biológicas, Universidad Técnica Particular de Loja, Ecuador.
Dra. Maritza Pupo, Profesora investigadora. Facultad de Biología. Universidad de La Habana, Cuba.

Dr. Fidel Ovidio Castro, Founder, Profesor investigador. Tecelvet, Chile.
Dra. Olga Moreno, Partner, Head Patent Division. Jarry IP SpA, Chile.

Dr. Carlos Borroto, Asesor de Transferencia de Tecnología. Dirección General at Centro de Investigaciones Científicas de Yucatán (CICY), México.
Dr. Javier Menéndez, Manager Specialist Process and Product 5cP. Sanoft Pasteur, Canadá.

Dr. Pedro Valiente, Profesor investigador. Facultad de Biología. Universidad de La Habana, Cuba.

Dr. Diógenes Infante, Prometeo / SENESCYT. Especialista de primer nivel en Biotecnología. Universidad de Yachay Tech, Ecuador.

Dra. Georgina Michelena, Profesora Investigador. Organización de las Naciones Unidas. (ONU), Suiza.

Dr. Francisco Barona, Profesor Asociado. Langebio Institute, México
Dr. Gustavo de la Riva, Profesor Investigador Titular. Instituto Tecnológico Superior de Irapuato, México.

Dr. Manuel Mansur, New Product Introduction Scientist (NPI) at Elanco Animal Health Ireland, Irlanda.

Dr. Rolando Pajón, Associate Scientist, Meningococcal Pathogenesis and Vaccine Researc. Center for Immunobiology and Vaccine Development, UCSF Benioff Children's Hospital Oakland", Estados Unidos.

Dra. Ileana Rosado Ruiz-Apodaca, Profesor / Investigador. Universidad de Guayaquil, Ecuador.

Dr. Carlos Eduardo Giraldo Sánchez, PhD, Profesor / Investigador. Universidad Católica de Oriente. Rionegro-Antioquia/Colombia.

Dr. Mario Alberto Quijano Abril, PhD, Profesor / Investigador. Universidad Católica de Oriente. Rionegro-Antioquia/Colombia.

Dr. Felipe Rojas Rodas, PhD, Profesor / Investigador. Universidad Católica de Oriente. Rionegro-Antioquia/Colombia.

Dra. Isabel Cristina Zapata Vahos, Profesor / Investigador. Universidad Católica de Oriente. Rionegro-Antioquia/Colombia.

Dr. Felipe Rafael Garcés Fiallos, PhD, Profesor / Investigador. Vicerrectorado de Investigación, Gestión Social del Conocimiento y Posgrado Universidad de Guayaquil (UG), Ecuador.

Dra. Celia Fernandez Ortega, PhD. Investigadora Titular. Centro de Ingeniería Genética y Biotecnología, Editora ejecutiva Biotecnología Aplicada, Cuba.

Dra. Ligia Isabel Ayala Navarrete, PhD. Profesor / Investigador. Universidad de las Fuerzas Armadas - ESPE, Ecuador.

Dr. Nalini kanta Sahoo, PhD. Professor & Head Department Marri Laxman Reddy Institute of Pharmacy, Hyderabad, Andhra Pradesh, India.

Dr. Saman Esmailnejad, Ph.D. Department of medical sciences, Tarbiat Modares University, Tehran, Iran.

Dr. Olukayode Karunwi, Ph.D. Research / Professor. Clemson University, Clemson, United States.

Associate Editor / Editor Asociado

Victor Santiago Padilla.

Redacción y Edición / Copyediting and corrections

Mg. Frey A. Narváez-Villa, Jefe del Fondo Editorial Universidad Católica de Oriente. Rionegro-Antioquia/Colombia.

MSc. José Enrique Alfonso Manzanet.

Diseño y Realización gráfica / Graphic design and production

DI. José Manuel Oubiña González.

Relaciones Públicas / Public relations

Camila Barranco Rodriguez.

Asistente de publicación / Publication assistant

Evelyn Padilla Rodriguez.

Instrucciones para los Autores

Los Trabajos serán Inéditos: Una vez aprobados, no podrán someterse a la consideración de otra revista, con vistas a una publicación múltiple, sin la debida autorización del Comité Editorial de la Revista. La extensión máxima será 8 cuartillas para los trabajos originales, 12 las revisiones y 4 las comunicaciones breves e informes de casos, incluidas las tablas y figuras. Los artículos se presentarán impresos (dos ejemplares). Todas las páginas se numerarán con arábigos y consecutivamente a partir de la primera. Estos deben acompañarse de una versión digital (correo electrónico o CD) en lenguaje Microsoft Word, sin sangrías, tabuladores o cualquier otro atributo de diseño (títulos centrados, justificaciones, espacios entre párrafos, etc.). Siempre se ha de adjuntar la carta del consejo científico que avala la publicación y una declaración jurada de los autores.

Referencias Bibliográficas. Se numerarán según el orden de mención en el texto y deberán identificarse mediante arábigos en forma exponencial. Los trabajos originales no sobrepasarán las 20 citas; las revisiones, de 25 a 50 y las comunicaciones breves e informes de casos.

En las Referencias en caso de que las publicaciones revisadas esten online se debe proveer un enlace consistente para su localización en Internet. Actualmente, no todos los documentos tienen DOI, pero si lo tienen se debe incluir como parte de la referencias. Si no tuviese DOI, incluir la URL.

Tablas, modelos y anexos: Se presentarán en hojas aparte (no se intercalarán en el artículo) y en forma vertical numeradas consecutivamente y mencionadas en el texto. Las tablas se ajustarán al formato de la publicación se podrán modificar si presentan dificultades técnicas.

Figuras: Las fotografías, gráficos, dibujos, esquemas, mapas, salidas de computadora, otras representaciones gráficas y fórmulas no lineales, se denominarán figuras y tendrán numeración arábica consecutiva. Se presentarán impresas en el artículo en páginas independientes y en formato digital con una resolución de 300 dpi. Todas se mencionarán en el texto. Los pies de figuras se colocarán en página aparte. El total de las figuras y tablas ascenderá a 5 para los trabajos originales y de revisión y 3 para las comunicaciones breves e informes de casos.

Abreviaturas y siglas: Las precederá su nombre completo la primera vez que aparezcan en el texto. No figurarán en títulos ni resúmenes. Se emplearán las de uso internacional.

Sistema Internacional de Unidades (SI): Todos los resultados de laboratorio clínico se informarán en unidades del SI o permitidas por este. Si se desea añadir las unidades tradicionales, se escribirán entre paréntesis. Ejemplo: glicemia: 5,55 mmol/L (100 mg/100 mL).

Para facilitar la elaboración de los originales, se orienta a los autores consultar los requisitos uniformes antes señalados disponibles en: [http://www.fisterra.com/recursos_web/mbelvancouver.htm#ilustraciones%20\(figura\)](http://www.fisterra.com/recursos_web/mbelvancouver.htm#ilustraciones%20(figura))

Los trabajos que no se ajusten a estas instrucciones, se devolverán a los autores. Los aceptados se procesarán según las normas establecidas por el Comité Editorial. El arbitraje se realizará por pares y a doble ciego en un período no mayor de 60 días. Los autores podrán disponer de no más de 45 días para enviar el artículo con correcciones, se aceptan hasta tres reenvíos. El Consejo de Redacción se reserva el derecho de introducir modificaciones de estilo y/o acotar los textos que lo precisen, comprometiéndose a respetar el contenido original.

El Comité Editorial de la Revista se reserva todos los derechos sobre los trabajos originales publicados en esta.

Bionatura

La **Revista Bionatura** es un medio especializado, interinstitucional e interdisciplinario, para la divulgación de desarrollos científicos y técnicos, innovaciones tecnológicas, y en general, los diversos tópicos relativos a los sectores involucrados en la biotecnología, tanto en Ecuador como en el exterior; así mismo, la revista se constituye en un mecanismo eficaz de comunicación entre los diferentes profesionales de la biotecnología.

Es una publicación sin ánimo de lucro. Los ingresos obtenidos por publicidad o servicios prestados serán destinados para su funcionamiento y desarrollo de su calidad de edición. (<http://revistabionatura.com/media-kit.html>)

Es una revista trimestral, especializada en temas concernientes al desarrollo teórico, aplicado y de mercado en la biotecnología.

Publica artículos originales de investigación y otros tipos de artículos científicos a consideración de su consejo editorial, previo proceso de evaluación por pares (peer review) sin tener en cuenta el país de origen.

Los idiomas de publicación son el Español e Inglés.

Los autores mantienen sus derechos sobre los artículos sin restricciones y opera bajo la política de Acceso Abierto a la Información, bajo la licencia de Creative Commons 4.0 CC BY-NC-SA (Reconocimiento-No Comercial-Compartir igual).

Esta revista utiliza Open Journal Systems, que es un gestor de revistas de acceso abierto y un software desarrollado, financiado y distribuido de forma gratuita por el proyecto Public Knowledge Project sujeto a la Licencia General Pública de GNU.

Nuestros contactos deben ser dirigidos a:
Revista Bionatura: editor@revistabionatura.com

ISSN: 1390-9347 (Versión impresa)

Formato: 21 x 29,7 cm

ISSN: 1390-9355 (Versión electrónica)

Sitio web: <http://www.revistabionatura.com>

Publicación periódica trimestral

Esta revista utiliza el sistema peer review para la evaluación de los manuscritos enviados.

Instrucciones a los autores en:

<http://revistabionatura.com/instrucciones.html>

Asistente de publicación / Publication assistant
Evelyn Padilla Rodriguez (sales@revistabionatura.com)

ÍNDICE / INDEX

-
- | | | |
|----------------|---|--------------|
| Article | Predicting mortality in critically ill patients with COVID-19 in the ICU from a secondary-level hospital in Ecuador | 2022.07.01.1 |
| | <i>Jorge Luis Vélez-Paez, Mario Patricio Montalvo, Fernando Esteban Jara, Santiago Aguayo-Moscoso, Wendy Tercero-Martínez, Lenin Stalin Saltos, Glenda Jiménez-Alulima, Estefanía Irigoyen-Mo-
gra, Evelyn Castro-Reyes, Christian Mora-Coello, Edgar López-Rondón, Patricio Toapanta, Eduardo
Vásconez-González, Esteban Ortiz-Prado</i> | |
| Article | Indicators to achieve a better positioning of Ecuadorian scientific journals | 2022.07.01.2 |
| | <i>Victor Santiago Padilla Yalitzá Therly Ramos Gil</i> | |
| Article | Evaluation of the water quality of some sulfur springs in Hammam Al-Alil sub-district in Nineveh governorate | 2022.07.01.3 |
| | <i>Hadeel Bassam Yahya, Yussra Al-Shaker, Rawaa M Hamoshi</i> | |
| Review | Efectos del material particulado sobre las células endoteliales, epiteliales y del sistema inmune
<i>Effects of particulate matter on endothelial, epithelial and immune system cells</i> | 2022.07.01.4 |
| | <i>Danna V. Cano-Granda, Mariana Ramírez-Ramírez, Diana M. Gómez-Gallego, and Juan C. Hernandez</i> | |
| Article | Study the relationship between <i>Helicobacter pylori</i> and bladder cancer | 2022.07.01.5 |
| | <i>Mohammad Heidari, Seyed Jalal Eshagh Hoseini, Hassan Fatemi Manesh</i> | |
| Article | Evaluation of secondary cancers, synchronous and metachronous with bladder cancer | 2022.07.01.6 |
| | <i>Seyed Jalal Eshagh Hoseini, Mohammad Heidari, Hassan Fatemi Manesh</i> | |
| Article | Effect of iodine-therapy on hyperthyroidism patients without pre-administration of anti-thyroid therapeutic options | 2022.07.01.7 |
| | <i>Homiera Rashidi, Bahman Ghaderian, Alireza Sedaghat, Mahmoud Latifi, Zohre Naimi</i> | |
| Article | Detection of biofilm formation of (<i>Serratia</i> and <i>E.coli</i>) and determination of the inhibitory effect of <i>Quercus</i> plant extract against these infectious pathogens | 2022.07.01.8 |
| | <i>Fatima Amer Abd Algabar, Batool Abdalameer Baqer</i> | |
| Article | Optimization of cephalosporin C acylase immobilization using crosslinked enzyme aggregates technique | 2022.07.01.9 |
| | <i>Julkipli Julkipli, Khaswar Syamsu and Ahmad Wibisana</i> | |

Article	Assessment of genetic fidelity of lacy tree philodendron (<i>Philodendron bipinnatifidum</i> Schott ex Endl.) micro propagated plants	2022.07.01.10
	<i>Mona S. Alwahibi, Asma Alhussein Alawaadh, Yaser Hassan Dewir, Dina A. Soliman, and Mayada Kadry Seliem</i>	
Article	Major Genetic Determinants of Extended-Spectrum β -Lactamase (ESBL), Carbapenemase, Fosfomycin and Colistin Resistance in <i>Escherichia Coli</i> from Intensive Care Unit	2022.07.01.11
	<i>Ahmed Mhawesh, Marwa khudair and Omer N. Abbas</i>	
Article	Identification of novel-vector control target proteins of <i>Aedes sp.</i> : A Systems Network Biology Approach	2022.07.01.12
	<i>Tammanna R. Sahrawat, Devika Talwar and Ritika Patial</i>	
Review	Microsphere: A Wander around Drug Delivery	2022.07.01.13
	<i>Anirban Karmakar, Soumya Dev Maity, Shayeree Barua, Raneet Das</i>	
Review	Tasa de retención de sellantes de resina en esmalte dental con alteraciones estructurales: una revisión sistemática	2022.07.01.14
	<i>Javier Jimémez-Díaz, Gabriela Curtze-Scotts, Guillermo Barahona-Fuentes</i>	
Article	Antibacterial and cytotoxic evaluation of sequential extract of <i>Moringa oleifera</i> leaves	2022.07.01.15
	<i>Usama Bin Naeem, Waqas Iftikhar, Mussarat Rafiq, Muhammad Babar Khawar</i>	
Clinical Report	Rara patología derivada de un anillo del cromosoma 15. Clínica, genómica e interactoma de proteínas de genes asociados al fenotipo <i>Rare pathology derived from a ring chromosome 15. Clinical, genomic and protein interactome of genes associated with the phenotype</i>	2022.07.01.16
	<i>César Paz-y-Miño, Camila Medranda, Alejandra Loaiza, Mishell Ponce, Paola E. Leone</i>	
Clinical Report	Coronavirus: First Report of a Sars-Cov-2 case In Ecuador. Are nutritional assessment and treatment helpful for a successful outcome?	2022.07.01.17
	<i>Ordoñez Martínez Mayra Graciela, Alemán Espinoza Washington René, Ulloa Correa José Efraín, Rodas Mireya, Sarango Sánchez Edwin Renato, Cucalón Gabriela, Frias-Toral Evelyn</i>	
Article	Dissecting the relationship between artificial insemination success and bull semen quality in the arid region of Tiaret (Algeria)	2022.07.01.18
	<i>Mohamed Achir, Khaled Taïbi, Leila Ait Abderrahim, Mohamed Boussaid, Kada Souana, Abdelkader Tadj, Toufik Benaïssa, Tayeb Gouchich</i>	
Article	Evaluation of X-ray ionizing radiation on <i>Plasmodium berghei</i> invasion of erythrocytes	2022.07.01.19
	<i>Carina Nava-Lausón, Lilian M. Spencer, Laszlo Sajo-Bohus, Jesús Dávila, Markus P. Tellkamp</i>	
Article	Identification of Some Breast Cancer Related Genes by RAPD Technique in Maysan Province, Iraq	2022.07.01.20
	<i>Zainab Zamil Gataa Allami, Maytham Abdulkadhim Dragh</i>	

Article	Detection of humoral immune response induced in horses vaccinated with inactivated Equine Herpes Virus Vaccine	2022.07.01.21
	<i>Mohamed Samy Abousenna , Heba A Khafagy, Nermeen Gouda Shafik, Neveen Mounir Abdelmotlib, Ibrahim Sayed Yahia</i>	
Article	Características de los pacientes con lumbalgia atendidos en un centro de atención primaria en Ecuador <i>Characteristics of patients with low background treated at a primary care center in Ecuador</i>	2022.07.01.22
	<i>Michelle Fuseau, David Garrido and Edgar Toapanta</i>	
Article	Study of effects Oat and Soybean on the Microbial and Sensory Analysis of Burgers (Beef, Chicken and Sheep)	2022.07.01.23
	<i>Hind Mohammed Saleh, Firas R. Jameel, Sara Thamer Hadi and Mohammed Majed Hamid</i>	
Letter to editor	A Single Web-Platform for Invitation or Advertisement of Online Courses and Webinars in These Covid Virus Time	2022.07.01.24
	<i>Anupam Saha</i>	
Article	The presence of Neopterin in the sera of a sample of Iraqi acromegalic patients (Type 2 diabetics and nondiabetics)	2022.07.01.25
	<i>Sabreen Hamodi Hamza, Zainab Fadhel Ashoor and Abbas Mahdi Rahmah</i>	
Article	Suitability of some well water for different human uses by studying some physicochemical properties	2022.07.01.26
	<i>Israa Salman Dalas; Muqdad Altae ,Raghad Mukdad Mahmood</i>	
Article	Mejoramiento del Rendimiento de un Motor Diésel mediante la adición de nanopartículas de ZnO al diésel <i>Diesel Engine Performance Improvement by adding ZnO nanoparticles to diesel fuel</i>	2022.07.01.27
	<i>Carlos Segovia, Ignacio Benavides, Jorge Melo, Víctor Montenegro</i>	
Article	Purification and characterization of L-asparaginase extracted from local Iraqi green beans (<i>Phaseolus vulgaris</i>)	2022.07.01.28
	<i>Nedhaal Suhail Zbar</i>	
Article	Epidemiological Molecular Analysis of <i>Acinetobacter baumannii</i> isolates using a multilocus sequencing typing and Global lineage	2022.07.01.29
	<i>Heba A. Kadhom and Munim R. Ali</i>	
Article	The influence of gamma rays and electric shock on seed germination and seedling growth in burdock plants	2022.07.01.30
	<i>Carina Nava-Lausón, Lilian M. Spencer, Laszlo Sajo-Bohus, Jesús Dávila, Markus P. Tellkamp</i>	
Article	Study single nucleotide polymorphism in Promoter region of UGT1A1 Gene in Iraqi Patients with Gilbert's syndrome	2022.07.01.31
	<i>Marwa A. Kubba, Abeer Ali Marhoon and Rafed Abbas Kadhum</i>	

Review	Recent advances on the development of a universal blood type <i>Esteban Guamba , Alejandra Cevallos</i>	2022.07.01.32
Review	Porous frameworks from Ecuadorian clays <i>María Calle Luzuriaga, Edward E. Ávila, Dario Alfredo Vilorio</i>	2022.07.01.33
Article	A16974C polymorphism of the IL-12 p40 gene in Cuban patients having recovered from COVID-19 <i>Estela Morales Peralta, Yáirma Zúñiga Rosales, Teresa Collazo Mesa, Elvia Nelemi Santos González, Yaira Hernández Pérez, María de los Angeles González Torres, Hilda Roblejo Balbuena, Beatriz Marcheco Teruel</i>	2022.07.01.34
Article	Temporal progress of web blight in three common bean genotypes on the central coast of Ecuador <i>Walter R. Chávez-García, Fiorella N. Mera-Vera, Diego Portalanza , and Felipe R. Garcés-Fiallos</i>	2022.07.01.35
Review	Temporal progress of web blight in three common bean genotypes on the central coast of Ecuador <i>Javiera Jiménez-Díaz , Gabriela Curtze-Scotts , Guillermo Barahona-Fuentes</i>	2022.07.01.36

ARTICLE / INVESTIGACIÓN

Predicting mortality in critically ill patients with COVID-19 in the ICU from a secondary-level hospital in Ecuador

Jorge Luis Vélez-Paez^{1,2}, Mario Patricio Montalvo¹, Fernando Esteban Jara¹, Santiago Aguayo-Moscoso¹, Wendy Tercero-Martínez¹, Lenin Stalin Saltos¹, Glenda Jiménez-Alulima¹, Estefanía Irigoyen-Mogro¹, Evelyn Castro-Reyes¹, Christian Mora-Coello¹, Edgar López-Rondón¹, Patricio Toapanta^{1,2}, Eduardo Vásconez-González³, Esteban Ortiz-Prado³

DOI. 10.21931/RB/2022.07.01.1

¹ Intensive Care Unit, Pablo Arturo Suárez Hospital, Quito, Ecuador.

² Faculty of Medicine, Universidad Central del Ecuador, Quito, Ecuador.

³ One Health Research Group, Faculty of Health Sciences, Medical School, Universidad de las Americas, Quito, Ecuador.

Corresponding author: jlvelez@uce.edu.ec

Abstract: Since its molecular isolation on January 7, 2020, the new SARS-CoV-2 coronavirus has spread rapidly, affecting regions such as Latin America. Ecuador received the worst outbreak globally if we count excess mortality per capita. This study describes the clinical, epidemiological and therapeutic characteristics of 89 patients admitted to an intensive care unit (ICU) in a second-level hospital in Quito, Ecuador. Methods: We conducted a retrospective cohort study. We collected data from health records of adult patients with severe COVID-19 admitted to an ICU in Quito, Ecuador, during the first five months of the SARS-CoV-2 outbreak. We used the Chi-square test or Fisher's exact statistics to analyze risk and associations between survivors and non-survivors. We used ROC curve analysis to predict mortality and determine cut-off points for mechanical, analytical, and cytometric ventilation parameters. We used the Wald test to evaluate the categorical predictors of the model at the multivariate level during the regression analysis. Results: 89 patients were recruited. The mean age of the patients was 54.72 years. Men represented 68.54% (n=61) and women 31.46% (n=28). Significant differences in mortality were observed (men 40.98% vs. women 17.76%). LDH and IL-6 at 24 hours after hospital admission were higher among non-survivors than survivors. Persistent hypercapnia (PaCO₂ >45 mmHg), a PaFiO₂ ratio of less than 140 mmHg, and positive end-expiratory pressure (PEEP) titration >9 mmHg were also associated with increased mortality. Conclusions: Elevated levels of LDH at 24 hours, IL-6 at 24 hours, lymphocyte and platelet count at 48 hours, neutrophil count at 48 hours and NLR are factors associated with higher motility, higher risk of failed extubation and reintubation in patients with acute respiratory distress syndrome due to COVID-19.

Key words: COVID-19, ICU, ROC curve, Mortality, Low-Middle Income Country.

Introduction

On 31 December, the Wuhan Municipal Health Committee informed the World Health Organization (WHO) that 27 people had been diagnosed with a type of pneumonia never described before¹. On 7 January, 2020, Chinese scientists had isolated and sequenced the etiological agent, a novel beta coronavirus later identified as SARS-CoV-2 (severe acute respiratory syndrome coronavirus type -two)². The genome of this RNA virus was made available on 12 January, 2020, allowing laboratories in different countries to produce specific primers for the infection diagnosis using real-time reverse transcription-polymerase chain reaction (RT-PCR)^{2,3}. On 11 March, 2020, the WHO declared COVID-19 a pandemic after the virus arrived in several countries rapidly⁴. Up to 5 October, 2020, more than 35 million people had been infected, causing more than 1 million deaths worldwide³.

In Latin America, a region with high levels of social inequality, mortality rates, and attack rate due to COVID-19, is devastating, especially for those living in poverty⁵. Households in the lowest income group have reduced access to health services, molecular diagnosis, and treatment. Health systems with scarce economic resources and disrupted contact tracing

capabilities are often incapable of controlling outbreaks at the community level, affecting mortality and hospital admission trends⁶.

In mid-February 2020, the disease reached Latin America and hit Ecuador abruptly. The first case in Ecuador was officially reported on 27 February, but the only scientific report suggests that the virus has entered the country weeks earlier⁷. In March, the virus had spread massively within Ecuador's coastal provinces, causing thousands of deaths each day in Ecuador, highlighting Guayaquil as the first COVID-19 epicenter in Latin America and the worst-hit country in the world⁸.

There is only one report exploring the epidemiological trends of COVID-19 in Ecuador, including a brief description of the clinical presentation among asymptomatic and mildly ill patients; nevertheless, no data is available in terms of the clinical features and outcome among critically ill patients⁷.

This study aims to present the outcome, and clinical characteristics of COVID-19 patients admitted to the intensive care unit in a secondary level hospital in Quito, Ecuador, from 1 April, 2020, to 31 July, 2020.

Citation: Vélez-Paez JL, Montalvo MP, Esteban Jara F, Aguayo-Moscoso S, Tercero-Martínez W, Stalin Saltos L, Jiménez-Alulima G, Irigoyen-Mogro E, Castro-Reyes E, Mora-Coello C, López-Rondón E, Toapanta P, Vásconez-González E, Ortiz-Prado E. Predicting mortality in critically ill patients with COVID-19 in the ICU from a secondary-level hospital in Ecuador. *Revis Bionatura* 2022;7(1) 1. <http://dx.doi.org/10.21931/RB/2022.07.01.1>

Received: 15 September 2021 / **Accepted:** 15 July 2022 / **Published:** 15 February 2022

Publisher's Note: Bionatura stays neutral with regard to jurisdictional claims in published maps and institutional affiliations.



Copyright: © 2022 by the authors. Submitted for possible open access publication under the terms and conditions of the Creative Commons Attribution (CC BY) license (<https://creativecommons.org/licenses/by/4.0/>).

Materials and methods

Setting

The study was carried out in the Intensive Care Unit in the secondary level hospital Pablo Arturo Suárez Hospital, Quito, Ecuador. Quito is the capital of Ecuador and has a population of 2.781.641. The city is located in the province of Pichincha and has an elevation of 2,850 m above sea level, becoming the second-highest capital city globally.

Study design

A retrospective cohort study of the clinical course and mortality due to COVID-19 among adult patients hospitalized and admitted to the ICU from 1 April to 31 July, 2020

Population and sample size

Every patient admitted to the ICU with a suspected diagnosis of COVID-19 within the established timeframe was initially included in the study. At the end of the study, we included 89 patients that fulfilled the inclusion criteria, while 12 were excluded from the study.

Inclusion criteria

Every patient admitted to the ICU unit with a positive molecular, serological, or clinical diagnosis of COVID-19 (characterized by: fever or chills, cough, dyspnea, anosmia, ageusia, sore throat, or myalgia) was included in the study. The clinical records (HC) of patients admitted with a confirmed result of COVID-19 by RT-PCR¹ or suggestive tomographic pattern (CO-RADS 4 or 5) were included, and cases with a presumptive diagnosis of COVID-19.

Exclusion criteria

Patients with a mild clinical presentation that were not admitted to the ICU or those with respiratory symptomatology that tested negative for SARS-CoV-2 infection through molecular testing (RT-PCR) or tomographic pattern not compatible with COVID-19 (CO-RADS 0 to 3).

Variables and measurements

Our team reviewed the electronic records of every patient that fulfilled the inclusion criteria. (Being admitted to the ICU was one of them)². Information concerning epidemiological, clinical, serological, and cytometric variables was collected. Every record was reviewed, and data were retrieved from admission to discharge or death in the ICU during the data collection period.

Statistical analysis

We performed a complete descriptive statistical analysis, calculating every qualitative variable's absolute and relative values. Mean, and standard deviation measures were used to describe differences and dispersion of the data set.

The assumption of normality of the quantitative variables was verified using the Shapiro test, where the t-test was used for parametric quantitative variables and the Mann Whitney test for those with non-parametric distributions.

We used the Chi-square test or Fisher's exact statistic to compare the proportion of survivors and non-survivors due to COVID-19. An odds ratio greater than one was used to indicate that the outcome was more likely to occur in one group.

We used the ROC curve analysis to predict mortality, determining cut-off points using the Youden index for the parameters related to mechanical ventilation and cytometric pa-

rameters. At the multivariate level, the Wald method forward logistic procedure regression was used, determining predictors of mortality for COVID-19. Statistical significance was established for p-value <0.05.

Ethical considerations

According to human research's local bioethical principles, anonymized, unidentifiable data from clinical records, excluding case reports, do not require internal review boards' approval. The physicians involved in collecting clinical data were also the only health providers accessing patients' clinical records.

Results

General results

During 121 days of follow-up, 89 patients with COVID-19 fulfilled the inclusion criteria. 68,54 % (n=61) were men and 31,46% women (n=28). There was no statistically significant difference in mean length of hospital stay (ALOS) between those who survived (9.31 days) versus those who died (10.29 days). The follow-up ended with 66.29% of patients (n=59) discharged from the ICU unit, while 33.71% of them (n=30) died due to COVID-19 (Table 1).

Age and sex differences

The average age of patients admitted to the hospital was 54.7 years, and survivors were 11 years younger (50.9) than non-survivors (62.2), and this difference was statistically significant (p-value: 0.001). Regarding gender, men were three times more likely to die (40.98%, n = 25) from COVID-19 compared to women (17.76%, n = 5) (p-value: 0.032).

Comorbidities and mortality risk

The most frequent comorbidity reported was hypertension (HT) in 20.22% (n=18) followed by obesity 16.85% (n=15) and diabetes mellitus (DM) 8.99% (n=8). The mean body mass index (BMI) was 30.84, with significant differences being observed between survivors (28,98) and non-survivors (31,99)⁵ being these differences statistically significant (p-value: 0.026).

Assessment of mortality indicators

The sequential organ failure assessment (SOFA) score at 24, 48, and 72 hours after admission was found to be 7.91, 6.14, and 5.46, respectively. The differences were statistically significant at 48 hours in survivors (SOFA=5.72) vs non-survivors (SOFA=7) and at 72 hours (SOFA= 4.93) versus (SOFA= 6.62) with a p-value of 0.038 and 0.010 respectively.

The APACHE II indicator was found to be higher among non-survivors (19.37) versus those who survived (17.42), although the differences were not statistically significant (p-value: 0.197) (Table 1).

Treatment and mortality

Seventy-two patients (80.9%) received systemic corticosteroid treatment⁷ (dexamethasone 6 mg daily up to 10 days), and among those, 25 patients (34.72%) did not survive while 47 (65.28%) survived. Low molecular weight heparin (LMWH) was administered to 69 patients (78.41%), and from this group, 59.42% (n=41) survived, and 40.58% died (n=28).

Ventilatory and respiratory parameters

To mitigate end-expiratory alveolar collapse, applied extrinsic PEEP values at 48 hours were significantly lower (7.89 cmH₂O) among survivors versus non-survivors (9.26 cmH₂O),

Clinical features	Total	Condition at discharge		p-value	OR (IC95%)
		Decease	Survivor		
Age (mean (SD)) years ^{1/}	54,72 (11,51)	62,23 (9,76)	50,9 (10,45)	0,000*	-
Sex (n (%)) ^{2/}					
Male	61 (68,54)	25 (40,98)	36 (59,02)	0,032**	3,19*** (1,07-9,53)
Female	28 (31,46)	5 (17,86)	23 (82,14)		
DM (%) ^{2/}					
Yes	8 (8,99)	2 (25,00)	6 (75,00)	0,712	-
No	81 (91,01)	28 (34,57)	53 (65,43)		
HTN (n (%)) ^{2/}					
Yes	18 (20,22)	8 (44,44)	10 (55,56)	0,281	-
No	71 (79,78)	22 (30,99)	49 (69,01)		
Obesity (n (%)) ^{2/}					
Yes	15 (16,85)	3 (20,00)	12 (80,00)	0,218	-
No	74 (83,15)	27 (36,49)	47 (63,51)		
BMI (mean (SD)) ^{3/}	30,84 (5,82)	31,99 (4,85)	28,98 (6,15)	0,026*	-
Apache II income (mean (SD)) ^{3/}	18,08 (5,84)	19,37 (6,08)	17,42 (5,65)	0,197	-
SOFA (mean (SD)) ^{3/}					
24 hours	7,91 (2,99)	8,33 (2,73)	7,69 (3,11)	0,251	-
48 hours	6,14 (2,54)	7 (2,61)	5,72 (2,41)	0,038*	-
72 hours	5,46 (2,84)	6,62 (2,76)	4,93 (2,74)	0,010*	-
Corticosteroid use (n (%)) ^{2/}	72 (80,90)	25 (34,72)	47 (65,28)	-	-
Heparin use Anticoagulation (n (%)) ^{2/}	69 (78,41)	28 (40,58)	41 (59,42)	-	-
Days of hospitalization (mean (SD)) ^{3/}	9,65 (5,44)	10,29 (5,66)	9,31 (5,34)	0,351	-

Note: SD = Standard Deviation; * significant differences in means, based on 1 / t test and 3 / Mann Whitney test; ** significant differences in the non-survivor condition, based on the Chi-square test or Fisher's exact statistic 2 /; *** OR = Odds Ratio significant, lower limit of the 95% confidence interval (95% CI) > 1

Table 1. Association between mortality and clinical characteristics.

and this difference was statistically significant (p-value: 0.015). The maximum PCO₂ at 72 hours was higher among non-survivors (49.34 mmHg), versus survivors (41.37 mmHg), and this difference was statistically significant (p-value: 0.026) (Table 2).

The PaO₂/FiO₂ ratio at 24 and 72 hours was always higher among survivors. For instance, non-survivors reported a PaO₂/FiO₂ of 127.77 mmHg and 136.36 mmHg at 24 and 72 hours, respectively, while survivors had values of 152.97 mmHg and 181.09 mmHg at the same time interval, both differences being statistically significant (p-value: 0.036 and <0.001 respectively).

Survivors remained intubated for seven days while non-survivors for ten days, a difference that is also statistically significant (p-value: 0.002).

Serological biomarkers

Mean lactate dehydrogenase levels (LDH) were higher among non-survivors (1025.47 U / L) versus survivors (891.10 U / L); Likewise, IL-6 presented was 137% higher among non-survivors (140.55 pg / ml) versus survivors (59.3 pg. / ml) (p-value: < 0.05). D-dimer and ferritin at 24 and 48 hours did not show significant differences (Table 3).

Flow cytometric analysis

Lymphocyte count at 48 hours presented a mean of 753.79 x 10³ / ml in survivors and 537.59 x 10³ / ml in non-survivors (p-value 0.006). Neutrophilia was found to be significantly higher among non-survivors at 24 hours (11,741.63 x 10³ / ml) in comparison with survivors (9,282.54 x 10³ / ml). For the neutrophil-lym-

phocyte ratio (NLR)⁸ at 24, 48 and 72, non-survivors had significantly higher NLR than survivors (p-value: < 0.001) (Table 4).

Platelet count at 48 hours shows that non-survivors had significantly lower platelet counts (320,103.45 x 10³ / ml) than survivors (388,172.41 x 10³ / ml).

Predictive factors for mortality

PEEP analysis.

The area of the receiver operating characteristic (ROC) curve for PEEP at 48 hours was 0.661 (95% CI 0.535-0.787), maximum PCO₂ at 72 hours 0.650 (95% CI 0.519-0.780), Pa-FiO₂ at 24 hours 0.636 (95% CI 0.508-0.765), and PaFiO₂ at 72 hours 0.747 (95% CI 0.638-0.857), these areas presented confidence intervals that do not include the value 0.5; therefore, be used to predict mortality for COVID-19.

The cut-off points to predict mortality in the ROC curve using the Youden index of the mechanical ventilation parameters were positive for mortality if 48-hour PEEP ≥8.50 cmH₂O, where the sensitivity was 54%, and specificity was 74% (Figure 1)⁹. Positive for mortality if: 72-hour peak PCO₂ ≥46.50 mmHg (sensitivity: 54%, specificity 77%), 24-hour PaFiO₂ ≤89 mmHg (sensitivity: 30%, specificity: 97%) and PaFiO₂ 72 hours ≤155.50 mmHg (sensitivity: 82%, specificity: 66%).

Biomarker analysis.

The area of the ROC curve for IL-6 was 0.675 (IC95%

Mechanical ventilation parameters	Total	Condition at discharge		p-value
		Decease	Survivor	
Ventilatory mode of admission (n (%)) ^{2/}				
Volume controlled	14 (15.73)	4 (28.57)	10 (71.43)	0.765
Pressure controlled	75 (84.27)	26 (34.67)	49 (65.33)	
Vt 24 hours (mean (SD)) ^{3/} ml/kg	403.15 (61.2)	398.33 (57.41)	405.59 (63.38)	0.761
Vt 48 hours (mean (SD)) ^{1/} ml/kg	417.69 (69.08)	411.9 (75.81)	420.63 (65.91)	0.582
Vt 72 hours (mean (SD)) ^{3/} ml/kg	424.41 (78.17)	434.21 (88.78)	418.57 (71.49)	0.222
PEEP 24 hours (mean (SD)) ^{3/} cmH2O	9.46 (2.09)	9.83 (2.28)	9.27 (1.99)	0.329
PEEP 48 hours (mean (SD)) ^{3/} cmH2O	8.35 (2.29)	9.29 (2.45)	7.89 (2.08)	0.015*
PEEP 72 hours (mean (SD)) ^{3/} cmH2O	7.81 (2.26)	8.46 (2.81)	7.43 (1.79)	0.227
24-hour plateau pressure (mean (SD)) ^{1/} cmH2O	23.19 (4.23)	23.73 (4.65)	22.92 (4.01)	0.391
48-hour plateau pressure (mean (SD)) ^{3/} cmH2O	21.77 (3.83)	22.07 (4.54)	21.61 (3.44)	0.637
72-hour plateau pressure (mean (SD)) ^{3/} cmH2O	21 (3.82)	22.11 (3.92)	20.35 (3.65)	0.074
Driving pressure 24 hours (mean (SD)) ^{3/} cmH2O	13.62 (3.28)	13.53 (3.56)	13.66 (3.17)	0.776
Driving pressure 48 hours (mean (SD)) ^{3/} cmH2O	13.33 (2.94)	13.07 (3.1)	13.47 (2.87)	0.252
Driving pressure 72 hours (mean (SD)) ^{3/} cmH2O	13.42 (3.24)	14 (3.55)	13.07 (3.02)	0.250
PCO ₂ 24 hours (mean (SD)) ^{3/} mmHg	45.77 (13.55)	45.28 (10.92)	46.01 (14.79)	0.969
PCO ₂ 48 hours (mean (SD)) ^{3/} mmHg	45.23 (12.63)	46.53 (12.07)	44.6 (12.95)	0.492
PCO ₂ 72 hours (mean (SD)) ^{3/} mmHg	44.03 (12.86)	49.34 (17.92)	41.37 (8.4)	0.026*
PaFiO ₂ 24 hours (mean (SD)) ^{3/} mmHg	144.47 (47.94)	127.77 (44.98)	152.97 (47.52)	0.036*
PaFiO ₂ 48 hours (mean (SD)) ^{3/} mmHg	160.78 (47.77)	147.89 (35.14)	167 (51.93)	0.192
PaFiO ₂ 72 hours (mean (SD)) ^{1/} mmHg	166.18 (54.96)	136.36 (41.04)	181.09 (55.25)	<0.001*
Prone ventilation (n (%)) ^{2/}	53 (59.55)	20 (37.74)	33 (62.26)	0.368
Days of pronation (mean (SD)) ^{3/}	2.38 (1.42)	2.43 (1.36)	2.35 (1.48)	0.827
Use of relaxant (n (%)) ^{2/}	55 (61.80)	17 (30.91)	38 (69.09)	0.477
Days with muscle relaxant (mean (SD)) ^{3/}	2.22 (1.46)	2.38 (1.77)	2.14 (1.3)	0.769
Days in MV (mean (SD)) ^{3/}	8.49 (5.67)	10.86 (5.26)	7.3 (5.54)	0.002*
Mechanical power 24 hours (mean (SD)) ^{3/} j/min	15.77 (4.59)	16.16 (4.26)	15.57 (4.77)	0.343
Mechanical power 48 hours (mean (SD)) ^{3/} j/min	14.92 (4.64)	14.64 (4.31)	15.07 (4.83)	0.961
Compliance 24 hours (mean (SD)) ^{3/} ml/cmH2O	26.49 (12.48)	26.17 (13.89)	26.66 (11.84)	0.742
Compliance 48 hours (mean (SD)) ^{3/} ml/cmH2O	27.42 (13.48)	29.61 (15.64)	26.2 (12.11)	0.428
Compliance 72 hours (mean (SD)) ^{3/} ml/cmH2O	34.32 (10.82)	34.45 (7.71)	34.24 (12.47)	0.575
VT x Kg 24 hours (mean (SD)) ^{3/}	6.97 (1.31)	6.91 (1.23)	7 (1.36)	0.888
VT x Kg 48 hours (mean (SD)) ^{3/}	7.94 (7.04)	7.1 (1.29)	8.4 (8.68)	0.812
VT x Kg 72 hours (mean (SD)) ^{3/}	8.53 (8.55)	7.71 (1.48)	9.05 (10.91)	0.353
Extubation (n (%)) ^{2/}				
Failed	20 (27.40)	14 (70.00)	6 (30.00)	0.000**
Successful	53 (72.60)	0 (0.00)	53 (76.81)	

Note: SD = Standard Deviation; * significant differences in means, based on 1 / t test and 3 / Mann Whitney test; ** significant differences in non-survivor condition, based on Chi-square test or Fisher's exact statistic 2 /

Table 2. Correlation between mortality and mechanical ventilation parameters.

Analytics parameters	Total	Condition at discharge		p-value
		Decease	Survivors	
D-dimer 24 hours (mean (SD)) ng / ml ^{2/}	3,237 (7,277)	4,947 (1,202)	2,382(2,581)	0,057
D-dimer 48 hours (mean (SD)) ng / ml ^{2/}	2,861 (2925)	3,594 (3,436)	2,478 (2,578)	0,185
Ferritin 24 hours (mean (SD)) ng / ml ^{2/}	1,085 (487)	1,223 (429,78)	1,015 (502)	0,094
Ferritin 48 hours (mean (SD)) ng / ml ^{2/}	1,086 (468)	1,158 (379,61)	1,051 (505)	0,388
LDH 24 hours (mean (SD)) U / L ^{2/}	936 (369)	1,025 (273,81)	891 (405)	0,003*
LDH 48 hours (mean (SD)) U / L ^{1/}	814 (271)	842 (259,05)	799 (280)	0,540
IL-6 (mean (SD)) pg. / mL ^{2/}	86 (14,7)	140 (20)	59 (98)	0,016*

Note: SD = Standard Deviation; * significant differences in means, based on 1 / t test and 2 / Mann Whitney test

Table 3. Correlation between mortality and analytical parameters.

Cytometry parameters	Total	Condition at discharge		p-value
		Decease	Survivors	
Lymphocytes 24 hours (mean (SD)) ^{2/}	849 (1383)	650(383)	950(1,673)	0,089
Lymphocytes 48 hours (mean (SD)) ^{2/}	681 (381)	537 (300)	753 (398)	0,006*
Lymphocytes 72 hours (mean (SD)) ^{2/}	771 (645)	594 (285)	856 (748)	0,079
Platelets 24 hours (mean (SD)) ^{2/}	366,078 (135,037)	338, 266 (137,929)	380,220 (132,481)	0,164
Platelets 48 hours (mean (SD)) ^{2/}	365,482 (139,212)	320,103(118,949)	388,172(143,9370)	0,043*
Platelets 72 hours (mean (SD)) ^{2/}	362,378(137,738)	324,107(120,235)	380,853(142,747)	0,055
Neutrophils 24 hours (mean (SD)) ^{2/}	10,111(4,457)	11,741 (4,649)	9,282(4,154)	0,013*
Neutrophils 48 hours (mean (SD)) ^{2/}	10,030 (4,585)	10,683 (4,059)	9,703(4,826)	0,322
Neutrophils 72 hours (mean (SD)) ^{2/}	9,841(4,204)	11,064 (4,375)	9,250(4,025)	0,063
Eosinophilic edges 24 hours (mean (SD)) ^{2/}	34,61(68,04)	27,8 (44,23)	38,07 (77,52)	0,922
Eosinophilic edges 48 hours (mean (SD)) ^{2/}	44,39 (87,52)	32,72 (56,89)	50,22 (99,32)	0,072
Eosinophilic edges 72hours (mean (SD)) ^{2/}	56,98 (104,83)	51,21 (86,85)	59,76 (113,1)	0,661
NLR 24 hours (mean (SD)) ^{2/}	18,54 (15,57)	23,8 (16,52)	15,87 (14,48)	0,002*
NLR 48 hours (mean (SD)) ^{2/}	18,96 (15,25)	26,01 (18,75)	15,44 (11,85)	0,000*
NLR 72 hours (mean (SD)) ^{2/}	18,68 (14,88)	22,64 (13,43)	16,77 (15,28)	0,004*

Note: SD = Standard Deviation; NLR = neutrophil / lymphocyte ratio; * significant differences in means, based on 1 / t test and 2 / Mann Whitney test

Table 4. Correlation between mortality and cytometric parameters.

0.542-0.809), and for LDH at 24 hours 0.691 (IC95% 0.580-0.803), these areas presented confidence intervals that do not include the value 0.5; therefore, they are significant in predicting mortality for COVID-19.

The cut-off points to predict mortality in the ROC curve using the Youden index of the analytical parameters were positive for mortality if IL-6 ≥ 117 pg / mL, where the sensitivity was 42%, and specificity was 91%. Regarding LDH, it was positive for mortality at 24 hours with a cut-off ≥ 783 U / L (sensitivity: 90%, specificity: 43%) (Figure 2).

The area of the ROC curve for NLR at 24 hours was 0.704 (95% CI 0.591-0.817), NLR at 48 hours¹⁰ 0.743 (95% CI 0.634-0.851), NLR at 72 hours 0.692 (95% CI 0.578-0.806), and platelets 48 hours¹¹ 0.633 (95% CI 0.508-0.759), these areas presented confidence intervals that do not include the value 0.5; therefore, they are significant to predict mortality for COVID-19 (Figure 3).

The cut-off points for predicting mortality in the ROC curve using the Youden index of the cytometry parameters were the following: Positive for mortality if NLR 24 hours¹³ ≥ 16.33 , where sensitivity was 73% and specificity 64%. Positive for mortality if NLR 48 hours ≥ 16.96 , where the sensitivity was 76% and specificity was 67%. Positive for mortality if NLR 72 hours ≥ 17.12 , where the sensitivity was 64% and specificity

74%. Positive for mortality if Platelets $\leq 364,000 \times 10^3$ ml, where the sensitivity was 79% and specificity 50%.

SOFA mortality prediction analysis.

For the SOFA mortality predictors, the cut-off point for COVID-19 was determined, the ROC curves showed for SOFA at 48 hours an area of 0.637 (95% CI 0.511-0.763), and for 72 hours of 0.675 (95% CI 0.556 -0.794), these areas were significant to predict mortality, the cut-off point established at 48 and 72 hours was positive for mortality if SOFA ≥ 6 , at 48 hours, the sensitivity of 79% and specificity 48% were obtained, at 72 hours the sensitivity was 69% and specificity 57% (Figure 4).

The results obtained showed that PaFiO₂ 72 hours ≤ 155.50 mmHg with p-value 0.009, IL-6 ≥ 117 pg. / mL with p-value 0.011, NLR 24 hours ≥ 16.33 with p-value 0.013 and NLR 72 hours ≥ 17.12 with p-value 0.005 are predictors of mortality for COVID-19; where values of PaFiO₂ 72 hours ≤ 155.50 mmHg, IL-6 ≥ 117 pg. / mL, NLR 24 hours ≥ 16.33 and NLR 72 hours ≥ 17.12 presented 9.24, 21.84, 6.13, and 13, 33 times more likely not to survive; the mechanical ventilation's cut-off points, analytical and cytometry parameters were determined (Table 5).

The results obtained showed that PaFiO₂ 72 hours ≤ 155.50 mmHg with p-value 0.009, IL-6 ≥ 117 pg. / mL with

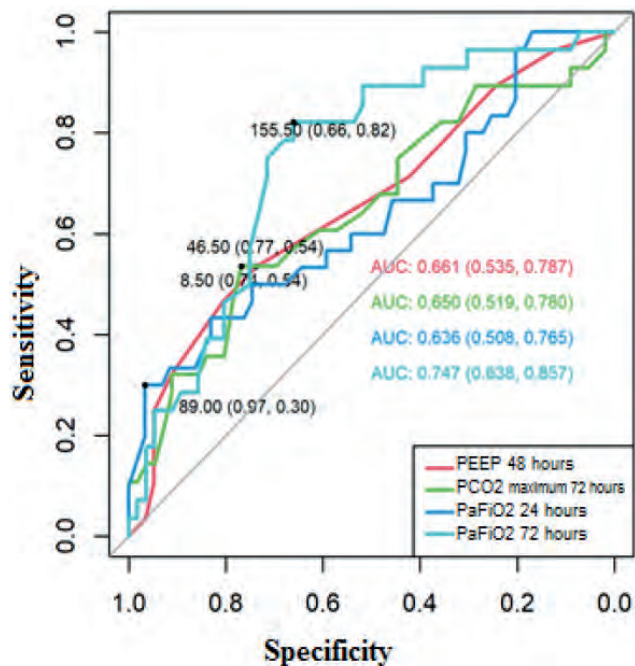


Figure 1. ROC curve to predict mortality for COVID-19, based on PEEP 48 hours, maximum PCO₂ 72 hours, PaFiO₂ 24 and 72 hours.

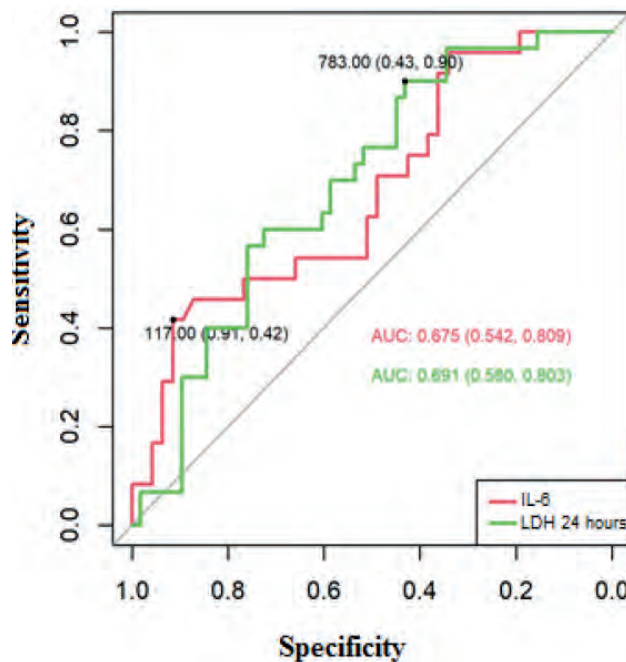


Figure 2. ROC curve to predict mortality for COVID-19, based on IL-6 and LDH at 24 hours.

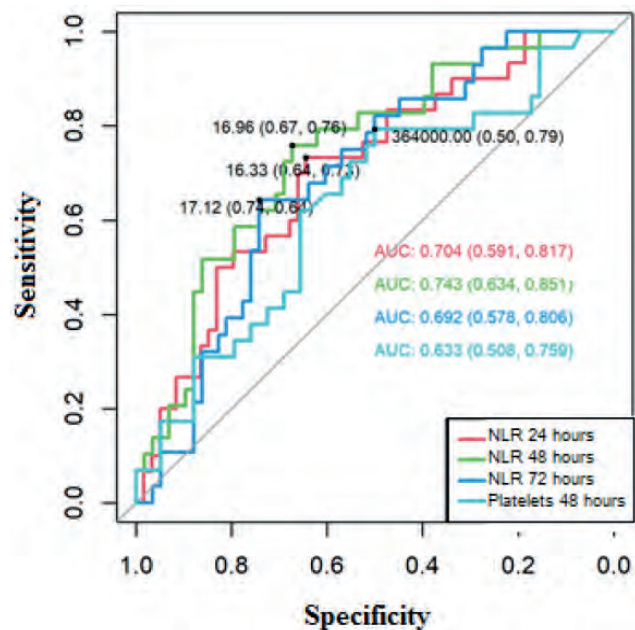


Figure 3. ROC curve to predict mortality for COVID-19, based on NLR (at 24, 48 and 72 hours¹⁴) and platelets at 48 hours¹⁶.

p-value 0.011, NLR 24 hours ≥ 16.33 with p-value 0.013 and NLR 72 hours ≥ 17.12 with p-value 0.005 are predictors of mortality for COVID-19; where values of PaFiO₂ 72 hours ≤ 155.50 mmHg, IL-6 ≥ 117 pg. / mL, NLR 24 hours ≥ 16.33 and NLR 72 hours ≥ 17.12 presented 9.24, 21.84, 6.13 and 13, 33 times more likely to not survive.

Discussion

This original research is the first report of the clinical characteristics of severely ill patients with COVID-19 who have been clinically managed in a secondary-level hospital ICU in

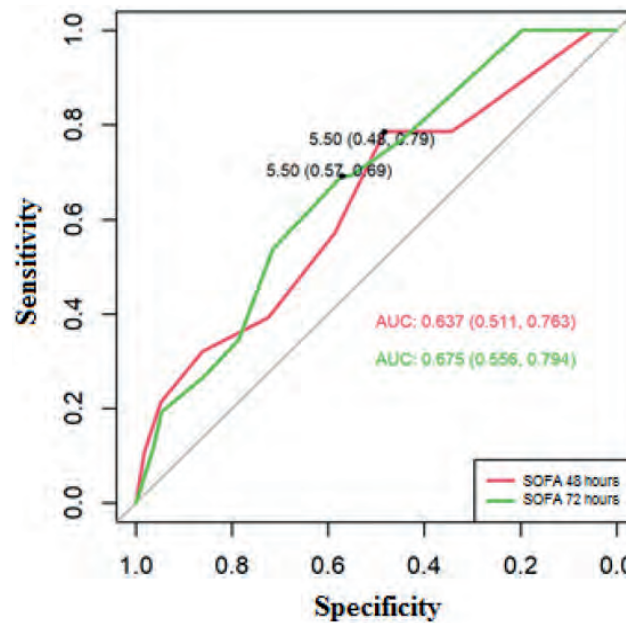


Figure 4. ROC curve to predict mortality for COVID-19, based on SOFA at 48 and 72 hours.

Quito, Ecuador. The results showed that older age and sex are positively associated with mortality. These results are similar to several reports available^{9,10}. The average age of our admitted patients was 54 years, considerably younger populations than other countries. In China, two reports found that the mean age of patients admitted to the ICU was between 64 and 66 years, on average ten years older than our population^{11,12}. In other continents, the age of the admitted patients is also higher. For instance, in Italy and Spain, the available information reports an average age of 63 years, while in the USA, the average age is 79 years^{10,13-16}.

Mejia *et al.* 2020 published the only available study with results similar to ours in a cohort of Peruvian patients. They

Variables	B	Wald	p-value	OR	95% CI-OR	
					Li	Ls
Inside the model						
PaFiO ₂ 72 hours ≤ 155,50 mmHg	2,22	6,74	0,009*	9,24**	1,73	49,49
IL-6 ≥ 117 pg./mL	3,08	6,54	0,011*	21,84**	2,06	231,85
NLR 24 hours ≥ 16,33	1,81	6,10	0,013*	6,13**	1,46	25,86
NLR 72 hours ≥ 17,12	2,59	7,85	0,005*	13,33*	2,18	81,56
Constant	-4,39	17,38	0,000*			
Excluded from the model						
PEEP 48 hours ≥ 8,50 cmH ₂ O		0,30	0,587			
Maximum PCO ₂ 72 hours > 46,50 mmHg		1,55	0,213			
PaFiO ₂ 24 hours ≤ 89 mmHg		2,63	0,105			
24-hour LDH ≥ 783 U / L		0,06	0,801			
NLR 48 hours ≥ 16,96		0,78	0,378			
Platelets ≤ 364,000 10 ³ ml		0,82	0,366			
SOFA 48 hours ≥ 6		0,71	0,399			
SOFA 72 hours ≥ 6		0,06	0,805			
Note: NLR = neutrophil / lymphocyte ratio; * significant variable p-value < 0.05, ** OR = significant odds ratio Li > 1; based on logistic regression forward procedure Wald method						

Table 5. Logistic regression to predict mortality for COVID-19, based on mechanical ventilation, analytical and cytometry parameters.

found that the median age of the admitted patients was 59 years¹⁷. Although there is no clear information on why older men are at higher risk of dying due to COVID-19, a higher proportion of comorbidities among men may play a significant role, and the presence of unhealthier lifestyles¹⁸, along with immunosenescence phenomena. It has also been hypothesized that men the angiotensin-converting enzyme-2 (ACE-2) receptor might play an important role. Previously published studies suggest that the ACE-2 receptor plays a role in other coronaviruses-related diseases such as Severe Acute Respiratory Syndrome (SARS) or Middle East Respiratory Syndrome (MERS), finding higher concentrations of ACE-2 receptors among men^{18,19}.

In terms of respiratory parameters, persisting hypercapnia for more than 72 hours, the PaFiO₂ ratio at 24 and 72 hours < 140 mmHg and PEEP greater than 9 cmH₂O were also associated with increased risk of mortality. External positive pressure ventilation increases intrathoracic pressure and does so more potently when the lungs are highly compliant²⁰. Moderate PEEP levels are required to ventilate adequately and achieve normoxia. In our results, maintaining PEEP levels greater than 8 mmHg after 48 hours was associated with a poorer prognosis. Although the impact of COVID-19 within the lungs is not quite the same as other diseases causing ARDS, the role of adequate ventilatory management is fundamental.

Gatinonni et al., defined two phenotypic patterns in the clinical presentation of COVID-19, a Low (L) phenotype in which there is low elastance, low shunt and poor recruit ability with little response to PEEP and a High (H) phenotype, with high elastance, high shunt and favorable response to alveolar recruitment with PEEP^{21,22}.

Regarding the presentation of the L and H phenotypes in ARDS due to COVID 19, we consider that their presentation was variable, if we take into account the relationship between

compliance and PaO₂ / FiO₂ as reported by Panwar²³, patients with lower PaO₂ / FiO₂, like those with low compliance died. However, these variables can be very heterogeneous because there could be H patterns with PaO₂ / FiO₂ greater than 150 and in other L phenotypes with PaO₂ / FiO₂ < 150 mmHg. Both PaO₂ / FiO₂ and compliance have always been considered a marker of severity; in our work, the patients who had lower values were the most serious and of them, those who died had low compliance from admission, as mentioned. In other studies, patients that improved PaO₂ / FiO₂ and compliance pattern L had better survival^{22,23}.

Our study also found that elevated levels of IL-6¹⁹, LDH at 24 hours, lymphopenia at 48 hours, neutrophilia at 24 hours, and high NLR from admission to 72 hours were also associated with more significant mortality. Previous works have evaluated this, which may indirectly indicate a reaction due to the massive inflammatory response or the cytokine storm constantly related with more severe clinical presentations^{24,25}. These results are similar to those previously reported worldwide; however, it is interesting to note that ferritin and the D-dimer biomarker have not achieved enough statistical power to predict mortality^{12,26}. Furthermore, our findings support the use of cytometric analysis that is often affordable and available in low-resource settings.

Several laboratory data are identified as predictors of severity and mortality in COVID-19, such as elevated D-dimer, lymphopenia, increased LDH, thrombocytopenia, increased C-reactive protein, elevated ferritin and IL-6, among others²⁷⁻³⁴. In our study, the factors associated with mortality were LDH values at 24 hours, IL-6, the lymphocyte and platelet count at 48 hours, the neutrophil count at 48 hours, and the NLR in all its measurements; the latter, together with IL-6, reached a predictive level. These results are consistent with the existing evidence in the world. Interestingly, D-dimer and ferritin at 24 and

48 hours did not present a significant association with mortality, a finding that contradicts the existing evidence at that time.

The most frequent comorbidities in our patients were: hypertension, obesity and diabetes mellitus (DM). For diabetes and hypertension, there was no statistically significant difference in terms of risk of mortality; nevertheless, when evaluating body mass index, higher BMI was associated with a greater risk of dying (Table 1), as described in other studies²⁶. A clinical report from Wang *et al.* showed statistically significant differences in terms of mortality among patients with chronic hypertension¹². On the other hand, other studies found that hypertension was not an independent factor in increasing mortality, opposing hypercholesterolemia and DM¹⁰.

In general terms, the overall mortality in our center seems to be adequate compared to other countries. In Ecuador, we found that 33.7% of patients succumbed in the ICU unit due to COVID-19. A recently published report from China, including 517 patients, reported an overall mortality rate of 37.7%^{12,13}. These numbers seem to be lower than other reports coming from Europe. For instance, in Italy, Grasselli *et al.* 2020 included 1,715 patients, and they found that the overall mortality was superior to 48%¹⁰. In Spain, a national cohort of 736 patients reported mortality rates greater than 42%¹⁴. On the other hand, information emerging from the USA shows that mortality was significantly lower in a cohort of 1,392 patients. They reported an overall mortality of 23.6%¹³.

In Latin America, reports are scarce. We found that in Peru, the overall mortality rate among severely ill COVID-19 patients was 32.4%³⁵. However, in this study, cut-off points for serological biomarkers and mechanical ventilation variables analysis were not determined, which might give a more in-depth insight into our results.

At the beginning of the pandemic, corticosteroids' use was controversial, and their use focused on quenching the so-called "cytokine storm"^{27,36-38}. During the first few months of the outbreak, few scientific societies recommended using systemic corticosteroids to treat ARDS. Nevertheless, in our hospital, we adopted the SARS and MERS guidelines, which could be associated with our relatively low mortality rates compared to other centers^{22,39-41}.

Limitations

Our results came from an intensive care unit of 7 beds. Therefore, collecting a representative sample was more prolonged than in other centers. It is essential to point out that a molecular analysis for COVID-19 using RT-PCR was not always available *in situ*; therefore, the diagnosis was based on radiological and clinical suspicion, and the confirmatory molecular or serological confirmation sometimes arrived days later.

Conclusions

The values of LDH at 24 hours, IL-6 the lymphocyte and platelet count at 48 hours, the neutrophil count at 48 hours, and the NLR are factors associated with mortality and were even determining factors for failure in the extubation and reintubation.

The clinical and physiopathological presentation of COVID-19 suggested a strong activation of the pro-inflammatory response; this meant that in our hospital, even without solid evidence, we indicated corticoids, a measure that was later validated by RCTs and meta-analyses. This would essentially justify the non-elevated mortality in our series of patients.

Although analytical markers such as IL 6 and LDH are

acceptable and well-known parameters for managing critical patients, their availability is not universal, and IL 6 is expensive. Finding a surrogate such as the NLR, which has a predictive value in its measurements at 24 and 72 hours that is not depreciable; makes the findings of this study relevant by providing a cost-effective instrument derived from the standard blood count to establish the risk of death and severity in COVID-19.

Ethics approval and consent to participate

According to human research's local bioethical principles, anonymized, unidentifiable data from clinical records, excluding case reports, do not require internal review boards' approval. The physicians involved in collecting clinical data were also the only health providers accessing patients' clinical records.

Availability of data and materials

The datasets used and analyzed during the current study are available from the corresponding author on reasonable request.

Competing interests

The authors declare no conflicts of interest.

Funding

This study did not receive any funding.

Authors' contributions

JLV was entirely responsible for conceptualizing the study and directing the team when collecting information. He drafted the first version of the manuscript and reviewed the final version. MPM, FEJ, SAM, WTM, LS, GJ, EI, EC, and CM were responsible for collecting information from the ICU unit and contributing equally to the data analysis. EVG was responsible for completing the dataset and completing the first draft of the manuscript. EOP was responsible for critically reviewing the first draft, completing the manuscript's final version, and critically reviewing the entire analytical process around data collection.

Acknowledgments

To all our collaborators, including medical, nursing and support staff who have spent months working day and night in the ICU without any proper resting, helping patients who are battling against COVID-19.

Bibliographic references

1. International Society for, Infectious Diseases. PRO/AH/EDR> COVID-19 update (59): global, cruise ship, WHO. 2020. <https://promedmail.org/promed-post/>. Accessed 30 September 2020.
2. CDC. 2019-nCoV Respuestas a las preguntas más frecuentes | CDC. CDC. 2020. <https://web.archive.org/web/20200318025404/https://www.cdc.gov/coronavirus/2019-ncov/faq-sp.html>. Accessed 30 Sep 2020.
3. Ortiz-Prado E, Simbaña-Rivera K, Gómez- Barreno L, Rubio-Neira M, Guaman LP, Kyriakidis NC, et al. Clinical, molecular, and epidemiological characterization of the SARS-CoV-2 virus and the Coronavirus Disease 2019 (COVID-19), a comprehensive literature review. *Diagn Microbiol Infect Dis.* 2020;98:115094.
4. OMS. Cronología de actuación ante el COVID-19 - OPS/OMS | Organización Panamericana de la Salud. <https://www.paho.org/es/panama/cronologia-actuacion-ante-covid-19>. Accessed 30 Sep 2020.
5. Ortiz-Prado E, Cevallos-Sierra G, Henríquez-Trujillo AR, Lowe R, Lister A. Covid-19 in Latin America. *The BMJ*; 2020. <https://blogs.bmj.com/bmj/2020/08/13/covid-19-in-latin-america/>. Accessed 3 Oct 2020.

6. Decerf B, Ferreira FH, Mahler DG, Sterck O. Lives and livelihoods: estimates of the global mortality and poverty effects of the Covid-19 pandemic. *The World Bank*; 2020.
7. Ortiz-Prado E, Diaz AM, Barreto A, Moyano C, Arcos V, Vasconez-Gonzalez E, et al. Epidemiological, socio-demographic and clinical features of the early phase of the COVID-19 epidemic in Ecuador. *medRxiv*. 2020.
8. Lima E, Vilela E, Peralta A, Rocha MG, Queiroz BL, Gonzalez MR, et al. Exploring excess mortality in Latin America in the context of covid pandemic: the cases of Brazil and Ecuador. 2020.
9. Palaodimos L, Kokkinidis DG, Li W, Karamanis D, Ognibene J, Arora S, et al. Severe obesity, increasing age and male sex are independently associated with worse in-hospital outcomes, and higher in-hospital mortality, in a cohort of patients with COVID-19 in the Bronx, New York. *Metabolism*. 2020;108:154262.
10. Grasselli G, Greco M, Zanella A, Albano G, Antonelli M, Bellani G, et al. Risk Factors Associated With Mortality Among Patients With COVID-19 in Intensive Care Units in Lombardy, Italy. *JAMA Intern Med*. 2020. doi:10.1001/jamainternmed.2020.3539.
11. Gao Q, Hu Y, Dai Z, Wu J, Xiao F, Wang J. The epidemiological characteristics of 2019 novel coronavirus diseases (COVID-19) in Jingmen, Hubei, China. *medRxiv*. 2020;:2020.03.07.20031393.
12. Wang Y, Lu X, Li Y, Chen H, Chen T, Su N, et al. Clinical Course and Outcomes of 344 Intensive Care Patients with COVID-19. *Am J Respir Crit Care Med*. 2020;201:1430-4.
13. Quah P, Li A, Phua J. Mortality rates of patients with COVID-19 in the intensive care unit: a systematic review of the emerging literature. *Crit Care*. 2020;24. doi:10.1186/s13054-020-03006-1.
14. Berenguer J, Ryan P, Rodríguez-Baño J, Jarrín I, Carratalà J, Pachón J, et al. Characteristics and predictors of death among 4035 consecutively hospitalized patients with COVID-19 in Spain. *Clin Microbiol Infect*. 2020;0. doi:10.1016/j.cmi.2020.07.024.
15. Richardson S, Hirsch JS, Narasimhan M, Crawford JM, McGinn T, Davidson KW, et al. Presenting Characteristics, Comorbidities, and Outcomes Among 5700 Patients Hospitalized With COVID-19 in the New York City Area. *JAMA*. 2020;323:2052-9.
16. Barrasa H, Rello J, Tejada S, Martín A, Balzikueta G, Vinuesa C, et al. SARS-CoV-2 in Spanish Intensive Care Units: Early experience with 15-day survival in Vitoria. *Anaesth Crit Care Pain Med*. 2020. doi:10.1016/j.accpm.2020.04.001.
17. Mejía F, Medina C, Cornejo E, Morello E, Vásquez S, Alave J, et al. Características clínicas y factores asociados a mortalidad en pacientes adultos hospitalizados por COVID-19 en un hospital público de Lima, Perú. 2020. doi:10.1590/SciELOPreprints.858.
18. Scully EP, Haverfield J, Ursin RL, Tannenbaum C, Klein SL. Considering how biological sex impacts immune responses and COVID-19 outcomes. *Nat Rev Immunol*. 2020;:1-6.
19. Sama IE, Ravera A, Santema BT, van Goor H, Ter Maaten JM, Cleland JG, et al. Circulating plasma concentrations of angiotensin-converting enzyme 2 in men and women with heart failure and effects of renin-angiotensin-aldosterone inhibitors. *Eur Heart J*. 2020;41:1810-1817.
20. Jardin F, Genevray B, Brun-Ney D, Bourdarias J-P. Influence of lung and chest wall compliances on transmission of airway pressure to the pleural space in critically ill patients. *Chest*. 1985;88:653-658.
21. Gattinoni L, Chiumello D, Caironi P, Busana M, Romitti F, Brazzi L, et al. COVID-19 pneumonia: different respiratory treatments for different phenotypes? *Springer*; 2020.
22. Montenegro F, Unigarro L, Paredes G, Moya T, Romero A, Torres L, et al. Acute Respiratory Distress Syndrome (ARDS) Caused by the Novel Coronavirus Disease (COVID-19): A Practical Comprehensive Literature Review. 2020.
23. Panwar R, Madotto F, Laffey JG, Van Haren FMP. Compliance Phenotypes in Early ARDS Before the COVID-19 Pandemic. *Am J Respir Crit Care Med*. 2020. doi:10.1164/rccm.202005-2046OC.
24. Sun X, Wang T, Cai D, Hu Z, Liao H, Zhi L, et al. Cytokine storm intervention in the early stages of COVID-19 pneumonia. *Cytokine Growth Factor Rev*. 2020.
25. Coperchini F, Chiovato L, Croce L, Magri F, Rotondi M. The cytokine storm in COVID-19: an overview of the involvement of the chemokine/chemokine-receptor system. *Cytokine Growth Factor Rev*. 2020.
26. Palaodimos L, Kokkinidis DG, Li W, Karamanis D, Ognibene J, Arora S, et al. Severe obesity, increasing age and male sex are independently associated with worse in-hospital outcomes, and higher in-hospital mortality, in a cohort of patients with COVID-19 in the Bronx, New York. *Metabolism*. 2020;108:154262.
27. CDC. Coronavirus Disease 2019 (COVID-19). Centers for Disease Control and Prevention. 2020. <https://www.cdc.gov/coronavirus/2019-ncov/hcp/clinical-guidance-management-patients.html>. Accessed 30 Sep 2020.
28. Ministerio de Sanidad. INFORMACIÓN CIENTÍFICA-TÉCNICA Enfermedad por coronavirus, COVID-19. 2020. <https://www.mscbs.gob.es/profesionales/saludPublica/ccayes/alertasActual/nCov/documentos/ITCoronavirus.pdf>. Accessed 30 Sep 2020.
29. BMJ. Coronavirus disease 2019 (COVID-19) - Symptoms, diagnosis and treatment | BMJ Best Practice US. *BMJ Best Practice*. 2020. <https://bestpractice.bmj.com/topics/en-us/3000168>. Accessed 30 September 2020.
30. McIntosh K. Coronavirus disease 2019 (COVID-19): Epidemiology, virology, and prevention - UpToDate. *UpToDate Inc*. 2020. <https://www.uptodate.com/contents/coronavirus-disease-2019-covid-19-epidemiology-virology-and-prevention>. Accessed 30 September 2020.
31. Cochrane. El valor D-dímero está asociado a la gravedad de los pacientes con la COVID-19. *cochrane.org*. 2020. [/es/recursos/evidencias-covid-19/el-valor-d-d%C3%ADmero-est%C3%A1-asociado-la-gravedad-de-los-pacientes-con-la](https://es/recursos/evidencias-covid-19/el-valor-d-d%C3%ADmero-est%C3%A1-asociado-la-gravedad-de-los-pacientes-con-la). Accessed 30 Sep 2020.
32. Lippi G, Favaloro EJ. D-dimer is Associated with Severity of Coronavirus Disease 2019: A Pooled Analysis. *Thromb Haemost*. 2020;120:876-8.
33. Nasiri MJ, Haddadi S, Tahvildari A, Farsi Y, Arbabi M, Hasanzadeh S, et al. COVID-19 Clinical Characteristics, and Sex-Specific Risk of Mortality: Systematic Review and Meta-Analysis. *Front Med*. 2020;7. doi:10.3389/fmed.2020.00459.
34. Xu L, Yaqian M, Chen G. Risk factors for severe corona virus disease 2019 (COVID-19) patients : a systematic review and meta analysis. *medRxiv*. 2020;:2020.03.30.20047415.
35. Benitez H, Vargaas E, Peña E, Taype A, Arrospide D, Castillo M, et al. Características clínicas, manejo y mortalidad de pacientes hospitalizados con COVID-19 en un hospital de referencia en Lima, Perú. *PRE-PRINT*. 2020.
36. WHO. Clinical management of COVID-19. *WHO*. 2020. <https://www.who.int/publications-detail-redirect/clinical-management-of-covid-19>. Accessed 30 September 2020.
37. Ministerios de Sanidad. Protocolo_manejo_clinico_ah_COVID-19.pdf. 2020. https://www.mscbs.gob.es/profesionales/saludPublica/ccayes/alertasActual/nCov/documentos/Protocolo_manejo_clinico_ah_COVID-19.pdf. Accessed 30 Sep 2020.
38. Ministerio de Sanidad. Manejo_urgencias_pacientes_con_COVID-19.pdf. 2020. https://www.mscbs.gob.es/profesionales/saludPublica/ccayes/alertasActual/nCov/documentos/Manejo_urgencias_pacientes_con_COVID-19.pdf. Accessed 30 Sep 2020.
39. Anesi G. Coronavirus disease 2019 (COVID-19): Critical care and airway management issues - UpToDate. *UpToDate Inc*. 2020. https://www.uptodate.com/contents/coronavirus-disease-2019-covid-19-critical-care-and-airway-management-issues?search=coronavirus-disease-2019-covid-19-%20critical-care-issues%5D&source=search_result&selectedTitle=1~150&usage_type=default&display_rank=1. Accessed 30 September 2020.
40. Alhazzani W, Møller MH, Arabi YM, Loeb M, Gong MN, Fan E, et al. Surviving Sepsis Campaign: guidelines on the management of critically ill adults with Coronavirus Disease 2019 (COVID-19). *Intensive Care Med*. 2020;46:854-87.
41. Wu C, Chen X, Cai Y, Xia J, Zhou X, Xu S, et al. Risk Factors Associated With Acute Respiratory Distress Syndrome and Death in Patients With Coronavirus Disease 2019 Pneumonia in Wuhan, China. *JAMA Intern Med*. 2020;180:934.

DE LA CURIOSIDAD ACADÉMICA A LA INNOVACIÓN TECNOLÓGICA



ESCUELA DE
CIENCIAS MATEMÁTICAS
Y COMPUTACIONALES



ESCUELA DE
CIENCIAS FÍSICAS
Y NANOTECNOLOGÍA



ESCUELA DE
CIENCIAS QUÍMICAS
E INGENIERÍA



ESCUELA DE
CIENCIAS DE LA TIERRA,
ENERGÍA Y AMBIENTE



ESCUELA DE
CIENCIAS BIOLÓGICAS
E INGENIERÍA

ARTICLE / INVESTIGACIÓN

Indicators to achieve a better positioning of Ecuadorian scientific journals

Victor Santiago Padilla*, Yalitza Therly Ramos Gil

DOI. 10.21931/RB/2022.07.01.2

Pontificia Universidad Católica del Ecuador Sede Ibarra, Imbabura, Ecuador.
Corresponding author: santiagopadillavictor@gmail.com

Abstract: Ecuador's scientific journals are not in a good position worldwide, as seen in the small number of journals indexed in impact databases. This research was carried out due to the current and prevailing need to improve the performance level of national scientific journals at the international level. This work sought to generate the information necessary for Ecuadorian scientific journals to have a greater scope considering the criteria for indexing in the Scopus, Clarivate Web of Science, Scielo, and Redalyc databases. This was determined based on the hypothesis: Failure to comply with the indicators for international scientific databases makes Ecuadorian journals not part of these collections. We identified differences between public and private institutions and the status of communication journals in compliance with the same criteria. We analyzed 55 Ecuadorian scientific journals already indexed in Latindex. The analysis was carried out by creating matrices that made it possible to quantify the fulfillment of the criteria, implementing a categorization of Yes for the journals that meet the indicator or NO for those that do not. Similarly, interviews were conducted with editors of the Ecuadorian journals with the best indexing to triangulate the information discussed in this research. The research showed that, although most magazines meet the vast majority of indexing criteria, the main problems are the geographic and institutional diversity of the editors and authors in the journals.

Key words: Databases, Indexing, Ecuadorian scientific journals, Scopus, Clarivate Web of Science, Scielo and Redalyc.

Introduction

Scientific journals are the basis of the knowledge community. They are in charge of collecting all the research that drives human beings as knowledge generators. These journals represent the vital means to disseminate research results and usually specialize in different disciplines or academic sub-disciplines¹.

Despite the importance of scientific journals, one of the problems within the academic context is identifying journals with a high impact. The great variety of journals at different levels of relevance leads to which articles provide a more significant impact and, therefore, better positioning in the ranking².

With the introduction of the 2008 Higher Education reform, scientific production in Ecuador experienced a turning point. From that date on, the national government required all higher education institutions to be directly linked and promote scientific and technological research³. The new requirements by said reform and the control of these, by the hand of the higher education agency, have led to an exponential growth in scientific production in the country since its creation⁴.

Despite this exponential growth in scientific publications in Ecuador, this positioning is inferior within Latin America, occupying in 2020 the 9th position in terms of publications and indexed scientific journals, with only 3 of the latter. However, the difference between the number of articles published by Ecuador (30775 publications) and Peru (36414 publications), the following country in the ranking, does not represent a significant difference, considering that the number of indexed Peruvian journals is 13⁵.

As observed in the aspects pointed out, we conducted this research due to the current and prevailing need to improve the

level of performance of Ecuadorian scientific journals. In this way, analyzing and evaluating the indicators that make a journal has a more significant impact will mean the creation of a basis for Ecuadorian scientific journals to have greater relevance in the future.

We considered all the information presented on the Scimago web page regarding the above. SCImago Journal Rank (acronym SJR) derived a positioning indicator for Latin American journals until 2020. The web analysis shows the status of Latin American journals indexed in the Scopus database, whose measurement reported the position of each of the countries related to scientific production during that year.

The first indicator analyzed was the number of indexed documents. Brazil was ranked with 1,145,853 documents, while in second and third place are Mexico with 387,111 and Argentina with 247,088. Below these positions in the top 10 indicators are Peru with 36 414 in 8th place and Ecuador in 9th place with 30 775 indexed documents. Uruguay closes the Top 10 with 23,887 documents⁶.

However, using the Scimago Journal Rank method and adding another indicator referring to the number of journals indexed in Scopus shows how the positions change. For example, Brazil remains in first place with 389 journals, while Colombia has 113 journals. However, Mexico and Chile are close behind with 111 and Chile with 109, occupying positions 3 and 4. At the same time, in positions 8 and 9 are Peru with 13 journals and Ecuador with 3 indexed journals⁶.

Therefore, the validity of the results of this research will provide relevant information so that scientific journals in Ecuador can consider obtaining a better positioning, both those that

Citation: Santiago Padilla V, Ramos Gil Y. T. Indicators to achieve a better positioning of Ecuadorian scientific journals. *Revis Bionatura* 2022;7(1). 2. <http://dx.doi.org/10.21931/RB/2022.07.01.2>

Received: 24 December 2021 / **Accepted:** 1 February 2022 / **Published:** 15 February 2022

Publisher's Note: Bionatura stays neutral with regard to jurisdictional claims in published maps and institutional affiliations.

Copyright: © 2022 by the authors. Submitted for possible open access publication under the terms and conditions of the Creative Commons Attribution (CC BY) license (<https://creativecommons.org/licenses/by/4.0/>).



are starting and those that have a history of academic dissemination. This will allow national research to have a greater reach and the Ecuadorian academic community to achieve a more significant international impact.

Materials and methods

Type of research

A basic approach and an explanatory level and field research are presented. Its purpose is to diagnose the situation of scientific journals in Ecuador and determine what parameters should be worked on to improve the positioning and indexing of journals.

Besides having a documentary and field design, the research was developed with a synchronic strategy, based on the current context, since the objective of defining "why" Ecuadorian scientific journals do not have better positioning was a primary element in the whole research process.

The data collection was derived from the field observation technique, allowing us to understand two phases of the research. The first one, to observe and interact directly with the organizational achievement of the subject of study, allowed to determine how it behaves in its specific environment with the general objective. The second phase made it possible to identify how the different variables in this environment can interact with the subject.

It is important to emphasize that the work is also configured with aspects of documentary research. To obtain the necessary data, texts, documents, and other documentary elements were used to analyze and interpret them critically to generate new knowledge.

Methods

A mixed approach (quantitative and qualitative) was chosen using the analytical-synthetic research method. The objective is to analyze all the leading databases' indexing criteria, synthesize the results, and propose new approaches and strategies to better position in Ecuadorian popular science journals. For this purpose, descriptive research was carried out to specify properties, characteristics and important features that make a scientific journal good positioning.

The use of this method involved collecting data from all available digital sources. The data synthesis will be displayed employing tables, charts, graphs, or any non-numerical form to facilitate understanding of the data collected. The studied indicators were obtained from the following databases: Scopus, Clarivate, Latindex, Scielo and Redalyc.

Population and sample

The sample size is 55 indexed Ecuadorian scientific journals. The journals were selected using a series of criteria detailed below. First, the journals of the institutions present in the Scimago university ranking were selected since this objectively gives us the context of the universities according to their scientific production, taking into account 3 parameters, performance in terms of research, innovation and social impact (De Moya Anegón et al., 2020). To reduce sample size and add another parameter to analyze, the institutions of the provinces of Ecuador where there were public and private institutions within the Scimago ranking were selected. Following these criteria, we chose journals of institutions from Pichincha, Guayas and Azuay.

We obtained a final sample size of 55 journals distributed among 15 institutions following this selection criterion. Of these, 7 institutions are public and have 27 journals in the sample, and 8 private institutions have 28 journals. This homogeneous distribution among the sample allows a comparison between the 2 types of institutions.

In addition to the 3 provinces mentioned, another selection criterion was included, which stipulated considering the geo-referential locality of the Universidad Católica del Ecuador, Ibarra campus through the university's journal, indexed in Latindex. This parameter inclusion was because the present research is part of a final degree work for obtaining the academic degree.

Content analysis

The content analysis was carried out based on compliance with the indexing criteria of the Scopus, Clarivate, Scielo and Redalyc databases. To quantify compliance with the criteria, we implemented a binary categorization system, assigning Yes for journals that meet the indicator or No for those that do not. All these data were then quantified to create graphs that allow a better understanding of the situation of Ecuadorian journals. The journals analyzed correspond to the last volume published.

The information necessary to achieve indexing is publicly available and provided by each database. Of the parameters for indexing, we only chose those explicitly verifiable on each journal's web page. Since there are several criteria for which the intervention of teams of evaluators from these databases is required, these more complex parameters occur in the final indexing process. Meanwhile, the parameters analyzed in this research work are those the journals are in the first steps of the indexing process. If the journals did not comply with these, the analysis would have stopped, and it would not be necessary to consider the more complex ones.

Semi-structured interviews

We realized semi-structured interviews with the editors of the journals with the best indexing in Ecuador. These interviews support the information gathered in the content analysis since some indexing indicators cannot be appreciated as external agents of the indexing evaluation entities. Likewise, the editors provide details about the management of a journal, specifically all those related to achieving indexing, maintaining its status, and improving the journal's quality constantly to achieve a more significant impact.

The interviews were conducted with a guide of topics to be covered. To make them more informal and obtain as much information as possible, they were conducted in conversation mode, interweaving the information provided by the interviewee with the topics and questions of interest for the research.

We conducted the interviews once we finished the statistical analysis. With the results of this analysis, it was possible to establish a conversation with each of the editors with complete knowledge of the journal's situation. We also inquired about the unfulfilled indicators or how they met specific parameters that the rest of the journals could not achieve.

Matrix

Four matrixes were created for each database since each has different indexing indicators. The following data were added to all the institutions in the sample: the province where they are located and the type of institution.

Interview Topics

A series of topics were determined to guide the conversation for the interviews. These were the following:

- Creation process
- Indexing problems
- Editorial committee
- Publication authors
- Number of articles and homogeneity
- Financing and support
- What the journal should improve
- Work between journals and faculties within the institution
- Other journals of the same institution

Results

Indicator matrix

Fifty-five journals indexed in Latindex were analyzed to check compliance with indexing indicators in the Scopus, Web of Science, Redalyc and Scielo databases. The parameters were compiled in a matrix of indicators. According to whether or not they met these criteria, they were marked with YES or NO criteria to quantify the total number of journals that met these indexing guidelines for each database. A total of 4 tables were created, each one specific to each database (see tables in annexes). Most journals met the vast majority parameters, so their inclusion in the analysis process is not statistically relevant.

Outstanding indicators

Once we collected all of the necessary data, we analyzed indicators using tables and their respective graphs to evaluate the Ecuadorian journals in terms of their indexing according to the indicators that stood out the most. It was also reviewed for a complete understanding and a deeper analysis to see any difference between public and private institutions. In addition, as this research is a thesis of the social communication career, the current situation of the country's communication journals will be analyzed. We rounded all values to the next higher value for calculating percentages, considering two significant figures.

Authors and editors diversity

Publishers and authors' geographic diversity are the parameters that stand out most for their non-compliance in the Scopus and Clarivate databases. At the same time, the Redalyc and Scielo databases have similar indicators, but they do not focus on geographic diversity but institutional diversity (Figure 1).

Information presentation on the website

Poor display of the journal's information on their websites was another indicator not fully met. Figure 2 shows the journals with web content in English and tables of contents and display formats.

Quantity and homogeneity of articles in the journal's issues

Other critical indicators to consider are the number of articles and their homogeneity to understand their impact on the journals' quality and scope (Figure 3).

Availability and visibility of the information

Regarding the parameters of information's availability and visibility on their digital platform, some missing criteria in several journals could also be appreciated, such as: Their document's digital preservation policy, whether they are hosted on an independent electronic platform, the presence of statistical data and the distinction of current indexing records (Figure 4).

Journal and author information

Finally, the journal and author information indicators have a significant percentage of non-compliances. These can be seen in Figure 5, which shows the use of bibliographic mas-headers, author identifiers, and digital resource identifiers present in the journals.

Discussion

Authors and editors diversity

One of the main points to achieve the indexing of scientific journals according to the indexing guidelines of the 4 databases analyzed, Scopus, Clarivate, Scielo and Redalyc, is the

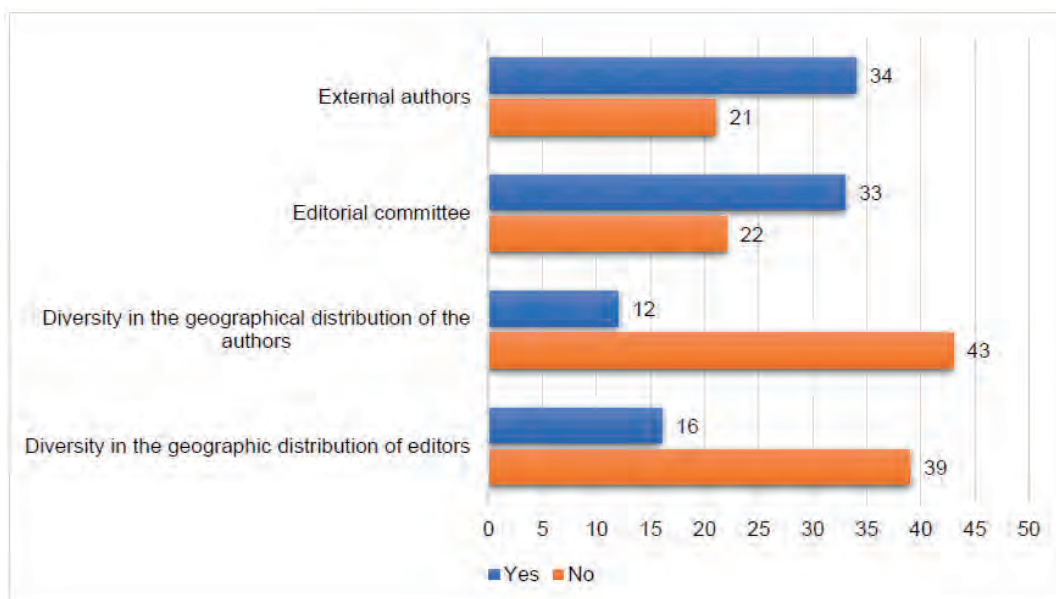


Figure 1. Authors and editors diversity.

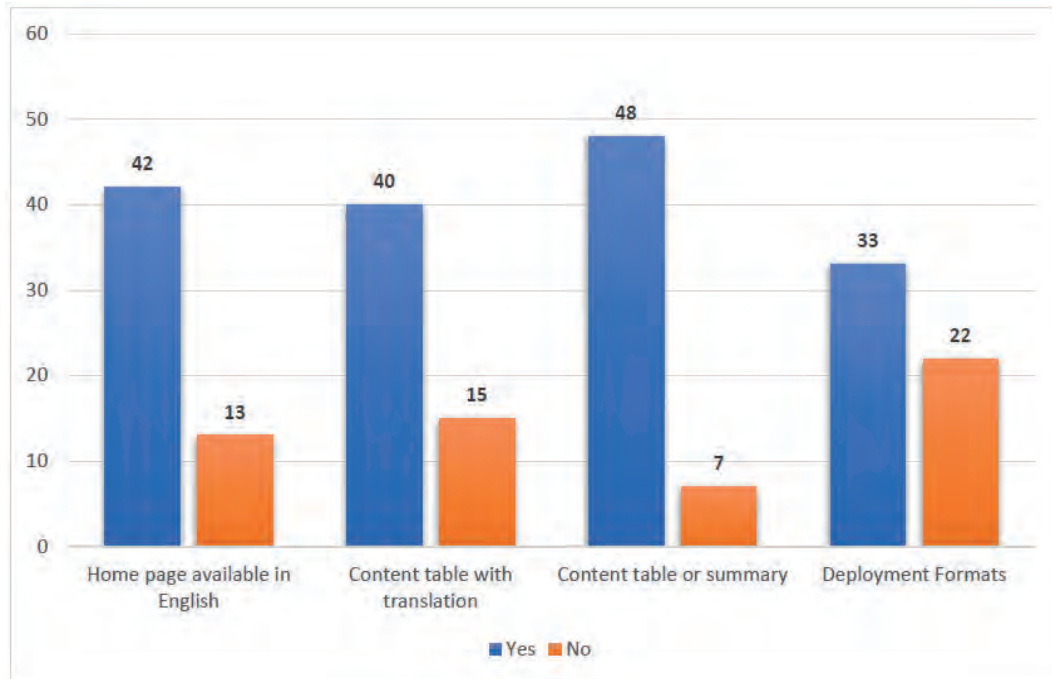


Figure 2. Information presentation on the website.

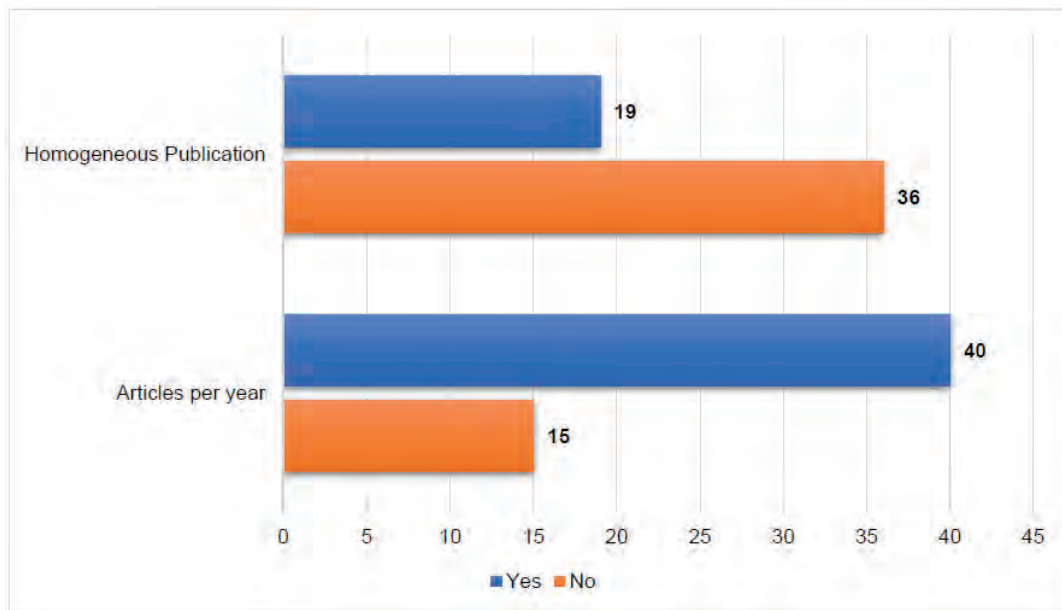


Figure 3. Quantity and homogeneity of articles in the journal's issues.

diversity of the editorial team and the diversity of the authors who publish in the journal. The relevance of the editorial's team geographical diversity is reflected when promoting the research output of the journals. Therefore, journals with an editorial team of various regions attract greater geographic diversity⁷.

Both Scopus and Clarivate require a minimum of 70% geographic diversity, both the journal editorial team and the authors publishing in the journal. As shown in Figure 1, most of the journals analyzed do not meet these indicators. Only 16 out of the 55 journals meet the editor's geographic diversity criterion equivalent to approximately 29% of the sample analyzed. This shows that there is little foreign participation in the editorial boards of Ecuadorian journals. At the same time, only 12 of the 55 journals (approximately 22%) have geographic diversity of publishers, which reveals practically no participation of fo-

reign authors in Ecuadorian journals. These percentages show a strong correlation between the editorial team's diversity and the authors' diversity of publications, as Demeter & Gaspar stated in their research in 2018.

The Redalyc and Scielo databases slightly change the requirement of this indicator, making it more local, and require that the journals have 70% of authors and editors from outside the publishing institution. As shown in Figure 1, concerning the previous indicators, there is an improvement; however, it continues to be a very negative factor for the journals, which prevents their indexing. As for the editors, 33 of the 55 journals (66%) comply with this requirement since they should only have less than 30% of their editorial board coming from the same institution. A similar situation arises with the author's distribution, where 34 out of 55 journals (approximately 62%) comply with the parameter of having less than 30% of their articles

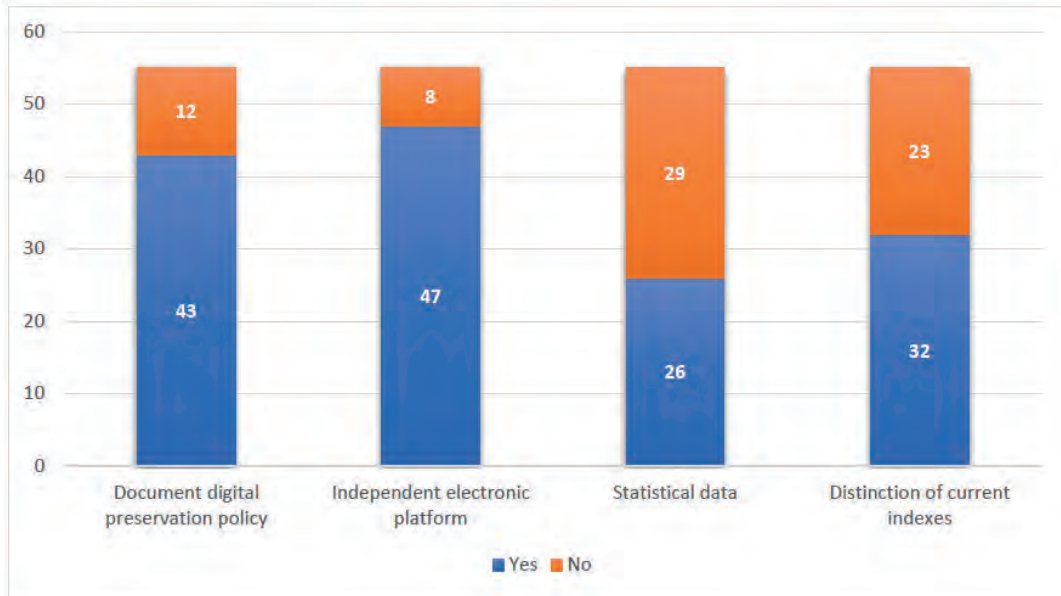


Figure 4. Availability and visibility of the information.

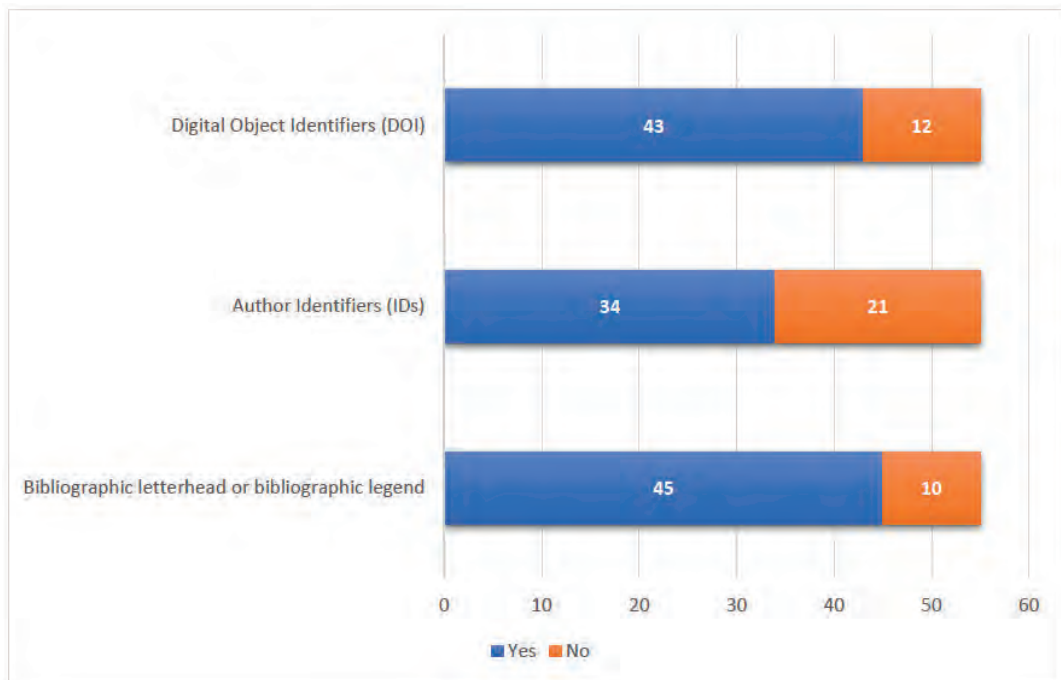


Figure 5. Journal and author information.

submitted by members of the same institution. This shows an improvement to the indicators of the geographical diversity of editors and authors. However, it is still a very high percentage of non-compliance requiring only the editorial board and publishing authors to be external to the publishing identity.

All the editors interviewed expressed that these indicators are the most important for indexing journals in impact databases. The editors of the journals La Granja and Bionatura (the only journals in the sample indexed in Scopus) emphasize that the creation of editorial committees is based on the journals' management of contacts since, in the beginning, these committees were formed by contacts close to the editors.

Regarding the criteria for the distribution of authors, the editors interviewed have a similar approach to that of the distribution of editorial committees. They affirm that the diversity of the editorial committees in conjunction with works such as

community managers and the use of social networks manage to attract the attention of potential authors to publish in their journals. Likewise, calls for papers such as the call for papers help receive articles. However, they emphasize that the vast majority comes from contacts and the rising journal's reputation.

They are comparing private and public institutions with these criteria. Regarding the geographic diversity of the editors, the private journals meet this criterion, with a total of 10 out of 28 journals (approximately 36%). In comparison, the public journals meet with 6 out of 27 journals (approximately 22%). Analyzing this parameter from the diversity of distribution of editors, in terms of whether they are part of the journal's institution or not, private journals comply with the parameter in 18 out of 28 journals (approximately 64%). In comparison, public journals comply with it in 15 out of 27 journals (approximately 56%). The distribution of authors presents a similar pano-

rama since private institutions have only 8 out of 28 journals (approximately 29%) that meet this criterion.

In contrast, public institutions have only 4 out of 27 journals (approximately 15%) that meet it. As for authors from the same country but outside the journal, both types of institutions comply with 17 out of 28 journals (approximately 61%) in the case of private journals and 17 out of 27 among public journals (approximately 63%). Our results showed no noticeable difference between the types of institutions; however, private institutions have higher compliance with these criteria.

Information presentation on the website

In recent decades, access to research articles has changed from print to digital sources, from closed to open access. Despite these changes and broader access to research results, there are still accessibility barriers regarding the formats available to access information⁸. English as the universal language of science has allowed scientists to communicate ideas freely and access the world's scientific literature⁹. These two previously mentioned characteristics are essential points to better indexing scientific journals since they should provide more feasible accessibility to the research present in each. These indexing points are the use of English in tables of contents and on the journal's home page, the display formats and the use of tables of contents or summaries.

In the journals analyzed, it can be seen in Figure 2, how a total of 40 of the 55 journals (73%) comply with the translation of the table of contents, and 42 of the 55 journals (76%) offer the possibility of translating the home page into English. This shows that the vast majority of the journals understand the importance of using the English language to achieve a greater reach for their publications. During the interviews conducted, some of the editors interviewed expressed that English was one of the journals' problems in achieving indexing in the Scopus database, which became one of the main criteria to be improved.

At the same time, as shown in Figure 2, 33 of the 55 journals (60%) present a diversity of display formats, which means that they have their articles in formats other than PDF, which is currently the most popular. Of the journals analyzed, many used other formats in previous issues. However, for the analysis presented, only the last published issue of the journal was considered, and at the time of the study, only 33 journals had at least one other format, other than PDF.

The use of tables of contents or summary is met in 87% (48 out of 55 journals) of the journals, making it an indicator that is met in the vast majority of cases. According to Ansoorge (2021)¹⁰, not presenting different display formats creates barriers for readers. For him, solutions exist; for example, OJS allows creating an HTML version of the article. Nevertheless, this requires some additional work from publishers and payment for the use of the platform, which is probably why many scientific journals prefer only to provide full-text articles in PDF format.

As for the comparison between private and public institutions, public universities have better compliance with all indicators except for the translation of the table of contents; however, it is a slight difference.

Quantity and homogeneity of articles in the journal's issues

For indexing, the databases analyzed require a minimum number of articles published per year by the journal and homogeneity in the number of articles published per year. Although the homogeneity criterion is not of transcendental importance since several of the journals analyzed that are indexed do not

meet it, the Redalyc database presents it as one of the highly valued criteria to be taken into account¹¹.

Of the 55 journals analyzed, 40 (73%) meet the requirement of having at least 16 articles per year (Figure 3). At the same time, only 19 of the 55 journals (35%) showed homogeneity in the number of articles between the volumes of the last complete year of publication (Figure 3). The lack of homogeneity in terms of publications has a simple solution: to publish homogeneously. However, part of the sample of the journals analyzed happens that to reach the 16 articles per year, they have to balance the publications between issues, i.e., if in the first issue they presented 6 articles, to meet the annual minimum, they must present 10. Some of the editors interviewed confirmed that when initiating the indexing processes of the journal, they did so, taking into account these indicators and planning the issues around this criterion.

They are analyzing the comparison between private and public institutions to fulfill these criteria. The difference between articles per year is minimal between the two types of institutions. Regarding homogeneity of publications, public institutions have worse performance, with only 22% of their journals meeting this criterion compared to 46% of the private ones. This shows that the editorial line in private journals emphasizes homogeneity of publication per year compared to public journals.

Information availability and visibility

This segment is about the availability and visibility of the information on the platform. The fulfillment of these criteria allows users to have deep knowledge about the journal they are reading or submit articles. Digital preservation allows maintaining access to digital materials beyond technological changes¹². This allows the prevalence of scientific articles for posterity. At the same time, the existence of digital preservation policies explicitly is an indication that allows journal users to detect whether the journal is predatory or not¹³. Hosting on electronic platforms independent from the university institution makes users interested in the journal arrive through a direct URL instead of entering from the university site, allowing faster and more efficient access. At the same time, the criteria: the presence of statistical data and distinction of current indexing records allow knowing both the statistics of the journal in terms of its performance and the quality of the journal since it allows knowing where it is indexed and the rank it occupies.

Regarding the criteria of digital preservation policy for documents and the use of independent digital platforms, compliance is very positive (Figure 4). This is seen with 43 out of 55 journals (78%) explicitly providing their digital document preservation policies and with 47 out of 55 journals (85%) complying with the use of independent digital platforms. Meanwhile, only 26 out of 55 journals (47%) show the use of some statistics on the web page and 32 out of 55 journals (58%) comply with the distinction of current records, i.e., to present explicitly, in detail and with links to the directories, databases and indexes in which they are found. Although compliance with the first two criteria is positive, some journals need to improve; however, compliance with statistics and the distinction of current records is low.

We can see varied differences when comparing public and private institutions with these criteria. Private institutions have better compliance in terms of the use of independent platforms, with 93% against 78% of the public ones and regarding the indicator of statistical data usage with 58% compliance against a low 37% by the public ones. In contrast, public insti-

tutions had a better percentage of compliance in presenting digital preservation policies for documents with 81% versus 75% for private institutions and with 63% of distinction of current records versus 54% for private institutions. The differences between the types of institutions are not significant.

Journal and author information

The last group of indicators, where the journal's criteria and author information are found, showed a percentage of non-compliance of more than 10% are those of the provision of information about the journal and the authors, visible in Figure 5. The DOI system identifies content objects in the digital environment with their names assigned to any entity for use in digital networks. It provides a simple method for accessing and reusing scholarly materials, facilitates data citation and thus increases the availability and recognition of research materials¹⁴. The use of ORCID, on the other hand, increases the discoverability of the authors' research results. It provides all the same information from works, awards and affiliations. This generates reliable profiles for researchers who publish in the journal and gives more credibility to the articles published before the readers¹⁵. In comparison, the use of bibliographic mastheads allows better identification of the particles present in the journal by having all the information available in this space.

As shown in Figure 5, compliance with the indicators: digital resource identifier and Bibliographic masthead are high. A total of 43 out of 55 journals (78%) comply with the use of DOI, while 45 out of 55 journals (81%) comply with the use of bibliographic mastheads. However, only 34 of 55 journals (62%) comply with author identifiers. While bibliographic mastheads are easy to resolve since it only involves adding them to the articles, the other two criteria are more complex. First, the DOI, the solution is simple, but it implies a monetary investment by the institutions since it is a paid service. At the same time, the use of identifiers by authors implies that they create the profiles and keep them updated.

Regarding compliance with author indicators, both types of institutions (public and private) are evenly matched, with private universities having 61% compliance and public universities 63% compliance. However, in the other indicators, it could be detected that private universities have a higher percentage of compliance, with 93% complying with the use of bibliographic headings and 82% complying with the use of DOI in comparison to 70% of public institutions complying with bibliographic headings and 74% with the use of DOI. These differences indicate that private universities have a slight advantage in managing journal and author information.

Conclusions

The main problems detected in the journals are the diversity of editors and authors. There are journals with editorial committees composed of editors from the same institution as the journal, which prevents them from being indexed in the Redalyc and Scielo databases. In terms of geographic diversity, the number of journals with editorial boards composed of editors from the same country is higher. This represents the main obstacle to progress indexing Scopus and Web of Science. As for the authors who publish in the journals, the panorama is the same as the editorial committees since they also present a high percentage of non-compliance.

The editorial directors of Ecuadorian journals interviewed for this research affirm that how they have managed to improve the diversity of editors and authors is based on the mana-

gement of contacts or networking. The editorial committees were formed based on working relationships managed by the editors, who, through networks generated during their professional life, have links with researchers and academics with the necessary reputation and experience to be members of the editorial committee. At the same time, as the editorial board is being formed, the new editors can search for and suggest possible candidates be part of the journal in the future.

Regarding authors in journals, the editors interviewed present a scenario very similar to the situation mentioned for publishers. A large number of the articles published are through the networking of the journal editors, since this way they can attract articles of more significant impact and scientific relevance. As journals gain reputation based on the indexing achieved and their good practices, they also increase the number of articles they receive in calls for papers. However, to obtain more citations and a more significant impact, editorial boards make an intense evaluation of which articles to publish to achieve that goal. This does not mean they do not publish the articles submitted through calls for papers. These articles are reviewed in-depth. The editorial teams maintain constant communication with the authors to correct errors and improve the publication.

Compliance with the indicators regarding the type of institution (public or private) showed no marked difference between the two types of institutions.

Recommendations

It is recommended that Ecuadorian journals build and develop their journals according to the indexing criteria in the central databases since these are designed with the objective that the journals have a more significant impact.

For future research, it is suggested to analyze the bibliometric indicators of Ecuadorian journals to know the country's situation in terms of these indicators since they are also an essential factor in determining how to improve the positioning and scope of scientific journals.

Acknowledgments

Special thanks to the ECOMS school of PUCESI for their constant support throughout the research process.

Bibliographic references

1. Mendoza, S., & Paravic, T. (2006). Origen, clasificación y desafíos de las Revistas Científicas. *Investigación y Postgrado*, 49-75.
2. Rodríguez Muñoz, R., Socorro Castro, A., & Espinoza Cordero, C. (2019). Análisis de Scimago Journal & Country Rank, utilidad para el desarrollo bibliométrico en la Universidad Metropolitana del Ecuador. *Publicando*, 58-68.
3. Balladares-Burgos, J., García-Naranjo, Á., & Granda-Villamar, C. (2020). Perspectivas de la producción científica en las universidades del Ecuador. *Revista Cátedra*, 3(2), 126-149.
4. Simbaña Gallardo, V. P., Espinosa Carrera, K. S., & Vinuesa Castillo, D. E. (2020). Perspectivas a la producción científica del Ecuador. *Tsafiqui - Revista Científica En Ciencias Sociales*, 11(14), 117-129. doi:<https://doi.org/10.29019/tsafiqui.v14i1.656>
5. Garcia-Bereguai, M. M. (2019). Revistas Indexadas en Scopus en Ecuador: La Asignatura Pendiente. *Revista Ecuatoriana de Neurología*, 13-14.
6. SCImago. (2020). SJR — SCImago Journal & Country Rank. Obtenido de <http://www.scimagojr.com>
7. Goyanes, M., & Demeter, M. (2020). How the Geographic Diversity of Editorial Boards Affects What Is Published in JCR-Ranked Communication Journals. *Journalism & Mass Communication Quarterly*, 97(4), 1123-1148. doi:10.1177/1077699020904169

8. Ribera, M., Pozzobon, R., & Sayago, S. (2019). Publishing accessible proceedings: the DSAI 2016 case study. *Universal Access in the Information Society*, 19(3), 557-569. doi:10.1007/s10209-019-00660-3
9. Márquez, M., & Porras, A. (2020). Science Communication in Multiple Languages Is Critical to Its Effectiveness. *Frontiers in Communication*, 5. doi:10.3389/fcomm.2020.00031
10. Ansoorge, L. (s.f.). Let's publish full-text scientific articles in HTML, not just PDF. *European Science Editing*. doi:10.3897/ese.2021.e75834
11. Redalyc. (2020). Postula tu revista. Recuperado el 5 de 12 de 2021, de <https://www.redalyc.org/postulacion.oa?q=criterios>
12. Saini, O. (2018). Understanding the Role of Institutional Repository in Digital Preservation in Academic Libraries: Review of Literature. *Library Philosophy and Practice* (e-journal), 1904. Obtenido de https://digitalcommons.unl.edu/libphilprac/1904/?utm_source=digitalcommons.unl.edu%2Flibphilprac%2F1904&utm_medium=PDF&utm_campaign=PDF-CoverPages
13. Laine, C., & Winker, M. (2017). Identifying predatory or pseudo-journals. *Biochemia Medica*, 27(2), 285-291. doi:10.11613/bm.2017.031
14. Wang, W., Deng, L., You, B., Zhang, P., & Chen, Y. (2017). Digital object identifier and its use in core Chinese academic journals: A Chinese perspective. *Learned Publishing*, 31(2), 149-154. doi:10.1002/leap.1137
15. Meadows, A. (25 de 08 de 2017). Ten reasons to get — and use — an ORCID iD! Obtenido de Elsevier Connect: <https://www.elsevier.com/connect/authors-update/ten-reasons-to-get-and-use-an-orcid-id!>

ARTICLE / INVESTIGACIÓN

Evaluation of the water quality of some sulfur springs in Hammam Al-Alil sub-district in Nineveh governorate

Hadeel Bassam Yahya, Yussra Al-Shaker, Rawaa M Hamoshi

DOI. 10.21931/RB/2022.07.01.3

Department of Environmental Sciences, College of Environmental Sciences and Technology, Mosul University, Iraq
Corresponding author: Hadeelalsaiigh2@gmail.com

Abstract: The research assessed the quality of mineral water in some sulfur springs in the Nineveh governorate, which are located in the Hammam Al-Alil sub-district on the right bank of the Tigris River. For that, monthly samples were collected from each site (45) water samples at a rate of (9) samples every month from three springs (3 samples \ Appointed) for five months from November (2020) until March (2021). The research aims to conduct a monthly study of water quality by conducting physical and chemical tests for the water of these springs, which included Temperature, Electrical Conductivity, Total Dissolved Solids, pH, Total Hardness, Total Alkalinity, Sulfate Ions, Phosphate Ions, Oils and Greases, as well as the tests. Biological measurement of the Total Count of bacteria. Where the temperature values ranged between (30.6-36.6) m, the Electrical Conductivity ranged between (2050.9-2688.4) $\mu\text{mhos/cm}$, while the values of Total Dissolved Solids were between (1025.4-2761) mg/liter, and the pH was between (6.8-7.3), concerning Total Hardness, its concentrations ranged between (820-1120) mg/liter during the study period, and the results showed that the Total Alkalinity concentrations were between (552-912) mg/liter in terms of calcium carbonate CaCO_3 , while the Sulfate and Phosphate ions were Between (1485 - 1712.1) and (0.020-0.069) mg/liter, respectively during the study period, the results indicated that the concentrations of oils and grease were between (0.08-0.27) mg/liter and finally the Total Count of bacteria ranged during the study period between (1.5 - 28) 10^5 cells. ML^{-1} .

Key words: Sulfur spring, Hammam Al-Alil, water quality.

Introduction

The water of springs is similar in its origin and composition to groundwater, where different water sources pass through the soil pores that filter the contents of pollutants and biological and non-biological plankton and dissolve many salts and elements present during their passage through the soil layers, which gives it a high percentage of salts, so it is called mineral water with hot water due to its high temperatures¹.

The water of the Springs flows from under the surface of the earth and is formed naturally in special water tanks and does not need to make changes or add chemicals, as the chemistry of mineral water and its size change from one place to another according to the conditions of its formation and the type of layers The formation in which this water is stored².

The presence of layers of gypsum rocks and the crater's formation under the earth's surface provided a suitable environment for the formation of sulfur with the help of particular types of anaerobic bacteria. As a result of this process, H_2S gas, which interacts with dissolved oxygen in the water, is released to form sulfuric acid H_2SO_4 , thus forming sulfuric acid water³.

Sulfur compounds are present in water either as sulfate (SO_4^{-2}) under aerobic conditions or hydrogen sulfide (H_2S) under anaerobic conditions resulting from *Desulfovibrio spp*⁴. but the most common is the sulfate ion SO_4^{-2} which is combined with the positive ions present in those waters and is widely present in most natural waters, and its concentrations range from a few milligrams to thousands per liter⁵.

Materials and methods

Study Area

The study area included several sulfur springs located in the Hammam Al-Alil area, which is about 30 km southeast of the city of Mosul, where they are located on the right bank of the Tigris River, as shown in Figure (1). Monthly samples were taken to study three sites, each Spring contains three sites, and this is shown in Table(1), and a hot, dry climate characterizes the region in summer and cold and rainy in winter, according to the data of the weather station in the city of Mosul.

Sample Collection

45 water samples were collected at a rate of 9 samples every month from three springs in Hammam Al-Alil area; namely, Ain Al-Fateh, Ain Zahra, and the last, Ain Fasusa, during five months for the period from November 2020 to March 2021, using sterile polyethylene bottles, with a capacity of (250) ml for biological tests, and a capacity (2) liters for chemical and physical tests by immersing the bottle after homogenizing it several times gradually so that its direction is facing the flow of water, where the sample was taken. Its oil was re-sealed tightly inside the water and closed with aluminum foil tightly closed and was kept in an iced cork box until it was transferred to the laboratory for physical and chemical tests. Its biological.

Citation: Yahya HB, Al-Shaker Y, Hamoshi RM. Investigation About the health of sulfur water and effect on tourist users in Hammam Al-Alil sub-district, Nineveh governorate. Revis Bionatura 2022;7(1). 3. <http://dx.doi.org/10.21931/RB/2022.07.01.3>

Received: 14 June 2021 / **Accepted:** 13 August 2021 / **Published:** 15 february 2022

Publisher's Note: Bionatura stays neutral with regard to jurisdictional claims in published maps and institutional affiliations.

Copyright: © 2022 by the authors. Submitted for possible open access publication under the terms and conditions of the Creative Commons Attribution (CC BY) license (<https://creativecommons.org/licenses/by/4.0/>).



Springs name	Coordinates	Sites
Fateh	36,167901N	site 1
	43,262666E	site 2
		site 3
Zahra	36,168054N	site 4
	43,262622E	site 5
		site 6
Fasosa	36,169029N	site 7
	43,261513E	site 8
		site 9

Table 1. Shows the names of sulfur springs

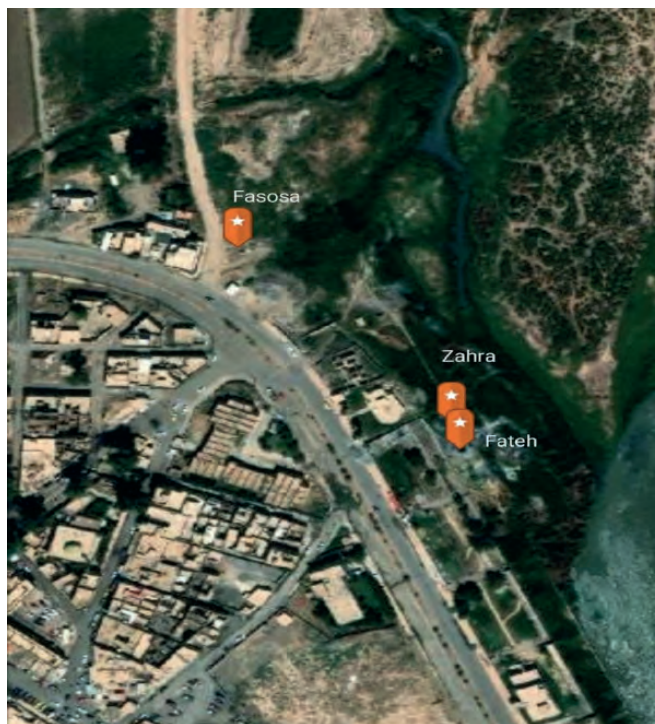


Figure 1. Shows the locations of the studied sulfur springs.

Types of Tests

A- Physical Tests

It includes the measurement of temperature using an alcohol thermometer, measured in degrees, the measurement of total dissolved solids using a T.D.S meter, expressed in mg/L, and the electrical conductivity measurement using an E.C meter in $\mu\text{m}\Omega/\text{cm}$

B- Chemical Tests

It includes measurement of the acidity function pH using a P.H. meter, total hardness by method with Na₂EDTA and measured in mg/l unit, total alkalinity in terms of CaCO₃ by the guide method and its unit mg/l, and determination of sulfate and phosphate represented by the unit mg/l by the spectroscopic method using Spectrophotometer, and finally, measuring oils and greases, and expressing the concentration in mg/l⁶.

C- Biological Tests

Bacteriological examinations were represented by the total number of bacteria, Total Plate Count (TPC) by dilutions to 10⁻⁵ dilutions and expressed in the cell. ml⁻¹.

Results

The properties of spring water depend on the chemical and physical properties and geochemical processes, which in turn depend on the physical and chemical properties of rocks and the chemical components of water and the velocity of water and human activities⁷.

Physical Tests

A-Temperature

Through the results shown in Table (2) and Figure (2), the

average temperatures of sulfur springs water during the study period ranged between (30.6-36.6) C, where the highest value was in site (2) and the lowest value in site (4). The high temperature of this water is attributed to the heat-emitting chemical reactions that accompany the dissolution and decomposition of the mineral materials that make up gypsum and dolomite rocks when water passes through them⁸.

B- Electric Conductivity

Figure (3) and Table (2) show the rates of electrical conductivity values during the study period, which ranged between (2050.9-2688.4) $\mu\text{m}\Omega/\text{cm}$, as it reached the highest value in the site (8) and the lowest value in the site (2) The reason for this is due to the geological and environmental formations of the studied areas⁹.

C- Total Dissolved Solid

It was found that the average values of T.D.S. ranged between (1025.4-2761) mg / l, where it was the lowest value in site (2) and the highest value in site (8), and the reason is due to the difference in the geological formations of the layers through which the water passes. With anhydrite and gypsum salts, it is characterized by high salt values¹⁰ Table No. (2) and Figure (4) show the average values.

Chemical Tests

A- pH

From Table (2) and Figure (5) the rates were between (6.8-7.3), as the highest value of the acidity function appeared in the two sites (6,4) and the lowest value was in the (9) site, which is low in fluctuation and the reason is due to the ability of an equation acidity of water and soils rich in carbonate and bicarbonate salts¹¹ As for the relative decrease of some values, it is due to the processes of biological decomposition and oxidation of organic materials in the event that oxygen concen-

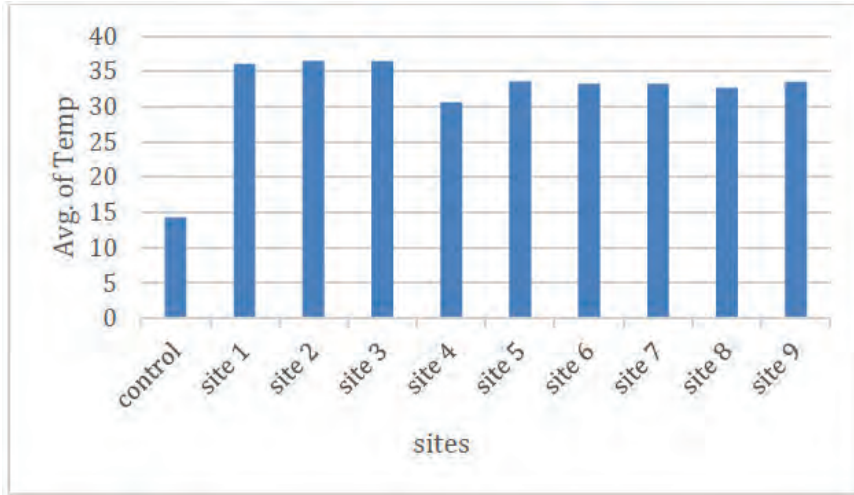


Figure 2. Shows the average temperature of the studied spring water.

Figure 3. Shows the E.C. rate of the studied spring water.

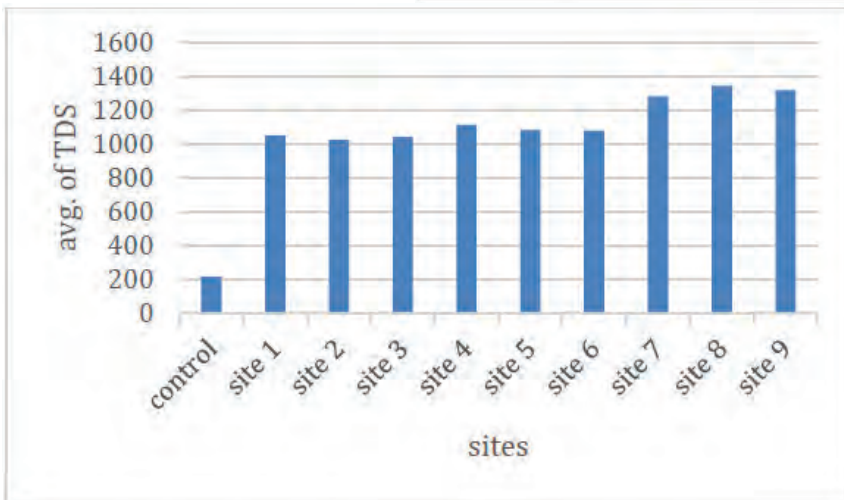
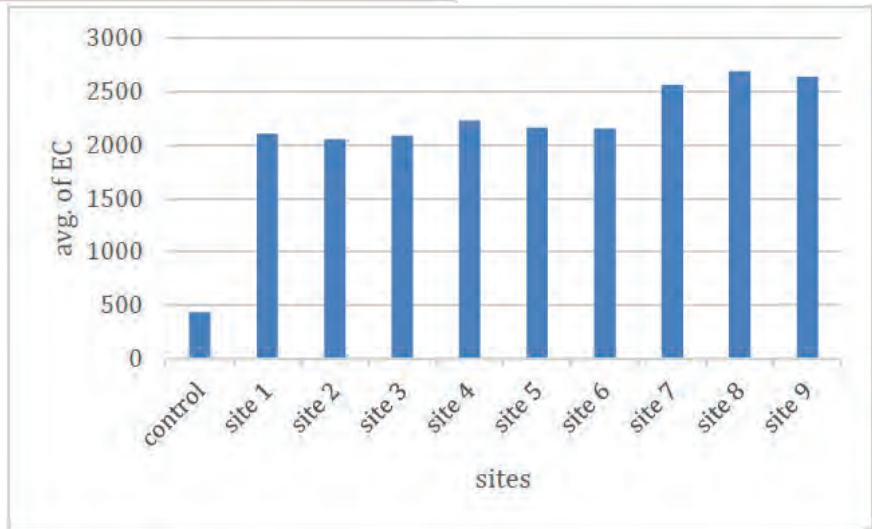


Figure 4. Shows the T.D.S. rate of the studied spring water.

trations drop to critical levels, which leads to the formation of many acidic and carboxylic compounds¹².

B- Total Alkalinity

The alkalinity is the amount of negative ions present in water and the resistance to hydrogen ions, and thus it is a measure of the water's susceptibility to the acidic equation¹³ bicarbonate because the pH values do not exceed 8.3¹⁴ The highest value was in site (9) and the lowest in site (4), where the rates were between (552-912) mg / l as shown in Table No. (2) and Figure No. (6).

C- Total Hardness

Through the results, it is clear that the average values of the total hardness ranged between (820-1120) mg / l during the study period, as it reached its lowest value in site No. (1) and its highest value in site (9), due to the reason for the presence of total hardness in water to positive ions, especially calcium and magnesium ions¹⁵ As the presence of calcium and magnesium ions depends on the geological nature of the land in which or through which water flows¹⁶ Table (2) and Figure (7) show the average values.

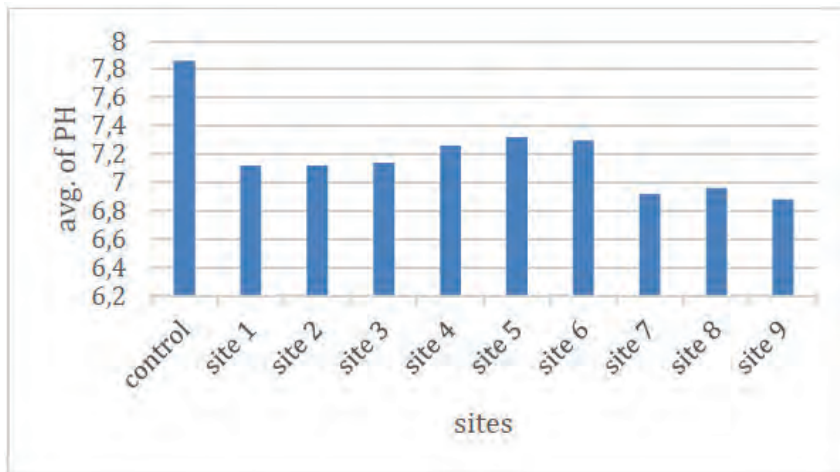


Figure 5. Shows the pH rate of the studied spring water.

Figure 6. Shows the total alkalinity rate as (CaCO₃) of the studied spring water.

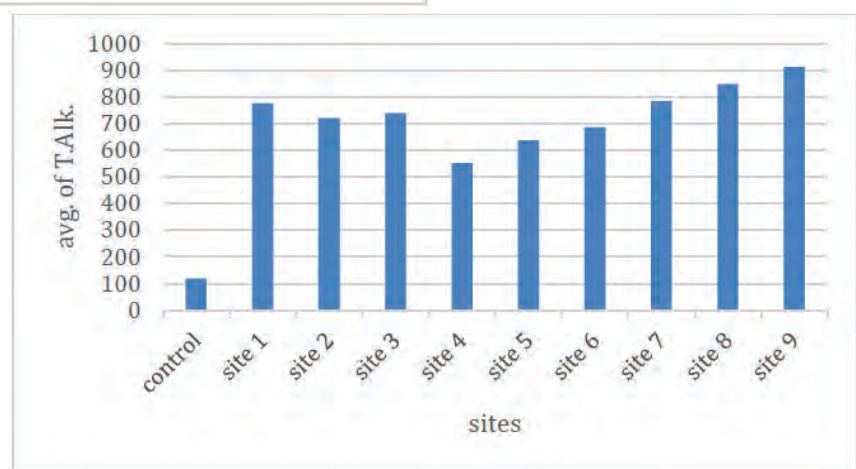


Figure 7. Shows the total hardness of the studied spring water.

D- Sulfate Ion SO₄⁻² Ions

The rates of sulfate ion concentrations during the study period ranged between (1485 - 1712.1) mg/L, where the highest value was in site (1) and the lowest value in site (8), as shown in Table (2) and Figure (8), and the reason for the presence of concentrations The sulfate ion indicates the nature of the geological rocks that make up the hole through which the water passes, as the decomposition of gypsum rocks and weathering processes are the main cause of the increase in sulfate concentrations in the study area¹⁷ in addition to the exposure of some sulfur minerals to oxidative conditions in the presence of water. And with Thiobacillus ferrooxidans, it leads to the release of ions of some chemical elements and the formation of sulfuric acid in sulfurous waters¹⁸.

E- Phosphate Ion PO₄⁻³ Ions

The results of the current study showed that the rate of phosphate concentrations ranged between (0.02-0.069) mg / l, where the highest value was at the site (9) and the lowest value at the site (6). Its adsorption by some clay minerals and organic compounds, which reduces its transmission to the aquatic environment¹⁹ as shown in Table No. (2) and Figure No. (9)

F- Grease & Oil

The results of the current study showed that the average concentration of oils and greases in the studied areas ranged between (0.15-0.17) mg / l, with the highest concentration in the sites (5,3,1) and the lowest concentration in the sites (7,6,4), and as it is shown in Figure (10) and Table (2), that the presence

of oils and grease in the water indicates that this water comes from layers containing oil, as evidenced by the presence of bitumen because the bitumen is one of the oil derivatives²⁰.

Biological Tests

A- The Total Bacteria Count (Total Plate Count)

The tests of the total number of bacteria are among the important indicators, which include the total of aerobic, facultative and non-autotrophic bacteria. These numbers are usually approximate, but most of them are due to the inability to provide a suitable nutrient medium for all species and the difficulty of providing appropriate conditions for their growth. One of the advantages of this group is that it can be detected easily²¹ and the results during the study period indicated that the numbers ranged between $(0-68) \times 10^5$ cells. ml⁻¹, as shown in Table No. (3) and Figure No. (11) shows the average number that was between $(1.5-28) \times 10^5$ cells. ml⁻¹.

Conclusions

The water of these springs is considered effective for the treatment of many diseases because it contains high concentrations of sulfates and salts, in addition to its high temperatures.

It is considered unsuitable for drinking if we take into account the sulfate concentration, apart from the rest of the cha-

racteristics, as it contains more than 400 mg/liter in addition to the taste and smell. It is also tough because it contains concentrations higher than 180 mg/liter and high salinity because it contains calcium and magnesium salts.

Funding

Self-funding.

Acknowledgments

In this section, we acknowledge any person who supports us to complete this project.

Conflicts of Interest

There is no conflict.

Bibliographic references

1. Al-Masry, Mohamed Said; Assaf, Huda. Sources of groundwater pollution. Prevention and safety. Damascus: The Atomic Energy Commission, (2007).
2. Matar, Iyad Abdel-Razzaq; Zidane, Tahseen Ali; Mahmoud, Bashar Abdel Aziz. Analytical comparative study of lime and sulfur spring water in Hit. Anbar University Journal of Pure Sciences, (2009).
3. Aswad, Khaled Galal; Mahmoud, Hazem Gomaa; Mohammed, Yasser Mayser. Study of the movement of some heavy metals in sulfur water in Al-Kasr village, northern Iraq. The Ninth Scientific Conference of the Dams and Water Resources Research Center, (2018).

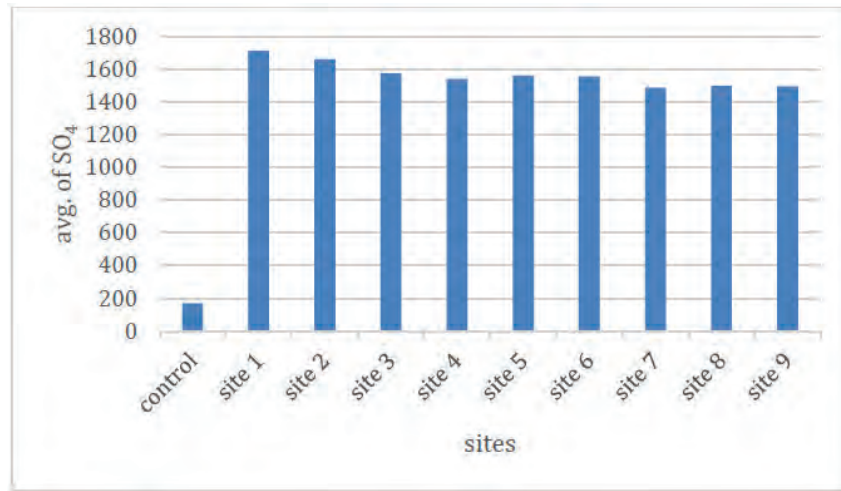


Figure 8. Shows the sulfate ion rate of the studied spring water.

Figure 9. Shows the sulfate ion rate of the studied spring water.

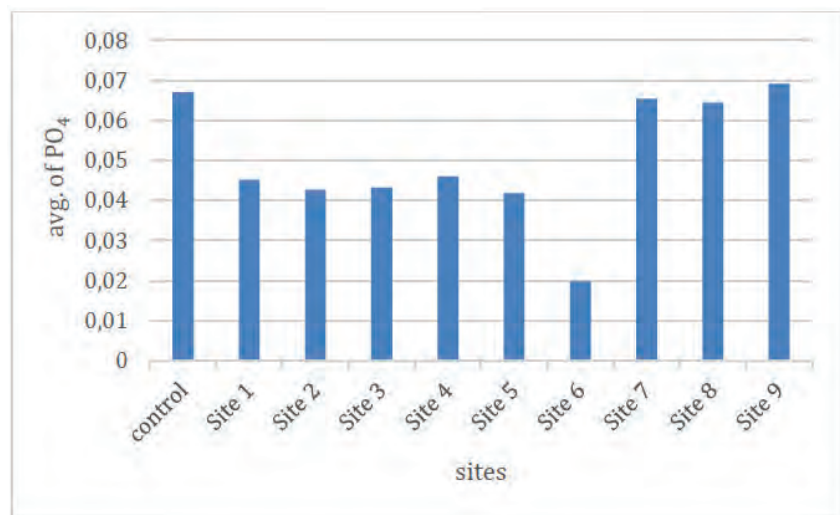


Figure 10. Shows the ratio of oils and greases to the studied spring water.

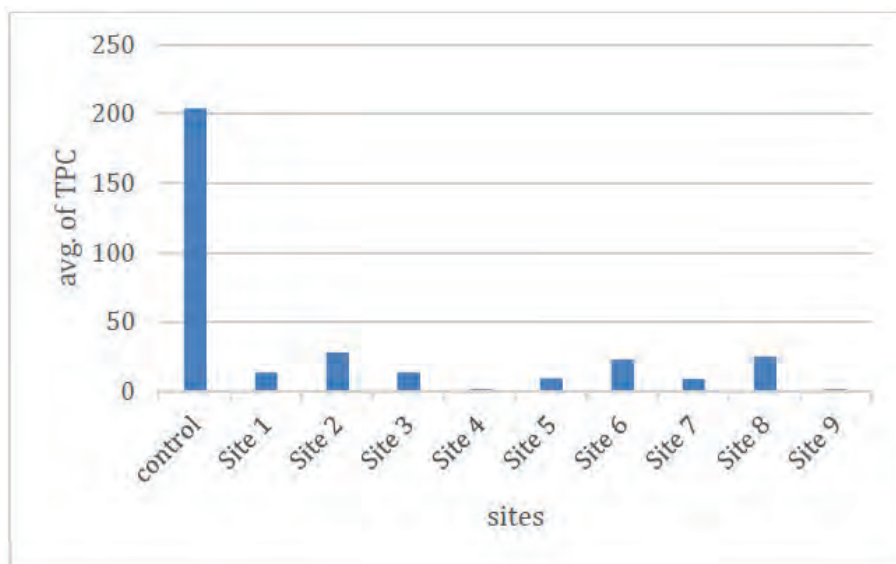
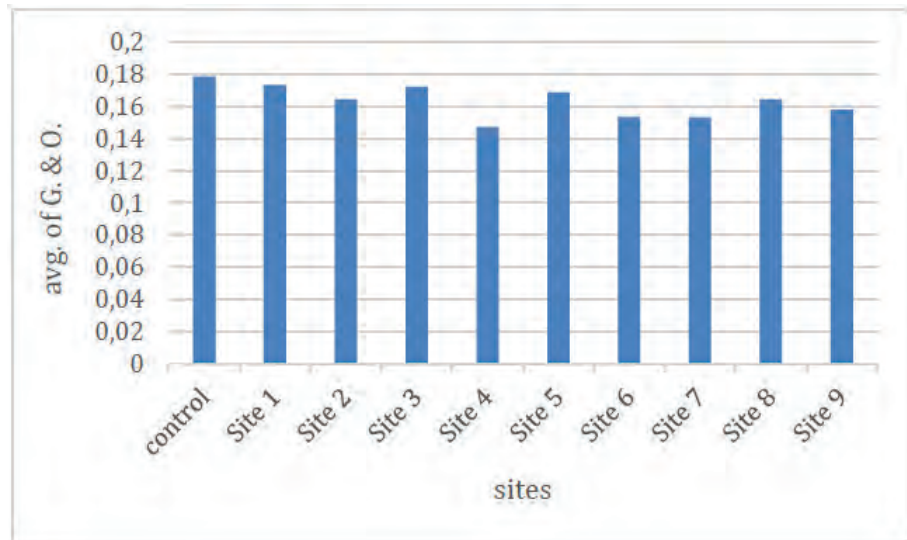


Figure 11. Shows the total bacteria count.

G.&O.	PO ₄ ⁻³	SO ₄ ⁻²	T.H	T.Alk.	T.D.S	E.C	pH	Temp.	month site
0.18	0.067	166.9	154.8	119	217.8	435.7	7.9	14.3	control
0.17	0.045	1712.1	820	776	1052.2	2104.4	7.1	36	site 1
0.16	0.043	1659	960	720	1025.4	2050.9	7.1	36.5	site 2
0.17	0.043	1572.6	1040	740	1042.2	2084.3	7.1	36.4	site 3
0.15	0.046	1538.5	940	552	1112.6	2225.4	7.3	30.6	site 4
0.17	0.042	1558.1	940	638	1081.8	2163.4	7.2	33.6	site 5
0.15	0.020	1553.4	940	686	1077.2	2154.4	7.3	33.3	site 6
0.15	0.065	1485	1020	784	1280	2559.8	6.9	33.2	site 7
0.16	0.064	1497.3	1020	848	1344.4	2688.4	7	32.6	site 8
0.16	0.069	1492.1	1120	912	1318.2	2635.9	6.8	33.5	site 9

Table 2. The chemical and physical examinations rate for the study sites.

avg.	3	2	1	12	11	month site
204	126	115	280	295	heavy	control
13.5	25	2	23	4	6	site 1
28	15	9	20	68	33	site 2
13.5	17	5	14	18	35	site 3
1.5	0	6	0	0	6	site 4
9.25	15	3	11	8	15	site 5
23	19	10	22	41	11	site 6
8.75	10	6	10	9	13	site 7
25.25	44	8	49	0	0	site 8
1.5	2	0	4	0	2	site 9

Table 3. Total number of bacteria (TPC) x 10⁵ cells.ml⁻¹ .

- Al-Allaf, T. A. M. A. Isolation and Identification of *Desulfovibrio* spp. from Hammam Al-Alil and Study some of the Environmental Properties of the Water in This Region, *Raf. J. Sci.*, (2018); Vol. 27, No.3, pp. 1-11, 2018.
- Mahe, Y. F., Perez, M. J., Tacheau, C., Fanchon, C., Martin, R., Rousset, F., & Seite, S. A new *Vitreoscilla filiformis* extract grown on spa water-enriched medium activates endogenous cutaneous antioxidant and antimicrobial defenses through a potential Toll-like receptor 2/protein kinase C, zeta transduction pathway. *Clinical, Cosmetic and Investigational Dermatology*, (2013); 6, 191-196.
- APHA, AWWA and WQPE "Stand Method for Examination of water and wastewater American Public Health Association, 23RD ed., Washington DC, U.S.A., (2017).
- Al-Taweel, Lama Saleh Jabbar. Study of some characteristics of sulfur spring water in Al-Hasya and Al-Khasf regions / Iraq, *Al-Qadisiyah Journal of Agricultural Sciences*, (2017); 2, 7-2.
- Al-Hamdani, Noor Ahmed Saadoun Applying water quality indicators to assess the water quality of a number of wells in the left coast of Mosul / Iraq. Master's thesis, College of Environmental Sciences and Technologies, University of Mosul,(2020).
- Al-Saffawi, A. Y. T. Water Quality of Nimrud District Wells Southeast of Mosul City for Drinking and Civil Purpose Using the Canadian Model of Water Quality. *Pakistan Journal of Analytical and Environmental Chemistry*, (2019); 20(1):75-81.
- Al-Saffawi, A. Y. T., and Al-Shuuchi, Y. T. M. Assessment of groundwater quality for irrigation by using water quality index (I.W.Q. index) in Al- Kasik district Northeastern of Mosul City. Iraq. *International Journal of Enhanced Research in Science, Technology and Engineering*, (2018);7(1): 76 – 81.
- Kevat, D., Dubey, M., Saxena, A. K. and GaurBiol, A. Assessment of Water Quality Index of Saank River, Morena, Madhya Pradesh. *International Journal of Science, Engineering and Technology Research (IJSETR)*, (2016) ; 5(8): 2563 – 2567.
- Sharaky, A. M., and Abdoun, S. H. Assessment of groundwater quality in Bahariya Oasis, Western Desert, Egypt. *Environmental Earth Sciences*, (2020);79(6): 1-14.
- Moses, A. N., and Ishaku, S. Evaluation of Physico-Chemical Properties of Well Water Qualities in Selected Villages in Zing Local Government Area of Taraba State, Nigeria. *International Journal of Contemporary Research and Review*, (2020); 11(03): 20282-20288.
- Fadipe, O. O., and Oladejo, K. T. Temporal Variation of groundwater resources in ilesa west local government, osun state Nigeria. *Nigerian Journal of Technology*, (2020); 39(1): 315-324.
- Verma, D. K., Bhunia, G. S., Shit, P. K., and Tiwari, A. K. Assessment of groundwater quality of the central Gangetic plain area of India using geospatial and W.Q.I. techniques. *Journal of the Geological Society of India*, (2018); 92(6): 743-752.
- Etikala, B., Golla, V., Arveti, N., Yenamala, S., Mannala, P., and Kumar, P. K. K. Statistical and Analytical Evaluation of Groundwater Quality of Atmakur Area, SPSR Nellore District, Andhra Pradesh, South India. In *Emerging Trends in Civil Engineering*, (2020); 61: 323-333. Springer, Singapore.
- Egbueri, J. C., Mgbenu, C. N., and Chukwu, C. N. Investigating the hydrogeochemical processes and quality of water resources in Ojoto and environs using integrated classical methods. *Modeling Earth Systems and Environment*, (2019); 5(4): 1443-1461.
- Duruibe, J. O., Ogwuegbu, M. O., and Ekwurugwu J. N. Heavy metal pollution and human biotoxic effects. *International Journal of Physical Sciences*, (2007); 2(5), 112-118.
- Asuma, O. O., Iserhien-Emekeme, R., Aweto, K. E., and Ofomola, M. O. Geophysical investigation of resistivity and groundwater quality in Ogbeloh coastal area of the western Niger Delta of Nigeria. *Applied Water Science*, (2020);10(2):1-9.
- Al Kubaisi, Rafea Kaduri; Zeidan, Ali Tahseen; Abbas, Fadel Firas. The effect of groundwater and sulfur springs on the water quality of the Euphrates River from the Syrian border to the Heet area in Anbar Governorate. *Anbar University for Pure Sciences*,(2007).
- Gomaa, Zuhair Gerges Evaluation of the performance efficiency of some sewage treatment plants in the city of Kirkuk. Master Thesis, College of Education for Pure Sciences, University of Mosul,(2017).

Biología para la producción y la vida



Técnicas Agrícolas | Cultivo de Tejidos | Bioproductos
Fitopatología/Microbiología | Biología Molecular | Biorremediación



REVIEW / ARTÍCULO DE REVISIÓN

Efectos del material particulado sobre las células endoteliales, epiteliales y del sistema inmune

Effects of particulate matter on endothelial, epithelial and immune system cells

Danna V. Cano-Granda^{1,2}, Mariana Ramírez-Ramírez^{1,2}, Diana M. Gómez², and Juan C. Hernandez² DOI: 10.21931/RB/2022.07.01.4¹ Grupo Inmunovirología, Facultad de Medicina, Universidad de Antioquia UdeA, Medellín, Colombia.² Infettare, Facultad de Medicina, Universidad Cooperativa de Colombia. Medellín, Colombia.Corresponding author: juankhernandez@gmail.com

Abstract: Particulate Matter (PM) is an air pollutant that is classified according to its aerodynamic diameter into particles with a diameter of less than 10 µm (PM10), a diameter of less than 2.5 µm (PM2.5), and particles ultra-fine with a diameter less than 0.1 µm (PM0.1). PM10 is housed in the respiratory system, while PM2.5 and 0.1 can pass into the circulation to generate systemic alterations. Although several diseases associated with PM exposure, such as respiratory, cardiovascular, and central nervous system, have been documented to cause 4.2 million premature deaths per year worldwide. Few reviews address cellular and molecular mechanisms in the epithelial and endothelial cells of the tissues exposed to PM, which can cause these diseases, this being the objective of the present review. For this, a search was carried out in the NCBI and Google Scholar databases focused on scientific publications that addressed the expression of pro-inflammatory molecules, adhesion molecules, and oxidative radicals, among others, and their relationship with the effects caused by the PM. The main findings include the increase in pro-inflammatory cytokines and dysfunction in the components of the immune response; the formation of reactive oxygen species; changes in epithelial and endothelial function, evidenced by altered expression of adhesion molecules; and the increase in molecules involved in coagulation. Complementary studies are required to understand the molecular effects of harmful health effects and the future approach to strategies to mitigate this response.

Key words: Air pollution, particulate matter, inflammation, endothelium, epithelium, oxidative stress, mutagenicity.

Resumen: El material particulado (PM, del inglés Particulate Matter) es un contaminante del aire que se clasifica según su diámetro aerodinámico en partículas con diámetro menor a 10 µm (PM10), diámetro menor a 2,5 µm (PM2.5) y las partículas ultra-finas con un diámetro menor a 0,1 µm (PM0.1). El PM10 se aloja en el sistema respiratorio, mientras que el PM2.5 y PM0.1 tienen la capacidad de pasar a la circulación, por lo que puede generar alteraciones sistémicas. Aunque se ha documentado varias enfermedades que se asocian a la exposición a PM, como respiratorias, cardiovasculares, y en el sistema nervioso central, que ocasionan en el mundo 4,2 millones de muertes prematuras al año. Hay pocas revisiones que aborden los mecanismos celulares y moleculares en células epiteliales y endoteliales de los tejidos expuestos al PM, que puedan ocasionar dichas enfermedades, siendo este el objetivo de la presente revisión. Para esta, se realizó una búsqueda en la base de datos del NCBI y Google Scholar enfocada en publicaciones científicas que abordaran la expresión de moléculas pro-inflamatorias, moléculas de adhesión y radicales oxidativos, entre otros, y su relación con los efectos ocasionados por el PM. Entre los principales hallazgos se destaca el aumento de citoquinas pro-inflamatorias y disfunción en los componentes de la respuesta inmune; la formación de especies reactivas del oxígeno; cambios en la función epitelial y endotelial, evidenciados por la alteración de la expresión de moléculas de adhesión; así como el incremento de moléculas implicadas en la coagulación. Se requieren estudios complementarios que contribuyan al entendimiento de los efectos moleculares asociados con los efectos deletéreos en la salud y el futuro planteamiento de estrategias para atenuar esta respuesta.

Palabras clave: Contaminación del aire, material particulado, endotelio, epitelio, inflamación, estrés oxidativo, mutagenicidad.

Introducción

La contaminación del aire incluye diversos componentes, entre los que se destacan gases, metales pesados, hidrocarburos aromáticos y PM¹. El PM, producido por el uso de diésel, polvo agrícola y de carreteras y partículas resultantes de actividades industriales, se clasifica según su diámetro aerodinámico en partículas con diámetro entre 2,5 y 10 µm (PM10), diámetro menor a 2,5 µm (PM2.5) y las partículas ultra-finas

con un diámetro menor a 0,1 µm (PM0.1)²⁻⁴. El PM tiene una composición variable que incluye, sulfatos, amonio, nitratos, cloro, carbono orgánico y material biológico (bacterias, esporas, polen)^{5,6}.

Los efectos que estos contaminantes del aire ocasionan en la salud humana, se han convertido en una alarma a nivel mundial, pues se estima que aproximadamente 4,2 millones

Citation: Cano-Granda D V, Ramírez-Ramírez M, Gómez-Gallego D M, Hernandez JC. Efectos del material particulado sobre las células endoteliales, epiteliales y del sistema inmune. *Revis Bionatura* 2022;7(1). 4. <http://dx.doi.org/10.21931/RB/2022.07.01.4> <http://dx.doi.org/10.21931/RB/2022.07.01.4>

Received: 1 June 2021 / **Accepted:** 27 July 2021 / **Published:** 15 February 2022

Publisher's Note: Bionatura stays neutral with regard to jurisdictional claims in published maps and institutional affiliations.

Copyright: © 2022 by the authors. Submitted for possible open access publication under the terms and conditions of the Creative Commons Attribution (CC BY) license (<https://creativecommons.org/licenses/by/4.0/>).



de muertes prematuras (que se produce antes de la edad promedio de muerte en una población determinada) pueden ser ocasionadas anualmente por la exposición a estos contaminantes⁷. La exposición a PM₁₀ y PM_{2.5} ha sido relacionada con diversas complicaciones sistémicas. Una vez el PM llega al sistema respiratorio, estas partículas pueden ser retenidas en el parénquima pulmonar, pasar por los alvéolos y ocasionar disminución de la función pulmonar, aparición y exacerbación del asma, enfermedad pulmonar obstructiva crónica (EPOC), aumento en la susceptibilidad a infecciones y alteración en el desarrollo del pulmón en niños⁸⁻¹². Aunque los mecanismos moleculares que explican estas patologías todavía no están muy bien descritos, algunos estudios han demostrado que, en células del epitelio respiratorio expuestas al PM, se da la liberación de las citoquinas inflamatorias IL-1 β , IL-6, IL-8, IL-25, IL-33, TNF- α , y GM-CSF, así como la liberación de Linfopoyetina Estromal Tímica (TSLP)¹³ que induce el reclutamiento de células efectoras de la respuesta alérgica¹⁴.

El PM puede además llegar a la circulación sanguínea, ocasionando alteraciones mitocondriales, daño oxidativo, mutagenicidad y genotoxicidad¹⁵, lo que se asocia con mayor riesgo de sufrir enfermedades cardiovasculares como infarto del miocardio, arritmias e insuficiencia cardíaca¹⁶, aterosclerosis, hipertensión, eventos coronarios e isquemias^{17,18}. El daño en el endotelio, ocasionado por la exposición a PM, puede contribuir al desarrollo de la enfermedad cardiovascular¹⁹, pues dicha exposición ocasiona la liberación de moléculas inflamatorias, como la IL-6 y la proteína C reactiva; esta última representa un marcador de enfermedad cardiovascular^{17,20,21}. Por otro lado, se ha encontrado que la exposición al PM genera alteración en los niveles de las moléculas implicadas en la coagulación^{22,23}, y la adhesión celular, afectando la integridad epitelial^{24,25} y la migración transendotelial de leucocitos²⁶⁻²⁸.

También se ha demostrado que la exposición a PM pue-

de ocasionar patologías metabólicas²⁹ y puede afectar otros sistemas como el nervioso; Por ejemplo, se ha asociado con alteraciones como depresión, ansiedad³⁰, trastorno por déficit de atención con hiperactividad³¹ y Alzheimer³². Además, en mujeres embarazadas puede causar parto prematuro y bajo peso al nacer en el neonato^{33,34}.

Aunque múltiples estudios han demostrado los efectos de la exposición al PM en la salud humana, no se encuentran muchos estudios que describan la asociación entre estos efectos y los mecanismos moleculares que podrían explicar la fisiopatología; por lo tanto, el objetivo de esta revisión es exponer las alteraciones celulares y moleculares en células epiteliales y endoteliales de los tejidos expuestos al PM y su posible asociación con las patologías previamente descritas.

En la figura 1 y tabla 1, se resumen los efectos de la exposición al PM en las células epiteliales y endoteliales.

Efectos inflamatorios del PM en células endoteliales y epiteliales

Una vez el PM es inhalado, entra en contacto con la mucosa respiratoria, en la que se encuentran células epiteliales y células del sistema inmune. En los pulmones, este PM es reconocido por los macrófagos, a través de sus receptores tipo Toll (TLR), principalmente TLR2 y TLR4, lo que induce la expresión de citoquinas como IL-1 β , IL-6, IL-8 y TNF- α , que regulan una respuesta inmune inflamatoria³⁵⁻³⁹. Al mismo tiempo, la exposición al PM estimula la activación de las células dendríticas⁴⁰, que pueden tomar el PM de la luz de las vías respiratorias, hacer presentación antigénica, y provocar un reclutamiento de Linfocitos T al pulmón⁴¹. Adicionalmente, el material particulado genera la producción de ROS, evento que conlleva al reclutamiento de neutrófilos a los pulmones⁴².

Se ha reportado que, en la línea de células epiteliales bronquiales humanas (BEAS-2B), la exposición al PM genera

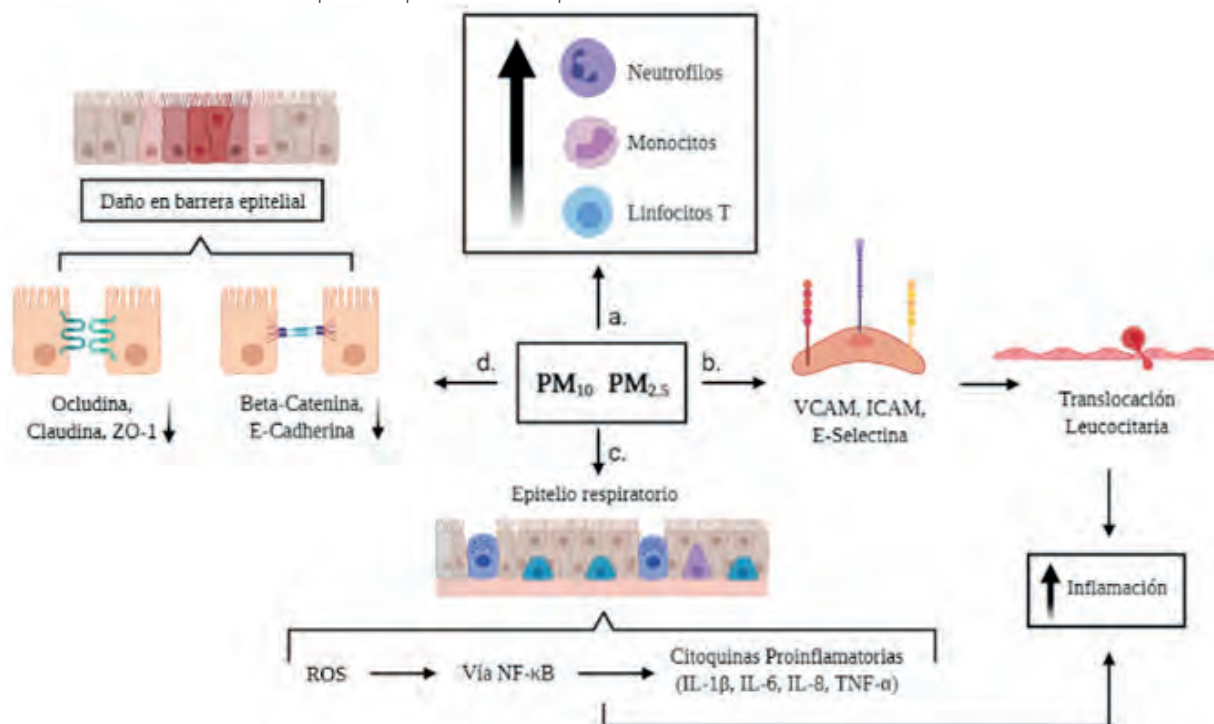


Figura 1. Efectos de la exposición al material particulado a) Produce un incremento en el reclutamiento de neutrófilos, monocitos y linfocitos T hacia el tracto respiratorio. b) Aumenta la migración transendotelial de leucocitos, al estimular la expresión de moléculas de adhesión como VCAM, ICAM-1 y E-selectina. c) Promueve la producción de especies reactivas del oxígeno (ROS) que conlleva a la activación de la vía NF- κ B, aumentando la liberación de citoquinas pro-inflamatorias. d) Genera disrupción de la barrera epitelial al disminuir las uniones intercelulares. Imagen creada con Biorender.com

Localización por tejido	Alteración	Efecto
Epitelio	Disminución de moléculas de adhesión ^{89,90} .	Afecta la integridad de la barrera epitelial ⁶⁷ .
	Alteración en la tasa de cobertura, la morfología y la función de los cilios ⁶⁹ .	Afecta la cobertura ciliar y su función ⁶⁹ .
	Cambio en la función mitocondrial ⁷¹ .	Afecta la fosforilación oxidativa, alterando la producción de ATP ⁷¹ .
Endotelio	Presencia de micropartículas circulantes ¹⁷ .	Inflamación, angiogénesis, trombosis, coagulación y regulación del tono muscular, formación de placas arterioescleróticas ⁸⁸ .
	Liberación de angiotensina ²⁰ .	Induce el incremento del sistema ACE ²⁰ .
	Alteración de moléculas de adhesión ²⁴ .	Incremento en la adhesión celular ²⁴ .
	Incremento de protrombina ⁸⁵ .	Desarrollo de la inflamación y la coagulación ⁸⁵ .
	Disminución del fibrinógeno ⁸⁵ .	Contrarresta la coagulación ⁸⁵ .
	Aumento de la endotelina -1 ⁸⁶ .	Favorece la vasoconstricción ^{86,91} .
	Disminución del factor de crecimiento endotelial vascular (VEFG) ⁸⁷ .	Afecta la angiogénesis ⁸⁷ .

Tabla 1. Efecto del PM en células epiteliales y endoteliales.

aumento de IL-1 β , IL-6 e IL-8 (quimioatrayente de neutrófilos). La IL-1 β induce el incremento de moléculas de adhesión como E-selectina e ICAM-1 (molécula de adhesión intercelular 1), las cuales favorecen la transmigración leucocitaria^{43,44}. Por su parte, la IL-6, estimula la producción de proteínas de fase aguda incluyendo la proteína C reactiva y proteínas implicadas en la coagulación⁴⁵. Se ha documentado además que la exposición al PM regula positivamente la expresión de TNF- α , a través de la vía de NF- κ B^{46,47}. Otras quimioquinas inducidas en respuesta al PM son MCP-1 (proteína quimioatrayente de monocitos 1)⁴⁸, que regula la migración e infiltración de los monocitos en las etapas tempranas de la exposición a PM⁴⁹, y CXCL1⁵⁰ implicada en el reclutamiento y activación de los neutrófilos⁵¹.

Mutagenicidad y genotoxicidad

El ciclo celular posee diversos mecanismos para el reconocimiento de cambios y reparación del ADN, desencadenados por errores en el proceso de replicación, que pueden ser inducidos por estímulos externos. Dentro de estos mecanismos, encontramos el sistema de respuesta al daño del ADN (DDR), del cual hacen parte la serina/treonina quinasa 1 (Chk1) y la serina/treonina quinasa 2 (Chk2), enzimas que han sido relacionadas además con la señalización de la respuesta inmune innata, es decir una señalización constante en respuesta al daño celular que incrementa la secreción de ciertas citoquinas⁵².

La exposición a PM puede ocasionar un incremento en la respuesta mitótica-apoptótica, arresto mitótico y necrosis celular, incidiendo en la disminución de la proliferación de células BEAS-2B, en las cuales, además, induce daño del DNA. Este daño en el DNA desencadena algunos mecanismos de respuesta, como ATM/Chk2, que se encarga del bloqueo de la mitosis cuando se ocasionan este tipo de daños a nivel molecular; sin embargo, en esta línea celular no se observa activación de ATR/Chk1, hecho que sugiere que la exposición a PM2.5 podría estar causando interferencias en esta respuesta y un incremento en la mutagénesis celular^{53,54}. Por otro lado,

en células alveolares tipo 1 (TT1), se alcanza a observar una respuesta genotóxica, controlada por la fosforilación de Chk1 y H2AX, esta última implicada en la señalización de la producción de rearrreglos en la cromatina^{54,55}.

NORAD es un ARN no codificante que se activa en respuesta al daño en el ADN⁵⁶, y se encuentra desregulado en varios tipos de cáncer⁵⁷. En cultivo de células epiteliales basales alveolares humanas A549 se ha demostrado que la exposición al PM causa una sobreexpresión del gen NORAD, generando un deslizamiento mitótico que finalmente conlleva a una aneuploidía en la célula⁵⁸. Por otro lado, en estas mismas células se ha demostrado la regulación positiva de LINC01816⁵⁹, el cual es un ARN no codificante, cuya regulación positiva se ha asociado a varios tipos de cáncer⁶⁰.

Radicales libres y estrés oxidativo

Bajo diversas condiciones metabólicas o de estrés celular, se da la formación de especies reactivas del oxígeno (ROS) que interactúan con proteínas, lípidos y ADN y generan daño celular^{61,62}. Se ha demostrado que la exposición a PM genera la producción de ROS en células del epitelio respiratorio, ocasionado por la inducción de la expresión de genes de la familia citocromo p450 como CYP1A1, CYP1B1^{63,64}, estas enzimas son las encargadas de metabolizar compuestos como los hidrocarburos aromáticos presentes en el PM y en este proceso forman metabolitos intermediarios inestables que contribuyen a la generación de estrés oxidativo y daño en el ADN⁶⁵. En A549, se encontró que posterior a la exposición a PM la mayoría de ROS producidos son: Peróxido de hidrógeno, radical hidroxilo y radical anión superóxido⁶⁶. En células BEAS-2B, se demostró que la exposición a PM2.5, incrementaba la fosforilación oxidativa, así como la masa mitocondrial, lo que resultó en una mayor producción de anión superóxido mitocondrial⁶⁷. Por otro lado, la producción de ROS desencadena la muerte celular, así como la activación de la vía ROS-MAPK-NF- κ B, que conlleva a la liberación de IL-1 β , IL-6, IL-8 y de otras moléculas como

la metalopeptidasa 9 de matriz (MMP-9) y la ciclooxigenasa 2 (COX-2)⁶⁸; estas últimas han sido asociadas a la fisiopatología de enfermedades cardiovasculares^{69,70}. Además, el estrés oxidativo se ha relacionado con enfermedades como la EPOC y su exacerbación, debido a que genera amplificación de la inflamación crónica, estimulación de la fibrosis y el enfisema⁷⁶.

Como respuesta al estrés oxidativo, se generan moléculas antioxidantes que contrarrestan los efectos negativos de ROS en el cuerpo humano⁷¹, sin embargo, en varias líneas de células epiteliales, como: células epiteliales bronquiales humanas (BEAS-2B), células epiteliales bronquiales/traqueales humanas sin ácido retinoico (NHBE) y células epiteliales bronquiales / traqueales humanas enfermas (COPD-DHBE), se ha demostrado una disminución de NRF2, posterior a la exposición de manera repetida a PM 2.5 a una concentración de 10 µg / cm²⁷². El factor de transcripción Nrf2 regula la expresión inducible de genes de enzimas detoxificantes y antioxidantes⁷³. Además, se observó que en células A549 posterior a la exposición a PM10, se presentó una disminución de manera concentración dependiente de enzimas antioxidantes, el glutatión reducido (GSH) presentó disminución a las 2 horas, mientras que las enzimas superóxido dismutasa (SOD), catalasa (CAT) a las 48 h⁷⁴.

Cambios en la función epitelial

El tejido epitelial es aquel que recubre todas las áreas externas del cuerpo, sus células están adheridas por medio de uniones intercelulares, como las uniones estrechas, las uniones adherentes, los desmosomas y los hemidesmosomas, las cuales permiten la integridad de la barrera epitelial^{25,77}.

En células del epitelio nasal humano, la expresión de moléculas ocludina, claudina 1 y proteína ZO, las cuales pertenecen a las uniones estrechas del epitelio se ven reguladas de manera negativa después de la exposición al PM2.5⁷⁸. Además, un estudio *in vitro* reportó una disminución progresiva, en función del tiempo de exposición al PM, en la E-cadherina y la Beta-catenina, moléculas que hacen parte de las uniones adherentes del epitelio⁷⁹. Asimismo, en un estudio en donde se evaluó la disrupción de la barrera epitelial en células del epitelio respiratorio se observó que el PM2.5 disminuye la resistencia transepitelial, al igual que la permeabilidad celular⁷⁸.

Los cilios, uno de los componentes fisiológicos del epitelio respiratorio, que tiene como función la remoción de restos celulares, microorganismos, partículas inhaladas y moco⁸⁰ también se ven afectados tras las exposición al PM; por ejemplo, en células del epitelio nasal este contaminante afecta la tasa de cobertura, la morfología y la función ciliar⁸¹. Por otro lado, en la línea celular A549 se ha demostrado que, la exposición a PM disminuye su capacidad de producir compuestos antimicrobianos como las β-defensinas, favoreciendo así la colonización bacteriana⁸².

En un estudio en células epiteliales bronquiales humanas se encontraron efectos a nivel mitocondrial, en donde el PM2.5 causó daño oxidativo, afectó la despolarización del potencial de membrana y la fosforilación oxidativa, lo que conllevó a una alteración en la producción de ATP⁷²; esto podría ser una explicación a la fisiopatología del desarrollo y exacerbación de la EPOC por la exposición al PM, pues esta enfermedad se ha relacionado con la disfunción mitocondrial^{83,84}. Asimismo, se demostró que la exposición al PM induce la expresión del gen Egr 1, que junto a la activación de NF-κB y AP-1 conllevan al incremento de interleuquinas pro-inflamatorias como IL-6 e IL-8 y a su vez al incremento en la producción de moco. Este gen está implicado en la regulación de la proliferación y diferenciación celular y se ha asociado con la patogénesis de enfermedades respiratorias, entre ellas la EPOC⁸⁵.

Cambios en la función endotelial

El endotelio es una capa que permite la separación de los tejidos sanguíneos, conformado por una monocapa de células endoteliales, las cuales forman el sistema circulatorio y que por ende abarca las arterias, venas y capilares⁸⁶. Se ha demostrado que el PM2.5, por su tamaño tienen la capacidad de pasar a circulación sistémica y generar daños en el endotelio⁸⁷. La exposición al PM2.5 genera ROS⁸⁸ y estimula la expresión de moléculas de adhesión como VCAM (molécula de adhesión celular vascular), la cual está implicada en la unión fuerte al endotelio y la migración transendotelial de los leucocitos^{43,89}. Otra molécula de adhesión que se incrementa por la exposición al PM es ICAM-1⁹⁰. El aumento de moléculas VCAM e ICAM-1 tras la exposición al PM2.5 aumenta significativamente el proceso de adhesión celular²⁶.

También se ha reportado que, después de la exposición *in vitro* a PM10, la expresión de la molécula E-selectina, implicada en el proceso primario de unión endotelio-células, aumenta en un 25%²⁷; lo que aumenta la Angiotensina II a nivel sistémico, e induce el incremento del sistema ACE (enzima convertidora de angiotensina)/ANGII (angiotensina II)/ AT1R (receptor de angiotensina)²². La Angiotensina II es una molécula conocida por su capacidad de aumentar la presión arterial, tanto ejerciendo una función de vasoconstricción como generando un descenso en la excreción de sal y agua en los riñones, que conlleva a un aumento del volumen del líquido extracelular y por ende la presión arterial⁹¹. En conjunto, estos efectos, tanto la alteración de moléculas de adhesión como el aumento en moléculas implicadas en la vasoconstricción, traen repercusiones a nivel del endotelio cardíaco debido a que este sistema genera un incremento en la producción de citoquinas pro-inflamatorias y moléculas de adhesión que puede llevar al desarrollo de enfermedades cardiovasculares^{92,93}. Los monocitos circulantes y los linfocitos T se unen a estas moléculas de adhesión y son redirigidos por citoquinas pro-inflamatorias y quimio-atrayentes a la íntima (capa más interna de los vasos sanguíneos), y eventualmente las células de la pared del vaso (denominadas células espumosas) mueren y liberan su contenido graso, ocasionando la calcificación con células del músculo liso y causando arteroesclerosis^{92,93}.

Se ha demostrado que las personas que se encuentran más expuestas al PM presentan un incremento en los niveles de los fragmentos de protrombina 1+2 en sangre, lo cual contribuye con el desarrollo de la inflamación e incremento de la coagulación⁹⁴. Además, se ha reportado una disminución en las concentraciones de fibrinógeno y factor VII, moléculas que pueden actuar de manera protectora frente a los efectos secundarios a la trombosis coronaria⁹⁵; y un aumento en la endotelina-1, un potente vasoconstrictor encargado de la regulación de la homeostasis vascular⁹⁶.

Por otro lado, en células endoteliales del cordón umbilical humano se demostró que, como consecuencia a la exposición con PM, hay una disminución del factor de crecimiento endotelial vascular (VEFG), el cual está implicado en la proliferación celular, migración y angiogénesis⁹⁷.

Por su parte, la proteína C reactiva, un reactante de fase aguda, es liberada como consecuencia del aumento de mediadores pro-inflamatorios y moléculas vasoactivas en células pulmonares endoteliales, ocasionado por el depósito de PM en los alvéolos; la liberación de esta molécula trae como consecuencia la activación de la respuesta innata y estrés oxidativo¹⁶.

Se ha documentado también que la exposición a PM aumenta las micropartículas circulantes, vesículas que se desprenden de las membranas de diversos tipos celulares, poste-

rior a la activación de procesos apoptóticos, y que ejercen un rol no solo en la formación de placas ateroscleróticas, sino también en la inflamación, angiogénesis, trombosis, coagulación y regulación del tono muscular^{19,98}. Estas micropartículas son liberadas principalmente tras la exposición a citoquinas pro-inflamatorias o agentes apoptóticos y una vez en circulación, disminuyen la acción de la sintetasa de óxido nítrico endotelial (eNOS), favoreciendo la agregación y adhesión plaquetaria, que finalmente resulta en la formación de trombos. Asimismo, aumentan la expresión de moléculas de adhesión en células endoteliales y sus receptores en monocitos, promoviendo así la inflamación vascular; y ejerciendo acción anti-angiogénica al fomentar la pérdida de factores de crecimiento e incrementar la expresión de moléculas como TNF- α e IP-10, que, en conjunto, llevan a una muerte prematura de origen cardíaco^{19,98}.

Conclusiones

En la actualidad, se han documentado varias enfermedades asociadas con la exposición al PM, así como los efectos a nivel molecular en células del epitelio y del endotelio. Entre las afecciones observadas en el tejido epitelial están el daño oxidativo y la despolarización del potencial de membrana, alteraciones que pueden explicar el desarrollo de enfermedades como la EPOC.

Además, a nivel endotelial, patologías como aterosclerosis y muerte cardiovascular prematura, se han asociado con el incremento de macropartículas circulantes, moléculas de adhesión, y del sistema ACE /ANGII, los cuales son inducidos tras la exposición al PM.

Finalmente, dada la gran diversidad de patologías que conlleva la exposición al PM, es importante la realización de más estudios que ayuden a correlacionar las patologías con las alteraciones a nivel molecular. En la literatura hay gran cantidad de reportes sobre alteraciones moleculares, el impacto a nivel celular y la respuesta inflamatoria, sin embargo, aún hacen falta estudios que logren generar una asociación de estas alteraciones con la fisiopatología de enfermedades previamente relacionadas a la exposición al PM, la realización de estos estudios podría dar paso a la generación de nuevas hipótesis en ensayos experimentales que permitan dilucidar los mecanismos moleculares subyacentes. Esto es importante debido a que podría propiciar el planteamiento de estrategias terapéuticas y medidas de salud pública que ayuden a mejorar la calidad de vida de las personas.

Funding

This research was funded by Minciencias, grant number 141580763047 and Universidad Cooperativa de Colombia.

Acknowledgments

Not applicable.

Conflicts of Interest

The authors declare no conflict of interest. The funders had no role in the design of the study; in the collection, analyses, or interpretation of data; in the writing of the manuscript, or in the decision to publish the results.

Referencias bibliográficas


1. NAAQS Table [Internet]. Available from: <https://www.epa.gov/criteria-air-pollutants/naaqs-table>

2. Conceptos básicos sobre el material particulado (PM, por sus siglas en inglés) [Internet]. Available from: <https://espanol.epa.gov/espanol/conceptos-basicos-sobre-el-material-particulado-pm-por-sus-siglas-en-ingles>
3. Partículas ultrafinas [Internet]. Available from: https://www.baaqmd.gov/about-air-quality/special-air-monitoring-projects/special-reports/ultrafine-particulate-matter?sc_lang=es-MX&switch_lang=true
4. Arias-Pérez RD, Tabora NA, Gómez DM, Narvaez JF, Porras J, Hernandez JC. Inflammatory effects of particulate matter air pollution. *Environ Sci Pollut Res* [Internet]. 2020 Sep 1; Available from: <http://link.springer.com/10.1007/s11356-020-10574-w>
5. Bedoya J. Comparación entre medidores Hi-Vol y PM10. 1993;108-11.
6. Harrison RM, Yin J. Particulate matter in the atmosphere: Which particle properties are important for its effects on health? *Sci Total Environ*. 2000;
7. Ambient (outdoor) air pollution [Internet]. Available from: [https://www.who.int/news-room/fact-sheets/detail/ambient-\(outdoor\)-air-quality-and-health](https://www.who.int/news-room/fact-sheets/detail/ambient-(outdoor)-air-quality-and-health)
8. Liu S, Zhou Y, Liu S, Chen X, Zou W, Zhao D, et al. Association between exposure to ambient particulate matter and chronic obstructive pulmonary disease: Results from a cross-sectional study in China. *Thorax*. 2017;
9. Gruzieva O, Bergström A, Hulchiy O, Kull I, Lind T, Melén E, et al. Exposure to air pollution from traffic and childhood asthma until 12 years of age. *Epidemiology*. 2013;
10. Samoli E, Nastos PT, Paliatatos AG, Katsouyanni K, Priftis KN. Acute effects of air pollution on pediatric asthma exacerbation: Evidence of association and effect modification. *Environ Res*. 2011;
11. Kim KH, Kabir E, Kabir S. A review on the human health impact of airborne particulate matter. *Environment International*. 2015.
12. Loaiza-Ceballos MC, Marin-Palma D, Zapata W, Hernandez JC. Viral respiratory infections and air pollutants. *Air Qual Atmos Heal* [Internet]. 2021 Sep 15; Available from: <https://link.springer.com/10.1007/s11869-021-01088-6>
13. De Grove KC, Provoost S, Brusselle GG, Joos GF, Maes T. Insights in particulate matter-induced allergic airway inflammation: Focus on the epithelium. *Clinical and Experimental Allergy*. 2018.
14. Cuelllar A. LINFOPOYETINA ESTROMAL TÍMICA REGULACIÓN DE LA RESPUESTA INMUNE Y LA ENFERMEDAD ALÉRGICA. *Pontif Univ javeriana*. 2007;
15. Feng S, Gao D, Liao F, Zhou F, Wang X. The health effects of ambient PM2.5 and potential mechanisms. *Ecotoxicology and Environmental Safety*. 2016.
16. Brook RD, Rajagopalan S, Pope CA, Brook JR, Bhatnagar A, Diez-Roux A V., et al. Particulate matter air pollution and cardiovascular disease: An update to the scientific statement from the American heart association. *Circulation*. 2010.
17. Simkhovich BZ, Kleinman MT, Kloner RA. Air Pollution and Cardiovascular Injury. *Epidemiology, Toxicology, and Mechanisms. Journal of the American College of Cardiology*. 2008.
18. Miller KA, Siscovick DS, Sheppard L, Shepherd K, Sullivan JH, Anderson GL, et al. Long-term exposure to air pollution and incidence of cardiovascular events in women. *N Engl J Med*. 2007;
19. Pope CA, Bhatnagar A, McCracken JP, Abplanalp W, Conklin DJ, O'Toole T. Exposure to Fine Particulate Air Pollution Is Associated with Endothelial Injury and Systemic Inflammation. *Circ Res*. 2016;
20. Ridker PM, Rifai N, Rose L, Buring JE, Cook NR. Comparison of C-reactive protein and low-density lipoprotein cholesterol levels in the prediction of first cardiovascular events. *N Engl J Med*. 2002;
21. Hu H, Wu J, Li Q, Asweto C, Feng L, Yang X, et al. Fine particulate matter induces vascular endothelial activation via IL-6 dependent JAK1/STAT3 signaling pathway. *Toxicol Res (Camb)* [Internet]. 2016;5(3):946-53. Available from: <https://academic.oup.com/toxres/article/5/3/946-953/5568598>
22. Xu X, Qimuge A, Wang H, Xing C, Gu Y, Liu S, et al. IRE1 γ /XBP1s branch of UPR links HIF1 α activation to mediate ANGII-dependent endothelial dysfunction under particulate matter (PM) 2.5 exposure. *Sci Rep* [Internet]. 2017 Dec 18;7(1):13507. Available from: <http://www.nature.com/articles/s41598-017-13156-y>

23. Chen R, Li H, Cai J, Wang C, Lin Z, Liu C, et al. Fine particulate air pollution and the expression of microRNAs and circulating cytokines relevant to inflammation, coagulation, and vasoconstriction. *Environ Health Perspect*. 2018;
24. Raudoniute J, Stasiulaitiene I, Kulvinskiene I, Bagdonas E, Garbaras A, Krugly E, et al. Pro-inflammatory effects of extracted urban fine particulate matter on human bronchial epithelial cells BEAS-2B. *Environ Sci Pollut Res* [Internet]. 2018 Nov 17;25(32):32277–91. Available from: <http://link.springer.com/10.1007/s11356-018-3167-8>
25. La célula. 3. Membrana celular:COMPLEJOS DE UNIÓN [Internet]. Available from: <https://mmegias.webs.uvigo.es/5-celulas/3-complejos.php>
26. Rui W, Guan L, Zhang F, Zhang W, Ding W. PM2.5-induced oxidative stress increases adhesion molecules expression in human endothelial cells through the ERK/AKT/NF- κ B-dependent pathway. *J Appl Toxicol*. 2016;
27. Alfaro-Moreno E, Martínez L, García-Cuellar C, Bonner JC, Clifford Murray J, Rosas I, et al. Biologic effects induced in vitro by PM10 from three different zones of Mexico City. *Environ Health Perspect*. 2002;
28. SANGUINETI AC, RODRÍGUEZ-TAFUR J. MOLECULAS DE ADHESION Y PIEL. *DERMATOLOGÍA Peru*. 1999;9.
29. He D, Wu S, Zhao H, Qiu H, Fu Y, Li X, et al. Association between particulate matter 2.5 and diabetes mellitus: A meta-analysis of cohort studies. *J Diabetes Investig*. 2017;
30. Braithwaite I, Zhang S, Kirkbride JB, Osborn DPJ, Hayes JF. Air pollution (Particulate matter) exposure and associations with depression, anxiety, bipolar, psychosis and suicide risk: A systematic review and meta-analysis. *Environmental Health Perspectives*. 2019.
31. Thompson JE. Airborne Particulate Matter. *J Occup Environ Med* [Internet]. 2018 May;60(5):392–423. Available from: <http://journals.lww.com/00043764-201805000-00002>
32. Kilian J, Kitazawa M. The emerging risk of exposure to air pollution on cognitive decline and Alzheimer's disease – Evidence from epidemiological and animal studies. *Biomedical Journal*. 2018.
33. Li X, Huang S, Jiao A, Yang X, Yun J, Wang Y, et al. Association between ambient fine particulate matter and preterm birth or term low birth weight: An updated systematic review and meta-analysis. *Environmental Pollution*. 2017.
34. Gómez-Gallego DM, Hernández JC, Ossa JAM la. Efectos adversos de la exposición prenatal al material particulado del aire sobre el feto y el recién nacido. *Iatreia* [Internet]. 2021 Sep 8;1(1 SE-Artículos de revisión). Available from: <https://revistas.udea.edu.co/index.php/iatreia/article/view/346016>
35. Shoefelt J, Mitkus RJ, Zeisler R, Spatz RO, Powell J, Fenton MJ, et al. Involvement of TLR2 and TLR4 in inflammatory immune responses induced by fine and coarse ambient air particulate matter. *J Leukoc Biol*. 2009;
36. Chi GC, Liu Y, MacDonald JW, Barr RG, Donohue KM, Hensley MD, et al. Long-term outdoor air pollution and DNA methylation in circulating monocytes: Results from the Multi-Ethnic Study of Atherosclerosis (MESA). *Environ Heal A Glob Access Sci Source*. 2016;
37. Filella X, Molina R, Ballesta AM. Estructura y función de las citoquinas. *Med Integr*. 2003;
38. Shi Y, Zhao T, Yang X, Sun B, Li Y, Duan J, et al. PM2.5-induced alteration of DNA methylation and RNA-transcription are associated with inflammatory response and lung injury. *Sci Total Environ*. 2019;
39. Soukup JM, Becker S. Human alveolar macrophage responses to air pollution particulates are associated with insoluble components of coarse material, including particulate endotoxin. *Toxicol Appl Pharmacol*. 2001;
40. Matthews NC, Pfeffer PE, Mann EH, Kelly FJ, Corrigan CJ, Hawrylowicz CM, et al. Urban Particulate Matter-Activated Human Dendritic Cells Induce the Expansion of Potent Inflammatory Th1, Th2, and Th17 Effector Cells. *Am J Respir Cell Mol Biol* [Internet]. 2016 Feb;54(2):250–62. Available from: <http://www.atsjournals.org/doi/10.1165/rcmb.2015-0084OC>
41. Glencross DA, Ho T-R, Camiña N, Hawrylowicz CM, Pfeffer PE. Air pollution and its effects on the immune system. *Free Radic Biol Med*. 2020 May;151.
42. Liu J, Li S, Fei X, Nan X, Shen Y, Xiu H, et al. Increased alveolar epithelial TRAF6 via autophagy-dependent TRIM37 degradation mediates particulate matter-induced lung metastasis. *Autophagy* [Internet]. 2021 Sep 15:1–19. Available from: <https://www.tandfonline.com/doi/full/10.1080/15548627.2021.1965421>
43. SANGUINETI AC R-TJ. MOLECULAS DE ADHESION Y PIEL. *DERMATOLOGÍA Peru*. 1999;9.
44. Wang G, Zhang G, Gao X, Zhang Y, Fan W, Jiang J, et al. Oxidative stress-mediated epidermal growth factor receptor activation regulates PM2.5-induced over-secretion of pro-inflammatory mediators from human bronchial epithelial cells. *Biochim Biophys Acta - Gen Subj* [Internet]. 2020 Oct;1864(10):129672. Available from: <https://linkinghub.elsevier.com/retrieve/pii/S0304416520301847>
45. Saavedra Ramírez PG, Vásquez Duque GM, González Naranjo LA. Interleucina-6: ¿amiga o enemiga? Bases para comprender su utilidad como objetivo terapéutico. *Iatreia*. 2011;
46. Yang J, Chen Y, Yu Z, Ding H, Ma Z. The influence of PM2.5 on lung injury and cytokines in mice. *Exp Ther Med* [Internet]. 2019 Aug 1; Available from: <http://www.spandidos-publications.com/10.3892/etm.2019.7839>
47. Varfolomeev E, Vucic D. Intracellular regulation of TNF activity in health and disease. *Cytokine* [Internet]. 2018 Jan;101:26–32. Available from: <https://linkinghub.elsevier.com/retrieve/pii/S1043466616304896>
48. Xu X, Jiang SY, Wang TY, Bai Y, Zhong M, Wang A, et al. Inflammatory Response to Fine Particulate Air Pollution Exposure: Neutrophil versus Monocyte. *PLoS One*. 2013;
49. Deshmane SL, Kremlev S, Amini S, Sawaya BE. Monocyte Chemoattractant Protein-1 (MCP-1): An Overview. *J Interf Cytokine Res* [Internet]. 2009 Jun;29(6):313–26. Available from: <http://www.liebertpub.com/doi/10.1089/jir.2008.0027>
50. Kumar RK, Shadie AM, Bucknall MP, Rutledge H, Garthwaite L, Herbert C, et al. Differential injurious effects of ambient and traffic-derived particulate matter on airway epithelial cells. *Respirology*. 2015;
51. Sawant K V, Poluri KM, Dutta AK, Sepuru KM, Troshkina A, Garofalo RP, et al. Chemokine CXCL1 mediated neutrophil recruitment: Role of glycosaminoglycan interactions. *Sci Rep*. 2016;
52. Rodier F, Coppé JP, Patil CK, Hoeijmakers WAM, Muñoz DP, Raza SR, et al. Persistent DNA damage signalling triggers senescence-associated inflammatory cytokine secretion. *Nat Cell Biol*. 2009;
53. Gualtieri M, Øvrevik J, Møllerup S, Asare N, Longhin E, Dahlman HJ, et al. Airborne urban particles (Milan winter-PM2.5) cause mitotic arrest and cell death: Effects on DNA, mitochondria, AHR binding and spindle organization. *Mutat Res - Fundam Mol Mech Mutagen*. 2011;
54. Marazita MC. P19INK4D y su fosforilación secuencial son críticas para el mantenimiento de la integridad del genoma [Internet]. 2010. Available from: https://bibliotecadigital.exactas.uba.ar/download/tesis/tesis_n4610_Marazita.pdf
55. Jarvis IWH, Enlo-Scott Z, Nagy E, Mudway IS, Tetley TD, Arlt VM, et al. Genotoxicity of fine and coarse fraction ambient particulate matter in immortalised normal (TT1) and cancer-derived (A549) alveolar epithelial cells. *Environ Mol Mutagen*. 2018;
56. Munschauer M, Nguyen CT, Sirokman K, Hartigan CR, Hogstrom L, Engreitz JM, et al. The NORAD lncRNA assembles a topoisomerase complex critical for genome stability. *Nature*. 2018;
57. Soghli N, Yousefi T, Abolghasemi M, Quej D. NORAD, a critical long non-coding RNA in human cancers. *Life Sci* [Internet]. 2021 Jan;264:118665. Available from: <https://linkinghub.elsevier.com/retrieve/pii/S0024320520314181>
58. Santibáñez-Andrade M, Sánchez-Pérez Y, Chirino YI, Morales-Bárceñas R, García-Cuellar CM. Long non-coding RNA NORAD upregulation induced by airborne particulate matter (PM10) exposure leads to aneuploidy in A549 lung cells. *Chemosphere*. 2020;
59. Kang D, Jung IB, Lee SY, Park SJ, Kwon SJ, Park DH, et al. Particulate matter less than 10 μ m (PM 10) activates cancer related genes in lung epithelial cells. *Inhal Toxicol* [Internet]. 2020 Dec 5;32(13–14):487–93. Available from: <https://www.tandfonline.com/doi/full/10.1080/08958378.2020.1850936>
60. Zhao H, Zhu X, Luo Y, Liu S, Wu W, Zhang L, et al. LINC01816 promotes the migration, invasion and epithelial-mesenchymal transition of thyroid carcinoma cells by sponging miR-34c-5p and regulating CRABP2 expression levels. *Oncol Rep* [Internet]. 2021 Mar 30;45(5):81. Available from: <http://www.spandidos-publications.com/10.3892/or.2021.8032>
61. Davies K. Free Radical Biology & Medicine. 2003.
62. Griffiths HR. Antioxidants and protein oxidation. In: *Free Radical Research*. 2000.

63. Gualtieri M, Longhin E, Mattioli M, Mantecca P, Tinaglia V, Mangano E, et al. Gene expression profiling of A549 cells exposed to Milan PM2.5. *Toxicol Lett.* 2012;
64. Abbas I, Badran G, Verdin A, Ledoux F, Rournie M, Lo Guidice JM, et al. In vitro evaluation of organic extractable matter from ambient PM2.5 using human bronchial epithelial BEAS-2B cells: Cytotoxicity, oxidative stress, pro-inflammatory response, genotoxicity, and cell cycle deregulation. *Environ Res.* 2019;
65. Hussain T, Al-Attas OS, Al-Daghri NM, Mohammed AA, De Rosas E, Ibrahim S, et al. Induction of CYP1A1, CYP1A2, CYP1B1, increased oxidative stress and inflammation in the lung and liver tissues of rats exposed to incense smoke. *Mol Cell Biochem [Internet].* 2014 Jun 21;391(1-2):127-36. Available from: <http://link.springer.com/10.1007/s11010-014-1995-5>
66. Mazuryk O, Stochel G, Brindell M. Variations in Reactive Oxygen Species Generation by Urban Airborne Particulate Matter in Lung Epithelial Cells—Impact of Inorganic Fraction. *Front Chem [Internet].* 2020 Dec 17;8. Available from: <https://www.frontiersin.org/articles/10.3389/fchem.2020.581752/full>
67. Sotty J, Kluzka J, De Sousa C, Tardivel M, Anthérieu S, Alleman L-Y, et al. Mitochondrial alterations triggered by repeated exposure to fine (PM2.5-0.18) and quasi-ultrafine (PM0.18) fractions of ambient particulate matter. *Environ Int [Internet].* 2020 Sep;142:105830. Available from: <https://linkinghub.elsevier.com/retrieve/pii/S0160412020317852>
68. Wang J, Huang J, Wang L, Chen C, Yang D, Jin M, et al. Urban particulate matter triggers lung inflammation via the ROS-MAPK-NF- κ B signaling pathway. *J Thorac Dis.* 2017;
69. Yabluchanskiy A, Ma Y, Iyer RP, Hall ME, Lindsey ML. Matrix metalloproteinase-9: Many shades of function in cardiovascular disease. *Physiology.* 2013.
70. Funk CD, FitzGerald GA. COX-2 inhibitors and cardiovascular risk. *Journal of Cardiovascular Pharmacology.* 2007.
71. Liguori I, Russo G, Curcio F, Bulli G, Aran L, Della-Morte D, et al. Oxidative stress, aging, and diseases. *Clin Interv Aging [Internet].* 2018 Apr;Volume 13:757-72. Available from: <https://www.dovepress.com/oxidative-stress-aging-and-diseases-peer-reviewed-article-CIA>
72. Leclercq B, Kluzka J, Anthérieu S, Sotty J, Alleman LY, Perdrix E, et al. Air pollution-derived PM2.5 impairs mitochondrial function in healthy and chronic obstructive pulmonary diseased human bronchial epithelial cells. *Environ Pollut.* 2018;
73. Königsberg Fainstein M. Nrf2: LA HISTORIA DE UN NUEVO FACTOR DE TRANSCRIPCIÓN QUE RESPONDE A ESTRÉS OXIDATIVO*. 2007;
74. Michael S, Montag M, Dott W. Pro-inflammatory effects and oxidative stress in lung macrophages and epithelial cells induced by ambient particulate matter. *Environ Pollut [Internet].* 2013 Dec;183:19-29. Available from: <https://linkinghub.elsevier.com/retrieve/pii/S0269749113000419>
75. Ionescu-Tucker A, Cotman CW. Emerging roles of oxidative stress in brain aging and Alzheimer's disease. *Neurobiol Aging [Internet].* 2021 Nov;107:86-95. Available from: <https://linkinghub.elsevier.com/retrieve/pii/S0197458021002402>
76. Barnes PJ. Oxidative stress-based therapeutics in COPD. *Redox Biol [Internet].* 2020 Jun;33:101544. Available from: <https://linkinghub.elsevier.com/retrieve/pii/S2213231720301610>
77. Pawlina W. *Histología Texto Y Atlas Correlación con Biología Molecular y Celular. Ross Histología texto y atlas.* 2015.
78. Zhao R, Guo Z, Zhang R, Deng C, Xu J, Dong W, et al. Nasal epithelial barrier disruption by particulate matter $\leq 2.5 \mu\text{m}$ via tight junction protein degradation. *J Appl Toxicol.* 2018;
79. Raudoniute J, Stasiulaitiene I, Kulvinskiene I, Bagdonas E, Garbaras A, Krugly E, et al. Pro-inflammatory effects of extracted urban fine particulate matter on human bronchial epithelial cells BEAS-2B. *Environ Sci Pollut Res.* 2018;
80. Pérez BF, Méndez GA, Lagos RA, Vargas MSL. Dinámica y patología del barrido mucociliar como mecanismo defensivo del pulmón y alternativas farmacológicas de tratamiento. *Rev Med Chil [Internet].* 2014 May;142(5):606-15. Available from: http://www.scielo.cl/scielo.php?script=sci_arttext&pid=S0034-98872014000500009&lng=en&nrm=iso&tlng=en
81. Jia J, Xia J, Zhang R, Bai Y, Liu S, Dan M, et al. Investigation of the impact of PM2.5 on the ciliary motion of human nasal epithelial cells. *Chemosphere.* 2019;
82. Rivas-Santiago CE, Sarkar S, Cantarella P, Osornio-Vargas Á, Quintana-Belmares R, Meng Q, et al. Air pollution particulate matter alters antimycobacterial respiratory epithelium innate immunity. *Infect Immun.* 2015;
83. Lerner CA, Sundar IK, Rahman I. Mitochondrial redox system, dynamics, and dysfunction in lung inflammaging and COPD. *Int J Biochem Cell Biol.* 2016;
84. Xiaoqin YJ, Wang X, Hu D. Mitochondrial alterations during oxidative stress in chronic obstructive pulmonary disease. *International Journal of COPD.* 2017.
85. Chen ZH, Kim HP, Sciruba FC, Lee SJ, Feghali-Bostwick C, Stolz DB, et al. Egr-1 regulates autophagy in cigarette smoke-induced chronic obstructive pulmonary disease. *PLoS One.* 2008;
86. Carvajal Carvajal C. El endotelio: estructura, función y disfunción endotelial. *Med Leg Costa Rica.* 2017;
87. Wang G, Zhang X, Liu X, Zheng J, Chen R, Kan H. Ambient fine particulate matter induce toxicity in lung epithelial-endothelial co-culture models. *Toxicol Lett.* 2019;
88. Long Y-M, Yang X-Z, Yang Q-Q, Clermont AC, Yin Y-G, Liu G-L, et al. PM2.5 induces vascular permeability increase through activating MAPK/ERK signaling pathway and ROS generation. *J Hazard Mater [Internet].* 2020 Mar;386:121659. Available from: <https://linkinghub.elsevier.com/retrieve/pii/S0304389419316139>
89. Zhang WC, Wang YG, Zhu ZF, Wu FQ, Peng YD, Chen ZY, et al. Regulatory T cells protect fine particulate matter-induced inflammatory responses in human umbilical vein endothelial cells. *Mediators Inflamm.* 2014;
90. Riggs DW, Zafar N, Krishnasamy S, Yeager R, Rai SN, Bhatnagar A, et al. Exposure to airborne fine particulate matter is associated with impaired endothelial function and biomarkers of oxidative stress and inflammation. *Environ Res [Internet].* 2020 Jan;180:108890. Available from: <https://linkinghub.elsevier.com/retrieve/pii/S0013935119306875>
91. Guyton A, Hall JE. *Tratado de fisiología medica.* 12th ed. 221 p.
92. Pacurari M, Kafoury R, Tchounwou PB, Ndebele K. The Renin-Angiotensin-Aldosterone System in Vascular Inflammation and Remodeling. *Int J Inflam [Internet].* 2014;2014:1-13. Available from: <http://www.hindawi.com/journals/ijji/2014/689360/>
93. Hurtubise J, McLellan K, Durr K, Onasanya O, Nwabuko D, Ndisang JF. The different facets of dyslipidemia and hypertension in atherosclerosis. *Curr Atheroscler Rep.* 2016;
94. Ellingsen DG, Chashchin M, Seljeflot I, Berlinger B, Chashchin V, Stockfelt L, et al. A study of atherothrombotic biomarkers in welders. *Int Arch Occup Environ Health.* 2019;
95. Rückert R, Ibaldo-Mulli A, Koenig W, Schneider A, Woelke G, Cyrys J, et al. Air pollution and markers of inflammation and coagulation in patients with coronary heart disease. *Am J Respir Crit Care Med.* 2006;
96. Finch J, Conklin DJ. Air Pollution-Induced Vascular Dysfunction: Potential Role of Endothelin-1 (ET-1) System. *Cardiovasc Toxicol.* 2016;
97. Shen C, Liu J, Zhu F, Lei R, Cheng H, Zhang C, et al. The effects of cooking oil fumes-derived PM 2.5 on blood vessel formation through ROS-mediated NLRP3 inflammasome pathway in human umbilical vein endothelial cells. *Ecotoxicol Environ Saf.* 2019;
98. Amabile N, Rautou PE, Tedgui A, Boulanger CM. Microparticles: Key protagonists in cardiovascular disorders. *Seminars in Thrombosis and Hemostasis.* 2010.
99. Chuang HC, Ho KF, Cao JJ, Chuang KJ, Ho SSH, Feng PH, et al. Effects of non-protein-type amino acids of fine particulate matter on E-cadherin and inflammatory responses in mice. *Toxicol Lett.* 2015;
100. Liu B, Wu S De, Shen LJ, Zhao TX, Wei Y, Tang XL, et al. Spermatogenesis dysfunction induced by PM2.5 from automobile exhaust via the ROS-mediated MAPK signaling pathway. *Ecotoxicol Environ Saf.* 2019;
101. Flores N. Endotelina-1: Vasoconstrictor Intrínseco Del Endotelio Vascular. *Rev Med.* 2013;



 ESCUELA DE
CIENCIAS BIOLÓGICAS
E INGENIERÍA



www.yachaytech.edu.ec

ARTICLE / INVESTIGACIÓN

Study the relationship between *Helicobacter pylori* and bladder cancerMohammad Heidari¹, Seyed Jalal Eshagh Hoseini^{2*}, Hassan Fatemi Manesh³

DOI. 10.21931/RB/2022.07.01.5

¹ Department of Pediatric Nephrology, School of Medicine, Qom University of Medical Sciences, Qom, Iran.² Department of Surgery, Qom University of Medical Sciences, Qom, Iran.³ Student Research Committee, Qom University of Medical Sciences, Qom, Iran.

Corresponding author: jalaleshaghoseini@gmail.com.

Abstract: Given that bladder cancer is one of the most common cancers, and *Helicobacter pylori* infection also has 30-80% prevalence in different communities, this study investigates the role of *H. pylori* in developing bladder cancer; From December 2013 to February 2020, 200 patients with bladder tumors who underwent bladder tumor resection through the urethra in Kamkar-Arabnia Hospital were included in this study. *H. pylori* Ab, IgA, and IgG tests were first requested from all patients. If their antibodies were positive, other periodic tests including creatinine-sodium-potassium, Prothrombin Time (PT), Prothrombin Time Test (PTT), and International Normalized Ratio (INR), urinalysis, and culture were taken. The obtained results were analyzed using SPSS software version 25, and in the chi-square test, $P < 0.05$ was considered a significant level; (3) Results: Based on laboratory findings, 66.5% of patients were *H. pylori* + ($p < 0.05$). The result of the PCR test was positive in 4% of all patients. Besides, 6% of patients who tested positive for *H. pylori* Ab also showed positive PCR tests. Further studies are needed to investigate the association between *H. pylori* infection and bladder tumors to evaluate the proper role of *H. pylori* in tumors of the urinary system, especially the bladder and prostate, which have not been treated or reduced by treating *H. pylori*.

Key words: *Helicobacter pylori*, Bladder cancer, Urinary system, Polymerase Chain Reaction.

Introduction

Most published research points to several factors that cause cancer, such as toxins, drugs, smoking, and obesity. However, there are few studies on cancer development through bacterial infections. Besides, the mechanisms of cancer through bacterial infections are not well understood. *H. pylori* are the first known bacterium to cause stomach cancer and may also be associated with cancer out of the human stomach¹. Therefore, there is a lot of focus and attention on *H. pylori* infection nowadays. This bacterium, which lives in the upper gastrointestinal tract, is found in half of the world's population. Its prevalence in geography, ethnicity, age, and socio-economic factors is very high in developing countries and less in developed countries^{2,3}. *H. pylori* is a gram-negative flagellate, microaerophilic, and helical bacterium that causes gastritis and can eventually cause stomach cancer⁴⁻⁷. Studies have recently shown that this bacterium also causes organs outside the digestive system^{6,8,9}. Other studies suggest that *H. pylori* may cause bladder and prostate inflammation or involve other organs¹⁰. On the other hand, vitamin D3 deficiency may also cause prostate cell proliferation and cancer¹¹. *H. pylori* infection causes chronic inflammation that can lead to metaplasia, dysplasia, and cancer^{6,10,12}. *H. pylori* infection is one of the risk factors in cancer development. However, its presence does not mean the definitive development of cancer¹³. The World Health Organization identifies it as a class 1 carcinogen because *H. pylori* in the stomach increase cancer risk by six times^{5,14}. Given that bladder cancer is one of the most common cancers and *H. pylori* infection also has 30-80% prevalence in different communities⁵, this study investigates the role of *H. pylori* in developing bladder cancer.

Materials and methods

Ethical consideration

The ethical committee approved this research's Qom University of Medical Sciences principles, Qom, Iran (Ethical number: IR.MUG.REC.1395.69). Additionally, Written consent was obtained from all patients included in the study.

Study design and patients

In a dissertation study from December 2013 to February 2020, 200 patients with bladder tumors referred to Kamkar-Arabnia Hospital, Qom, Iran, were assessed. After confirming the bladder tumor by cystoscopy¹⁵, patients underwent resection of the bladder tumor through the duct¹⁶.

Antibody detection

First, all patients underwent *H. pylori* antibody (Ab), Immunoglobulin A (IgA), and IgG tests¹⁷. For this purpose, peripheral blood was collected to determine anti-*H. pylori* IgG and IgA serum levels. ELISA method (Accubind®, USA) was used to determine serum anti-*H. pylori* IgG and IgA levels. The serum samples were diluted to 1/100. Other steps were performed according to the instructions of the manufacturer.

Complementary tests

After antibody detection, other periodic tests, including creatinine-sodium-potassium PT, A partial thromboplastin time (PTT), Prothrombin Time Test and INR (PT/INR), urinalysis, and culture were performed on patients with positive antibodies. Furthermore, Polymerase Chain Reaction (PCR) test was performed after the surgery¹⁸.

Citation: Heidari M, Eshagh Hosaini S K, Fatemi Manesh H. Study the relationship between *Helicobacter pylori* and bladder cancer. *Revis Bionatura* 2022 ;7(1). 5. <http://dx.doi.org/10.21931/RB/2022.07.01.5>

Received: 26 June 2021 / **Accepted:** 7 August 2021 / **Published:** 15 february 2022

Publisher's Note: Bionatura stays neutral with regard to jurisdictional claims in published maps and institutional affiliations.

Copyright: © 2022 by the authors. Submitted for possible open access publication under the terms and conditions of the Creative Commons Attribution (CC BY) license (<https://creativecommons.org/licenses/by/4.0/>).



DNA extraction

The removed bladder tissue was immediately frozen in liquid nitrogen and stored at -80°C until the experiment. A maximum of 25 mg of tissue was divided into small pieces and placed in a 1.5 mL microcentrifuge tube. Genomic DNA was extracted from the bladder tissues using the DNA extraction and purification kit (Qiagen, Valencia, CA). DNA was extracted directly from each tissue sample and used as a template to identify the specific *H. pylori* 16S rRNA gene. The quality and purity of extracted DNA samples were checked by gel electrophoresis and NanoDrop device (MA, USA), respectively¹⁹⁻²¹.

PCR procedure

H. pylori was identified using the 16S rRNA-based PCR (primers: HP-F: 5'-CTGGAGAGACTAAGCCCTCC-3' and HP-R: 5'-ATTACTGACGCTGATTGTGC-3')²². PCR circumstances and volumes were done according to described method²². Briefly, PCR was performed in of 50 μL volume. Ingredients were amplified in a device (Eppendorf Co., Germany) at several temperatures, including 1 cycle at 94°C for 2 min, 30 cycles of 30 s at 95°C , 30 s at 60°C , and 30 s at 72°C and another one cycle of 8 min at 72°C . Positive control was *H. pylori* 26695. The negative control was PCR-grade water (Thermo Fisher Scientific). Electrophoresis was performed by agarose gel (2.5%) at 120 V for 30 min. UVI doc system was applied for gel visualization^{23,24}.

Data analysis

Obtained data were analyzed by SPSS.V.25 according to the Chi-square test. $P < 0.05$ was level of significance^{25,26}.

Results

Table 1 shows the demographic characters of the studied patients and the distribution of *H. pylori*. The distribution of male and female patients amongst the examined population was 65% and 35%. One-hundred and thirty-three out of 200 (66.5%) examined samples were positive for *H. pylori*. Findings revealed that 85% of samples had positive homogeneity. Additionally, 87.5% of patients were cytologically positive. Besides, 82.5% of patients were diagnosed using ultrasonic technology. The majority of examined patients were educators (29%), followed by the farmer (28%) and labor (18.5%). Of the 200 patients in the study, 89 patients had high blood pressure ($p < 0.05$) and were taking aspirin (ASA). There were 120 smokers ($P < 0.05$). However, 25% of patients had no risk factor.

Figure 1 shows the age distribution of patients examined in the present study. The mean age was 67 years, and the ratio of men to women was 1.9. The prevalence of bladder cancer was significantly higher in men than in women ($P < 0.05$). 61-80 years old men have the highest cancer incidence ($P < 0.05$).

Table 2 shows the histopathological features of the bladder cancer examined in the present research. Transitional cell cancer (TCC) was the most commonly identified cancer type (87.5%), while adenocarcinoma (2.5%) was the less commonly identified.

Table 3 shows the German immune lab test findings for the detection of *H. pylori* amongst examined samples. A total of 133 out of 200 (66.5%) cases were recognized as *H. pylori*-positive using the German immune lab test ($P < 0.05$).

Table 4 shows the PCR results for the detection of *H. pylori* in diverse kinds of bladder cancers. The result of the PCR test was positive in 4% of all patients. Besides, 6% of patients who tested positive for *H. pylori* Ab also showed positive PCR results.

Discussion

Infectious diseases have been considered health-threatening issues in the last centuries²⁷⁻⁴⁰. Studies have shown that common organisms in saliva include three specimens of *H. pylori*, Campylobacter, and Neisseria cinerea, which are also present in the gastrointestinal tract. In vitro, these samples can catalyze many drugs and cause long-term gastrointestinal infections by causing nitrosamine compounds and gastric cancer⁴¹. However, in a study conducted by Heidari in Qom (2020), it was found that vitamin D3 deficiency plays a role in causing Benign prostatic hyperplasia (BPH) and possibly cancer¹¹. Also, in the study of Alireza Abdollahi *et al.* on 126 patients, 33.3% had prostatitis with pelvic pain, and 84 patients in the control group had no symptoms. All were positive for *H. pylori* and antibodies, although they had no prostatitis symptoms, detrimental to *H. pylori* in inflammatory prostate disease¹³. In this study conducted in Iran, many of these bacteria were identified in the prostate, BPH, and prostate cancer. *H. pylori* were examined by immunohistochemistry (IHC) and PCR, and the results were determined by DNA sequencing. However, *H. pylori* have been reported positively in one case immunohistochemistry¹³. In the study by Michaud *et al.* (2004), men with gastric tumors had a higher prevalence of bladder cancer, but cancer risk was not higher in patients with a duodenal ulcer⁴². Gastric ulcers were significantly more common among patients with gastric cancer than renal cancer. The gastric/duodenal ulcers proportion in the gastric group was 6.5, and the renal cancer group was 0.33⁴². In this study, *H. pylori* were identified as a risk factor for gastric and duodenal cancer. This bacterium causes stomach ulcers in the duodenum due to high acidity, but in the stomach, low acid production, gastritis, and ulcer disorders cause poor absorption of antioxidants, oxidative stress, and high levels of nitrates. Nitrates and nitrosamine compounds are also known as bladder carcinogens⁴². Due to this condition, it also occurs in the bladder as it does in the stomach. In this study, the condition closest to *H. pylori* was not correlated with gastric cancer, which seems to include a direct carcinogenic effect of the bacterium in the other studies was associated with *H. pylori* in 70-80% cases was positively correlated to gastric cancer⁴². Oral sex is one of the most common sex practices in the world. *H. pylori* transmitted via the act of sex through the urethra may lead to infection⁴². Several studies have shown that the transfer of bacterial metabolites of *H. pylori* can play a role in developing urinary tract cancers⁴³. Matsumoto's study showed that *H. pylori* infection caused Hodgkin's lymphoma, regressed by *H. pylori* treatment. Finally, further studies are needed to prove the role of *H. pylori* infection directly or indirectly in various tumors, including the urinary system⁴⁴.

Infection and chronic inflammation have been recognized as essential predisposing factors for carcinogenesis and tumors. International agency for cancer (IARC) research has estimated that approximately 11% of cancers are related to infectious diseases like bacteria, viruses, and parasites. Human cancer is caused by infectious agents such as *H. pylori*, Human papillomavirus (HPV), Epstein-Barr virus (EBV), Sickle hemoglobin (HbS), and Hepatitis C virus (HCV), and human immunodeficiency viruses (HIV)¹⁴. Chronic inflammations are accountable for about 25% of cancer cases. Environmental issues, including HCV, HPV, HBV, and *H. pylori* infections, may be accountable for around 65-80% of gastric cancers, 80% of hepatocellular cancers, and 90% of cervical cancers¹⁴. Under inflammation conditions, reactive oxygen species (ROS) and reactive nitrogen species (RNS) are made from inflammatory

Demographic characters	Frequency (%)
Total population	200
Male	130 (65%)
Female	70 (35%)
<i>H. pylori</i>-positive	133 (66.5%)
<i>H. pylori</i>-negative	67 (33.5%)
Homogeneity-positive	170 (85%)
Non-homogeneity	30 (15%)
Cytology-positive	175 (87.5%)
Cytology-negative	25 (12.5%)
Ultrasonic-positive	165 (82.5%)
Ultrasonic-negative	35 (17.5%)
Job title	
Educator	58 (29%)
Farmer	56 (28%)
Labor	37 (18.5%)
Hygienics	4 (2%)
Mechanic	15 (7.5%)
Driver	11 (5.5%)
Housewife	19 (9.5%)
High blood pressure with aspirin taking	89 (44.5%)
Smoking	120 (60%)
Without risk factor	50 (25%)

Table 1. Demographic characters of the studied patients and distribution of *H. pylori*.

and epithelial cells. These agents are capable of causing damage to various cellulars such as nucleic acids, proteins, and lipids. In this regard, *H. pylori* infection could affect the chronic bladder inflammation related to releasing large amounts of pro-inflammatory and vasoactive substances such as IL-1, IL-7, IL-1, and TNF- α or eicosanoids (leukotrienes, prostaglandins) and acute-phase proteins involved in the number of inflammatory diseases¹⁰. Besides, *H. pylori*-induced cytotoxin promotes intracellular survival of bacterium, modulates host immune responses, and induces autophagy because *H. pylori* as an intracellular microorganism invade and replicate in the cells. Compared to the translocation of *H. pylori* from the oral cavity to the stomach, *H. pylori* may reach the bladder through to the urethra, contaminated by saliva, and so on⁴⁵.

In the study by Heidari *et al.*¹¹, *H. pylori* infection was present in the urinary secretions of 8-hydroxy-2-deoxyguanosine, which causes DNA damage. In the 24-hour urine study of the subjects, 8ohdG was significantly higher in *H. pylori*-infected

individuals than in the control group. This study found that 8ohdG is one of the most abundant lesions in DNA. The 8ohdG generated by ROS is caused by a radical oxygen attack on DNA and interferes with DNA repair⁴³. This bacterium is significantly involved in developing bladder cancer and causes inflammation of the stomach, duodenum, and gall bladder⁴. *H. pylori*'s role in developing lower gastric lymphoma has also been identified⁴⁴. Recently, the association of this bacterium with urinary tract infection has been confirmed¹³. In a pilot study in patients with chronic prostatitis and pelvic pain, more people had a positive *H. pylori* antibody than in the control group^{45, 46}. However, it is not clear exactly how *H. pylori* are transmitted and why some individuals become symptomatic, and some do not⁴. Bacteria are likely to be transmitted through feces, mouth, saliva, and contaminated water and food⁴⁷. *H. pylori* is present in several locations, including adhesions to epithelial cells or inside vacuoles in epithelial cells. This bacterium stays in the lipid tissue and carbohydrates around the membrane

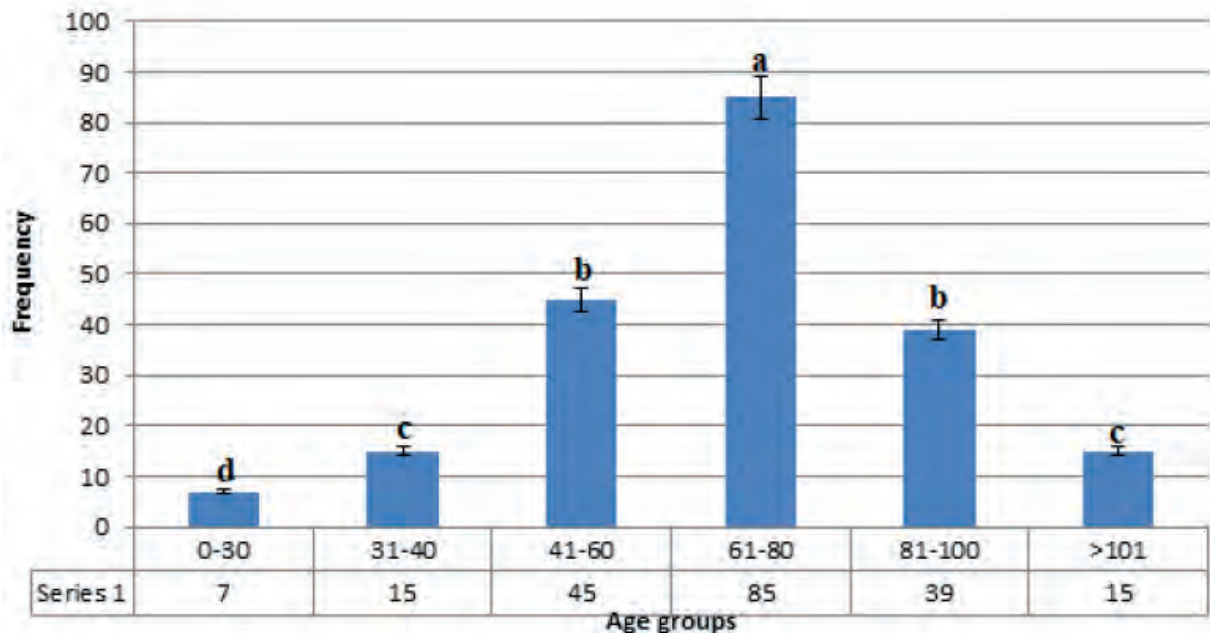


Figure 1. Age distribution of patients with bladder carcinoma. Dissimilar letters in each column show statistically significant differences ($P < 0.05$).

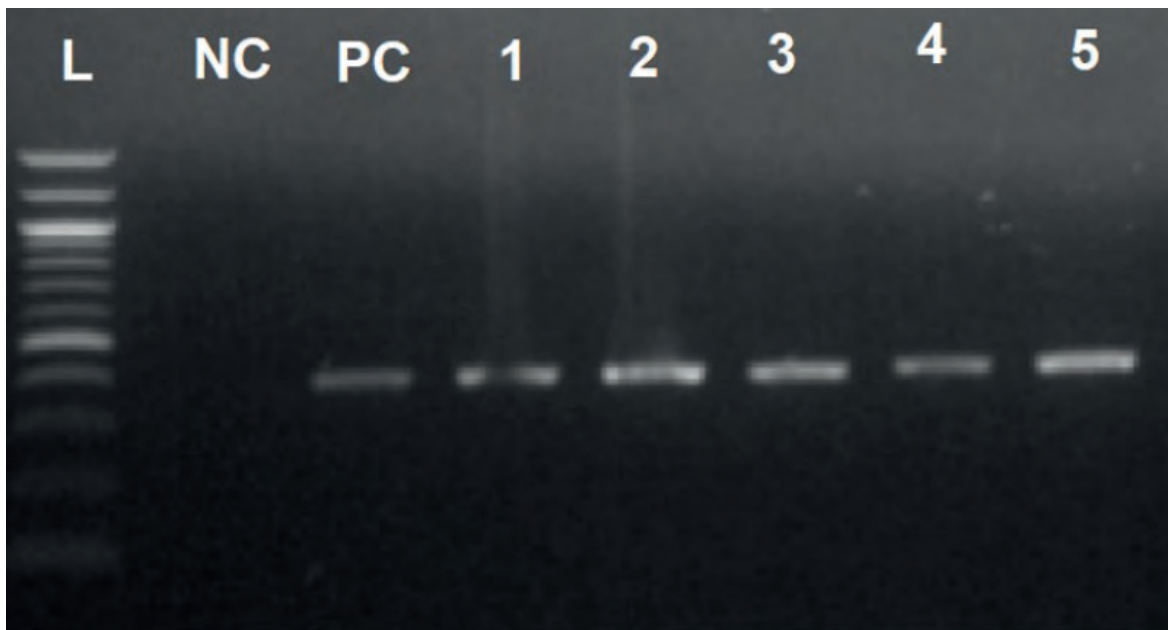


Figure 2. PCR electrophoresis. L: Ladder (100 bp), NC: Negative control, PC: Positive control, 1-5: Positive samples for *H. pylori* (446 bp).

by creating adhesion⁴⁵. The reason that suggests the role of *H. pylori* in the development of bladder disease is the observation of *H. pylori* in other organs associated with other cancers, and this case has been identified for a long time⁴⁸.

Bladder malt lymphoma also resolves after *H. pylori* treatment^{45,49}. Because *H. pylori* can cause infection into the bladder and prostate mucosa through the urethra (oral sex, anal sex, etc.) it causes chronic inflammation and the process of prostate and bladder cancer⁴⁵. Al-Marhoon, in various studies that have examined the association between *H. pylori* and urological diseases, has stated that the most crucial reason for the role of *H. pylori* in causing chronic inflammation is that it leads to lymphoma. In a study by Shria Kumar *et al.* on 371,813

people diagnosed with *Helicobacter pylori* infection, treatment of *H. pylori* infection reduced gastric cancer risk only if eradication was successful⁵⁰. As shown in the study of Heidari *et al.*, BCG injection effectively treated interstitial cystitis⁵¹. Bacillus Calmette-Guerin (BCG) injection can also be used to treat high-grade bladder cancers⁵². In this study, we had eight positive PCR cases of bladder tumors. Considering that there were 133 positive antibody tests in the study, the small number of patients due to infection is not conclusive. Of course, laboratory and individual disorders may play a role. Although, laboratory and individual disorders may play a role in this regard.

Type of cancer	No (%) patient
Transitional cell cancer (TCC)	175 (87.5)
Squamous cell carcinoma (SCC)	15 (7.5)
Adenocarcinoma	5 (2.5)
Mix	5 (2.5)

Table 2. Histological features of bladder cancer.

Table 3. Findings of the German immune lab test.

Total cases	<i>H. pylori</i> +	<i>H. pylori</i> -
200	133 (66.5%)	67 (33.5%)

	TCC	SCC	Adenocarcinoma	Mix
PCR +1	3	5	-	-

Table 4. PCR results for the detection of *H. pylori* in diverse bladder cancers.

Conclusions

The current research showed that *H. pylori* infections might predispose factors for bladder cancer. In this regard, a total of 133 out of 200 (66.5%) cases were recognized as *H. pylori*-positive using the German immune lab test ($P < 0.05$). Additionally, 6% of patients who tested positive for *H. pylori* Ab showed positive PCR results. Further studies are needed to investigate the association between *H. pylori* infection and bladder tumors. These studies should investigate the proper role of *H. pylori* in tumors of the urinary system, especially the bladder and prostate, which have not been treated or reduced by treating *H. pylori*.

Bibliographic references

- Yahaghi E, Khamesipour F, Mashayekhi F, Safarpour Dehkordi F, Sakhaei MH, Masoudimanesh M, Khameneie MK. Helicobacter pylori in vegetables and salads: genotyping and antimicrobial resistance properties. *BioMed Res Int*. 2014;2014.
- Atapour S, Dehkordi FS, Rahimi E. Detection of Helicobacter pylori in various types of vegetables and salads. *J J Microbiol*. 2014;7(5).
- Ranjbar R, Farsani FY, Dehkordi FS. Phenotypic analysis of antibiotic resistance and genotypic study of the *vacA*, *cagA*, *iceA*, *oipA* and *babA* genotypes of the Helicobacter pylori strains isolated from raw milk. *Antimicrob Res Infect Control*. 2018;7(1):1-4.
- Mousavi S, Dehkordi FS. Virulence factors and antibiotic resistance of Helicobacter pylori isolated from raw milk and unpasteurized dairy products in Iran. *J Venom Anim Tox Incl Trop Dis*. 2015;20:1-7.
- Mashak Z, Jafariaskari S, Alavi I, Shahreza MS, Dehkordi FS. Phenotypic and genotypic assessment of antibiotic resistance and genotyping of *vacA*, *cagA*, *iceA*, *oipA*, *cagE*, and *babA2* alleles of Helicobacter pylori bacteria isolated from raw meat. *Infect Drug Res*. 2020;13:257.
- Ranjbar R, Yadollahi Farsani F, Safarpour Dehkordi F. Antimicrobial resistance and genotyping of *vacA*, *cagA*, and *iceA* alleles of the Helicobacter pylori strains isolated from traditional dairy products. *J Food Safety*. 2019;39(2):e12594.
- Mousavi S, Safarpour Dehkordi F, Valizadeh Y. Genotyping of Helicobacter pylori strains isolated from raw milk and dairy products. *J Food Microbiol*. 2017;4(3):41-53.
- Kountouras J, Tsiaousi E, Trigonis S, Zavos C, Kouklakis G. Helicobacter pylori infection in a Greek cohort with biliary disease. *Br J Biomed Sci*. 2014;71(4):178-179. doi:10.1080/09674845.2014.11669984
- Houben GM, Hooi J, Hameeteman W, Stockbrugger RW. The frequency of Helicobacter pylori associated peptic ulcer disease and of autoimmune-associated conditions in gastric and renal cancer: a retrospective comparison in 267 patients. *Eur J Cancer Prev*. 1994 Dec;3 Suppl 2:75-9. doi: 10.1097/00008469-199412002-00014. PMID: 7735052.
- Witherell HL, Hiatt RA, Replogle M, Parsonnet J. Helicobacter pylori infection and urinary excretion of 8-hydroxy-2-deoxyguanosine, an oxidative DNA adduct. *Cancer Epidemiol Biomarkers Prev*. 1998;7(2):91-96.
- Heidari M, Hadi A. Relationship between Serum Level of Vitamin D in patients with BPH compared to healthy people in age group over 45. *Pak. J. Med. Health Sci*. 2020;14(2):1376-80.
- Brüggemann, H., & Al Zeer, M. A. (2020). Bacterial signatures and their inflammatory potentials associated with prostate cancer. *Apmis*, 128(2), 80-91.
- Abdollahi A, Etemadian M, Shoar S, Nozarian Z. Is Helicobacter pylori Infection a Risk Factor for Prostatitis? A Case-Control Study in a Referring Tertiary Care Center. *Iran J Pathol*. 2016;11(4):323-327.
- Sarker, K. K., Kabir, M. J., uddin Bhuyian, A. M., Alam, M. S., Chowdhury, F. R., Ahad, M. A., ... & Rahman, M. M. (2017). H. pylori infection and gastric cancer in Bangladesh: a case-control study. *International journal of surgery. Oncology*, 2(10), e44.
- Herr, H. W. (1990). Outpatient flexible cystoscopy and fulguration of recurrent superficial bladder tumors. *The Journal of urology*, 144(6), 1365-1366.
- Hall, R. R. (1992). Transurethral resection for transitional cell carcinoma. *Prob Urol*, 6, 460-471.
- Hirschl, A. M., & Makristathis, A. (2007). Methods to detect Helicobacter pylori: from culture to molecular biology. *Helicobacter*, 12, 6-11.
- Ho, S. A., Hoyle, J. A., Lewis, F. A., Secker, A. D., Cross, D., Mapstone, N. P., Dixon, M. F., Wyatt, J. I., Tompkins, D. S., & Taylor, G. R. (1991). Direct polymerase chain reaction test for detection of Helicobacter pylori in humans and animals. *Journal of clinical microbiology*, 29(11), 2543-2549. https://doi.org/10.1128/JCM.29.11.2543-2549.1991.
- Dehkordi FS, Valizadeh Y, Birgani TA, Dehkordi KG. Prevalence study of Brucella melitensis and Brucella abortus in cow's milk using dot enzyme-linked immunosorbent assay and duplex polymerase chain reaction. *J Pure Appl Microbiol*. 2014;8(2):1065-9.

20. Abdolmaleki Z, Mashak Z, Dehkordi FS. Phenotypic and genotypic characterization of antibiotic resistance in the methicillin-resistant *Staphylococcus aureus* strains isolated from hospital cockroaches. *Antimicrobial Resistance & Infection Control*. 2019;8(1):1-4.
21. Dehkordi FS, Momtaz H, Doosti A. Application of Real-Time PCR for detection of *Aspergillus* species in aborted ruminant fetuses. *Bulgar J Vet Med*. 2012;15(1):30-6.
22. Ho SA, Hoyle JA, Lewis FA, Secker AD, Cross D, Mapstone NP, Dixon MF, Wyatt JI, Tompkins DS, Taylor GR. Direct polymerase chain reaction test for detection of *Helicobacter pylori* in humans and animals. *J Clin Microbiol* 1991; 29: 2543-2549.
23. Rahi A, Kazemeini H, Jafariaskari S, Seif A, Hosseini S, Dehkordi FS. Genotypic and phenotypic-based assessment of antibiotic resistance and profile of staphylococcal cassette chromosome *mec* in the methicillin-resistant *Staphylococcus aureus* recovered from raw milk. *Infection and drug resistance*. 2020;13:273.
24. Dehkordi, F.S., Saberian, S., Momtaz, H. Detection and segregation of *Brucella abortus* and *Brucella melitensis* in Aborted Bovine, Ovine, Caprine, Buffalo and Camelid Fetuses by application of conventional and real-time polymerase chain reaction. *The Thai J Vet Med*. 2012;42(1):13.
25. Dehkordi FS, Khamesipour F, Momeni M. *Brucella abortus* and *Brucella melitensis* in Iranian bovine and buffalo semen samples: The first clinical trial on seasonal, Senile and geographical distribution using culture, conventional and real-time polymerase chain reaction assays. *Kafkas Univ Vet Fak Dergisi*. 2014;20(6):821-.
26. Dehkordi FS. Prevalence study of *Coxiella burnetii* in aborted ovine and caprine fetuses by evaluation of nested and real-time PCR assays. *American J Anim Vet Sci*. 2011;6(4):180-6.
27. Dehkordi FS, Tirgir F, Valizadeh Y. Effects of Guajol® ointment synthesized from medicinal smoke condensate of jennet feces on burn wound healing on Wistar rat. *Vet Res Forum*. 2017; 8(3):215.
28. Dehkordi FS, Tavakoli-Far B, Jafariaskari S, Momtaz H, Esmaeilzadeh S, Ranjbar R, Rabiei M. Uropathogenic *Escherichia coli* in the high vaginal swab samples of fertile and infertile women: virulence factors, O-serogroups, and phenotyping and genotyping characterization of antibiotic resistance. *New Microb New Infect*. 2020;38:100824.
29. Dehkordi FS, Haghighi N, Momtaz H, Rafsanjani MS, Momeni M. Conventional vs real-time PCR for detection of bovine herpes virus type 1 in aborted bovine, buffalo and camel fetuses. *Bulgar J Vet Med*. 2013;16(2):102-12.
30. Dehkordi FS, Yazdani F, Mozafari J, Valizadeh Y. Virulence factors, serogroups and antimicrobial resistance properties of *Escherichia coli* strains in fermented dairy products. *BMC Res Notes*. 2014;7(1):1-8.
31. Dehkordi FS, Barati S, Momtaz H, Ahari SN, Dehkordi SN. Comparison of shedding, and antibiotic resistance properties of *Listeria monocytogenes* isolated from milk, feces, urine, and vaginal secretion of bovine, ovine, caprine, buffalo, and camel species in Iran. *Jundishapur J Microbiol*. 2013;6(3):284.
32. Ghorbani F, Gheisari E, Dehkordi FS. Genotyping of *vacA* alleles of *Helicobacter pylori* strains recovered from some Iranian food items. *Trop J Pharm Res*. 2016;15(8):1631-6.
33. Dehkordi FS, Gandomi H, Basti AA, Misaghi A, Rahimi E. Phenotypic and genotypic characterization of antibiotic resistance of methicillin-resistant *Staphylococcus aureus* isolated from hospital food. *Antimicrob Res Infect Control*. 2017;6(1):1-1.
34. Dehkordi FS. Prevalence study of Bovine viral diarrhoea virus by evaluation of antigen capture ELISA and RT-PCR assay in Bovine, Ovine, Caprine, Buffalo and Camel aborted fetuses in Iran. *AMB Express*. 2011;1(1):1-6.
35. Dehkordi FS, Parsaei P, Saberian S, Moshkelani S, Hajshafiei P, Hoseini SR, Babaei M, Ghorbani MN. Prevalence study of *Theileria annulata* by comparison of four diagnostic Techniques in south-west Iran. *Bulgar J Vet Med*. 2012;15(2): 123-130.
36. Dehkordi FS, Haghighi Borujeni MR, Rahimi E, Abdizadeh R. Detection of *Toxoplasma gondii* in raw caprine, ovine, buffalo, bovine, and camel milk using cell cultivation, cat bioassay, capture ELISA, and PCR methods in Iran. *Foodborne Pathog Dis*. 2013;10(2):120-5.
37. Safarpordehkordi F, Yahaghi E, Khodaverdi Darian E. Prevalence of antibiotic resistance in *Escherichia coli* isolated from poultry meat supply in Isfahan. *Iran J Med Microbiol*. 2014;8(2):41-7.
38. Safarpour Dehkordi F, Hosseini S, Rahimi E, Momeni M, Yahaghi E, Khodaverdi Darian E. Investigate the frequency of virulence genes *Vibrio parahaemolyticus* isolated from fish, lobsters and crabs caught from Persian Gulf. *Iran J Med Microbiol*. 2014;8(2):1-7.
39. Safarpour Dehkordi F, Momtaz H, Esmailzade S, Khayyat Khameneie M, Yahaghi E. Detection of virulence factors of Uropathogenic *Escherichia coli* isolates from infertile women high vaginal swabs. *Iran J Med Microbiol*. 2014;7(4):1-8.
40. Nejat S, Momtaz H, Yadegari M, Nejat S, Safarpour Dehkordi F, Khamesipour F. Seasonal, geographical, age and breed distributions of equine viral arteritis in Iran. *Kafkas Univ Vet Fak Derg*. 2015;21(1):111-6.
41. Ziebarth, D., Spiegelhalder, B., & Bartsch, H. (1997). N-nitrosation of medicinal drugs catalyzed by bacteria from human saliva and gastrointestinal tract, including *Helicobacter pylori*. *Carcinogenesis*, 18(2), 383–389. <https://doi.org/10.1093/carcin/18.2.383>
42. Michaud DS, Mysliwiec PA, Aldoori W, Willett WC, Giovannucci E. Peptic ulcer disease and the risk of bladder cancer in a prospective study of male health professionals. *Cancer Epidemiol Biomarkers Prev*. 2004;13(2):250-254. doi:10.1158/1055-9965.epi-03-0174
43. Siomek A, Rytarowska A, Szaflarska-Poplawska A, et al. *Helicobacter pylori* infection is associated with oxidatively damaged DNA in human leukocytes and decreased level of urinary 8-oxo-7,8-dihydroguanine. *Carcinogenesis*. 2006;27(3):405-408. doi:10.1093/carcin/bgi238
44. Matsumoto, T., & Iida, M. (1997). Regression of mucosa-associated lymphoid-tissue lymphoma of rectum after eradication of *Helicobacter*. *The Lancet*. 350(9071), 115-116.
45. Brown L. M. (2000). *Helicobacter pylori*: epidemiology and routes of transmission. *Epidemiologic reviews*, 22(2), 283–297. <https://doi.org/10.1093/oxfordjournals.epirev.a018040>
46. Karatas, O. F., Turkay, C., Bayrak, O., Cimentepe, E., & Unal, D. (2010). *Helicobacter pylori* seroprevalence in patients with chronic prostatitis: a pilot study. *Scandinavian journal of urology and nephrology*, 44(2), 91-94.
47. Vaira, D., Holton, J., Menegatti, M., Gatta, L., Ricci, C., Ali, A., Landi, F., Moretti, C., & Miglioli, M. (1998). Routes of transmission of *Helicobacter pylori* infection. *Italian journal of gastroenterology and hepatology*, 30 Suppl 3, S279-S285.
48. Li, L. J., Shen, Z. J., Lu, Y. L., & Fu, S. Z. (2001). The value of endotoxin concentrations in expressed prostatic secretions for the diagnosis and classification of chronic prostatitis. *BJU international*, 88(6), 536–539. <https://doi.org/10.1046/j.1464-410x.2001.02354.x>
49. Colovic, M., Hadzi-Djokic, J., Cemerikic, V., Colovic, R., Jankovic, G., & Dacic, M. (1999). Primary MALT lymphoma of the kidney. *Hematology and cell therapy*, 41(5), 229-232.
50. Kumar, S., Metz, D. C., Ellenberg, S., Kaplan, D. E., & Goldberg, D. S. (2020). Risk Factors and Incidence of Gastric Cancer After Detection of *Helicobacter pylori* Infection: A Large Cohort Study. *Gastroenterology*, 158(3), 527–536.e7. <https://doi.org/10.1053/j.gastro.2019.10.019>
51. Heidari, M., Irani, D., & Khezri, A. (2005). THE efficacy of intravesical bacillus calmette-guerin in the treatment of female patient with interstitial cystitis. A double-blind, prospective, placebo controlled trial. *J Urol*. 1998;159(5):1483-7.
52. Godolo, G., Munari, F., Fassan, M. and de Bernard, M., 2015. Evaluation of the efficacy of the *H. pylori* protein HP-NAP as a therapeutic tool for treatment of bladder cancer in an orthotopic murine model. *J Vis Exp*. 2015;(99):e52743. doi:10.3791/52743.

ARTICLE / INVESTIGACIÓN

Evaluation of secondary cancers, synchronous and metachronous with bladder cancer

Seyed Jalal Eshagh Hoseini¹, Mohammad Heidari², Hassan Fatemi Manesh³

DOI. 10.21931/RB/2022.07.01.6

¹ Department of Surgery, Qom University of Medical Sciences, Qom, Iran.² Department of Pediatric Nephrology, School of Medicine, Qom University of Medical Sciences, Qom, Iran.³ Student Research Committee, Qom University of Medical Sciences, Qom, Iran.

Corresponding author: jalaleshaghoseini@gmail.com.

Abstract: The number of bladder cancer survivors worldwide is increasing due to the advancement of diagnostic methods and bladder cancer treatment. Besides, bladder cancer is the sixth most common cancer in Iran. Nowadays, many secondary cancers have been proven with bladder cancer. This study focused on synchronous and metachronous cancers with bladder cancer. This study was performed retrospectively. A total of 276 patients with a definitive diagnosis of bladder cancer were included in the study. Tumors were diagnosed using ultrasound and cystoscopy. Out of 276 patients with bladder tumor, 240 underwent resection, 25 underwent radical cystectomy, and 31 underwent chemotherapy in addition to resection. The mean age of patients was 65±3.9 years. Among the patients, 184 were male (67%), and 92 were female (33%). Smoking was the most common known risk factor. There were 165 smokers, 135 of whom were male and 30 female. Sixty-nine patients had no known risk factor ($P < 0.05$). Gastric cancer was the most common secondary cancer with bladder cancer in all individuals (5.7%). Prostate cancer (20%) in men and cervical cancer (11.9%) in women was the most common secondary cancer simultaneous with bladder cancer. Given the importance of SPC as a cause of cancer death, early detection and screening of primary cancer survivors will increase patients' life expectancy and quality of life.

Key words: Secondary cancers, synchronous, metachronous, bladder cancer.

Introduction

Bladder cancer is the most common malignancy of the urinary system and the 11th most common cancer in people. The prevalence of this cancer is increasing in different countries of the world. This cancer's mortality rate and incidence vary in different countries and regions. This difference depends on epidemiological data, social, cultural, and economic characteristics¹⁻². Bladder cancer is the sixth most common cancer in Iran. The prevalence of this cancer in Iran's population is 33.2 patients per 100,000 people³. Statistics indicate that this cancer has an increasing prevalence in Iran⁴ and registers more than 70,000 new cases and 30,000 deaths annually⁵. In general, 7.04% of cancers in Iran are associated with bladder cancer⁶. Bladder cancer's leading risk factor is smoking, accounting for 50-65% of all cases. Occupational or environmental toxins also play a significant role in causing this disease. In general, the risk factors for bladder cancer can be classified into three subtypes: genetic and molecular abnormalities, chemical or environmental exposure, and chronic irritation.

The bladder is an empty organ that stores urine in the lower abdomen. The urothelial cells of the bladder's lining are exposed to mutagenic substances secreted by the kidneys. These substances cause metaplasia and dysplasia changes and eventually bladder cancer. Most bladder tumors are transitional. In studies, bladder tumors have been synchronous and metachronous with other tumors. 90% of bladder cancers are diagnosed at 55 and above, and the disease is four times more common in men than women⁷⁻¹⁰. In general, the treatment

approach in bladder cancer is determined after determining the type of cancerous tissue. Treatments include bladder tumor resection, radical cystectomy, and complementary therapies such as single-dose intravesical immunotherapy with bacillus Calmette-Guérin (BCG) or intravesical chemotherapy¹¹. This study aimed to evaluate secondary tumors synchronous and metachronous with bladder tumors that, if diagnosed and treated in time, the disease will have a better prognosis, and the person will achieve better recovery.

Materials and methods

Ethics

This study was performed in the Center of Shohada Ashayer Khorramabad and Kamkar-Arabnia Hospital in Qom from 2006 to 2019. Written consent was obtained from all participants in the study. The personal information of patients included in the study was kept secret.

Study population and inclusion and exclusion criteria

In this study, 276 patients were included in the study. The inclusion criteria were those patients with significant bladder tumors. All types of bladder tumors were considered. These patients then underwent bladder tumor resection surgery based on a specialist diagnosis or, if necessary, radical cystec-

Citation: Eshagh Hosaini S K, Heidari M, Fatemi Manesh H. Evaluation of secondary cancers, synchronous and metachronous with bladder cancer. *Revis Bionatura* 2022;7(1). 6. <http://dx.doi.org/10.21931/RB/2022.07.01.6>

Received: 10 June 2021 / **Accepted:** 26 August 2021 / **Published:** 15 February 2022

Publisher's Note: Bionatura stays neutral with regard to jurisdictional claims in published maps and institutional affiliations.

Copyright: © 2022 by the authors. Submitted for possible open access publication under the terms and conditions of the Creative Commons Attribution (CC BY) license (<https://creativecommons.org/licenses/by/4.0/>).



tomy or additional treatments were considered for them¹³. Suspected patients to bladder cancer, which were referred to the hospital for cystoscopy and had consented to participate in the study were included in this survey. Patients without bladder tumors and those who don't have access to a definitive diagnosis were excluded from the survey.

Tumors diagnosis

Tumors were diagnosed using ultrasound and cystoscopy¹². Ultrasound was carried out with GE Voluson 730 using a convex probe with 5.3 Hz for all patients. A single individual carried out all ultrasounds. Afterward, the patients underwent cystoscopy conducted by a urologist who was not aware of the patients' ultrasound results. Afterward, tissue samples were prepared and sent to a pathology laboratory for pathological examinations. Olympus flexible fiberoptic cystourethroscopy was used for cystoscopy diagnosis of bladder tumors¹².

Study procedure

This study was performed retrospectively. The patients' information in the study was evaluated at intervals of about one year and five years after the diagnosis of bladder tumor in reading files, telephone calls, self-reports, and door-to-door visits for underlying diseases and secondary cancers. In case of the patient's presence and declaration of secondary cancer, the inclusion criteria were pathology reports, biopsy, endoscopy, and cancer-appropriate imaging in their medical records in the hospital. The subjects' underlying disease information in the study was recorded as a reading of hospital information.

Statistical analysis

According to the chi-square test, all data were then analyzed using SPSS software (version 22). P-value <0.05 was considered a significant level¹⁴⁻¹⁸.

Results

Demographic characters

Out of 276 patients with bladder tumor, 240 underwent resection, 25 underwent radical cystectomy, and 31 underwent chemotherapy in addition to resection. The mean age of patients was 65±3.9 (69 years). The youngest was 24 years old, and the oldest was 105 years old. Among the patients, 184 were male

(67%), and 92 were female (33%). Men's ratio to women was 2, and men 61-80 years old had the highest prevalence (P <0.05). Smoking was the most common known risk factor. There were 165 smokers, 135 of whom were male and 30 female. Sixty-nine patients had no known risk factor (P <0.05).

Bladder tumors frequency

Table 1 shows the frequency of bladder tumors amongst included patients. Findings showed that Transitional cell cancer (TCC) was the most frequently detected tumor amongst studied samples (88.60%) (P <0.05). However, adenocarcinoma was the less frequently detected tumor.

Job frequency

Table 2 shows the job frequency of included patients. Teachers (26.44%), farmers (23.18%), and workers (17.75%) were the most frequently determined jobs amongst the study population.

Age distribution

Table 3 shows the age distribution of examined patients. The majority of patients (30.79%) had 61-80 years old. Frequency of 0-30 and 101< years old patients were 3.26% and 8.33%, respectively.

Frequency of underlying diseases

Table 4 shows the frequency of underlying diseases amongst the studied patients. The most commonly identified underlying diseases amongst the studied patients were skeletal (35.14%), diabetes (18.47%), blood pressure (14.85%), and digestive (14.49%). Only 1.81% of examined patients had thyroid disorders. Additionally, only 2.53% of patients had pulmonary disease.

Other cancer distribution

Table 5 shows the frequency of other cancer types amongst the studied patients. In clinical, self-report and confirmed pathology examination, synchronous tumors, five years and if alive ten years after bladder tumor, diverse cancers were obtained. The most frequently detected cancer types were prostate (13.40%), stomach (5.79%), colon (4.34%), and cervix (3.98%). 63.40% of patients had no other cancers 5 years after the bladder tumor. No testicular tumor was clinically observed in the urogenital tract. Laryngeal and pancreatic tumors were also not observed in this study.

Type of cancer	Distribution (%)
Transitional cell cancer (TCC)	244 (88.40)
Squamous cell carcinoma (SCC)	21 (7.60)
Adenocarcinoma	5 (1.81)
Mix*	6 (2.17)
Total	276

Table 1. Frequency of bladder tumors amongst included patients.

Occupation	Jobs (%)							
	Housewife	Driver	Mechanic	Health/ Treatment	worker	Farmer	Teacher	Total
No.	36	16	28	10	49	64	73	276
	(13.04)	(5.79)	(10.14)	(3.62)	(17.75)	(23.18)	(26.44)	

Table 2. Job frequency of included patients.

Age groups (Year)	0-30	31-40	41-60	61-80	81-100	101<
Distribution (%)	9 (3.26)	38 (13.76)	64 (23.18)	85 (30.79)	57 (20.65)	23 (8.33)

Table 3. Age distribution of studied patients.

Underlying diseases	Skeletal	Thyroid	Digestive	Pulmonary	Cardiac	Prostate	Blood pressure	Diabetes	Colon disease
Frequency	97 (35.14)	5 (1.81)	40 (14.49)	7 (2.53)	13 (4.71)	12 (4.34)	41 (14.85)	51 (18.47)	10 (3.62)

Table 4. Frequency of underlying diseases amongst the studied patients.

Cancer types	Adrenal	Kidney	Cervix	Prostate	Breast	Brain	Thyroid	Lung	Liver	Colon	Stomach	No cancer
Frequency (%)	2 (0.72)	5 (1.81)	11 (3.98)	37 (13.40)	3 (1.08)	3 (1.08)	4 (1.44)	6 (2.17)	2 (0.72)	12 (4.34)	16 (5.79)	175 (63.40)

Table 5. Distribution of other cancer types among studied patients five years after bladder tumor.

Discussion

Despite high advances in the medical sciences¹⁹⁻²⁴, some diseases remain health-threatening²⁵⁻³⁰. The bladder is a hollow organ lined with mucous epithelial cells that stores urine for several hours. Mutagenic substances such as phenethylamines and benzene compounds and synthetic substances, chronic infection and inflammation cause metaplasia, dysplasia and eventually cancer and invasion to the underlying muscle tissue. According to the latest GLOBOCAN data, bladder tumors have 3% prevalence among tumors and increase in developed and developing countries. In the United States, bladder tumors are the sixth most common, mostly 55 years old, and are 2 to 4 times more common in men than women. In tumors with lower stage, the 5-year lifespan is 77%, and in metastatic cases, it is 5%. Cigarette tobacco is the most potent risk factor. Occupational and environmental factors contribute to about 20% of cases. Only about 7% of bladder tumors are inherited. In many cases, no specific exposure is found⁷.

Kotake *et al.*³¹ found that 376 patients with bladder tumors were analyzed for clinical cases. In their study, 299 patients were male, and 77 were female. The mean age of the subjects was 65.7 years. The most common synchronous tumors with bladder cancer in men were first gastric cancer (27.4%) and then prostate (15.3%), and in women, first cervical cancer (27.9%) and then gastric cancer (16.2%). Of the 119 cases, 58 were synchronous tumors, and 61 were metachronous

tumors. Bladder tumors in 85% of cases coincided with other urological tumors. Also, the ratio of secondary cancers to total cancers was 5.2%, and the ratio of secondary cancers with bladder cancer to total cancers was 15.9%³¹. In another study, multiple tumors were associated with prostate cancer in 93 patients (15.2%), and the organ most associated with prostate cancer was gastric cancer, followed by bladder, clone, and lung cancer. The mean age of the first, second, and third cancers was 72, 74 and 75 years. In 37 cases of death (71.4%) due to prostate cancer, the first and second cancers were about 20 months and about 8 months for third cancer. The primary stage in primary prostate tumors was lower than in secondary tumors. Survival rates were also reported to be better in this group. For this reason, it is recommended to consider the possibility of secondary cancers in primary ones³².

In a study in Taiwan conducted by Wu *et al.*³³ from 1987 to 2002 on 2109 patients, 99 patients were diagnosed with multiple secondary cancers with gastric tumors (4.7%). Secondary cancer (77.8%) was diagnosed 5 years before and after gastric cancer. 34.3% of patients were diagnosed with the synchronous tumor within one year. 77 male patients, prostate cancer, was the most common (19.5%), followed by colon cancers (18.2%) and liver (14.3%). In 22 female patients, colon cancer (31.9%) first followed by breast and cervical cancers (22.7%) had the highest prevalence rate³³. In another study in



Hungary, 77,504 autopsy cases were examined, of which 385 (4.2%) had double multiple primary malignant tumors. There was no significant difference in gender. Thyroid tumors were more commonly associated with lung, breast, and gastrointestinal tumors³⁴. In another study, secondary cancer was seen in 16.8% of kidney cancers, 12.5% of bladder cancers, and 21.8% of prostate cancers. The cause of recurrent tumor connections can be explained somewhat by the high average age (72 years). Uropoetic cancer was associated with lung cancer (the role of tobacco), gastrointestinal tumors (genetic or dietary factors), prostate cancer, bladder cancer, and hematologic malignancies. In this study, no association was found between testicular cancer and other malignancies³⁵.

In the study of Özdamar *et al.*³⁶ on 147 patients with genitourinary tumors, 6 patients had another tumor, 2 of which were concomitant and 4 of which were asynchronous. Cancer patients are at higher risk of secondary cancer than the general population. Secondary cancer may be diagnosed in long-term follow-up of cancer patients, or etiological factors may cause pleiotropic effects, or it may be due to treatments for first cancer. In a study in France, from 1989 to 2004, 10047 patients with bladder cancer were evaluated for secondary cancer. This study showed that the risk of new cancer among cancer survivors is 60% higher than the general population. Male patients also had a higher risk of prostate, head, neck, and lung cancers³⁷. In another study by T Fukagai *et al.*³⁸ in Japan from October 1980 to December 1994, 392 patients were treated for malignant neoplasms. 42 patients (10.6%) had multiple neoplasms, their mean age was 72.2 years, and 83% were male. Malignant neoplasms of the bladder, prostate, and kidney were observed in 19 (35%), 19 (35%), and 10 cases (11%), respectively. The incidence of prostate cancer was more associated with genitourinary organs than other primary malignant neoplasms. Other organs which had malignant neoplasms along with the genitourinary tract organs were the stomach (39%), lungs (12%), esophagus (9%), and pancreas (9%). Only 16 patients (35%) simultaneously had multiple malignancies neoplasms.

In a study by Whi-An Kwon *et al.*³⁹ in South Korea from 1993 to 2013, 48,875 people were investigated with an early diagnosis of bladder cancer. Bladder cancer survivors were at increased risk for some secondary cancers, particularly prostate and kidney, squamous cell carcinoma of the lung, and the lung's adenocarcinoma. In the cohort study by Eric Adjei Boakye *et al.*⁴⁰, 2903241 cancer patients were identified, of which 259685 (8.9%) developed secondary cancer (7.6% female and 10.3% male). Patients with smoking-related cancers had a higher risk of developing SPC than patients with non-smoking-related cancers. Besides, considering the infection of 30-80% of different communities with *H. pylori* and proving its role in the development of various cancers, including gastric cancer and its concurrence with bladder cancer in most studies^{41,42}, it seems that the prevalence of this infection also plays a role in the development of multiple secondary cancers.

However, specific research should assess other aspects and epidemiological properties of bladder cancer among the population. The study was limited to the low number of samples and low frequencies of studied groups.

Conclusions

Due to the increasing trend of bladder cancer worldwide and the evidence of concurrence or subsequent secondary cancers, identifying the causative agents and related risk fac-

tors can improve the prognosis of the disease and increase the life expectancy and quality of life of patients with this cancer. Therefore, it is essential to continuously monitor the risk of secondary cancer among bladder cancer survivors. On the other hand, owing to the growing number of cancer survivors cases and the SPC importance as a cancer death reason, there is a need to upsurge SPC screening and prevention.

Bibliographic references

1. Rozanec, José J., Fernando P. Secin. Epidemiología, etiología, prevención del cáncer vesical. *Arch Esp Urol*.2020; 73(10), 872-878.
2. Mathur, P., Sathishkumar, K., Chaturvedi, M., Das, P., Sudarshan, K.L., Santhappan, S., Nallasamy, V., John, A., Narasimhan, S., Roselind, F.S. Icmr-Nodir-Ncrp Investigator Group. 2020. Cancer statistics, report from national cancer registry programme, India. *JCO Global Oncol*. 2020;6:1063-1075.
3. Farmanfarma, K.K., MahdaviFar, N., Salehiniya, H. Bladder Cancer in Iran: An Epidemiological Review. *Res Report Urol*. 2020;12:91-103.
4. Hassanipour, S., Fathalipour, M., Salehiniya, H. The incidence of prostate cancer in Iran: a systematic review and meta-analysis. *Prostate Int*. 2018;6(2):41-45.
5. Ahmadi, M., Ranjbaran, H., Amiri, M.M, Nozari, J., Mirzajani, M.R., Azadbakht, M., Hosseinimehr, S.J. Epidemiologic and socioeconomic status of bladder cancer in Mazandaran Province, northern Iran. *Asian Pac J Cancer Prev*. 2012;13(10):5053-6.
6. Shakhssalim, N., Hosseini, S.Y., Basiri, A., Eshrati, B., Mazaheri, M. Soleimanirahbar, A. Prominent bladder cancer risk factors in Iran. *Asian Pacific J Cancer Prev*. 2010;11(3): 601-6.
7. Silverman, D.T., Hartge, P., Morrison, A.S. Devesa, S.S. Epidemiology of bladder cancer. *Hematol/Oncol Clin North Am*. 1992;6(1):1-30.
8. Kaufman, D.S., Shipley, W.U. Feldman, A.S. Bladder cancer. *The Lancet*. 2009;374(9685):239-249.
9. Sanli, O., Dobruch, J., Knowles, M.A., Burger, M., Alemozaffar, M., Nielsen, M.E. Lotan, Y. Bladder cancer. *Nature Rev Dis Primer*. 2017;3(1):1-19.
10. Jégu, J., Colonna, M., Daubisse-Marliac, L., Trétarre, B., Ganry, O., Guizard, A.V., Bara, S., Troussard, X., Bouvier, V., Woronoff, A.S. Velten, M. The effect of patient characteristics on second primary cancer risk in France. *BMC Cancer*. 2014;14(1):1-14.
11. DeGeorge, K.C., Holt, H.R. Hodges, S.C. Bladder cancer: diagnosis and treatment. *Am Family Physic*. 2017;96(8):507-514.
12. Herr, H.W. Outpatient flexible cystoscopy and fulguration of recurrent superficial bladder tumors. *J Urol*. 1990;144(6):1365-1366.
13. DeGeorge, K.C., Holt, H.R. Hodges, S.C. Bladder cancer: diagnosis and treatment. *Am Family Physician*. 2017;96(8):507-514.
14. Dehkordi FS, Momtaz H, Doosti A. Application of Real-Time PCR for detection of *Aspergillus* species in aborted ruminant foetuses. *Bulg J Vet Med*. 2012;15(1):30-6.
15. Dehkordi, F.S., Saberian, S., Momtaz, H. Detection and segregation of *Brucella abortus* and *Brucella melitensis* in Aborted Bovine, Ovine, Caprine, Buffaloes and Camelid Fetuses by application of conventional and real-time polymerase chain reaction. *The Thai J Vet Med*. 2012;42(1):13.
16. Dehkordi FS. Prevalence study of *Coxiella burnetii* in aborted ovine and caprine fetuses by evaluation of nested and real-time PCR assays. *American J Anim Vet Sci*. 2011;6(4):180-6.
17. Dehkordi FS, Tirgir F, Valizadeh Y. Effects of Guajol® ointment synthesized from medicinal smoke condensate of jennet feces on burn wound healing on Wistar rat. *Vet Res Forum*. 2017; 8(3):215.
18. Dehkordi FS, Tavakoli-Far B, Jafariaskari S, Momtaz H, Esmailzadeh S, Ranjbar R, Rabiei M. Uropathogenic *Escherichia coli* in the high vaginal swab samples of fertile and infertile women: virulence factors, O-serogroups, and phenotyping and genotyping characterization of antibiotic resistance. *New Microb New Infect*. 2020;38:100824.

19. Dehkordi FS, Haghighi N, Momtaz H, Rafsanjani MS, Momeni M. Conventional vs real-time PCR for detection of bovine herpes virus type 1 in aborted bovine, buffalo and camel fetuses. *Bulgar J Vet Med.* 2013;16(2):102-12.
20. Dehkordi FS, Yazdani F, Mozafari J, Valizadeh Y. Virulence factors, serogroups and antimicrobial resistance properties of *Escherichia coli* strains in fermented dairy products. *BMC Res Notes.* 2014;7(1):1-8.
21. Dehkordi FS, Barati S, Momtaz H, Ahari SN, Dehkordi SN. Comparison of shedding, and antibiotic resistance properties of *Listeria monocytogenes* isolated from milk, feces, urine, and vaginal secretion of bovine, ovine, caprine, buffalo, and camel species in Iran. *Jundishapur J Microbiol.* 2013;6(3):284.
22. Ghorbani F, Gheisari E, Dehkordi FS. Genotyping of *vacA* alleles of *Helicobacter pylori* strains recovered from some Iranian food items. *Trop J Pharm Res.* 2016;15(8):1631-6.
23. Dehkordi FS, Gandomi H, Basti AA, Misaghi A, Rahimi E. Phenotypic and genotypic characterization of antibiotic resistance of methicillin-resistant *Staphylococcus aureus* isolated from hospital food. *Antimicrob Res Infect Control.* 2017;6(1):1-1.
24. Dehkordi FS. Prevalence study of Bovine viral diarrhea virus by evaluation of antigen capture ELISA and RT-PCR assay in Bovine, Ovine, Caprine, Buffalo and Camel aborted fetuses in Iran. *AMB Express.* 2011;1(1):1-6.
25. Dehkordi FS, Parsaei P, Saberian S, Moshkelani S, Hajshafiei P, Hoseini SR, Babaei M, Ghorbani MN. Prevalence study of *Theileria annulata* by comparison of four diagnostic Techniques in south-west Iran. *Bulgar J Vet Med.* 2012;15(2): 123-130.
26. Dehkordi FS, Haghighi Borujeni MR, Rahimi E, Abdizadeh R. Detection of *Toxoplasma gondii* in raw caprine, ovine, buffalo, bovine, and camel milk using cell cultivation, cat bioassay, capture ELISA, and PCR methods in Iran. *Foodborne Pathog Dis.* 2013;10(2):120-5.
27. Dehkordi FS, Khamesipour F, Momeni M. *Brucella abortus* and *Brucella melitensis* in Iranian bovine and buffalo semen samples: The first clinical trial on seasonal, Senile and geographical distribution using culture, conventional and real-time polymerase chain reaction assays. *Kafkas Univ Vet Fak Derg.* 2014;20(6):821-8.
28. Dehkordi FS, Valizadeh Y, Birgani TA, Dehkordi KG. Prevalence study of *Brucella melitensis* and *Brucella abortus* in cow's milk using dot enzyme linked immuno sorbent assay and duplex polymerase chain reaction. *J Pure Appl Microbiol.* 2014;8(2):1065-9.
29. Safarpordehkordi F, Yahaghi E, Khodaverdi Darian E. Prevalence of antibiotic resistance in *Escherichia coli* isolated from poultry meat supply in Isfahan. *Iran J Med Microbiol.* 2014;8(2):41-7.
30. Safarpour Dehkordi F, Hosseini S, Rahimi E, Momeni M, Yahaghi E, Khodaverdi Darian E. Investigate the frequency of virulence genes *Vibrio parahaemolyticus* isolated from fish, lobsters and crabs caught from Persian Gulf. *Iran J Med Microbiol.* 2014;8(2):1-7.
31. Kotake, T. Kiyohara, H. Multiple primary cancers (MPC) associated with bladder cancer: an analysis of the clinical and autopsy cases in Japan. *JPN J Clin Oncol.* 1985;15:201-210.
32. Nakata, S., Takahashi, H., Takezawa, Y., Kobayashi, M., Suzuki, T., Kawashima, K. *Hinyokika kyo.* *Acta Urol JPN.* 200;46(6):385-391.
33. Wu, C.W., Lo, S.S., Chen, J.H., Hsieh, M.C., Li, A.F. Lui, W.Y. Multiple primary cancers in patients with gastric cancer. *Hepato-Gastroenterol.* 2006;53(69):463-467.
34. Tiszlavicz, L., Varga, Z. *Pajzsmirigyrákhoz társuló malignus tumorok autopsziás anyagban [Malignant tumors associated with thyroid cancer in an autopsy material]. Orvosi Hetilap.* 1991;132(11):575-578.
35. Laszlo, T. Istvan, S. *Urológiai multiplex tumorok autopsias anyagban. Orvosi Hetilap.* 1993;134(11):577-577.
36. Özdamar, A.S., Gültekin, E.Y. Gökalp, A. Multiple primary tumours of the urogenital system: our cases and a review of the literature. *Int Urol Nephrol.* 1997;29(5):511-515.
37. Muller, J., Grosclaude, P., Lapôtre Ledoux, B., Woronoff, A.S., Guizard, A.V., Bara, S., Colonna, M., Troussard, X., Bouvier, V., Trétarre, B. Velten, M. Trends in the risk of second primary cancer among bladder cancer survivors: a population based cohort of 10 047 patients. *BJU Int.* 2016;118(1):53-59.
38. Fukagai, T., Ishihara, M., Funabashi, K., Naitoh, Y., Maruyama, K. *Hinyokika kyo.* *Acta Urol Japonica.* 1996;42(3), 181-185.
39. Kwon, W.A., Joung, J.Y., Lim, J., Oh, C.M., Jung, K.W., Kim, S.H., Seo, H.K., Park, W.S., Chung, J., Lee, K.H. Won, Y.J. of second primary Cancer among bladder Cancer patients: a population-based cohort study in Korea. *BMC Cancer.* 2018;18(1):1-9.
40. Boakye, E.A., Wang, M., Sharma, A., Jenkins, W.D., Osazuwa-Peters, N., Chen, B., Lee, M. Schootman, M. Risk of second primary cancers in individuals diagnosed with index smoking-and non-smoking-related cancers. *J Cancer Res Clin Oncol.* 2020;146(7):1765-1779.
41. Al-Marhoon, M.S., Ouhtit, A., Al-Abri, A.O., Venkiteswaran, K.P., Al-Busaidi, Q., Mathew, J., Al-Haddabi, I., Shareef, O., Aquil, S., Rahman, K. Al-Hashmi, I. Molecular evidence of *Helicobacter pylori* infection in prostate tumors. *Current Urol.* 2014;8(3): 138-143.
42. Park, J.Y., Forman, D., Waskito, L.A., Yamaoka, Y., Crabtree, J.E. Epidemiology of *Helicobacter pylori* and CagA-positive infections and global variations in gastric cancer. *Toxins.* 2018;10(4):163.

ARTICLE / INVESTIGACIÓN

Effect of iodine-therapy on hyperthyroidism patients without pre-administration of anti-thyroid therapeutic options

Homiera Rashidi¹, Bahman Ghaderian², Alireza Sedaghat², Mahmoud Latifi³, Zohre Naimi^{2*}

DOI. 10.21931/RB/2022.07.01.7

¹ Associate Professor, Diabetes Research Center, Health Research Institute, Ahvaz Jundishapur University of Medical Sciences, Ahvaz, Iran.² Assistant Professor, Diabetes Research Center, Health Research Institute, Ahvaz Jundishapur University of Medical Sciences, Ahvaz, Iran.³ Department of Statistics and Epidemiology, Faculty of Public Health, Diabetes Research Center, Ahvaz Jundishapur University of Medical Sciences, Ahvaz, Iran.
Corresponding author: naimiz@gmail.com.

Abstract: Anti-thyroid treatment and radioiodine are mainly used treatments for patients with thyrotoxicosis. The effect of anti-thyroid drugs (ATDs) on radioactive iodine's therapeutic effectiveness in hyperthyroidism remains controversial. This study aimed to determine the treatment effectiveness and complications in patients with thyrotoxicosis receiving radioiodine treatment with or without adjunctive anti-thyroid drugs in a tertiary endocrinology center in Ahvaz, Iran. A total of 165 patients with thyrotoxicosis (50 males and 115 females) were recruited in this retrospective clinical study. These patients were divided into two groups: one group underwent natural iodine therapy without being treated with anti-thyroid drugs (N= 86), and the other group was first treated with anti-thyroid drugs and then treated with iodine (N= 79). Then, the frequency of euthyroidism, thyroid storm, thyroiditis, hypothyroidism and the time to reach euthyroidism is evaluated. The results showed no difference between the two groups when reaching the euthyroid and the mean numerical mean TSH at the time of hypothyroidism. However, the average dose of iodine received in the concomitant drug group was lower. No thyroid storm was observed in the two groups regarding complications after treatment. Also, the prevalence of hypothyroidism and thyroiditis were not significantly different between the two groups. Iodine therapy with and without the use of anti-thyroid drugs (ATD) in low-risk patients with thyrotoxicosis has no difference in treatment outcomes, response to treatment, and subsequent complications.

Key words: Anti-thyroid drugs, radioactive iodine (¹³¹I), Iodine therapy, thyrotoxicosis.

Introduction

Thyrotoxicosis is an excess thyroid hormone condition, a common disease, especially in women. The most common cause of thyrotoxicosis is Graves' disease. Other causes include toxic nodular hyperthyroidism and thyroiditis^{1,2}. Common signs of disease are fatigue, weight loss, tremor, anxiety, palpitations, disturbed sleep, sweating, heat intolerance, and polydipsia^{3,4}. The therapeutic possibilities for thyrotoxicosis treatment for these conditions, anti-thyroid drugs (ATD), thyroidectomy, and radioactive iodine ¹³¹I (RAI).⁵⁻⁷ early and timely treatment of hyperthyroidism also may prevent the progress of the disease⁸.

Each of the treatment modalities has particular efficacy limitations and potential adverse effects^{9,10}. The main clinical downside of ATD therapy is the high rate of hyperthyroidism recurrence when therapy is stopped¹¹⁻¹⁶. However, the ease of ATD treatment and the fact that the thyroid is not irreversibly compromised has rendered long-term, low-dose ATD treatment a rational choice for disease control¹¹. Radioactive iodine therapy is an essential definitive treatment of hyperthyroidism, used for more than six decades as first-line or second-line therapy, and ¹³¹I therapy is cost-effective, safe, and reliable^{5,12}. This data would be a valuable resource for physicians to involve patients in the shared decision-making process¹³. The effect of anti-thyroid drugs (ATDs) on radioactive iodine's therapeutic effectiveness in hyperthyroidism remains controversial¹⁴. So far, no study has been conducted in our country and this epi-

demiological region regarding the outcomes, results, and incidence of each of the possible complications in iodine therapy alone with and without anti-thyroid drug treatment of patients with thyrotoxicosis. This study aimed to assess the treatment effectiveness in patients with thyrotoxicosis receiving radioiodine treatment with or without adjunctive anti-thyroid drugs in a tertiary endocrinology center in Ahvaz, Iran.

Materials and methods

Ethics

The personal information of included individuals was kept secret. The ethical council approved the survey.

Inclusion criteria

According to our inclusion criteria, a total of 165 patients with thyrotoxicosis (50 males and 115 females) were recruited in the retrospective clinical study. Data on consecutive patients between 2015 to 2020 at the Endocrinology Clinics (Ahvaz, Iran) were retrospectively collected and reviewed. The diagnosis of thyrotoxicosis was performed according to the basis of elevated total T4 (TT4) and/or total T3 (TT3) values and TSH suppressed to < 0.01 mIU/L¹⁵.

Citation: Rashidi H, Ghaderian B, Sedaghat A, Latifi M, Naimi Z. Effect of iodine-therapy on hyperthyroidism patients without pre-administration of anti-thyroid therapeutic options. *Revis Bionatura* 2022;7(1). 7. <http://dx.doi.org/10.21931/RB/2022.07.01.7>

Received: 25 June 2021 / **Accepted:** 10 August 2021 / **Published:** 15 February 2022

Publisher's Note: Bionatura stays neutral with regard to jurisdictional claims in published maps and institutional affiliations.

Copyright: © 2022 by the authors. Submitted for possible open access publication under the terms and conditions of the Creative Commons Attribution (CC BY) license (<https://creativecommons.org/licenses/by/4.0/>).



Groups

All cases were divided into two groups: one group receiving the drug before iodine was considered (n=86), and the other group receiving only the iodine was defined (n=79). Inclusion Criteria were age between 18 to 65 years old and absence of comorbid diseases. Individuals over 65 years, patients with heart failure (Ejection fraction < 40%), pregnant women were excluded from this study. At the diagnosis and approximately 2 months intervals, serum- triiodothyronine (T3), thyroxine (T4), and TSH levels were analyzed.

These patients were divided into two groups: one group underwent natural iodine therapy without being treated with anti-thyroid drugs (N= 86). The other group was first treated with anti-thyroid drugs and then with iodine (N= 79). Then, the frequency of thyroid storm, thyroiditis and hypothyroidism, euthyroidism and the time to reach euthyroidism was examined using their evaluation. Euthyroidism was defined as T3, T4 serum levels within the normal range.

Questionnaire

A questionnaire was designed to retrospectively obtain all demographic, clinical, laboratory, and radiological results from the patients' medical records. All the experiments were performed according to the Ethical Committee's guidelines at the Ahvaz Jundishapur University of Medical Sciences, and all participants provided written informed consent.

Statistical analysis

Statistical analysis was performed using SPSS software (SPSS Inc, version 23, Chicago, IL, USA). Kolmogorov-Smirnov, and Shapiro-Wilk tests were used to test for the data normality. Central and descriptive statistics were reported for quantitative data. A Chi-square test was used to compare the ratio of complications in qualitative variables. P-value <0.05 was considered statistically significant¹⁶⁻¹⁹.

Results

Demographic characteristics

The median age in the iodine alone group and iodine with the drug group was 47.22±15.7 and 44.07±12.38. There was no statistically significant difference between the median ages of the two groups (P=0.15). The detail of the demographic characteristics of the study population is indicated in Table 1.

Comparison of the frequency of complications

Regarding the occurrence of complications after treatment, no thyroid storm was observed between the two groups, and the prevalence of hypothyroidism and thyroiditis were not significantly different between the two groups (Table 2).

The results showed no difference between the two groups when reaching the euthyroidism and the mean TSH at the time of hypothyroidism (P=0.11 and P=0.14, respectively).

Comparison time to euthyroidism & iodine dose

However, there was a significant difference in Iodine dose between the two groups (P=0.005), and the average dose of iodine received in the iodine with drug therapy group was lower than in the iodine alone group. The level of T3 at the beginning of the study was not significantly different between the two groups. However, the level of T4, which was significantly higher in the iodine alone group at the beginning of the study, showed a more significant decrease at the end of the treatment period than the iodine with drug therapy groups (Table 3).

The regression equation was used to find the correlation between levothyroxine administration and several variables.

Results of the regression equation

There was no significant correlation between that time and first T3, T4 variables, Iodine dose, thyrotoxicosis syndro-

Variable		Iodine alone group (N=86) (%)	Iodine with drug therapy (N=79) (%)
Age	≤30	13 (15.1)	12 (15.2)
	40-31	18 (20.9)	25 (31.6)
	50-41	25 (29.1)	15 (19)
	60-51	13 (15.1)	22 (27.8)
	>60	17 (19.8)	5 (6.3)
Sex	Male	21 (24.4)	29 (36.7)
	Female	65 (76.6)	50 (63.3)
Diabetes	No	82 (95.3)	76 (96.2)
	Yes	4 (4.7)	3 (3.8)
Hypertension	No	85 (98.8)	78 (98.7)
	Yes	1 (1.2)	1 (1.3)
Heart disease	No	82 (95.3)	78 (98.7)
	Yes	4 (4.7)	1 (1.3)
The clinical syndrome of thyrotoxicosis	Graves	32 (37.2)	46 (58.2)
	Toxic adenoma	2 (2.3)	3 (3.8)
	Hashitoxicosis	2 (2.3)	0 (0)
	multinodular goiter	50 (58.1)	30 (38)

Table 1. Demographic Characteristics of the study population.

Variable		Iodine alone group (%)	Iodine with drug therapy (%)	P-value
Hypothyroidism	No	31 (36.0)	31 (39.2)	0.67
	Yes	55 (64.0)	48 (60.8)	
Thyroiditis	No	86 (100.0)	78 (98.7)	0.47
	Yes	0 (0.0)	1 (1.3)	

Table 2. Comparison of the frequency of complications in the two groups.

Variable	Iodine therapy group (mean±SD)	Iodine with drug therapy group (mean±SD)	P-value
Euthyroidism Day	68.72±60.58	60.58±30.31	0.11
Iodine dose	23.8±8.7	19.86±9.21	0.005*

Table 3. Comparison time to euthyroidism & iodine dose between the two groups.

Variable	B	SD (Error)	P-value
T3 (first)	0.17	2.34	0.94
T4 (first)	-1.05	1.17	0.374
Iodine cumulative dose	0.004	1.21	0.99
Times of iodine therapy	-67.22	76.02	0.38
Euthyroidism day	0.76	0.32	0.024*
Type of thyrotoxicosis Syndrome	12.23	8.64	0.16
Age	-1.33	0.69	0.062
Sex	-22.46	22.73	0.32

Table 4. The results of the regression equation.

me, age, and sex ($P>0.05$). At the same time, Euthyroidism time showed a statistically significant correlation with the Levoday variable (levothyroxine onset time) ($P=0.024$) (Table 4).

Discussion

Several developments have been occurred in medical sciences²⁰⁻²⁵. However, there were so many defects regarding knowledge about diseases and their treatments²⁶⁻³⁴. Iodine therapy is the definitive treatment modality of hyperthyroidism³⁵; however, several concerns exist regarding this approach's efficacy³⁶. McDermott et al. believed that the possibility of thyroid dysfunction increases upon iodine therapy³⁷. This mainly occurs in high-risk patients such as the elderly, individuals with underlying heart diseases, and patients with enlarged thyroids. Therefore, these patients should undergo an anti-thyroid regimen before iodine therapy. However, our results have shown that iodine therapy alone could be safe with minimum side effects while generating similar treatment outcomes³⁷. In our study, no difference was observed in adverse effects such as thyroid storm, hypothyroidism and thyroiditis between the two study groups. The time point of achieving euthyroidism served as an independent and strong predictive factor for hypothyroidism development. This means that other variables, including age, gender, type of clinical syndrome, the initial number of T3 and T4, were not considered for predicting the development of hypothyroidism and initiation of Levothyroxine. Some studies have shown that ATDs can have a protective effect, which leads to a decrease in the thyroid gland's effective half-life and radioactive iodine uptake^{38,39}. A meta-analysis study investigated the effect of utilizing anti-thyroid drugs before iodine therapy and compared it with iodine therapy alone in grave patients.

Results have shown that administrating anti-thyroid drugs before iodine therapy increases treatment failure yet decreases subsequent hypothyroidism⁴⁰. Our results were not similar to those of the previous survey since we did not observe a difference in treatment responses, euthyroidism, and even subsequent hypothyroidism between them. The discrepancy could be explained as follow: First, in the mentioned study, the administered drug was PTU, while in our study, different types of drugs, and mostly methimazole, were utilized. In addition, Grave's disease was the only thyrotoxicosis syndrome evaluated in the mentioned study, but in our study, several thyrotoxicosis syndromes were assessed. Therefore, a separate study on Grave's patients treated with methimazole is suggested to evaluate the inconsistency of these results and investigate the effect of a special type of drug on the particular type of clinical syndrome.

Ding et al.⁴¹ conducted a study to evaluate long-term outcomes and immunity of iodine therapy without drug therapy. In their study, of 408 patients, 283 individuals were treated with iodine therapy, 15 of whom achieved complete remission and 47 partial remissions. Besides, no signs of disease relapse and recurrence were observed in patients treated with iodine alone. This study concluded that utilizing iodine therapy alone is safe and effective in treating patients with severe hyperthyroidism who are resistant to anti-thyroid drugs⁴¹. Similarly, our results have shown that administrating iodine therapy alone is safe in patients with thyrotoxicosis and, in terms of adverse effects, is similar to the combination therapy of drug and iodine therapy. In Ding et al.'s study, the follow-up period was longer, and the sample size was larger. Moreover, patients with heart disease and arrhythmia, hepatic dysfunctions, and over 65. Nevertheless, we excluded patients over 65 years and those with underlying heart disorders since they were considered a

high-risk group to treat using the iodine therapy without concomitant ATDs therapy.

There are several contradictions regarding the effect of anti-thyroid drugs and their impact on iodine therapy. Studies have shown that utilizing PTU (and not methimazole) before iodine therapy delays the therapeutic response. PTU is suggested to enhance thyroid tissue resistance against radioactive iodine^{5,42-44}. In a meta-analysis study performed on 1269 patients, drug therapy's risk of reducing the response to iodine therapy was approximately 1.28. After iodine therapy, the effect of hypothyroidism was not related to the type of drug used⁴⁰. The results of this meta-analysis were different from our study. Anti-thyroid drug treatment before iodine therapy did not affect the treatment results and subsequent complications in the current study.

Our study's limitation was the inclusion of low-risk patients in the study. In other words, it is unclear whether iodine therapy alone before ATD will have the same results in high-risk patients, such as the elderly, diabetic patients, and underlying heart disease. One of the study's strengths was evaluating different types of thyrotoxicosis syndromes, while most studies have been done on Graves' disease. The current study investigated the relations between T4, frequency of iodine therapy, iodine dose, time of euthyroidism, and hypothyroidism, which was for the first time. Our findings recommend comparing iodine therapy alone or ATD treatment before iodine therapy, with different drugs separately and in different thyrotoxicosis syndromes separately with a more significant number of subjects.

Conclusions

Iodine therapy with and without the anti-thyroid drug treatment in low-risk patients with thyrotoxicosis has no difference in therapy outcomes, response to treatment, and subsequent complications. The hypothyroidism time depends on the time of euthyroidism after receiving iodine in two groups. More quality randomized controlled trials are necessary to evaluate the quality of life, cost of the two treatments and more attention to confounding factors such as goiter size and thyroid uptake is recommended.

Acknowledgments

The authors would like to thank the staff of the Diabetes Research Center, Health Research Institute, Ahvaz Jundishapur University of Medical Sciences, Ahvaz, Iran.

Bibliographic references

1. Franklyn JA, Boelaert K. Thyrotoxicosis. *The Lancet*. 2012;379(9821):1155-66.
2. Burch HB, Cooper DS. Management of Graves disease: a review. *Jama*. 2015;314(23):2544-54.
3. Goichot B, Caron P, Landron F, Bouée S. Clinical presentation of hyperthyroidism in a large representative sample of outpatients in France: relationships with age, aetiology and hormonal parameters. *Clinical endocrinology*. 2016;84(3):445-51.
4. Pearce EN. Diagnosis and management of thyrotoxicosis. *Bmj*. 2006;332(7554):1369.
5. Iagaru A, McDougall IR. Treatment of thyrotoxicosis. *Journal of nuclear medicine*. 2007;48(3):379-89.
6. Wartofsky L, Glinoeer D, Solomon B, Nagataki S, Lagasse R, Nagayama Y, et al. Differences and similarities in the diagnosis and treatment of Graves' disease in Europe, Japan, and the United States. *Thyroid*. 1991;1(2):129-35.
7. Brito JP, Schilz S, Singh Ospina N, Rodriguez-Gutierrez R, Maraka S, Sangaralingham LR, et al. Anti-thyroid drugs—the most common treatment for Graves' disease in the United States: a nationwide population-based study. *Thyroid*. 2016;26(8):1144-5.
8. Ross DS. Radioiodine therapy for hyperthyroidism. *New England Journal of Medicine*. 2011;364(6):542-50.
9. Smith TJ, Hegedüs L. Graves' disease. *New England Journal of Medicine*. 2016;375(16):1552-65.
10. Eliasson M. Long-term prognosis after medical treatment of Graves' disease in a northern Swedish population 2000–2010. *Endocrinology*. 2014;170:419-27.
11. Orgiazzi J. Should protracted treatment with anti-thyroid drug (ATD) be considered as a routine strategy in patients with graves' disease who had a relapse after a first course of ATD? *Clinical Thyroidology*. 2015;27(11):302-5.
12. Silberstein EB, Alavi A, Balon HR, Clarke SE, Divgi C, Gelfand MJ, et al. The SNMMI practice guideline for therapy of thyroid disease with 131I 3.0. *Journal of Nuclear Medicine*. 2012;53(10):1633-51.
13. Azizi F, Malboosbaf R. Long-term anti-thyroid drug treatment: a systematic review and meta-analysis. *Thyroid*. 2017;27(10):1223-31.
14. Kartamihardja AHS, Massora S. The Influence of Antithyroid Drug Discontinuation to the Therapeutic Efficacy of 131I in hyperthyroidism. *World journal of nuclear medicine*. 2016;15(2):81.
15. Koulouri O, Moran C, Halsall D, Chatterjee K, Gurnell M. Pitfalls in the measurement and interpretation of thyroid function tests. Best practice & research Clinical endocrinology & metabolism. 2013;27(6):745-62.
16. Ghorbani F, Gheisari E, Dehkordi FS. Genotyping of vacA alleles of *Helicobacter pylori* strains recovered from some Iranian food items. *Trop J Pharm Res*. 2016;15(8):1631-6.
17. Nejat S, Momtaz H, Yadegari M, Nejat S, Safarpour Dehkordi F, Khamesipour F. Seasonal, geographical, age and breed distributions of equine viral arteritis in Iran. *Kafkas Univ Vet Fak Derg*. 2015;21(1):111-6.
18. Dehkordi FS, Momtaz H, Doosti A. Application of Real-Time PCR for detection of *Aspergillus* species in aborted ruminant foetuses. *Bulg J Vet Med*. 2012;15(1):30-6.
19. Dehkordi, F.S., Saberian, S., Momtaz, H. Detection and segregation of *Brucella abortus* and *Brucella melitensis* in Aborted Bovine, Ovine, Caprine, Buffaloes and Camelid Fetuses by application of conventional and real-time polymerase chain reaction. *The Thai J Vet Med*. 2012;42(1):13.
20. Dehkordi FS. Prevalence study of *Coxiella burnetii* in aborted ovine and caprine fetuses by evaluation of nested and real-time PCR assays. *American J Anim Vet Sci*. 2011;6(4):180-6.
21. Dehkordi FS, Tirgir F, Valizadeh Y. Effects of Guajol® ointment synthesized from medicinal smoke condensate of jennet feces on burn wound healing on Wistar rat. *Vet Res Forum*. 2017; 8(3):215.
22. Dehkordi FS, Tavakoli-Far B, Jafariaskari S, Momtaz H, Esmailzadeh S, Ranjbar R, Rabiei M. Uropathogenic *Escherichia coli* in the high vaginal swab samples of fertile and infertile women: virulence factors, O-serogroups, and phenotyping and genotyping characterization of antibiotic resistance. *New Microb New Infect*. 2020;38:100824.
23. Safarpourdehkordi F, Yahaghi E, Khodaverdi Darian E. Prevalence of antibiotic resistance in *Escherichia coli* isolated from poultry meat supply in Isfahan. *Iran J Med Microbiol*. 2014;8(2):41-7.
24. Dehkordi FS, Haghghi N, Momtaz H, Rafsanjani MS, Momeni M. Conventional vs real-time PCR for detection of bovine herpes virus type 1 in aborted bovine, buffalo and camel fetuses. *Bulg J Vet Med*. 2013;16(2):102-12.
25. Dehkordi FS, Yazdani F, Mozafari J, Valizadeh Y. Virulence factors, serogroups and antimicrobial resistance properties of *Escherichia coli* strains in fermented dairy products. *BMC Res Notes*. 2014;7(1):1-8.
26. Dehkordi FS, Barati S, Momtaz H, Ahari SN, Dehkordi SN. Comparison of shedding, and antibiotic resistance properties of *Listeria monocytogenes* isolated from milk, feces, urine, and vaginal secretion of bovine, ovine, caprine, buffalo, and camel species in Iran. *Jundishapur J Microbiol*. 2013;6(3):284.

27. Safarpour Dehkourdi F, Momtaz H, Esmailzade S, Khayyat Khameneie M, Yahaghi E. Detection of virulence factors of Uropathogenic *Escherichia coli* isolates from infertile women high vaginal swabs. *Iran J Med Microbiol.* 2014;7(4):1-8.
28. Dehkordi FS, Gandomi H, Basti AA, Misaghi A, Rahimi E. Phenotypic and genotypic characterization of antibiotic resistance of methicillin-resistant *Staphylococcus aureus* isolated from hospital food. *Antimicrob Res Infect Control.* 2017;6(1):1-1.
29. Dehkordi FS. Prevalence study of Bovine viral diarrhoea virus by evaluation of antigen capture ELISA and RT-PCR assay in Bovine, Ovine, Caprine, Buffalo and Camel aborted fetuses in Iran. *AMB Express.* 2011;1(1):1-6.
30. Dehkordi FS, Parsaei P, Saberian S, Moshkelani S, Hajshafiei P, Hoseini SR, Babaei M, Ghorbani MN. Prevalence study of *Theileria annulata* by comparison of four diagnostic Techniques in south-west Iran. *Bulgar J Vet Med.* 2012;15(2): 123-130.
31. Dehkordi FS, Haghighi Borujeni MR, Rahimi E, Abdizadeh R. Detection of *Toxoplasma gondii* in raw caprine, ovine, buffalo, bovine, and camel milk using cell cultivation, cat bioassay, capture ELISA, and PCR methods in Iran. *Foodborne Pathog Dis.* 2013;10(2):120-5.
32. Dehkordi FS, Khamesipour F, Momeni M. *Brucella abortus* and *Brucella melitensis* in Iranian bovine and buffalo semen samples: The first clinical trial on seasonal, Senile and geographical distribution using culture, conventional and real-time polymerase chain reaction assays. *Kafkas Univ Vet Fak Derg.* 2014;20(6):821-8.
33. Dehkordi FS, Valizadeh Y, Birgani TA, Dehkordi KG. Prevalence study of *Brucella melitensis* and *Brucella abortus* in cow's milk using dot enzyme linked immuno sorbent assay and duplex polymerase chain reaction. *J Pure Appl Microbiol.* 2014;8(2):1065-9.
34. Safarpour Dehkordi F, Hosseini S, Rahimi E, Momeni M, Yahaghi E, Khodaverdi Darian E. Investigate the frequency of virulence genes *Vibrio parahaemolyticus* isolated from fish, lobsters and crabs caught from Persian Gulf. *Iran J Med Microbiol.* 2014;8(2):1-7.
35. Ma C. The long term effects of radioiodine therapy versus anti-thyroid medications on Graves' disease. *Journal of Nuclear Medicine.* 2013;54(supplement 2):40-.
36. Braga M, Walpert N, Burch HB, Solomon BL, Cooper DS. The effect of methimazole on cure rates after radioiodine treatment for Graves' hyperthyroidism: a randomized clinical trial. *Thyroid.* 2002;12(2):135-9.
37. McDermott MT, Kidd GS, Dodson Jr LE, Hofeldt FD. Radioiodine-induced thyroid storm: case report and literature review. *The American journal of medicine.* 1983;75(2):353-9.
38. Moka D, Dietlein M, Schicha H. Radioiodine therapy and thyrostatic drugs and iodine. *European journal of nuclear medicine and molecular imaging.* 2002;29(2):S486-S91.
39. Mumtaz M, Lin LS, Hui KC, Khir ASM. Radioiodine I-131 for the therapy of Graves' disease. *The Malaysian journal of medical sciences: MJMS.* 2009;16(1):25.
40. Walter MA, Briel M, Christ-Crain M, Bonnema SJ, Connell J, Cooper DS, et al. Effects of anti-thyroid drugs on radioiodine treatment: systematic review and meta-analysis of randomised controlled trials. *Bmj.* 2007;334(7592):514.
41. Ding Y, Xing J, Fang Y, Wang Y, Zhang Y, Long Y. I-131 therapy for 345 patients with refractory severe hyperthyroidism: Without anti-thyroid drug pretreatment. *Experimental Biology and Medicine.* 2016;241(3):290-5.
42. Medghalchi, A., Akbari, M., Alizadeh, Y., Moghadam, R.S. The epidemiological characteristics of patients with thyroid eye disease in a referral center in northern Iran. *Journal of Current Ophthalmology,* 30(4), pp. 353-358
43. Imseis RE, Vanmiddlesworth L, Massie JD, Bush AJ, Vanmiddlesworth N. Pretreatment with propylthiouracil but not methimazole reduces the therapeutic efficacy of iodine-131 in hyperthyroidism. *The Journal of Clinical Endocrinology & Metabolism.* 1998;83(2):685-7.
44. Weaver JU, Razvi S. Dose of anti-thyroid drugs can effect remission in Grave's disease. *Endocrine journal.* 2005;52(1):159-.

ARTICLE / INVESTIGACIÓN

Detection of biofilm formation of (*Serratia* and *E.coli*) and determination of the inhibitory effect of *Quercus* plant extract against these infectious pathogens

Fatima Amer Abd Algabar¹, Batool Abdalameer Baqer²

DOI. 10.21931/RB/2022.07.01.8

¹ Lecturer, Middle Technical University, Baghdad, Iraq.² Lecturer, Al Mustansiriyah University, Baghdad, Iraq.

Corresponding author: fatimaamer@mtu.edu.iq

Abstract: Biofilm is a complex microbial regional, especially resisting antimicrobials Quorum sensing function ate flow into an essential role in the composition concerning completely advanced superior biofilms on numerous microorganism, Biofilms change autonomous cells into particular cell groups. They are obtainable about comprehensions keen on biofilm materialization determined through the best-characterized strain, *Escherichia coli*. The hastened biofilm obstacle of accord containing regular remedying decorates the requirement between significance with toughening modern rule approaches. By resources of the use of Congo process then PCR method since detection around biofilms arrangement, By way of the sunscreens of Quorum detecting were noticed over molecular finding using the PCR of the gene accountable for the structure of Biofilm in *Serratia* bacteria. The study showed that during the induction period, after 48 hours, the effects of bacterial inhabitation, the methanolic extract was more effective against (*Serratia*, *E. coli*) regarding superb consciousness (10, 20, 30 mg/l).

Key words: Biofilms 1, PCR 2, Plant Extract 3, Bacteria 4, Congo Methods.

Introduction

Biofilms remain communal of microbes involved to a superficial by polysaccharides, proteins, and nucleic acids¹. *E. coli* biofilm expansion is a complicated procedure that primes to striking constructions that are significantly used for sickness and causing solicitations (note the primary caused biofilm was produced to stash peptide antimicrobials to decrease corrosion². Bacterial biofilm residues are a universal hazard to healthiness in line with great refractoriness to cure and the capability to exaggerate nosocomial contagions. Therefore, exploration of original effectual molecules to confront this problem is significant³. The capability of antibacterial agents to constrain establishment of or annihilation of biofilms hold potential for decreasing establishment of outsides in addition to epithelial mucosa by microbes⁴.

Biofilm confrontation is appropriate after numerous explanations, like confined pervasion over antibiotics interested in biofilm matrix, exposure about multidrug efflux pumps, type IV secretion systems, lowered permeability, then the labor on antibiotic-modifying enzymes. After conservative management, the expanded biofilm hindrance improves the essential after improving current monitoring strategies⁵. Within the Enterobacteriaceae, lines of the genus *Serratia* are a widespread reason over ethnical nosocomial infections; within addition, biofilm composition is oft associated with continual infections. Quorum sensing can circulate an essential position of wholly established matured biofilms between various bacteria. For example, a breach of AHL production effects within the quick apprehension regarding biofilm improvement then the deficiency on mobile disintegration within filaments aggregates within *Serratia marcescens*⁶. The enzyme LuxS is accounta-

ble because of the manufacturing of autoinducer-2 (AI-2), a molecule so has been implicated in quorum sensing of many bacterial species. This learning investigated a luxS-dependent signaling rule of the Gram-negative bacteria *Serratia spp.*⁷. The outstanding capability of the plant sources to inhibit the early phase of biofilm establishment of the six bacterial isolates might be credited to interfering with forces (such as Brownian, sedimentation, Lifshitz-Van der Waals and electrostatic collaboration forces) that favor the deposition and adherence of bacteria to surfaces⁸.

This revision measured the capability of herb sources to terminate or avoid additional creation of conventional biofilms at 24 h and 48 h. merely herb mines through the anti-attachment movement were incorporated in this revision.

Materials and methods

Microorganisms in this study

20 isolates of distinctive class regarding pathogenic microorganism toughness (*E.coli* or *Serratia marcescens*) were removed beside particular scientific sources beyond Al-Kindy Teaching Hospital, depending on cultural, morphological or Vittek2 regulation characteristics.

Preparation regarding *Quercus* polyphenol extract

The spray-dried PE used to be arrived thru dehydration, namely described in Servili *et al.*¹⁰. The pattern was once shaken for 30 min or below centrifuged at 4500 rpm (10 min, 20°C). Once the pellet was re-extracted, the supernatants re-

Citation: Abd Algabar FA, Abdalameer Baqer B. Detection of biofilm formation of (*Serratia* and *E.coli*) and determination of the inhibitory effect of *Quercus* plant extract against these infectious pathogens. *Revis Bionatura* 2022;7(1). 8. <http://dx.doi.org/10.21931/RB/2022.07.01.8>

Received: 25 September 2021 / **Accepted:** 10 December 2021 / **Published:** 15 February 2022

Publisher's Note: Bionatura stays neutral with regard to jurisdictional claims in published maps and institutional affiliations.

Copyright: © 2022 by the authors. Submitted for possible open access publication under the terms and conditions of the Creative Commons Attribution (CC BY) license (<https://creativecommons.org/licenses/by/4.0/>).



united and constant after an aggregation over 50 mL within a volumetric flask.

Biofilm Production (Congo red test)

Mathur *et al.*¹¹ have described the approach because screening over biofilm formation. Plates have been inoculated with permanency with the aid of pure singular remoted colony or nursed aerobically for 24 - 48 hours at 37C°. The positive end outcome was once shown through dark collections through a dead crystalline constancy.

Detection of QS gene so is responsible on permanency durability Biofilm Production toughness by using Polymerase Chain Reaction method

PCR assay was once used following observe toughness QS genes (*lux s*) permanency into *Serratia Marcescens* isolates yet (carried abroad among a aggregation amount about 25µL, it was once created beyond 5µL regarding template DNA, 1µL over each over the primers, 12.5 green grasp mix. Then the aggregate used to be complete along 25µl over nucleases uninterrupted lotus tables (1)(2). DNA isolation was once made employing AccuPrep® Genomic DNA Extraction Kit strategies in imitation of preparing a luminous DNA for PCR beside the samples.

Agarose Gel Electrophoresis

When PCR magnification, agarose gel electrophoresis was implemented to check the existence of amplification. PCR was reliable on the extracted DNA criteria¹².

In vitro antibiofilm activity on sow permanency extract regarding Congo technique

Congo red agar technique One ml regarding clean leaves extracts was introduced according to Congo purple agar mediocre among panel fervor to uninteresting totally. Then bacteria used to be inoculating about Congo crimson agar aerobically because of 24 according to 48 h at 37°C¹³.

Statistical analysis

PCR production has been shipped for Sanger sequencing using ABI3730XL, computerized DNA sequences, with the aid of MacroGen Corporation – Korea. The results have been obtained by way of the e-mail below analyzed the usage of genius software program¹⁰.

Results and discussion

Detection of biofilm formation on Congo method

Biofilm-producing microorganisms are responsible for deep averse infections and are notoriously hard to eradicate. They show off hindrance according to antibiotics using more than a few techniques kind of confined entrance about antibiotic within biofilms, lowered growth dimensions then manifestation concerning resistance¹². Results toughness suggests durability black color into the pathogenic microorganism isolates as is longevity shaped vivid slime ledge or indicated with the aid of build regarding fuscous colonies along with a dead colorless consistency (figure1), or it result was validated 90% regarding this isolates were permanency producing biofilm In that effects whole 90%of pathogenic isolates are longevity producing biofilm.

Detection of QS gene by PCR technique

This approach is empathetic, easy to perform, specific because of gene families, and environment-friendly than the lousy techniques¹³. Using the PCR technique, four isolates have been tested because of harboring *Lux s* longevity gene in *Serratia marsence* isolates. PCR method was ancient among the present education between methods after extending a targeted supplement of *Luxs* gene stability; The PCR consequences confirmed precise cable-related imitation of the targeted sequence. PCR amplified regions revealed a molecular volume

Primer Name	Forward Primer	Reverse Primer	Predicted size (bp)	Reference Accession no	origin
luxS	TCATGGCATAACCATCACGG →	TCCAGAATGTGCTTGGCGAT←	360	Naba'a A. Muhammed1 et al.,2000)	Alpha DNA Co. (Canada)

Table 1. The following table illustrates the primer used in this study.

No.	Contents of the reaction mixture	Final concentration Pmol/ µl	The volume of the reaction mixture for a single tube(µl)
1	Green major mix	2x	12.5 µl
2	forward primer with(<i>lux s</i>) gene	0.4	1µl for each gene final volume 2 µl
3	Each reverse primer (<i>lux s</i>) gene	0.4	1µl for each gene final volume 2 µl
4	DNA pattern		5 µl
5	Nuclease free water		3.5µl

Table 2. Reaction Setup and Thermal Cycling Protocol Gene: luxS ng/µl ng/µl 2, Total volume 25.

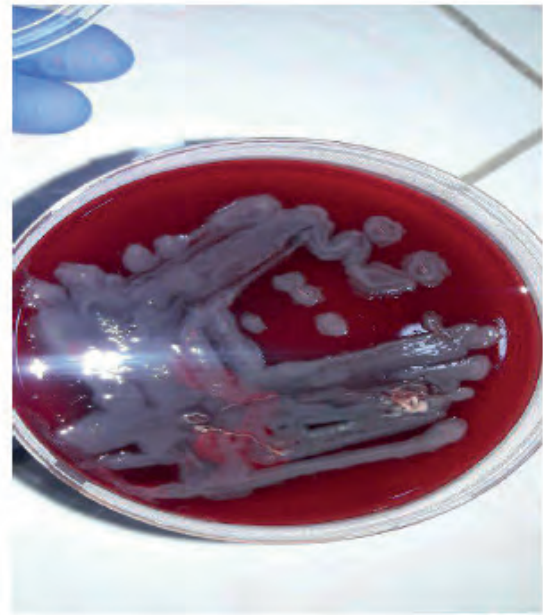
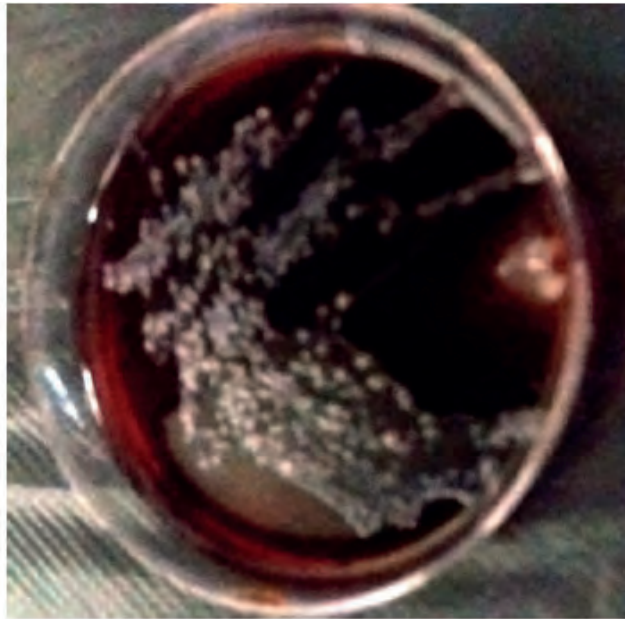


Figure 1. A- the effect of plant extract to inhibit biofilm Formation on Congo red.

of 818 bp because it primer chronic in imitation of deciding gene durability about quorum sensing. Permanency, namely shown within Figure (2).

Reticence of progress of pre-formed biofilms – calculation of obliteration of biofilm mass

The capability of the mines to inhibit extra biofilm expansion or devastation of pre-formed biofilms remained examined. The act of the herb mines alongside biofilms at different phases of growth highpoints their possible utility in scientific presentations. Such presentations might comfort to improve the immunological protection of diseased hosts against bacterial cell populations¹⁴, specifically those in biofilms, and following host allowance and decline of infection indications¹⁵. Results of the table.2 exhibit, figure ternary longevity excessive numerous plant extracts over several types concerning microorganisms examined and control¹⁶. These extracts show Felicitous stability antibacterial mission in struggle according to *E. coli* and *Serratia Marcescens* collectively including an inhibition zone used to be 14 mm. Yet, it had the harmful effect antibacterial undertaking among emulation according to *Serratia*; The study showed that the greater the induction period, after 48 hours, the effect of bacterial inhibition, The methanolic extract was more effective against (*Serratia, E. coli*) regarding superb consciousness (10,20,30 mg/l) (table 3).

Conclusions

Slight remained recognized nearly antimicrobial actions of the particular plant life in this revision. The effects displayed that elemental mines of the plants ensured decent action on the planktonic and sessile systems of the bacterial species examined. These effects bear implications for the growth then dissemination of biofilm clusters between these toughness isolates. These outcomes focus on using naturally occurring compounds of bury original as durability a potential power after barrier build regarding biofilm within pathogenic isolates.

Funding

This research received no external funding.

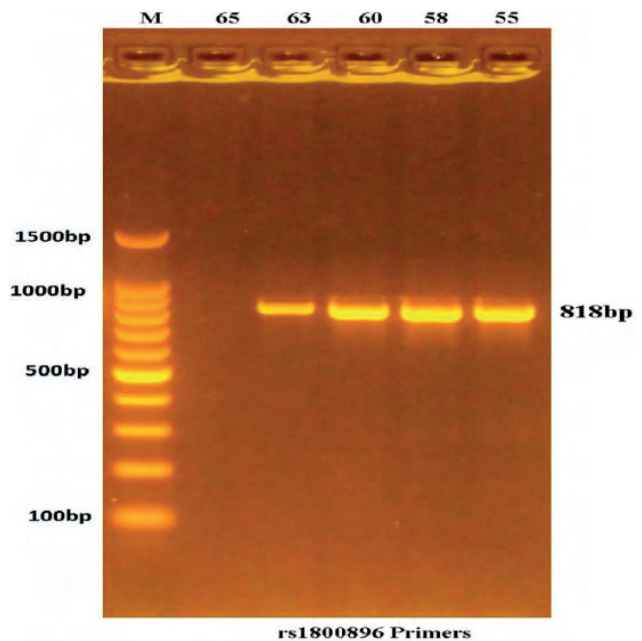


Figure 1. A- the effect of plant extract to inhibit biofilm Formation on Congo red.

Conflicts of Interest

The authors declare no conflict of interest.

Bibliographic references

1. Simões1, Lúcia Chaves2, et al. "Biofilm Interactions between Distinct Bacterial Genera Isolated from Drinking Water." Applied and Environmental Microbiology, vol. 73, no. 19, Oct. 2007, pp. 6192–200. DOI.org (Crossref), <https://doi.org/10.1128/AEM.00837-07>.
2. Rob Van Houdt1, et al. "Isolation and Functional Analysis of LuxS in *Serratia Plymuthica* RVH1." FEMS Microbiology Letters, vol. 262, no. 2, Sept. 2006, pp. 201–09, <https://doi.org/https://doi.org/10.1111/j.1574-6968.2006.00391.x>.
3. Roy1, Ranita2, et al. "Strategies for Combating Bacterial Biofilms: A Focus on Anti-Biofilm Agents and Their Mechanisms of Action." Virulence, vol. 9, no. 1, Dec. 2018, pp. 522–54. DOI.org (Crossref), <https://doi.org/10.1080/21505594.2017.1313372>.

Microbes	Control	10 mg/l	20mg/l	30mg/l	LSD value
<i>E. coli</i> (10 isolate)	0	7	9	13	2.88 *
<i>Ecoli</i> after 48hr	0	11	11	9	2.19 *
<i>Serratia Marcescens</i> (10 isolate),	0	11	12	12	2.04 *
<i>Serratia Marcescens</i> (48 hr)	0	14	13	14	3.52 *
<i>Ecoli</i> after 10 hr	0	0	6	10	3.08 *
<i>Serratia Marcescens</i> after 10hr	0	8	8	9	2.17 *
LSD value	--	3.61 *	3.09 *	3.73 *	---
* (P<0.05).					

Table 3. Antimicrobial Action of basic mines obtainable by inhibition zone diameter (mm).

- Nostro¹, Antonia², et al. "In Vitro Activity of Plant Extracts against Biofilm-Producing Food-Related Bacteria." *International Journal of Food Microbiology*, vol. 238, Dec. 2016, pp. 33–39. DOI.org (Crossref), <https://doi.org/10.1016/j.ijfoodmicro.2016.08.024>.
- Bavington¹, C2., and C3. Page. "Stopping Bacterial Adhesion: A Novel Approach to Treating Infections." *Respiration*, vol. 72, no. 4, 2005, pp. 335–44. DOI.org (Crossref), <https://doi.org/10.1159/000086243>.
- Quílez, A. M., et al. "Potential Therapeutic Applications of the Genus *Annona*: Local and Traditional Uses and Pharmacology." *Journal of Ethnopharmacology*, vol. 225, Oct. 2018, pp. 244–70. DOI.org (Crossref), <https://doi.org/10.1016/j.jep.2018.06.014>.
- Rice, S. A., et al. "Biofilm Formation and Sloughing in *Serratia Marcescens* Are Controlled by Quorum Sensing and Nutrient Cues." *Journal of Bacteriology*, vol. 187, no. 10, May 2005, pp. 3477–85. DOI.org (Crossref), <https://doi.org/10.1128/JB.187.10.3477-3485.2005>.
- Borges¹, Anabela², et al. "The Activity of Ferulic and Gallic Acids in Biofilm Prevention and Control of Pathogenic Bacteria." *Biofouling*, vol. 28, no. 7, Aug. 2012, pp. 755–67. DOI.org (Crossref), <https://doi.org/10.1080/08927014.2012.706751>.
- Mathur¹, T2., et al. "DETECTION OF BIOFILM FORMATION AMONG THE CLINICAL ISOLATES OF STAPHYLOCOCCI: AN EVALUATION OF THREE DIFFERENT SCREENING METHODS." *Indian Journal of Medical Microbiology*, vol. 24, no. 1, Jan. 2006, pp. 25–29. DOI.org (Crossref), [https://doi.org/10.1016/S0255-0857\(21\)02466-X](https://doi.org/10.1016/S0255-0857(21)02466-X).
- Servili¹, Maurizio², et al. "Improvement of Bioactive Phenol Content in Virgin Olive Oil with an Olive-Vegetation Water Concentrate Produced by Membrane Treatment." *Food Chemistry*, vol. 124, no. 4, Feb. 2011, pp. 1308–15. DOI.org (Crossref), <https://doi.org/10.1016/j.foodchem.2010.07.042>.
- Sedlackova¹, Tatiana², et al. "Fragmentation of DNA Affects the Accuracy of the DNA Quantitation by the Commonly Used Methods." *Biological Procedures Online*, vol. 15, no. 1, Dec. 2013, p. 5. DOI.org (Crossref), <https://doi.org/10.1186/1480-9222-15-5>.
- Wilmington¹, Delaware². "Interpretation of Nucleic Acid 260/280 Ratios." *Thermo Scientific T123 – TECHNICAL BULLETIN Nano-Drop Lite*, vol. T123– Rev 1/2012.
- Saiki¹, Randall K2., et al. "Primer-Directed Enzymatic Amplification of DNA with a Thermostable DNA Polymerase." *Science*, vol. 239, no. 4839, Jan. 1988, pp. 487–91. DOI.org (Crossref), <https://doi.org/10.1126/science.2448875>.
- Miladi¹, Hanene², et al. "Use of Carvacrol, Thymol, and Eugenol for Biofilm Eradication and Resistance Modifying Susceptibility of *Salmonella* Enterica Serovar Typhimurium Strains to Nalidixic Acid." *Microbial Pathogenesis*, vol. 104, Mar. 2017, pp. 56–63. DOI.org (Crossref), <https://doi.org/10.1016/j.micpath.2017.01.012>.
- Fatima Amer Abd Algabar¹. "Extraction of Staphyloxanthin from *Staphylococcus Aureus* and Studying Some Biological Effect of Staphyloxanthin Pigment." *Journal of Global Pharma Technology*, vol. 11, no. 04, 2019, pp. 491–96.
- Fatima Amer Abd Algabar¹. "Determine the Antibacterial Activity of Staphyloxanthin Produced by *Staphylococcus Aureus* against Some Bacteria." *Al-Nisour Journal for Medical Sciences*, vol. 1, no. 2, 2019, pp. 342–55.

ARTICLE / INVESTIGACIÓN

Optimization of cephalosporin C acylase immobilization using crosslinked enzyme aggregates technique

Julkipli Julkipli¹, Khaswar Syamsu¹ and Ahmad Wibisana^{2*}

DOI. 10.21931/RB/2022.07.01.9

¹Biotechnology Study Program, Graduate School, IPB University, IPB Dramaga Campus, Bogor, Indonesia.²The National Research and Innovation Agency (BRIN), Tangerang Selatan, Banten, Indonesia and Chemical Engineering Study Program, Pamulang University, Witana Campus, Tangerang Selatan, Banten, Indonesia.Corresponding author: ahmad.wibisana@brin.go.id

Abstract: Cephalosporin C acylase (CCA) is an essential enzyme for the one-step conversion of cephalosporin C into 7-aminocephalosporanic acid (7-ACA), an intermediate compound used to synthesize various semi-synthetic cephalosporin antibiotics. The industrial process prefers to use enzymes in immobilized form rather than soluble. A crosslinked enzyme aggregate (CLEAs) is a potential matrix-less enzyme immobilization technique to produce stable immobilized enzymes with high activity and low production costs. This study aimed to optimize the CCA immobilization using the CLEAs technique with Chitosan as a co-aggregate. The CCA lysate was obtained from harvesting CCA fermentation broth using a mutant strain of *Escherichia coli* through cell separation and lysis steps. Partially purified CCA by ammonium sulfate addition was conducted to obtain an active fraction of 20-60% saturation, followed by co-aggregation with Chitosan to form physical CCA aggregates. The aggregates were then immobilized by a crosslinking technique using glutaraldehyde to form CLEAs-CCA. Optimization of the immobilization process was carried out by Response Surface Methodology in three steps, (i) screening of the influencing factors, (ii) determining the level of the significant factors, and (iii) optimizing the immobilization condition. The CLEAs-CCA activity was used as a response parameter. Under optimum conditions, CLEAs-CCA activity obtained was 85.91 Ug⁻¹.

Key words: 7-aminocephalosporanic acid, cephalosporin C acylase, Chitosan, crosslinked enzyme aggregates, response surface methodology.

Introduction

Cephalosporins are antibiotics with a broad antibacterial spectrum and almost cover 50% of β -lactam antibiotics humans use^{1,2}. Most of them are derived from 7-aminocephalosporanic acid (7-ACA), a precursor compound generated from hydrolysis of cephalosporin C (CPC), a natural antibacterial obtained from *Acremonium chrysogenum* fermentation³. Therefore, it is essential to produce 7-ACA efficiently.

The industrial demands for efficient and environmentally friendly 7-ACA production have shifted from chemical to enzymatic processes. Initially, a two-step bioconversion using D-amino acid oxidase and glutaryl-7-aminocephalosporanic acid acylase was developed⁴. Recently, one-step bioconversion using cephalosporin C acylase (CCA, EC 3.5.1.11) has paid the attention of researchers because it is more efficient⁵.

The industrial application of enzymes is preferred in the immobilized rather than soluble form due to the more efficient bioconversion process⁶. Immobilization of enzymes on a matrix is a popular method. However, a dilution of enzyme up to 99% occurred, resulting in decreased activity⁷. In addition, the matrix used causes an increase in the enzyme cost and generates a waste matrix generated from the inactive biocatalyst⁸. To overcome these problems, enzyme immobilization by cross-linked enzyme aggregates (CLEAs) technique, a matrix-less immobilization approach, is a potential method to be applied⁷. It showed a simple, fast, and efficient method to immobilize

various enzymes⁹⁻¹⁰. To the best of our knowledge, there is no publication on the application of CLEA for CCA immobilization.

The CLEAs formation involves two critical steps, i.e., enzyme precipitation to form aggregates and crosslinking of the aggregates⁷. Ammonium sulfate and glutaraldehyde are often used as precipitation and crosslinker agents, respectively^{9,11,12}. However, crosslinking the enzyme with low superficial lysine residues with glutaraldehyde may cause weak enzyme binding, making it quickly released from its CLEAs¹³. The addition of co-aggregates, such as bovine serum albumin, poly-ethyleneimine, and poly-lysine, could form larger aggregates size and higher stability^{9,12,13}. Chitosan is a relatively inexpensive biopolymer (polyaminosaccharides, copolymers of N-acetyl-D-glucosamine and N-amino-D-glucosamine) with high availability rich in reactive amino groups, potentials to mediate the formation crosslinks between the aggregates^{14,15}.

In this research, optimization of the CCA immobilization by CLEAs technique using *Chitosan* as a co-aggregate was studied. Optimization was conducted with Response Surface Methodology (RSM), as it is an effective and widely used method for optimization in bioprocesses, including enzyme immobilization¹⁶⁻¹⁸. CLEAs-CCA (Ug-1) activity was used as a response. The experiments were carried out in three steps, namely, (i) screening of the influencing factors using 2ⁿ⁻² fractional factorial design (FFD), (ii) determining the level of significant fac-

Citation: Julkipli J, Syamsu K and Wibisana A. Optimization of cephalosporin C acylase immobilization using crosslinked enzyme aggregates technique. *Revis Bionatura* 2022;7(1). 9. <http://dx.doi.org/10.21931/RB/2022.07.01.9>

Received: 13 June 2021 / **Accepted:** 10 August 2021 / **Published:** 15 February 2022

Publisher's Note: Bionatura stays neutral with regard to jurisdictional claims in published maps and institutional affiliations.

Copyright: © 2022 by the authors. Submitted for possible open access publication under the terms and conditions of the Creative Commons Attribution (CC BY) license (<https://creativecommons.org/licenses/by/4.0/>).



tors using the steepest ascent method, and (iii) optimization of immobilization condition using RSM with Central Composite Design (CCD). CLEAs-CCA obtained were also evaluated for pH and temperature stability.

Materials and methods

Escherichia coli mutant as the CCA producer was provided by The National Research and Innovation Agency (BRIN), previously named was Biotech Center, Agency for the Assessment and Application of Technology - Indonesia. The culture was maintained in Miller Luria Bertani (LB) agar medium (Hi-media, Mumbai, India) pH 7.0, containing 100 $\mu\text{g mL}^{-1}$ ampicillin. The chemicals used were ammonium sulfate p.a (Merck, Germany), chitosan powder with a degree of deacetylation (DD) > 75% obtained from the local market, CPC-Na (Biorbyt, Netherlands), and 7-ACA (Tokyo Chemical Industry, Japan). Other chemicals such as 50% glutaraldehyde, absolute methanol, p-dimethylaminobenzaldehyde (p-DAB), NaOH granules, and acetic acid glacial were obtained from Sigma-Aldrich (Singapore).

CCA production

The CCA production method was adopted from Martius *et al.*¹⁹. A single colony of *E. coli* was selected and inoculated into 2 mL of fresh LB medium pH 7.0 containing ampicillin 100 $\mu\text{g mL}^{-1}$ and cultivated at 37°C overnight with shaking at 170 rpm. The seed culture was then prepared by suspending 0.5 ml of the overnight culture to 2 ml fresh LB medium pH 7.0 containing ampicillin of 100 $\mu\text{g mL}^{-1}$ and incubated at 37°C with shaking at 170 rpm in water bath. After two hours incubation ($\text{OD}_{600} \pm 0.6$), 0.5 ml of the seed culture was inoculated into a fresh 50 ml LB pH 7.0 containing ampicillin of 100 $\mu\text{g mL}^{-1}$ in a 250 ml Erlenmeyer flask and incubated at 37°C, shaken at 200 rpm until an OD_{600} of 0.6-0.8 was reached. The culture was then induced with lactose with a final concentration of 0.2% (w/v), and then cultivation was continued at 25°C with shaking at 200 rpm for 12 hours for CCA expression. The cells were harvested by centrifugation at 6,000 g, 4°C, for 10 minutes when the fermentation was finished. The pellets were then washed twice with a working buffer (0.1 M phosphate buffer pH 8.0) and then suspended in the same buffer containing 1 mM phenylmethylsulfonyl fluoride (PMSF). PMSF was used to inactivate the protease in cells. Cells were lysed by sonicating at 20 kHz, 25% amplitude, with a mode of 5 seconds "on" and 20 seconds "off" for 12 cycles using Misonix Sonicator XL2020 (Misonix, United States) in an ice bath. Cell debris was separated by centrifugation at 12,000 g, 4°C, for 5 minutes. CCA lysate was then stored at -20°C for further experiment.

Chitosan and glutaraldehyde solution preparation

The chitosan solution was prepared by Arsenault *et al.* method¹⁷. Chitosan powder was dissolved in 0.1 M HCl to obtain a specific concentration, stirring for 30 minutes, and then sonicated for one hour to dissolve Chitosan completely. The pH of the solution was adjusted to 5.5 by adding 1 N NaOH. Glutaraldehyde solution with a particular concentration (% w/v)

was prepared by weighing 50% glutaraldehyde solution and diluted with a working buffer.

CCA partial purification

Simple partial purification of CCA was carried out by precipitation technique using ammonium sulphate (AS)²⁰. AS powder was added slowly to 10 mL CCA lysate until it reached 20% saturation. The mixture was stirred continuously at a low speed at 40°C for 3 hours. The precipitate was separated by centrifugation at 10,000 g at 40°C for 15 minutes, and the supernatant was used for further fractionation. Precipitation was continued by adding AS to 60% saturation. The CCA aggregates of 20-60% saturation were separated by centrifugation and then resuspended in 40 mL of a working buffer. The suspension was used for CLEAs formation.

CLEAs-CCA formation method

The CLEAs formation method was adopted from Mageed *et al.*¹⁴ with slight modifications. A 0.5 mL chitosan solution was added to 1 mL of CCA aggregates suspension to obtain a final chitosan concentration in the range 1-5 mg mL^{-1} (x_1) according to the FFD factor level (Table 1). Chitosan is insoluble at pH above 6.5 and will aggregate with CCA aggregates. The aggregation was conducted by shaking at 150 rpm for 30-90 minutes (x_2). The co-aggregation allows CCA aggregates and Chitosan to interact electrostatically or hydrogen bonding. Furthermore, 0.5 mL of glutaraldehyde solution was added to obtain a final concentration in the range of 1-5 %, v/v (x_3) and then shaking at 200 rpm. Variation in suspension pH (x_4), crosslinking time (x_5), and crosslinking temperature (x_6) were carried out according to the range of each factor in the FFD (Table 1). In such a way, glutaraldehyde crosslinks of primary amine groups of enzyme and Chitosan. After the reaction was completed, the CLEAs-CCA was filtered using filter paper and washed with working buffer three times. The CLEAs-CCA was stored at -20°C for further analysis.

CLEAs-CCA activity determination

The CLEAs-CCA activity was determined using a micro-scale procedure according to Fernandez-Arrojo *et al.*²¹ with minor modifications. Twenty milligrams of CLEAs-CCA were added to a microtube containing 60 μL of CPC solution with a concentration of 20 $\mu\text{g mL}^{-1}$ in a working buffer (0.1 M phosphate buffer pH 8.5). The mixture was incubated in an incubator shaker at 37°C for 5 minutes. After the reaction was completed, 20 μL of the reactant was taken and mixed with 280 μL of stop solution (the solution consists of 0.5% p-DAB in absolute methanol: 0.05 M NaOH: 20% acetate acid glacial with ratio 1:2:4). The solution was left for 10 minutes at room temperature to develop color, and then the absorbance was measured at 415 nm.

Screening of factors

In the first step, factors affecting CLEAs-CCA immobilization were screened using the FFD experimental design. The factor screening plays an important role when many potential factors influence the response while the resource availability is limited²². FFD screened out the influencing factors based on

CLEAs-CCA activity was calculated using equation (1).

$$\text{CLEAs - CCA activity (Ug}^{-1}\text{)} = \frac{\mu\text{mol of 7 - ACA x dilution factor}}{\text{reaction time x wet weight of CLEAs - CCA (g)}} \quad (1)$$

Factors	symbol	Factor levels		
		+1	0	-1
Chitosan concentration (mgmL ⁻¹)	x ₁	5	3	1
Co-aggregation time (minutes)	x ₂	90	60	30
Glutaraldehyde concentration (% v/v)	x ₃	5	3	1
pH suspension	x ₄	9	8	7
Cross-linking time (minutes)	x ₅	240	150	60
Cross-linking temperature (°C)	x ₆	30	25	20

Table 1. Independent factors and their levels were used in the FFD experiment.

Run	Coded factor						Uncoded factor						CLEAs-CCA activity (Ug ⁻¹)
	x ₁	x ₂	x ₃	x ₄	x ₅	x ₆	x ₁	x ₂	x ₃	x ₄	x ₅	x ₆	
1	-1	-1	-1	-1	-1	-1	1	30	1	7	60	20	39.34
2	+1	-1	-1	-1	+1	-1	5	30	1	7	240	20	23.16
3	-1	+1	-1	-1	+1	+1	1	90	1	7	240	30	23.31
4	+1	+1	-1	-1	-1	+1	5	90	1	7	60	30	38.29
5	-1	-1	+1	-1	+1	+1	1	30	5	7	240	30	10.86
6	+1	-1	+1	-1	-1	+1	5	30	5	7	60	30	20.98
7	-1	+1	+1	-1	-1	-1	1	90	5	7	60	20	16.75
8	+1	+1	+1	-1	+1	-1	5	90	5	7	240	20	6.34
9	-1	-1	-1	+1	-1	+1	1	30	1	9	60	30	35.42
10	+1	-1	-1	+1	+1	+1	5	30	1	9	240	30	35.02
11	-1	+1	-1	+1	+1	-1	1	90	1	9	240	20	15.44
12	+1	+1	-1	+1	-1	-1	5	90	1	9	60	20	46.74
13	-1	-1	+1	+1	+1	-1	1	30	5	9	240	20	13.28
14	+1	-1	+1	+1	-1	-1	5	30	5	9	60	20	12.41
15	-1	+1	+1	+1	-1	+1	1	90	5	9	60	30	19.49
16	+1	+1	+1	+1	+1	+1	5	90	5	9	240	30	19.03
17	0	0	0	0	0	0	3	60	3	8	150	25	15.83
18	0	0	0	0	0	0	3	60	3	8	150	25	15.46
19	0	0	0	0	0	0	3	60	3	8	150	25	15.57
20	0	0	0	0	0	0	3	60	3	8	150	25	14.88
21	0	0	0	0	0	0	3	60	3	8	150	25	16.35
22	0	0	0	0	0	0	3	60	3	8	150	25	15.27

Table 2. Experimental FFD for factor screening and the result of CLEAs-CCA activity.

their main effects and excluded their interaction²³. By preliminary literature review, six independent factors and their levels were selected, and the screening experiment design is presented in Table 1. The FFD experiments consist of 22 runs (16 runs of two-level fractional factorial (2ⁿ⁻²) and 6 center point runs). The experimental design and the results are shown in Table 2.

Steepest ascent method

The level of significant factors obtained from the FFD experiment was initially optimized using the steepest ascent method to determine the center point of each factor. Sequential experiments were carried out by applying various influencing factors along the direction of the maximum increase in the

response as a rapid and efficient method for approaching the optimum neighborhood²⁴. Two points flanking the maximum response point of each factor are selected for the next optimization step.

Optimization immobilization conditions

The CCD with RSM was employed to optimize the two independent significant factors (glutaraldehyde concentration and crosslinking time). The other factors which have an insignificant effect were kept constant at the minimum level. The CCD and the result of the experiments are presented in Table 3.

The effect of significant factors was modeled with a second-order polynomial equation as given by equation (2).

$$Y = b_0 + b_i x_i + b_j x_j + b_{ij} x_i x_j + b_{ii} x_i x_i + b_{jj} x_j x_j + \varepsilon \quad (2)$$

Where Y represents the response predicted value, b_0 is a constant, b_i is the linear coefficient, b_{ij} is the interaction coefficient, b_{ii} and b_{jj} is the quadratic coefficient, and x_i, x_j are the coded level of the factors. Validation of optimum conditions obtained by the model was carried out by experiment with three replications. The relative error between predicted and experimental values was calculated by equation (3):

Statistical analysis

The effect of significant factors on CLEAs-CCA activity was analyzed using ANOVA and measured its relative significance based on an F-test with a confidence level of 95% (p-value < 0.050 is significant). The statistical analysis was carried out using Design-Expert version 12.0.11.0 software.

The immobilization yield and activity yield of CLEAs-CCA was determined according to equations (4) and (5)²⁵:

Characterization of CLEAs-CCA

pH stability

The pH stability assay was conducted by incubating CLEAs-CCA and free CCA at 4°C for 30 minutes in phosphate buffer solution (pH 7.5 and 6.5) and acetate buffer solution (pH 5.5 and 4.5). The pH of buffer solutions was adjusted to the desired value by adding HCl 1 N or NaOH 1 N. After the incubation, the sample was washed three times with a working buffer and measured the activity. The residual activity was expressed as a percentage of its maximum activity (equation 6).

Thermal stability

The thermal stability was evaluated by incubating CLEAs-CCA and free CCA at a temperature range of 35 - 65°C for 30 minutes. After incubation, the samples were cooled at 4°C, and the residual activities were determined.

Results

Screening of the influencing factors

The result of the screening experiment using FFD is shown in Table 2. The ANOVA of the first-order model and regression analysis of the variables (Table 4) revealed that the model

and the two factors (i.e., glutaraldehyde concentration and crosslinking time) have a significant effect (p-value < 0.050) on CLEAs-CCA activity. Other factors, namely, chitosan concentration, co-aggregation time, suspension pH, and crosslinking temperature, did not significantly affect the experimental range applied.

The linear model based on the significant factors was given in equation (7):

The model showed that glutaraldehyde concentration (x_3) and crosslinking time (x_5) have a negative value, which means both factors affect CLEAs-CCA activity inversely. Lower glutaraldehyde concentration and shorter crosslinking time would increase CLEAs-CCA activity. In addition, the FFD result showed a considerable variation in CLEAs activity, indicating that optimization of the significant factors would result in higher CLEAs-CCA activity.

Level determination of the significant factors for optimization

The two significant factors obtained from the FFD were applied simultaneously in the steepest ascent to determine their level used in optimization. Because the screening experiment still uses a wide range of factor levels, the significant factor level is still far from its optimum point. When predicted using response surface methodology, they need to be re-defined to obtain an accurate optimum point. The movement direction of the factors towards the area where the response increases rapidly can be assisted using the steepest ascent experiment. The experiment results showed that the maximum value of CLEAs-CCA activity was approximated to be in the range of the glutaraldehyde concentration 0.04-0.32% (v/v) and the crosslinking time 118-120 minutes (Fig.1). The insignificant factors, namely chitosan concentration, co-aggregation time, pH suspension, and crosslinking temperature, were kept constant at a minimum level (i.e., 1 mgmL⁻¹, 30 minutes, 7, and 20°C, respectively) during optimization.

Optimization of the immobilization conditions

The result of the CCD experiments is shown in Table 3. The ANOVA of the quadratic model (Table 5) demonstrated that the model was highly significant with a good coefficient determination, R² (0.986). It showed that the model fit with experimental data. The p-value of lack of fit, the variation of the

$$\text{Relative error (\%)} = \left| \frac{(\text{mean experimental value} - \text{predicted value})}{\text{mean experimental value}} \right| \times 100\% \quad (3)$$

$$\text{Immobilization yield (\%)} = \frac{\text{initial enzyme activity (U)} - \text{filtrate activity(U)}}{\text{initial enzyme activity (U)}} \times 100\% \quad (4)$$

$$\text{Activity yield (\%)} = \frac{\text{CLEAs activity (U)}}{\text{initial enzyme activity (U)} - \text{filtrate activity(U)}} \times 100\% \quad (5)$$

$$\text{Residual activity (\%)} = \frac{\text{activity of CLEAs} - \text{CCA}}{\text{activity of CLEAs} - \text{CCA}_{\text{max}}} \times 100\% \quad (6)$$

$$Y = 21.33 - 8.60x_3 - 5.19x_5 \quad (7)$$

model due to the model inadequacy, is 0.055, which implies that the lack of fit is insignificant. The value of 'Adequate Precision' 27.097 indicates an adequate signal. A value of 'Adequate Precision' > 4 is desirable.

A quadratic model equation fitted to the experimental data, given as coded factors, was shown in equation (8):

$$Y = 84.77 + 11.94x_3 - 4.24x_5 + 9.35x_3x_5 - 31.03x_3^2 - 14.93x_5^2 \quad (8)$$

The 3D surface plot of the quadratic model helps to investigate the desired response value and find the optimal operating conditions (Fig. 2). The peak of the curve is the maximum response obtained from the effect of significant factors and their interactions under optimal conditions. According to the quadratic model, the optimum condition for CLEAs-CCA immobilization was $x_3 = 0.18$ and $x_5 = -0.09$, or in actual value, glutaraldehyde concentration was 0.20 % (v/v) and crosslinking time was 119 minutes, with optimum predicted CLEA activity was 86.02 Ug^{-1} .

Validation of the model

A three-replicate experiment validated the prediction of CLEAs-CCA activity obtained under optimum conditions. As shown in Table 6, the experimental data were in good agreement with the predicted value in CLEAs-CCA activity. The relative error between predicted and experimental values fell

at 0.13%. It means that the results are within the confidence interval of 95%, confirming that the model is valid.

Stability of CLEAs-CCA

The thermal stability tests showed that free CCA had a slight decrease of activity (2.82%) after incubation at 45°C

compared to 35°C. However, at 55°C, its activity decreased sharply and only retained 4.57% activity. CLEAs-CCA showed better thermal stability and even showed an increase after incubation at 45°C. However, the CLEAs-CCA activity decreased after incubation at 55°C and retained only 25.87% activity. The experimental results are depicted in Figure 3a.

The pH stability tests also showed that CLEAs-CCA had better stability than free CCA. After incubation at pH 4.5 for 30 minutes, the CLEAs-CCA activity retained was 62.87%, while free CCA was 45.87 %. The experimental results are presented in Figure 3b.

Discussion

A simple immobilization technique and high enzyme stability are critical for enzymes in their production process. Im-

Run	Coded factor		Uncoded factor		CLEAs-CCA activity (Ug^{-1})
	x_3	x_5	x_3	x_5	
1	-1	-1	0.04	118.00	35.49
2	+1	-1	0.32	118.00	41.39
3	-1	+1	0.04	120.00	15.17
4	+1	+1	0.32	120.00	58.48
5	$-\alpha$	0	0.00	119.00	7.50
6	$+\alpha$	0	0.38	119.00	40.24
7	0	$-\alpha$	0.18	117.60	66.91
8	0	$+\alpha$	0.18	120.40	45.23
9	0	0	0.18	119.00	83.81
10	0	0	0.18	119.00	86.45
11	0	0	0.18	119.00	87.38
12	0	0	0.18	119.00	81.28
13	0	0	0.18	119.00	84.92

Table 3. CCD and experimental optimization result of CCA immobilization.

Factors	Coefficient estimate	F-value	p-value	Ranking
Model	21.33	6.59	0.0014*	significant
Chitosan concentration (x_1)	1.76	1.12	0.3059	4
Co-aggregation time (x_2)	-0.32	0.036	0.8512	6
Glutaraldehyde concentration (x_3)	-8.60	26.95	0.0001*	1
Suspension pH (x_4)	1.11	0.45	0.5118	5
Cross-linking time (x_5)	-5.19	9.80	0.0069*	2
Cross-linking temperature (x_6)	1.81	1.19	0.2919	3

*significant at a confidence level of 95%.

Table 4. ANOVA of the FFD screening experiments.

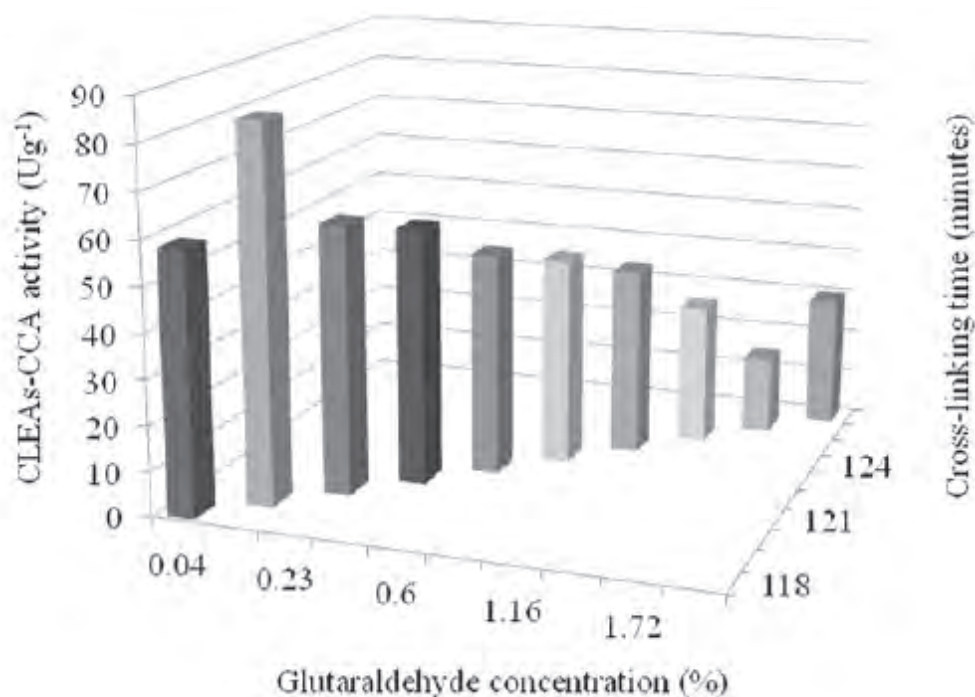


Figure 1. The steepest ascent experiment to determine the new level of significant factors is used in optimization.

Source	Sum of Squares	df	Mean square	F-value	p-value
Model	9172.43	5	1834.49	99.72	< 0.0001
Glutaraldehyde concentration (x₃)	1140.69	1	1140.69	62.01	0.0001
Cross-linking times (x₅)	143.64	1	143.64	7.81	0.0267
x ₃ x ₅	349.97	1	349.97	19.02	0.0033
x ₃ ⁵	6699.86	1	6699.86	364.20	< 0.0001
x ₅ ²	1550.93	1	1550.93	84.31	< 0.0001
Residual	128.77	7	18.40		
Lack of fit	106.01	3	35.34	6.21	0.0550*
Pure error	22.76	4	5.69		
Correction total	9301.20	12			
Standard deviation	4.29		R ²	0.986	
Mean	56.48		Adjusted R ²	0.976	
Coefficient of Variation (%)	7.59		Predicted R ²	0.915	
PRESS	789.41		Adequate Precision	27.097	

*insignificant at 95% confidence level, df: Degrees of freedom, PRESS: Predicted residual error sum of squares

Table 5. ANOVA for response surface quadratic model.

mobilizing enzymes using the CLEAs technique is a potential method to fulfill those demands. This technique involves only a simple preparation and does not require high purity of enzymes. In comparison, immobilization of CCA on the epoxy matrix was preceded by enzyme purification using immobilized metal affinity chromatography to obtain high purity enzyme^{4,26}. On the other hand, immobilization by the CLEAs technique does not require pure enzyme. The effect of enzyme purity on the CLEAs-penicillin G acylase (CLEAs-PGA) was studied by Rajendhran and Gunasekaran²⁷. The CLEAs-PGA generated from partially purified enzymes (enzyme purity 10 times higher than the initial crude enzymes) had 1.5 times higher activity than purified by the Ni-NTA chromatography technique (purity 31 times higher than the initial crude enzyme)²⁷. Therefore, com-

plex, high-cost, and time-consuming enzyme purification steps are unnecessary for CLEAs preparation.

In general, CLEAs formation involves two critical steps, i.e., enzyme precipitation to induce the physical enzyme aggregates formation and aggregates crosslinking to form permanently insoluble enzymes through covalent coupling of the aggregates while preserving their globular structure^{7,28}. The physical enzyme aggregates formation could be carried out by adding salts, organic solvents, or non-ionic polymers to enzyme solutions, as commonly used in protein purification. Partial purification of CCA using the salting-out method with the addition of AS was used in this study due to it being a simple method and relatively small effect on enzyme activity⁸. The active fraction of 20-60% saturation was used for CCA immo-

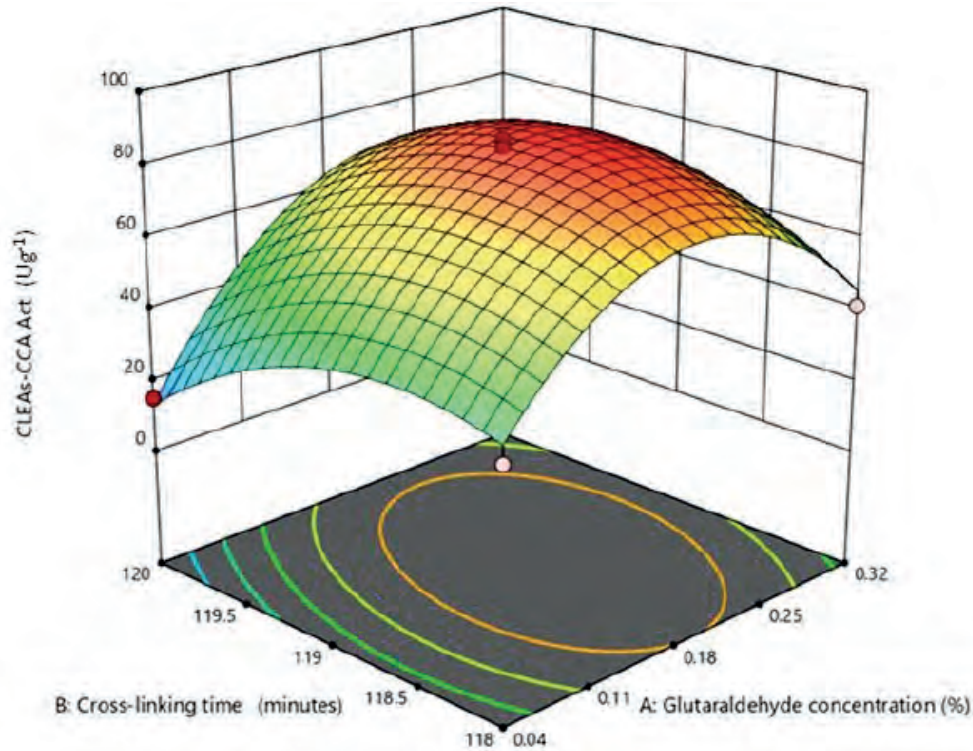


Figure 2. The 3D surface plot of the quadratic model.

Optimum factors level	Predicted value (Ug^{-1})	Experimental value (Ug^{-1})			Experimental mean value (Ug^{-1})	Relative error (%)
		1	2	3		
x_3 : 0.20 %	86.02	93,04	81,34	83,34	85.91	0.13
x_5 : 119 minutes						

Table 6. Experimental data at optimum conditions for model validation.

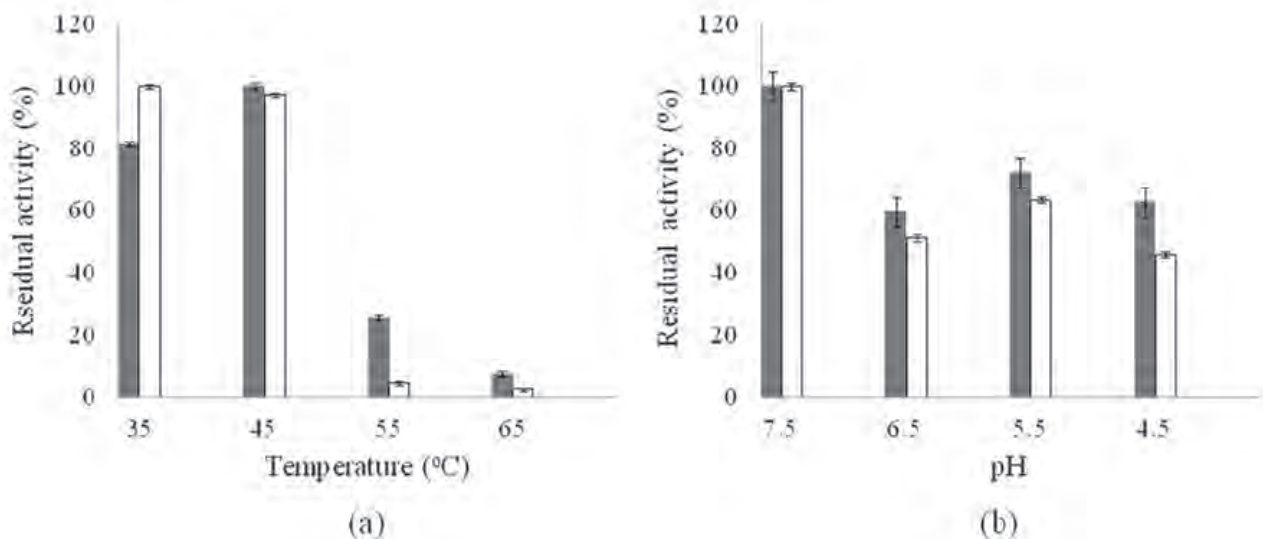


Figure 3. (a) Thermal stability test results; (b) pH stability test results; ■: optimized CLEAs-CCA; □: free CCA. Data are presented as mean values \pm S.E.

bilization. The partially CCA purification aimed to remove the contaminant protein in the lysate, such as esterase and β -lactamase, which are co-expressed when *E. coli* was used as an enzyme expression system²⁹. Both enzymes could hydrolyze CPC resulted in decreasing in yield of 7-ACA³.

The number of lysine residues on the enzyme surface

influences the effectiveness of crosslinking between crosslinkers and enzyme molecules. The amount of lysine residues also affects protein functionalization and enzyme immobilization^{30,31}. Lysine is the amino acid with an NH_2 (amino) side chain, the most reactive residue on the enzyme surface. Luo *et al.*³² reported that CCA contains only low (nine) superficial

lysine residues. Therefore, a co-aggregate compound rich in free amino groups, such as Chitosan, must be added before crosslinking. Chitosan as a co-aggregate can increase the effectiveness of crosslinking of CLEAs formation for various enzymes^{14,15}. In this study, the Chitosan with high DD (>75%) was mixed with the enzyme to provide an adequate number of free amino groups for crosslinking. DD is the ratio of N-amino-D-glucosamine to N-acetyl-D-glucosamine.

Glutaraldehyde is a widely applied bi-functional reagent for many CLEAs preparations since it is an efficient crosslinker with low cost and high availability³³. In this study, glutaraldehyde crosslinking was carried out at pH > 6.5. Under these conditions, the deprotonated amino group of Chitosan becomes more reactive as a nucleophilic agent⁶. Glutaraldehyde acts as an amino fixing arm to form an imine bond between the primary amino group of Chitosan and the enzyme, creating networks among them¹⁴. The reaction of primary amino groups of superficial lysine residues from neighboring enzyme molecules to glutaraldehyde can form inter- and intra-molecular aldol condensates, thereby increasing the stability of biocatalyst activity^{9,34,35}. However, the CLEAs formation using excessive glutaraldehyde would lead to enzyme inactivation due to its high reactivity and small size, allowing it to penetrate the enzyme's active site and access all essential amino acids involved in catalytic activity³⁶, leading the changes in intrinsic enzyme properties^{6,37,38}. In addition, more severe inactivation may occur for enzymes that have reactive amino acid residue in the vicinity of their active site³⁶. CCA has an essential N-terminal serine in its active site, which is susceptible to reacting with glutaraldehyde³⁸. He *et al.*³⁸ reported that crosslinking CCA with glutaraldehyde causes activity loss by 18% due to its excessive crosslinking. Therefore, adding Chitosan is necessary for crosslinking when glutaraldehyde is used. It could form reticulated covalent bonds between enzyme-enzyme, enzyme-polymer, and polymer-polymer, thereby increasing the number of crosslinks and reducing enzyme inactivation as well as increasing aggregate size. In this study, the particle size of CLEAs-CCA without chitosan addition was tiny and increased along with chitosan addition. The particle size of CLEAs is essential to facilitate mass transfer rate, product separation as well as its reusability after enzymatic processing¹².

Chitosan could also act as a coating agent for enzymes^{15,17}. As a poly-ionic biopolymer, Chitosan can interact with enzymes, preventing enzyme dissociation. Nevertheless, under certain conditions, such as low pH or high temperature, the biopolymer can be desorbed and lose its function as a protective layer. As a crosslinker agent, glutaraldehyde stabilizes CLEAs structure by crosslinking the biopolymer to the enzyme surface and among the biopolymers, avoiding the enzyme being re-dissolved during the buffer rinsing and their application^{14,33,34}.

This study used CCD for response surface optimization with two process variables (glutaraldehyde concentration and crosslinking time). It revealed that the optimized conditions were achieved at glutaraldehyde concentration 0.20% (v/v) and crosslinking time 119 minutes. The other factors were set at a minimum value: chitosan concentration 1 mgmL⁻¹, co-aggregation time 30 minutes, pH suspension 7, and crosslinking temperature 20°C. The maximum CLEAs-CCA activity achieved was 85.91 Ug⁻¹ (Table 6). Theoretically, at low glutaraldehyde concentration, one glutaraldehyde molecule reacts with a few amino groups of enzymes³³. Excessive interaction between residual amino acids on protein surface with glutaraldehyde must be avoided to maintain the catalytic activity of the immobilized enzyme. In addition, relatively low crosslinking

temperatures were used in this study to avoid CCA degradation. Within the temperature range used, maximum CLEAs activity was achieved in 2 hours.

The maximum activity of CLEAs-CCA obtained from this experiment was comparable and even exhibited slightly higher than that of immobilized CCA with matrix-binding obtained by Zhu *et al.*⁴ and Wei *et al.*²⁶, i.e., 81 Ug⁻¹ and 60 Ug⁻¹, respectively. However, the immobilization yield of CLEAs-CCA was 60.31%, and the activity yield was only 13.89%. Enzyme activity can be partially lost upon the precipitation and glutaraldehyde crosslinking step caused by the changes in intrinsic enzyme properties^{6,37,38}. Besides, the issues of diffusion and transport would arise since the pore sizes of the CLEAs may be small³⁹. However, the immobilization processes could promote enzyme resistance to pH or temperature changes and its repetitive use, making it more efficient than a free enzyme^{7,28}.

The poly-ionic biopolymer chitosan is essential to form larger particles and contributes to a stronger bond between the enzyme aggregates to obtain stable CLEAs^{12,33,34}. However, it becomes a part of the CLEAs non-catalytic structure, resulting in diluting the enzyme activity^{9,34}. Immobilized enzyme resulting from the origin CLEAs (without co-aggregate addition) was claimed as almost 100% undiluted, containing only enzyme and a tiny fraction of crosslinker⁷. Therefore, the dilution of CLEAs-CCA could be defined as the ratio of the bound enzyme and the quantity of Chitosan used. The addition of Chitosan as co-aggregate contributed to the enzyme dilution of 44.85%. However, this dilution effect is much lower than that of the matrix-bound immobilized enzyme, which causes the enzyme dilution up to 99%^{7,28}.

The thermal stability of the immobilized enzyme influences its industrial application⁴⁰. The rigid structure of CLEAs obtained by crosslinking is the reason for their increased stability^{7,8,14,18}. In addition, the thermal stability of the CLEAs can be generated by the effect of enzyme coating by Chitosan¹⁷. In this study, chitosan solution was prepared at pH 5.5 (pKa of Chitosan is around 6.5); therefore, Chitosan has a low negative charge. Electrostatic interaction and/or hydrogen bonding between the N-acetyl-D-glucosamine hydroxyl group of Chitosan and positively charged amino acid residues on the enzyme surface may occur, thereby increasing the thermal stability of CLEAs¹⁵. In addition, during the conversion CPC to 7-ACA, the pH of the solution tends to decrease due to the by-products accumulation, resulting in a decrease in the hydrolysis rate and enzyme stability⁴¹. The CLEAs-CCA showed good stability at low pH up to 4.5; therefore, product inhibition related to low pH could be minimized.

Conclusions

The maximum CLEAs-CCA activity of 85.91 26 Ug⁻¹ was obtained with the optimized immobilization conditions: glutaraldehyde concentration 0.2% (v/v) and crosslinking time 119 minutes. Chitosan as co-aggregate increases the number of crosslinks, which is indicated by the formation of larger particles size and increasing CLEAs-CCA stability. CLEAs-CCA immobilization also succeeded in reducing enzyme dilution up to 55.15%.

Author Contributions

Conceptualization and methodology, J.J. and A.W.; performing experiments and analyzing data, J.J.; writing—original draft preparation, J.J.; writing—review and editing, A.W. and K.S.; supervision, A.W. and K.S. All authors have read and

agreed to the published version of the manuscript.

Funding

This research received no external funding.

Acknowledgments

The author thanks BRIN, Indonesia, to facilitate these experiments.

Conflicts of Interest

The authors declare no conflict of interest.

Bibliographic references

- Selvi, A.; Das, D.; Das, N. Potentiality of yeast *Candida* sp. SMN04 for degradation of cefdinir, a cephalosporin antibiotic: kinetics, enzyme analysis and biodegradation pathway. *Environ. Technol* 2015, 36, 3112-24. doi: 10.1080/09593330.2015.1054318.
- Collignon, P.J.; Conly, J.M.; Andremont, A.; McEwen, S.A.; Aida-Kane, A. World Health Organization ranking of antimicrobials according to their importance in human medicine: A critical step for developing risk management strategies to control antimicrobial resistance from food animal production. *Clin. Infect. Dis* 2016, 63, 1087-93. doi: 10.1093/cid/ciw475.
- Pollegioni, L.; Rosini, E.; Molla, G. Cephalosporin C acylase: dream and/or reality. *Appl. Microbiol. Biotechnol* 2013, 97, 2341-55. doi: 10.1007/s00253-013-4741-0.
- Zhu, X.; Luo, H.; Chang, Y.; Su, H.; Li, Q.; Yu, H.; Shen, Z. Characteristic of immobilized cephalosporin C acylase and its application in one-step enzymatic conversion of cephalosporin C to 7-aminocephalosporanic acid. *World J. Microb. Biot* 2011, 27, 823-9. doi: 10.1007/s11274-010-0523-3.
- Gröger, H.; Pieper, M.; König, B.; Bayer, T.; Schleich, H. Industrial landmarks in the development of sustainable production processes for the β -lactam antibiotic key intermediate 7-aminocephalosporanic acid (7-ACA). *Sustain. Chem. Pharm* 2017, 5, 72-9. doi: 10.1016/j.scp.2016.08.001.
- Mateo, C.; Palomo, J.M.; Fernandez-Lorente, G.; Guisan, J.M.; Fernandez-Lafuente, R. Improvement of enzyme activity, stability and selectivity via immobilization techniques. *Enzyme Microb. Technol* 2007, 40, 1451-63. doi: 10.1016/j.enzmictec.2007.01.018.
- Cao, L.; van Langen, L.; Sheldon, R.A. Immobilised enzymes: carrier-bound or carrier-free? *Curr. Opin. Biotechnol* 2003, 14, 387-94. doi: 10.1016/s0958-1669(03)00096-x.
- Velasco-Lozano, S.; López-Gallego, F.; Mateos-Díaz, J.C.; Favela-Torres, E. Cross-linked enzyme aggregates (CLEA) in enzyme improvement – a review. *Biocatalysis* 2016, 1, 166-77. doi: 10.1515/boca-2015-0012.
- Wilson, L.; Illanes, A.; Soler, L.; Henríquez, M.J. Effect of the degree of crosslinking on the properties of different CLEAs of penicillin acylase. *Process Biochem* 2009, 44, 322-6. doi: 10.1016/j.procbio.2008.11.010.
- Razib, M.S.M.; Rahman, R.N.Z.R.A.; Shariff, F.M.; Ali, M.S.M. Biochemical and structural characterization of crosslinked enzyme aggregates (CLEAs) of organic solvent tolerant protease. *Catalysts* 2020, 10, 55-70. doi: 10.3390/catal10010055.
- Talekar, S.; Joshi, A.; Joshi, G.; Kamat, P.; Haripurkar, R.; Kamble, S. Parameters in preparation and characterization of cross linked enzyme aggregates (CLEAs). *RSC Adv.* 2013, 3, 12485. doi: 10.1039/c3ra40818c.
- Ye, J.; Li, A.; Chu, T.; Pan, X.; He, B. Poly-lysine supported cross-linked enzyme aggregates of penicillin G acylase and its application in synthesis of beta-lactam antibiotics. *Int. J. Biol. Macromol.* 2019, 140, 423-8. doi: 10.1016/j.ijbiomac.2019.08.021.
- Shah, S.; Sharma, A.; Gupta, M.N. Preparation of crosslinked enzyme aggregates by using bovine serum albumin as a proteic feeder. *Anal. Biochem* 2006, 351, 207-13. doi: 10.1016/j.ab.2006.01.028.
- Mageed, H.; Ezz, N.; Radwan, R. Bio-inspired trypsin-chitosan crosslinked enzyme aggregates: a versatile approach for stabilization through carrier-free immobilization. *BioTechnologia* 2019, 100, 301-9. doi: 10.5114/bta.2019.87589.
- Grajales-Hernandez, D.; Armendariz-Ruiz, M.; Velasco-Lozano, S.; Lopez-Gallego, F.; Mateos-Diaz, J.C. Chitosan-based CLEAs from *Aspergillus niger* type A feruloyl esterase: high-productivity biocatalyst for alkyl ferulate synthesis. *Appl. Microbiol. Biotechnol* 2020, 104, 10033-45. doi: 10.1007/s00253-020-10907-2.
- Wibisana, A.; Sumaryono, W.; Mirawati, S.T.; Pudjilestari, S.P. Optimization of surfactin production by *Bacillus amyloliquefaciens* MD4-12 using response surface methodology. *Microbiol. Indones* 2015, 9, 120-8. doi: 10.5454/mi.9.3.4.
- Arsenault, A.; Cabana, H.; Jones, J.P. Laccase-based CLEAs: Chitosan as a novel crosslinking agent. *Enzyme Res* 2011, 2011, 376015. doi: 10.4061/2011/376015.
- Mahmod, S.S.; Yusof, F.; Jami, M.S.; Khanahmadi, S. Optimizing the preparation conditions and characterization of a stable and recyclable crosslinked enzyme aggregate (CLEA)-protease. *Bioresour. Bioprocess* 2016, 3, 3-13. doi: 10.1186/s40643-015-0081-5.
- Martius, E.; Wibisana, A.; Ardiani, Y. The optimization of soluble cephalosporin C acylase expression in *E. coli*. *Int. J. Eng. Sci* 2018, 7, 29-34. doi: 10.9790/1813-0703012934.
- Wingfield, P.T. Preparation of soluble proteins from *Escherichia coli*. *Curr. Protoc. Protein Sci* 2015, 78, 6.2.1-6.2.22. doi: 10.1002/0471140864.ps0602s78.
- Fernandez-Arrojo, L.; Santos-Moriano, P.; Rodriguez-Colinas, B.; Ballesteros, A.O.; Plou, F.J. Micro-scale procedure for enzyme immobilization screening and operational stability assays. *Biotechnol. Lett* 2015, 37, 1593-600. doi: 10.1007/s10529-015-1835-z.
- Li, R.; Lin, D.K.J. Variable selection for screening experiments. *Qual. Technol. Quant. Manag* 2009, 6, 271-80. doi: 10.1080/16843703.2009.11673199.
- Gunst, R.F.; Mason, R.L. Fractional factorial design. *WIREs Comp. Stats* 2009, 1, 234-44. doi: 10.1002/wics.027.
- Chen, H.; Zhang, J.; Dang, Y.; Shu, G. Optimization for immobilization of β -galactosidase using plackett-burman and steepest ascent. *J. Chem. Pharm* 2014, 6, 612-6. doi: 10.1007/s10529-015-1835-z.
- Sheldon, R.A.; van Pelt, S. Enzyme immobilisation in biocatalysis: why, what and how. *Chem. Soc. Rev* 2013, 42, 6223-35. doi: 10.1039/c3cs60075k.
- Wei, Y.; Luo, H.; Chang, Y.; Yu, H.; Shen, Z. Reversible immobilization of cephalosporin C acylase on epoxy supports coated with polyethyleneimine. *Biocatal. Biotransformation* 2016, 33, 250-9. doi: 10.3109/10242422.2016.1168814.
- Rajendhran, J.; Gunasekaran, P. Application of crosslinked enzyme aggregates of *Bacillus badius* penicillin G acylase for the production of 6-aminopenicillanic acid. *Lett. Appl. Microbiol* 2007, 44, 43-9. doi: 10.1111/j.1472-765X.2006.02043.x.
- Sheldon, R.A. CLEAs, combi-CLEAs and 'smart' magnetic CLEAs: Biocatalysis in a bio-based economy. *Catalysts* 2019, 9, 261-91. doi: 10.3390/catal9030261.
- Sonawane, V.C. Enzymatic modifications of cephalosporins by cephalosporin acylase and other enzymes. *Crit. Rev. Biotechnol* 2006, 26, 95-120. doi: 10.1080/07388550600718630.
- Campanella, B.; Bramanti, E. Detection of proteins by hyphenated techniques with endogenous metal tags and metal chemical labelling. *Analyst* 2014, 139, 4124-53. doi: 10.1039/c4an00722k.
- Sheldon, R.A. Enzyme immobilization: The quest for optimum performance. *Adv. Synth. Catal* 2007, 349, 1289-307. doi: 10.1002/adsc.200700082.
- Luo, H.; Zhao, H.; Chang, Y.; Wang, Q.; Yu, H.; Shen, Z. Oriented immobilization and characterization of a poly-lysine-tagged cephalosporin C acylase on glyoxyl agarose support. *Appl. Biochem. Biotechnol* 2015, 175, 2114-23. doi: 10.1007/s12010-014-1411-3.
- Barbosa, O.; Ortiz, C.; Berenguer-Murcia, Á.; Torres, R.; Rodrigues, R.C.; Fernandez-Lafuente, R. Glutaraldehyde in bio-catalysts design: a useful crosslinker and a versatile tool in enzyme immobilization. *RSC Adv* 2014, 4, 1583-600. doi: 10.1039/c3ra45991h.

34. Wahab, M.K.H.A.; El-Enshasy, H.A.; Bakar, F.D.A.; Murad, A.M.A.; Jahim, J.M.; Illias, R.M. Improvement of crosslinking and stability on crosslinked enzyme aggregate (CLEA)-xylanase by protein surface engineering. *Process Biochem* 2019, 86, 40-9. doi: 10.1016/j.procbio.2019.07.017.
35. Migneault, I.; Dartiguenave, C.; Bertrand, M.J.; Waldron, K.C. Glutaraldehyde: Behavior in aqueous solution reaction with protein, and application to enzyme crosslinking. *BioTechniques* 2004, 37, 790-802. doi: 10.2144/04375RV01.
36. Mateo, C.; Palomo, J.M.; van Langen, L.M.; van Rantwijk, F.; Sheldon, R.A. A new, mild crosslinking methodology to prepare cross-linked enzyme aggregates. *Biotechnol. Bioeng* 2004, 86, 273-6. doi: 10.1002/bit.20033.
37. Velasco-Lozano, S.; Lopez-Gallego, F.; Vazquez-Duhalt, R.; Mateos-Diaz, J.C.; Guisan, J.M.; Favela-Torres, E. Carrier-free immobilization of lipase from *Candida rugosa* with polyethyleneimines by carboxyl-activated crosslinking. *Biomacromolecules* 2014, 15, 1896-903. doi: 10.1021/bm500333v.
38. He, H.; Wei, Y.; Luo, H.; Li, X.; Wang, X.; Liang, C.; Chang, Y.; Yu, H.; Shen, Z. Immobilization and stabilization of cephalosporin C acylase on aminated support by crosslinking with glutaraldehyde and further modifying with aminated macromolecules. *Biotechnol. Prog* 2015, 31, 387-95. doi: 10.1002/btpr.2044.
39. Garcia-Galan, C.; Berenguer-Murcia, Á.; Fernandez-Lafuente, R.; Rodrigues, R.C. Potential of different enzyme immobilization strategies to improve enzyme performance. *Adv. Synth. Catal* 2011, 353, 2885-904. doi: 10.1002/adsc.201100534.
40. Chapman, J.; Ismail, A.; Dinu, C. Industrial applications of enzymes: Recent advances, techniques, and outlooks. *Catalysts* 2018, 8, 238-65. doi: 10.3390/catal8060238.
41. Xiao, Y.; Huo, X.; Qian, Y.; Zhang, Y.; Chen, G.; Ouyang, P.; Lin, Z. Engineering of a CPC acylase using a facile pH indicator assay. *J. Ind. Microbiol. Biotechnol* 2014, 41, 1617-25. doi: 10.1007/s10295-014-1501-9.

ARTICLE / INVESTIGACIÓN

Assessment of genetic fidelity of lacy tree philodendron (*Philodendron bipinnatifidum* Schott ex Endl.) micro propagated plants

Mona S. Alwahibi¹, Asma Alhussein Alawaadh¹, Yaser Hassan Dewir^{2*}, Dina A. Soliman¹, and Mayada Kadry Seliem³

DOI. 10.21931/RB/2022.07.01.10

¹ Department of Botany and Microbiology, College of Science, King Saud University, Riyadh 11495, Saudi Arabia.² Plant Production Department, College of Food and Agriculture Sciences, King Saud University, Riyadh 11451, Saudi Arabia and Department of Horticulture, Faculty of Agriculture, Kafrelsheikh University, Kafr El-Sheikh 33516, Egypt.³ Ornamental and Floriculture Department, Horticulture Research Institute, Antoniadis, Alexandria 21599, Egypt.
Corresponding author: ydewir@ksu.edu.sa

Abstract: Tissue culture is a potent means for producing clonally propagated plants. However, genetically identical regenerants are of great concern due to their economic consequences. Therefore, polymerase chain reaction (PCR)-based molecular markers are employed to detect somaclonal variations. In this study, the genetic fidelity of *in vitro* raised *Philodendron bipinnatifidum* clones, and their mother plant was tested using 11 randomly amplified polymorphic DNA (RAPD) markers. The RAPD decamers produced 92 amplicons with 8.4 bands ranging from 260-5000 bp. The bands varied from one to fifteen for primer 8 and primer 7, respectively. The genetic similarity between the micro propagated plantlets and mother plant of *P. bipinnatifidum* was nearly 100%, assuring uniformity and true-to-type regenerated plantlets for this commercially crucial ornamental plant.

Key words: Araceae, genetic fidelity, micropropagation, polymorphism, RAPD analysis.

Introduction

Rapid clonal propagation is one of the most extensively used approaches of biotechnology. *In vitro* plants undergo several subculture cycles before their rooting, and acclimatization and cytogenetic variations may occur in this long process¹. Somaclonal variations can be a valuable source for new genetic material² and might be advantageous for crop improvement³. However, its occurrence in micro propagated plants results in undesirable plant off-types, limiting its applications in the tissue culture industry. Therefore, the most critical concern has been the maintenance of genetic uniformity and the production of true-to-type plants. The influence of *in vitro* culture conditions i.e., culture media, type of explant, and subculture cycles, may lead to genomic variation in the regenerated plantlets. Therefore, assessment of genetic stability is a prerequisite while performing micropropagation⁴.

Several methods were available to assess regenerated plants' genetic fidelity, such as morphological characteristics, cytological and flow cytometry analysis⁵. DNA based molecular markers emerged as the most suitable genetic tools to determine the genetic variation among regenerated plants⁶. Molecular markers such as randomly amplified polymorphic DNA (RAPD)⁷, amplified fragment length polymorphism (AFLP)⁸, simple sequence repeat (SSR)⁹ and inter simple sequence repeats (ISSR)^{10,11} are used for determining the genetic fidelity of micro propagated plants. Cost-effectiveness is a major checkpoint in micropropagation. Because of the simplicity and cost effectiveness of RAPD technique, it is used for genetic stability analysis, amplifying the different regions of the genome¹² in several plant species^{4,6,13,14}.

Lacy tree philodendron (*Philodendron bipinnatifidum*

Schott Ex Endl.), formerly known as *P. selloum* K. Koch, is a self-heading ornamental plant species that can reach heights of 4–5 m and possesses deeply cut, green to dark green leaves that can grow up to 1 m in length. Conventional propagation does not encourage the multiplication of the species¹⁵. Therefore, *in vitro* propagation methods can be utilized to facilitate the continuous generation of high-quantity and high-quality plant materials compared with traditional vegetative propagation. Our previous report established an efficient micropropagation protocol for lacy tree philodendron through axillary shoot regeneration with a 100% rooting and acclimatization¹⁵. Therefore, the objective of this study was to assess the genetic fidelity of the regenerants to assure the production of genetically identical plantlets.

Materials and methods

Plant material

The mother plant of *P. bipinnatifidum* (Figure 1 A) and ten micro propagated plantlets through axillary shoot proliferation¹⁵ were randomly selected and used as plant material in this study. The axillary shoots were multiplied on MS medium¹⁶ that contained 6-benzylaminopurine (1 mg·L⁻¹) and indole-3-butyric acid (0.5 mg·L⁻¹) for 6 wks (Figure 1 B). These *in vitro* shoots were kept in our laboratory for nine subculture cycles, *in vitro* plantlets rooted on MS medium that contained naphthalene acetic acid (1 mg·L⁻¹) for 6 wks (Figure 1 C) and acclimatized in a 1:1 (v:v) mixture of peat moss and perlite for

Citation: Alwahibi MS, Alawaadh AA, Dewir YH, Soliman DA, and Seliem MK. Assessment of genetic fidelity of lacy tree philodendron (*Philodendron bipinnatifidum* Schott ex Endl.) micro propagated plants. *Revis Bionatura* 2022;7(1). 10. <http://dx.doi.org/10.21931/RB/2022.07.01.10>

Received: 17 June 2021 / **Accepted:** 20 August 2021 / **Published:** 15 February 2022

Publisher's Note: Bionatura stays neutral with regard to jurisdictional claims in published maps and institutional affiliations.

Copyright: © 2022 by the authors. Submitted for possible open access publication under the terms and conditions of the Creative Commons Attribution (CC BY) license (<https://creativecommons.org/licenses/by/4.0/>).



30 d (Figure 1 D) as described by Alawaadh *et al.*¹⁵. Young fresh leaves of the mother plant and clonal regenerants were thoroughly cleaned, washed with sterile distilled water, and kept in liquid nitrogen until molecular analysis.

Genomic DNA isolation

Genomic DNA was isolated from fresh leaves of both mother plants and micro propagated plants by using the cetyltrimethylammonium bromide (CTAB) method¹⁷. Approximately 100-150 mg of leaves were ground using 600 μ L of pre-heated (65°C) extraction buffer (2% CTAB, 20 mM EDTA, 100 mM Tris-HCl, 1.4 M NaCl, 2% polyvinylpyrrolidone (PVP), 0.2% mercaptoethanol), transferred to a centrifuge tube (2 mL) and incubated for 30 min in a 65°C water bath, the samples were inverted every 5 min. 600 μ L of chloroform-isoamyl alcohol (24: 1) was added and mixed by inverting the tubes carefully 10 times, and the cells were centrifuged at 12000 rpm for 10 min at room temperature. The supernatant was collected and carefully mixed with a two-thirds volume of ice-cold isopropanol, and the DNA samples were collected by centrifuging for 10 min. RNaseA (10 μ g/ml) was added to the 50 μ L of TE buffer (10 mM Tris and 0.1 mM EDTA) before dissolving the DNA to remove any RNA in the preparation, and the mixture was incubated at 37 °C for 30 min. 100 μ L and 750 μ L of 3 M sodium acetate and absolute ice-cold ethanol were added. The DNA was collected by high-speed centrifugation for 10 min, and then carefully washed with ice-cold absolute and 70% ethanol and centrifuged at 12000 rpm for 10 min. Finally, the samples were dried at room temperature and dissolved in 50-100 μ L of TE buffer. The quality and concentration of DNA were determined by EMLEN photometer P330.

PCR conditions

11 decamer RAPD primers (Macrogen Korea) were used for DNA amplification. PCR reaction was carried out in a volume of 20 μ L. PCR was performed as follows: 94°C for 5 min; followed by 35 cycles of 94°C for 1 min, specific annealing temperature (Ta) according to the primer sequence for 30 sec and 72°C for 3 min and the final extension step at 72°C for 10 min. Amplification was carried out in MJ Mini Bio RAD, thermal cycler in 25 μ L reaction volume containing the following reagents: 1.0 μ L of dNTPs (10 mM), 1.0 μ L of MgCl₂ (25 mM), 5 μ L of 10x buffer, 1.0 μ L of primer (10 pmol), 1.0 μ L of DNA (25 ng μ L⁻¹), 0.3 μ L of taq polymerase (5 u μ L⁻¹) and 15.7 dd.H₂O.

Gel electrophoresis and genetic analysis

The RAPD products were electrophoresed in 1.5 % agarose gel containing Red safe dye in TAE buffer (40 mM Tris-acetate, 20 mM glacial acetic acid, 1 mM EDTA, pH 7) at 75 V. The gels were documented using a gel documentation system (UVITEC, UK) and according to an analysis by Phoretix program 1D gel analysis software version 4.01. Two repeats were performed to confirm the results. The bands obtained by scoring the RAPD profiles were treated as binary characters and coded accordingly (presence = 1, absence = 0). The genotypes showing similarity in their RAPD characteristics were grouped using UPGMA (Unweighted Paired Group with Arithmetic Average) The SPSS-10 package was used for statistical analysis.

Results

Assessment of genetic fidelity was performed on the *P. bipinnatifidum* micro propagated plantlets using RAPD analysis

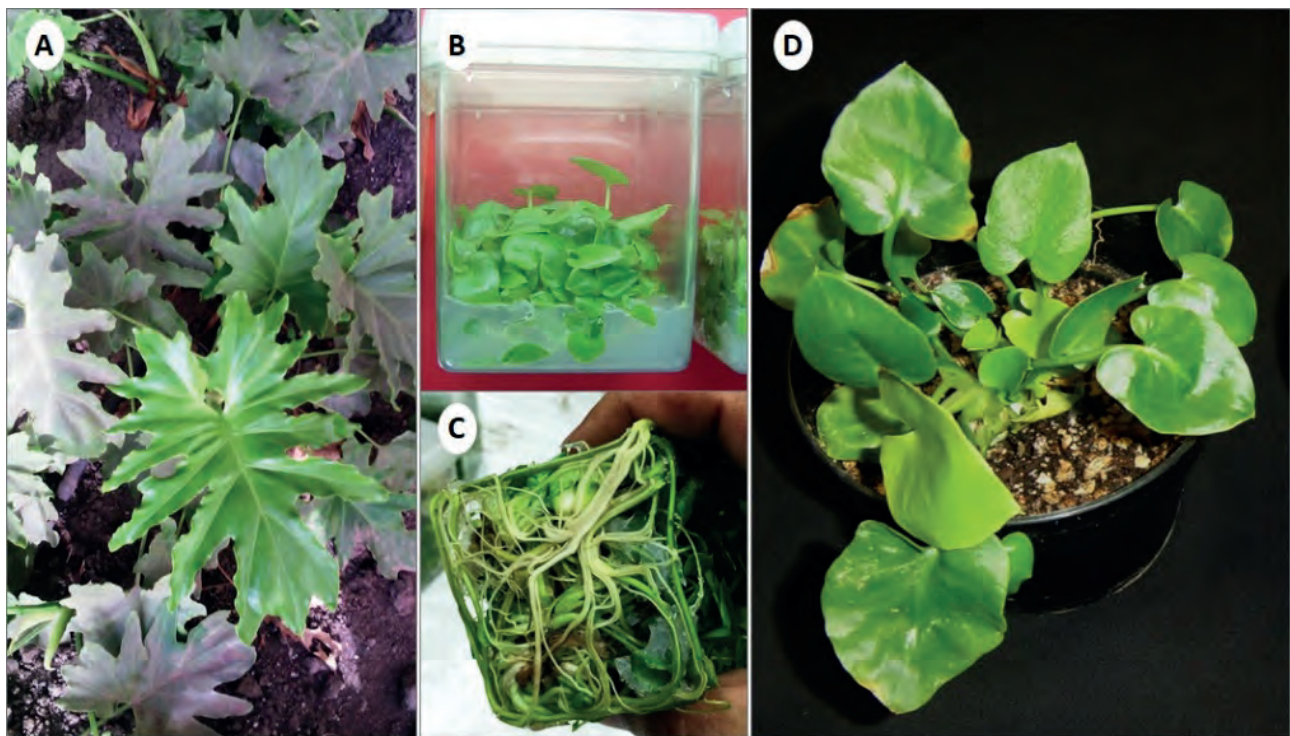


Figure 1. Micropropagation of *Philodendron bipinnatifidum* (A) Mother plant, (B) Shoot multiplication in gelled culture, full-strength Murashige and Skoog medium that contained 6-benzylaminopurine (1 mg·L⁻¹) and indole-3-butyric acid (0.5 mg·L⁻¹), after 6 wks of culture, (C) In vitro plantlets rooted on Murashige and Skoog medium that contained naphthalene acetic acid (1 mg·L⁻¹), after 6 wks of culture, (D) Acclimatized plantlet in a 1:1 (v:v) mixture of peat moss and perlite, after 30 d. (Unpublished photographs).

Primers code	Primer sequences (5'-3')	No. of scorable band per primer	Size range for amplified products	No. of monomorphic bands	Polymorphism (%)
1	CAGGCCTTTC	11	500-3000	11	0
2	AGTCAGCCAC	8	500-2500	8	0
3	AATCGGCTG	4	500-1500	4	0
4	AGGGGTCTTG	5	400-1900	5	0
5	GGGTAACGCC	8	300-1500	8	0
6	TCGCGATAG	11	350-5000	10	9.1
7	CAGCACCCAC	15	270-1800	15	0
8	TTCCGAACCC	1	1000	1	0
9	AGCCAGCGAA	7	260-1500	7	0
10	GACCGCTTGT	8	500-2000	8	0
11	GTGCAACGTG	14	400-3000	12	14.3
Total		92		89	3.3



Table 1. RAPD primers were used for testing the genetic fidelity of *Philodendron* micro propagated plants.

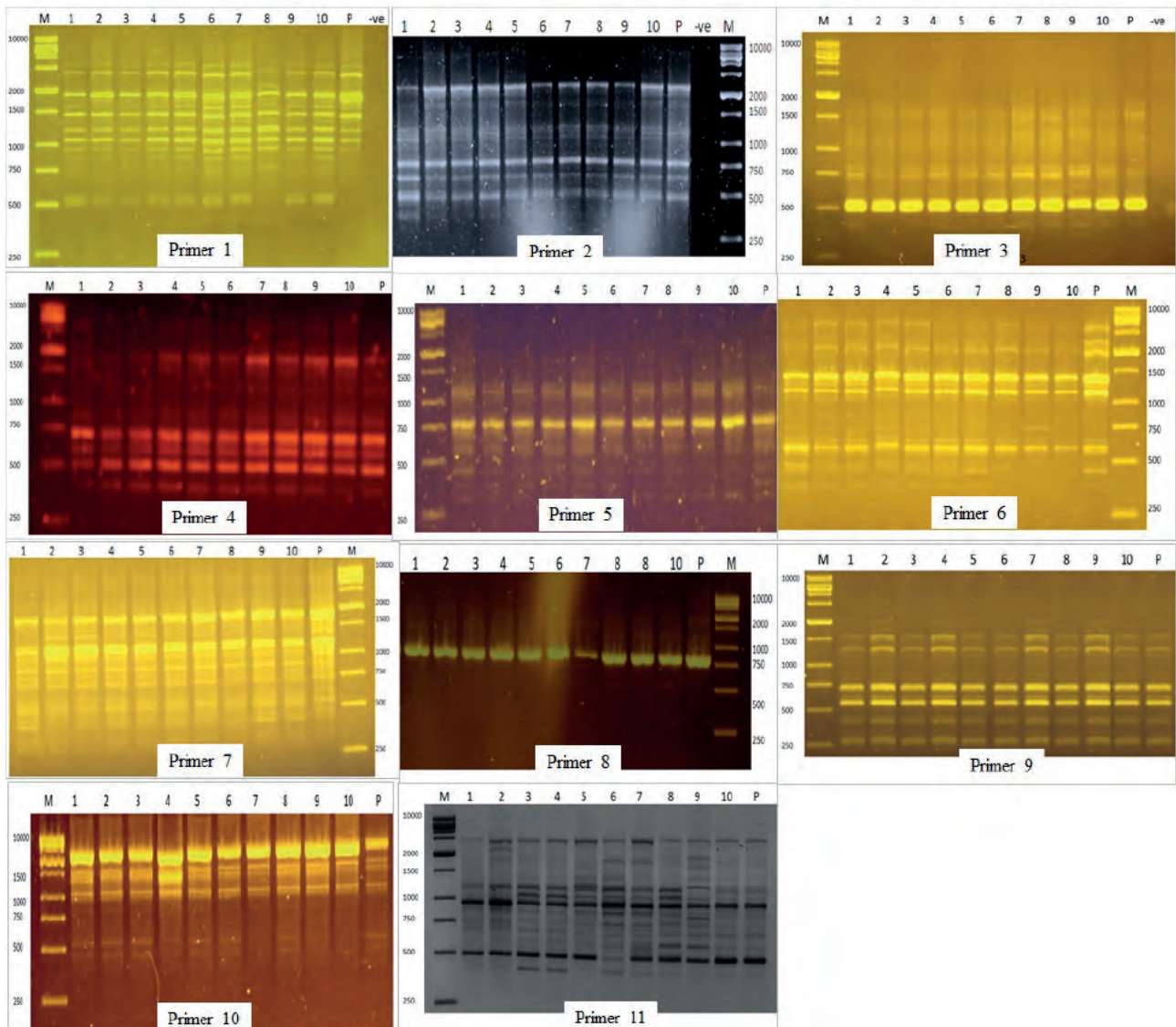


Figure 2. DNA Amplification pattern obtained with RAPD primers. Lane M- DNA ladder; Lane-P D.N.A. from mother plant; Lane 1-10 DNA from micropropagated plants.

	Mother plant	Clone 1	Clone 2	Clone 3	Clone 4	Clone 5	Clone 6	Clone 7	Clone 8	Clone 9	Clone 10
Clone 1	1.00	1.00	0.99	0.99	0.99	0.99	0.99	0.99	0.99	0.99	1.00
Clone 2	0.99	0.99	1.00	0.98	0.98	0.98	0.98	0.98	0.98	0.98	0.99
Clone 3	0.99	0.99	0.98	1.00	1.00	1.00	1.00	1.00	1.00	0.98	0.99
Clone 4	0.99	0.99	0.98	1.00	1.00	1.00	1.00	1.00	1.00	0.98	0.99
Clone 5	0.99	0.99	0.98	1.00	1.00	1.00	1.00	1.00	1.00	0.98	0.99
Clone 6	0.99	0.99	0.98	1.00	1.00	1.00	1.00	1.00	1.00	0.98	0.99
Clone 7	0.99	0.99	0.98	1.00	1.00	1.00	1.00	1.00	1.00	0.98	0.99
Clone 8	0.99	0.99	0.98	1.00	1.00	1.00	1.00	1.00	1.00	0.98	0.99
Clone 9	0.99	0.99	0.98	0.98	0.98	0.98	0.98	0.98	0.98	1.00	0.99

Table 2. Similarity coefficient among the screened plants based on RAPD analysis.

with 11 RAPD primers (Table 1; Figure 2). The selected primers gave 92 scorable bands with an average of 5.8 bands ranging from 260-5000 bp. The bands varied from 1 to 15 for primer 8 and primer 7, respectively.

RAPD amplification pattern obtained with all primers except for primers 6 and 11 revealed that all bands produced by micro propagated plants were monomorphic and similar to that of the mother plant. Primer 6 amplified 10 monomorphic bands and one unique polymorphic band (750 bp) produced by *in vitro* propagated clone 9. Primer 11 produced 14 scorable bands, out of which 12 were monomorphic while two were polymorphic. A unique band with a molecular size of 2400 bp was produced only in propagated clone 2, whereas micro propagated clones 3,4,5,6,7,8 produced a band with a molecular size of 1000 bp. Of the 11 primers analyzed, nine primers showed 0% polymorphism, while primers 6 and 11 showed 9.1% and 14.3% polymorphism, respectively. The genetic similarity between the micro propagated plantlets and the mother plants ranged from 0.98 to 1.00, with an average of 0.99 (Table 2).

Discussion

High genetic fidelity and true-to-type clones are critical for commercial micropropagation to maintain the essential characteristics of the mother plant¹. Phenotypic variations such as abnormal leaf shape and dwarf growth indicate off-type clones. However, the absence of these morphological abnormalities does not guarantee true-to-type regenerated plantlets; therefore, molecular markers should be utilized to assure their clonal fidelity. It has been reported that although *in vitro* regenerated *Philodendron micans* plantlets phenotypically resembled mother plants, they showed a high frequency of ploidy change suggests the occurrence of somaclonal variation¹⁸. The author indicated that analysis of 20 randomly selected *Philodendron micans* plantlets using DNA flow cytometry showed that two were mixoploid. RAPD profiles of the randomly selected clones of *Philodendron* 'Xanadu' different ages compared to the mother plant were identical, thus assuring a genetic fidelity-maintained protocol for this commercially important plant¹⁹. RAPD molecular marker was used to assess genetic fidelity in other micro propagated plant species belonging to the Araceae family, such as *Aglaonema* 'Valentine'¹⁷ where all tested plantlets were highly uniform or identical to the mother plant. Conversely, for *Anthurium Andreanum* Bicolour 'Agniho-tri', RAPD analysis revealed variations in band pattern of the regenerated plantlets²⁰.

Genetic variation is a common phenomenon observed in

plants regenerated from tissue cultures³. Various factors such as genotype, explant type, culture periods and growth regulators combinations and concentrations may disturb the internal polarity and physiology of the explants^{21,22} and could also influence the stability of tissue cultured plants^{22,23}. Therefore, limiting the number of subculture cycles could maintain clonal characteristics. For example, DNA polymorphism (20%) was reported in protocorm like-bodies of *Phalaenopsis gigantea* after 20 wks of culture on a medium containing 4.5 μM thidiazuron and 65.5 μM chitosan while reducing the culture period to 16 wks resulted in no variations²⁴. However, the amenability to *in vitro* induced mutagenic effect is species-dependent. Borsari *et al.*²⁵ reported no polymorphism in micro propagated blackberry plants (*Rubus fruticosus*) for 12 subcultures during 30 months of *in vitro* multiplication.

Conclusions

The genetic fidelity of micropropagated *P. bipinnatifidum* clones was confirmed by using PCR-based RAPD analysis. Polymorphism detected among these clones was negligible. The micropropagation protocol can successfully be employed for commercial application without any risk of genetic instability.

Author Contributions

Conceptualization, MSA, AAA and YHD; methodology, MSA and AAA; software, MSA and AAA; validation, YHD, DAS and MKS; formal analysis, MSA, AAA and YHD; investigation, MSA and AAA; resources, MSA and YHD; data curation, MSA and AAA; writing—original draft preparation, MSA, AAA and YHD; writing—review and editing, MSA, AAA, YHD; DAS and MKS; visualization, DAS and MKS; project administration, MSA and YHD; funding acquisition, MSA. All authors have read and agreed to the published version of the manuscript.

Funding

This research was funded by the Deanship of Scientific Research at King Saud University for funding this work through research group NO (RGP-1435-086).

Institutional Review Board Statement

Not applicable.

Informed Consent Statement

Not applicable.

Data Availability Statement

All data are presented within the article.

Acknowledgments

The authors extend their appreciation to the Deanship of Scientific Research at King Saud University for funding this work through research group NO (RGP-1435-086).

Conflicts of Interest

The authors declare no conflict of interest. The funders had no role in the design of the study; in the collection, analyses, or interpretation of data; in the writing of the manuscript, or in the decision to publish the results.

Bibliographic references

- Dewir YH, Nurmansyah, Naidoo, Y, Teixeira da Silva, JA. Thidiazuron-induced abnormalities in plant tissue cultures. *Plant Cell Reports*. 2018. 37: 1451-1470.
- Podwyszyńska M, Niedoba, K, Korbin, M, Marasek, A. Somaclonal variation in micropropagated tulips determined by phenotype and DNA markers. *Acta Horticulturae*. 2006. 714: 211-220.
- Krishna H, Alizadeh, M, Singh, D, Singh, U, Chauhan, N, Eftekhari, M, Sadh, RK Somaclonal variations and their applications in horticultural crops improvement. *3 Biotech*. 2016. 6: 54.
- Rai MK, Phulwaria, M, Harish, Gupta, AK, Shekhawat, NS, Jaiswal, U. Genetic homogeneity of guava plants derived from somatic embryogenesis using SSR and ISSR markers. *Plant Cell, Tissue and Organ Culture*. 2012. 111: 259-264.
- Kanchanapoom K, Chunui, P, Kanchanapoom, K. Micropropagation of *Anubias barteri* var. nana from shoot tip culture and the analysis of ploidy stability. *Notulae Botanicae Horti Agrobotanici Cluj-Napoca*. 2012. 40: 148-151.
- Sharma S, Sudheer Pamidimarri, D.V.N., Vijay Anand, KG, Reddy, MP. Assessment of genetic stability in micropropagules of *Jatropha curcas* genotypes by RAPD and AFLP analysis. *Industrial Crops and Products*. 2011. 34: 1003-1009.
- El-Mahrouk ME, Dewir, YH, Naidoo, Y. Micropropagation and genetic fidelity of the regenerants of *Aglaonema 'valentine'* using randomly amplified polymorphic D.N.A. *HortScience*. 2016. 51: 398-402.
- Dann AL, Wilson, CR. Comparative assessment of genetic and epigenetic variation among regenerants of potato (*Solanum tuberosum*) derived from long-term nodal tissue-culture and cell selection. *Plant Cell Reports* 2011. 30: 631-639.
- Stimela T, Kasili, RW, Mamati, EG. Pomegranate micropropagation, callogenesis and genetic integrity assessment using simple sequence repeat markers. *Journal of Agricultural Science* 2019. 11: 237-250.
- Kumar Mishra A, Nath Tiwari, K, Mishra, P, Kumar Tiwari, S, Kumar Mishra, S, Singh, J. Factors affecting the efficiency of in vitro regeneration from seedling-derived nodal explants of *Nyctanthes arbortristis* L. and evaluation of genetic fidelity. *Plant Biosystems* 2020. 154: 197-205.
- Vemula S, Koppula, T, Jogam, P, Mohammed, M. In vitro high frequency multiplication and assessment of genetic fidelity of *Corallocarpus epigaeus*: An endangered medicinal plant. *Vegetos*. 2020. 33: 63-73.
- Asthana P, Jaiswal, VS, Jaiswal, U. Micropropagation of *Sapindus trifoliatus* L. and assessment of genetic fidelity of micropropagated plants using RAPD analysis. *Acta Physiologiae*. 2011. 33:1821-1829.
- Ahmad, N, Anis, M. An efficient in vitro process for recurrent production of cloned plants of *Vitex negundo* L. *European Journal of Forest Research*. 2011. 130: 135-144.
- Ramesh, M, Vijayakumar, KP, Karthikeyan, A, Pandian, SK. RAPD based genetic stability analysis among micropropagated, synthetic seed derived and hardened plants of *Bacopa monnieri* (L.): a threatened Indian medicinal herb. *Acta Physiologiae Plantarum* 2011. 33: 163-171.
- Alawaadh AA, Dewir, YH, Alwihibi, MS, Aldubai, AA, El-Hendawy, S, Naidoo, Y. Micropropagation of lacy tree *Philodendron* (*Philodendron bipinnatifidum* Schott ex Endl.). *HortScience* 2020. 55: 294-299.
- Murashige T, Skoog, F. A revised medium for rapid growth and bioassays with tobacco tissue cultures. *Physiologiae Plantarum* 1962. 15: 473-497.
- Doyle JJ, Doyle, JJ. Isolation of plant DNA from fresh tissue. *Focus* 1990. 12: 13-15.
- Xiong ZJ. Regeneration of *Philodendron Micans* K.koch through protocorm-like bodies and improvement of plant form using growth regulators. MSc thesis, University of Florida, USA. 2009.
- Gangopadhyay G, Bandyopadhyay, T, Gangopadhyay, SB, Mukherjee, KK. Luffa sponge - A unique matrix for tissue culture of philodendron. *Current Science* 2004. 86: 315-319.
- David A, Madappa, MB, Bopaiah, AK. RAPD Analysis of rapidly multiplied in vitro plantlets of *Anthurium andreaeanum* Bicolour Var *Agnihotri*. *IOSR-J.B.B*. 2015. 1: 10-14.
- Lal D, Singh, N. Mass multiplication of *Celastrus paniculatus* Willd an important medicinal plant under in vitro conditions using nodal segments. *Journal of American Science*. 2010. 6: 55-61.
- Premvaranon P, Vearasilp, S, Thanapornpoong, S, Karladee, D, Gorinstein, S. In vitro studies to produce double haploid in *Indica* hybrid rice. *Biologia* 2011. 66: 1074-1081.
- Bairu MW, Aremu, AO, van Staden, J. Somaclonal variation in plants: causes and detection methods. *Journal of Plant Growth Regulation*. 2011. 63: 147 - 173.
- Samarfard S, Kadir, MA, Kadzimin, SB, Saud, HM, Ravanfar, SA, Danaee, M. In vitro propagation and detection of somaclonal variation in *Phalaenopsis gigantea* as affected by chitosan and thidiazuron combinations. *HortScience* 2014. 49: 82-88
- Borsai O, Hârța, M, Szabo, K, Kelemen, CD, Andrean, FA, Codrea, MM, Clapa, D Evaluation of genetic fidelity of in vitro-propagated blackberry plants using RAPD and SRAP molecular markers. *Horticultural Science*. 2020. 47: 21-27.

ARTICLE / INVESTIGACIÓN

Major Genetic Determinants of Extended-Spectrum β -Lactamase (ESBL), Carbapenemase, Fosfomycin and Colistin Resistance in *Escherichia Coli* from Intensive Care Units

Ahmed Mhawesh^{1*}, Marwa khudair² and Omer N. Abbas³

DOI. 10.21931/RB/2022.07.01.11

¹ Dept. of Med. and Mol. Biotech., College of Biotechnology, Al-Nahrain University, Baghdad, Iraq.² DNA forensic Center for Research and Training, Al-Nahrain University, Baghdad, Iraq.³ Post Graduate, Dept. of Quality Control, Grain Board of Iraq, Ministry of Trade, Baghdad, Iraq.Corresponding author: alshammariahmed.a.m@gmail.com

Abstract: *Escherichia coli* (*E. coli*) strains placed in predominant nosocomial bacteria in intensive care units (ICUs), resulting in severe drug-resistant infections. Non-susceptibility to β -lactams and last-line drugs such as Fosfomycin and Colistin cause limited availability of infections eradication. The objective of this study included the determination of genes encoding extended-spectrum β -lactamase (ESBL), Carbapenemase, Colistin, and Fosfomycin resistance in clinical isolates of *E. coli* in ICUs. A total of 200 *E. coli* isolates were identified from ICU settings. The CTXM-1, SHV, IMP and OXA-48 genes were detected for β -lactamases using the polymerase chain reaction (PCR) technique. The fosA3 and mcr-1 and mcr-2 genes were also detected for resistance against Fosfomycin and Colistin. The CTX-M1, SHV, IMP and OXA-48 genes were detected in 60 (30%), 56 (28%), 28 (14%) and 4 (8%) of isolates. none of the *E. coli* isolates had the mcr-2 and fosA3 genes. Despite the existence of resistance genes to the third-generation antibiotics and Carbapenemase s, any isolates had genes for resistance to Fosfomycin and Colistin. More studies are needed to follow the resistance genes against last-resort antibiotics.

Key words: *Escherichia coli*, beta-lactamase, Fosfomycin, Colistin, ESBLs.

Introduction

Escherichia coli (*E. coli*) organism is known as the cause of wound and urinary infections, pneumonia, meningitis, sepsis, etc., so it is unique along with other members of the normal intestinal flora¹⁻⁵. This bacterium is facultatively anaerobic, oxidase negative and catalase-positive. *E. coli* is one of the most common microorganisms in the normal intestinal flora of humans and warm-blooded animals⁶⁻⁹. It colonizes in the host intestine a few days after birth. Today, the increasing spread of antibiotic-resistant bacteria is one of the problems of human society. Bacteria can be resistant to different types of antibiotics through different mechanisms¹⁰⁻¹³. One of the most common antibiotic resistance mechanisms, especially in Gram-negative bacteria, is the production of beta-lactamase enzymes. They are enzymes that cause the beta-lactam antibiotic ring's cleavage, such as Penicillins and cephalosporins, to inactivate these drugs, thereby protecting the bacteria against the drug.

Extended-spectrum beta-lactamase (ESBL) enzymes are beta-lactamases that hydrolyze Penicillins, first-, second-, and third-generation cephalosporins, as well as aztreonam, but do not affect carbapenems (such as imipenem) and cephamycins (such as cefoxitin)^{7,10,11}.

Despite the measures that have been taken in developing broad-spectrum antimicrobials, the emergence and spread of bacterial resistance is a concern^{1,3,6,10,11}. Gram-negative spp is one of the significant barriers to properly treating infectious diseases. Among them, those that produce ESBLs restricted

treatment of menacing infections. *E. coli* is a common species in the production of ESBL enzymes and is a major cause of nosocomial infections^{14,15}. On the other hand, resistance to carbapenems is a severe issue that is caused by various enzymes. Intensive care units are basic settings where the resistant strains spread. Major ESBL and Carbapenemase genes include CTX-M, SHV, TEM, IMP, VIM and OXA-48, which are spread with various resistance levels^{1,3,10,11,14}. The aim of our study included detection of genes encoding ESBLs (SHV and CTX-M1), Carbapenemase s (OXA-48 and IMP1), Colistin and Fosfomycin among *E. coli* from ICU settings.

Materials and methods

Bacterial isolates and patients

450 stool samples were initially collected and cultured onto the blood agar and MacConky media (MERK, Germany). Suspected colonies were subjected to the IMVIC test to identify them. These tests included indole production, motility in the SIM medium, vogues pro square and citrate consumption. 200 *E. coli* was determined using biochemical tests from ICU settings. Patients included 84 males and 112 females with an age mean of 52.21 years. All the patients had more than 24h of hospitalization.

Citation: Mhawesh A, khudair M, Abbas ON. Major Genetic Determinants of Extended-Spectrum β -Lactamase (ESBL), Carbapenemase, Fosfomycin and Colistin Resistance in *Escherichia Coli* from Intensive Care Units. *Revis Bionatura* 2022;7(1). 11. <http://dx.doi.org/10.21931/RB/2022.07.01.11>

Received: 20 June 2021 / **Accepted:** 10 November 2021 / **Published:** 15 February 2022

Publisher's Note: Bionatura stays neutral with regard to jurisdictional claims in published maps and institutional affiliations.

Copyright: © 2022 by the authors. Submitted for possible open access publication under the terms and conditions of the Creative Commons Attribution (CC BY) license (<https://creativecommons.org/licenses/by/4.0/>).



Phenotypic detection of ESBLs

The production of ESBLs enzymes was confirmed using the synergy and combine tests. The synergy test included a culture of isolate onto the Mueller Hinton agar and placing two disks co-amoxiclav and ceftazidime near each other. Additionally, the combined disk included placement of ceftazidime disk and a blank disk that contained clavulanic acid. Any increase in the inhibition zone exhibited the production of ESBLs.

DNA isolation

The total genomic DNA was extracted using the boiling method. After preparation of bacterial suspension from a single colony of isolates in DDH₂O, each tube was boiled for 10min and centrifuged at 10,000rpm for 5min. The supernatant was used as a DNA template. The quantification of the DNA load was evaluated using the 260/280 ratio and Nano-drop device to be >1.8.

Detection of ESBLs and Carbapenemase genes

The ESBL and Carbapenemase genes, including CTX-M, SHV, IMP and OXA-48 were detected using PCR and using specific primers shown in table 1. The PCR conditions included 94°C for 3min, and a 30 cycle of 94°C, annealing for 45s, 72°C for 1min and final extension of 72°C for 10min. The master mix

(6μL), template DNA (1μL), each F and R primer (1μL) and DD-H₂O (5μL) were mixed in the reaction tube.

Detection of mcr-1, mcr-2 and fosA3 genes

The PCR assay was employed for the amplification of Fosfomycin (fosA3) and Colistin (mcr-1, mcr-2) resistant genes using specific primer sequences and annealing shown in table 2.¹⁹.

The thermal cycle for detecting mcr-1 and mcr-2 genes was similar to that of previous, but the annealing temperature included 56°C and 58°C. The PCR products were run onto the 1% gel agarose in 1X Tris Borate EDTA (TBE) and visualized using safe dye.

Data analysis

The prevalence of genes was analyzed by SPSS version 20, and the un-paired T-test and ANOVA options were used for assessment of significance defining <0.05 cut-off value.

Results

Patients and isolates

Of 200 patients, 84 males and 112 females with a mean

Primers	Sequence 5'----3'	Annealing T	Amplicon size (bp)	Reference
<i>bla_{SHV}</i>	F: GCCGGGTTATTCTTATTTGTCGC R: ATGCCGCGCCAGTCA	56	1016	16,17
<i>Bla_{IMP}</i>	F: GGGTGGGGCGTTGTTCCTA R: TCTATTCCGCCCGTGTCTGC	62	198	
<i>bla_{CTXM}</i>	F: CGCTTTGCGATGTGCAG R: ACCGCGATATCGTTGGT	59	500	18
<i>bla_{OXA-48}</i>	F: CGCCCGCGTCGACGTTCAAGAT R: TCGGCCAGCAGCGGATAGGACAC	65	484	17

Table 1. Specific primers for detection of CTX-M, SHV, IMP and OXA-48 genes.

primer	Sequence: 5' to 3'	Product size (bp)	Reference
<i>fosA3</i>	F: GGCATTTTATCAGCAGT R: AGACCATCCCCTTG TAG	350	This study
<i>mcr-1</i>	F: AGTCCGTTTGTCTTGTGGC R: AGATCCTTGGTCTCGGCTTG	320	This study
<i>mcr-2</i>	F: CAAGTGTGTTGGTCGCAGTT R: TCTAGCCCGACAAGCATAACC	715	This study

Table 2. The primer sequences for the detection of Fosfomycin and Colistin resistance genes.

age of 52.21 years were included. The previous hospitalization was determined in 177 of them ($p < 0.001$). All the patients had more than 24h of hospitalization. Moreover, 189 ($p < 0.0001$) of them had previous beta-lactam administration. The age range of patients and rate of ESBLs production has been depicted in table 3. 70 patients were infected with ESBL-producing *E. coli*.

As shown in table 3, the age range 51-60 years were significantly more infected with ESBL-producing *E. coli*, but other age groups were not significantly associated with the ESBL production.

Age range (years)	ESBL (%)	p value
<10	0	Non-S
11-20	0	Non-S
21-30	5	Non-S
31-40	18	Non-S
41-50	20	Non-S
51-60	50	0.031, S
61-70	7	Non-S
>70	0	Non-S

Table 3. The age range of patients and ESBL production.

DESBL and Carbapenemase genes

The CTX-M1, SHV, IMP and OXA-48 genes were detected in 60 (30%), 56 (28%), 28 (14%) and 4 (8%) of isolates (figures 1-4).

Notably, three isolates had all the CTX-M1, SHV, IMP, and OXA-48 genes. The patients had ages >60 years and had previous hospitalization and antibiotic consumption.

The association of ESBL genes with previous hospitalization and antibiotic prescription has been depicted in table 4. As shown, there was a significant relationship between the previous hospitalization and antibiotic prescription and the rate of ESBL production ($p < 0.0001$).

PCR detection of mcr-1, mcr-2 and fosA3 genes

None of the *E. coli* isolates had the mcr-1, mcr-2 and fosA3 genes.

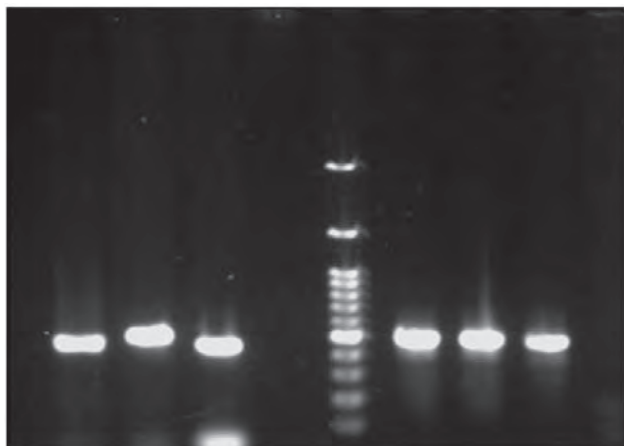


Figure 1. PCR gel electrophoresis of CTX-M1 with 500 bp size.

Discussion

Despite the fact that infectious diseases and their treatment have always been considered throughout human history, their changes and mutations have caused failure in their eradication^{1,6,10,11}. On the other hand, even this has caused new strains, and their prevalence has increased the range of these diseases in new forms. Microbial strains which produce enzymes hydrolyzing broad-spectrum antimicrobials are a concern. Gram-negative species are one of the significant barriers to the definitive treatment of infectious diseases²⁰⁻²². *E. coli* is a common species in the production of ESBL enzymes and is the main cause of nosocomial infections, especially urinary tract infections and sepsis, viscera, liver abscesses, cholangitis and cholecystitis and pancreatic abscesses. Therefore, due to the growing number of these strains in nosocomial infections and ICU centers, determining the pattern of *E. coli* resistance genes encoding ESBLs and Carbapenemase enzymes in clinical samples was one of the objectives of this study.

In this study, the rate of CTX-M SHV ESBLs included 30% ($n=60$) and 28% ($n=56$), respectively. The production of ESBL enzymes is encoded by several genetic factors that produce over 340 different types of beta-lactamase enzymes. These enzymes are classified into different classes based on their genetic identification and similarity. There are different reports of the prevalence of these enzymes in the Enterobacteriaceae family in the world. Studies in other parts of the world have reported a different prevalence. It seems that the emergence and spread of ESBL-bearing bacteria are often due to the widespread use of beta-lactam drugs so that today we see an increasing number of these bacteria in various parts of hospitals such as ICUs. In a study by Tasli *et al.* in Turkey, the production of ESBL in *E. coli* strains was equal to 17% 23, and in the study of Villegas in Colombia, it was reported 3.4% 24.

On the other hand, the Zhou study in Shanghai showed that 47.4% of *E. coli* isolated from patients produced these enzymes¹⁹. In another study by Wu *et al.* in Taiwanese hospitals, ESBL-producing *E. coli* was 18.18% as one of the most abundant ESBL-producing isolates 25. In Lebanon, the rate was 28.1%. This rate is much lower in Japan, less than 0.1% in *E. coli* and 0.3% in *Klebsiella spp.* Elsewhere in Asia, it has been reported from 4.8% to 28%^{25,26}. Comparison of these results shows that the rate of ESBL in isolated strains from different countries and in one country from one hospital to another va-

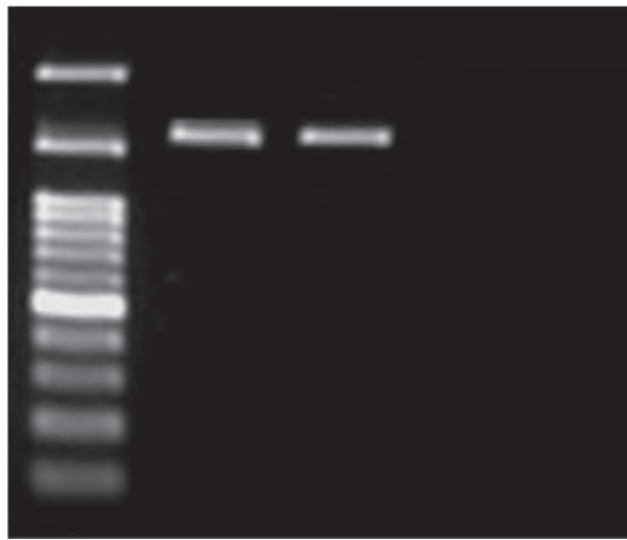


Figure 2. PCR gel electrophoresis of SHV with 1016 bp size.

ESBL genes	Previous hospitalization	Prior antibiotic use	p value
CTX-M1	58/60 (96.7%)	51/60 (85%)	<0.0001
SHV	54/56 (96.4%)	49/56 (7.5%)	<0.0001

Table 4. The association of ESBL genes with previous hospitalization and antibiotic prescription.

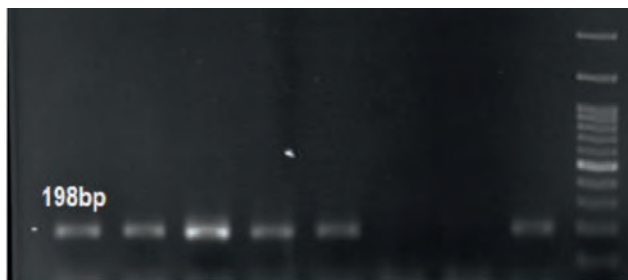


Figure 3. PCR gel electrophoresis of IMP with 198 bp size.

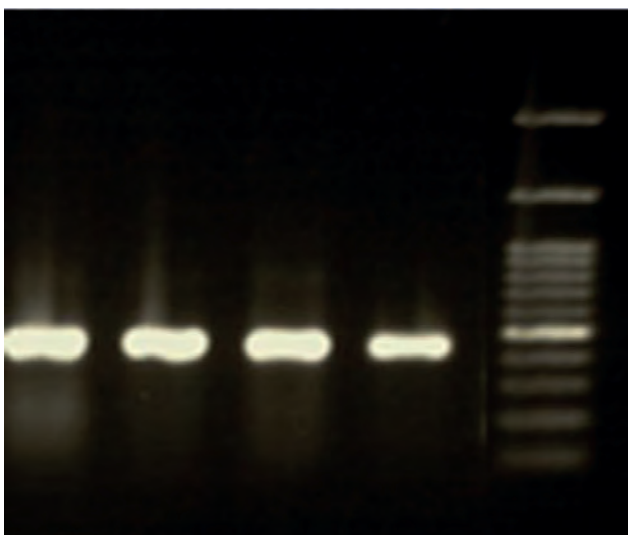


Figure 4. PCR gel electrophoresis of OXA-48 gene with 484 bp size.

ries depending on the infection control system and patient's treatment method in each hospital. Various risk factors are involved in increasing the number of ESBL-producing bacteria, such as long-term hospital stay, overuse of antibiotics (including third-generation cephalosporins), use of vascular and urinary catheters, and prolonged ICU storage history of surgery and irrational and inadequate use of antimicrobial treatments. This study also observed that prior hospitalization and antibiotic usage are significant risk factors.

We also observed that the IMP and OXA-48 genes were detected in 28 (14%) and 4 (8%) isolates, respectively. Fortunately, none of the isolates had genes encoding Fosfomycin (fosA3) and Colistin (mcr-1 and mcr-2) resistance.

Conclusions

In this study, a high rate of *E. coli* isolates from ICU were ESBL-producing by amplifying CTX-M and SHV genes. Fortunately, none of the isolates had genes encoding Fosfomycin (fosA3) and Colistin (mcr-1 and mcr-2) resistance. More studies are needed to follow the resistance genes against last-resort antibiotics.

Informed Consent Statement

Not applicable.

Data Availability Statement

The results of this study will be found under the rules of the journal and related link.

Acknowledgments

To my colleagues working in laboratories inside my college and to those who helped me collect samples and resources.

Conflict of interest

None to declare.

Bibliographic references

1. Hamadamin HA, Baban ST, Hussien BM, Ali FAJJoKMCV. Distribution of blaTEM Gene among Escherichia Coli Strains Isolated from Different Clinical Samples in Erbil City. 2019;7(1).
2. Mahon CR, Lehman DC, Manuselis G. Textbook of diagnostic microbiology-e-book: Elsevier Health Sciences; 2018.
3. Kalantar D, Mansouri S. Emergence of multiple β -lactamases produced by Escherichia coli clinical isolates from hospitalized patient in Kerman, Iran. 2010.
4. Owaif HAA, Mhawesh AA, Abdulateef SAJAoTM, Health. The role of BipA in the regulation of K1 capsular polysaccharide production of uropathogenic Escherichia coli. 2019;22:201-209.
5. King JE, Owaif HAA, Jia J, Roberts ISJI, immunity. Phenotypic heterogeneity in expression of the K1 polysaccharide capsule of uropathogenic Escherichia coli and downregulation of the capsule genes during growth in urine. 2015;83(7):2605-2613.
6. Drawz SM, Bonomo RAJCMr. Three decades of β -lactamase inhibitors. 2010;23(1):160-201.
7. Palzkill TJAotNYAoS. Metallo- β -lactamase structure and function. 2013;1277:91.
8. Owaif HAHA. Regulation of Transcription of the Escherichia coli Group 2 Capsule Gene Clusters: The University of Manchester (United Kingdom); 2017.
9. Jaber AM, Aal Owaif HJPA. Detection Of Genes Involved In Biofilms Formation By Escherichia Coli Isolated From Patients Suffering Of Urinary Tract Infections. 2020;20(2):5987-5992.
10. Liu Y-Y, Wang Y, Walsh TR, et al. Emergence of plasmid-mediated Colistin resistance mechanism MCR-1 in animals and human beings in China: a microbiological and molecular biological study. 2016;16(2):161-168.
11. Al-Bdery ASJ, Mohammad GJ, Hussien BJGR. Vancomycin and linezolid resistance among multidrug-resistant Staphylococcus aureus clinical isolates and interaction with neutrophils. 2020;21:100804.
12. Mhawesh AA, Aal Owaif HA, Abdulateef SAJJoPHR, Development. In vitro Experimental Research for Using the Silver Nanoparticles as Plasmid Curing Agent in Some Types of Multi-Antibiotic Resistant Pathogenic Bacteria. 2019;10(8).
13. Mhawesh AA, Hussein HA, Abdullah MN. GENE EXPRESSION OF MIR-7 IN LOCAL ISOLATES OF STAPHYLOCOCCUS AUREUS.
14. Al-Sa'ady AT, Mohammad GJ, Hussien BMJGR. Genetic relation and virulence factors of Carbapenemase β -producing Uropathogenic Escherichia coli from urinary tract infections in Iraq. 2020;21:100911.

15. Ali FA, Hussen BM, Zaki SMJAoTM, Health. Molecular detection of bla ctx-m gene among pseudomonas aeruginosa strains isolated from different clinical samples in erbil city. 2020;23:231-231.
16. Rayamajhi N, Kang SG, Lee DY, et al. Characterization of TEM-, SHV-and AmpC-type β -lactamases from cephalosporin-resistant Enterobacteriaceae isolated from swine. 2008;124(2):183-187.
17. Alkhudhairy MK, Alshadeedi SM, Mahmood SS, Al-Bustan SA, Ghasemian AJMp. Comparison of adhesin genes expression among Klebsiella oxytoca ESBL-non-producers in planktonic and biofilm mode of growth, and imipenem sublethal exposure. 2019;134:103558.
18. Kanaan MHG, Al-Shadeedi SM, Al-Massody AJ, Ghasemian AJCi, microbiology, diseases i. Drug resistance and virulence traits of Acinetobacter baumannii from Turkey and chicken raw meat. 2020;70:101451.
19. Ahmed AM, Nakano H, Shimamoto TJJoAC. The first characterization of extended-spectrum β -lactamase-producing Salmonella in Japan. 2004;54(1):283-284.
20. Balaky STJ, Abdulkhalik H, Hussen BM, Hassan H, Mawlood AHJZJoP, Sciences A. Molecular Identification of Acinetobacter baumannii and Acinetobacter genomic species 13TU Using PCR. 2019;31(1):17-22.
21. Hussen BM, Al-Marzoqi AH, Ghasemian AJJoGC. Assessment of oncogenic role of intestinal microbiota in colorectal cancer patients. 2020:1-6.
22. Hussen BMJZJoP, Sciences A. Evaluating the prevalence of virulence factor gene and biofilm production in Pseudomonas aeruginosa isolated from different clinical samples. 2020;32(4):108-113.
23. Tasli H, Bahar IHJJjoid. Molecular characterization of TEM-and SHV-derived extended-spectrum beta-lactamases in hospital-based Enterobacteriaceae in Turkey. 2005;58(3):162.
24. Villegas MV, Correa A, Perez F, et al. Prevalence and characterization of extended-spectrum β -lactamases in Klebsiella pneumoniae and Escherichia coli isolates from Colombian hospitals. 2004;49(3):217-222.
25. Rosenthal VD, Maki DG, Jamulitrat S, et al. International nosocomial infection control consortium (INICC) report, data summary for 2003-2008, issued June 2009. 2010;38(2):95-104. e102.
26. Ling TK, Xiong J, Yu Y, et al. Multicenter antimicrobial susceptibility survey of gram-negative bacteria isolated from patients with community-acquired infections in the People's Republic of China. 2006;50(1):374-378.

ARTICLE / INVESTIGACIÓN

Identification of novel-vector control target proteins of *Aedes sp.*: A Systems Network Biology Approach

Tammanna R. Sahrawat, Devika Talwar and Ritika Patial

DOI. 10.21931/RB/2022.07.01.12

³Centre for Systems Biology and Bioinformatics, UIEAST, Panjab University, Chandigarh, India.
Corresponding author: tammanna@pu.ac.in

Abstract: *Aedes* is an important vector for various viruses that cause dengue, chikungunya and zika, which affect human health globally. Due to regular outbreaks of these diseases worldwide, there is a need to identify essential vector proteins that are critical for the survival of the vector, which may be targeted to control the spread of vector-borne disease (VBD). *In silico* computational methods involving comparative proteomics, analysis of orthologous proteins common amongst members of *Aedes* genus and protein-protein interaction (PPI) pathway were used to identify essential proteins that could act as novel therapeutic candidates. Twenty-three conserved proteins between *A. aegypti* and *A. albopictus* were identified from a BLASTP search with an e-value threshold of 0.005, and their PPI networks were constructed in the STRING database. The merged network was analyzed using various Cytoscape plugins viz. ClusterONE, Cytohubba and MCODE. Thirty-one hub proteins were identified from the system's network biology analysis, and detailed data and literature mining were carried out. Twelve novel vector-control target proteins of *A. aegypti*, having no human homologs, were determined in the present study that can effectively act as potential therapeutic candidates for drug design and vaccine development.

Key words: Vector-borne disease (VBD), Therapeutic candidates, Network Systems Biology, Protein-protein interactions (PPI), Computational biology.

Introduction

Vector-borne diseases (VBD) are significant contributors to the global disease burden and account for more than 17% of all infectious diseases, causing more than 700000 deaths annually¹. An important taxon of arthropods that affects human health globally by acting as a vector of arthropod-borne viruses are mosquitoes belonging to the *Aedes* genus. It's been over five decades that *Aedes*-borne diseases, such as dengue, Zika, chikungunya, and yellow fever, have emerged and re-emerged globally^{2,3}. The global population at risk is expanding in concert with changes in the distribution of two key vectors: *Aedes aegypti* and *Aedes albopictus*. Their desiccation-resistant eggs facilitate the invasion of *Aedes* into new areas, and the distribution of these species is largely driven by both human movement and the presence of a suitable climate⁴.

Dengue virus has been reported to cause about 390 million human infections per year; the chikungunya virus spread worldwide in the early 2000s, with recent reports of the spread of Zika virus, while yellow fever has resurged in Africa and America. In most cases, vector control is the only means to cope with various foreign diseases.

The feeding preference of *Aedes* is only mammalian species, including birds, mammals and humans, which increases during the multiplication phase of their life cycle. The transmission of viruses from the mosquitoes to the organisms sharing the same niche is due to the bite of the infected vector, which releases the virus into the body of the recipient organism. *Aedes aegypti* was earlier found in forested territories, utilizing tree openings as natural surroundings as their habi-

tat⁵. Now, they have transformed and evolved along with the increasing urbanization and have found their habitat in leftover jars, tires, broken water-filled buckets and even in the tanks or ponds having stagnant water. They usually prefer areas where they can easily find their host and feed on them eventually⁶.

Another member of the *Aedes* genus is now listed as one of the top 100 invasive species by the Invasive Species Specialist Group⁷ on account of being a suitable vector for causing human diseases chikungunya virus, dengue virus, and dirofilariasis is *A. albopictus*. Experimental evidence has shown that its preferred host is humans, but being an opportunistic feeder, it can depend upon other hosts such as domestic and wild animals, birds, reptiles, and amphibians for its food cycle^{8,9}.

Vector-borne diseases (VBD) are a worldwide concern and a significant cause of human morbidity and mortality, causing immeasurable suffering and impeding economic development. To protect humans from these destructive diseases, controlling insect vectors is often the most suitable and sometimes the only option available. Many control strategies have been designed and followed since centuries ago, but despite such efforts and programs, mosquito-borne diseases are prospering throughout the world¹⁰.

The amalgamation of "omics" data with computational biology tools in network systems biology offers the advantage of speedy identification of critical vector proteins necessary for the survival of the vectors, which may play an essential role in controlling vector populations. *In silico* methods such as comparative and subtractive genomics can be effectively be used

Citation: Sahrawat TR, Talwar D and Patial R. Identification of novel-vector control target proteins of *Aedes sp.*: A Systems Network Biology Approach. *Revis Bionatura* 2022;7(1). 12. <http://dx.doi.org/10.21931/RB/2022.07.01.12>

Received: 2 August 2021 / **Accepted:** 18 November 2021 / **Published:** 15 February 2022

Publisher's Note: Bionatura stays neutral with regard to jurisdictional claims in published maps and institutional affiliations.

Copyright: © 2022 by the authors. Submitted for possible open access publication under the terms and conditions of the Creative Commons Attribution (CC BY) license (<https://creativecommons.org/licenses/by/4.0/>).



to identify proteins/genes of vectors that are non-homologous to their human hosts. These proteins/genes may then be targeted using drugs and vaccines by inhibiting critical vector pathways and preventing host-seeking and feeding behaviors.

The present study was undertaken to identify critical vector-control target proteins for the *Aedes* genus using a network systems biology approach. Such an approach offers the opportunity to ascertain potential targets for drug development and vaccine design that would facilitate the production of novel therapeutics specific against the disease-carrying vectors.

Materials and methods

Proteome data mining

The UniProt KB database (<https://www.uniprot.org>)¹¹ was used to extract proteins present in vector *Aedes aegypti* and for functional annotation of the essential proteins along with eggNOG (<http://eggnog5.embl.de>)¹².

BLAST

Basic alignment search tool¹³ was used to identify non-human homologs proteins of *Aedes aegypti*. This was followed by the identification of conserved essential proteins amongst two central disease-causing species of the *Aedes* genus, namely *Aedes aegypti* and *Aedes albopictus*.

Vector specific pathway analysis using KEGG

Complete form (KEGG)¹⁴ was used to ascertain the metabolic pathways of non-homologous essential proteins that were identified in the previous step.

Sub-cellular location prediction

To predict the subcellular location of the essential proteins, a consensus was drawn from the results obtained from UniProt¹¹, Cello¹⁵, I-loc animal¹⁶, SherLoc2¹⁷ and Wolf PSORT¹⁸.

Host-vector protein-protein interactions

STRING

(Search Tool for the Retrieval of Interacting Genes/Proteins) (<https://string-db.org/>) (version 11.0) database was used to build protein-protein interaction networks of essential proteins of *Aedes aegypti* and their interacting partners. The networks obtained were analyzed using Cytoscape (version 3.8.0) and its various plugins such as ClusterONE, CytoHubba, MCODE¹⁹.

ClusterONE

(<http://apps.cytoscape.org/apps/clusterone>). ClusterONE (Clustering with Overlapping Neighborhood Expansion) was used to identify highly connected regions in the form of clusters that were based on weighted graphs with associated confidence values²⁰.

CytoHubba

(<http://apps.cytoscape.org/apps/cytohubba>). CytoHubba with the scoring method of maximal clique centrality (MCC) was used to rank hub genes²¹.

MCODE

(<http://apps.cytoscape.org/apps/mcode>). MCODE (Molecular Complex Detection) was used to find highly connected regions called clusters based solely on connectivity data²².

Results

Proteome data mining for identification of non-human homologs

UniProt KB was used to retrieve proteins present in *Aedes aegypti*. To increase reliability and reduce redundancy in data mining, only the reviewed 253 protein data entries were selected. All the 253 protein sequences of *A. aegypti* were subjected to a BLASTP search against the host proteome of *Homo sapiens* with an e-value threshold of 0.005²³. A total of 24 proteins of *A. aegypti* that showed "no significant similarity" to humans were shortlisted as non-human homologs (Table 1). After that, these proteins were analyzed using computational biology approaches to identify essential proteins of *Aedes* genus that may act as potential drug and vaccine targets.

Identification of essential proteins in *Aedes aegypti*

The presence of orthologous proteins between two or more species indicates their essentiality for the survival of the genus. Orthologous proteins are known to retain equivalent functions in different organisms²⁴. Due to the absence of any information about the essential proteins/genes of *A. aegypti* in DEG (Database of Essential Genes), various bioinformatics tools were used to identify the orthologues. Twenty-four proteins of *A. aegypti* (Table 1) were subjected to a manual BLASTP search with e-value threshold of 0.005, to identify conserved proteins against proteome of another *Aedes* genus member i.e. *A. albopictus*. Unique orthologues proteins were selected manually using a cut-off $\geq 50\%$ identity between *A. aegypti* and *A. albopictus*. Twenty-three proteins (except TKSIA_AEDAE) were identified as conserved essential proteins common between the *Aedes* species. These conserved proteins may be critical for the survival and pathogenicity of members of *Aedes* genus (Table 1).

Vector specific pathway analysis and sub-localization prediction

The 23 proteins identified as conserved essential proteins were then categorized as "pathway dependent" or "pathway independent" using UniProt KB GO and KEGG pathway database, and their subcellular location was determined by drawing consensus amongst results obtained from UniProt, Cello, I-loc animal, SherLoc2 and Wolf PSORT. Out of the 23 proteins, 20 were found to be pathway independent, and 3 proteins, namely DEFA_AEDAE, DEFB_AEDAE and DEFC_AEDAE were found pathway dependent, involved in innate immunity²⁵. All these 23 proteins of *A. aegypti* that were absent in human hosts were further explored using a network systems biology approach to identify critical vector target proteins that can act as drug and vaccine targets to curb the spread of VBDs.

Host-vector protein-protein interactions

Construction of gene interaction network

The interaction network for the 23 essential proteins of *Aedes aegypti* was constructed using the STRING database. On analysis, it was observed that HPEP_AEDAE and BURS_AEDAE were absent, while DEFA_AEDAE and DEFB_AEDAE were represented as the same protein in STRING results for *Aedes sp.* Therefore the resulting PPI network had 20 proteins that showed no significant interactions amongst themselves since these proteins were involved in different pathways of survival and pathogenesis of the vector (Figure 1). Three

1	COMM2_AEDAE	9	ATP8_AEDAE	17	DEFC_AEDAE
2	V15A1_AEDAE	10	SNPF_AEDAE	18	CECA_AEDAE
3	OBP45_AEDAE	11	V15A3_AEDAE	19	VIT1_AEDAE
4	NPF_AEDAE	12	PBAN_AEDAE	20	DEFB_AEDAE
5	LCK_AEDAE	13	DEFA_AEDAE	21	ALL3_AEDAE
6	ALL2_AEDAE	14	OR4_AEDA	22	SHAKB_AEDAE
7	CORZ_AEDAE	15	V15A2_AEDAE	23	HPEP_AEDAE
8	BURS_AEDAE	16	ORCO_AEDAE	24	TKSIA_AEDAE*

* rejected because it was not common between the *Aedes aegypti* and *A. albopictus* species

Table 1. Essential proteins common in both *Aedes aegypti* and *Aedes albopictus*.

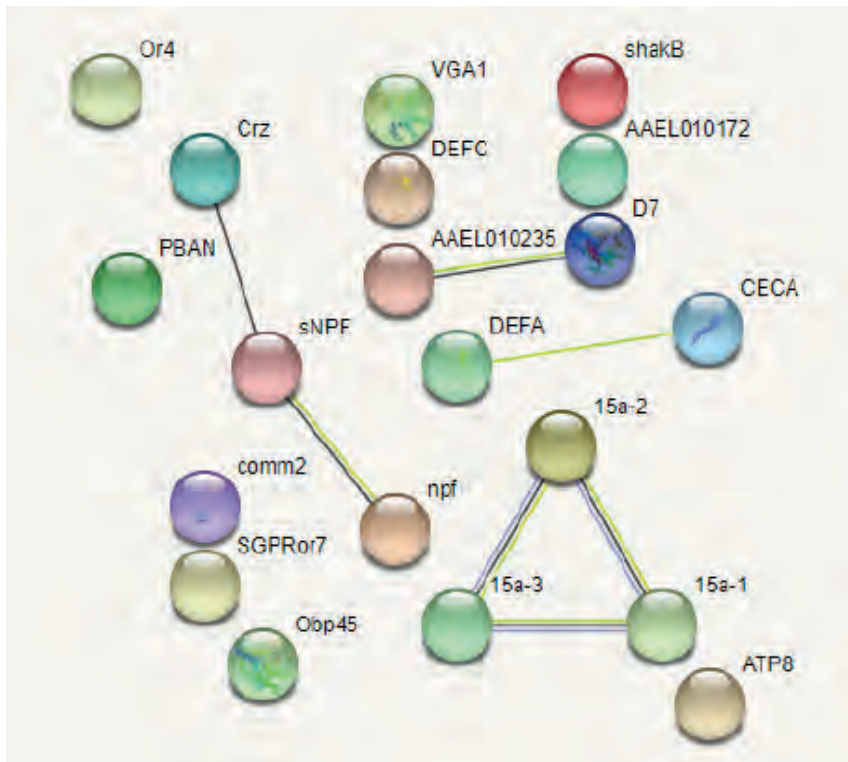


Figure 1. Intra-species interactions amongst *Aedes* proteins constructed in the STRING database.

PPIs were observed, i.e., ALL2_AEDAE (D7) and ALL3_AEDAE (AAEL010235) that are salivary gland allergens and reported to be involved in blood-feeding of the human host^{26,27}; CORZ_AEDAE (crz) and NPF_AEDAE with SNPF_AEDAE, in which all are neuropeptides with CORZ being involved in heart contraction²⁸; V15A1_AEDAE (15a-1), V15A2_AEDAE (15a-2) and V15A3_AEDAE (15a-3) are proteins involved in oogenesis and therefore may act as an essential control point in the reproduction of *Aedes* mosquito^{29,30}.

To better understand the interactions of the essential proteins with other proteins of *A. aegypti*, interaction networks of each of the 20 proteins were built individually in STRING and were imported and merged into a single network using Cytoscape software. The resulting merged network contained 96 edges (representing genes/proteins) and 243 nodes (representing interactions between genes/proteins) (Figure 2). This network was further analyzed using various plugins of Cytoscape to identify essential proteins of *A. aegypti*.

On analysis of the merged network with Cytoscape plugin ClusterONE, color-coded nodes were obtained in which red and grey nodes represent highly significant genes and outliers, respectively (Figure 3). Eleven clusters were obtained that had a significant P-value (<0.05) (Table 2), but only three top-ranked clusters having the most significant number of nodes and edges were further studied.

Another Cytoscape plugin MCODE was used to find clusters or highly connected regions in the protein-protein interaction network in which node colors represent the node score and range from black to red (lowest to highest, respectively), while white indicates a score of zero (Figure 4). Eleven clusters were also obtained from MCODE, out of which the first three clusters were considered as significant based on the higher number of nodes and edges (Table 3).

To further validate the results of genes identified as essential using Cytoscape plugins- ClusterONE and MCODE another plugin CytoHubba was used to analyse the merged

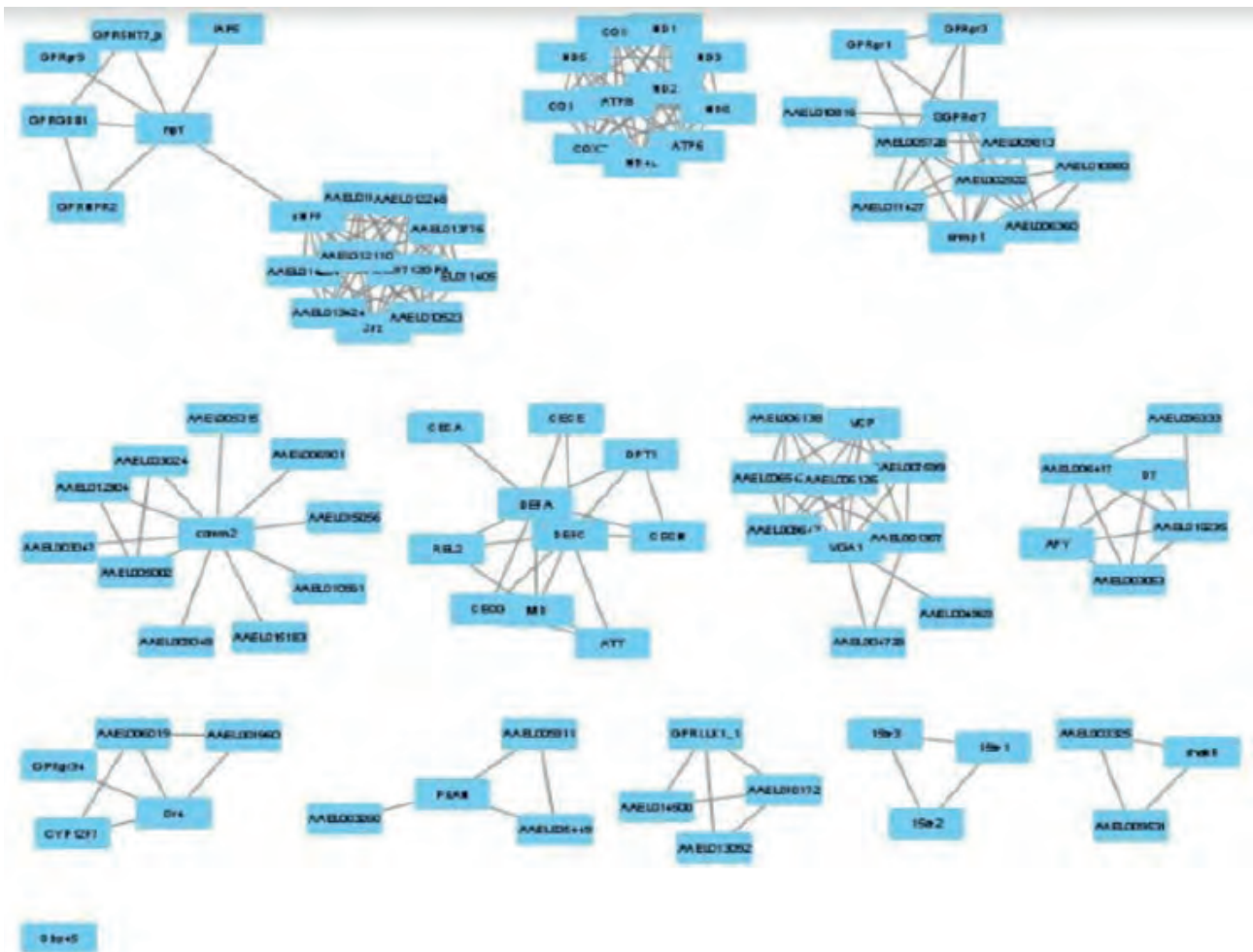


Figure 2. Merged PPI network having 96 nodes, 243 edges in Cytoscape.

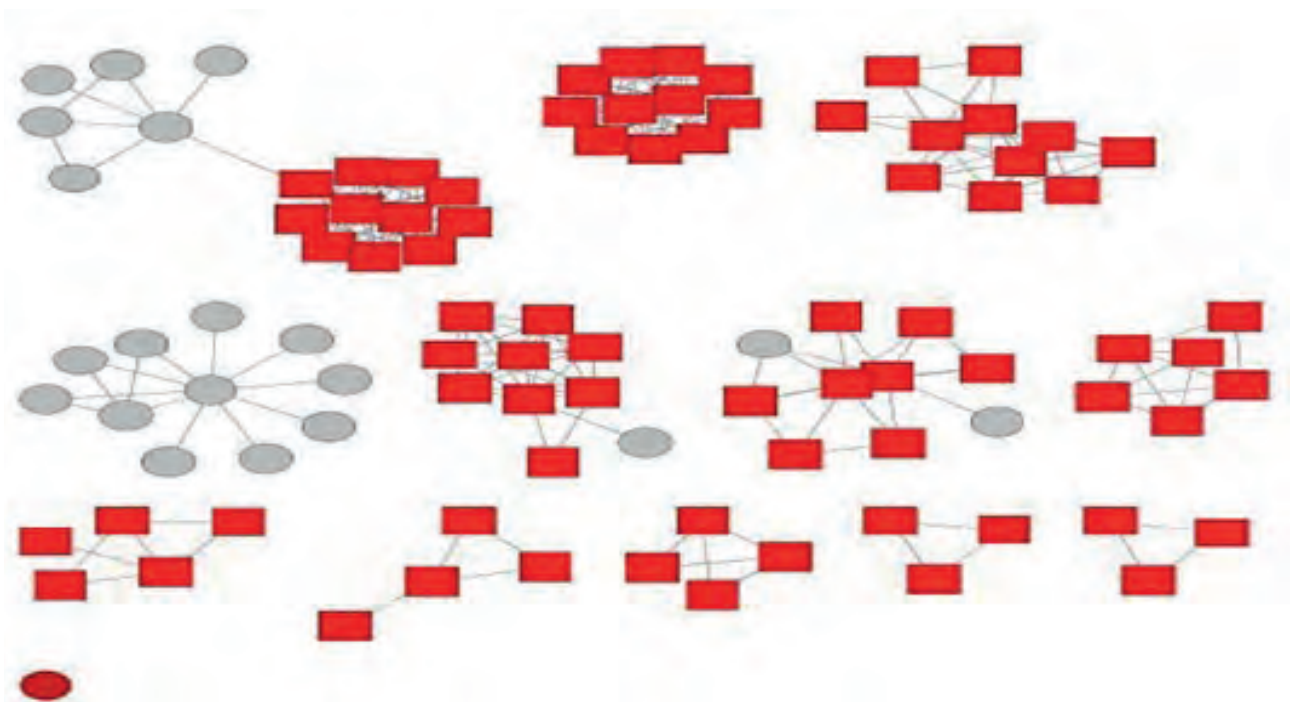


Figure 3. ClusterONE results were obtained by analyzing the interaction network.

PPI network (Figure 2) to identify the "Hubs" which represent the highly connected nodes. A hub is more likely to be essential because it has more interactions and, therefore, a higher likelihood to engage in an essential interaction³¹. The network obtained showed genes/proteins color-coded with highly significant genes in red (31 genes), orange and least significant in yellow (Figure 5).

The proteins present in the three top-ranked clusters obtained from ClusterONE and MCODE were identical, as were the 31 top-ranked genes obtained from CytoHubba, thereby validating our results obtained from different Cytoscape plugins that use different methods to identify hub proteins that can further be explored to act as putative target proteins for vector control (Table 4).

Data mining of shortlisted proteins

UniProtKB was used to retrieve information, such as target name, associated metabolic pathway, length, molecular weight, subcellular location etc., of the identified 31 essential genes of *Aedes* genus that code for non-homologous human proteins. Thereafter, a rigorous manual search in PDB was done to identify any structural homologs amongst the proteins of *Aedes* genus with its human host as unintended binding of the drug/vaccine, designed for *Aedes* to the structurally similar proteins of the human host could have devastating effects in the hosts, since structurally similar and related proteins may have similar binding sites with capabilities to recognize chemically similar ligands³².

Out of 31 proteins of *Aedes* only 9 proteins did not have any structural homology with humans in PDB. These 09 proteins shortlisted three other proteins, namely BRUS_AEDAE,

HPEP_AEDAE (that had no entries in STRING database), and ALL3_AEDAE (salivary gland allergen reported to have binary interactions with 2 human proteins, namely COA1 and CO2A3) were analyzed for their biological function in UniProt. Therefore, 12 proteins were shortlisted as novel vector-control target proteins of *A. aegypti* that had no human homologs and could effectively act as potential drug and vaccine targets (Table 5) to prevent the outbreak of VBDs by controlling the vector population of *Aedes*.

Literature mining of critical vector-control target proteins of *A. aegypti*

In the present study to identify critical vector-control target proteins for *Aedes* genus that can be used as potential targets for vaccine and drug development, we identified 12 proteins, out of which 5 proteins are neuropeptides. Two uncharacterized proteins, AAEL013776_AEDAE and AAEL013424_AEDAE, need to be further solved in structure and function to predict their importance in vector metabolic activities and survival.

Neuropeptides are one of the most diverse classes of signaling molecules and play a significant role in regulating a wide range of physiological processes in *Aedes* mosquitoes such as host-seeking behavior, blood-feeding, molting sex-specific processes, including reproduction³³. Regulatory peptides act as neurochemicals, and hormones govern these processes in mosquitoes. These peptides are processed, stored, and released within the nervous system as neurotransmitters and from the midgut endocrine system and neurosecretory cells as circulating hormones. They exert their action by binding to membrane receptors, most often to G-protein coupled re-



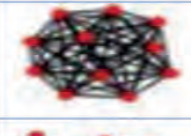




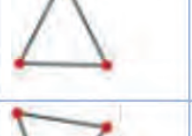



Sr. No.	Clusters	No. of Nodes	P-value	Sr. No.	Clusters	No. of Nodes	P-value
1		11	2.705E-6	7		5	0.004
2		11	4.222E-6	8		4	0.010
3		11	1.231E-5	9		4	0.010
4		9	8.122E-5	10		3	0.023
5		8	3.882E-4	11		3	0.023
6		6	0.001				

Table 2. Eleven clusters having significant P-value (<0.05) obtained from ClusterONE.

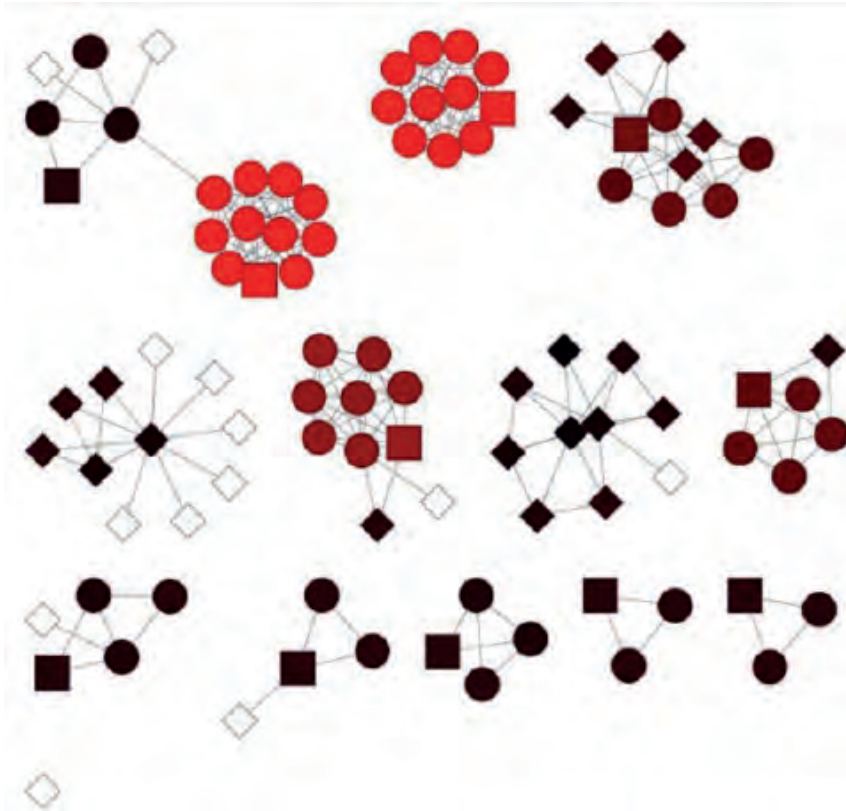


Figure 4. MCODE results obtained by analyzing the PPI network.

No.	Clusters	Nodes	Edges	S. No.	Clusters	Nodes	Edges
1		11	55	7		4	5
2		11	55	8		4	5
3		8	27	9		3	3
4		5	10	10		3	3
5		6	12	11		3	3
6		4	5				

Table 3. Eleven clusters were obtained from the interaction network.

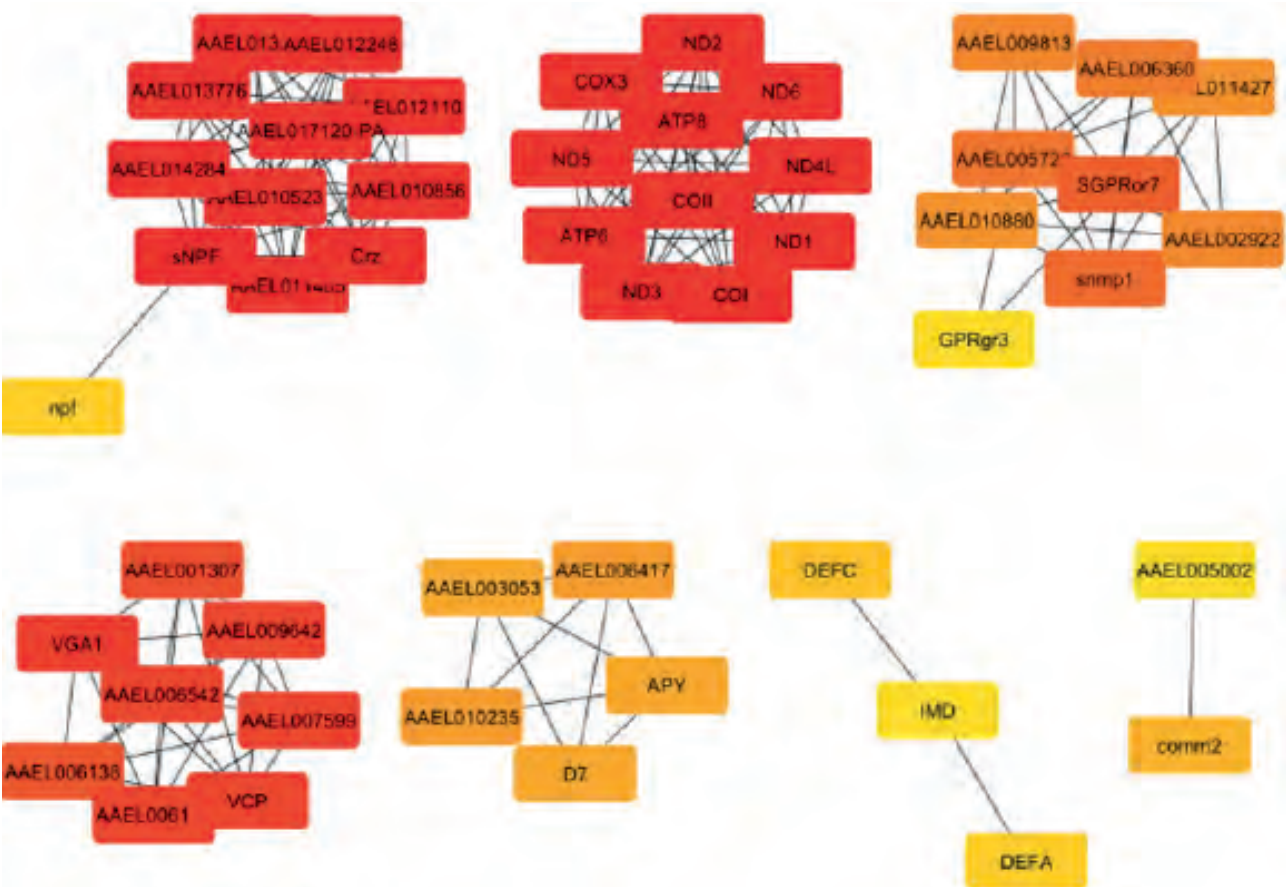


Figure 5. Graphical view of ranked hub nodes obtained from Cytoscape plugin Cytohubba with color-coding highly essential (Red) - less essential (Yellow).

ceptors (GPCRs) and, to a lesser extent, to receptor tyrosine kinases³⁴.

Host seeking is a fundamental aspect of mosquito and vertebrate host interactions, and the process is reported to be regulated by head peptide (HPEP_AEDAE), a neuropeptide encoded by gene *HP-1* in blood-fed female *A. aegypti*, and also other sex-specific processes as it was found to be expressed in larvae and males. Ingestion of a blood meal has been reported to trigger egg maturation in *A. aegypti*, and after that, females show a marked decrease in responses to host emanations that initially stimulated host-seeking behavior³⁵.

Short neuropeptide F (sNPF_AEDAE), a member of the neuropeptide F/Y superfamily, was isolated from adult *A. aegypti*, and NPF-like immunostaining was observed in the brain and midgut of adults and larvae. The reported fluctuations in the concentrations of sNPF reflect changes in the regulatory role of this peptide in digestive processes and the reproductive cycle with a sudden drop once a blood meal was imbibed²⁸.

Proteins such as odorant receptors (ORs) play critical roles in olfactory behaviors, including a co-receptor, designated ORCO_AEDAE, expressed in most olfactory sensory neurons in both adults and larvae, and is highly conserved among the order Diptera to which the *Aedes* genus belongs. It plays a crucial role in forming a ligand-gated ion channel to generate signals to induce behavioral responses, including host-seeking and host selection³⁶.

The arthropod saliva contains proteins delivered into the bite wound that can modulate the host's hemostatic and immune responses to facilitate blood meal intake and pathogen transmission. *Aegyptin* (ALL3_AEDAE), an abundantly expressed salivary protein of *A. aegypti*, is a collagen-binding

protein that inhibits platelet aggregation and adhesion, thereby playing a significant and nonredundant role in successful feeding^{29,37}. It has been reported to have interactions with the human collagen alpha-1 (I) and (III) chains i.e., COA1_HUMAN & CO2A3_HUMAN, respectively, thereby helping to transmit the pathogen in the vector saliva to the human host.

Gonadotropin-releasing hormone-related peptide Corazonin (CRZ) has been shown to have roles in pigmentation, ecdysis or act as a cardio stimulatory factor while its receptor-CRZR is expressed in the primary sex organs of adult male and female mosquitoes. This indicates a potential physiological role of CORZ_AEDAE in regulating reproductive biology in *A. aegypti*³⁷.

The gene encoding vitellogenin (Vg), a significant yolk protein precursor (YPP) in most oviparous animals, is expressed in extra ovarian tissues in a sex-, tissue- and stage-specific manner. Steroid hormones play a critical role in the regulation of Vg genes. In egg-laying vertebrates, estrogen triggers the transcription of the Vg³⁸. Before blood-feeding, ovary maturation remains at a previtellogenic state of arrest, and the production of vitellogenin (VIT1_AEDAE), the major yolk protein precursor, by the fat body is tightly repressed. After a blood meal, multiple regulatory factors act synergistically to trigger vitellogenin protein synthesis in the fat body. The vitellogenin proteins are then released into the hemolymph and taken up by the developing oocytes via receptor-mediated endocytosis. Therefore, stringent control of the expression of the Vg gene in mosquitoes is tied to the availability of a blood meal³⁰.

Two other unreviewed proteins shortlisted in the present study, namely Q17715_AEDAE and Q17712_AEDAE have reported lipid transporter activity, and on the investigation of their

ClusterONE		CytoHubba		MCODE	
		RANK	Protein		
Cluster 1	ND1	1	sNPF	ND1	Cluster 1
	ND3	2	AAEL017120-PA	ND3	
	ND5	2	AAEL010856	ND2	
	ND6	2	AAEL014284	ND6	
	ATP6	2	AAEL012248	ATP6	
	ND4L	2	AAEL012110	ND4L	
	COX3	2	AAEL013424	COX3	
	COI	2	AAEL010523	COi	
	ATP8	2	AAEL013776	ND5	
	ND2	2	AAEL011405	COii	
	COII	2	Crz	ATP8	
		2	COii		
Cluster 2	AAEL012248	2	COi	AAEL010856	Cluster 2
	AAEL012110	2	ND1	AAEL012248	
	AAEL014284	2	ND2	AAEL013776	
	AAEL010856	2	COX3	AAEL011405	
	AAEL011405	2	ND5	AAEL010523	
	Crz	2	ND3	AAEL017120-PA	
	AAEL013776	2	ND4L	AAEL012110	
	AAEL010523	2	ATP6	AAEL013424	
	AAEL017120-P A	2	ATP8	AAEL014284	
	sNPF	2	ND6	Crz	
	AAEL013424	23	VGA1	sNPF	
		24	AAEL007599		
Cluster 3	AAEL010816	24	VCP	VCP	Cluster 3
	SGPRor7	24	AAEL009642	VGA1	
	GPRgr1	24	AAEL006542	AAEL007599	
	AAEL011427	24	AAEL006126	AAEL001307	
	AAEL002922	29	AAEL001307	AAEL006126	
	AAEL006360	30	AAEL006138	AAEL009642	
	Smp1	31	SGPRor7	AAEL006542	
	AAEL009813			AAEL006138	
	AAEL005278				
	AAEL010880				
	GPRgr3				

Table 4. Top interacting Genes retrieved from Cytoscape plugins.

S. No.	Entry name	Non homologous protein target name	Uniprot id	Associated metabolic pathway (Uniprot/EggNOG)	Length	Molecular weight
1.	ATP8_AEDAE	ATP synthase protein 8	B0FWC9	• Energy production and conversion	53	6435
2.	AAEL013776_AEDAE	Uncharacterized protein	Q16167	• Translation • ribosomal structure and biogenesis	140	15642
3.	AAEL013424_AEDAE	Uncharacterized protein	Q16J76	• Function unknown	173	18946
4.	CORZ_AEDAE	Pro-corazonin	Q17AN4	• Corazonin receptor binding • Neuropeptide signaling • Positive regulation of heart contraction	137	15559
5.	SNPF_AEDAE	Short neuropeptide F	A0SIX6	• Neuropeptide signaling • Regulation of multicellular organism growth • Regulation of response to food	215	24637
6.	VIT1_AEDAE	Vitellogenin-A1	Q16927	• Lipid transporter activity • Nutrient reservoir activity	2169	252892
7.	Q177I5_AEDAE	AAEL006126-PA	Q177I5	• Lipid transporter activity	2087	242048
8.	Q177I2_AEDAE	AAEL006138-PA	Q177I2	• Lipid transporter activity	2142	249436
9.	BURS_AEDAE	Bursicon	P85316	• Cuticle pigmentation • Chitin-based cuticle sclerotization • Signal transduction • Hormone activity	163	17719
10.	ALL3_AEDAE	30 kDa salivary gland allergen Aed a 3	AAEL010235	• Causes an allergic reaction in humans by interaction with COA1_HUMAN & CO2A3_HUMAN	273	29155
11.	HPEP_AEDAE	Head peptide	Q9GQV7	• Neuropeptide signaling pathway • Negative regulation of host-seeking behavior	128	14605
12.	ORCO_AEDAE	Odorant receptor coreceptor	Q178U6	• Detection of chemical stimulus involved in sensory perception of smell • Signal transduction • Eating behavior	478	54277

Table 5. Non-homologous proteins of *A. aegypti* with reference to humans as potential drug and vaccine targets from unique pathways.

families and domains using InterPro, Pfam and Prosite databases, they were found to be related to vitellogenin, thereby indicating that they might also be involved in the process of oogenesis.

Bursicon is a neuropeptide hormone consisting of two subunits, burs α and burs β , members of the cystine-knot protein (CKP) family that usually form dimers (homo- or heterodimers) and are responsible for certain biological functions by binding to specific receptors. Zhang *et al.* (2017) report that the biological significance of bursicon extends beyond its classical developmental roles in cuticle tanning and wing expansion to mediating prophylactic immunity during molting periods. Bursicon (BURS_AEDAE) homodimers were shown to induce expression of AMP genes *via* Relish2 in *A. aegypti* as prophylactic immunity to protect mosquitoes during the vulnerable stages of each molt³⁹.

The F_1-F_0 ATP synthase is a large multi-subunit enzyme that uses the proton gradient generated by the respiratory chain to synthesize ATP. F_1 -ATP synthase region is composed of five different subunits (α , β , γ , δ , ϵ) assembled as a complex of three alternating α and β subunits together with a single unit of each of the other three subunits⁴⁰. It was initially believed that F_1-F_0 ATP synthase was strictly confined to the mitochondrial inner membrane. But for a wide variety of normal cells, including endothelial cells, adipocytes, keratinocytes, and hepatic cells, active ATP synthase activity on the cell surface has been documented⁴¹. Fongsaran *et al.* (2014) reported that ATP8 β plays a role in Chikungunya virus (CHIKV) infection of mosquito cells⁴¹, and there is evidence showing that the same protein is involved in the internalization of white spot syndrome virus (WSSV) to shrimp cells⁴², and possibly binding of dengue virus to insect cells⁴³, suggests that this is a conserved virus-arthropod interaction. Therefore, by targeting ATP8_AEDAE, the interaction of the pathogens and the mosquito vector can be disrupted and thereby, transmission to the human host may be effectively prevented.

Furthermore, targeting proteins involved in various physiological processes such as reproductive (CORZ_AEDAE and VIT1_AEDAE), immune (BURS_AEDAE) and metabolic activities (ATP8_AEDAE) can affect the survival of the vectors and thereby contain the spread of VBDs by controlling vector population.

Concomitantly, blood-feeding on humans also propagates disease transmission because the mosquito ingests the pathogen from an infected human and transmits it to new hosts during subsequent blood meals. The concentration of Head peptide and sNPF are higher in mosquitoes before blood feeding i.e., during the host-seeking phase and following blood meal, their concentrations fall^{44,45}. Therefore, Head peptide (HPEP_AEDAE), sNPF (SNPF_AEDAE), ORCO (ORCO_AEDAE) and ALL3 (ALL3_AEDAE) may also prove useful targets for blocking host-seeking and biting behavior, thereby preventing the transmission of pathogens from vector to the human host and thus constitute an alternative strategy to curb the disease.

Conclusions

The proteins identified in the present study can develop novel strategies to target critical vector components to successfully block the development of the vector or pathogen/parasite in its vector.

Funding

The authors would like to acknowledge the fun-

ding received under grant no. S&T&RE/Rp/147(19-20) San/10/2019/1703-1710 from Department of Science and Technology and Renewable Energy, U.T, Chandigarh, India under the short term research project scheme along with Panjab University Chandigarh for providing the infrastructure for the research work.

Informed Consent Statement

Not applicable.

Acknowledgments

The authors would like to acknowledge their parent institute, Panjab University Chandigarh, for providing the infrastructure for the work.

Conflicts of Interest

The authors declare no conflict of interest.

Bibliographic references

1. WHO. Vector borne diseases Report available at <https://www.who.int/news-room/fact-sheets/detail/vector-borne-diseases>.
2. Roiz D, Wilson AL, Scott TW, Fonseca DM, Jourdain F, Müller P, Velayudhan R, Corbel V. Integrated Aedes management for the control of Aedes-borne diseases. *PLoS neglected tropical diseases*. 2018 Dec 6;12(12):e0006845.
3. Mayer SV, Tesh RB, Vasilakis N. The emergence of arthropod-borne viral diseases: A global prospective on dengue, chikungunya and zika fevers. *Acta tropica*. 2017 Feb 1;166:155-63.
4. Kraemer MU, Reiner RC, Brady OJ, Messina JP, Gilbert M, Piggott DM, Yi D, Johnson K, Earl L, Marczak LB, Shirude S. Past and future spread of the arbovirus vectors *Aedes aegypti* and *Aedes albopictus*. *Nature microbiology*. 2019 May;4(5):854-63.
5. Weaver SC, Reisen WK. Present and future arboviral threats. *Antiviral research*. 2010 Feb 1;85(2):328-45.
6. Barrera R, Amador M, Diaz A, Smith J, Munoz Jordan JL, Rosario Y. Unusual productivity of *Aedes aegypti* in septic tanks and its implications for dengue control. *Medical and veterinary entomology*. 2008 Mar;22(1):62-9.
7. Invasive Species Specialist Group. Global Invasive Species Database – *Aedes albopictus* 2009.
8. Eritja R, Escosa R, Lucientes J, Marques E, Roiz D, Ruiz S. World-wide invasion of vector mosquitoes: present European distribution and challenges for Spain. *Biological invasions*. 2005 Mar;7(1):87-97.
9. Turell MJ, Dohm DJ, Sardelis MR, O'guinn ML, Andreadis TG, Blow JA. An update on the potential of North American mosquitoes (Diptera: Culicidae) to transmit West Nile virus. *Journal of medical entomology*. 2005 Jan 1;42(1):57-62.
10. Tolle MA. Mosquito-borne diseases. *Current problems in pediatric and adolescent health care*. 2009 Apr 1;39(4):97-140.
11. UniProt Consortium. UniProt: a worldwide hub of protein knowledge. *Nucleic acids research*. 2019 Jan 8;47(D1):D506-15.
12. Huerta-Cepas J, Szklarczyk D, Heller D, Hernández-Plaza A, Forslund SK, Cook H, Mende DR, Letunic I, Rattei T, Jensen LJ, von Mering C. eggNOG 5.0: a hierarchical, functionally and phylogenetically annotated orthology resource based on 5090 organisms and 2502 viruses. *Nucleic acids research*. 2019 Jan 8;47(D1):D309-14.
13. Madden T. The BLAST sequence analysis tool. In: *The NCBI Handbook* [Internet]. 2nd edition 2013 Mar 15. National Center for Biotechnology Information (US).
14. Kanehisa M. The KEGG database In: *Novartis Foundation Symposium*.
15. Yu CS, Cheng CW, Su WC, Chang KC, Huang SW, Hwang JK, Lu CH. CELLO2GO: a web server for protein subCELLular LOcalization prediction with functional gene ontology annotation. *PLoS one*. 2014 Jun 9;9(6):e99368.

16. Lin WZ, Fang JA, Xiao X, Chou KC. iLoc-Animal: a multi-label learning classifier for predicting subcellular localization of animal proteins. *Molecular BioSystems*. 2013;9(4):634-44.
17. Briesemeister S, Blum T, Brady S, Lam Y, Kohlbacher O, Shatkay H. SherLoc2: a high-accuracy hybrid method for predicting subcellular localization of proteins. *Journal of proteome research*. 2009 Nov 6;8(11):5363-6.
18. Fu SC, Imai K, Horton P. Prediction of leucine-rich nuclear export signal containing proteins with NESsential. *Nucleic acids research*. 2011 Sep 1;39(16):e111-.
19. Mering CV, Huynen M, Jaeggi D, Schmidt S, Bork P, Snel B. STRING: a database of predicted functional associations between proteins. *Nucleic acids research*. 2003 Jan 1;31(1):258-61.
20. Nepusz T, Yu H, Paccanaro A. Detecting overlapping protein complexes in large protein interaction networks. *Nature methods*. 2012 May;9(5):471.
21. Chin CH, Chen SH, Wu HH, Ho CW, Ko MT, Lin CY. cytoHubba: identifying hub objects and sub-networks from complex interactome. *BMC systems biology*. 2014 Dec;8(4):1-7.
22. Bader GD, Hogue CW. An automated method for finding molecular complexes in large protein interaction networks. *BMC bioinformatics*. 2003 Dec; 4(1):1-27.
23. Singh S, Malik BK, Sharma DK. Metabolic pathway analysis of *S. pneumoniae*: an in silico approach towards drug-design. *Journal of bioinformatics and computational biology*. 2007 Feb;5(01):135-53.
24. Gabaldón T, Koonin EV. Functional and evolutionary implications of gene orthology. *Nature Reviews Genetics*. 2013 May;14(5):360-6.
25. Merkl SH, van Rij RP. Beyond RNAi: antiviral defense strategies in *Drosophila* and mosquito. *Journal of insect physiology*. 2013 Feb 1;59(2):159-70.
26. Oktarianti R, Senjarini K, Hayano T, Fatchiyah F. Proteomic analysis of immunogenic proteins from salivary glands of *Aedes aegypti*. *Journal of infection and public health*. 2015 Nov 1;8(6):575-82.
27. Chagas AC, Ramirez JL, Jasinskiene N, James AA, Ribeiro JM, Marinotti O, Calvo E. Collagen-binding protein, Aegyptin, regulates probing time and blood feeding success in the dengue vector mosquito, *Aedes aegypti*. *Proceedings of the National Academy of Sciences*. 2014 May 13;111(19):6946-51.
28. Stanek DM, Pohl J, Crim JW, Brown MR. Neuropeptide F and its expression in the yellow fever mosquito, *Aedes aegypti*. *Peptides*. 2002 Aug 1;23(8):1367-78.
29. Engelmann F. Insect vitellogenin: identification, biosynthesis, and role in vitellogenesis. In *Advances in Insect Physiology* 1979 Jan 1 (Vol. 14, pp. 49-108). Academic Press.
30. Marti n D, Wang SF, Raikhel AS. The vitellogenin gene of the mosquito *Aedes aegypti* is a direct target of ecdysteroid receptor. *Molecular and cellular endocrinology*. 2001 Feb 22;173(1-2):75-86.
31. He X, Zhang J. Why do hubs tend to be essential in protein networks?. *PLoS Genet*. 2006 Jun 2;2(6):e88.
32. Govindaraj RG, Brylinski M. Comparative assessment of strategies to identify similar ligand-binding pockets in proteins. *BMC bioinformatics*. 2018 Dec;19(1):1-7.
33. Predel R, Neupert S, Garczynski SF, Crim JW, Brown MR, Russell WK, Kahnt J, Russell DH, Nachman RJ. Neuropeptidomics of the mosquito *Aedes aegypti*. *Journal of proteome research*. 2010 Apr 5;9(4):2006-15.
34. Riehle MA, Garczynski SF, Crim JW, Hill CA, Brown MR. Neuropeptides and peptide hormones in *Anopheles gambiae*. *Science*. 2002 Oct 4;298(5591):172-5.
35. Stracker TH, Thompson S, Grossman GL, Riehle MA, Brown MR. Characterization of the AeaHP gene and its expression in the mosquito *Aedes aegypti* (Diptera: Culicidae). *Journal of medical entomology*. 2002 Mar 1;39(2):331-42.
36. Liu H, Liu T, Xie L, Wang X, Deng Y, Chen CH, James AA, Chen XG. Functional analysis of Orco and odorant receptors in odor recognition in *Aedes albopictus*. *Parasites & vectors*. 2016 Dec;9(1):1-0.
37. Oryan A, Wahedi A, Paluzzi JP. Functional characterization and quantitative expression analysis of two GnRH-related peptide receptors in the mosquito, *Aedes aegypti*. *Biochemical and biophysical research communications*. 2018 Mar 4;497(2):550-7.
38. Wetekam W, Mullinix KP, Deeley RG, Kronenberg HM, Eldridge JD, Meyers M, Goldberger RF. Effect of estrogen on gene expression: purification of vitellogenin messenger RNA. *Proceedings of the National Academy of Sciences*. 1975 Sep 1;72(9):3364-8.
39. Zhang H, Dong S, Chen X, Stanley D, Beerntsen B, Feng Q, Song Q. Relish2 mediates bursicon homodimer-induced prophylactic immunity in the mosquito *Aedes aegypti*. *Scientific reports*. 2017 Feb 22;7(1):1-9.
40. Leyva JA, Bianchet MA, Amzel LM. Understanding ATP synthesis: structure and mechanism of the F1-ATPase. *Molecular membrane biology*. 2003 Jan 1;20(1):27-33.
41. Fongsaran C, Jirakanwisal K, Kuadkitkan A, Wikan N, Wintachai P, Thepparit C, Ubol S, Phaonakrop N, Roytrakul S, Smith DR. Involvement of ATP synthase subunit in chikungunya virus entry into insect cells. *Archives of virology*. 2014 Dec;159(12):3353-64.
42. Paingankar MS, Gokhale MD, Deobagkar DN. Dengue-2-virus-interacting polypeptides involved in mosquito cell infection. *Archives of virology*. 2010 Sep 1;155(9):1453-61.
43. Zhan W, Wang X, Chi Y, Tang X. The VP37-binding protein F1ATP synthase subunit involved in WSSV infection in shrimp *Litopenaeus vannamei*. *Fish & shellfish immunology*. 2013 Jan 1;34(1):228-35.
44. Christ P, Reifenrath A, Kahnt J, Hauser F, Hill SR, Schachtner J, Ignell R. Feeding-induced changes in allatostatin-A and short neuropeptide F in the antennal lobes affect odor-mediated host seeking in the yellow fever mosquito, *Aedes aegypti*. *PLoS one*. 2017 Nov 22;12(11):e0188243.
45. Duvall, L. B., Ramos-Espiritu, L., Barsoum, K. E., Glickman, J. F., & Vosshall, L. B. (2019). Small-molecule agonists of *Ae. aegypti* neuropeptide Y receptor block mosquito biting. *Cell*, 176(4), 687-701.

Docencia, investigación,
extensión y proyección
social al servicio del territorio



Fortalezas institucionales

- > Biotecnología
- > Limnología
- > Derechos Humanos – Posconflicto
- > Internacionalización
- > Inclusión Social
 - SER – Servicio Educativo Rural
 - Educación de Alfabetización
- > MII S – Instituto de formación para el trabajo y el desarrollo humano
- > Formación humanística “Ruta Humanística en el currículo - Cátedra abierta Maestra de la Sabiduría”
- > Investigación y desarrollo tecnológico
- > Comprometida con la calidad
- > Centro de Estudios Territoriales
- > Biodiversidad
 - Herbario
 - Ictiología
 - Fitoteca

Áreas del conocimiento

- Ciencias Agropecuarias
 - Ciencias de la Educación
 - Ciencias de la Salud
 - Ciencias Económicas y Administrativas
 - Ciencias Sociales
 - Derecho
 - Ingenierías
 - Teología y Humanidades
- > 26 programas de pregrado
 - > 16 programas de posgrado
 - 1 doctorado
 - 8 maestrías
 - 7 especializaciones

www.uco.edu.co  Universidad Católica de Oriente  @uconio



“Servicio educativo con calidad en
Personas, procesos y servicios”

Contacto institucional Universidad Católica de Oriente
Sector 3, Cra. 46 No. 40B 50 - PBX: +(57)(4) 569 90 90. Ext. 604
Fax: +(57)(4) 501 09 72 - Email: uco@uco.edu.co



REVIEW / ARTÍCULO DE REVISIÓN

Microsphere: A Wander around Drug Delivery

Anirban Karmakar^{1*}, Soumya Dev Maity², Shayeree Barua³, Raneet Das⁴

DOI. 10.21931/RB/2022.07.01.13

¹B.Pharm, Bharat Technology, Uluberia, Howrah – 711316, WB.²B. Pharm, School Of Pharmacy, Techno India University, Salt Lake Sec-V, Kolkata - 700091, WB.³M.Pharm, Pharmaceutics, Gupta College of Technological Sciences, Ashram More, GT Road, Asansol - 713301, WB.⁴Assistant Professor, Department Of Pharmaceutics, Radha Govind University, Ramgarh, Jharkhand.

Corresponding author: anirban.karmakar.ak@gmail.com

Abstract: Microspheres have free-flowing powder characteristics consisting of synthetic polymers and proteins with a particle size of 1-1000 µm. Microsphere improves bioavailability, stability and targets the drug to a selected site at a predetermined rate. Sorts of microspheres are bioadhesive, floating, radioactive, polymeric, and biodegradable microspheres. Therefore, the array of practices for the groundwork of microspheres offers a chance to regulate drug administration properties and develop the therapeutic efficacy of a given drug. The microsphere is spherical microparticles & is employed where predictable & consistent particle area is vital. The microspheres have the drug located centrally within the particle encased within the unique polymeric membrane. The present review highlights various sorts of microspheres, different methods of preparation, their applications, and various parameters to gauge their efficiency. Microspheres have received much attention not just for prolonged release but also for targeted medicine. A systematic review of one of the most promising drug delivery systems should be easier to read than the medical research articles, as they target a wider audience. The systematic reviews of the microparticles conclude that spherical microspheres & are accustomed to delivering the drug at the target site with specificity if modified and take care of the specified concentration at the location of interest without the untoward effects presented during a consistent therapy to help research and retrieval of health.

Key words: Microsphere, Microparticles, Ionotropic Gelation, Microsphere Formulation, Microsphere Evaluation, Review Microspheres.

Introduction

Microparticles drug delivery system is one of the processes to provide the sustained and managed to ship of medication to long periods, as small particles of solids or tiny droplets of beverages surrounded employing partitions of natural and artificial polymer films of various thickness and degree of permeability performing as a release charge controlling substance¹. Originally practice of albumin microparticles in drug delivery systems was advised by Kramer in 1974². Microparticles are well-defined as particulate dispersions or solid particles by size in the range of 1 – 1000 micrometer³ where the drug is dissolved and entrapped, encapsulated or attached to a microparticles matrix⁴. Varying upon the preparation method, microparticles, microspheres, or microcapsules can be gained⁵. Microparticles are micrometric matrix systems and are efficiently sphere-shaped in shape⁶. Microparticles are the polymeric entities in which the drug is physically and homogeneously dispersed, whereas microcapsules are micrometric reservoir systems, and microcapsules may be globular or non-globular in shape³. Microcapsules are structures in which the drug is limited to a hollow surrounded by an exclusive polymer membrane. Microcapsules size 100-150 micrometer⁷. The microencapsulation technology allows protection of medication from the environment, stabilization of sensitive drug substances, elimination of incompatibilities, or masking of unsightly flavor⁸. Hence, they play an improved bioavailability of conven-

tional drugs and minimize side effects. Treatment is restricted to solid consideration. A more comprehensive and far-reaching approach and venture are critically required for suitable countermeasures and readiness⁹. Microparticles are also a valuable way of turning in APIs, which might be pharmacological lively but are difficult to supply due to confined solubility in water. In such tablets, attaining high C_{max}, T_{max} and AUC is problematic. Consequently, a need exists for fast-release products containing those agents. Microparticles-based formulations can offer a steady drug awareness within the blood or target tablets to precise cells or organs¹⁰. In recent years biodegradable polymeric microparticles, mainly those coated with a hydrophilic polymer which includes polyethylene glycol, known as long-circulating particles, have been used as potential drug delivery devices for of their ability to distribute for a prolonged period objected to a particular organ, and their proficiency in delivering proteins, peptides and genes¹¹.

Microparticles offer a way to supply macromolecules by spreading routes and efficiently managing the discharge of such pills or drugs¹². Additionally, it can be used to ship vaccines and molecules inclusive of DNA for use in gene therapy. Macromolecules offer adequate safety of encapsulated markers towards degradation, the opportunity of controlled and local shipping of the drug over intervals starting from a few hours to months, and smooth management. Controlled drug

Citation: Karmakar A, Dev Maity S, Barua S, Das R. Microsphere: A Wander around Drug Delivery. *Revis Bionatura* 2022;7(1). 13. <http://dx.doi.org/10.21931/RB/2022.07.01.13>

Received: 25 August 2021 / **Accepted:** 20 November 2021 / **Published:** 15 February 2022

Publisher's Note: Bionatura stays neutral with regard to jurisdictional claims in published maps and institutional affiliations.

Copyright: © 2022 by the authors. Submitted for possible open access publication under the terms and conditions of the Creative Commons Attribution (CC BY) license (<https://creativecommons.org/licenses/by/4.0/>).



delivery structures could be instrumental in supplying the optimal therapy for a given drug molecule. Each drug has a distinguishing 'minimum effective concentration', below which no therapeutic effect is detected and a specific 'minimum toxic concentration' above which undesired side effects arise. The range between is so-called the 'therapeutic range' or 'therapeutic window'. Varying upon the type of drug and biological factors, this therapeutic window could be thin⁵. The most advantageous effect of many clinical cares is obtained by keeping the drug attention inside the therapeutic variety over a sustained time frame⁵. Every scientist reconciles whether and what to decrypt and how to display it¹³. This is chiefly proper for potent drugs, together with anti-cancer drugs. Management of the entire drug dose straight away the use of conventional pharmaceutical dosage, the whole quantity is rapidly launched into the belly, absorbed into the bloodstream, and dispensed at some stage in the human frame. Therefore, the rate at which the drug is the movement website is often improved. Depending on the therapeutic range and dispensed dose, the risk of toxic side effects can be considerable.

The concentration decreases again as no continuous drug supply is provided, and the human body eliminates the active agent. This results in a shifting concentration of the drug levels in the plasma, and the therapeutic range is reached through a brief period¹⁴. This represents a pressing test to the pharmaceutical business to create practical conveyance frameworks for the proficient conveyance of this mind-boggling restorative in a naturally dynamic shape. Their need is the clinical and remedial districts has heightened the examination¹⁵. The hydrophilic and lipophilic drug may be fused or entrapped into moderately high-performance polymeric microparticles. Those styles of drug service structures have proved to be extra physico-chemically solid than liposomes both in vivo and throughout storage¹¹. Pharmacy discipline plays a fundamental role in patient healthcare. It is a considerable discipline that is present worldwide. With the propagation of the Internet and the growth in computer technology and manufacturing, the ratio of price to performance decreases¹⁶. The work done would su-

rely help in academic purpose and the reference to be used in the future development when all is said in done component of an expanded conveyance framework is progressively seen as a favorable answer for natural medications¹⁷.

Drug Delivery Systems

Novel drug delivery system

Several drug delivery and drug-directed systems are developed to minimize drug degradation, drug adverse effects, and surge the drug bioavailability (quantity of drug available at a site targeted section). Site precise drug delivery may be either active or passive procedure¹⁸.

Drug Delivery Carriers

Colloidal drug carrier techniques such as micellar solutions, liquid crystal dispersions, vesicles, and nanoparticle dispersions comprising tiny particles of 10–400 nm diameter show great promise as drug delivery systems. When budding these formulations, the goal is to gain systems with optimized drug loading and release properties, extended shelf-life and low toxicity¹⁹.

Micelles

Micelles formed by self-assembly of amphiphilic block co-polymers (5-50 nm) in aqueous solutions are of great interest for drug delivery applications²⁰. The drug or the medication may be physically entrapped in the middle of block copolymer micelles and transported at concentrations that may exceed their intrinsic water- solubility^{21,22}.

Liposome

Liposome serves lipoidal vesicles (lipid bilayer), which serve as drug providers to improve the shipping of pharmaceutical drugs²³. Liposomes are small lipoidal vesicles enclosing an aqueous solution inner a hydrophobic membrane. To deliver the molecules to the focused website online, the lipid bilayer

Demographic characters			
variant	groups	frequency	percent
gender	male	27	45.0
	female	33	55.0
	Total	60	100.0
residence	Urban	34	56
	Rural	26	43
	Total	60	100
employment	employ	16	26.7
	Not employ	44	73.3
	Total	60	100

Table 1. The demographic characters.

N=60	Intervention group			Control group		
	before	after	p-value	before	after	p-value
weight	85.75	84.85	<0.0001	86.30	87.08	<0.0001
Waist circumference	103.97	101.62	<0.0001	106.30	106.36	0.895
B.M.I.	31.11	30.40	<0.0001	32.27	32.55	<0.0001
FBS	176.93	141.4	<0.0001	183.36	192.40	0.035

*Significant P value < 0.05

Table 2. Comparisons characteristics of the study group before and after the intervention.

N=60	Intervention group Mean SD	Control group Mean SD	P-Value
Weight change	-0.89 ± 0.79	0.79 ± 0.88	<0.0001
Waist circumference changes	-2.35 ± 1.16	0.07 ± 2.75	<0.0001
BMI change	-0.71 ± 0.37	0.28 ± 0.88	<0.0001
FBS change	-35.07 ± 32.34	9.03 ± 22.36	<0.0001

* Significant P value < 0.05

Table 3. Shows the difference between the intervention and the control group in the mean change of the characteristics study group.

can fuse with different bilayers, including the cell membrane; for that reason, liposomes act as drug providers for drug shipping for drug delivery²³.

Hydrogels

Hydrogels are three-dimensional cross-linked water-soluble polymers²⁴. various combinations of polymers are formulated for novel drug delivery devices as novel drug delivery systems²³. numerous tablets formulated as hydrogels consist of Riboflavin, Salicylic acid, Simvastatin^{22,23}.

Nano Particles

Nanoparticles are amorphous or crystalline compounds starting from 10-200 nm, which are novel drug gadgets used for novel drug delivery systems²⁵. Nanoparticles adsorb or encapsulate the drug, thus protecting against chemical or enzymatic degradation^{26,27}. Diverse Nano gadgets for drug shipping include Nanotubes, quantum dots, Nanorobots, den dimers, Nanowires, Nanoshells and Nanopores²³. The discharge of the drug from the formulation is by controlled diffusion. Thus the discharge of the drug happens from the core, across the polymer matrix or membrane²³. Hence, the membrane acts as a barrier for drug release²⁸. therefore solubility and diffusivity of drug in polymer membrane will become the figuring out element for drug release^{23,29}.

Materials Used For Preparation Of Microsphere

Microspheres used typically are made with polymers that have manifold blessings. Those are reliable means to supply

the drug to the target website online with specificity if changed and keep the desired awareness on the web page of the hobby without untoward results³⁰. Strong biodegradable microspheres have the capacity during the particle-matrix for the controlled launch of drug³¹. Microspheres received much attention now for extended-release and for concentrating on anti-cancer drugs to the tumor³². the dimensions, surface fee, and floor hydrophilicity of microspheres have been attained to be crucial in regulating the fate of particles in vivo studies at the macrophage uptake of microspheres have verified their ability in concentrated on tablets to pathogens residing intracellularly³³. Microspheres made with polymers are classified into two types:

Synthetic Polymer

Synthetic polymers are divided into two types.

Non-biodegradable polymers

Some examples are Polymethyl methacrylate (PMMA) and Acrolein Glycidyl methacrylate and Epoxy polymers.

Biodegradable polymers

Some examples being Lactides as well as Glycolides with their co-polymers, Poly-alkyl cyano acrylates and Poly-anhydrides.

Natural polymers

Natural polymers gained from diverse sources like proteins, carbohydrates and chemically modified Carbohydrates,

Proteins like Albumin, Gelatin, and Collagen. Carbohydrates like Agarose, Carrageenan, Chitosan, and Starch. Chemically modified carbohydrates like Poly dextran, Poly starch³⁴. The health benefits are rewarding which gives an extra boost to use this items on daily basis keeping in check the over consumption³⁵.

Types Of Microspheres

Bio adhesive microspheres

Adhesion may be defined as sticking the drug to the membrane by using the sticking belongings of the water-soluble polymers³⁶. Adhesion of drug shipping device to the mucosal membrane consisting of buccal, rectal, ocular, and nasal can be labeled as bio adhesion³⁷. These microspheres show off a prolonged residence time at the website of software and motive intimate contact with the absorption web page, producing higher healing motion³⁸.

Magnetic microspheres

This kind of delivery system could be very a great deal essential which localizes the drug to the sickness or disease site³⁹. This large amount of freely circulating drug can be replaced via a smaller quantity of magnetically centered drug³⁹. Magnetic carriers hold magnetic responses to a magnetic area from integrated materials used for magnetic microspheres like chitosan, dextran⁴⁰. Therapeutic or healing magnetic microspheres are used to supply chemotherapeutic agents to liver tumors⁴⁰. Drugs like proteins and peptides also can be targeted through this system⁴¹. Diagnostic microspheres, used for imaging liver metastases and also can be used to extricate bowel loops from other abdominal systems by using forming nano-sized debris supramagnetic iron oxides⁴².

Floating microspheres

In floating kinds, the majority density is much less than the gastric fluid and stays buoyant within the stomach without affecting gastric emptying rate⁴³. The drug is launched slowly on the favored charge, and the gadget is determined to be floating on gastric content material, increasing gastric juice and increasing fluctuation in plasma⁴⁴. Moreover, it also reduces the possibility of dose dumping. It produces a prolonged therapeutic impact and consequently reduces dosing frequencies³⁷. Drug (ketoprofen) is given within the shape of floating microspheres^{42,45}.

Radioactive microspheres

Radioembolization treatment microspheres sized 10-30 nm are more significant than the capillaries' diameter and get tapped inside the first capillary bed once they come across. They may be injected into the arteries that cause them to tumors of the hobby, so these kinds of conditions radioactive microspheres deliver excessive radiation doses to the targeted regions without unfavorable the everyday surrounding tissues⁴⁴. It varies from drug delivery systems because radioactivity is not discharged from microspheres but acts from within a typical radioisotope distance and atypical kinds of radioactive microspheres are α emitters, β emitters, γ emitters⁴⁴.

Polymeric microspheres

The distinctive kinds of polymeric microspheres may be classified as biodegradable and synthetic polymeric microspheres^{42,44,46}.

Biodegradable polymeric microspheres

Natural polymers such as starch are worked with the concept that they are biodegradable, biocompatible, and also bioadhesive in the environment. Biodegradable polymers prolong the house time when touched with mucous membrane due to its high degree of swelling belongings with an aqueous medium, resulting in gel formation. The rate and quantity of drug release are measured using the polymer's concentration and the release pattern in a sustained way. The primary disadvantage is that in scientific use, drug loading performance of biodegradable microspheres is complicated and challenging to control the drug release⁴⁷, but it provides a wide range of applications in the microsphere-primarily based treatment⁴⁴.

Synthetic polymeric microspheres

Synthetic polymeric microspheres are broadly utilized in medical utility; moreover, that extensively utilized as a bulking agent, fillers, embolic particles, drug delivery vehicles⁴⁸ and proved to be safe and biocompatible, but the focal disadvantage of this kind of microspheres tends to migrate away from the injection site and lead to embolism, potential risk, and further organ damage^{44,46}.

Preparation Of Microspheres

Ionotropic gelation technique

The gelation technique has been enhanced through several inspired methodological modifications⁴⁹. Ionotropic gelation via electrospraying and spinning disc processing produces nanoparticles with a more uniform distribution. Hydrophobic and hydrophilic drugs can be encapsulated with high efficiency by emulsification followed by ionic gelation⁴⁹. Ionotropic gelation is based on the competence of polyelectrolytes to cross-link in the authority of counter ions to form hydrogels⁵⁰. The natural polyelectrolytes inspite, having a property of coating on the drug core and acting as release rate retardants, contains certain anions on their organic structure. These anions form a meshwork structure by combining with the polyvalent cations and inducing gelation by binding mainly to the anion blocks^{51,52}.

Single Emulsion Method

The microparticulate carriers of the natural polymers, carbohydrates, & proteins are prepared. The microparticulate carriers of natural polymers like proteins and carbohydrates are prepared by one emulsion technique^{36,53-55}. The natural polymers are dissolved or dispersed during an aqueous medium followed by dispersion in a non-aqueous medium like oil. Next, cross-linking of the dispersed globule is administered. The cross-linking is often achieved through warmth or using chemical cross-linkers. The chemical cross-linking agents used are formaldehyde, glutaraldehyde, and acid chloride. Heat denaturation isn't suitable for thermolabile substances. Chemical cross-linking suffers the disadvantage of excessive exposure of active ingredients to chemicals added during preparation and then subjected to centrifugation, washing, and separation. The character of the surfactants wont to stabilize the emulsion phases can significantly influence the dimensions, surface morphology, size distribution, drug loading and release, and bio performance of the ultimate product. Schematic description of the Single Emulsion Method is given in Fig No. 1.

Double Emulsion Method

This method of microspheres preparation involves the formation of multiple emulsions or double emulsions of type

w/o/w and is the most acceptable match to the water-soluble drugs, peptides, proteins, and vaccines. This method is often used with both naturals also as synthetic polymers. The aqueous protein solution is dispersed within the lipophilic organic continuous phase. This protein solution may enclose the active constituents. Schematic description of the Double Emulsion Method is given in Fig No. 2^{36,53-55}.

Polymerization Method

It is administered with the aid of the usage of exceptional techniques as bulk, suspension, precipitation, emulsion, and micellar polymerization methods. In bulk, a monomer or an aggregate of monomers alongside the initiator or catalyst is typically heated to initiate polymerization. The polymer so obtained could also be molded as micro-spheres. Schematic description of the Polymerization Method is given in Fig No. 3^{36,54}.

Phase Separation and Coacervation Method

This process is predicated on the principle of decreasing the polymer's solubility within the organic phase, which affects the formation of a polymer-rich phase called the coacervates. During this method, drug particles are dispersed during a polymer solution, and an incompatible polymer is brought to the device, making the primary polymer for the section separation. Schematic description of the Phase Separation and Coacervation method is given in Fig No. 4^{36,53-55}.

Spray Drying and Spray Congealing

These methods have supported drying the mist of polymer and drugs within the air. Depending upon removal of the solvent or cooling of the answer, these two processes are named spray drying and spray congealing. Microparticles are separated from the recent air by the cyclone separator while

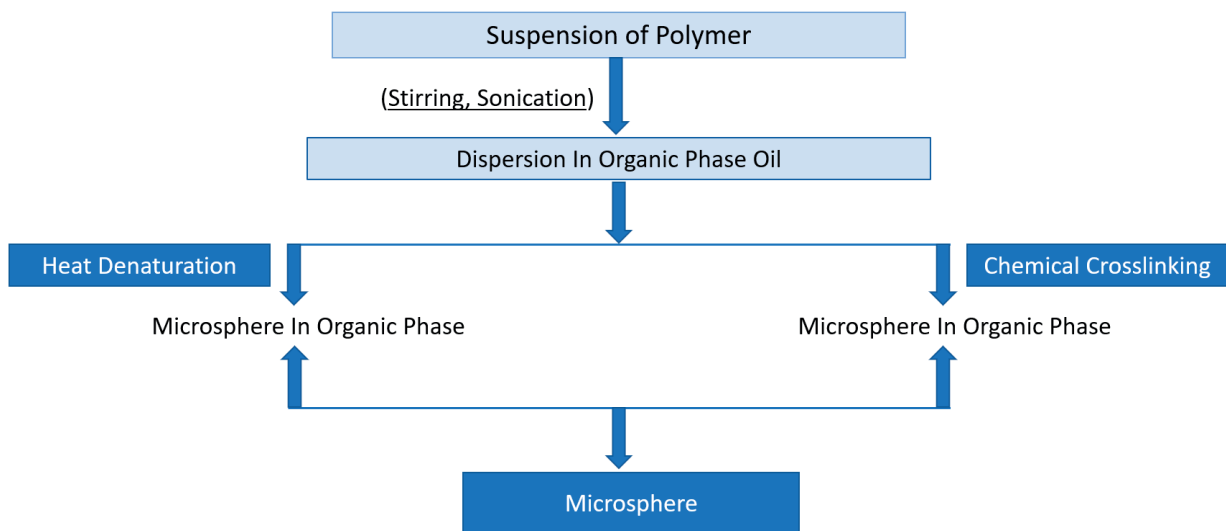


Figure 1. Single Emulsion method.

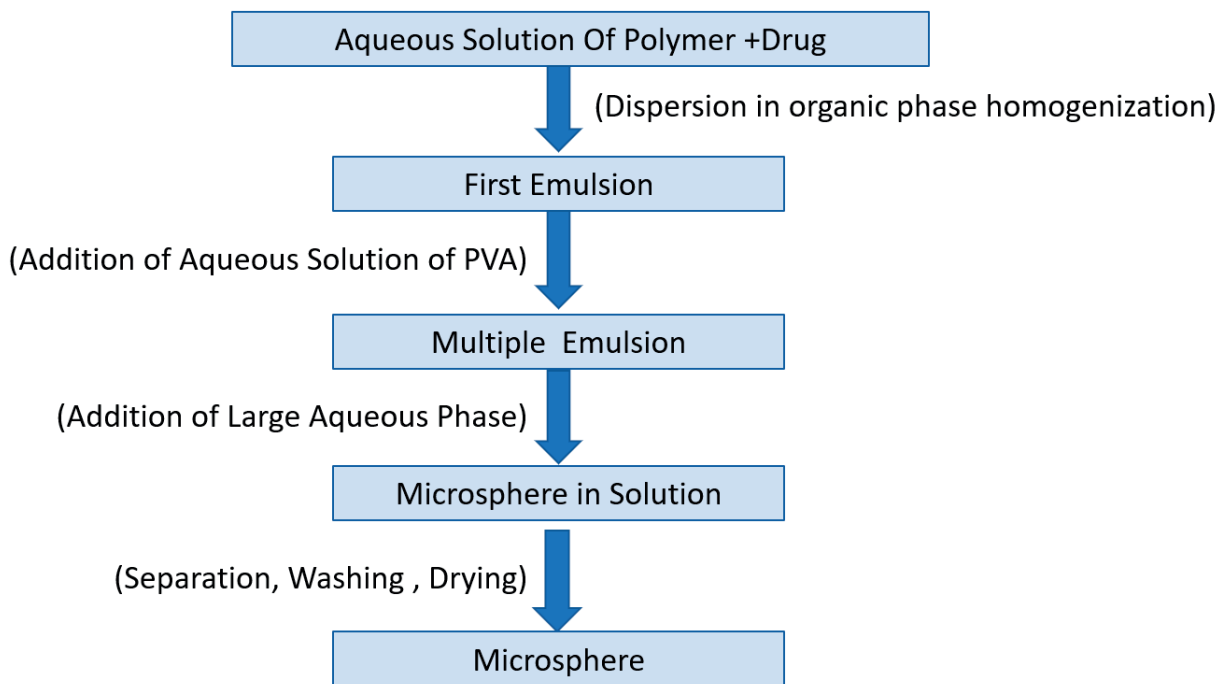


Figure 2. Double Emulsion method.

the traces of solvent are eliminated using vacuum drying. One of the principal advantages of the technique is the feasibility of operation below aseptic situations^{36,53-55}. The spray drying process is employed to encapsulate diverse penicillins. Thiamine mononitrate and sulphathiazole are encapsulated inside the mixture of mono and di-glycerides of stearic acid and palmitic acid using spray congealing. However, very speedy solvent evaporation results in the formation of porous microparticles. Schematic description of the Spray Drying and Spray Congealing method is given in Fig No. 5.

Other techniques are Wax Coating and Hot melt method, Air Suspension, Solvent Extraction, Precipitation, Freeze Drying⁵⁶.

Methods Of Preparation Of Microspheres by Iontropic Gelatin Technique

The microsphere of the test drug is prepared by ionotropic gelation technique using different proportions of polymers (sodium alginate and guar gum). Sodium alginate was dissolved in distilled water (10ml) in desired concentration and heated to make a liquid solution. Heated the desired quantity of guar gum in 10ml of water, mixed the sodium alginate solution, and prepared the polymer solution. Then the drug is brought

into the polymer answer. Make five extraordinary types of formula in line with the ratio of Sodium Alginate: Guar gum is 1:1, 2:1, 3:1, 4:1, 5:1. The gelation medium became prepared by dissolving calcium chloride (five% w/v). The homogenous alginate solution turned into extruded using a 21G syringe needle into the gelation medium. The space among the threshold of the needle and plane of gelation medium changed into about 10cms. The gel microspheres shaped have been left in the answer with mild stirring for 30 min at room temperature to improve mechanic strength⁵⁷. After that, microspheres are gathered and washed with distilled water two times, dried at room temperature for 24 hours, and stored in desiccators^{58,59}. Gels are well known to depend on solvents and preparation methods. For example, PVA hydrogels prepared with free-thaw cycling show exciting transparency features and a high modulus⁶⁰.

Evaluation Study Of Microspheres

Particle Size Analysis

Microspheres were separated into different size fractions by sieving for 10 minutes using a mechanical shaker (Geologists Syndicate Pvt Ltd, India) containing standard sieves

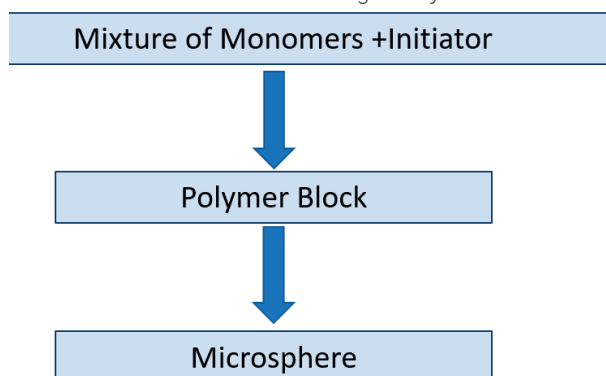


Figure 3. Polymerization method.

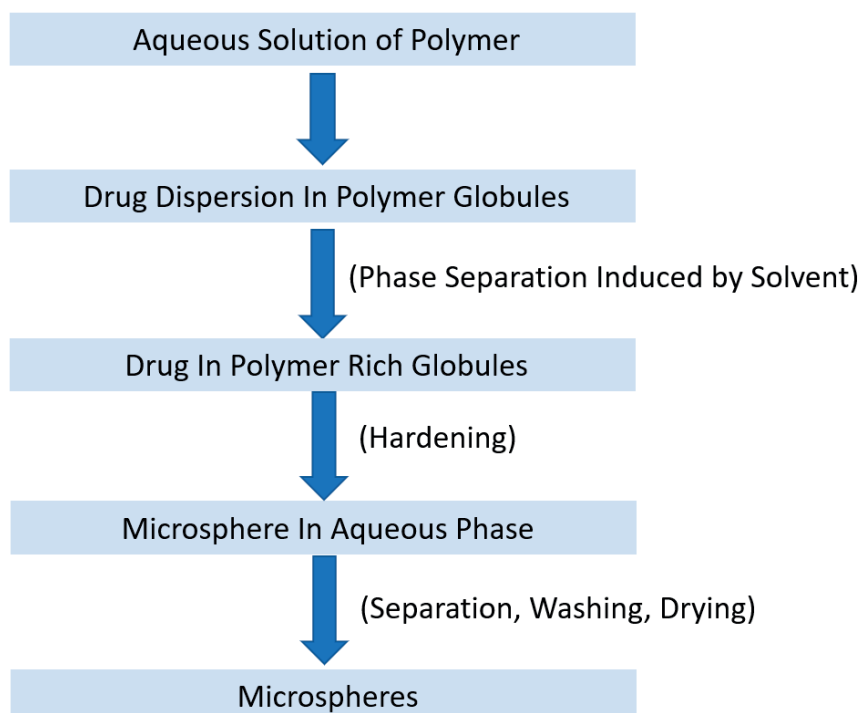


Figure 4. Phase Separation and Coacervation method.

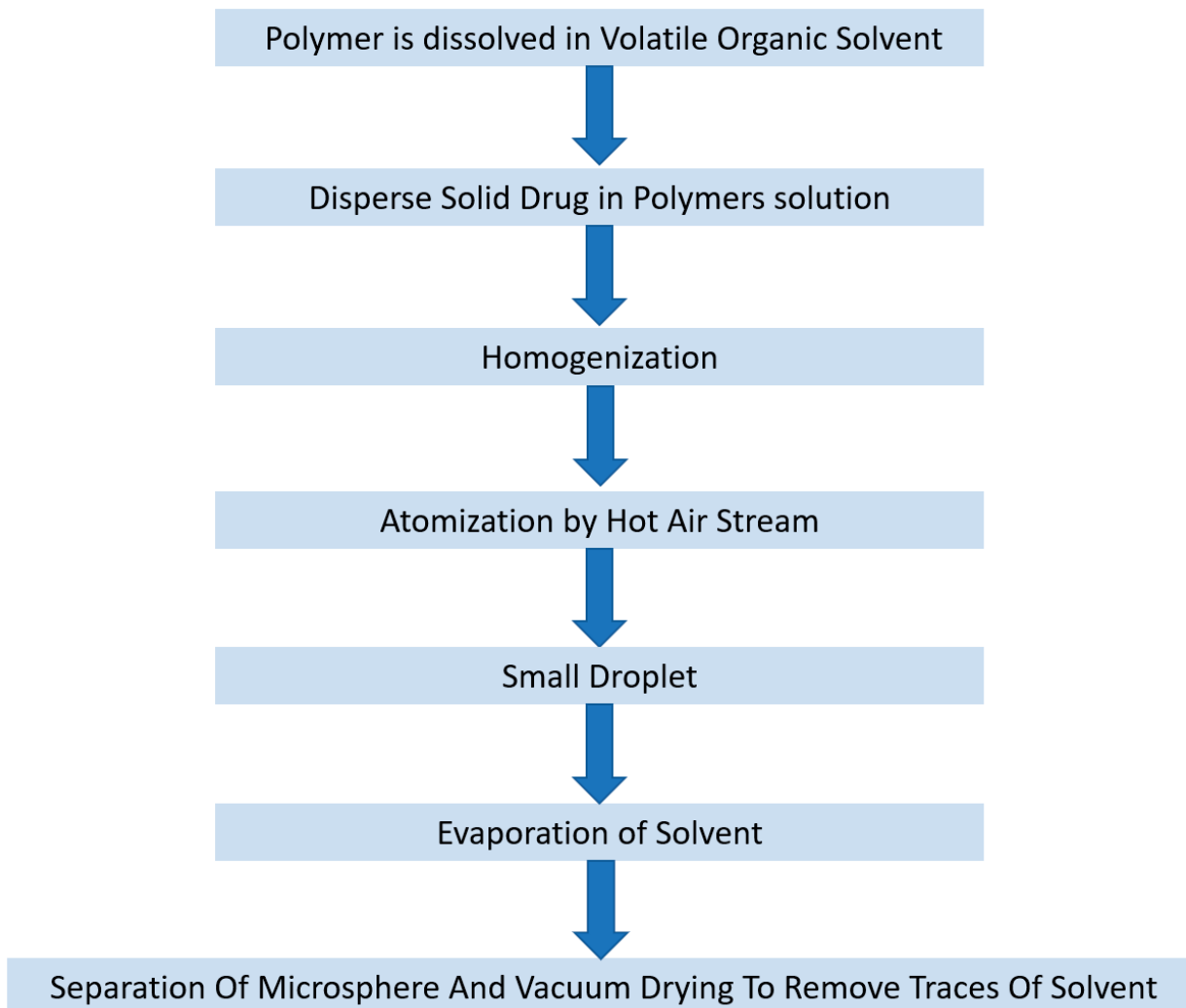


Figure 5. Spray Drying and Spray Congealing.

having a mesh size of #16, #18, and SS#25. The particle size distribution of the microspheres for all the formulations was determined, and the mean particle size of microspheres was calculated using the following formula⁶¹. Mean particle size = \sum (mean particle size of the fraction \times weight fraction) / \sum (weight fraction). Scanning Electron Microscopy is generally used to determine the particle's size and shape. The particle size can be determined by using light electron microscopy^{29,62}.

Surface morphology

The samples for the SEM evaluation had been prepared with the aid of sprinkling the microspheres on one facet of the adhesive stub. Then the microspheres were blanketed with gold earlier than microscopy. Finally, the morphology and size of the microspheres had been observed with the scanning electron microscope (FEI Quanta- 2 hundred MK2, Netherlands)⁶³.

Drug entrapment efficiency, drug loading

The amount of drug present in the Sodium Alginate and Guar Gum microspheres can be determined by taking the acknowledged quantity of microspheres wherein 100 mg of the drug needs to be present theoretically⁶⁴. Then, the microspheres were beaten, and the powdered microspheres were taken and dissolved in one hundred ml of phosphate buffer (pH7.4) solution and stirred for 15 minutes with a c program language period of five mins and allowed to hold for twenty-four hours.

Then the solution was filtered through Whitman No.1 filter paper. Then the absorbance became measured spectro-photometrically at 320nm in opposition to phosphate buffer (pH7.4) answer as clean with the help of UV double beam spectrophotometer, and concentrations had been determined by using the simultaneous equation: $Y = mx + c$

DEE (%) = [Experimental drug Content / Initial Drug Content into the Formulation] \times 100

Drug Loading (%) = $[Q_m / W_m] \times 100^{10}$

Where, W_m = weight of the microspheres;

Q_m = quantity of the drug present in the microspheres

FTIR Studies

The infrared (IR) spectra were recorded using an FTIR spectrophotometer (Perkin Elmer Spectrum GX) by the KBr pellet in the wavelength region between 4000 and 400 cm^{-1} ⁶⁵. The spectra obtained for metronidazole and physical mixtures of metronidazole with polymers were compared to check the compatibility of the drug with polymers^{62,64}.

In vitro drug release study

Dissolution studies were performed using an automated assembly comprising a dissolution bath (Pharmatest PTW III) and a UV visible spectrophotometer. For the first series of experiments, either 125 mg of drug or weighed quantities of microspheres containing 100 mg of test drug were placed in

six separate 1-liter containers containing aqueous phosphate buffer (0.2 M monobasic and 0.2 M dibasic sodium phosphate mixed to solve with pH 8). For the second series of experiments, dissolution media comprised five different buffer solutions, all prepared at pH 8, incorporating a range of cations and anions. The buffers consisted of the following pairs of compounds titrated together to achieve pH 8 solutions at 37°C: 0.2 M monobasic and 0.2 M dibasic sodium phosphate, 0.2 M monobasic and 0.2 M dibasic potassium phosphate, 0.1 M citric acid and 0.2 M dibasic sodium phosphate, 0.1 M MOPS and 0.1 M MOPS sodium salt and finally, 0.1 M tris and 0.1 M hydrochloric acid. Finally, for the third series of experiments, drug release studies were conducted for test drugs contained within stearic acid microspheres using a sodium phosphate buffer over a range of sodium and phosphate concentrations (0.01 M to 0.8 M and 0.02 M to 0.2 M, respectively). During all dissolution testing, a constant stirring speed and temperature were maintained at 200 rpm and 37°C, respectively. Changes in the absorbance values at 235 nm were recorded for 20 minutes at two-minute intervals. Results are replicated (n=6) for statistical analysis, and a mean value for absorbance was then calculated to obtain the percentage of drug released for each time interval. It should be noted that before drug release experiments, it was found that the presence of the drug and/or microspheres did not affect the pH of the dissolution media under any conditions investigated in this research. A solution of pH 8 was chosen to optimize the solubility of the drug^{62,64}. Various limitations relating to atmosphere, edaphic, generation, and innovation viewpoints as specified underneath frustrates higher efficiency⁶⁶.

Angle Of Repose

Firstly, measure the height (h) of the microsphere pile from the ground's peak⁶⁴. Then measured the horizontal distance (d) from the middle of the pile to the edge. Then use the formula

$$\text{Angle of Repose} = \tan^{-1}(2h/d)$$

Bulk Density and Tapped Density

The bulk density is received by adding a regarded powder mass to a graduated cylinder. The tapped density is obtained by robotically tapping a graduated cylinder containing the microspheres until little similar volume change is determined. The tapped density is calculated as mass divided with the aid of the very last volume of the powder^{67,68}.

Swelling study (degree of swelling)

Microspheres (one hundred mg) had been positioned in a little extra distilled water, 0.1N HCL, and PBS (pH 7. four) and allowed to swell to consistent weight. The microspheres were separated and blotted with filter paper, and their modifications in weight modifications had been computed at a c program language length of 10 minutes and recorded. The diploma of swelling (A) changed into then calculated from the components: $A = Wg - WO / WO$ in which WO is the preliminary weight of the beads, and Wg is the burden of the beads at equilibrium swelling within the medium^{53,54,64,69}.

Percentage Yield

The prepared microspheres were wholly dried in an oven maintained at 37°C for 24 hours and then weighted^{54,64,69}. The percentage yield of microspheres was calculated according to the following equation: % Yield = (Practical Yield / Theoretical Yield) * 100

Discussion

This review article reflects upon the ionotropic gelation technique of Microsphere formulation. Future possible advancements with microsphere drug delivery were based on the information and knowledge; progress is possible. An individual should enrich the knowledge of different subjects. The more people gain knowledge, the more contribution can be expected to this subject⁷⁰. A microsphere is a process in which drug particles can be encapsulated in a biodegradable polymer or a synthetic polymer that can be used as a delivery system. A controlled or sustained drug delivery system or insoluble drugs has become a significant concern for all in the pharmaceutical field because of its expenses, time-consuming, and development process^{71,72}. In this pharmaceutical field, the microsphere plays a significant role where different kinds of problems can be solved quickly, such as it can be used to increase the bio-availability of the highly insoluble drugs in nature²¹. In the pharmaceutical measurements shapes that contain it as one of a kind dynamic standard with very productive outcomes for the particular motivations behind its outline⁷³.

Cancer is considered a common disease in the whole world. Currently, chemotherapy is considered one of the most common treatments by almost all doctors in this situation. HER2, human epidermal growth factor 2, is a marker for breast cancer that is overexpressed by 25% - 30% for invasive breast cancers. Anti-cancer drugs loaded with albumin microsphere can show the effect against human epidermal growth factor 2 (HER2) and a relatively new type of "targeted" cancer therapy for breast cancer treatment^{74,75}. These assumptions may seem restrictive, but they are satisfied for many natural systems, and in any case, the resulting expressions yield invaluable insights⁷⁶.

In this fast living world, we find discoveries of different kinds of drugs almost every day that lead to more effective results. Every drug has its gains and drawbacks; working with a microsphere can open many different sections to deal with the drugs that possess different kinds of problems. Researchers are working hard for more betterment of this work, and betterment is such a process that shall be ever-growing⁷⁷. Above mentioned suggestions, recommendations, research depend on our statistical surveying, which is restricted as far as anyone is concerned, and capacity and the discoveries from this investigation are probably going to factor unequivocally into essential arranging⁷⁸.

On the other hand, vaccines are considered one of the most efficient and inexpensive ways to immunize and control infectious diseases. The dose of the vaccine can be encapsulated by a layer of polymer or a biodegradable polymer, which in turn helps in the controlled release of the antigen in the body, and therefore the multiple dosage forms of the vaccine can be reduced as low as a single dosage form⁷⁹. More studies are required in this field for a better palliative approach. Compartment displaying is broadly utilized and a matter of worry in restorative sciences⁸⁰.

Conclusions

Microspheres (Few Lab Prepared Microspheres is given in Fig No. 6.) are characteristically free-flowing powders having a particle size starting from 1-1000 μm consisting of proteins or synthetic polymers where the range of techniques for the preparation of microspheres provides multiple options to regulate as drug administration aspects and to reinforce the



Figure 6. Few Lab Prepared Microspheres.

therapeutic efficacy of a given the drug. Although there is a variety of difficulties to be figured out to achieve prolonged gastric retention, an excessive number of companies are that specializes in commercializing this system due to their advantages of sustained and controlled-release action, reduced dose frequency, improved steadiness, dissolution rate, and bioavailability the microspheres drug delivery system is that the hottest drug delivery system. Compared to standard dosage forms, these delivery systems offer numerous advantages, including improved efficacy, reduced toxicity, improved patient compliance, and convenience. Such systems frequently use macromolecules as carriers for the drugs. Microspheres by ionotropic gelation technique promise a possible approach for gastric retention. By combining various other strategies, within the future, the microspheres will find a prominent & central place within the novel drug delivery, particularly within the diagnostics, diseased cell sorting, gene & genetic materials, targeted, safe, effective & specific in vitro delivery & supplements because the miniature versions of the diseased tissues & organ within the body.

Author Contributions

Anirban Karmakar: Literature Review & Investigation, Writing – Original Draft Preparation & corresponding author. Soumya Dev Maity: Software, Editing, Correction, Software and other essentials. Raneet Das: Data Curator, Acquiring Permissions, Visualization, Writing – Reviewing and Editing. Shayere Barua: Writing – Reviewing and Editing, Reformatting.

Funding

Authors declare no such funding related to this article.

Acknowledgments

The authors are very thankful to Suprodip Mandal (Assistant Professor, Department Of Pharmacognosy, School Of Pharmacy, Techno India University, Salt Lake Sec-V, Kolkata) for his professional devotion vigor and his guidance during this project.

Conflicts of Interest

Authors do not claim any conflict of interest.

Bibliographic references

1. Devi J, Muthu AK. Isolation and characterization of active components derived from whole-plant of *Saccharum spontaneum* (linn.). 2015;7:197-203.
2. Kramer PA. Albumin Microspheres as Vehicles for Achieving Specificity in Drug Delivery. *Journal of Pharmaceutical Sciences*. 1974;63(10):1646-1647. doi:10.1002/jps.2600631044
3. Singh MN, Hemant KSY, Ram M, Shivakumar HG. Microencapsulation: A promising technique for controlled drug delivery. *Res Pharm Sci*. 2010;5(2):65-77.
4. Nikam PM, Gondkar SB, Saudagar RB. Nanocrystal Drug Delivery System: A Review. *Rese Jour Pharmaceut Dosag Form and Technol*. 2016;8(2):122. doi:10.5958/0975-4377.2016.00016.1
5. Padalkar DrA, Shahi S, Thube patil M. Micro particles: An approach for betterment of drug delivery system. *International Journal of Pharma Research and Development – Online*. 2011;3:March/012.
6. Bidyut Das, Juti Rani Devi. MICROPARTICULATE DRUG DELIVERY SYSTEM- A REVIEW. *World Journal of Pharmaceutical and Life Sciences WJPLS*. 2(6):243-258.
7. Bharath S. *Pharmaceutical Technology: Concepts and Applications*. Pearson Education India; 2013. Accessed June 10, 2021. <https://books.google.co.in/books?id=akQ8BAAQAQBAJ&pg=PA189&lpg=PA189&dq=%22Microcapsules+are+systems+in+which+the+drug+is+confined+to+a+cavity+surrounded+by+a+unique+polymer+membrane.%22+source=bl&ots=ICKJp05OJb&sig=ACfU3U2lIR3TVz-3CYMWxMG5y66vIGjVfAw&hl=en&sa=X&ved=2ahUKewiQ1or-JzYTWAhXs7HMBHdphD5QQ6AEwAnoECAEQAw#v=onepage&q&f=false>
8. Drx Rather Ishfaq. microparticulate drug delivery system ppt. Presented at the: 04:10:21 UTC. Accessed June 10, 2021. <https://www.slideshare.net/DrxRatherIshfaq/ishfaq-ahmad-rather-power-presentation>
9. Saha A, Debnath B. The obscure impact of Nipah virus. *RB*. 2019;4(1). doi:10.21931/RB/2019.04.01.13
10. Spain SG, Yaşayan G, Soliman M, Heath F, Saeed AO, Alexander C. Nanoparticles for Nucleic Acid Delivery. In: *Comprehensive Biomaterials*. Elsevier; 2011:389-410. doi:10.1016/B978-0-08-055294-1.00133-1
11. Gupta P, Vermani K, Garg S. Hydrogels: from controlled release to pH-responsive drug delivery. *Drug Discovery Today*. 2002;7(10):569-579. doi:10.1016/S1359-6446(02)02255-9
12. study of microparticle preparation by the solvent evaporation method using focused beam reflectance measurement (fbm) - pdf free download. accessed june 10, 2021. <https://docplayer.net/29309088-Study-of-microparticle-preparation-by-the-solvent-evaporation-method-using-focused-beam-reflectance-measurement-fb.html>
13. Saha A, Chatterjee A, Chowdhury S. An Overview on the Role of Transcription in Medical and Computer Application. *CiiT International Journal of Artificial Intelligent Systems and Machine Learning*. 2018;10(10):230-238. doi:AIML102018004
14. Bankar S.K, Chaudhari A.V, Mahale N.B, Chaudhari S.R. A Review on Orodispersible Tablets Prepared Using Spray Dried Sustained Release Microparticles. *JADD*. 1(2):82-95.
15. Saha A, Bhattachajee S, Mukherjee S. Research and Review: Drugs and Drugs Development Based on Protein Drug Delivery System. *Research and Advances in Pharmacy and Life Sciences*. 2019;1(1):1-13. doi:http://doi.org/10.5281/zenodo.1
16. Saha A, Chatterjee A, Ghosh M. An Overview On The Utility Of Computer Application In The Pharmacy World And Its Significance. *IRJPS*. 2018;5(3):1628-1635. doi:10.21276/irjps.2018.5.3.9
17. Saha A, Debnath B. Research And Review: Drugs And Drugs Development Based On Novel Drug Delivery System. *Research & Review: Drugs and Drugs Development*. 2018;1(1):1-13. doi:10.5281/ZENODO.1477186
18. Hennink WE, van Nostrum CF. Novel cross-linking methods to design hydrogels. *Advanced Drug Delivery Reviews*. 2002;54(1):13-36. doi:10.1016/S0169-409X(01)00240-X

19. Sharma J, Kalra S, Sharma A, Rani S. Colloidal Drug Carriers. *The Internet Journal of Family Practice*. 2009;9(2). Accessed June 10, 2021. <http://ispub.com/IJFP/9/2/10130>
20. Recent Advances in Novel Drug Delivery Systems. *AZoNano.com*. Published March 25, 2006. Accessed June 10, 2021. <https://www.azonano.com/article.aspx?ArticleID=1538>
21. Tiwari G, Tiwari R, Sriwastawa B, et al. Drug delivery systems: An updated review. *Int J Pharm Investig*. 2012;2(1):2-11. doi:10.4103/2230-973X.96920
22. Kabiri K, Omidian H, Hashemi SA, Zohuriaan-Mehr MJ. Synthesis of fast-swelling superabsorbent hydrogels: effect of cross-linker type and concentration on porosity and absorption rate. *European Polymer Journal*. 2003;39(7):1341-1348. doi:10.1016/S0014-3057(02)00391-9
23. Kotturi N. Research and Reviews: Journal of Pharmaceutics and Nanotechnology. 2015;3(2):4.
24. Ahmed EM. Hydrogel: Preparation, characterization, and applications: A review. *Journal of Advanced Research*. 2015;6(2):105-121. doi:10.1016/j.jare.2013.07.006
25. Singh A, Garg G, Sharma P. NANOSPHERES: A NOVEL APPROACH FOR TARGETED DRUG DELIVERY SYSTEM. 5(3):5.
26. novel drug delivery system. *vibdoc.com*. Accessed June 10, 2021. <https://vibdoc.com/novel-drug-delivery-system.html>
27. Surabhi Mehra, Ashok Kumar, Shamsheer S Kanwar. Synthesis of an Antioxidant n-propyl Gallate by Magnetic Iron Nanoparticles-bound Lipolase. *Research & Reviews: Journal of Pharmaceutics and Nanotechnology*.
28. Drug Release - an overview | ScienceDirect Topics. Accessed June 10, 2021. <https://www.sciencedirect.com/topics/nursing-and-health-professions/drug-release>
29. Alvarez-Lorenzo C, Concheiro A. Reversible adsorption by a pH- and temperature-sensitive acrylic hydrogel. *Journal of Controlled Release*. 2002;80(1-3):247-257. doi:10.1016/S0168-3659(02)00032-9
30. Hadpad Shobha, Jadhav Shital. Microspheres - a novel drug delivery system. 1. Accessed June 10, 2021. https://www.ejbps.com/ejbps/abstract_id/5821
31. B. Sree Giri Prasad, V. R. M Gupta, N. Devanna, K. Jayasurya. MICROSPHERES AS DRUG DELIVERY SYSTEM – A REVIEW. *Journal of Global Trends in Pharmaceutical Sciences*. Accessed June 10, 2021. <https://1library.net/document/yrk5l0jz-microspheres-as-drug-delivery-system-a-review.html>
32. Midha K, Nagpal M, Arora S. Microspheres: a recent update. *International Journal of Recent Scientific Research*. 2015;6(8).
33. Byrne ME, Park K, Peppas NA. Molecular imprinting within hydrogels. *Advanced Drug Delivery Reviews*. 2002;54(1):149-161. doi:10.1016/S0169-409X(01)00246-0
34. Acharya A, Mohan H, Sabharwal S. Radiation induced polymerization and cross-linking behavior of N-hydroxy methyl acrylamide in aqueous solutions. *Radiation Physics and Chemistry*. 2002;65(3):225-232. doi:10.1016/S0969-806X(02)00271-2
35. Saha A, Das M, Das A, Mandal S. Dietetic Benefits of Yogurt Based Beverage (Lassi) Becoming Fact-Finding Probe in Research. *IJPR*. 2021;13(03):1150-1156. doi:10.31838/ijpr/2021.13.03.157
36. Ganesan P, Deepa John AJ, Sabapathy L, Duraikannu A. Review on Microsphere. *American J of Drug Discovery and Development*. 2014;4(3):153-179. doi:10.3923/ajdd.2014.153.179
37. A.G. Chintale, V.S. Kadam, K.S. Maske, D.B. Raut, S.V. Kale, S.D. Rai. Recent Advances in Microsphere Drug Delivery System: A Review. Accessed June 10, 2021. https://rjptonline.org/HTML_Papers/Research%20Journal%20of%20Pharmacy%20and%20Technology_PID_2013-6-4-11.html
38. Gavalvi KV, Kengar MD, Chavan KV, Anekar VP, Khan NI. A Review on Microsphere and its Application. *Asian Jour Pharmac Res*. 2019;9(2):123. doi:10.5958/2231-5691.2019.00020.0
39. Chandna A, Batra D, Kakar S, Singh R. A review on target drug delivery: magnetic microspheres. *Journal of Acute Disease*. 2013;2(3):189-195. doi:10.1016/S2221-6189(13)60125-0
40. Hamad Farah F. Magnetic Microspheres: A Novel drug delivery system. *japlr*. 2016;3(4). doi:10.15406/japlr.2016.03.00067
41. chitra singh, suresh purohit, madhu singh, b.l.pandey. design and evaluation of microspheres:a review. *journal of drug delivery research*. 2(2). Accessed June 10, 2021. https://www.academia.edu/5260698/Design_and_evaluation_of_microspheres_a_review
42. Pal K, Banthia AK, Majumdar DK. Preparation and characterization of polyvinyl alcohol-gelatin hydrogel membranes for biomedical applications. *AAPS PharmSciTech*. 2007;8(1):21. doi:10.1208/pt080121
43. Kaushik A, Tiwari A, Gaur A. Role of excipients and polymeric advancements in preparation of floating drug delivery systems. *Int J Pharma Investig*. 2015;5(1):1. doi:10.4103/2230-973X.147219
44. Tarun Virmani, Jyoti Gupta. Pharmaceutical application of microspheres: an approach for the treatment of various diseases. *ijpsr*. 8(8). doi:10.13040/ijpsr.0975-8232.8(8).3252-60
45. Mukund JY, Kantilal BR, Sudhakar RN. Floating microspheres: a review. *Braz J Pharm Sci*. 2012;48(1):17-30. doi:10.1590/S1984-82502012000100003
46. Horii F, Hu S, Ito T, et al. Cross polarization/magic angle spinning 13C n.m.r. study of solid structure and hydrogen bonding of poly(vinyl alcohol) films with different tacticities. *Polymer*. 1992;33(11):2299-2306. doi:10.1016/0032-3861(92)90520-7
47. Manoj kumar das, abdul baquee ahmed, dipankar saha. microsphere a drug delivery system—a review. *international journal of current pharmaceutical research*. 11(4):34-41.
48. Manish Jamini, Saurabh Rawat. A Review on Microsphere. *Research Journal of Pharmaceutical, Biological and Chemical Sciences*. 4(1). Accessed June 10, 2021. https://www.academia.edu/6790961/A_Review_on_Microsphere
49. Desai KG. Chitosan Nanoparticles Prepared by Ionotropic Gelation: An Overview of Recent Advances. *Crit Rev Ther Drug Carrier Syst*. 2016;33(2):107-158. doi:10.1615/CritRevTherDrugCarrierSyst.2016014850
50. Ganesh N. S., G.Bharathi, Hanumanthachar Joshi, Jayanthi C, Devendra Pratap Singh. buoyant multiparticulate drug delivery - a focus on hydrogel beads. *woorlidd j jooourrnaall ooff pphhaarrrmmaac y y aanndd pphhaarrrmmaacceeuttiiccaall ssciiieen nccceess*. 2(2). accessed june 10, 2021. https://www.academia.edu/5741871/buoyant_multiparticulate_drug_delivery_a_focus_on_hydrogel_beads_wjpps?auto=download
51. j.s. patil, m.v. kamalapur, s.c. marapur, d.v. kadam. ionotropic gelation and polyelectrolyte complexation: the novel techniques to design hydrogel particulate sustained, modulated drug delivery system: a review. *digest journal of nanomaterials and biostructures*. 5(1):241-248.
52. Peppas NA, Merrill EW. Development of semicrystalline poly(vinyl alcohol) hydrogels for biomedical applications. *J Biomed Mater Res*. 1977;11(3):423-434. doi:10.1002/jbm.820110309
53. Mahale MM, Saudagar RB. Microsphere: A Review. *Journal of Drug Delivery & Therapeutics*. 2019;9(3-s):854-856. doi:http://dx.doi.org/10.22270/jddt.v9i3
54. NR K. Microsphere: A Brief Review. *AJBPS*. 2015;05(47):13-19. doi:10.15272/ajbps.v5i47.713
55. Patil NV, Wadd NV, Thorat SS, Upadhye SS. Microspheres: A Novel Drug Delivery System. *Am J Pharm Tech Res*. 2020;10(02):286-301.
56. Oakenfull D, Scott A. Gelatin gels in deuterium oxide. *Food Hydrocolloids*. 2003;17(2):207-210. doi:10.1016/S0268-005X(02)00053-X
57. Ajaykumar Tiwari, Gaurang Patel, Nirav Rabadia. FORMULATION AND EVALUATION OF FLOATING MICROSPHERE H2RECEPTOR BLOCKER RANITIDINE HCLBY IONIC GELATION METHOD. *International Journal Of Pharmaceutical Sciences And Research*. 3. Accessed June 10, 2021. <https://1library.net/document/zkeljx1z-formulation-evaluation-floating-microsphere-receptor-blocker-ranitidine-gelation.html>
58. Syed Ershad, V Sai Kishore, U Kartheek, M Sandeep, K Prameela Rani, K Adithya. Preparation and Evaluation of Floating Microspheres of Ritonavir. *Research And Reviews:Journal Of Pharmacy And Pharmaceutical Sciences*. 2013;3(1). Accessed June 10, 2021. <https://www.rroij.com/open-access/preparation-and-evaluation-of-floating-microspheres-of-ritonavir-5-11.pdf>

59. Pal K, Pal S. Development of Porous Hydroxyapatite Scaffolds. *Materials and Manufacturing Processes*. 2006;21(3):325-328. doi:10.1080/10426910500464826
60. Rinku khurana, Alka Ahuja, Roop K. Khar. Development And Evaluation of Mucoadhesive Films Of Miconazole Nitrate. *Indian Journal Of Pharmaceutical Sciences*. Accessed June 11, 2021. <https://ijpsr.com/bft-article/buccal-patches-a-review/?view=fulltext>
61. BC Behera, SK Sahoo, S Dhal, BB Barik, BK Gupta. Characterization Of Glipizide-Loaded Polymethacrylate Microspheres Prepared By An Emulsion Solvent Evaporation Method. *Tropical Journal of Pharmaceutical Research*. 7. Accessed June 10, 2021. <http://www.bioline.org.br/request?pr08003>
62. Pal K, Banthia AK, Majumdar DK. Development of carboxymethyl cellulose acrylate for various biomedical applications. *Biomed Mater*. 2006;1(2):85-91. doi:10.1088/1748-6041/1/2/006
63. Yaswanth Allamneni, B V V K Reddy, P Dayananda Chary, Venkata Balakrishna Rao N, S Chaitanya Kumar, Arun Kumar Kalekar. Performance Evaluation of Mucoadhesive Potential of Sodium Alginate on Microspheres Containing an Anti-Diabetic Drug: Glipizide. *International Journal of Pharmaceutical Sciences and Drug Research*.:115-122.
64. Mazumder R, Allamneni Y, Firdous SM, Parya H, Chowdhury AD. Formulation, development and in-vitro release effects of ethylcellulose coated pectin microspheres for colon targeting. *Asian J Pharm Clin Res*. 2013;6(5):138-144.
65. Ramana G, Krishna Chaitanya A. Preparation and In-vitro characterization of ethylcellulose coated pectin alginate microspheres of 5-fluorouracil for colon targeting. *Journal Of Applied Pharmaceutical Science*. Accessed June 10, 2021. <https://1library.net/document/yn4e6rjz-journal-of-applied-pharmaceutical-science.html>
66. Saha A, Mandal S. Nutritional Benefit of Soybean and Its Advancement in Research. *SFP*. 2019;5:6-16. doi:10.18052/www.scipress.com/SFP.5.6
67. Bulk and Tapped Density. *Particle Analytical*. Accessed June 10, 2021. <https://particle.dk/methods-analytical-laboratory/bulk-and-tapped-density/>
68. Falk B, Garramone S, Shivkumar S. Diffusion coefficient of paracetamol in a chitosan hydrogel. *Materials Letters*. 2004;58(26):3261-3265. doi:10.1016/j.matlet.2004.05.072
69. Sharma N, Purwar N, Gupta PC. MICROSPHERES AS DRUG CARRIERS FOR CONTROLLED DRUG DELIVERY: A REVIEW. *IJPSR*. 2015;6(12):4579-4587. doi:10.13040/IJPSR.0975-8232.6(11).4579-87
70. Saha A, Das A, Mandal S. Reading Journals of Different Spectrum: Necessities and Importance. *IJNHS*. 2021;2(1):1-4.
71. Ju X-J, Chu L-Y. Lab-on-a-chip fabrication of polymeric microparticles for drug encapsulation and controlled release. In: *Microfluidics for Pharmaceutical Applications*. Elsevier; 2019:217-280. doi:10.1016/B978-0-12-812659-2.00009-0
72. Kakkar V, Wani SUD, Gautam SP, Qadrie ZL. ROLE OF MICROSPHERES IN NOVEL DRUG DELIVERY SYSTEMS: PREPARATION METHODS AND APPLICATIONS. *Int J Curr Pharm Sci*. Published online May 15, 2020:10-15. doi:10.22159/ijcpr.2020v12i3.38326
73. Saha A, Jana M, Das A. Comparative In Vitro Evaluation Of Two Commercially Available Brands Of Pantoprazole And Domperidone Capsules. *IRJPS*. 2018;5(2):1500-1505. doi:10.21276/irjps.2018.5.2.13
74. Rajput M, Agrawal P. Microspheres in cancer therapy. *Indian J Cancer*. 2010;47(4):458. doi:10.4103/0019-509X.73547
75. King J, Quinn R, Glenn DM, et al. Radioembolization with selective internal radiation microspheres for neuroendocrine liver metastases. *Cancer*. 2008;113(5):921-929. doi:10.1002/cncr.23685
76. Saha A, Bhattacharjee S. Research and Review: Based on Distillation, Distillation Types and Advancements: A Short Summary. *Journal of Advances in Pharmacy Practices*. 2019;1(1):8-16. doi:10.5281/ZENODO.2545018
77. Jana M, Mandal S, Das A, Das M, Saha A. Granulation strategy holding a dynamic rhythm in herbal pharmaceuticals. *PHARMA-WAVE*. 2020;13:9-24.
78. Saha A, Das A, Dutta S, Mandal S. A Competitive Analysis Of Top Ten Pharmaceutical Companies In India. *RB*. 2021;6(2):1865-1872. doi:10.21931/RB/2021.06.02.30
79. Eldridge JH, Staas JK, Meulbroek JA, McGhee JR, Tice TR, Gilley RM. Biodegradable microspheres as a vaccine delivery system. *Molecular Immunology*. 1991;28(3):287-294. doi:10.1016/0161-5890(91)90076-V
80. Saha A, Bhattacharjee S, Jana M, Mandal S. Research And Review: Advancement In The Pharmacokinetics Of One Compartment Modeling. *IJNHS*. 2020;1(2):7-18.

REVIEW / ARTÍCULO DE REVISIÓN

Tasa de retención de sellantes de resina en esmalte dental con alteraciones estructurales: una revisión sistemática

Retention rate of resin sealants in dental enamel with structural alterations: a systematic review

Javiera Jiménez-Díaz¹, Gabriela Curtze-Scotts¹ and Guillermo Barahona-Fuentes^{2*}

DOI. 10.21931/RB/2022.07.01.14

¹ Universidad Andrés Bello, Facultad de Odontología, Viña del Mar, Chile.² Grupo de Investigación en Salud, Actividad Física y Deporte ISAFYD, Universidad de Las Américas, sede Viña del Mar, Chile.
Corresponding author: danielbarahonaf@gmail.com

Resumen: Los sellantes de resina han sido utilizados de manera preventiva y terapéutica en esmalte dental. Este último puede presentar distintas condiciones en su estructura. En este sentido, la retención adhesiva en esmalte sano posee amplia evidencia en su efectividad, no así en esmalte con alteraciones estructurales. De esta manera, se hace relevante conocer la retención adhesiva de estos materiales y cómo se comportan en el tiempo en esmalte con variaciones en su composición. Determinar la tasa de retención que presentan los sellantes de resina en esmalte dental con alteraciones estructurales. El estudio forma parte de una revisión sistemática, que sigue el protocolo PRISMA. Se examinaron artículos publicados entre 2010 y 2020 sobre el comportamiento retentivo de los sellantes de resina en esmalte dental con alteraciones estructurales. La búsqueda electrónica fue realizada en Web of Science, Scopus, PubMed y Medline. Se incorporaron aquellos artículos que utilizaron sellantes de resina en esmalte dental con alteraciones estructurales en ensayos clínicos. Resultados: Se encontraron ocho artículos. Estos fueron estratificados según la superficie de aplicación; (i) superficie cariada, (ii) superficie con fluorosis y (iii) superficie con hipomineralización incisivo molar. Se evidenció que la tasa de retención de los sellantes de resina sobre esmalte cariado es de un 80% en promedio, en esmalte con fluorosis dental un 67,5% y esmalte con hipomineralización incisivo molar 72% a los 2 años de su aplicación. El comportamiento retentivo de sellantes de resina sobre esmalte con alteraciones estructurales es adecuada para las tres superficies de aplicación. Sin embargo, se requiere de mayores estudios respecto a fluorosis dental e hipomineralización incisivo molar. La mayor evidencia sobre la tasa de retención se encontró en superficies cariadas.

Palabras clave: Sellantes de resina, Retención adhesiva, Caries dental, Fluorosis dental, Hipomineralización incisivo molar.

Abstract: Resin sealants have been used preventively and therapeutically in tooth enamel. The latter can present different conditions in its structure. In this sense, adhesive retention in enamel has ample evidence of its effectiveness, but not in enamel with structural alterations. In this way, it is relevant to know the adhesive retention of these materials and how they behave over time in enamel with variations in its composition. To determine the retention rate of resin sealants in tooth enamel with structural alterations. The study is part of a systematic review following the PRISMA protocol. Articles published between 2010 and 2020 on the retentive behavior of resin sealants in dental with structural alterations were examined. The electronic search was carried out in Web of Science, Scopus, PubMed and Medline. Those articles that used resin sealants in dental enamel with structural alterations were incorporated in clinical trials. Results: Eight articles were found. These were stratified according to the application surface; (i) carious surface, (ii) surface with fluorosis and (iii) surface with hypomineralization of the molar incisor. It was evidenced that the retention rate of resin sealants on decayed enamel is 80% on average, in enamel with dental fluorosis 67.5% and enamel with hypomineralization of the molar incisor 72% 2 years after their application. The retentive behavior of resin sealants on enamel with structural alterations is adequate for the three application surfaces. However, further studies are required regarding dental fluorosis and molar incisor hypomineralization. The most significant evidence on the retention rate was found on various surfaces.

Key words: Resin sealants, Adhesive retention, Dental Caries, Dental fluorosis, Molar incisor hypomineralization.

Introducción

El esmalte dental es la estructura más dura y mineralizada en todo el cuerpo humano, en cuya composición encontramos un 95% de estructura mineral, mientras que un 5% corresponde a agua y materia orgánica¹. Defectos en el desarrollo de este tejido mineralizado ocurren debido a desequilibrios biológicos que afectan a las células involucradas en la formación y maduración del esmalte; los ameloblastos¹. La extensión del defecto del esmalte depende de la intensidad del factor etiológico, así como del período de tiempo durante el cual estuvo presente en la etapa de desarrollo del diente².

El esmalte dental es la estructura más dura y mineralizada en todo el cuerpo humano, en cuya composición encontramos un 95% de estructura mineral, mientras que un 5% corresponde a agua y materia orgánica¹. Defectos en el desarrollo de este tejido mineralizado ocurren debido a desequilibrios biológicos que afectan a las células involucradas en la formación y maduración del esmalte; los ameloblastos¹. La extensión del defecto del esmalte depende de la intensidad del factor etiológico, así como del período de tiempo durante el cual estuvo presente en la etapa de desarrollo del diente².

Citation: Jiménez-Díaz J, Curtze-Scotts G, Barahona-Fuentes G. Tasa de retención de sellantes de resina en esmalte dental con alteraciones estructurales: una revisión sistemática *Revis Bionatura* 2022;7(1). 14. <http://dx.doi.org/10.21931/RB/2022.07.01.14>

Received: 20 August 2021 / **Accepted:** 30 November 2021 / **Published:** 15 February 2022

Publisher's Note: Bionatura stays neutral with regard to jurisdictional claims in published maps and institutional affiliations.



Copyright: © 2022 by the authors. Submitted for possible open access publication under the terms and conditions of the Creative Commons Attribution (CC BY) license (<https://creativecommons.org/licenses/by/4.0/>).

Aquellos defectos que ocurren durante la etapa de maduración dan como resultado un volumen regular de esmalte, pero con una mineralización insuficiente, lo que se conoce como hipomineralización³. Dentro de los defectos de hipomineralización dental podemos nombrar la hipomineralización incisivo molar (MIH) y fluorosis dental (FD)³. MIH corresponde a un defecto del desarrollo cualitativo y de origen sistémico del esmalte, donde puede verse afectado uno o más molares permanentes, con o sin afeción de los incisivos permanentes³. En comparación a un esmalte sano, los dientes afectados por MIH presentan una variación y disposición prismática distinta, histológicamente hablando, y muestra propiedades mecánicas menores, en términos de módulo de elasticidad⁴. Por otro lado, la FD se refiere a las alteraciones que ocurren como resultado del consumo excesivo de flúor durante la formación dental³, dejándolo con un menor contenido mineral y una porosidad aumentada⁵. En este sentido, en un estudio realizado por Gu *et al.*⁶, consideraron que un esmalte con alto contenido de flúor produce una mayor resistencia al grabado ácido necesario para la retención de materiales, logrando menos irregularidades superficiales y por tanto una adhesión más débil⁶.

Así como podemos encontrar alteraciones del desarrollo, el esmalte dental también puede presentar lesión de caries, y que puede ser categorizada dependiendo de su ubicación anatómica en la pieza dental, según su severidad, profundidad de penetración en los tejidos y estado de actividad⁷. Esta lesión presenta un volumen mineral heterogéneo con un contenido mineral más bajo en su capa superficial, permitiendo el movimiento de agua y ácidos hacia el interior a través de sus poros, lo que podría explicar la extensión que puede alcanzar la lesión cariosa⁸, la que suele producirse principalmente en fosas y fisuras⁹.

Los sellantes se han utilizado como un material que se introduce en las fosas y fisuras oclusales de aquellos dientes que son susceptibles a generar caries, el cual forma una capa que protege y previene la acumulación de biofilm facilitando la desorganización de este durante el cepillado¹⁰. Asimismo, estos aíslan las bacterias presentes lo que produce un efecto terapéutico inactivando la lesión de caries¹⁰. El uso de sellantes también se ha considerado para el tratamiento preventivo en dientes que presenta MIH, cuyas superficies son más susceptibles al desarrollo de lesiones cariosas¹¹, al igual que aquellas superficies que presentan FD, en las que se ha encontrado una relación positiva respecto al desarrollo de lesión de caries, sobre todo en áreas altamente fluoradas⁵.

El éxito de los sellantes de fosas y fisuras depende, en gran medida, de su retención a largo plazo¹². Una pérdida parcial del material sellador conduce a la ocurrencia de una filtración marginal y, en consecuencia, a desarrollar una lesión de caries asociada al sellante¹¹. Existen variables que contribuyen a mejorar o disminuir la retención del sellante como lo son las propiedades del esmalte dental, el tratamiento de superficie realizado y la habilidad del operador¹³. Sin lugar a dudas, el tipo de material sellador y su viscosidad, así como la resistencia al desgaste del material son factores contribuyentes a la retención y prevención de caries¹³. En este sentido, Gu *et al.*⁶, consideran una variable importante la superficie de esmalte en la que se quiere conseguir la adhesión⁶. En el caso del esmalte dental sano, y gracias al grabado ácido y la disolución de cristales de apatita, se obtiene una superficie irregular en la que el sellante de resina puede penetrar, generando así una retención micromecánica efectiva^{6,14}. Al respecto, De Munk *et al.*¹⁵ concluyeron en una revisión sistemática que la mayoría de los estudios de durabilidad de la adhesión consideran la unión a esmalte dental sano como fuerte y estable¹⁵, mientras que

Kotsanos *et al.*¹⁶ encontraron que los sellantes en niños afectados por MIH tenían una mayor probabilidad de requerir un nuevo tratamiento, en comparación con el grupo de control. Asimismo, se ha evidenciado que la fuerza de unión del sellante de resina en esmalte hipomineralizado es significativamente menor que la de esmalte sano¹⁷, por lo que los sellantes de fisura en dientes con caries sufrirán mayores microperforaciones en comparación con los aplicados en superficies dentales sanas⁶. Sin embargo, la evidencia de la retención y longevidad de estos sellantes para el tratamiento de esmalte dental con alteraciones estructurales es limitada e inconclusa¹⁸.

En relación a la información disponible, se puede evidenciar que el comportamiento retentivo de sellantes de resina en esmalte dental sano se ha estudiado desde hace varios años y se encuentra bastante bien descrito, no así lo que se refiere al comportamiento de estos materiales en esmalte con alteraciones estructurales, donde la información es limitada. Consecuentemente, el objetivo de esta revisión consistió en determinar la tasa de retención que presentan los sellantes de resina en esmalte dental con alteraciones estructurales.

Materiales y métodos

Fuentes de información y búsqueda

Para desarrollar esta revisión sistemática, se llevó a cabo una búsqueda orientada por referencias en distintas bases de datos y buscadores electrónicos: Web of Science (WoS), Scopus, PubMed y Medline. En cada una de las bases de datos consultadas, se realizaron búsquedas en los campos del título, resumen y palabras clave. Los límites de búsqueda fueron: artículos publicados en los últimos diez años (enero de 2010 a mayo de 2020). La búsqueda bibliográfica de los estudios fue realizada en conformidad con las directrices de revisiones sistemáticas y metaanálisis (PRISMA)¹⁹. Para este propósito, la población, la intervención, los comparadores y los resultados (PICO) se establecieron de la siguiente manera: (i) Esmalte dental con alteraciones estructurales (Caries dental, Fluorosis, Hipoplasias, Hipomineralizaciones) de niños, adolescentes, adultos y adultos mayores; (ii) Solo aquellas intervenciones que hayan evaluado retención adhesiva de forma clínica; (iii) Los comparadores fueron estudios que hayan utilizado sellantes de resina y; (iv) Los resultados de retención hayan sido positivos o negativos. Por lo anterior, las siguientes palabras clave fueron combinadas con los operadores booleanos (AND/OR): ("Pit and fissure sealant" OR "Resin sealant" OR "Composite sealant" OR "Dental sealants") AND ("Dental caries" OR "Dental Enamel Hypoplasia" OR "Dental Fluorosis" OR "Hypocalcification" OR "Hypomineralization" OR "Hypomaturation" OR "Molar Incisor Hypomineralization") AND ("Adhesive retention" OR "Retention rate"). Cabe mencionar que todos los términos utilizados para la búsqueda, fueron términos asociados a las variables de estudio y que no necesariamente debían ser términos MeSH.

Criterios de elegibilidad

La elegibilidad de cada uno de los estudio fue evaluada según los siguientes criterios de inclusión: a) estudios que hayan presentado como diseño ensayo clínico; b) artículos que incluyan la aplicación de sellantes sobre esmalte dental con alteraciones estructurales (Caries dental, Fluorosis, Hipoplasias, Hipomineralizaciones) de niños, adolescentes, adultos y adultos mayores; c) estudios de retención adhesiva evaluada clínicamente; d) estudios que utilizaron sellantes de resina; e)

estudios que estuviesen publicados en idioma inglés, español, portugués, francés y alemán; y f) artículos publicados durante los últimos 10 años (2010 a 2020).

Los estudios que presentaron las siguientes características, fueron excluidos: a) artículos a los que no se pueda acceder y que no contengan abstract; y b) estudios realizados en dientes de animales. Dos autores realizaron la búsqueda y revisaron los estudios; ambos decidieron si la inclusión de los artículos era apropiada. En caso de algún desacuerdo entre estos, se consultó con el tercer autor.

Evaluación de la calidad metodológica de los estudios

La calidad metodológica y el riesgo de sesgo de cada estudio científico seleccionado y que cumplieron con los criterios de inclusión para la revisión, fueron evaluados utilizando el manual de Cochrane²⁰. Dos autores llevaron a cabo la evaluación de sesgo, en caso de algún desacuerdo, se consultó al tercer autor de la revisión. El riesgo de sesgo fue dividido en seis dominios diferentes: i) sesgo de selección correspondiente a la generación de secuencia aleatoria y ocultamiento de la asignación de la muestra; ii) sesgo de realización ya sea el cegamiento de los participantes y/o el personal del estudio; iii) sesgo de detección según el cegamiento de la evaluación de los resultados entregados; iv) sesgo de desgaste correspondiente a información de los datos de resultados incompletos; v) sesgo de notificación que forma parte del informe selectivo; y vi) otros tipos de sesgo como la declaración de conflicto de intereses. Para cada uno de los ítems, se consideró la respuesta a una pregunta; cuando la pregunta fue respondida con un "Sí", el sesgo fue bajo; cuando era "No", el sesgo era alto; y cuando no estaba claro, el posible sesgo estaba relacionado con la falta de información o incertidumbre.

Resultados

Selección de estudios

Luego de la búsqueda electrónica se encontraron 86 artículos, de estos 31 fueron duplicados. Los 55 artículos restantes fueron filtrados por títulos y resúmenes, quedando así 20 estudios para lectura y análisis completo. Luego de revisar los 20 artículos resultantes, 13 fueron eliminados por no contar con los criterios de inclusión. Se incluyó 1 artículo por búsqueda de referencias bibliográficas orientada. Finalmente, la cantidad total de estudios científicos incluidos para esta revisión sistemática fue de 8 artículos. La estrategia de búsqueda y la selección de los estudios se presentan en la Figura 1.

Los ocho artículos se estratificaron de acuerdo a la superficie de aplicación: (i) Superficie cariada ($n = 6$), (ii) Superficie con Fluorosis ($n = 1$) y (iii) Superficie con Hipomineralización incisivo molar ($n = 1$).

La tasa de retención observada en los estudios para sellantes de resina aplicados sobre superficies cariadas (entre ICDAS 1-4), varía entre un 69,7% y un 97,3%. En cuanto a la tasa de retención observada en el estudio de superficie con fluorosis, esta es de un 67,5%. Finalmente, la tasa de retención es de un 72% para el estudio de superficie con MIH. Los resultados se encuentran resumidos en la Tabla 1, mientras que las características generales de los artículos evaluados son presentados en la Tabla 2.

Evaluación de la calidad metodológica y detección del riesgo de sesgo para los estudios individuales

La evaluación de la calidad metodológica y la detección

del riesgo de sesgo de los ocho estudios seleccionados para esta revisión sistemática, evidenciaron que los estudios desarrollados por Fragelli *et al.*¹⁸, Hasanuddin *et al.*²⁷ y Nardi *et al.*²⁵ detectaron un alto riesgo de sesgo para el dominio de sesgo de selección y para el dominio de sesgo de detección. Mientras que Muñoz *et al.*²⁴ presentaron un alto riesgo de sesgo para el criterio de selección y Honkala *et al.*²² evidenciaron un riesgo de sesgo alto correspondiente al sesgo de detección. Asimismo Erdemir *et al.*²¹, Fragelli *et al.*¹⁸, Hasanuddin *et al.*²⁷, Muñoz *et al.*²⁴ y Nardi *et al.*²⁵ mostraron un riesgo de sesgo poco claro para el sesgo de realización. Del mismo modo, Erdemir *et al.*²¹, Fragelli *et al.*¹⁸ y Hasanuddin *et al.*²⁷ obtuvieron un riesgo de sesgo poco claro para el sesgo de notificaciones. También Hasanuddin *et al.*²⁷, Muñoz *et al.*²⁴ y Nardi *et al.*²⁵ mostraron un riesgo de sesgo poco claro para otros tipos de sesgos. Por último Muller Bolla *et al.*²³ y Ntaoutidou *et al.*²⁶, fueron los únicos estudios que evidenciaron un riesgo de sesgo bajo para cada uno de los dominios. Los detalles completos de cada estudio y dominio se presentan en Figura 2 y Figura 3.

Discusión

Al término de esta revisión sistemática, se pudo observar que los dientes tratados con un sellante de resina independiente del tipo de alteración estructural que presentaba el diente, evidenciaron una tasa de retención de alrededor del 70% a los 2 años de su aplicación clínica^{18,21-27}.

En un estudio realizado por Honkala *et al.*²² la evidencia científica demostró que posterior a 12 meses de seguimiento, existe un 73% de retención en los sellantes de resina. Esto podría explicarse, debido a que las fallas de sellado ocurren dentro del primer año de aplicación y ésta aumenta a medida que transcurre el tiempo²⁸. En este sentido, al compararse la retención adhesiva de un sellante de resina vs una resina flow, no se encontraron diferencias significativas, excepto en molares superiores, donde Tetric Evo Flow tuvo una retención significativamente mejor a los 24 meses (88,5%)²¹. Por otra parte Oba *et al.*²⁹ evidenciaron que un sellante convencional presentaba mayor retención a los 12 meses en comparación a dos resinas flow, mientras que a los 24 meses de seguimiento no existieron diferencias significativas entre ambos materiales. En base a esto, se hace relevante considerar el tiempo de seguimiento para la evaluación de la retención del sellante, debido a que algunos autores, consideran que 12 meses de seguimiento es un tiempo corto para proporcionar evidencia suficiente y que sería ideal extenderse en años³⁰.

En cuanto a las tasas de retención de los sellantes en lesiones microcavitadas, esta fue de 77% en selladores a base de resina y de un 83% en los selladores de GI, evidenciando diferencias no significativas entre ambos grupos ($p = 0,48$)²⁴. Esto podría explicarse por otros estudios donde se sugieren que las superficies desmineralizadas pueden disminuir la longevidad del sellante de resina¹, debido que la microinfiltración ocurre con mayor frecuencia alrededor de lesiones cariosas selladas que en superficies selladas sanas¹¹. En un ensayo clínico Jaafar *et al.*³¹ estudiaron el comportamiento retentivo de un sellante de resina v/s un sellante de ionómero sobre lesiones incipientes de caries, y observaron diferencias estadísticamente significativas a los 3 meses (93,33% vs 77,77%) y 6 meses (75,56% vs 48,88%), a favor a los sellantes resinosos. Por tanto, existen indicios de que el comportamiento retentivo de sellantes de resina suele mostrar mejores resultados sobre lesiones de caries incipientes que sobre lesiones microcavitadas.

En relación a los sellantes de resina que dentro de su

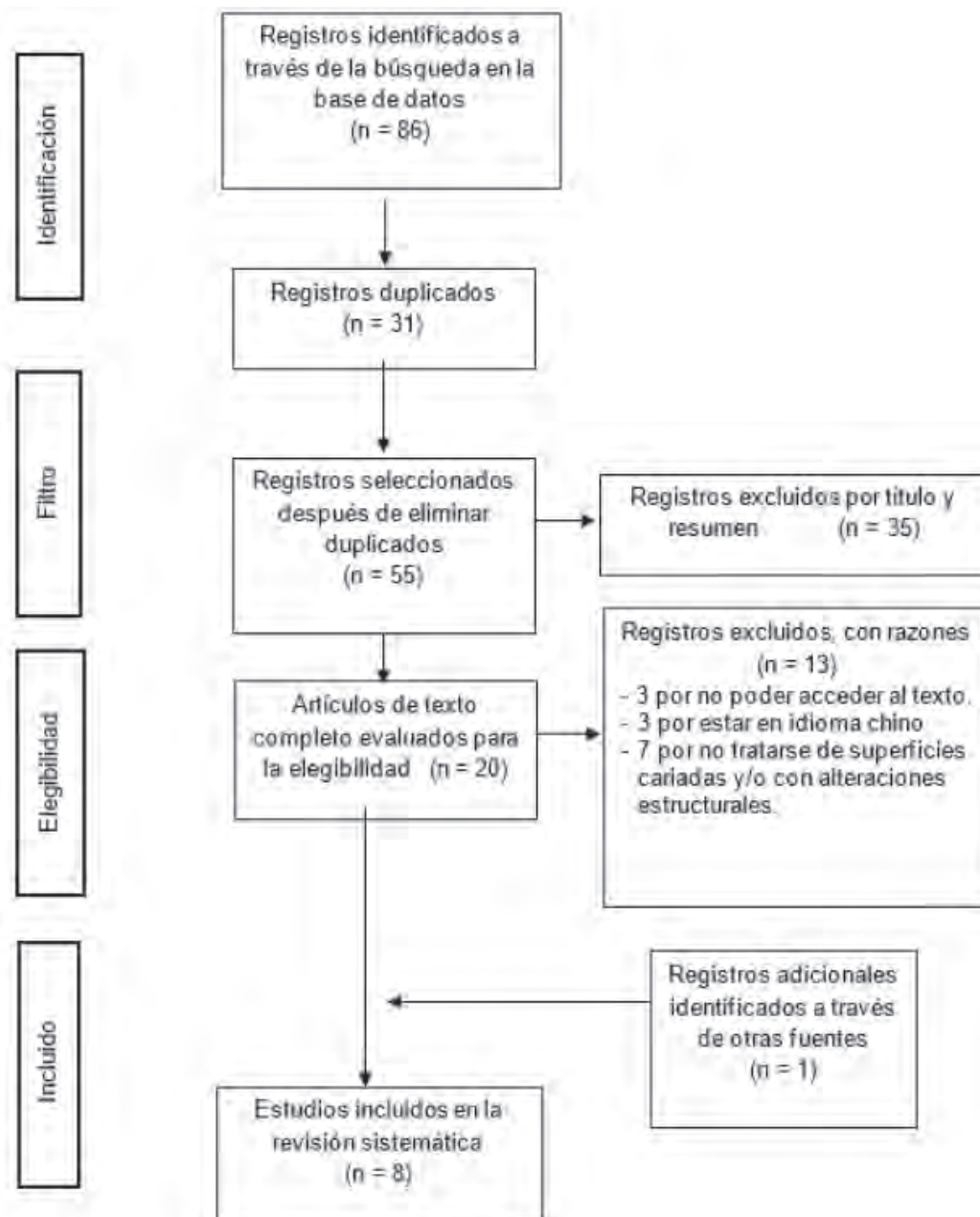


Figura 1. Diagrama de flujo de la estrategia de búsqueda.

Autor	Año publicación	Retención	Seguimiento clínico
Superficies cariadas			
Erdemir et al. ²¹	2014	85.4%- 88.5%	24 meses
Honkala et al. ²²	2015	73%	12 meses
Muller Bolla et al. ²³	2018	70%	24 meses
Muñoz et al. ²⁴	2019	77%	24 meses
Nardi et al. ²⁵	2018	85,9% - 97,3%	12 meses
Ntaoutidou et al. ²⁶	2018	69,7%	18 meses
Superficie con Fluorosis			
Hasanuddin et al. ²⁷	2014	67,5%	12 meses
Superficie con MIH			
Fragelli et al. ¹⁸	2017	72%	18 meses

MIH: (Hipomineralización incisivo molar)

Tabla 1. Resumen de resultados en términos de retención y seguimiento clínico para sellantes de resina aplicados en superficies de esmalte con alteraciones estructurales.

Autor	Objetivo	Muestra	Protocolo de aplicación	Método de evaluación	Resultados
Superficie cariada					
Erdemir et al. 2014.²¹	Evaluar la tasa de retención y efecto de prevención de caries de un composite fluido (Tetric Evo Flow) en comparación con un sellante de resina convencional (Heliobond F) en una población joven durante un periodo de 24 meses	De un total de 220 dientes en 34 pacientes con al menos 2 caries de fosas y cavidades no cavitadas en el primer y segundo molar fueron seleccionados para este ensayo aleatorizado de diseño de boca dividida (117 molares superiores y 103 inferiores) fueron sellados con Tetric Evo Flow (n=110) y Heliobond F (n=110).	Se realizó profilaxis con piedra pómez y posterior lavado de spray aire-agua por 60 s. Los dientes se aislaron con algodón y eyector de saliva. Se aplicó ácido fosfórico al 37% por 60 s, se enjuagó con spray aire-agua por 30 s y se secó por 20 s. Para Tetric Evo Flow, se aplicó adhesivo Excite, volatilizó por 2-3 s y se fotocuró por 20 s, se aplica resina fluida, que fue polimerizada por 20 s. Heliobond F fue aplicado en superficie, se dejó esparcir por 15 s y fue fotocurado por 20 s. Para todos se realizó chequeo y ajuste de oclusión.	Todas las restauraciones de selladores se evaluaron clínicamente en 1, 6, 12 y 24 meses. La evaluación fue en términos de retención y presencia de caries.	No hubo diferencias significativas en la evaluación de tasa de retención para cada periodo de evaluación, en la habilidad de prevención de caries y tampoco en si el material fue aplicado en un diente superior o inferior (p > 0,05) excepto en molares superiores a los 24 meses, donde Tetric Evo Flow tuvo una mejor retención (p < 0,05).
Honkala et al. 2015.²²	Medir el efecto preventivo de caries de los sellantes aplicados en superficies oclusales de molares primarios, en comparación con las aplicaciones de barniz de flúor, y evaluar la tasa de retención de los sellantes después de 1 año.	106 niños fueron incluidos. 266 superficies fueron selladas y a 266 superficies se le aplicó barniz de flúor de molares primarios con códigos de caries ICDAS de 0-4.	El sellante utilizado fue ClinproTM fotopolimerizable, y el barniz de flúor fue DuraShield.	Evaluación clínica 1 año después de la primera examinación.	Hubo diferencias significativas en cuanto a presencia de caries, presentándose más en superficies barnizadas v/s superficies selladas (p < 0,001). En tasa de retención, el 73% fue completamente retenido, 15,1% parcialmente retenido, 10,1% perdido y 1,7% perdido y llenado.
Muller Bolla et al. 2018.²³	Evaluar la efectividad de los selladores dentales para prevenir la aparición de lesiones cariosas ICDAS 3-6. Determinar la efectividad por tipo de sellador, con y sin fluoruro. También se evaluó tasa de retención y factores de riesgo.	663 pares de dientes en 400 niños (5 a 15 años) considerados con alto ICR y presentaban molares permanentes libres de caries o afectados por lesiones ICDAS 1-2.	Luego de limpieza profiláctica, el diente a sellar se aisló con rollos de algodón. La superficie oclusal se secó y se grabó con gel de ácido fosfórico al 37% por 20 s, seguido de enjuague por 20 s con jeringa de aire y agua sin aceite. Luego sellador a base de resina se aplicó en la superficie oclusal del diente.	Examen visual utilizando los criterios ICDAS 3-6 en los molares permanentes a los 6, 12, 18 y 24 meses de seguimiento. La tasa retentiva se evaluó visualmente como total o no. El sellador se consideraba parcialmente perdido si no cubría todas las fosas y fisuras oclusales.	Los molares sellados tenían un menor riesgo de lesiones ICDAS 3-6 que los molares no sellados (p < 0,0001), en el grupo que incluye solo molares permanentes con lesiones ICDAS 1-2 hubo un efecto preventivo menor que en el grupo sin lesiones ICDAS 1-2 (p < 0,0001). El efecto del sellador era similar independientemente de si contenía fluoruros o no (p < 0,0001) y la pérdida de sellador no se asoció con el riesgo de caries. La tasa de retención total de los sellantes fue del 70% a los 2 años de seguimiento.
Muñoz et al. 2019.²⁴	Comparar la progresión de las lesiones cariosas y la retención de material entre los selladores basados en resina y GI, para el tratamiento de las lesiones cariosas oclusales ICDAS 3 en escolares.	41 niños que tenían 151 lesiones ICDAS 3. Sellador a base de resina (n = 76) y sellador GI (n = 75).	Esmalte oclusal se grabó con ácido ortofosfórico al 37% por 15 s, luego se enjuagó durante 30 s con agua y se secó al aire por 15 s. Se fotopolimerizó por 20 s a 1 cm de la superficie del diente. Grupo de selladas con GI, el esmalte se acondicionó con ácido poliacrílico usando cepillo, se frotó sobre la lesión por 15 s, se lavó con algodón humedecido por 5 s y se seca al aire por 5 s.	Evaluación clínica y radiográfica a los 12 y 24 meses. Se evaluó progresión de lesión, retención e integridad de materiales.	Lesiones progresivas a ICDAS 5, fue ns entre los grupos. La retención fue de 77% en selladores a base de resina y de un 83% en los selladores GI, siendo ns entre los grupos.
Nardi et al. 2018.²⁵	Evaluar la retención de un sellador de resina opaco y uno transparente y comparar su efectividad a los 6 y 12 meses. Evaluar la posibilidad de utilizar una cámara intraoral basada en fluorescencia a través del sellador transparente a monitorizar la desmineralización del esmalte.	42 pacientes (20 hombres y 22 mujeres) con al menos dos molares con código ICDAS 0, 1, 2. Se evaluaron un total de 150 dientes sellados en el estudio. En 77 casos se usó el sellador transparente, mientras que en 73 se aplicó el sellador opaco.	Se aplicó sellador en dientes, con un aumento de 3,5X. Después de colocar la goma dique, las fisuras se limpiaron con rotifex y pasta abrasiva sin fluoruro, se enjuagó con agua y secado al aire. Se acondicionó de 20 a 30 s con ácido fosfórico al 37% seguido de pulverización de agua por 60 s y se secado al aire, seguido de aplicación de sellador, fotocurado y control oclusal.	Seguimiento clínico a los 6 y 12 meses realizado por experto para evaluar la retención del sellador y monitorear cualquier tendencia de desmineralización bajo el sellador transparente utilizando mediciones de fluorescencia	La diferencia de retención fue ns a los 6 meses. A los 12 meses aumento significativo (p = 0,006) en efectividad clínica de sellador opaco.
Ntaoutidou et al. 2018.²⁶	Evaluar clínicamente las tasas de retención y el efecto de prevención de caries de un sellador de fosas y fisuras a base de resina con rellenos de cemento con GI pre-reaccionado (S-PRG), en comparación con un sellador a base de resina convencional durante un periodo de 18 meses.	81 niños, 6 a 12 años. Se colocaron un total de 218 sellantes en ambos grupos en los primeros molares permanentes con código ICDAS 0 o 1. GE: 105 dientes con sellador de GI pre-reaccionado (S-PRG) y GC: 113 dientes con sellador convencional de resina.	GE, se aplicó imprimación sobre superficie del esmalte con microbrush, se dejó sin remover por 5 s y se secó al aire, se aplicó directamente desde la jeringa en fosas y fisuras y se curó con luz por 10 s. GC, se aplicó gel de ácido ortofosfórico al 37% por 30 s al diente. Se enjuagó y secó al aire. El sellador se aplicó directamente desde la jeringa a todas las fisuras y luego se foto polimerizó con unidad de curado dental por 30 s.	Evaluación clínica a los 6, 12 y 18 meses en términos de formación de caries basada en ICDAS II y retención de sellador de acuerdo a los siguientes criterios: 1. Retención total 2. Pérdida parcial 3. Pérdida total.	A los 6 meses, las tasas de retención completas fueron del 82,2% para el GC y de un 16,5% para el GE, siendo la diferencia significativa (p < 0,001). A los 12 meses, las tasas respectivas fueron 72,2% y 8,7% (p < 0,001). Mientras que al final de los 18 meses, las tasas de retención generales para GC y GE fueron 69,7% y 6,9%, respectivamente (p < 0,001).

Tabla 2. Características de los ensayos clínicos de sellantes de resina aplicados en superficies de esmalte con alteraciones estructurales.

cm; (centímetros), CST; (técnica convencional de sellantes de fisuras), EST; (técnica de sellado con esmalteplastia), GC; (grupo control), GE; (grupo experimental), GI; (ionómero de vidrio), ICDAS; (Sistema Internacional de Detección y Evaluación de Caries), ICR; (Riesgo de caries individual), MIH; (Hipomineralización incisivo molar), ns; (no significativo), s; (segundos).

Hasanuddin et al. 2014.²⁷	Evaluar y comparar la retención y la aparición de caries después de la colocación de sellantes de fisuras Clinpro y Fuji VII.	80 escolares con fluorosis dental leve a moderada fueron asignados al GE1 (sellante Clinpro) y al GE2 (sellante Fuji VII) con 40 niños en cada grupo.	En ambos grupos, los sellantes de fisuras se aplicaron mediante CST en un lado, y EST en el otro lado del mismo arco. La única modificación en la técnica fue un aumento en el tiempo de grabado a 35-40 s para todos los grupos. En el GE2, EST se realizó mediante el uso de una fresa antes del grabado y la colocación del sellante. En todos los sujetos, el aislamiento se logró mediante cotones de algodón y eyector.	La retención y la aparición de caries se evaluó clínicamente a los 7 días, 1, 3, 6 y 12 meses.	El GE1 mostró una tasa de retención mayor en comparación con GE2 ($p < 0,05$).
Superficie con Hipomineralización Incisivo Molar					
Fragelli et al. 2017.¹⁸	Evaluar la supervivencia del sellador en los primeros molares permanentes afectados por MIH y comparar la tasa de supervivencia con los selladores aplicados a los molares sanos a los 18 meses de seguimiento.	41 primeros molares permanentes. (GC: 16 dientes no afectados por MIH y GE: 25 afectados por MIH).	Se aplicó una profilaxis, anestesia infiltrativa, goma dique, aplicación de ácido fosfórico al 35% durante 30 s, enjuague extenso y chorro de aire durante 5 s, aplicación de sellador de resina (Fluorshield, Dentsply) fotopolimerización durante 20 s eliminación de la goma dique, examen del contacto oclusal y pulido final.	Evaluación clínica por un examinador calibrado a los 1, 6, 12 y 18 meses bajo luz artificial y después de profilaxis, que consideró: forma anatómica, adaptación marginal, textura superficial, decoloración marginal, retención y presencia de lesiones cariosas secundarias.	No se encontraron diferencias significativas entre GC y GE

Tabla 2. Características de los ensayos clínicos de sellantes de resina aplicados en superficies de esmalte con alteraciones estructurales.

cm; (centímetros), CST; (técnica convencional de sellantes de fisuras), EST; (técnica de sellado con esmalteplastia), GC; (grupo control), GE; (grupo experimental), GI; (ionómero de vidrio), ICDAS; (Sistema Internacional de Detección y Evaluación de Caries), ICR; (Riesgo de caries individual), MIH; (Hipomineralización incisivo molar), ns; (no significativo), s; (segundos).

	a. Generación de secuencia aleatoria (sesgo de selección)	a. Oculamiento de la asignación (sesgo de selección)	b. Cegamiento de los participantes y personal del estudio (sesgo de realización)	c. Diferencias sistemáticas entre grupos en la forma en que los resultados fueron obtenidos (sesgo de detección)	d. datos incompletos por abandonos del estudio (sesgo de desgaste)	e. Diferencias sistemáticas entre los resultados presentados y los no presentados (sesgo de notificación)	f. Otros tipos de sesgos
Erdemir et al. 2014. ⁽²¹⁾	✓	✓	⊖	✓	✓	⊖	✓
Fragelli et al. 2017. ⁽¹⁸⁾	✗	✗	⊖	✗	✓	⊖	✓
Hasanuddin et al. 2014. ⁽²⁷⁾	✗	✗	⊖	✗	✓	⊖	⊖
Honkala et al. 2015. ⁽²²⁾	✓	✓	✓	✗	✓	✓	✓
Muller-Bolla et al. 2018. ⁽²³⁾	✓	✓	✓	✓	✓	✓	✓
Muñoz et al. 2019. ⁽²⁴⁾	✓	✗	⊖	✓	✓	✓	⊖
Nardi et al. 2018. ⁽²⁵⁾	✗	✗	⊖	✗	✓	✓	⊖
Ntaoutidou et al. 2018. ⁽²⁰⁾	✓	✓	✓	✓	✓	✓	✓

Figura 2. Evaluación del riesgo de sesgo siguiendo el manual Cochrane en los artículos incorporados para la revisión sistemática.

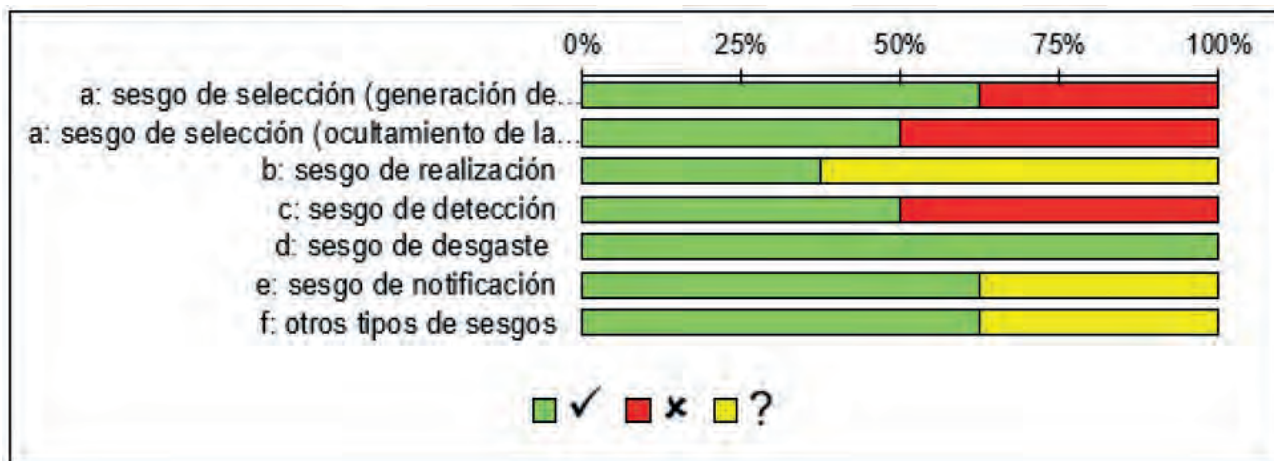


Figura 3. Gráfica que identifica el riesgo de sesgo a juicio de los autores acerca de cada dominio de riesgo de sesgo presentado como porcentaje en los artículos incluidos.

composición presentan flúor, se ha evidenciado que la tasa de retención de los sellantes fue de un 70% a los 2 años independientemente si contenían fluoruro, en aquellos dientes sanos o con lesiones ICDAS 1-2, existiendo una tendencia a un menor riesgo entre los dientes que recibieron sellante con flúor, y la pérdida del sellante no se asoció con el riesgo de caries²³. En contraste con lo anterior, un estudio realizado por Ganss *et al.*³² evidenciaron una tasa de retención de sellantes con liberación de flúor del 38% para Helioseal F y del 60% para Fissurit F aislados con rollos de algodón al cabo de un año de seguimiento clínico, esta diferencia en la tasa de retención pudo haber sido modificado por el aislamiento del diente al momento de ser aplicado el sellante, debido a que los hallazgos sugieren que la colocación de goma dique aumenta la tasa de retención, la calidad del sellador y puede reducir factores dependientes del material que se consideran una causa de fallas del sellante³². Por otra parte, al evaluarse la retención de un sellante de resina opaco y uno transparente (ambos con flúor), se evidenció que a los 12 meses existió un aumento significativo en la efectividad clínica del sellante opaco²⁵. Asimismo, Ntaoutidou *et al.*²⁶ evaluaron la tasa de retención de un sellante de resina que contenía rellenos de cemento de GI pre-reaccionado (S-PRG) con liberación de flúor, y lo compararon con un sellante a base de resina convencional, donde se mostró una mejor tasa de retención en el sellante de resina convencional a los 6, 12 y 18 meses. Pese a lo anterior, se ha demostrado que la capacidad de evaluar adecuadamente la retención en selladores opacos es mucho menos propensa a errores que con los selladores transparentes²⁵. Esto se debe principalmente a la dificultad en la detección clínica de selladores transparentes durante el seguimiento²⁵. Estos resultados podrían explicarse por posibles deficiencias en la capacidad de grabado del cebador de autograbado del GE²⁶. En este sentido, es bien sabido que la unión al esmalte se logra mediante la formación de tags de resina en el esmalte grabado y la longitud de estos tags se correlaciona con la fuerza de unión³³. Junto con lo anterior, existe un cuestionamiento sobre la efectividad de los adhesivos de autograbado, ya que la mayoría no son tan ácidos como el ácido fosfórico³⁴. Esto queda demostrado en un estudio donde se descubrió que la penetración de los materiales adhesivos era significativamente mayor cuando se aplicaba sobre esmalte grabado con ácido fosfórico que con adhesivos autograbantes³⁵. A diferencia de estos y otros hallazgos^{26,35}, Feigal *et al.*³⁶ encontraron que el adhesivo autograbante Prompt L-Pop fue tan efectivo como el ácido fosfórico solo para la colocación del

sellante evaluado durante un período de 24 meses. Estos resultados podrían explicarse por la agresividad particular del adhesivo de autograbado utilizado en este estudio, que es muy similar al ácido fosfórico, con un pH de 1³⁷. Pese a esto, aún son necesarias más investigaciones futuras para confirmar la superioridad de los sellantes de resina con flúor^{23,38}.

Por otra parte, la tasa de retención en dientes con fluorosis, se ha demostrado que el sellante a base de resina (Clinpro) presenta una retención total del 67,5%²⁷. Este resultado podría estar relacionado con el hecho de que se realizó un grabado aumentado con ácido fosfórico al 37%⁶. En este sentido, Gu *et al.* estudiaron la unión de fuerza microtensil utilizando diferentes concentraciones de ácido fosfórico en dientes con fluorosis, al término del estudio se pudo evidenciar que la fuerza de unión fue menor en diente que presentaban mayores cantidades de fluorosis⁶. Esto podría indicar que se hace necesario la remoción de un esmalte aprismático que podría influenciar negativamente la retención³⁹.

En los tratamientos de aplicación con Fuji VII, la técnica de esmalteplastía mostró mejores resultados retentivos en comparación a la técnica de aplicación convencional²². Esto podría explicarse por el hecho de que el sellante puede tener más acceso a la fisura cuando se elimina esmalte alrededor de esta³⁹. Esto se relaciona con un estudio realizado por Hatirli *et al.*¹⁴ donde la técnica esmalteplastía mejoró significativamente la profundidad de penetración de los selladores por sobre otras técnicas. En este sentido, se podría deducir que una forma efectiva de aumentar la retención de sellantes de resina en superficies con fluorosis sería aumentando el área de superficie de adhesión⁶. Sin embargo, esto sería opuesto a lo que dictan las técnicas mínimamente invasivas cuyo objetivo es la conservación de tejido con la mínima pérdida posible⁴⁰, por lo que se hace relevante seguir investigando sobre otras técnicas para mejorar la retención en este tipo de sustrato.

Respecto a la tasa de retención de sellante de resina en dientes afectados por MIH, no se encontraron diferencias significativas en comparación a dientes no afectados¹⁸. Esto se puede deber a que se produjo una adherencia del sellante en la superficie del esmalte, que pudo haber sido remineralizada por tratamientos preventivos previos con barniz de flúor¹⁸. En relación a lo anterior, Fütterer *et al.* evidenciaron que un tratamiento preventivo con barniz de flúor favorecía la remineralización y disminuía el riesgo de fracturas y lesiones cariosas en los dientes afectados por MIH¹¹. Asimismo, Lygidakis *et al.*⁴¹ evidenciaron que los sellantes de fisuras con MIH en 54 niños

con molares con opacidades oclusales, presentaron una alta retención al utilizarse adhesivos de 5ta generación antes de colocar el sellador. En contraparte, un estudio de Kotsanos *et al.*¹⁶ se evidenció que los sellantes aplicados en 35 molares con MIH no presentaron retención después de un período de tiempo. Sin embargo, estos autores¹⁶, no realizaron un tratamiento previo de superficie a diferencia de Lygidakis *et al.*⁴¹. Esto puede sugerir que independientemente de la superficie en la cual se aplique el sellante, existiría una tasa de retención mayor si se realiza un tratamiento de superficie previo^{18,41}. Pese a esto, la información sobre adhesión en esmalte hipomineralizado es aún limitada, especialmente en lo que respecta al uso de sellantes.

Dentro de las limitaciones de esta revisión sistemática se puede mencionar que no se pudo acceder a todos los textos que se abarcaron durante la búsqueda metodológica, ya sea por estar en un idioma fuera de los criterios de inclusión o por la imposibilidad de acceso al texto completo. Otra limitación importante en esta revisión, fue el número limitado de estudios que evaluaron la tasa de retención en superficie con fluorosis dental²⁷ y superficie con hipomineralización incisivo molar¹⁸, así como la limitada cantidad de ensayos clínicos relacionados con estos dos tipos de alteraciones de esmalte.

Se sugiere para futuras investigaciones realizar estudios de ensayos clínicos por sobre estudios *in vitro* en dientes afectados con hipomineralización incisivo molar y con fluorosis dental. Además, se sugiere a los investigadores prolongar el tiempo de seguimiento clínico de los pacientes, tanto para este tipo de superficies como para superficies cariadas.

Conclusiones

Al término de la revisión se evidenció que el comportamiento retentivo de los sellantes de resina sobre esmalte con alteraciones estructurales es adecuada y óptima a los 2 años de su aplicación clínica tanto para superficies cariadas, superficies con fluorosis, como también superficies con MIH. Pese a esto, se requieren de más estudios respecto a la tasa de retención en fluorosis dental y MIH, donde la información científica es aún limitada. Por otra parte, la mayor evidencia sobre la tasa de retención se encontró en superficies cariadas, la cual presenta un mejor comportamiento retentivo independientemente de su tiempo de seguimiento.

Contribuciones de los autores

Conceptualización, J.J.-D y G.C.-S.; metodología, G.B.-F.; validación, J.J.-D., G.C.-S y G.B.-F.; análisis formal, J.J.-D y G.C.-S.; investigación, J.J.-D., G.C.-S y G.B.-F.; redacción — preparación del borrador original, J.J.-D., G.C.-S y G.B.-F.; redacción — revisión y edición, G.B.-F.; visualización, J.J.-D y G.B.-F.; supervisión, G.B.-F.; administración de proyecto, G.B.-F.; Todos los autores han leído y aceptado la versión publicada del manuscrito.

Financiamiento

Esta investigación no recibió financiamiento externo.

Declaración de la Junta de Revisión Institucional

No aplica.

Declaración de consentimiento informado

No aplica.

Declaración de disponibilidad de datos

No aplica.

Conflicto de intereses

Los autores declaran no poseer conflictos de intereses.

Referencias bibliográficas

- Świetlicka I, Kuc D, Świetlicki M, et al. Near-Surface Studies of the Changes to the Structure and Mechanical Properties of Human Enamel under the Action of Fluoride Varnish Containing CPP-ACP Compound. *Biomolecules*. 2020;10(5). doi:10.3390/biom10050765
- Krishnaji Musale P, Shrikant Soni A, Sunil Kothare S. Etiology and Considerations of Developmental Enamel Defects in Children: A Narrative Review. *J Pediatr Rev*. 2019;7(3):141-150. doi:10.32598/jpr.7.3.141
- da Cunha Coelho ASE, Mata PCM, Lino CA, et al. Dental hypomineralization treatment: A systematic review. *J Esthet Restor Dent*. 2019;31(1):26-39. doi:10.1111/jerd.12420
- Ethennawy K, Schwendicke F. Managing molar-incisor hypomineralization: A systematic review. *J Dent*. 2016;55:16-24. doi:10.1016/j.jdent.2016.09.012
- Revelo-Mejia IA, Hardisson A, Rubio C, Gutiérrez ÁJ, Paz S. Dental fluorosis: the risk of misdiagnosis—a Review. *Biol Trace Elem Res*. 2020;1-9.
- Gu M, Lv L, He X, Li W, Guo L. Effect of phosphoric acid concentration used for etching on the microtensile bond strength to fluorotic teeth. *Medicine (Baltimore)*. 2018;97(35).
- Chenicheri S, Usha R, Ramachandran R, Thomas V, Wood A. Insight into oral biofilm: primary, secondary and residual caries and phyto-challenged solutions. *Open Dent J*. 2017;11:312.
- Gan SC, Fok ASL, Sedky RA, Sukumaran P, Chew HP. Sorptivity of water in enamel for categorizing caries lesions. *Dent Mater*. 2020;36(11):1379-1387.
- Sreedevi A, Mohamed S. Sealants, pit and fissure. In: *StatPearls [Internet]*. StatPearls Publishing; 2019.
- Cvikl B, Moritz A, Bekes K. Pit and fissure sealants—a comprehensive review. *Dent J*. 2018;6(2):18.
- Fütterer J, Ebel M, Bekes K, Klode C, Hirsch C. Influence of customized therapy for molar incisor hypomineralization on children's oral hygiene and quality of life. *Clin Exp Dent Res*. 2020;6(1):33-43.
- Rani BSK, Viswambharapanicker S, Mattumathody S, Muralidharan A, Dinsha ARN, Saluja P. Assessment of shear bond strength and marginal sealing ability of pit and fissure sealants: An *in vitro* study. *J Contemp Dent Pract*. 2018;19(6):642-646. doi:10.5005/jp-journals-10024-2312
- Singh A, Patil V, Juyal M, Raj R, Rangari P, others. Comparative evaluation of occlusal pits and fissures morphology modification techniques before application of sealants: An *In vitro* study. *Indian J Dent Res*. 2020;31(2):247.
- Hatirli H, Yasa B, Yasa E. Microleakage and penetration depth of different fissure sealant materials after cyclic thermo-mechanic and brushing simulation. *Dent Mater J*. 2018;37(1):15-23. doi:10.4012/dmj.2016-234
- DeMunck J, Van Landuyt K, Peumans M, et al. A critical review of the durability of adhesion to tooth tissue: Methods and results. *J Dent Res*. 2005;84(2):118-132. doi:10.1177/154405910508400204
- Kotsanos N, Kaklamanos EG, Arapostathis K. Treatment management of first permanent molars in children with Molar-Incisor Hypomineralisation. *Eur J Paediatr Dent*. 2005;6(4):179-184.
- Lagarde M, Vennat E, Attal J, Dursun E. Strategies to optimize bonding of adhesive materials to molar-incisor hypomineralization-affected enamel: A systematic review. *Int J Paediatr Dent*. 2020;30(4):405-420.
- Fragelli CMB, Feltrin J, Bussaneli DG, Jeremias F, Cordeiro L. Survival of sealants in molars affected by molar-incisor hypomineralization. *Braz Oral Res*. 2017;31:1-9.

19. Moher D, Shamseer L, Clarke M, et al. Preferred reporting items for systematic review and meta-analysis protocols (PRISMA-P) 2015 statement. *Syst Rev*. 2015;4(1):1-9. doi:10.1186/2046-4053-4-1
20. Higgins JPT, Green S editors. *Cochrane Handbook for Systematic Reviews of Interventions*. 5th ed. London: Chichester, UK: Wiley; 2011.
21. Erdemir U, Sancakli HS, Yaman BC, Ozel S, Yucel T, Yildiz E. Clinical comparison of a flowable composite and fissure sealant: A 24-month split-mouth, randomized, and controlled study. *J Dent*. 2014;42(2):149-157. doi:10.1016/j.jdent.2013.11.015
22. Honkala S, Elsalhy M, Shyama M, Al-Mutawa S, Boodai H, Honkala E. Sealant versus fluoride in primary molars of kindergarten children regularly receiving fluoride varnish, One-year randomized clinical trial follow-up. *Caries Res*. 2015;49(4):458-466. doi:10.1159/000486426
23. Muller-Bolla M, Courson F, Lupi-Pégurier L, et al. Effectiveness of Resin-Based Sealants with and without Fluoride Placed in a High Caries Risk Population: Multicentric 2-Year Randomized Clinical Trial. *Caries Res*. 2018;52(4):312-322. doi:10.1159/000486426
24. Muñoz-Sandoval C, Gambetta-Tessini K, Giacaman RA. Microcavitated (ICDAS 3) carious lesion arrest with resin or glass ionomer sealants in first permanent molars: A randomized controlled trial. *J Dent*. 2019;88:103163. doi:10.1016/j.jdent.2019.07.001
25. Nardi GM, Mazur M, Corridore D, et al. Clinical comparison between an opaque and a clear pit and fissures sealants: a 12-month split-mouth, randomized controlled study. *Clin Ter*. 2018;169(1):5-9. doi:10.7417/T.2018.2046
26. Ntaoutidou S, Arhakis A, Tolidis K, Kotsanos N. Clinical evaluation of a surface pre-reacted glass (S-PRG) filler-containing dental sealant placed with a self-etching primer/adhesive. *Eur Arch Paediatr Dent*. 2018;19(6):431-437. doi:10.1007/s40368-018-0379-z
27. Hasanuddin S, Reddy ER, Manjula M, Srilaxmi N, Rani ST, Rajesh A. Retention of fissure sealants in young permanent molars affected by dental fluorosis: a 12-month clinical study. *Eur Arch Paediatr Dent*. 2014;15(5):309-315. doi:10.1007/s40368-014-0116-1
28. Anauate-Netto, C. Borelli, L. Amore, R. Di Hipolito, V. D Alpino P. Caries progression in non-cavitated fissures after infiltrant application: a 3-year follow-up of a randomized controlled clinical trial. 2017:442-454.
29. Oba, A. A., Sönmez, I. Ş., Ercan, E., & Dülgergil T. Comparison of retention rates of fissure sealants using two flowable restorative materiales and conventional resin sealant.pdf. *Med Princ Pract*. 2012;21(3):234-237.
30. Martignon S, Zarta OL. The use of adhesive systems under fissure sealants improves their retention, with etch-and-rinse performing better than self-etching adhesive systems. *J Evid Based Dent Pract*. 2017;17(1):56-58.
31. Jaafar N, Ragab H, Abedrahman A, Osman E. Performance of fissure sealants on fully erupted permanent molars with incipient carious lesions: A glass-ionomer-based versus a resin-based sealant. *J Dent Res Dent Clin Dent Prospects*. 2020;14(1):61-67. doi:10.34172/joddd.2020.009
32. Ganss C, Klimek J, Gleim A. One year clinical evaluation of the retention and quality of two fluoride releasing sealants. *Clin Oral Investig*. 1999;3(4):188-193. doi:10.1007/s007840050100
33. Perdigão J. Resin infiltration of enamel white spot lesions: An ultramorphological analysis. *J Esthet Restor Dent*. 2020;32(3):317-324.
34. Ranka CP, Somasundaram R. An Update Review of Self Etching Primers in Orthodontics. *J Adv Med Dent Sci Res*. 2020;8(11):87-91.
35. Suda S, Tsujimoto A, Barkmeier WW, et al. Comparison of enamel bond fatigue durability between universal adhesives and two-step self-etch adhesives: effect of phosphoric acid pre-etching. *Dent Mater J*. 2018;37(2):244-255.
36. Feigal RJ, Quelhas I. Clinical trial of a self-etching adhesive for sealant application: success at 24 months with Prompt L-Pop. *Am J Dent*. 2003;16(4):249-251.
37. Jamadar A, Vanti A, Uppin V, Pujar M, Ghivari S, Vagarali H. Comparative evaluation of shear bond strength of sixth-and seventh-generation bonding agents with varying pH--An in vitro study. *J Conserv Dent JCD*. 2020;23(2):169.
38. Ahovuo-Saloranta A, Forss H, Walsh T, Nordblad A, Mäkelä M, Worthington H V. Pit and fissure sealants for preventing dental decay in permanent teeth. *Cochrane Database Syst Rev*. 2017;2017(7). doi:10.1002/14651858.CD001830.pub5
39. Garg N, Mayall SS, Pathivada L, Yeluri R, others. Combined Effect of Enamel Deproteinization and Intermediate Bonding in the Retention of Pit and Fissure Sealants in Children: A Randomized Clinical Trial. *J Clin Pediatr Dent*. 2018;42(6):427-433.
40. Frencken JE. Atraumatic restorative treatment and minimal intervention dentistry. *Br Dent J*. 2017;223(3):183.
41. Lygidakis NA, Dimou G, Stamataki E. Retention of fissure sealants using two different methods of application in teeth with hypomineralised molars (MIH): a 4 year clinical study. *Eur Arch Paediatr Dent*. 2009;10(4):223-226. doi:10.1007/BF03262686

ARTICLE / INVESTIGACIÓN

Antibacterial and cytotoxic evaluation of sequential extract of *Moringa oleifera* leaves

Usama Bin Naeem¹, Waqas Iftikhar¹, Mussarat Rafiq² and Muhammad Babar Khawar^{3*}

DOI. 10.21931/RB/2022.07.01.15

¹ Department of Pharmacology and Toxicology, Faculty of Biosciences, University of Veterinary and Animal Sciences Lahore, Pakistan.² Cell and Molecular Biology Lab, Institute of Zoology, University of the Punjab, Lahore, Pakistan.³ Department of Zoology, University of Narowal, Narowal-Pakistan.

Corresponding author: babar.khawar@ucp.edu.pk

Abstract: *Moringa Oleifera* is an interesting plant used in Asian traditional medicine. In this study, *in vitro* antibacterial and cytotoxic evaluation of sequential extracts (aqueous, ethanol, and chloroform) of *Moringa Oleifera* was carried out. The antibacterial analysis was estimated with minimum inhibitory concentration (MIC) by micro dilution of *Moringa Oleifera* against common poultry pathogens *Clostridium perfringens* type A and *Escherichia coli*, while cytotoxic evaluation was estimated by the reduction in cell viability due to apoptosis or necrosis by metabolic events in the presence and absence of crude extracts or tested component. The aqueous extract shows the highest percentage yield (45/50gm) succeeded by ethanol extract (5.5gm/50gm) and chloroform extract (0.2gm/50gm). In our study, the zone of inhibition of sequential extracts of *Moringa Oleifera* against *Haemophilus* species are highest for chloroform (17mm), intermediate for ethanol (13mm), and lowest for aqueous extract (12.3mm). For chloroform extract the CSP was calculated at 10 different concentrations, 2000 µg/ml, 1000µg/ml, 500µg/ml, 250µg/ml, 125µg/ml, 62.5µg/ml, 31.25µg/ml, 15.63µg/ml, 7.81µg/ml and 3.91µg/ml. The results for cell survival percentage (CSP) in the present research are 26%, 46%, 58%, 55%, 60%, 63%, 62%, 59%, 68% and 82% respectively. The CSP results of chloroform extract indicated that it is toxic for cells at ≥1000µg/ml. At 1000µg/ml concentration CSP was 46% which is > 50% and therefore it is cytotoxic. At higher concentrations, chloroform is more cytotoxic than hexane because at > 1000µg/ml the cell survival percentage was recorded to be < 50%. For ethanol extract CSP was calculated at 10 concentrations, 6000µg/ml, 3000µg/ml, 1500µg/ml, 750µg/ml, 375µg/ml, 187.5µg/ml, 93.75µg/ml, 46.85µg/ml, 23.43µg/ml and 11.71µg/ml. The CSP values are 18%, 48%, 60%, 58%, 69%, 56%, 59%, 74%, 57% and 78% respectively which indicate that at concentrations ≥3000µg/ml the chloroform extract is toxic for cells. At a concentration less than 3000µg/ml, the CSP is more than 50%. So, as compared to hexane and chloroform, ethanol extract is less toxic at higher concentrations. Cytotoxicity of aqueous extract was calculated at 10 concentrations, 5000µg/ml, 2500µg/ml, 1250µg/ml, 625µg/ml, 312.5µg/ml, 156.25µg/ml, 78.125µg/ml, 39.06µg/ml, 19.53µg/ml and 9.76µg/ml. The CSP values are 8%, 18%, 42%, 56%, 54%, 59%, 55%, 62% 59% and 66% respectively. At a concentration ≥625µg/ml, the aqueous extract is toxic for cells. The CSP at 625µg/ml is 42%, hence toxic for cells. The cell survival percentage is more than 50% at a concentration > 625µg/ml, indicating that aqueous extract is more toxic to the cell than the rest of the three (Hexane, Chloroform, Ethanol extracts) at higher concentrations.

Key words: *Moringa oleifera*, poultry pathogens, minimum inhibitory concentration, antibacterial, cytotoxicity, cell survival percentage.

Introduction

"The tree of life" named *Moringa oleifera*, is regarded as one of the most valuable and useful trees because its all parts can be used for medication and food^{1,2}. The leaves of *Moringa* are eaten either cooked or fresh in salads. Leaves in the form of dried powder can be stored without losing nutritional value for months. However, it is essential to screen *Moringa oleifera* for antimicrobial properties and investigate its sanitizing /preservative potential³. In developing countries, untreated water-borne life-threatening infections are increasing⁴. World Health Organization (WHO) has warned that microbial resistance to typical water treatment mechanisms is increasing, and medicinal plants offer a good source of choice. The assessment of all the drugs is based on phytochemical and pharmacological approaches, which lead to the drug discovery

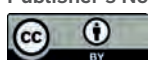
referred to as natural product screening⁵. Antibacterial resistance is a global problem; strategies to improve the current situation include controlling infections and minimizing the incidence of bacterial resistance by making new findings and innovations in antibacterial antibiotics and chemotherapeutic agents⁶. Almost 20% of the plants found in the world have been investigated through pharmacological or biological tests, and a considerable number of new antibiotics are synthesized using natural or semi-synthetic resources⁷. Due to the high cost of antibacterial medicines in developing countries like Pakistan, a significant portion of the population uses medicinal plants as medicaments against infectious diseases.

Citation: Bin Naeem U, Iftikhar W, Rafiq M, Babar Khawar M. Antibacterial and cytotoxic evaluation of sequential extract of *Moringa oleifera* leaves. *Revis Bionatura* 2022;7(1). 15. <http://dx.doi.org/10.21931/RB/2022.07.01.15>

Received: 25 August 2020 / **Accepted:** 20 November 2021 / **Published:** 15 February 2022

Publisher's Note: Bionatura stays neutral with regard to jurisdictional claims in published maps and institutional affiliations.

Copyright: © 2022 by the authors. Submitted for possible open access publication under the terms and conditions of the Creative Commons Attribution (CC BY) license (<https://creativecommons.org/licenses/by/4.0/>).



Materials and methods

All experimental work was performed at the Department of Pharmacology and Toxicology, UVAS, Lahore. The fresh mature leaves of *Moringa Oleifera* were shadow dried at room temperature. Leaves were turned in powder form and stored in a dry place. Soxhlet apparatus as done by (8) with slight modification was used to collect the sequential extracts from dried leaves powder of *Moringa Oleifera* and dried through the rotary evaporator. For further analysis, sequential extracts were used to estimate the antibacterial activity. Cytotoxicity was conducted by colorimetric analysis, MTT (methyl thiazole tetrazolium) assay in vitro.

Antibacterial activity

Identification based on Biochemical tests

All the selected microorganisms, *Staphylococcus aureus*, *Escherichia coli*, *Salmonella enterica*, *Clostridium perfringens* type A, *Haemophilus spp.*, were biochemically characterized by a series of biochemical tests performed for Gram reaction, catalase test, carbohydrate (lactate) fermentation, IMViC tests (Indole test, Methyl Red test, Citrate utilization test, Voges-Proskauer test) and oxidase test as per the standard methods reported in The "Bergey's Manual of Determinative Bacteriology"⁹.

Antimicrobial susceptibility testing (AST) by Agar well diffusion method

Plant extract containing antimicrobial constituents is allowed to soak or diffuse properly in the agar medium on a plate with fresh growth of test microorganisms. A zone of inhibitions is produced circularly due to inhibition of the confluent lawn of growth. The zone of inhibition's diameter is measured in mm.

Minimum inhibitory concentration (MIC) calculation by Micro dilution method

96-well plates were used and labeled for every three isolates of a microorganism and their crude extracts. 100µl MHB media was introduced to each well up to 12th well by sterile micropipette. 100µl of each plant extract was added to the first well, mixed properly, and then serially two-fold diluted up to 10th well by taking 100µl from first well and shifted to second well then took a sample from the second well and shifted to third well and so on. The sample taken from the 10th well was discarded at the end. Now, 100µl of suspension inoculum was introduced up to the 11th well. Standardized inoculum and broth media presence in the 11th well was considered positive control while only broth media presence in the 12th well was considered a negative control.

The final volume in each well was 200µl, except in the 12th well, which has 100µl. The plates were wrapped, labeled, and incubated for 24 hours at 37°C. The plate's optical density (OD value) was measured using an ELISA reader at 595nm wavelength. Note the MIC endpoints as the lowest concentration of crude extract where no visible growth was shown¹⁰. The experiment was performed in triplicate, and the results were noted in mean ± standard deviation format. The data was analyzed statistically by using one-way ANOVA, and the treatment means were compared by Duncan's Multiple Range (DMR) posthoc test at significance level P ≤0.05¹¹.

Cytotoxic evaluation

Preparation of MTT dye

In a sterile test tube, 50 mg of MTT dye was taken. 0.22 µm syringe was used to filter water and then added to test tube containing MTT dye. The prepared MTT dye was stored at 4°C for further use.

Vero cell line

The Vero cell line was taken from WTO-QOL (Quality Operation Laboratory) UVAS, Lahore. For future use in research, it was cryopreserved by a method described by Day and Stacey, 2007¹².

Cell line revival

The cryovial labeled Vero cells were removed from the liquid nitrogen container. Cells were decontaminated with 70% isopropyl alcohol and then thawed at 37°C in a water bath. The Vero cells suspension was shifted to a centrifuge tube containing cell culture media from cryovial. After centrifugation, the supernatant was discarded to remove DMSO, and pellets of Vero cells were resuspended by adding 5ml of cell culture media (M-199). The Vero cells were transferred to the Carrel cell flask for further use.

Vero cell's seeding in 96-well cell culture plate

Vero cells suspension (100 µl) was seeded in 96 well plates in a safety cabinet aseptically. The plates seeded with Vero cells were incubated in 5% CO₂ for 72 hours at 37°C, and an inverted microscope for a complete monolayer was used to monitor cell plates.

Cell survival percentage

Calculation of cell survival percentage:

$$CSP = \frac{\text{Mean OD of test} - \text{Mean OD of negative control}}{\text{Mean OD of positive control}} \times 100$$

Statistical analysis

The parameters analyzed in all experiments were subjected to SPSS for windows version 16, SPSS inc, Chicago, IL, USA). One-way ANOVA analyzed the zone of inhibition and minimum inhibitory concentrations and then the means were compared with Duncan's Multiple Range (DMR) posthoc test at significance level P ≤0.05¹³.

Results

Selected bacteria identification

Staphylococcus aureus (*S. aureus*), *Salmonella enterica* (*S. enterica*), *Escherichia coli* (*E. coli*), *Clostridium perfringens* (*C. perfringens*) type A, and *Haemophilus* species (isolated from poultry) were collected from the Microbiology department of UVAS, Lahore. These bacteria were cultured. Microscopic evaluation and biochemical characterization were performed to confirm these bacteria. The summary of the biochemical test is shown in Table 1.

Minimum inhibitory concentration (MIC) values

Antibacterial activity of *Moringa oleifera* sequential leaves and root extracts against common poultry pathogens was evaluated using the MIC method. Minimum inhibitory concentrations of *Clostridium perfringens* and *Escherichia coli* were

Test performed	<i>Clostridium perfringens</i>	<i>Escherichia coli</i>
Gram Staining	+	-
Indole test	-	+
Lactose fermentation	+	+
Catalase test	-	+
Methyl Red test	-	+
Voges- Proskauer test	-	-
Citrate test	-	-

Table 1. Summary of biochemical test performed.

measured) and results are summarized in Tables 2 and 3, respectively. Means minimum inhibitory concentration of all extracts (chloroform, ethanol, and aqueous) differ non-significantly, as showed by ANOVA and Duncan's test. Minimum inhibitory concentration values were recorded highest for aqueous (5000µg/mL), while lowest for hexane (1250µg/mL), chloroform (1250µg/mL) and ethanol (1250µg/mL). So, hexane, chloroform, and ethanol were active at their respective lowest concentrations.

Cytotoxicity assay

Assay for cytotoxicity was performed by MTT assay using Vero cell lines for sequential extracts (Hexane, Chloroform, Ethanol, and Aqueous) of *Moringa oleifera* roots. Every extract was evaluated using different concentrations. Cell survival percentage and results were indicated as mean optical density \pm standard deviation. CSP was calculated with the help of the optical density of each extract tested.

This means having the same superscripts differ non-significantly and with different superscripts differ significantly. This means having the same superscripts differ non-significantly and with different superscripts differ significantly.

Chloroform extract was safe at concentrations of 500µg/ml, 250µg/ml, 125µg/ml, 62.5µg/ml, 31.25µg/ml, 15.63µg/ml, 7.81µg/ml and 3.91µg/ml where cell survival percentage was more than 50% and the values are 58%, 55%, 60%, 63%, 62%, 59%, 68% and 82% respectively while it was toxic at the concentrations of 2000 µg/ml, 1000µg/ml where cell survival percentage was less than 50% i.e., 26% and 46% respectively, and results are summarized in Table 4.

Ethanol extract was safe at conc. of 1500µg/ml, 750µg/ml, 375µg/ml, 187.5µg/ml, 93.75µg/ml, 46.85µg/ml, 23.43µg/ml and 11.71µg/ml where cell survival percentage was more than 50% and the values are 60%, 58%, 69%, 56%, 59%, 74%, 57% and 78% respectively while it was toxic at the concentrations of 6000µg/ml, 3000µg/ml where cell survival percentage was less than 50% i.e., 18% and 48% respectively and results are represented in Table 5.

Aqueous extract was safe at concentrations of 625µg/ml, 312.5µg/ml, 156.25µg/ml, 78.125µg/ml, 39.06µg/ml, 19.53µg/ml and 9.76µg/ml where cell survival percentage was more than 50% and the values are 56%, 54%, 59%, 55%, 62%, 59% and 66% respectively while it was toxic at the concentrations of 5000µg/ml, 2500µg/ml, 1250µg/ml where cell survival percentage was less than 50% i.e., 8%, 18% and 42% respectively as summarized in Table 6.

Discussion

The current study was designed to determine the antibacterial activity of *Moringa oleifera* against common poultry pathogens *C. perfringens* type A, *E. coli*, *Haemophilus species*, *S. enterica*, and *S. aureus*. Well-diffusion method for qualitative and minimum inhibitory concentration (micro-broth dilution method) for the quantitative study was performed to find out antibacterial activity of sequential extracts using hexane, chloroform, ethanol, and aqueous solvents. These minimum inhibitory concentrations were evaluated for cytotoxicity.

The aqueous extract shows the highest percentage yield (45/50gm) succeeded by ethanol extract (5.5gm/50gm), hexane extract (0.2gm/50gm), and chloroform extract (0.2gm/50gm). The percentage yield was 90%, 11%, 0.8%, 0.4% respectively. In a study the extraction of *Astragalus Root* was carried out with two-fold 95% ethanol, and the yield obtained was 17.1%. The extraction was carried out for three days at room temperature. The filtrate then collected was concentrated under pressure and stored for further use. The yield obtained was closely related to our study's ethanol extract, which was reported 11%¹³.

For *Clostridium* species, culture characteristics, gram staining, different biochemical tests such as Lipase test, Esculin Hydrolysis test, Catalase test, Indole test, Voges- Proskauer test Starch hydrolysis test Motility test, and Methyl Red test were performed¹⁴.

Different biochemical tests were used for the identification of *Escherichia coli*. MacConkey's agar and Eosin methylene Blue agar were used to observe colony characters. Gram staining was also performed. To identify bacteria motility test by hanging drop method, mannitol, sucrose, lactose, maltose and dextrose fermentation, voges procure, indole, methyl red, and Catalase tests were used¹⁵. *E. coli* isolates are catalase-positive, as tested in another study¹⁶.

The minimum inhibitory concentration of sequential extracts of *Moringa Oleifera* leaves against *Clostridium perfringens* are highest for aqueous (5000µg/mL), while lowest for chloroform (1250µg/mL) and ethanol (1250µg/mL). So, chloroform and ethanol are active at their lowest concentration, the MIC values against *Escherichia coli* are highest for aqueous (3333.33µg/mL), medium for ethanol (2500µg/mL) while lowest for chloroform (208µg/mL).

For chloroform extract the CSP was calculated at 10 concentrations, 2000 µg/ml, 1000µg/ml, 500µg/ml, 250µg/ml,

Serial no.	Plant Extract	MIC Values (µg/ml)	Mean MIC ± standard deviation
1	Chloroform	1250	1250 ± 0.00 a
1250			
1250			
2	Ethanol	1250	1250 ± 0.00 a
1250			
1250			
3	Aqueous	5000	5000 ± 0.00 a
5000			
5000			

Table 2. Values of MIC for sequential extracts (Chloroform, Ethanol and Aqueous) of *Moringa oleifera* leaves against *Clostridium perfringens* isolates (n=3).

Serial no.	Plant Extract	MIC Values (µg/ml)	Mean MIC ± standard deviation
1	Chloroform	156.25	208.33 ± 90.21 a
312.5			
156.25			
2	Ethanol	5000	2500 ± 2165.1 ab
1250			
1250			
3	Aqueous	2500	3333.33 ± 1443.37 b
2500			
5000			

Table 3. Values of MIC for sequential extracts (Chloroform, Ethanol and Aqueous) of *Moringa oleifera* leaves against *Escherichia coli* isolates (n=3).

125µg/ml, 62.5µg/ml, 31.25µg/ml, 15.63µg/ml, 7.81µg/ml and 3.91µg/ml. The results for cell survival percentage (CSP) in the present research are 26%, 46%, 58%, 55%, 60%, 63%, 62%, 59%, 68% and 82% respectively. The CSP results indicate that chloroform extract is toxic to cells at concentration ≥1000µg/ml. CSP at 1000µg/ml is 46% means toxic to cell because value is less than 50%. At a concentration less than 1000µg/ml the CSP is more than 50%. So, at higher concentrations chloroform is more cytotoxic to cell than hexane.

The CSP for Ethanol extract was calculated at 10 concentrations, 6000µg/ml, 3000µg/ml, 1500µg/ml, 750µg/ml, 375µg/ml, 187.5µg/ml, 93.75µg/ml, 46.85µg/ml, 23.43µg/ml and 11.71µg/ml. The CSP values are 18%, 48%, 60%, 58%, 69%, 56%, 59%, 74%, 57% and 78% respectively which indicates that chloroform extract at concentration ≥3000µg/ml is 48% so cytotoxic. At a concentration less than 3000µg/ml the CSP is more than 50%. Ethanol as compared to hexane and chloroform is less toxic to cell at higher concentration. Cytotoxicity of aqueous extract was calculated at 10 concentrations, 5000µg/

ml, 2500µg/ml, 1250µg/ml, 625µg/ml, 312.5µg/ml, 156.25µg/ml, 78.125µg/ml, 39.06µg/ml, 19.53µg/ml and 9.76µg/ml. The CSP values are 8%, 18%, 42%, 56%, 54%, 59%, 55%, 62% 59% and 66% respectively. The resulted values indicate that aqueous extract is cytotoxic at concentration ≥625µg/ml. The CSP at 625µg/ml is 42% which means it is toxic to the cells. At a concentration ≥625µg/ml the CSP is more than 50%. So, aqueous extract is more toxic to cell as compared to the rest of two (chloroform, ethanol extracts) at higher concentration.

Conclusions

The current study aimed to evaluate cytotoxic and antibacterial activities of different extracts of *Moringa Oleifera* against common poultry pathogens. Sequential extraction with ethanol, chloroform and aqueous solvents was prepared, and antibacterial activity was evaluated by using agar well diffusion. A micro broth dilution test was used to evaluate the MIC of plant extracts. The extracts exhibiting antimicrobial activity were

Sr. No.	Concentrations µg/ml	Mean ± SD	CSP
1	2000	0.179±0.06	26
2	1000	0.245±0.02	46
3	500	0.284±0.05	58
4	250	0.275±0.04	55
5	125	0.291±0.02	60
6	62.5	0.303±0.02	63
7	31.25	0.300±0.12	62
8	15.63	0.289±0.03	59
9	7.81	0.32±0.08	68
10	3.91	0.365±0.02	82
Positive control	20% DMSO	0.330±0.04	
Negative control	Cell Culture Media	0.094±0.01	

Table 4. CSP Values of Chloroform extract of *Moringa Oleifera* leaves at different concentrations by MTT assay.

Sr. No.	Concentrations µg/ml	Mean ± SD	CSP
1	5000	0.117±0.03	8
2	2500	0.153±0.04	18
3	1250	0.240±0.02	42
4	625	0.293±0.02	57
5	312.5	0.286±0.04	55
6	156.25	0.303±0.02	59
7	78.125	0.290±0.02	56
8	39.06	0.315±0.00	63
9	19.53	0.301±0.06	59
10	9.77	0.326±0.05	66
Positive control	20% DMSO	0.366±0.02	
Negative control	Cell Culture Media	0.086±0.03	

Table 6. Cell survival percentage of aqueous extract of *Moringa oleifera* Leaves.

further evaluated for cytotoxicity by using an MTT assay on the Vero cell line. Cell culture media was prepared, cell lines were propagated, the monolayer was formed. This monolayer was exposed to plant extract dilutions. After 24-48 hours, MTT dye was introduced, and cell survival percentage was calculated. SPSS software was used to analyze data. Results MTT assay and antibacterial activity were compared using DMR posthoc test. All extracts inhibited the growth of *Clostridium perfringens* and *Escherichia coli* except aqueous extract, which

Sr. No.	Concentrations µg/ml	Mean ± SD	CSP
1	6000	0.155±0.03	18
2	3000	0.258±0.04	48
3	1500	0.298±0.02	60
4	750	0.291±0.03	58
5	375	0.329±0.04	69
6	187.5	0.285±0.02	56
7	93.75	0.295±0.04	59
8	46.88	0.346±0.03	74
9	23.43	0.287±0.03	57
10	11.72	0.36±0.03	78
Positive control	20% DMSO	0.341±0.04	
Negative control	Cell Culture Media	0.094±0.01	

Table 5. Values for cell survival percentage of *Moringa Oleifera* leaves Ethanol extract of at various concentrations by MTT assay.

shows no zones of inhibition against *C. perfringens*. MIC values were higher for aqueous extract against all selected bacteria and lowest for chloroform against *E. coli* (208.3µg/ml); *Moringa Oleifera* leaves showed antibacterial activity against all selected pathogens. Chloroform extract showed more significant antibacterial activity than ethanol and aqueous. Cytotoxicity values for chloroform extract are safer than the other two extracts. *Moringa Oleifera* may be used to design traditional medicines for the development of therapeutic agents which will be more safe, effective, and economical.

Author Contributions

U. B. N.; W. I.; M.R.; and M. B. K. proposed the concept of this study. U. B. N. and W. I. did the experimental research. U. B. N.; W. I. and M.R. analyzed the results and wrote the initial draft. M.B.K. reviewed, finalized the manuscript, and supervised the study.

Funding

This research received no external funding.

Acknowledgments

The authors are thankful to the Vice-chancellor of the University of Veterinary and Animal Sciences Lahore, Pakistan, for supporting this study's accomplishment.

Conflicts of Interest

The authors declare no conflict of interest.

Bibliographic references

- Moyo, B.; Masika, P.J.; Hugo, A.; Muchenje, V. Nutritional characterization of *Moringa (Moringa oleifera Lam.)* leaves. *Afr. J. Biotechnol.* 2011, 10, 12925-12933.
- Ma, Z. F.; Ahmad, J.; Zhang, H.; Khan, I.; Muhammad, S. Evaluation of phytochemical and medicinal properties of *Moringa (Moringa oleifera)* as a potential functional food. *S. Afr. J. Botany.* 2020, 129, 40-46.

3. Bukar, A.; Uba, A; Oyeyi, T.I. Phytochemical analysis and antimicrobial activity of parkia biglobosa (Jacq.) Benth. Extracts against some food – borne microorganisms. *Adv. Environ. Biol.* 2010, 74-80
4. Al-Bari, M.; Sayeed, M.; Rahman, M.; Mossadik, M. Characterization and antimicrobial activities of a phenolic acid derivative produced by *Streptomyces bangladesiensis*, a novel species collected in Bangladesh. *Res. J. Med. Med. Sci.* 2006, 1, 77- 81.
5. Foye, W.O.; Lemke, T.L.; Williams, D.A. *Foye's Principles of Medicinal Chemistry*, 6th Ed.; Lippincott Williams and Wilkins: Philadelphia, 2008; pp 44-45.
6. Danso, A.A. Interpretation of low praziquantel cure rates of *Schistosoma mansoni*. *Trends Parasitol.* 2002, 18, 95- 143.
7. Mothana, R.A.; Lindequist, U. Antimicrobial activity of some medicinal plants of the island Soqotra. *J. Ethnopharmacol.* 2005, 96(1-2), 177-181.
8. Balachandar, S.; Jagadeeswari, M.; Dhanabalan, R.; Meenachi, M. 2012. Antimicrobial Activity of *Astragalus membranaceus* against Diarrheal Bacterial Pathogens. *Int. J. Pharm.* 2012, 2(2), 2416-418.
9. Lederberg, J. Isolation and characterization of biochemical mutants of bacteria. *Methods Med. Res.* 1950, 3(195), 5-22.
10. Andrews, J. M. (2001). Determination of minimum inhibitory concentrations. *J. antimicrob. Chemother.* 2001, 48(suppl_1), 5-16.
11. Dzomba, P.; Muchanyereyi, N. Potential antimicrobial plant extract based therapeutics from *temnocalyx obovatus* roots. *Eur. J. Med. Chem.* 2012, 209-215
12. Day, J. G.; Stacey, G. *Cryopreservation and freeze-drying protocols. Methods in molecular biology.* Humana Press: New York, 2007
13. Wang, Y.; Auyeung, K.K.; Zhang, X.; Ko, J.K. *Astragalus saponins modulates colon cancer development by regulating calpain-mediated glucose-regulated protein expression.* *BMC Complement. Altern. Med.* 2014, 1-12.
14. Chaturvedi, A.; Shukla, S. Occurance of *Clostridium* species in different dairy products and its associated health risk. *Int. J. Recent Sci. Res.* 2015, 2, 2827-2829.
15. Zinnah, M.; Bari, M.; Islam, M.; Hossain, M.; Rahman, M.; Haque, M.; Babu, S.; Ruma, R.; Islam, M. Characterization of *Escherichia coli* isolated from samples of different biological and environmental sources. *Bangladesh J. Vet. Med.* 2007, 5 (1), 25-32.
16. Soomro, A.; Arain, M.; Khaskheli, M.; Bhutto, B. Isolation of *Escherichia coli* from raw milk and milk products in relation to public health sold under market conditions at Tandojam. *Pak. J. Nutr.* 2002, 1 (3), 151-152.

CLINICAL REPORT / REPORTE DE CASO

Rara patología derivada de un anillo del cromosoma 15. Clínica, genómica e interactoma de proteínas de genes asociados al fenotipo

Rare pathology derived from a ring chromosome 15. Clinical, genomic and protein interactome of genes associated with the phenotype

César Paz y Miño^{1,2,3*}, Camila Medranda⁴, Alejandra Loaiza⁴, Mishell Ponce⁴, Paola E. Leone²

DOI. 10.21931/RB/2022.07.01.16

¹ Academia Ecuatoriana de Medicina, calles Sodiro y Valparaíso, Pabellón 4. 170136 Quito, Ecuador.² Sociedad Ecuatoriana de Genética Humana, Ecuador.³ Facultad de Ciencias de la Salud Eugenio Espejo, Universidad UTE, Quito, Ecuador.⁴ Genomics Lab. Amazonas N39-82 y Pereira. Edificio Casa Vivanc, Ecuador.Corresponding author: genetica_medica@cesarpazymino.com

Resumen: Se presenta el caso de una paciente de sexo femenino de cuatro años y dos meses de edad, quien consultó por un fenotipo especial: Retraso psicomotor, talla corta, microcefalia, orejas grandes y de implantación baja, frente pequeña, arcos superciliares prominentes, comisura labial abierta, hipertelorismo ocular, cuello corto, hipertelorismo mamario y pectus excavatum. El objetivo de este trabajo es analizar una paciente con rasgos fenotípicos inusuales, a través del examen físico, análisis comparativo con otros casos, y estudios genéticos. El estudio citogenético reveló un cariotipo en mosaico, mos 46,XX,r(15)(q26.3)/46,XX con la presencia del anillo en 83%. El estudio de arrays de mapeo genético identificó la pérdida de 3,5 Mb en 15q26.3. Entre los genes perdidos en la región terminal de 15q, se evidenció una interacción entre sus productos proteicos según el análisis por STRING. Este es el segundo caso de anillo del cromosoma 15 informado en el Ecuador, y sería el centésimo primero en el mundo desde 1966. El fenotipo especial de estos individuos se relaciona con la cantidad de material genético perdido. Los genes implicados en la formación del anillo, así como las proteínas que determinarían estos genes y las relaciones en distintas vías celulares, son analizados *in silico* con la finalidad de comprender la fisiopatología de este trastorno. Su diagnóstico es mayoritariamente postnatal por lo cual el enfoque clínico difiere individualmente de acuerdo a los síntomas y signos que se presenten.

Palabras clave: 46,XX,r(15)(q26.3), anillo del cromosoma 15, mosaico, array de mapeo genético, interactoma.

Abstract: The case of a 4-year-two-month-old female patient is presented, who consulted for a special phenotype: psychomotor retardation, short stature, microcephaly, large and low-set ears, small forehead, prominent brow ridges, labial commissure open, ocular hypertelorism, short neck, mammary hypertelorism and pectus excavatum. The objective of this study is to analyze a patient with unusual phenotypic traits, through physical examination, comparative analysis with other cases, and genetic studies. The cytogenetic study revealed a mosaic karyotype, mos 46,XX,r(15)(q26.3)/46,XX with the presence of the ring in 83%. The genetic mapping array study identified the loss of 3.5 Mb in 15q26.3. Among the genes lost in the terminal region of 15q, an interaction between their protein products was evidenced according to the STRING analysis. This is the second case of a ring chromosome 15 reported in Ecuador. And it would be the 101st in the world since 1966. The special phenotype of these individuals is related to the amount of genetic material lost. The genes involved in the formation of the ring, as well as the proteins that determine these genes and the relationships in different cellular pathways, are analyzed *in silico* in order to understand the pathophysiology of this disorder. Its diagnosis is mostly postnatal, so the clinical approach differs individually according to the symptoms and signs that appear.

Key words: 46,XX,r(15)(q26.3), ring chromosome 15, mosaic, genetic mapping array, interactome.

Introducción

Los cromosomas en anillo son anomalías cromosómicas estructurales inestables, producidos por roturas terminales en uno o ambos brazos cromosómicos seguidas de un evento de fusión de los extremos rotos¹, o por un reordenamiento inversión-duplicación-delección², los que pueden desencadenar la pérdida o ganancia de material genético. Los cromosomas en anillo también pueden formarse por la fusión de secuencias subteloméricas como por la fusión entre telómeros, lo que no

ocasionaría pérdida de material genético^{3,4}, como se observa en pacientes con fenotipo normal, pese al anillo.

En general, el fenotipo de los casos con anillo del cromosoma 15, r(15), presenta retraso del crecimiento, bajo peso al nacer, retraso mental variable, microcefalia, hipertelorismo y fascias triangulares⁵.

El cromosoma 15 en anillo constituye una alteración estructural rara, siendo su prevalencia menor de uno en un

Citation: Paz y Miño C, Medranda C, Loaiza A, Ponce M, Leone PE. Rara patología derivada de un anillo del cromosoma 15. Clínica, genómica e interactoma de proteínas de genes asociados al fenotipo. *Revis Bionatura* 2022;7(1). 16. <http://dx.doi.org/10.21931/RB/2022.07.01.16>

Received: 30 June 2021 / **Accepted:** 7 November 2021 / **Published:** 15 February 2022

Publisher's Note: Bionatura stays neutral with regard to jurisdictional claims in published maps and institutional affiliations.



Copyright: © 2022 by the authors. Submitted for possible open access publication under the terms and conditions of the Creative Commons Attribution (CC BY) license (<https://creativecommons.org/licenses/by/4.0/>).

millón, afectando con más frecuencia al sexo femenino en comparación con el masculino. Se han reportado cien casos alrededor del mundo desde 1966 hasta la fecha, uno de ellos en Ecuador en el año 2018⁶⁻⁸. El presente caso que informamos constituye el segundo de esta patología en el país.

Si bien el diagnóstico prenatal para este tipo de anomalías es posible mediante pruebas especializadas como amniocentesis, ultrasonido y análisis de vellosidades coriónicas; los resultados obtenidos con estas pruebas sólo pueden ser reconfirmados después del nacimiento y a lo largo de la infancia evaluando la aparición y desarrollo de características clínicas congruentes con esta enfermedad⁹. El fenotipo final dependerá del porcentaje de mosaico del anillo que presente el paciente y de la cantidad delecionada de material genético al momento de la formación del anillo.

El objetivo de este trabajo es describir un nuevo caso de una paciente de cuatro años dos meses con rasgos fenotípicos inusuales, que acudió voluntariamente a realizarse una evaluación genética, estudios citogenéticos y moleculares, con la finalidad de entender su patología y analizar su origen y comportamiento genético.

Caso clínico

La probandus acude por primera vez a consulta genética a los cuatro años dos meses de edad, es de sexo femenino, fue producto de una tercera gestación. La madre de 27 años y padre de 30 años de edad aparentemente sanos, sin anomalías conocidas y no consanguíneos.

La paciente proviene de la ciudad de Quito ubicada en la región Sierra del Ecuador; de acuerdo a la ancestría de la población ecuatoriana, la paciente es mestiza¹⁰.

La paciente nació por parto vaginal a las 40 semanas de

gestación reportando un peso de 1.134 g, perímetro cefálico de 31 cm y APGAR de 8-10. Asiste a consulta genética por presentar problemas en su fenotipo: Retraso psicomotor y del desarrollo, bajo peso al nacer (14.2 Kg <percentil 10), talla corta (105 cm <percentil 3), microcefalia (48 cm <percentil 10), retraso mental, frente pequeña, hipertelorismo ocular, arcos supraciliares prominentes, orejas grandes y de implantación baja, filtrum corto, labios hipoplásicos, comisura labial abierta, nariz pequeña, cuello corto, hipertelorismo mamario y pectus excavatum (Figura 1).

Análisis del fenotipo

Se listó las características físicas de todos los casos con anillo del cromosoma 15 descritos en la literatura⁶⁻⁸. Se comparó el fenotipo de la paciente con el de la lista de los 100 casos anteriores.

Estudio genético

Tanto a la probandus como a sus padres se les tomó muestras de sangre periférica con heparina y se realizó los estudios citogenéticos utilizando el protocolo estándar del laboratorio; cultivo de 72 horas en medio RPMI-1640, enriquecido con Suero bobino fetal 15%, fitohemaglutinina, antibiótico y antimicótico. Se realizó la cosecha con colchicina y fijador de Carnoy; extensión de portaobjetos y bandedo GTG (Giemsa-Tripsina-Giemsa). Se contabilizaron 100 metafases por individuo.

Para los estudios moleculares se empleó muestras de sangre periférica obtenidas mediante punción venosa y tratadas con ácido etilendiaminotetraacético (EDTA) como anticoagulante. Se utilizaron 200 µl de muestra para la extracción de ADN utilizando el kit comercial Purelink Genomic DNA (Invitrogen®, Life Technologies, CA, USA). La concentración y pureza del material genético se valoró utilizando NanoDrop 2000c Spectrophotometer (Thermo Fisher Scientific Inc., MA, USA)¹⁰.



Figura 1. Fotografía de la paciente. A) Vista frontal. B) Vista lateral.

Se realizó el análisis de los componentes de la ancestría genética, por tipificación de 46 marcadores informativos de ancestría autosómica, basados en inserción y delección¹⁰. Para describir el estado de las regiones cromosómicas involucradas en el anillo se emplearon arrays de mapeo genético CytoScan 750K (Affymetrix, Santa Clara, CA, USA) según las instrucciones del fabricante (Affymetrix, Santa Clara, CA, USA). Para los genes implicados en la región de pérdida cromosómica se aplicó el análisis bioinformático STRING¹¹.

Resultados

El análisis de las características físicas descritas en los 100 casos informados en la literatura, reveló 52 rasgos (6-8), 12 de ellos presentes en la actual paciente. La probandus presentó también 6 signos no descritos en otros pacientes (Tabla 1).

El estudio de ancestría de la paciente muestra la siguiente composición étnica: Nativoamericano 62%, Europeo 32% y Afr descendiente 6%.

El estudio citogenético de la paciente evidenció dos líneas celulares: normal de 46 cromosomas en el 17% de las metafases analizadas y una con la presencia del cromosoma 15 en anillo (Figura 2) en el 83%, con un cariotipo: mos 46,XX,r(15)(q26.3) [83]/46,XX¹⁷. Los cariotipos de los padres fueron normales: 46,XX y 46,XY.

El estudio de arrays de mapeo genético mostró una delección terminal en 15q26.3 (Figura 3), de 3.459.037 pb con la pérdida de una copia de 29 genes localizados en esta región (desde 98.970.003 pb a 102.429.040 pb) (Tabla 2).

Entre los 29 genes perdidos en la región de 15q26.3 se evidenció una interacción entre nueve de sus productos proteicos según el análisis por STRING (Figura 4). Los otros 20 genes tienen acciones individuales y no presentaron interacciones.

Discusión

Los componentes de la ancestría genética de la paciente es similar a la paciente que describimos anteriormente con cromosoma 15 en anillo⁶ y conforme a la composición étnica del individuo ecuatoriano promedio¹⁰. Se ha informado en muchos casos de la literatura, que el componente genético de ancestría podría determinar prevalencias diferentes según las regiones del mundo. Aunque no es definitivo, la presencia de dos casos en población ecuatoriana es llamativa⁶.

Se han descrito diferentes mecanismos de formación de los cromosomas en anillo (1-4); nuestra paciente presenta un anillo producto de la delección terminal de los brazos cortos y largos del cromosoma 15¹.

Las características clínicas de los casos con anillo del cromosoma 15 demuestran una gran variabilidad del fenotipo, es así que comparamos el de la actual paciente con el de los cien casos informados en la literatura⁶⁻⁸. Encontramos un total de 52 rasgos, de los cuales el más común es el retraso del crecimiento, presente en el 75% del total de casos con cromosoma 15 en anillo, nuestra paciente también mostró esta característica. La frecuencia de los otros rasgos se observan en la Tabla 1: bajo peso al nacer, microcefalia, retraso mental, cara triangular, clinodactilia, braquimesofalangia, retraso en el desarrollo, trastorno del lenguaje, talla corta al nacer, manchas café con leche, puente nasal ancho, paladar ojival, edad ósea retrasada, retraso psicomotor, hipertelorismo ocular, orejas de implantación baja, micrognatia, manos pequeñas, filtrum corto, boca con comisuras dobladas hacia abajo, retrognatia, cuello corto, sobrepeso, hipotonía, pliegues epicánticos, problemas de alimentación, frente prominente, crecimiento desproporcionado de las extremidades, estrabismo, nariz pequeña, hernia diafragmática, cabello escaso, fisura palpebral corta, escoliosis, hipoplasia mamaria, comunicación interauricular, aracnodactilia, hipoplasia ovárica, genitales hipoplásicos, braquicefalia, hipoplasia de labios, pliegue palmar único, conducto arterioso persistente, defecto septal ventricular, pecho en escudo, falange dismórfica, pliegue palmar anormal en los dedos, hipoplasia uterina, comportamiento agresivo, hallux varus y discriminación visual.

Nuestra paciente presentó solo 12 de estas 52 características: retraso del crecimiento, bajo peso al nacer, microcefalia, retraso mental, retraso psicomotor y del desarrollo, hipertelorismo ocular, orejas de implantación baja, filtrum corto, labios hipoplásicos, cuello corto y nariz pequeña. El fenotipo de la paciente mostró adicionalmente frente pequeña, arcos superciliares prominentes, orejas grandes, comisura labial abierta, hipertelorismo mamario y pectus excavatum.

Como diagnóstico diferencial, al no haber un fenotipo clásico de los pacientes con anillo del cromosoma 15, solamente se puede referir a síndromes polimalformativos o de fenotipo inespecífico no caracterizado. El fenotipo de los pacientes con anillos en general y del cromosoma 15 en particular, es muy variado y no es estándar. Se los puede agrupar como dismorfismos en estudio, posiblemente por cromosomopatías.

Los anillos dicéntricos o multicéntricos, anillos grandes o pequeños, como se muestran en la Figura 2, no están contemplados en el cariotipo de la paciente como líneas celulares, por estar presentes en un porcentaje menor al 3%, que es lo que al menos deberían superar para ser considerados como una línea celular. Son solamente variaciones del propio anillo que se forman por la dinámica de este tipo de alteraciones cro-



Figura 2. Diferentes tipos de cromosomas 15 en anillo encontrados en la paciente. Cromosoma normal, cromosoma en anillo monocéntrico y cromosoma en anillo dicéntrico. Las flechas señalan los puntos de rotura.

Características clínicas	Caso actual	Porcentaje de casos clínicos informados en la literatura (ref. 6-8)
Retraso del crecimiento	+	75
Bajo peso al nacer	+	44
Microcefalia	+	41
Retraso mental	+	41
Cara triangular	-	33
Clinodactilia	-	33
Braquimesofalangia	-	32
Retraso en el desarrollo	+	29
Trastorno del lenguaje	-	27
Talla corta al nacer	+	25
Manchas café con leche	-	25
Puente nasal ancho	-	22
Paladar ojival	-	21
Edad ósea retrasada	-	21
Retraso psicomotor	+	20
Hipertelorismo ocular	+	19
Orejas de implantación baja	+	18
Micrognatia	-	16
Manos pequeñas	-	12
Filtrum corto	+	10
Boca con comisuras dobladas hacia abajo	-	10
Retrognatia	-	10
Cuello corto	+	10
Sobrepeso	-	10
Hipotonía	-	10
Pliegues epicánticos	-	9
Problemas en la alimentación	-	9
Frente prominente	-	8
Crecimiento desproporcionado de las extremidades	-	8
Estrabismo	-	7
Nariz pequeña	+	7
Hernia diafragmática	-	7
Cabello escaso	-	6
Fisuras palpebrales cortas	-	6
Escoliosis	-	6
Hipoplasia mamaria	-	6
Comunicación interauricular	-	6
Aracnodactilia	-	6
Hipoplasia ovárica	-	6
Genitales hipoplásicos	-	6
Braquicefalia	-	5
Hipoplasia de labios	+	5
Pliegue palmar único	-	5
Conducto arterioso persistente	-	5
Defecto septal ventricular	-	5
Pecho en escudo	-	5
5ª Falange dismórfica	-	5
Pliegues palmares dactilares anormales	-	5
Hipoplasia uterina	-	5
Comportamiento agresivo	-	5
Hallux valgus	-	1
Distinción visual disminuida	-	1
Frente pequeña	+	0
Arcos superciliares prominentes	+	0
Orejas grandes	+	0
Comisura labial abierta	+	0
Hipertelorismo mamario	+	0
Pectum excavatum	+	0

Tabla 1. Comparación de los rasgos fenotípicos entre la actual paciente y los 100 casos informados en la literatura con cromosoma 15 en anillo.

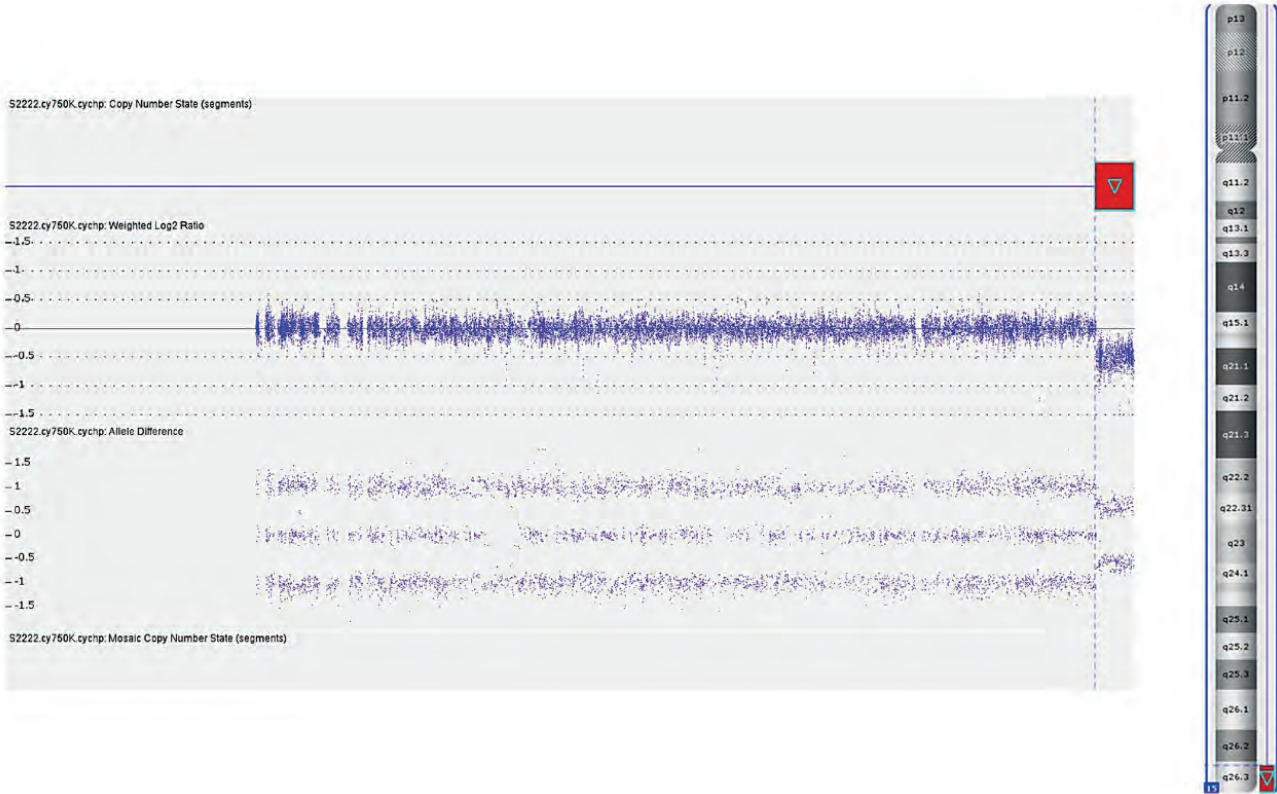


Figura 3. Representación del número de copias del cromosoma 15 por array de mapeo genético. Los resultados se muestran para la relación log 2 (una medida del número de copias cromosómicas; eje Y) frente a la posición genómica en el cromosoma 15 (línea azul, número de copias 2 y cuadro rojo, deleción de una copia; eje X).

Región cromosómica	Pares de bases	Alteración genética	Número de copias	Genes
15q26.3	98.970.003-102.429.040	Pérdida	1	<i>FAM169B, IGF1R, MIR4714, PGPEP1L, SYNM, TTC23, LRRC28, HSP90B2P, MEF2A, LYSMD4, DNM1P46, ADAMTS17, SPATA41, CERS3, PRKXP1, LINS1, ASB7, ALDH1A3, LRRK1, CHSY1, VIMP, SNRPA1, PCSK6, LOC100507472, TM2D3, TARSL2, OR4F6, OR4F15, OR4F13P</i>

Tabla 2. Genes involucrados en la deleción del cromosoma 15 en anillo en la paciente.

mosómicas (rotura-reunión), y que antiguamente generaron discusiones científicas porque se pensaba que algo tenían que ver con el fenotipo. Este tipo de dinamismo del anillo, se lo puede observar y es gráficamente llamativo, pero no se asocia al fenotipo final^{2,6,17}.

La diversidad de características clínicas descritas en los casos con cromosoma 15 en anillo podría asociarse a la cantidad de material genético delecionado. Es frecuente encontrar el punto de rotura en 15q26 aunque se ha identificado en distintas bandas y sub-bandas del brazo largo del cromosoma 15.

Para determinar la longitud de la pérdida en el cromosoma 15 se ha empleado los arrays de mapeo genético, con los cuales no solo se ha definido el tamaño de la pérdida, sino que en algunos casos se ha identificado microduplicaciones que han estado asociadas a características clínicas consistentes con la duplicación de 15q26 como problemas cardíacos y renales^{6,7}.

En nuestra paciente, la región delecionada de 3.459.037 pb de 15q26.3 contiene 29 genes. Entre ellos sobresalen: el receptor del factor de crecimiento similar a la insulina 1 (IGF1R). La haploinsuficiencia de este gen por deleción de 15q26

puede causar retraso del crecimiento pre y postnatal, situación descrita en 1991 y confirmada recientemente con el empleo de varias metodologías entre ellas: citogenética convencional, arrays de mapeo genético y secuenciación completa del exoma¹². CHSY1, este gen codifica un miembro de la familia de la condroitina N-acetilgalactosaminiltransferasa. Estas enzimas poseen actividad dual glucuroniltransferasa y galactosaminiltransferasa y desempeñan papeles críticos en la biosíntesis del sulfato de condroitina, un glicosaminoglicano involucrado en muchos procesos biológicos que incluyen la proliferación celular y morfogénesis. La expresión disminuida de este gen puede desempeñar un papel en el cáncer colorrectal, y las mutaciones en este gen son una causa del síndrome de braquidactilia preaxial a través de la modulación de la señalización NOTCH¹³.

Otros genes, ubicados en la región delecionada, son PGPEP1L y TTC23 descritos frecuentemente en el llamado Síndrome de deleción del cromosoma 15q26-qter también conocido como Síndrome de deleción telomérica 15q, caracterizado por presentar varios síntomas entre ellos el más frecuente, el retraso del crecimiento pre y postnatal¹⁴.

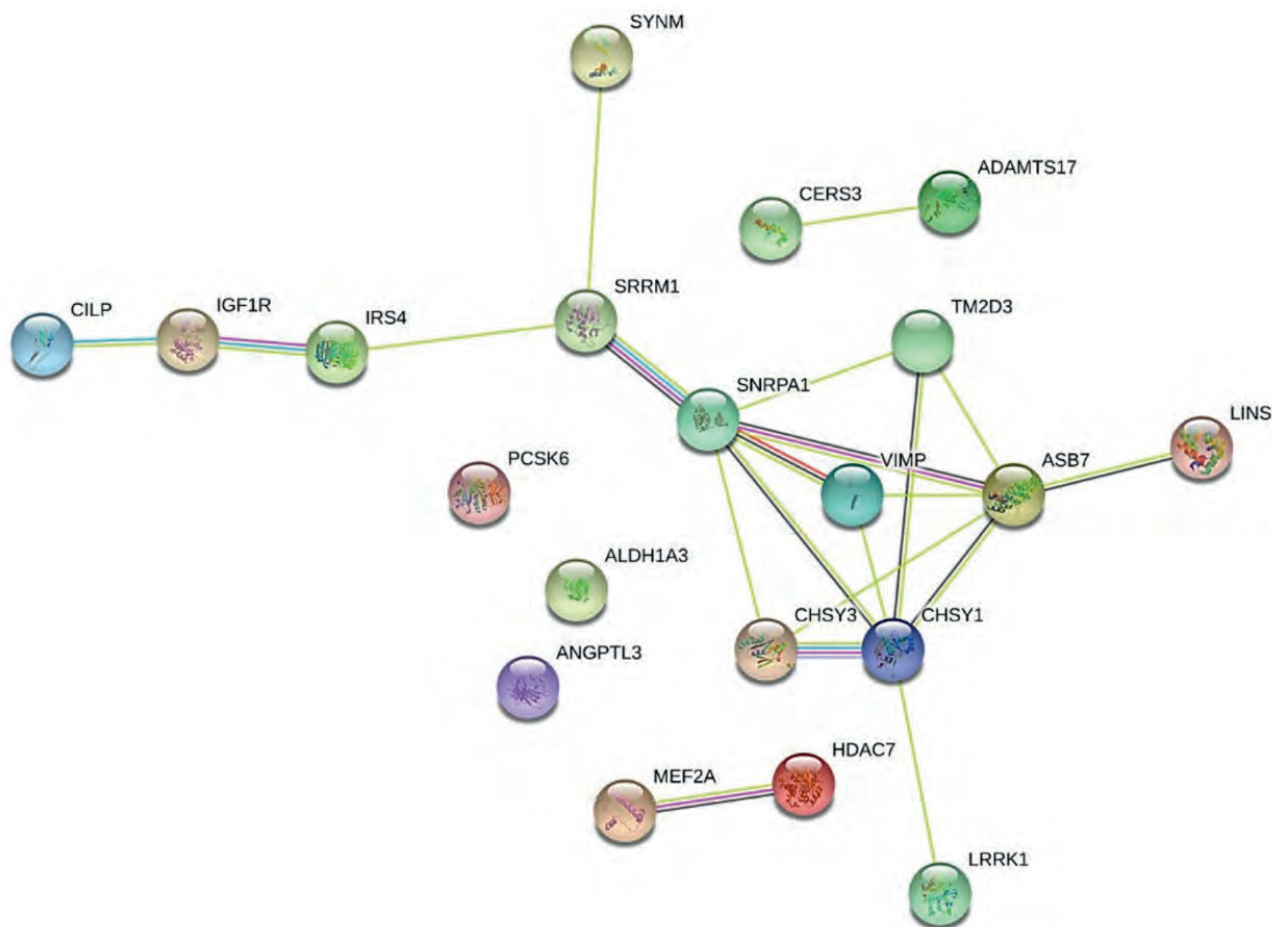


Figura 4. Interactoma de proteínas producto de los genes localizados en la región delecionada del cromosoma 15q26. Líneas celestes, interacciones determinadas en bases de datos seleccionadas; líneas rosadas, interacciones determinadas experimentalmente; líneas de otros colores, interacciones previstas por vecindad de genes, fusiones de genes y homología de proteínas.

Al analizar los productos proteicos de los genes localizados en la zona de deleción en 15q26.3, se evidenció interacciones en 9 proteínas y de estas relaciones destaca IGF1R con CILP e IRS4. CILP, proteína de la capa intermedia del cartílago, que aumenta en el cartílago de la osteoartritis temprana. Este tipo de artritis guarda una relación notable con la edad y es mucho más frecuente en mujeres que en varones. Tiene la capacidad de suprimir la proliferación inducida por IGF1 y la síntesis de proteoglicanos sulfatados, e inhibe la autofosforilación de IGF1R inducida por ligando¹⁵. IRS4, actúa como una interfaz entre múltiples receptores de factores de crecimiento que poseen actividad tirosina quinasa, como el receptor de insulina, IGF1R y FGFR1, y una red compleja de moléculas de señalización intracelular que contienen dominios SH2¹⁶.

Aunque existe una pérdida de material genético, y eso implica la disminución de funciones proteicas importantes, no encontramos una red de interacción precisa. Muchas proteínas actúan solas. Adicionalmente, la pérdida es en heterocigosis, por tanto, el alelo perdido en la deleción cromosómica, podría ser compensado en función con el alelo sobrante, esto podría explicar la alta variación de los fenotipos¹².

La pérdida de 3,5 Mb de 15q26.3 afecta la producción de proteínas eficaces, y el estudio de las redes de interacción de las proteínas alteradas, por esta haploinsuficiencia, evidencia el funcionamiento de cada gen dentro de un proceso biológico, que en este caso se tratan de interacciones establecidas en base a datos seleccionados y a determinados experimentalmente¹².

La variabilidad clínica observada en nuestra paciente y en todos los casos informados respondería al tamaño de la pérdida de ADN del cromosoma 15 involucrado en el anillo. Al igual que hemos analizado en otros casos de cromosomas en anillo^{2,6,17}, la heterogeneidad clínica y la frecuencia baja de la mayoría de características nos lleva a pensar que es muy difícil describir un fenotipo estándar y conceptualizar un Síndrome del anillo¹⁸, nos reafirmamos que el fenotipo alterado está definido principalmente por la cantidad de material genético involucrado en la formación del anillo y la pérdida de los genes de la región específica.

Conclusiones

La utilización de herramientas citogenéticas y moleculares convencionales ha permitido el progreso del diagnóstico genético y una mejor comprensión de los síndromes genéticos. Todos los reordenamientos por los que pasa un cromosoma para adquirir una estructura de anillo presentan un patrón similar. Comienza con una rotura de ambos segmentos terminales con la posterior unión de los extremos rotos. Sin embargo, el fenotipo de un paciente con un cromosoma 15 en anillo es muy variable y no hay mucha información disponible sobre la pérdida de material genético en estos casos. Aunque se ha informado desde 1966 casos similares al presente, solamente un par de ellos hacen referencia a la cantidad de pérdida del material genético^{6,7,8}. Este caso clínico es un nuevo aporte a la comprensión científica de los anillos cromosómicos y es el se-

gundo reporte de un paciente ecuatoriano con un cromosoma 15 en anillo, aplicando herramientas citogenéticas y moleculares

Referencias bibliográficas

1. Guilherme RS, Meloni VFA, Kim CA, Pellegrino R, Takeno SS, Spinner NB, Contlin LK, Christofolini DM, Kulikowski LD, Melaragno MI. Mechanisms of ring chromosome formation, ring instability and clinical consequences. *BMC Med Genet.* 2011;12:171-7.
2. Paz-y-Miño C, Proaño A, Verdezoto S, García JL, Hernández-Rivas JM, Leone PE. Clinical, cytogenetic, and molecular findings in a patient with ring chromosome 4: case report and literature review. *BMC Med Genomics.* 2019;12(1):167.
3. Côté GB, Katsantoni A, Deligeorgis D. The cytogenetic and clinical implications of a ring chromosome 2. *Ann Genet.* 1981;24:231-5.
4. Sigurdardottir S, Goodman BK, Rutberg J, Thomas GH, Jabs EW, Geraghty MT. Clinical, cytogenetic and fluorescence in situ hybridization findings in two cases of "complete ring" syndrome. *Am J Med Genet.* 1999;87:384-90.
5. Butler MG, Fogo AB, Fuchs DA, et al. Two patients with ring chromosome 15 syndrome. *Am J Med Genet.* 1988;29:149-54.
6. Paz-y-Miño C, Guevara-Aguirre J, Paz-y-Miño A, Velarde F, Armendáriz-Castillo I, Yumiceba V, Hernández JM, García JL, Leone PE. Ring chromosome 15 - cytogenetics and mapping arrays: a case report and review of the literature. *J Med Case Rep.* 2018;12(1):340-9.
7. Shao HY, Wang HL, Wu H, Liu XY, Miao ZY. Clinical, cytogenetic and molecular analyses of a rare case with ring chromosome 15 and review of the literature. *Taiwan J Obstet Gynecol.* 2020;59(6):980-4.
8. Zhang J, Yang Y, Zhang J, Wang S, Yao F, Zhang Y, Jiang S. Molecular cytogenetic study of a case with ring chromosome 15. *Zhonghua Yi Xue Yi Chuan Xue Za Zhi.* 2021;38(3):238-41 [En Chino].
9. Liu YH, Chang SD, Chen FP. Increased fetal nuchal fold leading to prenatal diagnosis of ring chromosome 15. *Prenat Diagn.* 2001;21(12):1031-3.
10. Zambrano AK, Gaviria A, Cobos-Navarrete S, Gruezo C, Rodríguez-Pollit C, Armendáriz-Castillo I, García-Cárdenas JM, Guerrero S, López-Cortés A, Leone PE, Pérez-Villa A, Guevara-Ramírez P, Yumiceba V, Fiallos G, Vela M, Paz-y-Miño C. The three-hybrid genetic composition of an Ecuadorian population using AIMS-InDels compared with autosomes, mitochondrial DNA and Y chromosome data. *Sci Rep.* 2019;9(1):9247.
11. STRING CONSORTIUM 2021. [Internet]. [Consultado 2 May 2021]. Disponible en: https://string-db.org/cgi/input?sessionId=bREgW3EM4iOP&input_page_show_search=on.
12. Ocaranza P, Golekoh MC, Andrew SF, Guo MH, Kaplowitz P, Saal H, Rosenfeld RG, Dauber A, Cassorla F, Backeljauw PF, Hwa V. Expanding genetic and functional diagnosis of IGF1R haploinsufficiencies. *Horm Res Paediatr.* 2017;87:412-22.
13. Tian J, Ling L, Shbout M, Lee H, O'Connor B, Merriman B, Nelson SF, Cool S, Ababneh OH, Al-Hadidy A, Masri A, Hamamy H, Reversade B. Loss of CHSY1, a secreted FRINGE enzyme, causes syndromic brachydactyly in humans via increased NOTCH signaling. *Am J Hum Genet.* 2010;87(6):768-78.
14. MalaCards. Human Disease Database: Chromosome 15q26-qter Deletion syndrome. 2021. [Internet]. [Consultado Jun 2021]. Disponible en: https://www.malacards.org/card/chromosome_15q26_qter_deletion_syndrome.
15. Liu L, He J, Liu C, Yang M, Fu J, Yi J, Ai X, Miao Liu M, Yong Zhuang Y, Zhang Y, Huang B, Li C, Zhou Y, Feng C. Cartilage intermediate layer protein affects the progression of intervertebral disc degeneration by regulating the extracellular microenvironment (Review). *Int J Mol Med.* 2021;47(2):475-84.
16. Heinen CA, de Vries EM, Alders M, Bikker H, Zwaveling-Soonawala N, van den Akker ELT, Bakker B, Hoorweg-Nijman G, Roelfsema F, Hennekam RC, Boelen A, van Trotsenburg ASP, Fliers E. Mutations in IRS4 are associated with central hypothyroidism. *J Med Genet.* 2018;55(10):693-700.
17. Paz-y-Miño C, Benítez J, Ayuso C, Sanchez-Cascos A. Ring chromosome 6: clinical and cytogenetic behaviour. *Am J Med Genet.* 1990;35:481-3.
18. Kosztolányi G. Does "ring syndrome" exist? An analysis of 207 case reports on patients with a ring chromosome. *Hum Genet.* 1987;75:174-9.

CLINICAL REPORT / REPORTE DE CASO

Coronavirus: First Report of a Sars-Cov-2 case In Ecuador. Are nutritional assessment and treatment helpful for a successful outcome?

Ordoñez Martínez Mayra Graciela¹, Alemán Espinoza Washington René^{1,2}, Ulloa Correa José Efraín¹, Rodas Mireya², Sarango Sánchez Edwin Renato², Cucalón Gabriela³, Frias-Toral Evelyn⁴

DOI. 10.21931/RB/2022.07.01.17

¹Hospital Alcívar, Coronel 2207 y Cañar. Guayaquil, Ecuador.

²School of Medicine, Universidad Espíritu Santo - Ecuador, Samborondón, Ecuador.

³ESPOL Polytechnic University, Escuela Superior Politécnica del Litoral, ESPOL, Lifescience Faculty, Campus Gustavo Galindo, Guayaquil, Ecuador.

⁴Universidad Católica Santiago de Guayaquil, Av. Pdte. Carlos Julio Arosemena Tola, Guayaquil 090615, Ecuador.

Corresponding author: mg_ordonez@hotmail.com

Abstract: Due to the globalized world in which we live, there are more excellent migratory movements and an increase in emerging diseases. During the past year, the significant impact of the coronavirus has been evident. It was previously designated 2019-nCoV and was identified as the cause of a cluster of pneumonia cases in Wuhan in late 2019. In February 2020, the World Health Organization (WHO) declared the COVID-19 coronavirus disease 2019, which causes severe acute respiratory syndrome (SARS-CoV-2). This outbreak's scope and ultimate effect remain unclear due to the fast spreading of new virus variants worldwide and the limitations to reaching a sufficient vaccination rate in low-income countries. We want to report the first case of COVID-19 in Ecuador and the lessons learned from its management.

Key words: Coronavirus, severe acute respiratory syndrome.

Introduction

A new variant for coronavirus emerged at the end of 2019, which was designated 2019-nCoV. It was identified as the cause of a cluster of pneumonia cases in Wuhan, China, and rapidly spread throughout China and worldwide. In February 2020, the World Health Organization (WHO) declared the COVID-19 disease¹, coronavirus disease 2019, which causes severe acute respiratory syndrome (SARS-CoV-2)². This outbreak's scope and ultimate effect are unclear as the situation rapidly evolves into new virus variants. We report the first case of COVID-19 in Ecuador to see retrospectively the actions taken to control its dissemination nationwide.

CASE REPORT

A 71-year-old woman was hospitalized in February 2020 for moderate-intensity headache, dry cough, non-quantified fever, progressive dyspnea, diaphoresis, and a feeling of restlessness. Something remarkable is that she came from Spain 8 days before. She had a medical history of hypertension and ischemic cerebrovascular event.

At her physical examination, bilateral sub-crepitant rales were found up to lung medium fields, leg edema (+++). Her temperature was 101.3 F, blood pressure 140/90 mmHg, heart rate 102 beats per minute, respiratory rate 28 per minute, oxygen saturation 88% at rest in room air, no reports of weight variations at admission or tobacco and alcohol consumption.

The patient was monitored with O₂ supply by mask at 10 liters per minute, improving saturation to 93%. Laboratory tests were done as presented in Table 1.

On admission, the chest X-ray showed bilateral basal and perihilar alveolar opacities with left basal confluent. Blood and urine culture tests and tests for Influenza A and B were negatives. Unfortunately, due to COVID 19 tests in Ecuador, it was impossible to perform the test from the patient's admission. The echocardiogram reported pulmonary hypertension with 59 mmHg.

High-resolution chest computerized tomography (CT) showed a left basal laminar pleural effusion, ground-glass opacities associated with thickening interlobular septa and bilateral bronchial dilatations (Figure. 1).

The patient was transferred to ICU with initial diagnoses of Acute Hypoxemic Respiratory Failure plus Severe Acute Pneumonia of the Community with a CURB-65 score: 2 (Mortality 6.8% - intermediate risk) / SOFA score: 2 (≤33.3% mortality) / APACHE II score: 12 (predicted mortality rate 14.6%) and Acute Pulmonary Edema. In the ICU, antibiotic treatment was started with Meropenem and Furosemide, and routine protocols were established. Also, the patient received enteral nutrition by nasogastric tube with a specialized formula low in carbohydrates, modified fat, and fiber (providing 1 cal/mL, 245 cal/250 mL. Caloric Distribution: Protein 16.8%, carbohydrates 34.2%, fat 49%) combined with a ready to use protein module made of soy (protein 6.8 gr and carbohydrates 0.4 gr) diluted in 200 cc of water every 8 hours by intermittent infusion. The patient received non-invasive ventilation (NIV) due to O₂ saturation that dropped to 90% and tachypnea to improve the ventilatory pattern.

Citation: Ordoñez Martínez M G, Alemán Espinoza W R, Ulloa Correa J E, Rodas M, Sarango Sánchez E R, Cucalón G, Frias-Toral E. Coronavirus: First Report of a Sars-Cov-2 case In Ecuador. Are nutritional assessment and treatment helpful for a successful outcome? *Revis Bionatura* 2022;7(1). 17. <http://dx.doi.org/10.21931/RB/2022.07.01.17>

Received: 9 July 2021 / **Accepted:** 31 October 2021 / **Published:** 15 February 2022

Publisher's Note: Bionatura stays neutral with regard to jurisdictional claims in published maps and institutional affiliations.



Copyright: © 2022 by the authors. Submitted for possible open access publication under the terms and conditions of the Creative Commons Attribution (CC BY) license (<https://creativecommons.org/licenses/by/4.0/>).

The patient continued with no improvement, so treatment for typical and atypical germs was extended, along with antiviral coverage (Linezolid, Clarithromycin, Oseltamivir). In addition, a real-time multiplex RT-PCR of a nasal swab respiratory panel is performed, the result of which was negative for arbovirus, variants of coronavirus (229E, HKU1, NL63, OC43), adenovirus, influenza (A / H1, / H3, B), parainfluenza 1a/4, respiratory syncytial virus, rhinovirus, enterovirus and atypical germs (*Bordetella pertussis*, *Chlamydomydia pneumoniae*, *Mycoplasma pneumoniae*).

Between the 2nd and 3rd days of hospitalization, the patient remained in isolation in ICU, maintaining saturation but without radiological improvement. Finally, on the 4th day of hospitalization, the patient is anxious and does not tolerate NIV mask, her PO₂ decreases, leukocytes dropped to 9400, Neutrophils 85% (Table 1). Due to her hypoxemia and irregular ventilatory pattern, the patient is intubated with pressure-controlled ventilation (PCV), under sedation, and analgesia with midazolam and fentanyl.

Parameters/Date	2/22/20	2/24/20	2/26/20	2/28/20
Leucocyte (10 ³)	17.96	16.7	9.40	10.7
Neutrophils	15.79	15.0	6.71	9.17
Lymphocytes	1.65	1.07	0.89	0.94
Platelets (k/ul)	364	452	571	598
Hemoglobin (g/dl)	11	10.9	10.8	9.9
Hematocrit	32%	30%	30%	28%
Procalcitonin (ng/mL)	0.34	0.5	0.6	
CRP (mg/dl)	42	---	29	28
D-dimer (ng/dl)	2098			
Arterial Blood Gas				
pH	7.5	7.5	7.48	7.5
pCO ₂	27	36	42	41
pO ₂	126	129	61	112
SatO ₂	97%	99%	93%	99%
PAFI	206	211		
HCO ₃ (mmol/L)	21	28	31	32

Table 1. Summary of Laboratory test.

On the 5th day of admission, a bronchoalveolar lavage (BAL) is performed. Samples are sent to the National Institute of Public Health and Research (INSPI) to determine the RT-PCR of SARS-CoV-2 after coordination with the Ministry of Public health and reported positive. Then the patient was referred to a Contingency Hospital assigned for confirmed COVID-19 cases according to the Ecuadorian Ministry of Public Health (MPH) guidelines (Figure. 2).

Discussion

The coronavirus is still a public health emergency of international concern, with more than 152 million cases reported in 192 countries and regions³. Despite the great efforts to improve the vaccination rates in different nations, those with limited

resources, as Ecuador, are dealing with this implacable virus and its new variants. The constant increasing COVID-19 cases, the attempts to return to normal economic activities, poverty, the Alfa, Beta, Gamma, Delta and other new variants are some of the factors that have severely affected the Ecuadorian health system. As a result, more hospital sections have been assigned to these patients; ICU beds, ventilators, O₂ tanks, medicines, and all resources needed for their treatment are not enough. Unfortunately, this scenario is common in many countries in South America and other regions⁴. Hence, several governments have implemented quarantine measurements and flight restrictions, among other dispositions, to control this inexorable enemy.

Individuals exposed to COVID-19 cases must strictly follow the isolation and the guidelines defined by the MPH to control the virus spreading, especially since there are new, more virulent strains. Complications such as severe pneumonia, respiratory failure, acute respiratory distress syndrome (ARDS), and cardiac injury, including fatal outcomes, occur three to six days after suspected exposure.

As seen in the timeline (Figure. 2), 13 days after the onset of the symptoms, the patient was diagnosed with COVID-19. During that time, the "patient zero" made a series of contacts between family and friends in 2 very crowded cities from Ecuador. In that way, the primarily spread person-to-person through respiratory droplets was initiated. Notably, this person was among several that arrived in the country through the first 15 days of February. This time of the year is prevalent to receive travelers from Spain, Italy, and the United States.

This case report highlights the importance of clinicians obtaining a recent history of travel or exposure to COVID-19 positive cases in any patient presenting acute disease symptoms for early recognition. Also, to ensure proper identification and prompt isolation of patients at risk for 2019-nCoV infection to help reduce further transmission. As for the community, people should be advised to practice social distance, wear a medical mask, diligent hand washing, respiratory hygiene to contain their respiratory secretions, and seek medical attention in case of suspicion⁵.

Nutritional assessment and treatment are still not part of the routine protocols in many institutions worldwide, as demonstrated by the nutritional papers⁶. After all these months, where more knowledge around COVID-19 has been developed, the profound impact of nutritional status on these patients has been shown. Many researchers have highlighted the direct connection between an altered nutritional status with prolonged stay, more significant admission in the ICU, and higher mortality rates⁷. In Ecuador, a multidisciplinary group elaborated the guidelines for assessment and treatment of COVID-19 cases, and throughout the guideline, it has been emphasized the fundamental role of the nutritional status for a patient's prognosis⁸. This nutritional approach also applies to cancer patients who have been severely affected by this pandemic, as it was published by Rodríguez *et al.*⁹.

While the governments are making exceptional attempts to reach herd immunization, it remains imperative not to forget the fundamental things to prevent COVID-19 infection and treat them through a nutritional assessment. It can be determined if there is any degree of malnutrition as recommended by the ESPEN guidelines to do the needed corrections to improve the patient's prognosis¹⁰. Remarkably, these guidelines were developed in collaboration with WHO representatives, one of the leading institutions about this disease.

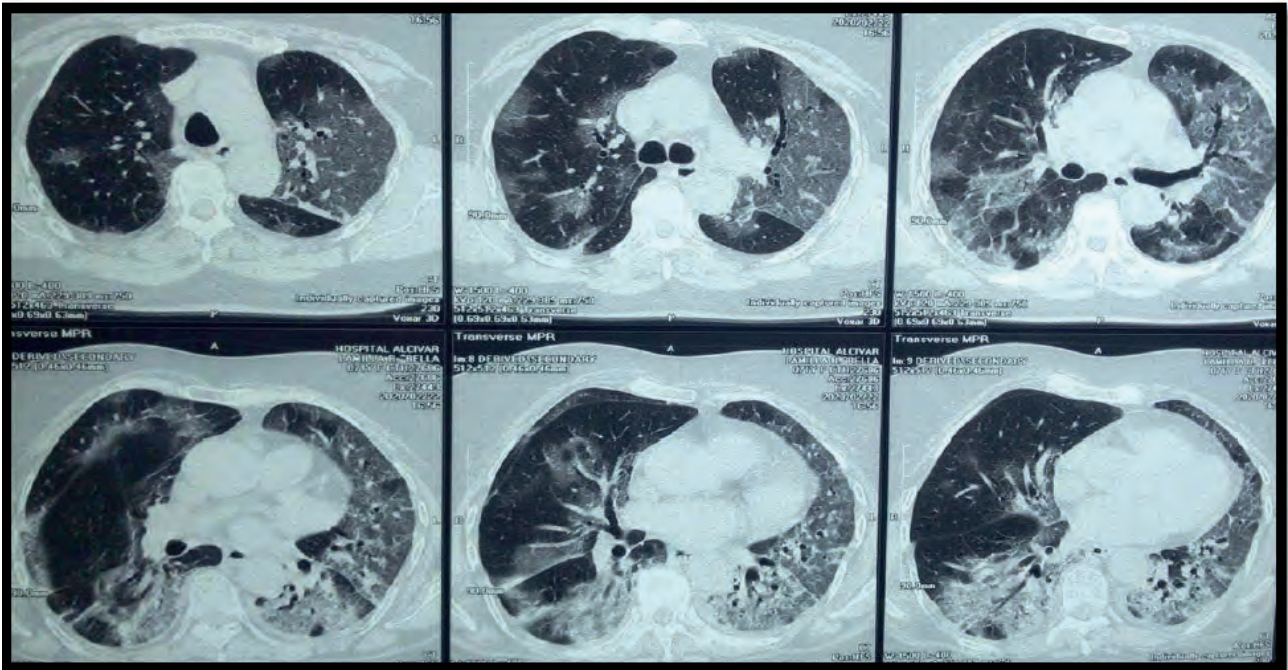


Figure 1. Chest CT scan showing left basal laminar pleural effusion, ground-glass opacities associated with thickening interlobular septa and bilateral bronchial dilatations.

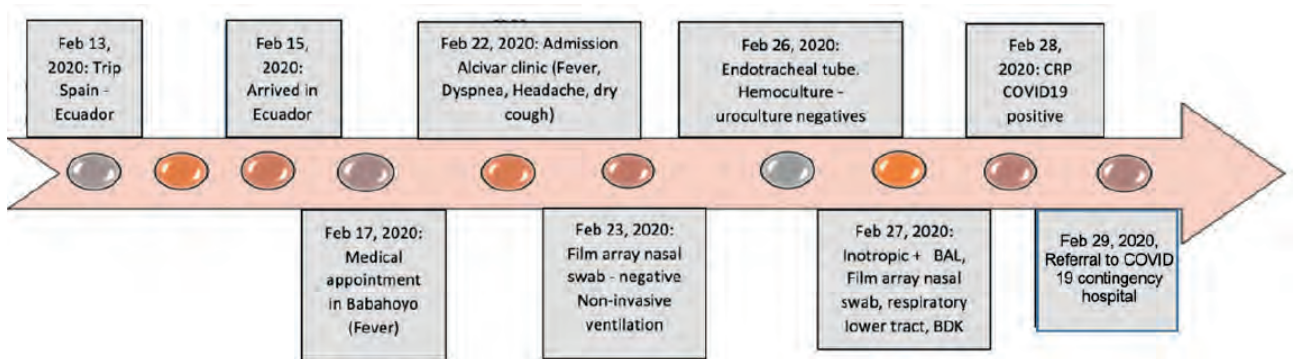


Figure 2. Timeline of significant events in the reported case. BAL: bronchoalveolar lavage.

Conclusions

We hope this case can emphasize the relevance of initiating an early diagnosis and installing correct protocols to control COVID-19 dissemination. Also, it stresses that nutritional assessment and intervention are essential pillars to prevent and contribute to the integral management of these patients, especially in countries where the vaccination rates, due to several reasons, are not as fast as the number of positive cases.

Statement of authorship

All authors contributed equally to this case-report communication.

Funding Source

None

Statement of Ethics

The patient provided both verbal and written informed consent to publish the case, including the publication of images.

Declaration of Competing Interest

We have no competing interests to disclose.

Acknowledgments

None

Bibliographic references

1. Cucinotta D, Vanelli M. WHO Declares COVID-19 a Pandemic. *Acta Biomed.* 2020 Mar 19;91(1):157-160. doi: 10.23750/abm.v91i1.9397. PMID: 32191675; PMCID: PMC7569573.
2. Coronaviridae Study Group of the International Committee on Taxonomy of Viruses. The species Severe acute respiratory syndrome-related coronavirus: classifying 2019-nCoV and naming it SARS-CoV-2. *Nat Microbiol.* 2020 Apr;5(4):536-544. doi:10.1038/s41564-020-0695-z. Epub 2020 Mar 2. PMID: 32123347; PMCID: PMC7095448.
3. Dong E, Du H, Gardner L. An interactive web-based dashboard to track COVID-19 in real time. *Lancet Inf Dis.* 20(5):533-534. doi: 10.1016/S1473-3099(20)30120-1
4. Alava JJ, Guevara A. A critical narrative of Ecuador's preparedness and response to the COVID-19 pandemic. *Public Health Pract (Oxf).* 2021 Nov;2:100127. doi: 10.1016/j.puhip.2021.100127. Epub 2021 Apr 23. PMID: 33907741; PMCID: PMC8062908.

5. Cuéllar L, Torres I, Romero-Severson E, Mahesh R, Ortega N, Pungitore S, et al. Excess deaths reveal the true spatial, temporal, and demographic impact of COVID-19 on mortality in Ecuador. medRxiv [Preprint]. 2021 Mar 1:2021.02.25.21252481. doi: 10.1101/2021.02.25.21252481. PMID: 33688690; PMCID: PMC7941667.
6. Cereda E, Klersy C, Hiesmayr M, Schindler K, Singer P, Laviano A, et al. NutritionDay Survey Collaborators. Body mass index, age and in-hospital mortality: The NutritionDay multinational survey. Clin Nutr. 2017 Jun;36(3):839-847. doi: 10.1016/j.clnu.2016.05.001. Epub 2016 May 15. PMID: 27236599.
7. Yu Y, Ye J, Chen M, Jiang C, Lin W, Lu Y, et al. Malnutrition Prolongs the Hospitalization of Patients with COVID-19 Infection: A Clinical Epidemiological Analysis. J Nutr Health Aging. 2021;25(3):369-373. doi: 10.1007/s12603-020-1541-y. PMID: 33575730; PMCID: PMC7709472.
8. Ministry of Health. Consenso interino multidisciplinario informado en La evidencia sobre El tratamiento de COVID19. Ecuador: Government of Ecuador, 2020.
9. Rodriguez D, Guerrero M, Maldonado M, Herrera S, Frías E, Santana, S. Recomendaciones en el tratamiento nutricional para pacientes oncológicos ante covid-19. J Health Med Sci. 2020; 6(4):303-314.
10. Barazzoni R, Bischoff SC, Breda J, Wickramasinghe K, Krznaric Z, Nitzan D, et al; endorsed by the ESPEN Council. ESPEN expert statements and practical guidance for nutritional management of individuals with SARS-CoV-2 infection. Clin Nutr. 2020 Jun;39(6):1631-1638. doi: 10.1016/j.clnu.2020.03.022. Epub 2020 Mar 31. PMID: 32305181; PMCID: PMC7138149.

ARTICLE / INVESTIGACIÓN

Dissecting the relationship between artificial insemination success and bull semen quality in the arid region of Tiaret (Algeria)

Mohamed Achir, Khaled Taïbi*, Leila Ait Abderrahim, Mohamed Boussaid, Kada Souana, Abdelkader Tadj, Toufik Benaïssa, Tayeb Gouchich

DOI. 10.21931/RB/2022.07.01.18

³Faculty of Life and Natural Sciences, University of Tiaret, 14000, Algeria.
Corresponding author: khaledtaibi@hotmail.com

Abstract: Despite being subject to prior assortment, frozen bull sperms commercialized for artificial insemination may present certain morphological defects. The present study aims (i) to assess the artificial insemination success of the most common cattle breeds in Algeria and (ii) to evaluate the possible effects of commercialized bull's semen quality on this operation. Artificial insemination was assessed through four years of field monitoring by inseminating different cattle breeds of normal fertility. However, semen quality was evaluated using light microscopy by measuring viability, motility, and morphological abnormalities of spermatozoa. Field study revealed a high percentage of normal calving in red and white Holstein breed (44.83 %) against the high percentage of embryonic mortality (46.43 %) and calving with a malformation (10.71 %) in Montbéliarde breed. Semen quality assessment revealed that sperm viability and motility were higher in Holstein breeds than in Montbéliarde. Furthermore, significant differences between semen bulls were found in the proportion of abnormal spermatozoa; a higher rate of sperms with the abnormal head was observed in the black and white Holstein breed (69.3±10.98 %). However, the percentage of abnormal sperms with tail defects was higher in the Montbéliarde breed (67.5±10.74 %). The lousy quality of the selected semen and/or the poor handling and storage of frozen semen constitute a determinant factor that hinders the success of artificial insemination in the arid region of Tiaret (Algeria).

Key words: Dairy and beef cattle, artificial insemination, sperm abnormalities, calving, embryogenic mortality, Tiaret, Algeria.

Introduction

Livestock production significantly reinforces the socio-economic lives of people throughout the creation of employment opportunities and deliverance of household incomes, mainly in undeveloped countries. Furthermore, several products and by-products derived from livestock have a significant nutritional and economic value, such as meat and milk, which constitute veritable protein sources for consumers¹. However, the development of livestock productivity is faced with several constraints, especially in arid and semiarid regions, limiting severely sustainable livestock production.

Indeed, the livestock farming sector has experienced several biotechnological progressions during the last decades with the primary goal of enhancing productivity and improving genetic gain². In this sense, artificial insemination was the most common biotechnology practiced in farm animals, particularly dairy cattle, to improve breeding and obtain genetic advances³. The wide use of bovine artificial insemination as efficient reproductive biotechnology is due mainly to the development of cryopreservation methods ensuring spermatozoa viability, from the best breeding bulls, after long periods of storage that can be used to inseminate thousands of cows worldwide⁴. The latest available statistics of the National Center for Artificial Insemination and Genetic Improvement (2017) have reported a success rate of the whole national insemination program ranging from 45% to 48% in Algeria.

Several factors are responsible for the success of artificial insemination outcomes and require appropriate attention, such as female physiology, farm management and quality of semen used in the programs⁵. Though selected beforehand, frozen bull spermatozoa commercialized for artificial insemination may present specific morphological abnormalities³. Abnormal spermatozoa might reflect troubles in the spermatogenesis process that affect normal spermatozoa of the same ejaculate^{6,7}. In general, poor spermatozoa morphology constitutes a good indicator of low fertility rate⁸ this is why it is essential to analyze spermatozoa morphology to predict fertilizing capacity⁹.

Therefore, the aim of this study is (i) to evaluate the success of artificial insemination program in the arid regions of Tiaret (Algeria), throughout field monitoring carried out in fifteen pilot farms during the period 2016-2019, then (ii) to assess the quality of commercialized bull semen used in reproductive programs in Algeria throughout the estimation of morphological abnormalities of the most common dairy and beef breeds bulls to determine the possible presence of variations between them, regarding the proportion of abnormal spermatozoa.

Citation: Achir M, Taïbi K, Ait Abderrahim L, Boussaid M, Souana K, Tadj A, Benaïssa T, Gouchich T. Dissecting the relationship between artificial insemination success and bull semen quality in the arid region of Tiaret (Algeria). *Revis Bionatura* 2022;7(1). 18. <http://dx.doi.org/10.21931/RB/2022.07.01.18>

Received: 10 June 2021 / **Accepted:** 15 October 2021 / **Published:** 15 February 2022

Publisher's Note: Bionatura stays neutral with regard to jurisdictional claims in published maps and institutional affiliations.

Copyright: © 2022 by the authors. Submitted for possible open access publication under the terms and conditions of the Creative Commons Attribution (CC BY) license (<https://creativecommons.org/licenses/by/4.0/>).



Materials and methods

The scientific committee approved the study for ethical criterion in the department of Natural and Life Sciences, Ibn Khaldoun University of Tiaret (Algeria) (Ref. 05/SCDNLS/2018).

Bull semen samples

The present study was performed on certified frozen semen straws belonging to selected dairy and beef breeds obtained from the National Center for Artificial Insemination and Genetic Improvement (Algiers, Algeria). Frozen semen samples of breeding bulls were produced in 0.25 µl straws where each straw contained approximately 25 million spermatozoa. The semen samples were frozen with the same routine cryopreservation technology using the same extender.

Our study involved three bulls selected by the National Center for Artificial Insemination and Genetic Improvement according to their performance representing the three most common breeds in Algeria, namely the bull *Jetstream* for Montbéliarde breed, *Jopic* for Red and white Holstein breed and *Jukebox* for Black and white Holstein breed.

Field monitoring of artificial insemination

The field monitoring of the artificial insemination success using the selected semen was conducted from 2016-2019 in fifteen dairy farms located in the region of Tiaret. A total of 86 cows known to be of normal fertility were selected for the study encompassing the main frequent dairy breeds in the region, i.e., 29 black and white Holstein, 29 red and white Holstein and 28 Montbéliarde cows.

All the farms subject to this study have the same management model; livestock buildings are similar in design, hygienic conditions and alimentation. Besides, health care was supervised by veterinarians. It should also be noted that cows were inseminated with semen originating from the same batch of tested samples.

Semen quality analysis

For semen analysis, straws were thawed at 37 °C for 30 seconds, then they were maintained at the same temperature during the processing. The percentage of spermatozoa motility in each semen sample (around 10 µL) was determined using a phase-contrast microscope supplied with a warm stage adjusted to 37 °C.

After that, bull semen samples were diluted and fixed in pre-warmed (37 °C) formaldehyde-PBS. At that point, a smear from diluted semen was made on a glass slide then was stained by eosin (1.67%) and nigrosin (10%) stain according to the protocol established by Moskovtsev and Librach (10). In this sense, at least 200 spermatozoa cells were examined per slide from each bull sample at 400x and 1000x magnification using a phase-contrast microscope (Leica DM2500; Wetzlar, Germany) to assess their viability and morphological abnormalities. The number of spermatozoa cells bearing head, midpiece and tail morphological abnormalities were recorded as previously described by Menon, Barkema¹¹.

Data analysis

Data were subjected to a one-way analysis of variance to determine the effect of breed type on the measured parameters. Comparison between breeds was carried out using the test of Duncan. The significant differences between means and percentages were determined at the $P < 0.05$ level. In all cases, data were examined for normality and homogeneity of variances and identified for any violations of assumptions. The statistical analyses were performed using the computing environment R (R Development Core Team, 2013).

Results

Field monitoring

Field monitoring of the artificial insemination operation carried out during 2016-2019 has raised several concerns (Table 1). The percentage of normal calving was comprised between the high value of 44.83% noticeable for the red and white Holstein breed and low values of 25% and 27.59% distinguished respectively in Montbéliarde and black and white Holstein breeds. Furthermore, a higher proportion of embryonic mortality was recorded in the Montbéliarde breed (46.43%) in comparison to red and white (20.69%) and black and white Holstein breeds (17.24%). Besides, it should be noted that a significant proportion of 10.71% of calving with malformation has been registered in the Montbéliarde breed.

Semen analysis

Semen analysis has revealed that individual spermatozoa motility was significantly higher in Holstein breeds (46.37±11.22% in red and white and 46.28±12.94% in black and white Holstein respectively) in comparison to Montbéliarde (34.74±8.46%). By the same, red and white (41.48±5.3%) and black and white Holstein breeds (41.33±17.2%) have demonstrated high spermatozoa viability when compared with the Montbéliarde breed (29.31±6.54%).

The most frequent spermatozoa morphological abnormalities found in the head, midpiece and tail are shown in Tables 2, Figure 1. The black and white Holstein breed was characterized mainly by spermatozoa head defects, while red and white Holstein and Montbéliarde breeds were characterized mainly by spermatozoa tail defects. Significant differences between breeds were found in the proportion of spermatozoa with abnormal head (p -value<0.001***); a higher rate was observed in black and white Holstein breed (69.3±10.98%) while it was around 34.54±18.01% and 25.28±8.95% respectively in red and white Holstein and Montbéliarde breeds. Remarkably, the percentage of spermatozoa with abnormal midpieces was comparable among the examined breeds (p -value>0.05 non-significant). However, the percentage of abnormal spermatozoa with tail defects was significantly higher in the Montbéliarde breed (67.5±10.74%) followed by the red and white Holstein breed (46.15±17.68%) while the lowest percentage was recorded in black and white Holstein breed (24.47±9.95%). Taking

Breed	Normal calving	Embryonic mortality	Gravid	Calving with malformation
Black and white Holstein	8 (27.6%) ^a	5 (17.2%) ^a	12 (41.4%) ^c	/
Red and white Holstein	13 (44.8%) ^b	6 (20.7%) ^a	10 (34.5%) ^b	/
Montbéliarde	7 (25%) ^a	13 (46.4%) ^b	5 (17.9%) ^a	3 (10.7%)

Table 1. Field monitoring of the cows inseminated artificially by the selected bull semen breeds in the region of Tiaret, Algeria.

Breed	Individual spermatozoa motility (%)	Spermatozoa viability (%)	Head defects (%)	Midpiece defects (%)	Tail defects (%)
Black and white Holstein	46.28±12.94 ^b	41.33±17.2 ^b	69.3±10.98 ^c	23.42±6.59 ^a	24.47±9.95 ^a
Red and white Holstein	46.37±11.22 ^b	41.48±5.3 ^b	34.54±18.01 ^b	25.79±6.87 ^a	46.15±17.68 ^b
Montbéliarde	34.74±8.46 ^a	29.31±6.54 ^a	25.28±8.95 ^a	36.95±12.76 ^b	67.5±10.74 ^c

Table 2. Individual spermatozoa motility, spermatozoa viability and morphological abnormalities of the selected bull semen used for artificial insemination programmes in Algeria.

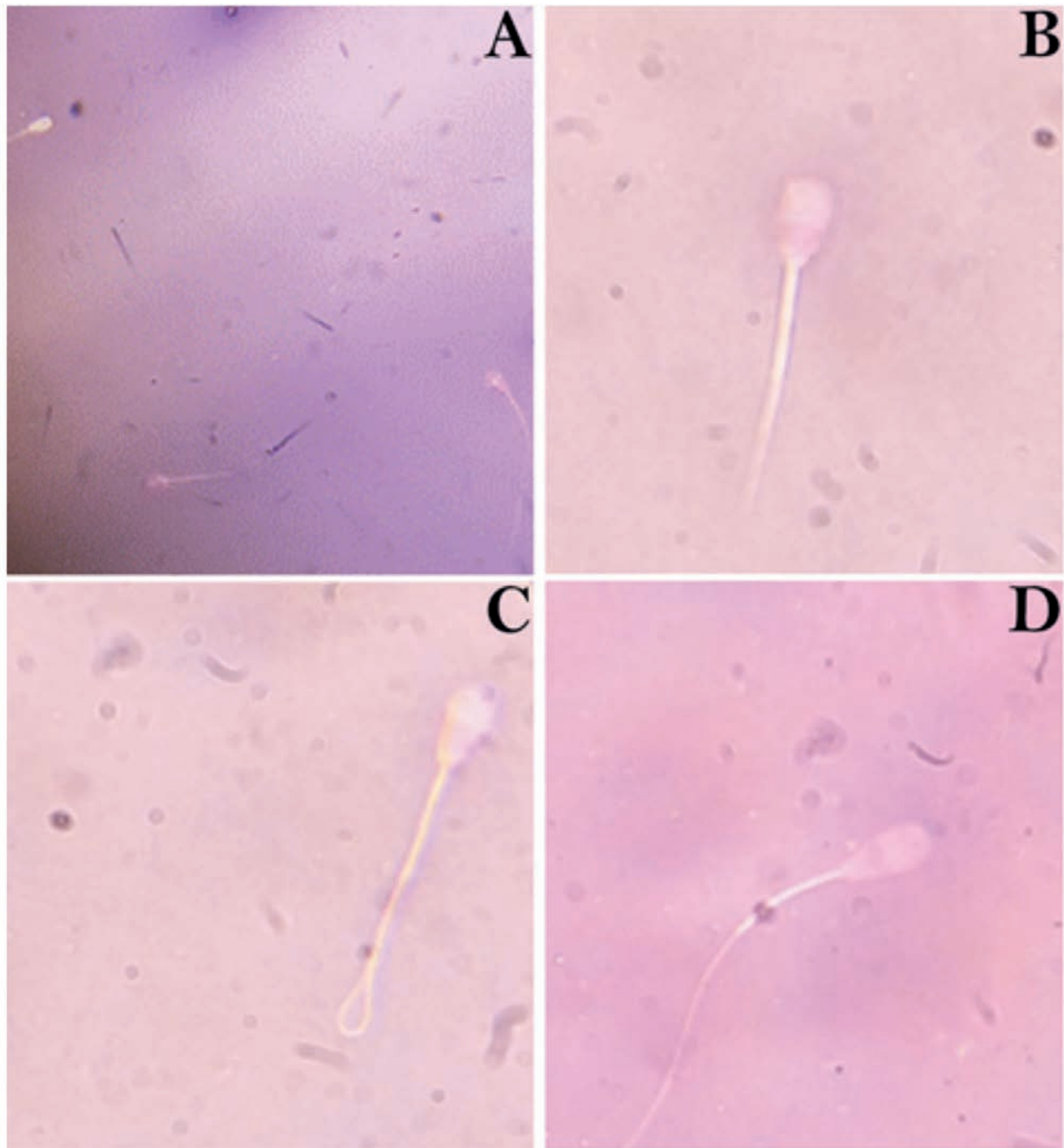


Figure 1. Semen morphology in frozen/thawed bull doses for artificial insemination. A: normal spermatozoa; B: Head defect; C: Tail defect; D: midpiece defect.

all together, the statistical correlation based on the coefficient of Pearson has demonstrated a significant positive correlation between individual spermatozoa motility and spermatozoa viability (r -value=0.61**) alongside a significant negative correlation among spermatozoa head defects and spermatozoa tail defects (r -value=0.84**).

Discussion

Artificial insemination is widely practiced as reproductive biotechnology to manage a large number of cows reducing animal handling and labor¹². The present study aims to assess the rate of success of the artificial insemination program on the most common cattle breeds raised in the arid region of Tiaret (Algeria) throughout field monitoring carried out for almost five consecutive years. In addition, the quality of the commercialized bull semen was also evaluated to examine its effects on this operation.

Several factors might determine the success rate of bovine artificial insemination programs, such as female physiology, cattle breed, suckling, size of ovulatory follicle and timing of insemination¹³. The obtained results revealed a high percentage of normal calving in red and white Holstein breeds. However, the percentage of embryonic mortality and/or calving with malformation was higher in the Montbéliarde breed.

It should be noted that embryonic mortality is very difficult to diagnose since it can generally be infectious (less than 30%) and non-infectious (more than 70%) causes¹⁴. Uterine contamination by pathogens leads to endometritis and might also induce a direct cytolytic effect on the embryo, systemic effects via septicemias, viremias or toxemias on the dam¹⁵. Viruses, bacteria, protozoa, and probably mycoplasma pass in the uterus through the hematogenous way or the vagina. However, non-specific pathogens, primarily bacteria, enter the uterus by ascending infection. Furthermore, non-infectious causes of early embryonic death are chromosomal aberrations or external factors, e.g., high ambient temperature, nutritional factors and maternal factors¹⁶.

The Montbéliarde breed belongs to the group of Pie Rouge breeds (Simmental and Fleckvieh families). In addition to its milk and meat being highly appreciated by consumers, Algerian farmers prefer to raise Montbéliarde cows because of their excellent hardiness and adaptability to local environmental conditions compared to the Holstein breeds¹⁷.

Semen quality assessment revealed that spermatozoa viability and motility were higher in Holstein breeds than in Montbéliarde. Rodríguez-Martínez¹⁸ has reported that measured spermatozoa motility in bulls is significantly correlated to fertility even for post-thawed semen.

A higher proportion of spermatozoa with the abnormal head was observed in the black and white Holstein breed, while the percentage of abnormal spermatozoa with tail defects was higher in the Montbéliarde breed. These results clearly illustrate the terrible quality of the selected semen and/or the poor handling and storage of commercial frozen semen, which dramatically reduced the chance of success of artificial insemination programs in Algeria. Hallap, Jaakma¹⁹ reported a high percentage of spermatozoa with standard head and tail morphology in Estonian Holstein bulls. In general, scrotal circumference, as the most accessible measure of a bull's ability to produce adequate spermatozoa, correlates positively with testicular volume and semen quality²⁰ and negatively with the occurrence of spermatozoa defects²¹.

It is known that morphologically abnormal spermatozoa

can diminish fertilization rates and embryonic development²². The maximum acceptable value for spermatozoa abnormalities percentage ranges between 25% and 30%³. In general, bull semen is classified as satisfactory if it contains at least 70% morphologically normal spermatozoa, with less than 20% of spermatozoa with an abnormal head¹¹. Unfortunately, the results indicated that more than two folds significantly exceed these levels for the three tested breeds.

Morphologically abnormal spermatozoa resulting from an abortive apoptotic mechanism or genetic origin are usually characterized by highly damaged DNA²³. Most abnormalities of the spermatozoa head are closely associated with reduced fertility since the spermatozoa head comprises the genetic material and key effectors of fertilization¹¹. Similar observations have been made by Johnson²⁴ and Ostermeier, Sargeant²⁵ regarding abnormal condensation of chromatin and abnormal nuclear shape from a part and bulls' fertility from another part. Thundathil, Palasz²⁶ have demonstrated that spermatozoa with abnormal heads reduce fertilization and embryonic development, consequently leading to cleavage failure. Spermatozoa with abnormal midpiece or tail are either non-motile or have abnormal motility; usually, aberrations of these parts occur as spermatogenesis defects and affect spermatozoa motility¹¹.

Besides, the process of freezing and thawing might induce irreversible damages to spermatozoa membranes, resulting in either the occurrence of spermatozoa abnormalities or cell death¹⁸. John Morris, Acton²⁷ has reported that at rapid cooling rates, the cell damage to spermatozoa is a result of an osmotic imbalance encountered during thawing, rather than intracellular ice formation. In addition, Ghirardosi, Fischman³ have attributed the high occurrence of abnormal head spermatozoa to the adverse effects of cryopreservation. Furthermore, Bacinoglu, Taş²⁸ demonstrated that morphological abnormalities present in frozen and thawed semen were significantly lower in high-fertile bulls.

According to our records, this study represents the first analysis of morphological spermatozoa abnormalities in doses of bovine semen promoted for artificial insemination currently marketed in Algeria.

Conclusions

The present study evaluated the artificial insemination success of the most common cattle breeds raised in Algeria through four years of field monitoring and assessed the quality of commercialized bull's semen used in this operation.

Overall, the present study results have demonstrated a high percentage of normal calving in red and white Holstein breeds. However, embryonic mortality and calving with malformation were higher in the Montbéliarde breed. Besides, assessment of semen quality revealed high spermatozoa viability and motility in Holstein breeds compared to Montbéliarde. In addition, the rate of spermatozoa with the abnormal head was higher in the black and white Holstein breed, while the percentage of abnormal spermatozoa with tail defects was higher in the Montbéliarde breed.

In general, it appears that the bad quality of the selected semen and/or the poor handling and storage of frozen semen constitute a determinant factor that hinders the success of artificial insemination in Algeria. Therefore, spermatozoa morphology assessments are highly recommended before processing and freezing and even in post-thawed commercial doses. Further studies regarding the modalities of distribution

and processing are also recommended, so that in the future, the use of bull semen with high percentages of spermatozoa abnormalities might be avoided.

Bibliographic references

- Mudzengi CP, Dahwa E, Kapembeza CS. Livestock Feeds and Feeding in Semi-arid Areas of Southern Africa. 2020. In: Livestock Health and Farming [Internet]. Available from: <https://www.intechopen.com/books/livestock-health-and-farming/livestock-feeds-and-feeding-in-semi-arid-areas-of-southern-africa>.
- Göncü S, Güngör C. The Innovative Techniques in Animal Husbandry. 2018. In: Animal Husbandry and Nutrition [Internet]. [4-22].
- Ghirardosi MS, Fischman ML, Jorge AE, Chan D, Cisale H. Relationship between morphological abnormalities in commercial bull frozen semen doses and conception rate. 2018;50(3):e12884.
- Ugur MR, Saber Abdelrahman A, Evans HC, Gilmore AA, Hitit M, Arifiantini RI, et al. Advances in Cryopreservation of Bull Sperm. *Front Vet Sci*. 2019;6:268-.
- Jemal H, Lemma A. Review on Major Factors Affecting the Successful Conception Rates on Biotechnological Application (AI) in Cattle. *The Journal of medical research*. 2015;15(3):29-37.
- Sharpe RM. Environmental/lifestyle effects on spermatogenesis. *Philos Trans R Soc Lond B Biol Sci*. 2010;365(1546):1697-712.
- Massart A, Lissens W, Tournaye H, Stouffs K. Genetic causes of spermatogenic failure. *Asian J Androl*. 2012;14(1):40-8.
- Attia S, Katila T, Andersson M. The Effect of Sperm Morphology and Sire Fertility on Calving Rate of Finnish Ayrshire AI Bulls. *Reproduction in domestic animals = Zuchthygiene*. 2016;51(1):54-8.
- Saacke RG. Sperm morphology: Its relevance to compensable and uncompensable traits in semen. *Theriogenology*. 2008;70(3):473-8.
- Moskovtsev SI, Librach CL. Methods of sperm vitality assessment. *Methods in molecular biology (Clifton, NJ)*. 2013;927:13-9.
- Menon AG, Barkema HW, Wilde R, Kastelic JP, Thundathil JC. Associations between sperm abnormalities, breed, age, and scrotal circumference in beef bulls. *Can J Vet Res*. 2011;75(4):241-7.
- Oliveira LZ, de Arruda RP, de Andrade AFC, Celeghini ECC, dos Santos RM, Beletti ME, et al. Assessment of field fertility and several in vitro sperm characteristics following the use of different Angus sires in a timed-AI program with suckled Nelore cows. *Livestock Science*. 2012;146(1):38-46.
- Meneghetti M, Filho OGS, Peres RFG, Lamb GC, Vasconcelos JLM. Fixed-time artificial insemination with estradiol and progesterone for *Bos indicus* cows I: Basis for development of protocols. *Theriogenology*. 2009;72(2):179-89.
- Vanroose G, de Kruif A, Van Soom A. Embryonic mortality and embryo-pathogen interactions. *Anim Reprod Sci*. 2000;60-61:131-43.
- Blackwell TE, Werdin RE, Eisenmenger MC, FitzSimmons MA. Goitrogenic effects in offspring of swine fed sulfadimethoxine and ormetoprim in late gestation. *Journal of the American Veterinary Medical Association*. 1989;194(4):519-23.
- Shah BR. Factors Leading to Early Embryonic Death Nepalese Veterinary Journal. 2019;36:118-25.
- Allouche L, Madani T, Mechmeche M, Bouchemal A. Reproductive performance of Montbeliard cows reared under subtropical environment: effects of heat stress and acclimatization duration. *Livestock Research for Rural Development*. 2018;30.
- Rodríguez-Martínez H. Laboratory semen assessment and prediction of fertility: still utopia? *Reproduction in domestic animals = Zuchthygiene*. 2003;38(4):312-8.
- Hallap T, Jaakma U, Rodriguez-Martinez H. Changes in semen quality in Estonian Holstein AI bulls at 3, 5 and 7 years of age. *Reproduction in domestic animals = Zuchthygiene*. 2006;41(3):214-8.
- Benia AR, Taïbi K, Ait-Amrane A, Belhamiti T, Hammoudi SM, Kaidi R. Study of seasonal sexual activity variations in Algerian rams: Sexual behaviour, testosterone concentration control and environmental factors. *African Journal of Biotechnology*. 2013;12(41):6042-8.
- Kastelic JP, Cook RB, Pierson RA, Coulter GH. Relationships among scrotal and testicular characteristics, sperm production, and seminal quality in 129 beef bulls. *Can J Vet Res*. 2001;65(2):111-5.
- Walters AH, Eyestone WE, Saacke RG, Pearson RE, Gwazdauskas FC. Bovine embryo development after IVF with spermatozoa having abnormal morphology. *Theriogenology*. 2005;63(7):1925-37.
- Enciso M, Cisale H, Johnston SD, Sarasa J, Fernández JL, Gosálvez J. Major morphological sperm abnormalities in the bull are related to sperm DNA damage. *Theriogenology*. 2011;76(1):23-32.
- Johnson WH. The significance to bull fertility of morphologically abnormal sperm. *The Veterinary clinics of North America Food animal practice*. 1997;13(2):255-70.
- Ostermeier GC, Sargeant GA, Yandell BS, Evenson DP, Parrish JJ. Relationship of bull fertility to sperm nuclear shape. *Journal of andrology*. 2001;22(4):595-603.
- Thundathil J, Palasz AT, Mapletoft RJ, Barth AD. An investigation of the fertilizing characteristics of pyriform-shaped bovine spermatozoa. *Anim Reprod Sci*. 1999;57(1-2):35-50.
- John Morris G, Acton E, Murray BJ, Fonseca F. Freezing injury: the special case of the sperm cell. *Cryobiology*. 2012;64(2):71-80.
- Bacinoglu S, Taş M, Cirit U, Özdaş OB, Ak K. The potential fertility estimation capacity of the hypoosmotic swelling test, the thermal stress test and a modified cervical mucus penetration test in the bovine. *Anim Reprod Sci*. 2008;104(1):38-46.

ARTICLE / INVESTIGACIÓN

Evaluation of X-ray ionizing radiation on *Plasmodium berghei* invasion of erythrocytes

Carina Nava-Lausón¹, Lilian M. Spencer^{1,4*}, Laszlo Sajo-Bohus², Jesús Dávila³, Markus P. Tellkamp⁴ DOI. 10.21931/RB/2022.07.01.19¹ Cell Biology Department, Simón Bolívar University, Valle de Sartenejas, Caracas, Venezuela.² Physics Department, Simón Bolívar University, Valle de Sartenejas, Caracas, Venezuela.³ Radiotherapy Service Gurve, La Trinidad, Caracas, Venezuela.⁴ School of Biological Sciences and Engineering, Yachay Tech University, San Miguel de Urcuquí, Ecuador.Corresponding author: lspencer@yachaytech.edu.ec

Abstract: Developing new strategies for designing effective vaccines has become a priority for parasitologists worldwide. There is high interest in designing a vaccine against malaria since it is considered one of the most prevalent infectious diseases in the tropics. We evaluated the effects of X-rays irradiation on the erythrocytic stage of *Plasmodium berghei* ANKA merozoites and schizonts using doses of ionizing radiation ranging between 10 and 300 Gy on parasitized red blood cells (PRBC) to study the attenuating effects of radiation on the merozoites. Parasitic activity diminution was observed starting at 50 Gy, and the dose for complete attenuation was established at 200 Gy, corresponding with a 100% survival rate of mice. *In vivo* invasion experiments and immunofluorescence assays (IFA) showed inhibition of merozoite invasion of the host red blood cells (RBC). Nonetheless, immunization with irradiated parasitized red blood cells (IPRBC) was ineffective in protective assays. We perform cytoadherence and inhibition of cytoadhesion assays on irradiated merozoites. The results showed that high irradiation doses caused an unspecific cellular adhesion phenomenon independent of the ICAM-1 and CD36 interaction, which was determined by Cytoadhesion assays. Our results show that, even though X-ray irradiation is an effective method to induce complete parasite attenuation, it might affect the parasite's membrane surface structures triggering unspecific adhesion.

Key words: Malaria vaccine, LINAC X-ray ionizing radiation, *Plasmodium berghei*, erythrocyte membrane modification.

Introduction

Malaria is one of the most prevalent infectious diseases in the tropics. It is caused by a protozoan parasite of the genus *Plasmodium* and is responsible for millions of cases every year. In 2017, 228 million people were diagnosed with malaria, and around 435,000 malaria deaths were reported¹.

Plasmodium species are protozoan parasites that belong to the phylum *Apicomplexa* and display a complex life cycle that involves an invertebrate vector (female *Anopheles* mosquito) and a vertebrate host. In its vertebrate host, the *Plasmodium* parasite goes through two stages: in the first stage, sporozoites invade hepatocytes and undergo asexual multiplication into merozoites; in the second, merozoites are released into the bloodstream, where they invade erythrocytes. Inside red blood cells (RBC), merozoites reproduce asexually for a second time, forming the merozoite-RBC complex, also called schizont. These merozoite-filled RBCs burst open, releasing more infectious merozoites that rapidly invade uninfected RBCs to repeat their asexual erythrocytic cycle^{2,3,4}.

X-ray irradiation is one of the most commonly used methods to achieve effective attenuation of the *Plasmodium* parasite during the design of malaria vaccines^{3,5}. Many studies have reported the use of irradiation of *Plasmodium* sporozoites to achieve parasite attenuation⁶. However, inoculation of radiation-attenuated sporozoites (RAS) provides poor protection against a second challenge with the natural parasite⁷. A study in 2013 by Seder *et al.* used an intravenous (IV) inoculation with

RAS to achieve a greater immunological response, obtaining the most promising results in fighting malaria reinfection⁸, yet some concerns remain on the IV administration route and the low rate of success obtained in the trials.

Administration of malaria vaccine RTS-S or Mosquirix (RTS, S) has resulted in a 60% decrease in the disease's clinical manifestations, but meningitis cases have also been reported in African children who have received this vaccine^{9,10}.

Researchers have also reviewed candidate proteins belonging to the merozoite stage, and they have been shown to mediate immunity against the invasion of the erythrocyte¹¹. However, there are no reports on merozoite attenuation as a strategy for malaria vaccine design. Therefore, this work aimed to determine the effects of high doses of ionizing radiation on the merozoite stage in the *Plasmodium berghei*-rodent model and assess this approach's potential to determine the effect of irradiation on the parasite's membrane. In particular, we considered the effect of radiation on cell adherence.

Materials and methods

Plasmodium berghei ANKA strain and *in vitro* culture

Ten-week-old female BALB/c mice, bred under pathogen-free conditions, were obtained from the Simón Bolívar

Citation: Nava-Lauson, C.; Spencer, L.M.; Sajo-Bohus, L., Davila, J. and Tellkamp, M. Evaluation of X-ray ionizing radiation on *Plasmodium berghei* invasion of erythrocytes. *Revis Bionatura* 2022;7(1). 19. <http://dx.doi.org/10.21931/RB/2022.07.01.19>

Received: 8 August 2021 / **Accepted:** 25 October 2021 / **Published:** 15 February 2022

Publisher's Note: Bionatura stays neutral with regard to jurisdictional claims in published maps and institutional affiliations.



Copyright: © 2022 by the authors. Submitted for possible open access publication under the terms and conditions of the Creative Commons Attribution (CC BY) license (<https://creativecommons.org/licenses/by/4.0/>).

University's Animal Housing Facility and subsequently infected with the lethal strain *Plasmodium berghei* ANKA. Blood draws were performed on Krebs' glucose solution (KGS) containing heparin (1:20 dilution of Sodium heparin 1000 U.I./ml) and passed through columns of fibrous cellulose powder (CF 11, Sigma®) to remove leukocytes^{12,13}. For schizont purification, parasitized red blood cells (PRBC) were isolated using Percoll-Krebs gradient¹². Merozoites and schizonts were evaluated by short culture *in vitro* as previously described by Spencer and co-workers¹⁴. The ethical review board approved all animal experiments of Simón Bolívar University.

Parasitological evaluation of radiated and parasitized red blood cells

We used a VARIAN Clinac Trilogy® 2100 model X-ray machine at 6MV to irradiate schizonts using doses between 10 and 300 Grays (10, 30, 50, 80, 100, 120, 200 300 Gy). Following the irradiation process, BALB/c mice were inoculated intra-peritoneally (IP) with 5x10³ Irradiated Parasitized Red Blood Cells (IPRBC). After inoculation, parasitaemia was assessed daily on blood smears obtained from the mice tails, stained with Giemsa stain and viewed under a light microscope at 1000 magnification¹⁵. All experiments were repeated in triplicate using groups of five BALB/c mice for each irradiation dose.

After two months, the mice that survived inoculation with the IPRBCs were infected with the *P. berghei* ANKA lethal strain with 5x10³ infected RBCs, and their parasitaemia was assessed daily again. All experiments were repeated three times with groups of five BALB/c mice for each irradiation dose.

Indirect immunofluorescence assay

The effect of irradiation on the merozoite membrane was evaluated using an indirect immunofluorescence assay (IFA)¹⁶. We used blood smears of mice inoculated with IPRBCs obtained 10 days post-infection and fixed with acetone. Immune sera acquired from experimental mice inoculated with different doses of IPRBC were used as sources for primary antibodies.

Afterward, we incubated the samples with FITC-labeled anti-mouse IgG (Sigma®) as a secondary antibody, and the smears were observed with an Optika® microscope XDS-3FL model at 400X magnification. Micrographic pictures were acquired using the OptikPro7® software.

Indirect enzyme-linked immunosorbent assay

Enzyme-linked immunosorbent assay (ELISA), indirect type, was performed to evaluate recognition of superficial antigens present on the schizonts in BALB/c mice infected with *P. berghei* ANKA¹⁷. Microplates (96-wells, Nunc®) were coated with 2x10⁵ PRBC per well (100 µL) and blocked by the addition of 3% bovine serum albumin (BSA) in phosphate buffer saline (PBS). Next, hyper-immune sera (HiS) obtained from mice previously inoculated with IPRBC at different doses of radiation (80, 100, 200 and 300 Gy) were added 1:100 as a source of primary antibodies and incubated at 37°C for 1 hour. Wells were washed three times with washing buffer (PBS-Tween 0.005%) and samples were incubated with 100 µL/well of horseradish peroxidase (HRP)-conjugated goat anti-mouse polyvalent immunoglobulin (IgG; H+L) (Sigma®), 1:1000 and incubated for 1 hour at 37°C.

Finally, after washing the wells with PBS-Tween 0.005%, we added 100 µL/well of azino-bis (3-ethylbenz-thiazoline-6-sulfonic acid) (ABTS, Sigma®) as substrate in 0.05 M phosphate-citrate buffer (pH 5.0) containing 0.05% w/v H₂O₂. The reaction was stopped by the addition of 50 µl 2M H₂SO₄ per well. The plates were read at 405 nm in a microplate reader (Bio-RAD i-Mark®) using the Titer-soft Software Flow to measure the absorbance. Percentages and dilutions were standardized in preliminary tests. The cut-off point was calculated using absorbance (O.D., optical density) ± 3 standard deviations from sera of 10 uninfected mice (data not shown).

Western blot assay

The immunodetection of polypeptides in hyperimmune sera obtained from mice previously inoculated with IPRBC was achieved by Western blot assays. We prepared a *P. berghei* so-

Demographic characters			
variant	groups	frequency	percent
gender	male	27	45.0
	female	33	55.0
	Total	60	100.0
residence	Urban	34	56
	Rural	26	43
	Total	60	100
employment	employ	16	26.7
	Not employ	44	73.3
	Total	60	100

Table 1. The demographic characters.

N=60	Intervention group			Control group		
	before	after	p-value	before	after	p-value
weight	85.75	84.85	<0.0001	86.30	87.08	<0.0001
Waist circumference	103.97	101.62	<0.0001	106.30	106.36	0.895
B.M.I.	31.11	30.40	<0.0001	32.27	32.55	<0.0001
FBS	176.93	141.4	<0.0001	183.36	192.40	0.035

*Significant P value < 0.05

Table 2. Comparisons characteristics of the study group before and after the intervention.

N=60	Intervention group Mean SD	Control group Mean SD	P-Value
Weight change	-0.89 ± 0.79	0.79 ±0.88	<0.0001
Waist circumference changes	-2.35 ±1.16	0.07 ±2.75	<0.0001
BMI change	-0.71 ±0.37	0.28 ±0.88	<0.0001
FBS change	-35.07 ±32.34	9.03 ±22.36	<0.0001

* Significant P value < 0.05

Table 3. Shows the difference between the intervention and the control group in the mean change of the characteristics study group.

luble antigen (PbSA) by sonication of purified schizonts suspended in lysis buffer containing 50mM Tris-HCl pH 8.0, 5mM EDTA, 5mM EGTA, 0.05% Tween 20 and 1% complete protease inhibitor cocktail (SC-29130, Santa Cruz Biotechnologies®). The polypeptides of PbSA were separated by SDS-polyacrylamide (12%) gels at 100 V for 1 hour and then electrophoretically transferred to a nitrocellulose membrane¹⁸. A pre-stained protein ladder from Invitrogen® (170-10 kDa) was used as marker.

After transfer, blots were blocked by incubation with a 3% non-fat milk powder solution in PBS, and proteins were detected with 1:100 primary antibodies dilution (hyper-immune sera from mice previously inoculated with IPRBC at 80, 200 and 300 Gy) by incubating for 1 hour. Blots were subsequently incubated with anti-mouse immunoglobulin conjugated to horseradish peroxidase (Sigma®) at 1:1000 dilution. Antibody binding was detected by incubating in a solution of 3 mg/ml 4-chloro-1-naphthol in methanol, mixed with 50 mL of 50 mM Tris-HCl pH 7.5 and 30 µL of 30% H₂O₂. The reaction was stopped by washing with H₂O¹⁹.

Cytoadhesion and cytoadhesion inhibition assays

Cytoadhesion assays were performed *in vitro* on 24-well plates on which VERO cells had been cultured to confluence. Then, 2x10⁵ IPRBC with irradiation doses of 80, 120 and 200 Gy were added to each well and cells were allowed to cytoadhere for 2 h at 37°C²⁰. RBCs were used as negative control and PRBC as a positive control. Unattached cells were removed by washing with PBS, and attached cells were fixed for 1h

with 2.5% glutaraldehyde (Sigma®). The IPRBC and PRBC were first incubated with the respective hyper-immune sera at 1:10 dilution for 1 hour²¹. Adherent IPRBC, PRBC and RBC on VERO cells were counted under a light microscope in 4 randomly selected fields at 400X magnification (OptikPro 7®). To calculate the number of IPRBC that adhere to VERO cells, counts were recorded in 5 different microscope fields, and each assay was performed in triplicate.

Statistical analysis

Each experimental value is presented as the mean of five replicates ± standard deviation. Once normality and homogeneity criteria were met, statistical analyses were carried out by ANOVA and Tukey Test using confidence level at 95%. All statistical analyses were performed using R in its version 3.2.3.

Results

Evaluation of IPRBC in experimental protective assays

The daily monitoring of parasitaemia is shown in Fig. 1, where we assessed the parasitaemia percentage (%) as a function of days post-infection. Figure 1A suggests reducing parasitaemia percentages in peripheral blood as radiation doses increase. Moreover, animals inoculated with IPRBC with 50 Gy survived four days longer than other experimental groups. As shown in fig. 1B, treatments with 80, 120 and 200 Gy accom-

plished complete control of parasitaemia on days 26, 23 and 20 post-infection, respectively. We observed a survival rate of 33.3% (5 out of 15 mice) for irradiation with 80 Gy; 66.6% (10 out of 15 mice) for doses of 120 Gy, and 100% for irradiation with 200 Gy. Statistical analyses with ANOVA and Tukey tests showed no significant differences between control, 10 Gy and 30 Gy treatments. These results showed that the minimum radiation intensity to attenuate *Plasmodium berghei* schizont was 50 Gy. However, the most efficient attenuation dose was 200 Gy, which resulted in a 100% survival rate. In the case of a dose of 300 Gy, all mice died around day 11.

The experimental group that survived IRBC infection with 200 Gy were re-infected with the *P. berghei* strain ANKA, and the parasitaemia percentage was monitored daily as shown in figure 2. It is important to note that sixty days after IPRBC inoculation, we did not observe any parasitaemia on surviving mice. Strikingly, none of the experimental animals survived the second immunological challenge with the lethal strain of *P. berghei* ANKA, and all mice died within 18 days post-infection (Fig. 2). Of note, experimental animals previously inoculated with IPRBC with 200 Gy died four days later than those of the control group. These results suggest that immunization with IPRBC did not provide protective immunity.

Immunofluorescence assays showed X-ray treatment has an inhibitory effect on the *Plasmodium berghei* merozoite invasion to the RBC. Fig. 3 shows control merozoites have invaded the host RBC after 10 days (panel A), while schizonts irradiated with 120 Gy remain outside the RBC (panel B).

Indirect ELISA

Indirect ELISA experiments were performed to determine the capacity of sera from mice inoculated with IPRBC to recognize naturally occurring PRBC as antigen. The results are presented in Fig. 4, which plots absorbance vs. different hyper-immune sera used. These results suggest that radiation might cause damages to the RBC membrane, and therefore, the surface antigens recognized by the antibodies are affected. The recognition epitopes for the irradiated RBC are different, and therefore, the antibodies do not recognize the antigen in the natural state of PRBCs without radiating. Fig. 4 shows a gradual decrease in absorbance concerning immune sera from IRBCs; when the radiation increases, sera from IRBC recognized less the antigenic surface of PRBCs.

Western blot assay

To evaluate the recognition of the antigenic surface by the IPRBC sera, we used PbSA as antigen and hyper-immune sera from experimental mice previously inoculated with IPRBC at different radiation doses. The PbSA polypeptide pattern was recognized by the hyper-immune sera of *P. berghei* infected mice. Antibodies showed 3 separate protein bands with apparent weights of 103 kDa, 45-49 kDa, and 19 kDa (Fig. 5; lane 2). However, the hyper-immune sera of mice inoculated with IPRBC recognized only the 19 kDa polypeptide (Fig. 5; lanes 3, 4 and 5). The blotting also reveals weaker bands for the 45-49 kDa protein of all hyper-immune sera from the IPRBCs with different radiation doses tested.

MSP-1 is known to be one of the most characteristic pro-

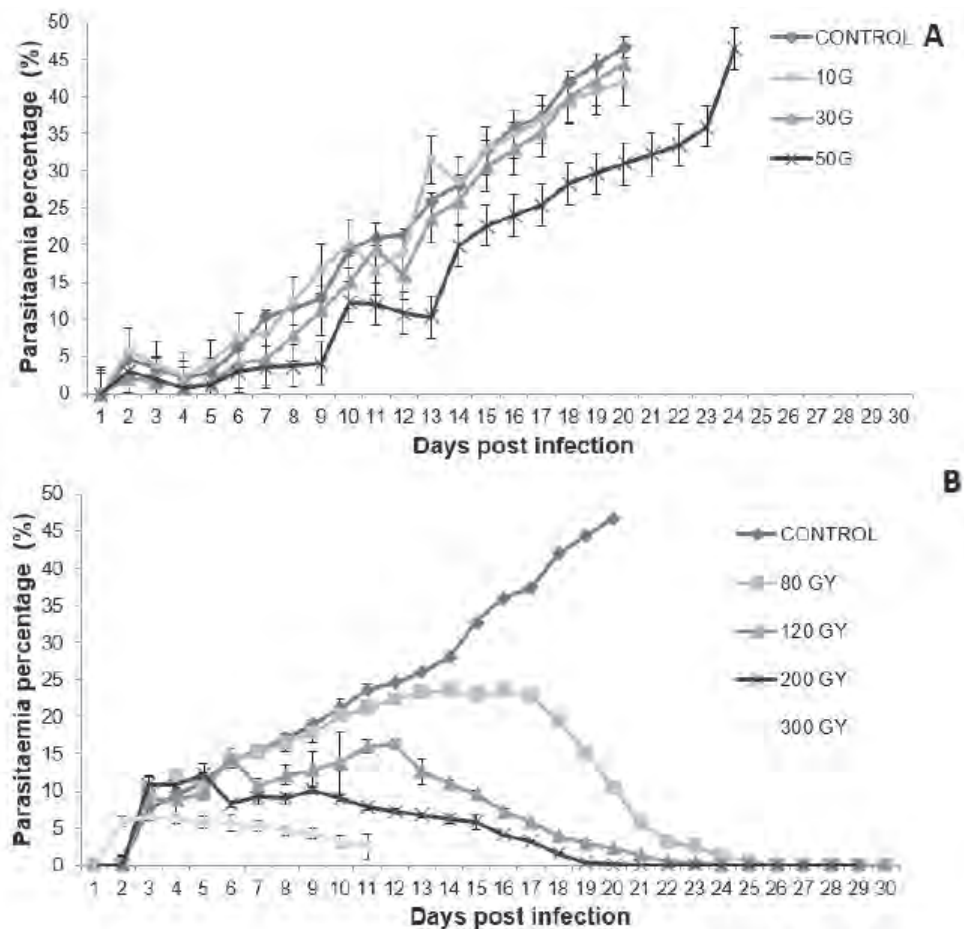


Figure 1. Percentage of parasitaemia observed in BALB/c mice infected with IPRBC, treated with different irradiation doses. We evaluated two independent experiments: A. 10, 30 and 50 Gy, and B. 80, 120, 200 and 300 Gy. The control is the non-irradiated parasites as active infection. Each experiment was assessed with 5x10³ IPRBC/mice in three groups of five animals per group.

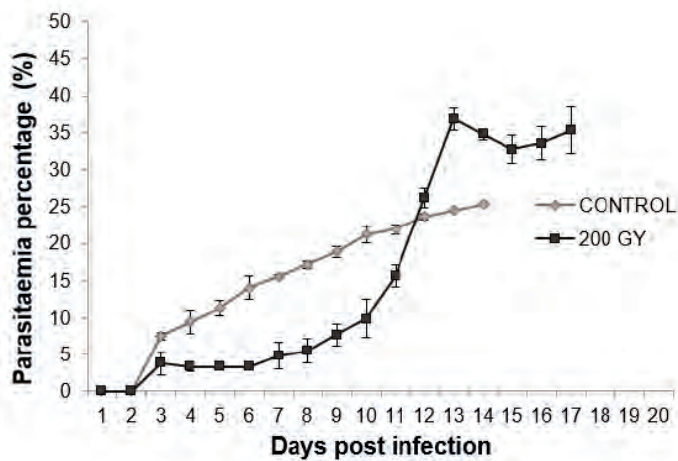


Figure 2. Parasitaemia percentage observed in BALB/c mice re-infected with lethal strain *Plasmodium berghei* ANKA. For each experiment, mice were inoculated with 5×10^3 parasites/mouse in a control (naïve mice) and 200Gy treatment, using two groups of five animals each.

A

B

C

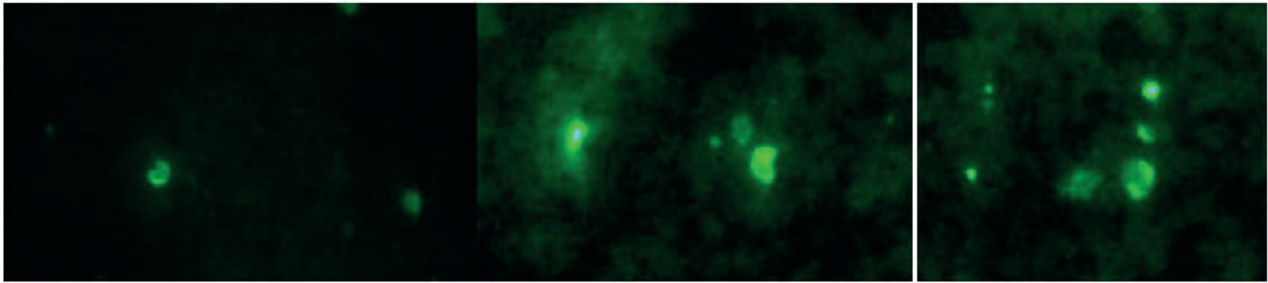


Figure 3. Immunofluorescence patterns on hyper-immune sera from infected mice; antibodies reactive to MSP-1 were applied to methanol-acetone-fixed smears of erythrocytes infected with *P. berghei* ANKA. A. positive control with PRBC; B. IPRBC with 120 Gy and C. IPRBC with 200 Gy. In panels, B and C show merozoites outside the RBC.

teins on the surface of merozoites and has been described as a potent immune inducer for protective immunity^{7,22}. The 45-49 and 19 kDa protein bands recognized by hyper-immune sera correspond to polypeptides associated with the MSP-1 protein after proteolytic cleavage²³⁻²⁶. A weaker recognition of the 45-49 kDa protein band suggests that the MSP-1 polypeptide may have undergone alterations in its structure caused by X-ray radiation (lanes 3, 4 and 5). Furthermore, the apparent weight band of 103 kDa was not recognized or very weak by the sera from the different radiation doses.

Cytoadhesion assay *in vitro*

We modified the protocol described by Pouvelle and co-workers by using epithelial cells (VERO) instead of endothelial cells to perform the cytoadhesion assays²⁰ (See figure 6). Both cell lines (endothelial and Vero) are reported to express the Intracellular Adhesion Molecule 1 (ICAM-1) and CD54; which mediates the adhesion between PRBC and cellular receptors^{27,28}. Additionally, epithelial cells express CD36, which acts as a secondary binding molecule for PRBC in natural malarial infections^{27,28}.

Figure 6 showed a decrease in cytoadhesion for radiations of 80 (98.8 IPRBC / field) and 120 Gy (72.4 IPRBC / field) concerning positive control. Figure 6. E shows that the adhesion levels for schizonts irradiated with 200 Gy (195 IPRBC/ field) are 1.4 times greater than the positive control of parasitized red blood cells (140 GRP / field).

Discussion

We evaluated the effects of high X-rays doses (80, 100,

120, 150, 180, 200 and 300 Gy) on experimental groups of BALB/c mice infected with 5×10^5 IPRBC¹⁴. Our results showed a typical parasitaemia curve in positive controls as shown in Fig. 1. The treatment with 120 Gy accomplished the complete control of parasitaemia on the 13th day post-infection, resulting in survival rates over 50% (8/15). Another relevant observation was that mice inoculated with IPRBC at 300 Gy died around day 11 post-infection with low levels of parasitaemia (between 1.5 and 4% parasitaemia). This suggests that death is not directly related to malaria infection but to the effect of radiation on IPRBCs. Based on the results obtained from cytoadherence assays (Fig. 6). We suggest this decrease in cytoadhesion is probably due to damage caused by radiation on the cell membranes (for both parasites and RBC). Our hypothesis is supported by the studies of Claessens and Rowe, in which the inhibition of ICAM-1 in *Plasmodium falciparum* sporozoites causes a decrease in the number of parasites attached to HBEC cells²⁹. The observation of IPRBC confirmed this remarkable result aggregates on smears from experimental animals monitored for parasitaemia (data not shown). Consequently, we suggest that death, even at low levels of parasitaemia in peripheral blood, is caused by bloodstream blockage on the microvasculature, indicating a dose-dependent parasite attenuation by ionizing radiation.

IFA show a decrease in merozoite invasion capacity of RBC in a radiation-dependent manner that correlates with the low levels of parasitaemia (less than 15%) circulating in peripheral blood on the 10th day post-inoculation (Fig. 1.B, 120 and 200Gy). We suggest X-rays might alter the conformation of surface antigen as MSP-1 antigen on the parasite's membrane^{5,23,24}, which is no longer recognized by antibodies from IPRBC hyperimmune sera as proven by western blot assays

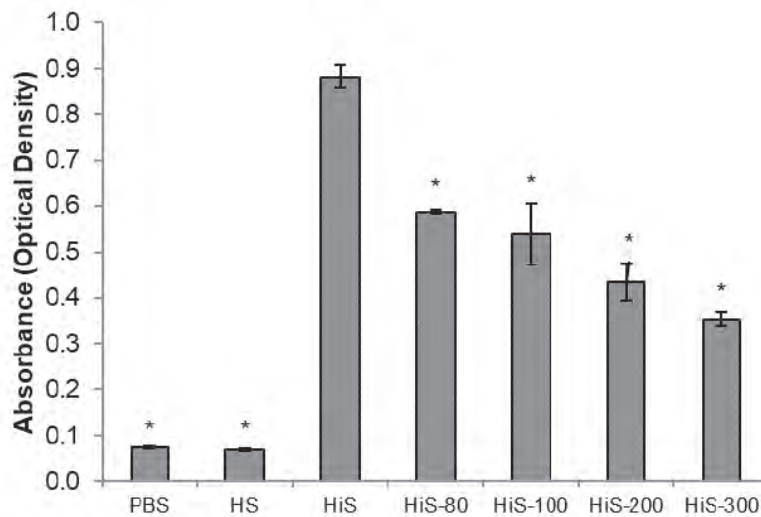


Figure 4. Indirect ELISA tests with PRBC as antigen. PBS was used as buffer control, healthy sera (HS) as negative control and hyper-immune sera (HiS) as positive control. Hyper-immune sera extracted from mice previously inoculated with IPRBC treated with different doses of radiation: 80 Gy (HiS-80), 200 Gy (HiS-200) and 300 Gy (HiS-300) were evaluated for primary antibodies. Bars represent the standard error for each treatment. The cut-off value is located at an absorbance of 0.08 D.O. The asterisks indicate significant differences with respect to positive control by ANOVA and Tukey statistical analyses ($p < 0.005$).

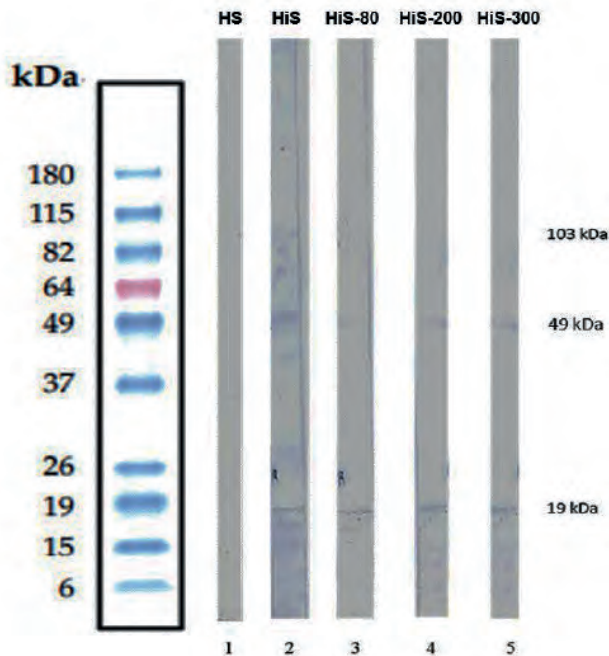


Figure 5. Western blot using PbSA as antigen and hyper-immune sera extracted from mice previously inoculated with IPRBC at different doses: 80 Gy (HiS-80), 200 Gy (HiS-200) and 300 Gy (HiS-300). Healthy sera (HS) were used as negative control and hyper-immune sera (HiS) as positive control.

(figure 5). Therefore, these results are evidence for the effect of high doses of X-rays on *Plasmodium berghei* merozoites invasion and suggest that death in experimental animals is not a consequence of malaria infection. An inverse correlation between radiation intensity and absorbance obtained by indirect ELISA suggests X-rays may also cause damages on the schizont's membranes and modify the MSP-1 antigen^{5,7,24}, thus diminishing the capability of hyperimmune sera to recognize natural PRBC membranes. The absorbance obtained from HiS as a positive control was 0.88 D.O. This value decreases gradually when radiation intensity rises until it reaches a value of 2.5 times lower at HiS-300 (0.35 D.O.) (Fig.4). In consequence, as the radiation applied to PRBC increases, the surface proteins suffer alterations, diminishing their capacity to activate the humoral response³⁰. This could explain the changes observed during the secondary challenge (Fig. 1) and could be the reason for the failure to maintain protection against *P. berghei* ANKA infection.

The results of the cytoadhesion tests are presented in Fig. 6. The black arrows show the number of adhered IPRBCs per field decreases with the treatments of 80 Gy (IPRBC-80) and 120 Gy (IPRBC-120) compared to the positive control

(PRBC). Cytoadherence of PRBCs to host cells depends on different proteins that play a relevant role in malaria pathogenicity. Some of those proteins are expressed by the parasite early, such as trophozoite³¹. However, the 200 Gy radiation (IPRBC-200) showed an increase of adhered cells 2 times higher than IPRBC-120, suggesting the adhesion is unspecific and is not mediated by receptors.

Conclusions

Attenuation of *Plasmodium berghei* merozoites was observed with X-ray doses starting at 50 Gy, and the effective dose of attenuation was 200 Gy for inoculation with 5×10^3 IPRBC/mice resulting in 100% survival. Moreover, the results of IFAs showed that this effect was caused by an inhibition of merozoite invasion to the host RBC. Nonetheless, this irradiation dose was not effective in protective assays because of the alterations suffered by the membrane structure, as showed in western blot and cytoadhesion tests.

In addition, the cytoadherence results demonstrated that high doses of irradiation cause an unspecific cellular adhesion

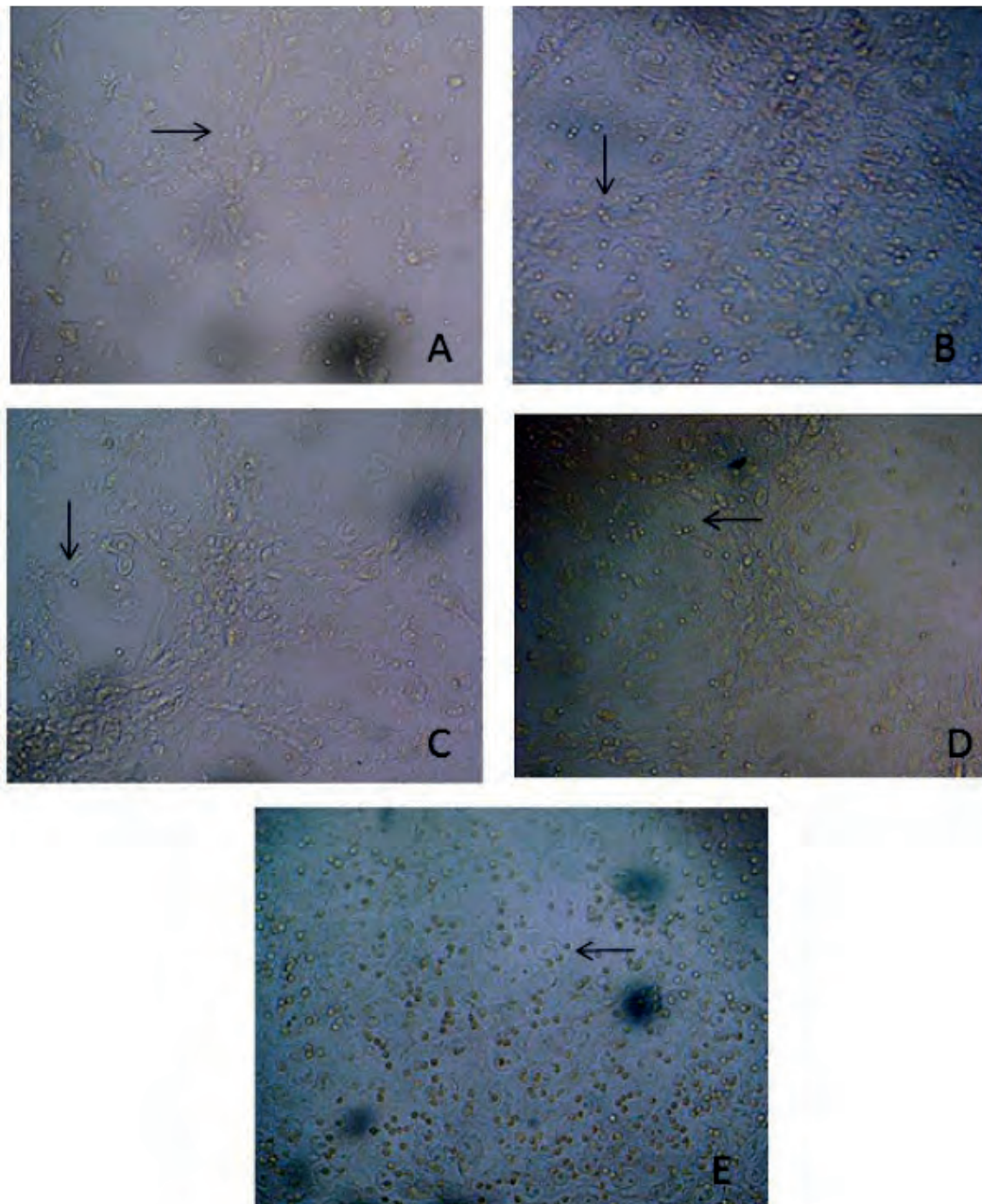


Figure 6. *In vitro* microagglutination test for IPRBC on VERO cells observed under a light microscope at a magnification of 400X. Panel A corresponds to the negative control, with healthy red blood cells. Panel B is a positive control, PRBCs (parasitized red blood cells) without radiation exposure. Panel C corresponds to IPRBC receiving radiation of 80 Gy. Panel D corresponds to IPRBCs subjected to radiation of 120 Gy, and panel E corresponds to IPRBCs irradiated with a dose of 200 Gy. The arrows point to the parasitized and irradiated RBCs on VERO cells.

independent of ICAM-1 and CD36. This unspecific adhesive effect increased in a radiation dependent manner as a possible result of alterations on the integrity of erythrocytic membrane structures. Therefore, this study suggests that radiation of merozoites and schizonts are not an effective strategy for the design of a malaria vaccine.

Author Contributions

Conceptualization, LMS. CNL and LMS performed all experiments. Irradiation protocols performed by JD. Writing—review and editing, LMS; CNL; LS and MPT. Funding acquisition, LS and LMS. All authors have read and agreed to the published version of the manuscript.

Funding

This study was financed by a grant from FONACIT (Fondo Nacional de Ciencia, Innovación y Tecnología), No. 29407-2269, Venezuela.

Institutional Review Board Statement

The experiments described in this study were carried out following the laboratory's standards and the Bioethics Committee of the Simón Bolívar University.

Acknowledgments

We would like to thank Dr. Juan C. Piña-Crespo, Beatriz Pernia and Sophya Alchali for helpful suggestions and critical reading of the manuscript.

Conflicts of Interest

The authors declare no conflict of interest.

Bibliographic references

1. WHO (World Health Organization) [Internet]. World malaria report 2018. [July 2021]. Available from: <https://www.who.int/malaria/media/world-malaria-report-2018/en/>.
2. Cherfas J. Malaria vaccines: the failed promise. *Science*. 1990;247(4941):402-403.
3. Carvalho LJM, Daniel-Ribeiro CT, Goto H. Malaria Vaccine: Candidate Antigens, Mechanisms, Constraints and Prospects. *Scand J Immunol*. 2002;56(4):327-343.
4. Thera MA, Plowe CV. Vaccines for Malaria: How Close Are We? *Annu Rev Med*. 2012;63(1):345-357.
5. Chattopadhyay R, Conteh S, Li M, James ER, Epstein JE, Hoffman SL. The Effects of radiation on the safety and protective efficacy of an attenuated *Plasmodium yoelii* sporozoite malaria vaccine. *Vaccine*. 2009;27(27):3675-3680.
6. Duffy PE, Sahu T, Akue A, Milman N, Anderson C. Pre-erythrocytic malaria vaccines: identifying the targets. *Expert Rev Vaccines*. 2012;11(10):1261-1280.
7. Purcell LA, Yanow SK, Lee M, Spithill TW, Rodriguez A. Chemical Attenuation of *Plasmodium berghei* sporozoites induces sterile immunity in mice. *Infect Immun*. 2008;76(3):1193-1199.
8. Seder RA, Chang LJ, Enama ME, Zephir KL, Sarwar UN, Gordon IJ, et al. Protection against malaria by intravenous immunization with a nonreplicating sporozoite vaccine. *Science*. 2013;341(6152):1359-1365.
9. Schwartz L, Brown GV, Genton B, Moorthy VS. A review of malaria vaccine clinical projects based on the WHO rainbow table. *Malar J*. 2012;11(1):11.
10. Sackey AH. Musings on malaria morbidity and mortality after the new Mosquirix[®] vaccine. *Ghana Med J*. 2019;53(2):87-188.
11. Beeson JG, Drew DR, Boyle MJ, Feng G, Fowkes FJ, Richards JS. Merozoite surface proteins in red blood cell invasion, immunity and vaccines against malaria. *FEMS Microbiol Rev*. 2016;40(3):343-72.
12. Richards WH, Williams SG. The removal of leucocytes from malaria infected blood. *Ann trop med parasitol*. 1973;67(2):249-250.
13. Sayles PC, Wassom DL. Are antibodies important in mice infected with *Plasmodium yoelii*? *Parasitol Today*. 1992;8(11):368-370.
14. Spencer LM, Quintana D, Hidalgo L. An assay to evaluate the inhibition of invasion in vitro of *P. yoelii* strain with different monoclonal antibodies raised against MSP-119. *Biomédica* [Internet]. 2008 [July 2020];19(1):45-51. Available from: <https://dialnet.unirioja.es/servlet/articulo?codigo=6058430>
15. Spencer LM, Ogun SA, Fleck SL, Ling IT, Scott-Finnigan TJ, Blackman MJ, et al. Passive immunization with antibodies against three distinct epitopes on *Plasmodium yoelii* merozoite surface protein-1 suppresses parasitemia. *Infect Immun*. 1998;66(8):3925-3930.
16. Voller A, O'Neill P. Immunofluorescence method suitable for large-scale application to malaria. *Bull World Health Organ*. 1971;45(4):524-529.
17. Bidwell DE, Bartlett A, Voller A. Enzyme Immunoassays for Viral Diseases. *J Infect Dis*. October 1977;136(2): S274-S278.
18. Laemmli UK. Cleavage of structural proteins during the assembly of the head of bacteriophage T4. *Nature*. 1970;227(5259):680-685.
19. Blackman MJ, Ling IT, Nicholls SC, Holder AA. Proteolytic processing of the *Plasmodium falciparum* merozoite surface protein-1 produces a membrane-bound fragment containing two epidermal growth factor-like domains. *Mol Biochem Parasitol*. 1991;49(1):29-33.
20. Pouvelle B, Fusaï T, Lépolard C, Gysin J. Biological and biochemical characteristics of cytoadhesion of *Plasmodium falciparum* infected erythrocytes to chondroitin-4-sulfate". *Infect Immun*. 1998;66(10):4950-4956.
21. Hasler T, Handunnetti SM, Aguiar JC, Schravendijk MR, Greenwood BM, et al. In vitro resetting, cytoadherence and microagglutination properties of *Plasmodium falciparum* infected erythrocytes from Gambian and Tanzanian patients. *Blood*. 1990;76(9):1845-1852.
22. IAEA (International Atomic Energy Agency). Radiation Biology: a handbook for teachers and students. Vol 42 [Internet]. Vienna, Austria: IAEA Publishing Section; 2010 [cited 2021 July 29]. Available from: <https://www.iaea.org/publications/8219/radiation-biology-a-handbook-for-teachers-and-students>
23. Holder AA, Freeman RR. Protective Antigens of Rodent and Human Bloodstage Malaria. *Philos. Trans R Soc Lond B Biol Sci*. 1984;307(1131):171-177.
24. McBride JS, Heidrich HG. Fragments of the polymorphic Mr 185 000 glycoprotein from the surface of isolated *Plasmodium falciparum* merozoites form an antigenic complex. *Mol Biochem Parasitol*. 1987;23(1):71-84.
25. Holder AA, Blackman MJ, Burghaus PA, Chappel JA, Ling IT, McCallum-Deighton N, et al. A malaria merozoite surface protein (MSP1)-structure, processing and function. *Mem Inst Oswaldo Cruz*. 1992;87(3):37-42.
26. Chappel JA, Egan AF, Riley EM, Druilhe P, Holder AA. Naturally acquired human antibodies which recognize the first epidermal growth factor-like module in the *Plasmodium falciparum* merozoite surface protein 1 do not inhibit parasite growth in vitro. *Infect Immun*. 1994;62(10): 4488-4494.
27. Rothlein R, Dustin ML, Marlin SD, Springer TA. A human intercellular adhesion molecule (ICAM-1) distinct from LFA-1. *J Immunol*. 1986;137(4):1270-1274.
28. Ho M, White NJ. Molecular mechanisms of cytoadherence in malaria. *Am J Physiol Cell Physiol*. 1999;276(6):C1231-C1242.
29. Claessens A, Rowe JA. Selection of *Plasmodium falciparum* Parasites for Cytoadhesion to Human Brain Endothelial Cells. *J Vis*. 2012; 59:7-1.
30. Brown A, Turner L, Christoffersen S, Andrews KA, Szestak T, Zhao Y, Larsen S, Craig AG, Higgins MK. Molecular architecture of a complex between an adhesion protein from the malaria parasite and intracellular adhesion molecule 1. *J Biol Chem*. 2013; 288(8):5992-6003.
31. Lee WC, Russell B, Rénia L. Sticking for a cause: the falciparum malaria parasites cytoadherence paradigm. *Front Immunol*. 2019; 10:1444.

ARTICLE / INVESTIGACIÓN

Identification of Some Breast Cancer Related Genes by RAPD Technique in Maysan Province, Iraq

Zainab Zamil Gataa Allami*, Maytham Abdulkadhim Dragh

DOI. 10.21931/RB/2022.07.01.20

³Department of Biology, College of Science, University of Misan, Maysan, Iraq.
Corresponding author: zainabzamil @ uomisan.edu.iq

Abstract: Breast cancer is a heterogeneous disease regarding its morphology, invasive behavior, metastatic capacity, hormone receptor expression and clinical outcome. Many risk factors for breast cancer, including genetic factors, account for 25-30% of the incidence. About 15-30% of breast cancer is heritable due to known familiar highly penetrates genes and the others are sporadic; It is worthy to state that this study was the first in the world to include amplified genes as a PCR template to determine the relationship between their polymorphism and breast cancer incidence using, RAPD of amplified genes. The study was designed first to evaluate the association of ABCG2 gene polymorphism beside miRNA-152 and ER- α using the RAPD technique with breast cancer incidence in Maysan province women, and second to use those genes as indicators for breast cancer prediction and diagnosis. The study included 100 patients with breast cancer and 30 control healthy women, and then all samples were amplified by conventional PCR by specific F and R primer for (ABCG2, ER- α , miRNA-152) genes and then the best (20 PCR product) from which was chosen as the template for PCR RAPD PCR technique. The results revealed there are significant differences ($P < 0.05$) in the unique band of ABCG2 at marker OPAA 11, OPU 15, OPAA 17, significant differences ($P < 0.05$) in the total band of ER- α at marker OPAA11, significant differences in the polymorphic band of ER- α at marker OPU 15, significant differences in the unique band of ER- α at marker OPAA11, OPU 15, and significant differences ($P < 0.05$) in the bands that had been size (50-60) bp, (140 - 150) bp, (170-180) bp of miRNA-152 at marker OPAA 17, OPD 18 between breast cancer patients and control. Our study proved the relationship between genetic polymorphism of breast cancer-related genes (ABCG2, ER- α , miRNA-152) and a higher incidence of cancer; The current study recommends employing these results for future prediction and diagnosis of breast cancers.

Key words: Polymorphism, Iraqi, Breast cancer, Drug resistance gene, Estrogen receptor α gene, regulatory gene.

Introduction

Breast cancer (BC) is the most common type of cancer among women worldwide. It accounts for 15% of cancer deaths among women and is the leading cause of cancer death in females worldwide¹. In Iraq, it is the most typical type of female malignancy, accounting for approximately one-third of the registered female cancers according to the Iraqi cancer registry in 2004^{2,3}. About 5-10% of breast cancer is inherited⁴; while 90-95% is sporadic and revealed randomly and is not predetermined genetically^{5,6}.

The alteration in the expression of ATG5, caspase 3, and Bax genes can cause induction of both apoptosis and necrosis in human cancer cells⁷. The susceptibility genes are considered a critical risk factor for hereditary and sporadic breast cancer. However; The genesis of breast cancer is usually cumulative mutations of different genes⁸. Several genes linked to breast cancer have been found⁹. Such as the ABCG2 gene that is located on the human chromosome at the locus 4q 22.1¹⁰⁻¹². ABCG2 belongs to a sizeable ATP-binding cassette (ABC) transporters affecting P - glycoprotein (P-gp), overexpression of ABC transporters, increased anti-apoptotic machinery, DNA damage repair machinery, and enhanced drug inactivation mechanism are concerned in the intrinsic or acquired resistance

to chemotherapy^{13,14}. ER- α gene is located on chromosome 6q25.1, ER α receptor superfamily has the primary function in the development and progression of cancer, it also stimulates mammary epithelial tissue proliferation and differentiation through combining with estrogen¹⁵⁻¹⁷. However, the allele variant is associated with BC risk in different populations¹⁸. miRNA -152 gene is situated on chromosome 17q21.32^{19,20}, which has the primary function in regulating biological processes such as differentiation, proliferation, and apoptosis^{21,22}.

RAPD technique (Random Amplified polymorphic DNA) can be defined as a DNA fingerprinting technique based on Polymerase Chain Reaction (PCR) amplification of random fragments of genomic DNA with single short primers (markers) of arbitrary nucleotide sequences^{23,24}. RAPD is a semi-quantitative method more used to detect genetic alterations or polymorphisms in genetic mapping, taxonomy and phylogenetic studies and later in genotoxicity and carcinogenesis studies²⁵. Applying RAPD analysis is used in the studies in genetic instability or genetic alterations of breast cancer²⁶.

In this study, we performed a new procedure with some modifications to the traditional RAPD technique when we used the amplified gene as a template in RAPD. This procedure re-

Citation: Gataa Allami Z, Abdulkadhim Dragh M. Identification of Some Breast Cancer Related Genes by RAPD Technique in Maysan Province, Iraq. *Revis Bionatura* 2022;7(1). 20. <http://dx.doi.org/10.21931/RB/2022.07.01.20>

Received: 15 August 2021 / **Accepted:** 20 October 2021 / **Published:** 15 February 2022

Publisher's Note: Bionatura stays neutral with regard to jurisdictional claims in published maps and institutional affiliations.

Copyright: © 2022 by the authors. Submitted for possible open access publication under the terms and conditions of the Creative Commons Attribution (CC BY) license (<https://creativecommons.org/licenses/by/4.0/>).



sulted in more accuracy and more yielded specific data. We named it PCR-RAPD-PCR (PRP). This study aims to evaluate the genetic polymorphism of the BC gene in breast cancer women patients in Maysan province, south of Iraq.

Materials and methods

Study sites

The study was undertaken in the genetic engineering laboratory/ Department of Biology / College of Science/Misan University. A total of (100) blood samples were collected from the breast cancer women patients and (30) healthy in Maysan Health Directorate/ AL-Sader Teaching Hospital /AL-Shifa Tumor Treatment Center in/ AL-Amarah city (sub-districts of Maysan province/south of Iraq).

Samples collection and identification

100 blood samples (2-3 mL) were collected from each breast cancer female patient (in case patient woman in good healthy) or blood samples (1mL) were collected from each breast cancer patient woman (in case the patient woman in critical condition). Blood samples were collected from each woman patient through the median cubital vein or carpal veins (according to a health condition) into EDTA-containing tubes and were stored at -20°C till DNA extraction.

Genomic DNA isolation

All samples were collected from the breast cancer women patients at a different time for three months (September to November). All samples were kept under the same condition. DNA was extracted from whole blood by using the gSYNCTM DNA Extraction Kit Functional Test Data (Geneaid, Taiwan).

Column purification

FGenomic DNA was isolated from the blood sample. The amount of isolated DNA was varied from 523.92 to 887.12 ng/ μ L DNA and an absorbance ratio of A260/280 was obtained in the range of 1.71–1.98 according to (27).

Polymerase chain reaction for isolated PCR product (specific BC genes)

Isolated DNA from all 100 women BC Patient and 30 normal; genomic DNA samples were prepared by pooling the same amount of genomic DNA from each individual. The DNA fragments of the PCR product of BC genes were amplified through the polymerase chain reaction technique. The following components: 2.5 μ L primer F, 2.5 μ L primer R, 2.5 μ L Nuclease free water, 12.5 μ L GO Taq [®]G2 Green master mix, and 5 μ L DNA template were added for each 25 reaction mixture. The primer sequences are shown in Table 1.

The PCR reaction consisted of 35 cycles following three

essential steps: initial denaturation (5 min at 94°C), DNA denaturation (1 min at 94°C), primer annealing ABCG2 (45 sec at gradient 53.5 -58.5°C), primer annealing ER- α (45 sec at gradient 52-58°C), primer annealing miRNA -152 (15 sec at 65°C), and primer extension (1 min at 72°C). There was a Final extension cycle for 7 min at 72°C. The size of the amplified PCR product was subjected to electrophoresis in 1.2 % agarose gel, 1X TBE buffer with ethidium bromide 2%, at 80 V for 60 min. The bands were visualized under ultraviolet trans-illumination and photographed in Gel-Doc equipment. The PCR product with a clear band was later used as a template in the PCR - RAPD - PCR Technique.

Purify PCR Product by gel extraction

PCR products were obtained after a conventional PCR run; PCR products were extracted from an agarose gel after gel electrophoresis for breast cancer-related genes using the E.Z.N.A. [®] Gel Extraction kit protocol (OMEGA BIO-TEK, USA).

Column Purification

PCR product (specific gene) was isolated from the DNA gel extraction, the amount of isolated DNA PCR product (specific gene) was varied from 523.92-887.12 ng/ μ L and absorbance ratio of A260/280 was obtained in the range of 1.71-1.98.

PCR- RAPD- PCR Technique

The isolated PCR product from all women BC Patient and normal DNA; the same best 40 PCR product (20 patient and 20 control) of ABCG2, ER- α , miRNA-152 genes were chosen for PCR RAPD PCR. The RAPD primer sequencing in the PCR-RAPD-PCR is shown in (Table 2).

The reaction mixture (20 μ L) consisted of template PCR product 2.5 μ L, 2.5 μ L (OPAA11, OPU15, OPAA17, OPD18) RAPD primer, 7.5 μ L Nuclease free water, and 7.5 μ L GO Taq [®]G2 Green master mix. The mixture was incubated in the TECHNE prime thermal cycler (with heating lid) programmed for (35-40) cycles, each one consisting of as following: a denaturation step (1 min at 94°C), one annealing step (30 sec at gradient 36-39°C) and an extension step (1 min at 72°C). After the cycling, a final extension for 1.30 min at 72°C was followed by slow cooling to 10°C. Four RAPD primers: (OPAA11, OPU15, OPAA17, OPD18) were used in the amplifications. The primers were obtained from the AUGCT DNA SYN Biotechnology /China company.

Electrophoretic analysis

The reaction products were separated by electrophoresis on an agarose gel (2 %) containing ethidium bromide (2%) were prepared in 1X TBE buffer. The DNA ladder size marker used in this study contained many discrete bands (in base pair) 1500, 1000, 900, 800, 700, 600, 500, 400, 300, 200,100,75,50 and 25 bp from the nearest distance to the well to the far one from the well respected. This ladder was used as a molecular size indicator in the experiments of this study. The DNA fragments

primer	Sequence	GC%	Length (Base)		References
ABCG2	5-AAAT GTTCATAG CCAGTTTCTTGGA-3 3-ACAGTAATGTCGAAGTTTTTATCGCA-5	35.29 %	F:25	R:26	28
miRNA-152	5-TCTGTCATGCACTGACTGCTC-3 3GGGCATGCTTCTGGAGTCTA-5	53.65 %	F:21	R:20	29
ER- α	5-ATG CGC TGC GTC GCC TCTAA-3 3-CTG CAG GAA AGG CGA CAG CT-5	60 %	F:20	R:20	30

Table 1. Sequence of ABCG2, miRNA-152, ER- primers, GC% and length.

Primers	Primers Sequences	GC%	Length (Base)
OPAA11	5-ACCCGACCTG-3	80 %	10 Base
OPU15	5-ACGGGCCAGT -3	70 %	10 Base
OPAA17	5-GAGCCCGACT -3	70%	10 Base
OPD18	5-GAGAGCCAAC- 3	60%	10 Base

Table 2. Sequence of RAPD primers, GC% and length.

obtained were visualized under ultraviolet light. The molecular sizes of DNA bands were estimated according to the standard curve representing the relationship between molecular band size of the ladder measured by base pairs and distance of migration bands³¹.

Statistical analysis

The relationship between the polymorphic, monomorphic, unique band and RAPD primer of the breast cancer patient and control was assessed using the X^2 test; $P < 0.05$ was considered statistically significant.

Results

PCR-RAPD-PCR

We determined three genes related to breast cancer (BC), the ABCG2 associated with drug resistance. The ER- α and miRNA -152 genes are associated with receptor estrogen response and regulatory gene. We performed a conventional PCR assay and yielded a single band at approximately 300 bp, 500 bp, 180 bp, respectively. The genetic polymorphism of included genes was done by four RAPD primers (OPAA11, OPU15, OPAA17, and OPD18). We were using amplified BC genes as the template in the PCR-RAPD-PCR technique (PRP). The results of PRP showed that RAPD primers were able to generate polymorphic, monomorphic, unique bands with different ratios between BC patients and control, as shown in figure (1).

Detection primer efficiency and discriminatory power among BC related genes

Our finding showed a difference in the primer discriminatory power among BC related genes in the patient and control; whereas the high discriminatory power in the patient was 40% at OPU15 of ABCG2, the highest primer discriminatory power in control was 42.85 at OPAA11 of ABCG2; the highest primer efficiency in the patient was 0.028 at OPU 15 of ABCG2; while the highest primer efficiency in the control was 0.078 at OPU15 of ER- α , as shown in figure (2).

Detection genetic polymorphism of breast cancer-related genes

The overall number of bands in the BC patients were (214, 149, 298) band for ABCG2, mi-RNA, ER- α genes respectively, with the total number of bands (661) while the total bands of the control were (162, 93, 128); with Overall total number of (383) band, as shown in figure (2,3).

The total polymorphic bands in the BC patient of ABCG2, ER- α , mi-RNA 152 genes were (15, 18, 8) respectively, while in control were (14, 34, 0) bands; The total monomorphic bands in ABCG2, ER- α , mi-RNA 152 genes of the patients were (12, 16, 8) respectively; while in control were (16, 0, 12) bands; The total unique bands in ABCG2, ER- α , mi-RNA 152 genes were (10, 5, 2) bands in a patient; while in control were (6, 7, 0)

bands, as shown in figure (3) and table (3, 4, 5, 6, 7, 8, 9, 10, 11).

The results showed similarity between patients and control regarding total band percentages, the differences between the two groups were not significant. These results compared between 214 bands in patients and 164 bands in control. The results showed no significant differences in polymorphic bands between patients and control regarding the gene ABCG2. Results were compared between 15 bands in patients and 14 bands in control, as shown in table 4.

While significant differences ($P < 0.05$) appeared between patients and control in unique bands with the primer OPAA11, OPAA17 and OPU15. The results were compared between 10 bands of patients and 6 bands of control, as shown in table 5.

As for monomorphic bands, no significant differences were found between the two groups of patients and control of different markers. These results were compared between 12 bands in patients and 16 bands in control, as shown in table 6.

The total number of bands were similar between patients and control for the gene ER α , except for the primer OPAA11, which revealed a significant difference ($P < 0.05$) between the two groups, for this, we can consider this primer differentiating between patients and control from the genetic view. These results compared between 298 in patients and 128 in control, as shown in table 7.

As for the polymorphic bands, the table below showed a significant difference ($P < 0.05$) between patients and control only for the primer OPU15, while the rest primers were not. The results were compared between 18 bands in patients and 34 bands in control, as shown in table 8.

When examining the unique bands, a significant difference ($P < 0.05$) between patients and control for the primers OPAA11 and OPU15. These results were compared between 5 bands in patients and 7 bands in control, as shown in table 9.

All patients showed monomorphic bands, while no monomorphic bands were found in the control group for all primers. When using the Chi-square test to compare patients and control, we noticed the following: The table below includes Chi-square values, data referred to (*) significantly different on the level of 5% while data referred to (**) significantly different on the level of 1%. Thus the patient group was significantly different from the control group in total bands for OPAA17 and OPD18, while bands were similar in both OPAA11 and OPU15, as shown in table 10.

There were no significant differences in total bands between the two groups for all the primers. The percentage of total bands was calculated from the total bands of each group (it was 149 in patients and 93 in control). The main difference between the two groups is that there were polymorphic bands in patients and not found in the control group, as shown in table 11.

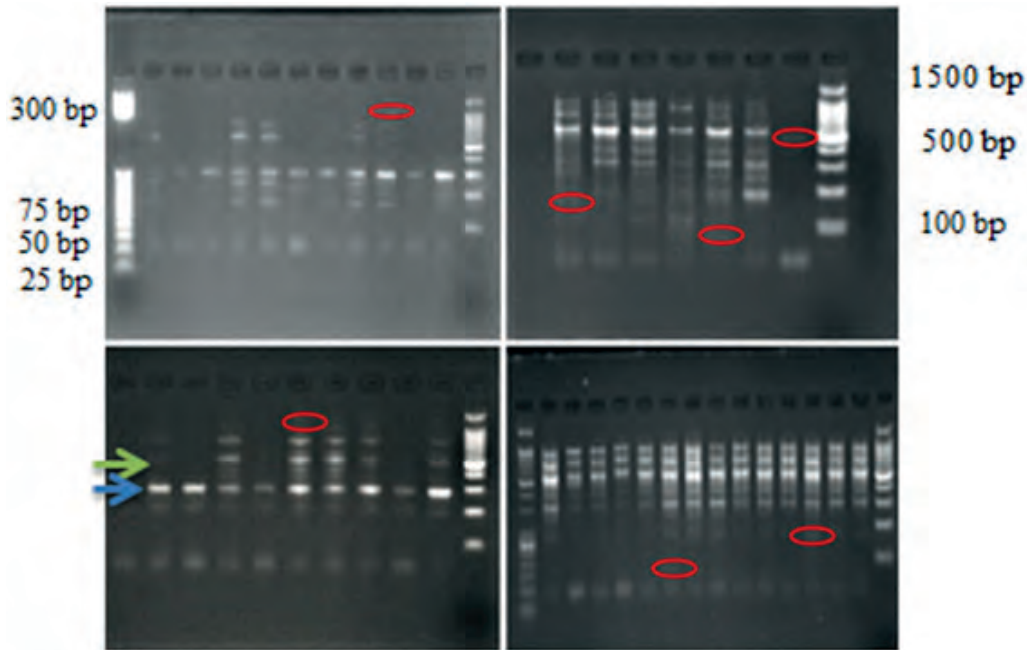


Figure 1. PCR assay for BC-related gene with RAPD primer. Agarose gel of 2% loaded with DNA ladder of (25-1100 bp). And four RAPD primers (OPAA11, OPU 15, OPAA17 and OPD 18) were used. Red circles refer to unique bands. The green arrow refers to the polymorphic band. The Blue arrow refers to the monomorphic band.

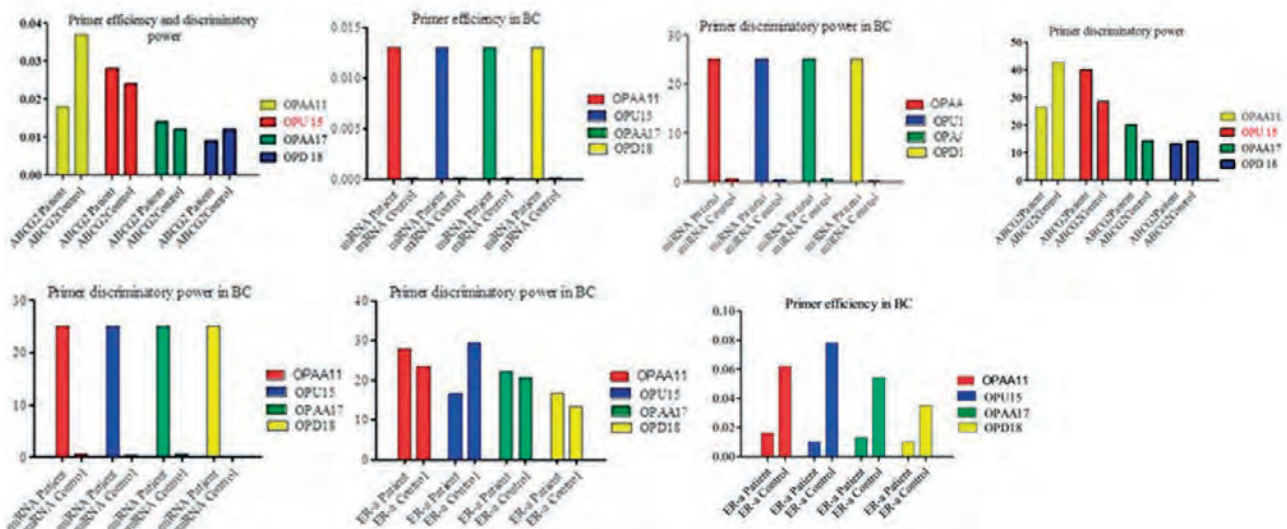


Figure 2. RAPD primer efficiency and discriminatory power in breast cancer-related genes in BC patients and control.

Discussion

To our knowledge, this is the first study that attempts to estimate the possible role of a polymorphism of the ABCG2, ER- α , miRNA 152 between the BC patients and control by PCR- RAPD- PCR technique.

One of the most common malignancies in women is Breast cancer, with an incidence rate double that of ovarian, stomach, colorectal and cervical cancer and about triple that of lung cancer. Many methods were used to study genetic polymorphism of the genes related to breast cancer, and although the RAPD technique was considered random with reduced reproducibility, we chose it as a rapid and low price technique³² to gain an initial idea of our data to know the next step of testing. Despite that, we performed a new procedure with some modifications in the traditional RAPD technique when we used the

amplified gene as a template in RAPD. This procedure resulted in more bands yielded with more accuracy and specific data. The current study found that the number of bands per primer for each gene was high; this improved RAPD successfully increased the number of RAPD bands produced from a given PCR Product. Therefore, we applied the PCR - RAPD - PCR technique with 3 specific BC genes (ABCG2, ER- α , mi-RNA-152) to generate more bands for detecting genomic alterations in human breast cancer.

Present results showed a reasonable degree of genetic polymorphism detected between normal and breast cancer patients. Our results showed the high genetic polymorphism in breast cancer patients: The total number of bands in the breast cancer patients of (ABCG2, ER- α ,miRNA 152) were (214, 298,149) respectively, while the total bands in control were (162, 128, 93) respectively. The total number of bands of the genetic polymorphism of the breast cancer were 69 when used extracted total

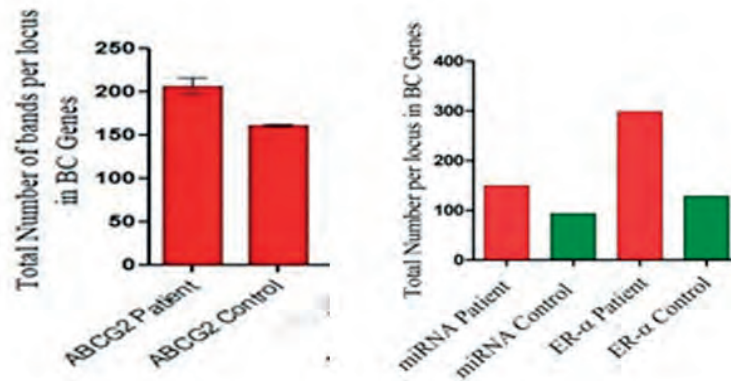


Figure 3. ABCG2, miRNA 152, ER- genes with the total bands per locus in the BC patients and control.

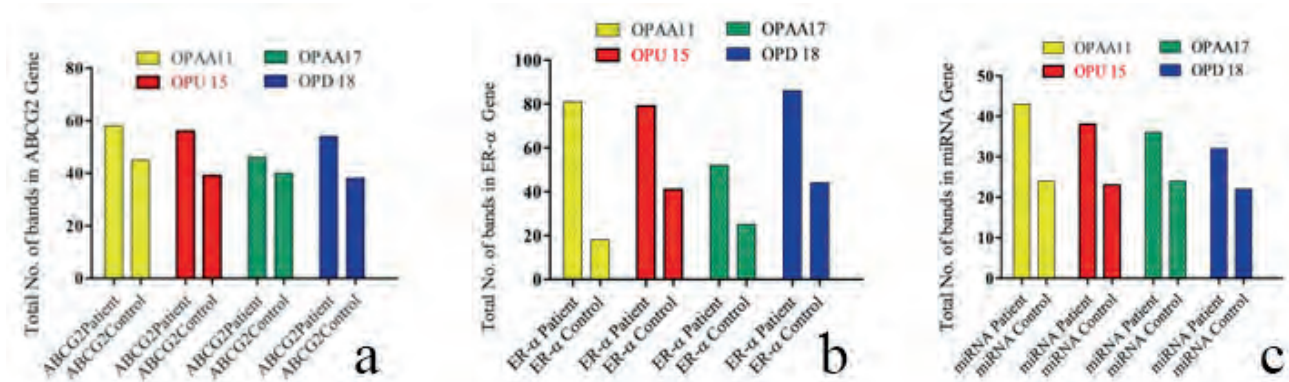


Figure 4. Total number of bands from RAPD primers in breast cancer patient and control ;(a) ABCG2;(b) ER- ; (c) miRNA.

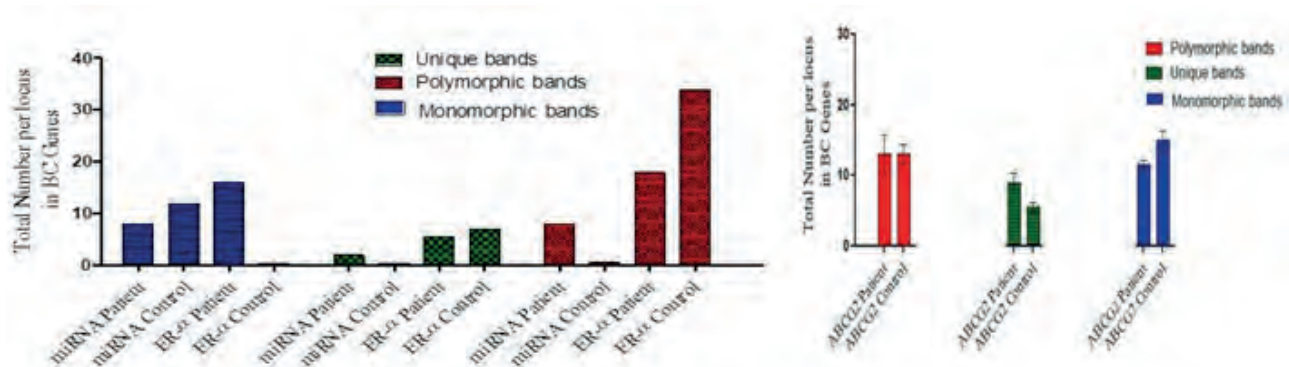


Figure 5. The ability of RAPD primers to generate polymorphic, monomorphic and unique bands.

Markers	Patients ABCG2	Control ABCG2	Chi- Squares	P- value
OPAA11	27.102	27.777	0.008	not significant
OPU15	26.168	24.074	0.087	not significant
OPAA17	21.495	24.691	0.221	not significant
OPD18	25.233	23.456	0.064	not significant

Table 3. Band percentages of patients and control of different markers of ABCG2 gene.

Markers	Patients ABCG2	Control ABCG2	Chi- Squares	P- value
OPAA11	26.6	42.857	3.77	not significant
OPU15	40	28.571	1.90	not significant
OPAA17	20	14.285	0.95	not significant
OPD18	13.3	14.285	0.032	not significant

Table 4. Percent of polymorphic bands of different markers of the gene ABCG2 in patients and control groups.

Markers	Patients ABCG2	Control ABCG2	Chi- Squares	P- value
OPAA11	10	33.33333333	12.56410256	< 0.05
OPU15	0	33.33333333	33.33333333	<0.05
OPAA17	50	0	50	< 0.05
OPD18	40	33.33333333	0.606060606	not significant

Table 5. Percent of unique bands of different markers of the gene ABCG2 in patients and control groups.

Markers	Patients ABCG2	Control ABCG2	Chi- Squares	P- value
OPAA11	25	25	0	not significant
OPU15	25	25	0	not significant
OPAA17	25	25	0	not significant
OPD18	25	25	0	not significant

Table 6. Monomorphic band percentages of different markers of ABCG2 gene in patients and control.

Marker	Era patients	Era Control	Chi- Squares	P- value
OPAA11	27.18120805	14.0625	4.172769839	< 0.05
OPU15	26.51006711	32.03125	0.520717025	not significant
OPAA17	17.44966443	19.53125	0.117168506	not significant
OPD18	28.8590604	34.375	0.481158247	not significant

Table 7. Total band percentages of patients and control of different markers of the gene Era.

Marker	Era patients	Era Control	Chi- Squares	P- value
OPAA11	1.677852349	6.25	2.636847058	not significant
OPU15	1.006711409	7.8125	5.252029483	< 0.05
OPAA17	1.342281879	5.46875	2.500023411	not significant
OPD18	2.013422819	7.03125	2.783803254	not significant

Table 8. Percent of polymorphic bands of different markers of the gene ERa in patients and control groups.

Marker	Era patients	Era Control	Chi- Squares	P-value
OPAA11	40	14.28571429	12.18045113	< 0.05
OPU15	0	14.28571429	14.28571429	< 0.05
OPAA17	20	28.57142857	1.512605042	not significant
OPD18	40	42.85714286	0.098522167	not significant

Table 9. Percent of unique bands of different markers of the gene ERa in patients and control groups.

bp	OPAA11	OPU15	OPAA17	OPD18
	Chi-squares values			
50-60	0.602433	2.839489	23.66898**	25.06026**
140-150	0.602433	1.033991	5.002315*	4.804468*
170-180	0.326397	1.714199	7.259259**	7.929468**

Table 10. Chi-Squares values between patients and control group (miRNA gene) similar bands.

Markers	Chi-Squares	P-value
OPAA11	0.1704	Not significant
OPU15	0.0118	Not significant
OPAA17	0.0541	Not significant
OPD18	0.1052	Not significant

Table 11. Chi-Squares values between patients and control group (miRNA gene) total bands.

DNA as a template and 6 arbitrary primers 2. The total amplified bands were 72 in the breast cancer patient, 28 in control when extracted total DNA as a template and five arbitrary primers³³.

Our results and modification referred to the success of PCR RAPD PCR in generating a more significant number of bands by using PCR product (specific gene) as a template instead of total DNA extracted in the study of the genetic polymorphisms of the breast cancer-related genes and their relationship to breast cancer in Maysan province /south of Iraq.

Our results showed the full polymorphic bands in the breast cancer patient of ABCG2, ER- α , miRNA 152 genes were (15,18,8), while in control were (14,34,0), whereas the polymorphic band may be referred to heterozygous genomic regions of the PCR-RAPD-PCR profile.

The total monomorphic bands in the breast cancer patient of ABCG2, ER- α , miRNA -152 genes were (12,16,8) bands, while in control were (16,0,12) bands, whereas the monomorphic band may be referred to homogenous genomic regions of the PCR- RAPD- PCR profile.

The total unique bands in the breast cancer patient of ABCG2, ER- α , miRNA 152 genes were (10,5,2) in the breast cancer patient while (6,7,0) bands were in control.

Our results showed significant differences ($P < 0.05$) in the unique band of ABCG2 at marker OPAA 11; OPU 15; OPAA 17 between breast cancer patients and control.

Our results showed significant differences ($P < 0.05$) in the total ER- α at marker OPAA11; Our results showed significant differences in the polymorphic band of ER- α at marker OPU 15 between breast cancer patients and control. Our results showed significant differences in the unique band of ER- α at marker OPAA11; OPU 15 between breast cancer patients and control.

Our results showed there are significant differences in the bands that had been size (50-60) bp ; (140 - 150) bp ; (170-180) bp of miRNA-152 at marker OPAA17; OPD 18 between breast cancer patients and control. We suggested that the differences in the number of bands between breast cancer patients and control are probably due to the nucleotides sequence of the primers (markers) and on the genotype of the breast cancer patients. It is noteworthy, the number of compatible sites of primer in the (ABCG2, ER- α , mi-RNA-152) genes of the breast cancer patients which is affected by different types of mutations and translocations, this will affect the primer (marker) and the template interaction sites and will result in the loss or profit of bands; as a result, this will leads to differences in the number of amplified bands the ability of RAPD analysis to detect the genetic instability or genetic alterations which represents the differences between a standard and malignant cell that may comprise insertion, deletion and alteration in the oncogenes or suppressor genes that could cause cancer²⁵.

Our results showed differences in the size of the fragments between patients and control might be referred to the polymorphism that includes the differences in molecular weights of amplified bands which product from multiple types of mutations and translocations occurred, thus causing mobility shift of bands and probably cause the addition of new bands³⁴⁻³⁸.

Our finding showed differences in the primer discriminatory power between patient and control; our results showed that the high discriminatory power in breast cancer patients was 40% at OPU15 of ABCG2, the highest primer discriminatory power was in contrast the control was 42.85% at OPAA11of ABCG2. The primer's capacity to show polymorphisms in comparison to polymorphisms shown by all primers is called primer discriminatory power^{2,39}.

Our results showed that the highest primer efficiency in the breast cancer patient was 0.028 at OPU15 of the ABCG2

gene; while the highest primer efficiency in the control was 0.078 at OPU15 of ER- α gene. The primer efficiency values range from (0 -1) and are defined as the measure of the primer's ability to result in polymorphisms⁴⁰.

Conclusions

Our results proved the accuracy of our modification in the traditional RAPD technique, which yielded more specific bands related to genes; this test also showed us high polymorphism in patients compared to control, which may be related to mutations or mutations modifications. Although our study did not include genes concerned with family history incidence of breast cancer, we suggested from our data that most breast cancers in Iraqi women are not family related but rather drug resistance and estrogen response. We can predict and early diagnose breast cancer upon analysis of our chosen genes; our study allows us to employ these genes in the early prediction of breast cancer.

Authors contributions

Conceptualization, MAD and ZZG; methodology, MAD; software, ZZG; validation, ZZG and MAD; formal analysis, ZZG; investigation, MAD; resources, ZZG; data curation, MAD; writing—original draft preparation, ZZG; writing review and editing, MAD; visualization, ZZG; supervision, MAD; project administration, MAD. All authors have read and agreed to the published version of the manuscript.

Funding

This research received no external funding.

Institutional Review Board

Both the Misan health directorate and AL-Shifa Tumor Treatment center had been informed about the study's aims before collecting blood samples, all declare their agreement of giving samples (255; 13/9/2020). The study follows the rules of scientific research of Misan University, Iraq.

Informed Consent

Informed consent was obtained from all subjects involved in the study. The patient's consent was oral.

Acknowledgment

Many profound thanks to Maysan Health Directorate/ AL-Sader Teaching Hospital /AL-Shifa Tumor Treatment Center, especially Assist. Prof. Dr. Haider Sadun Qasim and all the staff of the /AL-Shifa Tumor Treatment center to facilitate the collection of blood samples and provide support to graduate students. My thanks and appreciation to all breast cancer women patients and ordinary people for their consent to draw blood samples. Also, we would like to express thanks to the genetic engineering laboratory/Department of Biology/College of Science/Misan University and all the staff of the genetic engineering laboratory; thank you to M.SC.Shaima Rabie Bannon.

Conflicts of interest

The authors declare no conflict of interest.

Bibliographic references

- Jin Y. Blood DNA methylation as a surrogate epigenetic biomarker in study of night shift work and breast cancer. Doctoral dissertation, Yale University, 2020.

2. Ismaeel HM. Identification of genomic markers by RAPD-PCR Primers in Iraq Breast Cancer patients. *Iraq J Sci.* 2013;54:97-104.
3. Mohammed ZA. Determination of Serum IL-8 Level in Women with Breast Cancer and Their Correlation With Disease Progression. *Iraqi Journal of Cancer and Medical Genetics.* 2018 Jan 12;4(2).
4. Al Hannan F, Keogh MB, Taha S, Al Buainain L. Characterization of BRCA1 and BRCA2 genetic variants in a cohort of Bahraini breast cancer patients using next generation sequencing. *Molecular genetics & genomic medicine.* 2019 Jul;7(7):e00771.
5. Antoniou A, Pharoah PD, Narod S, Risch HA, Eyfjord JE, Hopper JL, Loman N, Olsson H, Johannsson O, Borg Å, Pasini B. Average risks of breast and ovarian cancer associated with BRCA1 or BRCA2 mutations detected in case series unselected for family history: a combined analysis of 22 studies. *The American Journal of Human Genetics.* 2003 May 1;72(5):1117-30.
6. Sabra SA, Saad AA, Abd El Moneim NA, Hemida MA, Moussa N, Haroun M. Evaluation of breast cancer regarding molecular and immunochemical markers. *International Journal of Immunotherapy and Cancer Research.* 2020 Feb 20;6(1):001-9.
7. Banoun SR, Ghasemian A. The Characters of Graphene Oxide Nanoparticles and Doxorubicin Against HCT-116 Colorectal Cancer Cells In Vitro. *Journal of Gastrointestinal Cancer.* 2021 Mar 19:1-5.
8. Xie Z. A systematic review: breast cancer susceptibility genes. In: *E3S Web of Conferences 2020 (Vol. 218).* EDP Sciences.
9. Sun YS, Zhao Z, Yang ZN, Xu F, Lu HJ, Zhu ZY, Shi W, Jiang J, Yao PP, Zhu HP. Risk factors and preventions of breast cancer. *International journal of biological sciences.* 2017;13(11):1387.
10. Ni Z, Mark ME, Cai X, Mao Q. Fluorescence resonance energy transfer (FRET) analysis demonstrates dimer/oligomer formation of the human breast cancer resistance protein (BCRP/ABCG2) in intact cells. *International journal of biochemistry and molecular biology.* 2010;1(1):1.
11. Haider AJ, Briggs D, Self TJ, Chilvers HL, Holliday ND, Kerr ID. Dimerization of ABCG2 analysed by bimolecular fluorescence complementation. *PLoS One.* 2011 Oct 3;6(10):e25818.
12. Chen L, Manautou JE, Rasmussen TP, Zhong XB. Development of precision medicine approaches based on inter-individual variability of BCRP/ABCG2. *Acta Pharmaceutica Sinica B.* 2019 Jul 1;9(4):659-74.
13. Manandhar S, Kim CG, Lee SH, Kang SH, Basnet N, Lee YM. Estrogen 1 regulates cancer cell stemness in doxorubicin-resistant breast cancer cells. *Oncotarget.* 2017 Sep 19;8(41):70521.
14. Nayak D, Tripathi N, Kathuria D, Siddharth S, Nayak A, Bharatam PV, Kundu C. Quinacrine and curcumin synergistically increased the breast cancer stem cells death by inhibiting ABCG2 and modulating DNA damage repair pathway. *The international journal of biochemistry & cell biology.* 2020 Feb 1;119:105682.
15. Ponglikitmongkol M, Green S, Chambon P. Genomic organization of the human oestrogen receptor gene. *The EMBO journal.* 1988 Nov;7(11):3385-8.
16. Abd Ellatif M, Zahran MA, Denaiwar A, Elbaz A, Abdel Azeez HA. Study of polymorphism of the estrogen receptor alpha gene as a genetic marker for the risk of breast cancer. *IJCEBS.* 2016;4:16-22.
17. Al-Amri RJ, Alotibi MK, Al-Raddadi RI, Shebli WT, Fallatah EI, Alhujaily AS, Mohamed HS. Estrogen Receptor 1 Gene (ESR1) rs2234693 Polymorphism and Breast Cancer Risk in Saudi Women. *Asian Pacific Journal of Cancer Prevention: APJCP.* 2020 Nov;21(11):3235.
18. Chauhan P, Yadav R, Kaushal V, Kadian L. Evaluation of genetic polymorphism in estrogen receptor gene as breast cancer risk. *Biomed Res.* 2019;30:72.
19. Zhou X, Zhao F, Wang ZN, Song YX, Chang H, Chiang Y, Xu HM. Altered expression of miR-152 and miR-148a in ovarian cancer is related to cell proliferation. *Oncology reports.* 2012 Feb 1;27(2):447-54.
20. Liu X, Li J, Qin F, Dai S. miR-152 as a tumor suppressor microRNA: Target recognition and regulation in cancer. *Oncology letters.* 2016 May 9;11(6):3911-6.
21. Md J. lund aH: Microrna and cancer. *Mol oncol.* 2012;6:590-610.
22. Ge S, Wang D, Kong Q, Gao W, Sun J. Function of miR-152 as a tumor suppressor in human breast cancer by targeting PIK3CA. *Oncology research.* 2017;25(8):1363.
23. Kumar NS, Gurusubramanian G. Random amplified polymorphic DNA (RAPD) markers and its applications. *Sci Vis.* 2011 Jul;11(3):116-24.
24. Sharma M, Singh D. Utility of random amplified polymorphic DNA (RAPD) in forensic entomology. *Int J Sci Res Sci Technol.* 2017;3(1):56-8.
25. Atienzar FA, Jha AN. The random amplified polymorphic DNA (RAPD) assay and related techniques applied to genotoxicity and carcinogenesis studies: a critical review. *Mutation Research/Reviews in Mutation Research.* 2006 Nov 1;613(2-3):76-102.
26. Novikov VV, Shumilova SV, Novikov DV, Kalugin AV, Fomina SG, Karaulov AV. Genetic Instability in Locus rs5498 E469K (A/G) of ICAM-1 Gene in Patients with Colorectal Cancer and Breast Cancer. *Bulletin of experimental biology and medicine.* 2016 Apr;160(6):811-3.
27. Surzycki S. Basic techniques in molecular biology. *Springer Science & Business Media;* 2012 Dec 6.
28. Wu H, Liu Y, Kang H, Xiao Q, Yao W, Zhao H, Wang E, Wei M. Genetic variations in ABCG2 gene predict breast carcinoma susceptibility and clinical outcomes after treatment with anthracycline-based chemotherapy. *BioMed research international.* 2015 Nov 8;2015.
29. Nguyen-Dien GT, Smith RA, Haupt LM, Griffiths LR, Nguyen HT. Genetic polymorphisms in miRNAs targeting the estrogen receptor and their effect on breast cancer risk. *Meta gene.* 2014 Dec 1;2:226-36.
30. Sato H, Nogueira-de-Souza NC, D'Amora P, Silva ID, Girão MJ, Schor E. Intron 1 and exon 1 alpha estrogen receptor gene polymorphisms in women with endometriosis. *Fertility and sterility.* 2008 Dec 1;90(6):2086-90.
31. Sambrook J, Russell DW. *Molecular cloning: A laboratory manual.* Mol. Cloning A Lab. Man. 2001.
32. Bidet P, Lalande V, Salauze B, Burghoffer B, Avesani V, Delmée M, Rossier A, Barbut F, Petit JC. Comparison of PCR-ribotyping, arbitrarily primed PCR, and pulsed-field gel electrophoresis for typing *Clostridium difficile*. *Journal of clinical microbiology.* 2000 Jul 1;38(7):2484-7.
33. Al-Askeri MA. Genetic Polymorphism in Iraqi Females Diagnosed with Breast Cancer Using Random Amplification of Polymorphic DNA Technique. *INTERNATIONAL JOURNAL OF PHARM-TECH RESEARCH.* 2016;9(11):312-6.
34. Misra A, Sulaiman IM, Sinha S, Sarkar C, Mahapatra AK, Hasnain SE. Genetic alterations in brain tumors identified by RAPD analysis. *Gene.* 1998 Jan 5;206(1):45-8.
35. Ong TM, Song B, Qian HW, Wu ZL, Whong WZ. Detection of genomic instability in lung cancer tissues by random amplified polymorphic DNA analysis. *Carcinogenesis.* 1998 Jan 1;19(1):233-5.
36. Papadopoulos S, Benter T, Anastassiou G, Pape M, Gerhard S, Bornfeld N, Ludwig WD, Dörken B. Assessment of genomic instability in breast cancer and uveal melanoma by random amplified polymorphic DNA analysis. *International journal of cancer.* 2002 May 10;99(2):193-200.
37. Xian ZH, Cong WM, Zhang SH, Wu MC. Genetic alterations of hepatocellular carcinoma by random amplified polymorphic DNA analysis and cloning sequencing of tumor differential DNA fragment. *World Journal of Gastroenterology: WJG.* 2005 Jul 14;11(26):4102.
38. Ibrahim M, Saleh N, Archoukieh E, Al-Obaide H, Al-Obaidi M, Said H. Detection of Novel Genomic Polymorphism Detection of Novel Genomic Polymorphism in Acute Lymphoblastic Leukemia by Random Amplified Polymorphic DNA Analysis. *int. J. can. Res.* 2010;6:19-26.
39. Grundmann H, Schneider C, Hartung D, Daschner FD, Pitt TL. Discriminatory power of three DNA-based typing techniques for *Pseudomonas aeruginosa*. *Journal of Clinical Microbiology.* 1995 Mar;33(3):528-34.
40. Newton CR, Graham A. *Polymerase chain reaction.* Bios. Scientific Publishers Ltd., Oxford, UK. 1997.

ARTICLE / INVESTIGACIÓN

Detection of humoral immune response induced in horses vaccinated with inactivated Equine Herpes Virus Vaccine

Mohamed Samy Abousenna^{1*}, Heba A Khafagy¹, Nermeen Gouda Shafik¹, Neveen Mounir Abdelmotilib², Ibrahim S. Yahia^{3,4,5}

DOI. 10.21931/RB/2022.07.01.21

¹ Central Laboratory for Evaluation of Veterinary Biologics, Agriculture Research Center, P.O.Box 131 El-Seka El-Baida ST., Abbassia, 11318, Cairo, Egypt.² Arid Lands Cultivation Research Institute, City of Scientific Research and Technological Application, Bourg EL-Arab, Alexandria, Egypt.³ Laboratory of Nano-Smart Materials for Science and Technology (LNSMST), Department of Physics, Faculty of Science, King Khalid University, Saudi Arabia.⁴ Research Center for Advanced Materials Science (RCAMS), King Khalid University, Abha 61413, P.O. Box 9004, Saudi Arabia.⁵ Nanoscience Laboratory for Environmental and Bio-medical Applications (NLEBA), Semiconductor Lab., Department of Physics, Faculty of Education, Ain Shams University, Roxy, 11757 Cairo, Egypt.

Corresponding author: mohamedsamya2020@hotmail.com

Abstract: Equine herpesviruses (EHV1 and EHV4) are essential in horses. Repeated cases of infection and abortion in mares who have regularly vaccinated impetus us to determine to investigate the humoral immune response after post-vaccination with the same inactivated vaccine and the best vaccination protocol. Twelve healthy susceptible horses were divided into four groups (3 horse /group). The first group was vaccinated I/M with inactivated Equine Herpes (type 1 and 4), where each horse was inoculated with a single dose (2ml/ dose /horse). The second group was vaccinated with inactivated Equine Herpes (type 1 and 4) then a booster dose after two months. The third group was vaccinated with inactivated Equine Herpes (type 1 and 4) followed by two booster doses at two months intervals. Three horses were kept as a negative control in the fourth group. Serum samples were tested for the EHV and antibodies using virus Neutralization Test (VNT) and ELISA; it was found that VNT against EHV-1 indicated that the neutralizing antibody titer value ≥ 4 fold titer rise had been demonstrated at 28th-day post-vaccination for all vaccinated horse groups, it was demonstrated that the vaccinated horse group (1) indicated the significant greater titer values compared to other vaccinated groups and showed protective titer value till the end of the experiment (6 months post-vaccination), There is an agreement in titer values between ELISA and VNT tests for EHV was observed, but it could not reveal the same antibodies, where the ELISA measures antibodies against EHV1-4. It was concluded that the single-dose vaccination protocol was more appropriate for horse vaccination than other vaccination protocols.

Key words: Equine Herpesvirus, Rhinopneumonitis, Serological test, vaccine.

Introduction

Equine herpesvirus 1, 4 (EHV-1 and EHV-4) is an equine viral infectious disease that is endemic in most territories. The virus belongs to the family Herpesviridae¹. It is transmitted by inhalation of aerosols of virus-laden respiratory secretions². The disease causes respiratory illness, abortion, and occasionally neonatal mortality in horses. Abortion in mares usually occurs after two to four weeks of infection in the third trimester of the gestation period³. The morbidity rate is increased in young horses sharing the same air space. The primary infection source could be the placental fluids and aborted tissues of infected mares, where it contains a highly high payload of EHV⁴. Although equine Herpesvirus disease has variable clinical manifestations, EHV-1 is a significant cause of neurological disease in horses⁵. Vaccination is an essential tool in disease control. The available commercial vaccines have two antigen content found in inactivated form for prevention and protection from respiratory illness and abortion due to infection, but there is no instruction or evidence about vaccine efficacy to prevent the neurologic form⁶. Although horses were vaccinated with inactivated Equine Herpes virus vaccine, a repeated cases of abortion occurred. So this study prompted us to investigate

the immune response duration post-vaccination with inactivated Equine Herpesvirus vaccine and the most suitable time for booster dose to determine the best vaccination protocol. Serum antibody levels against EHV 1-4 could be screened by virus neutralization test (VNT)⁷ and ELISA⁸.

Materials and methods

Virus

A freeze-dried local strain of EHV type 1 was used for the virus-neutralizing test. It was obtained from Equine Vaccine Research Dept., Veterinary Serum and Vaccine Research Institute (VSVRI), Abbassia, Cairo, according to Magda⁹.

Tissue culture

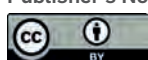
African green monkey kidney cells (Vero) were obtained from the Foreign Animal Disease Diagnostic Laboratory (FA-DDL), Plum Island, USA, and used for virus propagation and virus neutralization test (VNT)

Citation: Abousenna, M.S.; Khafagy, H.A.; Shafik, N.G.; Abdelmotilib, N.M.; Yahia, I.S. Detection of humoral immune response induced in horses vaccinated with inactivated Equine Herpes Virus Vaccine. *Revis Bionatura* 2022;7(1). 21. <http://dx.doi.org/10.21931/RB/2022.07.01.21>

Received: 20 August 2021 / **Accepted:** 20 November 2021 / **Published:** 15 February 2022

Publisher's Note: Bionatura stays neutral with regard to jurisdictional claims in published maps and institutional affiliations.

Copyright: © 2022 by the authors. Submitted for possible open access publication under the terms and conditions of the Creative Commons Attribution (CC BY) license (<https://creativecommons.org/licenses/by/4.0/>).



Inactivated Equine Herpesvirus Vaccine

The local commercial inactivated Equine Herpesvirus (type 1 and 4) was used in this study had been evaluated and approved before by Central Laboratory for Evaluation of Veterinary Biologics, (CLEVB).

Animals and Vaccination Protocols

Twelve healthy susceptible horses, between 6 and 10 years old, with low neutralizing antibody titers (< Log₁₀ 0.6 TCID₅₀) against EHV-1¹⁰) were divided into four groups (3 horse /group). The first group was vaccinated I/M with inactivated EHV1-4 vaccine, where each horse was inoculated with a single dose (2ml/ dose /horse). The second group was vaccinated with inactivated EHV1-4 vaccine then a booster dose after two months. The third group was vaccinated with inactivated EHV1-4 vaccine followed by two booster doses at two months intervals. Three horses were kept as a negative control in the fourth group.

All animal groups were kept in a designated area for CLEVB at the animal facility house of the government veterinary hospital, Abbasia, Cairo, Egypt.

Evaluation of Humoral immune response

Virus Neutralization Test (VNT)

Serum samples were tested for the EHV-1 and antibodies using the virus Neutralization Test (VNT) and expressed as a neutralizing index according to Senthil and Parames¹¹.

ELISA Kit

Equine Herpesvirus type 1 and 4 Differentiating test – Svanova lot, A69377- REF, 10-3100-02. It was supplied by

the Central Laboratory for Evaluation of Veterinary Biologics (CLEVB). The antibody values were measured at a 450 nm absorbance reading of each well. According to the manufacturer's instructions, positive values were considered from a cut off 0.2.

Results

Table 1 shows the VNT results against EHV-1 for the vaccinated horse groups (1,2 and 3) with inactivated EHV (1 and 4) vaccine, all vaccinated horse groups indicated an increase in titer values at 3 months post-vaccination, the groups (2 and 3) showed a slight decrease in antibody titer values after 2nd dose of vaccination compared to group (1). In contrast, the 3rd dose of vaccination in group (3) indicated a decrease in antibody titer values below the protective value (≥ 4 fold titer rise) compared to groups (1 and 2), which was demonstrated at 5 months post-vaccination. The vaccination protocol was used in the group (1) to afford high antibody titer compared to other vaccination protocols.

Table 2 shows the ELISA results against EHV 1 and 4 for the vaccinated horse groups (1,2 and 3) with inactivated EHV (1 and 4) vaccine, all vaccinated horse groups indicated an increase in mean ELISA values at 2 months post-vaccination, the groups (2 and 3) showed a decrease in mean ELISA values after 2nd dose of vaccination compared to group (1). In contrast, the 3rd dose of vaccination in group (3) indicated a decrease in mean ELISA values similar to group (2) mean ELISA values, demonstrated at 5 months post-vaccination. The vaccination protocol was used in the group (1) to afford high antibody titer compared to other vaccination protocols.

Time of Sampling	Group 1	Group 2	Group 3	Group 4 (control)
Zero day	0.3	0.2	0.3	0.3
Vaccination (2ml/ dose /horse)				
14 th DPV	1.2	0.9	1.14	0.3
28 th DPV	1.8	1.5	1.68	0.6
2MPV	2.04	1.92	2.04	0.4
Booster dose				
3MPV	2.4	2.04	2.1	0.3
4MPV	2.28	1.8	1.86	0.5
Booster dose				
5MPV	1.92	1.68	1.44	0.5
6MPV	1.8	1.5	1.08	0.4

DPV: Days post-vaccination - MPV: Month's post-vaccination.

Response rate ≥ 4 fold titer rise

Group 1: EHV inactivated single vaccine dose.

Group 2: EHV inactivated vaccine with a booster after two months.

Group 3: EHV inactivated vaccine with two booster doses two months interval

Control: Negative control without injection

Table 1. Virus neutralizing antibody titer in vaccinated horses with inactivated Equine Herpes virus vaccine.

Time of Sampling	Group 1	Group 2	Group 3	Group 4 (control)
Zero day	0.25	0.19	0.23	0.2
Vaccination (2ml/ dose /horse)				
14th DPV	0.89	0.78	0.88	0.18
28thDPV	1.28	1.19	1.22	0.21
2MPV	1.53	1.45	1.58	0.22
Booster dose				
3MPV	1.29	0.9	0.96	0.22
4MPV	0.85	0.56	0.67	0.23
Booster dose				
5MPV	0.76	0.33	0.25	0.21
6MPV	0.65	0.35	0.17	0.22

DPV: Days post-vaccination - MPV: Month's post-vaccination.

Group 1: EHV inactivated single vaccine dose.

Group 2: EHV inactivated vaccine with a booster after two months.

Group 3: EHV inactivated vaccine with two booster doses two months interval

Control: Negative control without injection

Table 2. Seroconversion of horses vaccinated with inactivated Equine Herpes virus vaccine tested by ELISA.

Discussion

Hygienic measures and vaccination control EHV1 and EHV4 infections. Commercial vaccines, either inactivated or modified live virus (MLV), have been shown to afford protection for vaccinated animals, lessening EHV-related respiratory disease, neurological disease, and abortion under experimental conditions¹². Many studies have demonstrated the humoral responses of on-field vaccinated horses using serological assays¹³.

This study compared different vaccination protocols using inactivated EHV1-4 vaccine, and the humoral immune responses were screened post-vaccination to demonstrate the best vaccination protocol using VNT and ELISA.

The VNT was carried out for detection of neutralizing antibody against EHV-1 for serum samples of vaccinated horse groups (1,2 and 3) within 6 months post- vaccination, the results of VNT indicated that the neutralizing antibody titer value ≥ 4 fold titer rise (the response rate. (4)) has been demonstrated at 28th day post vaccination for all vaccinated horse groups, it was demonstrated that the vaccinated horse group (1) indicated greater titer values compared to other vaccinated groups and showed protective titer value till the end of the experiment (6 months post vaccination), while the vaccinated horse groups (2 and 3) indicated apparent decrease in antibody titer values after 2nd dose of vaccination, furthermore subsequent decrease in antibody titer values was demonstrated after 3rd dose of vaccination in vaccinated horse group(3), as shown in table No.(1), interestingly, similar study demonstra-

ted that horses received three doses of inactivated EHV-1 vaccine, a month apart, the Geometric mean (GM) titer increased to the response rate after the first dose, but no evident titer rises were observed after the second and third doses¹⁴.

There is an agreement in titer values between ELISA and VNT tests for EHV was observed, but it could not reveal the same antibodies, where the ELISA measure antibodies against EHV1-4 as shown in table No. (2) while VNT measure antibodies against EHV1 only, a similar study demonstrated it was observed no correlation in the antibody titer values between ELISA and SN tests for EHV1. This could be justified that the SN test measured the antibodies differ from those measured by ELISA¹⁵.

The obtained results of our study showed a clear difference in immune response between three vaccination protocols which was explained by other studies, the immune response was not observed post-vaccination—especially the effect of booster dose vaccination. This failure of the humoral immune response probably due to the type of vaccine, a study used a modified live vaccine (MLV) and an inactivated vaccine, the serum neutralization (SN) assays indicated high SN titer values in MLV vaccinated mares when compared to those vaccinated with the inactivated vaccine, this could be explained that the antibody response is probably vaccine-type dependent¹³⁻¹⁶ in another study, the hypothesis of the decrease in antibody titer after the first inoculation of the vaccine has a neutralizing action could be accepted but it does not work or justify

the decrease of antibody titer values after subsequent ones of vaccination. This reduction of antibody titer values followed by subsequent ones could be explained by the antibodies interference hypothesis due to the presence of a high titer of anti-EHV4 antibodies which has an antigenic correlation with EHV1. In another study showed that the failure of immune response had a different hypothesis, it could be a different antigen structure between vaccinal strain and the virus used in VNT, and inappropriate vaccine formulation, or by the high antibody titer before vaccination¹⁵.

Conclusions

It was concluded that the single-dose vaccination protocol was more appropriate for horse vaccination than other vaccination protocols, thus affording higher antibody titers, longer immunity duration and economic wise; therefore, further investigation is desperately needed to assess the cellular immune response post-vaccination and its role in horse protection.

Author Contribution

Experiments were designed by NGS and MSA; the experiments were performed HAK, NMA and MSA. NMA accomplished data analysis. ISY and MSA. HAK and MSA wrote the manuscript.

Institutional Review Board Statement

Institutional Animal Care and Use Committee at Central Laboratory for Evaluation of Veterinary Biologics approved the research manuscript, and it has been reviewed under our research authority and is fulfilling bioethical standards.

Data Availability Statement

All data generated or analyzed during this study are included in this published article.

Acknowledgments

The authors express their appreciation to the Deanship of Scientific Research at King Khalid University for funding this work through the research groups program under grant number R.G.P.2/111/41. The authors extend their appreciation to the Deputyship for Research and Innovation, Ministry of Education, in Saudi Arabia, for funding this research work through the project number: (IFP-KKU-2020/9).

Conflicts of Interest

The authors declare no conflict of interest.

Bibliographic references

1. ICTV Taxonomy (html). International Committee on Taxonomy of Viruses (ICTV). Retrieved 17 January (2019). <https://talk.ictvonline.org/>.
2. Goodman, L.B.; Loregian, A.; Perkins, G.A.; Nugent, J.; Buckles, E.L.; Mercorelli, B.; Kydd, J.H.; Palu, G.; Smith, K.C.; Osterrieder, N. & Davis-Poynter, N.A point mutation in a herpesvirus polymerase determines neuropathogenicity. *PLoS Pathogen*.2007, 3 (11), e160.
3. Carter, G.R.; Flores, E.F.; Wise, D.J."Herpesviridae". A Concise Review of Veterinary Virology. Retrieved 2006-06-08.
4. OIE. Organization for Animal Health. Equine rhinopneumonitis-Infection with equine herpesvirus-1 and -4. En: OIE. World Organization for Animal Health. Manual of diagnostic tests and vaccines for terrestrial animals (mammals, birds, bees). Paris:OIE;

- 2018,Chapter 3.5.9. p 1320-1332
5. Goehring, L.S.; van Winden, S.C.; van Maanen, C.; Sloet vaOldruijtenborgh-Oosterbaan, M.M. Equine herpesvirus type1-associated myeloencephalopathy in The Netherlands: a four-year retrospective study (1999 –2003). *J. Vet. Intern. Med.* 2006, 20:601–607.
6. Laura, B.; Goodman, A.B.; Christine, W.A.; Edward, J.; Dubovi, A.B.; Carvel, G.A.B. and Bettina, W.A.B. Immunological Correlates of Vaccination and Infection for Equine Herpesvirus 1, *Clinical and Vaccine Immunology* 2011,p. 235–241
7. Thomson GR, Mumford JA, Campbell J, Griffiths L and Clapham P. Serological detection of equid herpesvirus 1 infections of the respiratory tract. *Equine Vet. J.*2011, 8, 58–65.
8. Crabb, B.S. and Studdert, M.J. Equine herpesviruses 4 (equine rhinopneumonitis virus) and 1 (equine abortion virus). *Adv. Virus Res.* 1995, 45, 153–190.
9. Magda, A.K.; Maysa, H.; Safaa, A.W.; Nehal, S.S.; Nashwa, K.M.; Heba, E.; Sohair, E. and Eman, E. Prospective studies of equine herpesvirus-1 myelo encephalo pathy in Egypt 2012 "IPPo logia, Anno24,n.3-4 settembre- dicembre 2013, p. (25-31).
10. Charles, W.; Purdy, D.; Shirley, J.; Williams, F. and Grant, B.S. Equin rhinopneumonitis virus (Herpes virus type1) Attenuation in stable monkey cell line *Am. j. Vet. Res.* 1977, 38 (8):1211- 1215.
11. Senthil, N.R. and Parames, W. Seroprevalence of equine herpes virus (EHV-1) in equidae using serum neutralization test. *J. of Res Agric Animal Sci.*2014, 2 (5):04-06 .
12. Heldens, J.G.M.; Hannant, D.; Cullinane, A.A.; Prendergast, M.J.; Mumford, J.A.; Nelly, M.; Kydd, J.H.; Weststrate, M.W. and Van den Hoven, R. Clinical and virological evaluation of the efficacy of an inactivated EHV1 and EHV4 whole virus vaccine (Duvaxyn EHV1.4). Vaccination/challenge experiments in foals and pregnant mares. *Vaccine* 2001, 19, 4307–4317.
13. Bresgen C, Lämmer M, Wagner B, Osterrieder N, Damiani AM Serological responses and clinical outcome after vaccination of mares and foals with equine herpesvirus type 1 and 4 (EHV-1 and EHV-4) vaccines. *Vet. Microbiol.* 2012, 160, 9–16.
14. Bannai, H.; Tsujimura, K.; Nemoto, M. et al. Epizootiological investigation of equine herpesvirus type 1 infection among Japanese racehorses before and after the replacement of an inactivated vaccine with a modified live vaccine. *BMC Vet Res* 15, 280 (2019). <https://doi.org/10.1186/s12917-019-2036-0>
15. Attili, A.R.; Colognato, R.; Preziuso, S.; Moriconi, M.; Valentini, S.; Petrin, S.; De Mia, G.M.; Cuteri, V. Evaluation of Three Different Vaccination Protocols against EHV1/EHV4 Infection in Mares: Double Blind, Randomized Clinical Trial. *Vaccines*. 2020; 8(2):268. <https://doi.org/10.3390/vaccines8020268>.
16. Mumford, E.L.; Traub-Dargatz, J.L.; Carman, J.; Callan, R.J.; Collins, J.K.; Goltz, K.L.; Romm, S.R.; Tarr, S.F.; Salman, M.D. Occurrence of infectious upper respiratory tract disease and response to vaccination in horses on six sentinel premises in northern Colorado. *Equine Vet. J.* 2003, 35, 72–77.
17. Foote, C.E.; Love, D.N.; Gilkerson, J.R. and Whalley, J.M. Serological responses of mares and weanlings following vaccination with an inactivated whole virus equine herpesvirus 1 and equine herpesvirus 4 vaccine. *Vet. Microbiol.* 2002, 88 , 13–25.

REVIEW / ARTÍCULO DE REVISIÓN

Características de los pacientes con lumbalgia atendidos en un centro de atención primaria en Ecuador

Characteristics of patients with low back pain treated at a primary care center in Ecuador

Michelle Fuseau¹, David Garrido² and Edgar Toapanta³

DOI. 10.21931/RB/2022.07.01.22

¹ Instituto Nacional de Reumatología del Uruguay, Uruguay.² Hospital de Clínicas Dr. Manuel Quintela, Uruguay.³ Coordinación Zonal 1 Salud, Ecuador.

Corresponding author: michellefuseau@gmail.com

Resumen: La lumbalgia constituye un problema de salud pública por su alta prevalencia y carga de la enfermedad. Este estudio tuvo como objetivo determinar las características de los pacientes con lumbalgia atendidos en el centro de salud N1 de Ibarra, entre enero 2017 y noviembre 2020. Se incluyeron 2055 consultas por lumbalgia, observándose un incremento durante el período de estudio, a excepción del año 2020 (53,78% menos consultas que en 2019). La consulta por lumbalgia fue significativamente más frecuente en mujeres que hombres (64,18% vs. 35,82%; z-score 12,87, p<0,05). La edad en hombres (mediana 49 años, rango intercuartílico 30,75 años) fue significativamente mayor (p=0,003) que en mujeres (mediana 46 años, rango intercuartílico 25 años). La frecuencia acumulada de consultas fue mayor entre los 28-60 años, en su mayoría (67,98%) por lumbalgia no especificada. El 4,79% de las consultas fueron referidas al segundo nivel de atención, donde la mayoría (69,77%) tuvo una codificación diagnóstica de lumbalgia específica. Sobre las consultas subsiguientes (220 pacientes), la mayoría tuvieron 2 (9,05%) y menos frecuente ≥ 3 (1,65%) consultas por año. En conclusión, se observó un incremento en la frecuencia de consultas por lumbalgia, predominante en los grupos en edad laboral, con un bajo porcentaje referido al segundo nivel de atención.

Palabras clave: Lumbalgia, epidemiología, recurrencia, Ecuador.

Abstract: Low back pain is a public health problem due to its high prevalence and burden of the disease. This study aimed to determine the characteristics of patients with low back pain treated at the Centro de Salud N1 from Ibarra, between January 2017 and November 2020. Two-thousand fifty-five consultations for low back pain were included, observing an increase during the study period, except for 2020 (53.78% fewer consultations than 2019). Consultation for low back pain was more frequent in women than men (64.18% vs 35.82%; z-score 12.87, p <0.05). The age in men (median 49 years, interquartile range 30.75 years) was significantly higher (p=0.003) than in women (median 46 years, interquartile range 25 years). The cumulative frequency of consultations was higher between 28-60 years, mostly (67.98%) due to unspecified low back pain. Four-point seventy-nine percent of the consultations were referred to secondary care, where most (69.77%) had a specific diagnostic coding for low back pain. Regarding subsequent consultations (220 patients), most had 2 (9.05%) and less frequent ≥ 3 (1.65%) yearly consultations. In conclusion, there was an increase in the frequency of consultations for low back pain, predominant in the working-age groups, with a low percentage referred to secondary care.

Key words: Low back pain, epidemiology, recurrence, Ecuador.

Introducción

El dolor lumbar o lumbalgia es un síntoma común y uno de los motivos de consulta más frecuentes en atención primaria de salud. Se estima una incidencia del 5% por año, con una prevalencia del 60 al 70% a lo largo de la vida; siendo más frecuente en mujeres y a mayor edad, con su punto máximo entre los 80 a 89 años^{1,2}.

Las causas de lumbalgia aguda (duración menor a 12 semanas) son inespecíficas hasta en 95% de los casos, es decir sin una causa anatómico patológica atribuible, por lo cual generalmente remite en días a semanas. Sin embargo, múltiples factores biofísicos, psicológicos, sociales, comorbilidades y mecanismos de procesamiento del dolor, contribuyen tanto a la experiencia del dolor como a la transición a un dolor persistente e incapacitante³. De este modo, la lumbalgia es una de

las principales causas de años vividos con discapacidad, siendo más frecuente entre los 45 a 49 años; por tanto, la mayor carga de la enfermedad afecta a la población en edad laboral².

Teniendo en cuenta su alta prevalencia, la repercusión sobre el bienestar general y las actividades diarias, el ausentismo laboral y la gran carga económica a las personas, familias y gobiernos, la lumbalgia constituye un problema de salud pública⁴.

Dado que la mayoría de los pacientes con lumbalgia son asistidos en centros de atención primaria de salud, es importante conocer las características de la población atendida, como punto de partida para plantear estrategias de promoción, prevención y atención en salud. El objetivo del presente estudio es determinar las características de los pacientes con

Citation: Abousenna, M.S.; Khafagy, H.A.; Shafik, N.G.; Abdelmotlib, N.M.; Yahia, I.S. Detection of humoral immune response induced in horses vaccinated with inactivated Equine Herpes Virus Vaccine. *Revis Bionatura* 2022;7(1). 22. <http://dx.doi.org/10.21931/RB/2022.07.01.22>

Received: 20 August 2021 / **Accepted:** 20 November 2021 / **Published:** 15 February 2022

Publisher's Note: Bionatura stays neutral with regard to jurisdictional claims in published maps and institutional affiliations.

Copyright: © 2022 by the authors. Submitted for possible open access publication under the terms and conditions of the Creative Commons Attribution (CC BY) license (<https://creativecommons.org/licenses/by/4.0/>).



lumbalgia atendidos en el centro de salud N1 de Ibarra durante el período enero 2017 a noviembre 2020.

Materiales y métodos

Este es un estudio de tipo observacional y descriptivo, en el que se consideró como unidad de análisis todas las consultas médicas codificadas como lumbalgia con los códigos M54.5 lumbago no especificado, M54.4 lumbago con ciática, M51.1 trastornos de disco lumbar y otros con radiculopatía, y M51.0 trastornos de discos intervertebrales lumbares y otros con mielopatía, correspondientes a la codificación de la Clasificación Internacional de Enfermedades versión 10 (CIE-10), realizadas en el centro de salud N1 (CSN1) de la ciudad de Ibarra, Ecuador.

Localización

Ibarra es la capital de la provincia de Imbabura, localizada en su cantón homónimo, encontrándose al norte de Ecuador, y que posee una población de aproximadamente 180 000 habitantes en su área urbana. Las parroquias urbanas del cantón Ibarra incluyen Alpachaca, El Sagrario, San Francisco, Priorato, y Caranqui. El CSN1 tiene un área de influencia de aproximadamente 95 000 habitantes, que corresponden a la parroquia El Sagrario con sus 21 barrios, parroquia de San Francisco con sus 17 barrios, y a 9 comunidades rurales.

Población de estudio

Pacientes que consultaron por lumbalgia en el CSN1 de Ibarra desde enero 2017 hasta noviembre 2020, cuyo motivo de consulta primario fue lumbalgia, independientemente de su edad. Los criterios de exclusión fueron, pacientes atendidos por lumbalgia como motivo de consulta secundario.

Recolección de datos

Se recopiló la información registrada en la base de datos del Registro Diario Automatizado de Consultas y Atenciones Ambulatorias (RDACAA) en los años 2017 y 2018, y de la Plataforma de Registro de Atención en Salud (PRAS) en el 2019 y 2020.

VARIABLES ANALIZADAS

Se incluyeron las siguientes variables; sexo, edad, etnia, nacionalidad, CIE-10 diagnóstico, referencia al 2do nivel de atención, número de consulta, número de pacientes con consultas subsecuentes.

Análisis estadístico

El análisis fue realizado mediante SPSS V.25, y la tabulación inicial de los datos mediante Excel 2013.

Se analizaron las variables cuantitativas utilizando la mediana junto con rango intercuartílico (RIC) y su representación gráfica mediante diagramas de cajas y bigotes, mientras que las variables cualitativas fueron representadas mediante frecuencias y porcentajes. Para la representación de la edad, como variable continua, se usaron histogramas y polígonos de frecuencia. Para la representación de la frecuencia acumulada se utilizaron ojivas.

Para la comparación entre variables cuantitativas de dos grupos, y dado que solo poseemos los datos muestrales, se utilizó la prueba t de Student (t) para diferencia de medias comparando las varianzas mediante el test de Fisher (F), y para la comparación entre 3 o más grupos se utilizó el test ANOVA. El uso de pruebas paramétricas en muestras grandes

sobre el uso de pruebas no paramétricas, independientemente de su distribución, se basa en la recomendación de Fagerland, M.W.⁵.

Para la comparación de las proporciones en un mismo grupo, se utilizó z score utilizando la ecuación:

$$z = \frac{(p - \pi)}{\sqrt{(\pi(1 - \pi)/n)}}$$

Donde p es la proporción de eventos en el grupo y π la proporción que corresponde a la hipótesis nula (para este caso, consideramos una proporción esperada de mujeres de 0,49, según lo reportado por el Instituto Nacional de Estadística y Censos del Ecuador).

Para comparar las proporciones entre dos grupos independientes, se utilizó chi cuadrado

Aspectos éticos

Dado que este estudio parte de una fuente secundaria de datos, los pacientes incluidos en el estudio no fueron sometidos a ningún tipo de intervención. Se cumplió con las medidas de protección a la confidencialidad, ya que no se registró ni reveló ningún dato personal que pudiera identificar al paciente.

Resultados

Las características de los pacientes atendidos por lumbalgia en el CSN1 durante el período 2017-2020 se detallan en la tabla 1. Se incluyeron 2055 consultas por lumbalgia durante el período de estudio. Se excluyeron 383 consultas por lumbalgia, debido a que el motivo de consulta fue secundario.

La consulta por lumbalgia fue más frecuente en mujeres (64,18%) que en hombres (35,82%), siendo esta diferencia mayor en comparación a la proporción esperada de mujeres ($p < 0,05$).

Aunque la etnia mestiza fue la más frecuente, su proporción disminuyó a lo largo de los años. Otras nacionalidades han aumentado su proporción durante el período de estudio.

En cuanto a la codificación diagnóstica, la mayoría de las consultas (67,98%) fueron por lumbalgia no especificada.

La referencia al segundo nivel de atención se registró en el 4,79% de las consultas por lumbalgia. De ellos, la mayoría (69,77%) tuvo una codificación diagnóstica de lumbalgia específica.

Consultas subsecuentes

El 17,18% del total de consultas incluidas correspondieron a una morbilidad subsecuente; entre ellas, la mayoría tuvieron 2 (9,05%) y menos frecuente 3 o más (1,65%) consultas por año. Entre quienes tuvieron 3 o más consultas subsecuentes, la mayoría fueron mujeres (58,82%), con una mediana de edad de 44 años en mujeres y de 53 años en hombres.

Distribución de las consultas por frecuencias acumuladas

Las medianas de edad según los años de estudio fueron 45 años, 46 años, 46 años, y 49 años, para 2017, 2018, 2019 y 2020, respectivamente, evidenciándose una tendencia creciente con respecto a la edad ($F = 2,94$, $p = 0,032$), como se muestra en la figura 1.

La frecuencia acumulada de consultas tanto en hombres como en mujeres fue mayor en los grupos de edad intermedios (28 a 60 años) (figura 2, A).

La edad en hombres (mediana 49 años, RIC 30,75 años) fue significativamente mayor ($p = 0,003$) que en mujeres (mediana 46 años, RIC 25 años) (figura 2, B).

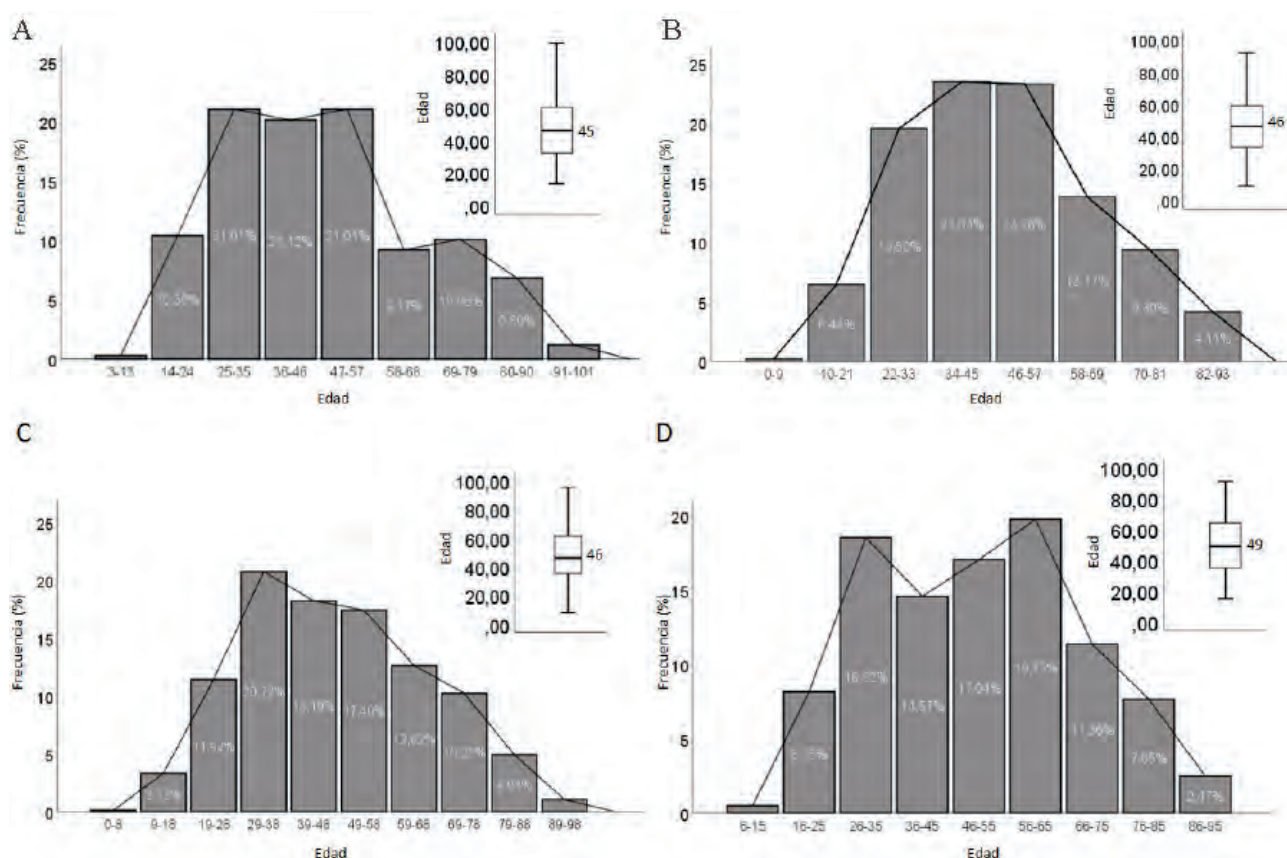


Figura 1. Distribución de la frecuencia de consultas por lumbalgia por grupos de edad. A. Año 2017, B. Año 2018, C. Año 2019, Año 2020.

La frecuencia acumulada de consultas subsecuentes aumentó con la edad, alcanzando su punto máximo entre los 50 a 60 años y luego disminuyeron gradualmente (figura 2, C). La mediana de edad en el grupo de morbilidad subsecuente fue significativamente mayor que en el grupo de primera consulta (53 y 45 años, respectivamente; $t=5,12$, $p<0,01$) (figura 2, D).

Discusión

A nivel mundial, el número prevalente de personas con lumbalgia ha aumentado significativamente a lo largo de los años². Similarmente, en el presente trabajo se observó un incremento en el número de consultas por lumbalgia durante el período de estudio, a excepción del año 2020, en el que se redujeron a aproximadamente la mitad en comparación al 2019. Esto podría explicarse por el menor número de meses incluidos durante el año 2020 (enero-noviembre), así como por la menor asistencia de pacientes ocasionada por la emergencia sanitaria por SARS-CoV-2.

La lumbalgia se presentó en una relación mujer-hombre 2:1, similar al estudio de Guevara et al. realizado en el cantón Cuenca, Ecuador⁶. Otros estudios realizados en centros de atención primaria o en la comunidad, tanto en Ecuador como en otros países, también han señalado la mayor frecuencia de lumbalgia en mujeres, aunque generalmente sin encontrar diferencias estadísticamente significativas^{7,8}. Por el contrario, en algunos estudios donde el sexo masculino se encontró como un posible factor de riesgo para lumbalgia, se resalta que fueron realizados en población en edad laboral o con riesgo ocupacional⁹.

La frecuencia acumulada de consultas en hombres y mujeres aumentó con la edad, siendo mayor en edades intermedias, y descendiendo progresivamente a partir de los 60 años, similar al trabajo de Pérez J., realizado en un centro de salud de Cuenca, Ecuador⁸. Aunque a diferencia de nuestros hallazgos, a nivel mundial se ha reportado un descenso en la frecuencia de lumbalgia a edades más tardías (70 a 80 años), todos los trabajos coinciden en señalar su mayor frecuencia en los grupos en edad laboral, uno de los motivos por lo cual la lumbalgia se considera un problema de salud pública^{2,7,10}.

En cuanto a las consultas subsecuentes por lumbalgia, el promedio anual durante el período de estudio (17,18%) fue menor a lo reportado por otros trabajos, donde las estimaciones de recurrencia a 1 año oscilan entre el 24 al 80%¹¹. Estas diferencias probablemente se deben a la falta de uniformidad en la definición de lumbalgia recurrente, como lo señala la revisión sistemática de Da Silva T et al.¹², por lo cual no es posible obtener estimaciones sólidas del riesgo y factores pronósticos de lumbalgia recurrente, sin embargo, el único predictor señalado consistentemente en otros trabajos fue la historia de episodios previos de lumbalgia.

Entre quienes tuvieron 3 o más consultas subsecuentes durante 1 año, la mayoría fueron mujeres jóvenes, a diferencia de lo reportado por Beaudet N., donde las mujeres de 65 años o más tuvieron 1,35 veces más riesgo de consultar 3 o más veces¹³.

En cuanto a la codificación diagnóstica, si bien la mayoría de las consultas fueron por lumbalgia no especificada, el porcentaje de lumbalgias específicas (32,02%) fue mayor a lo informado en otras series (5-10%)¹⁴. No obstante, consideramos que esto se debe a la codificación diagnóstica aplicada y no ne-

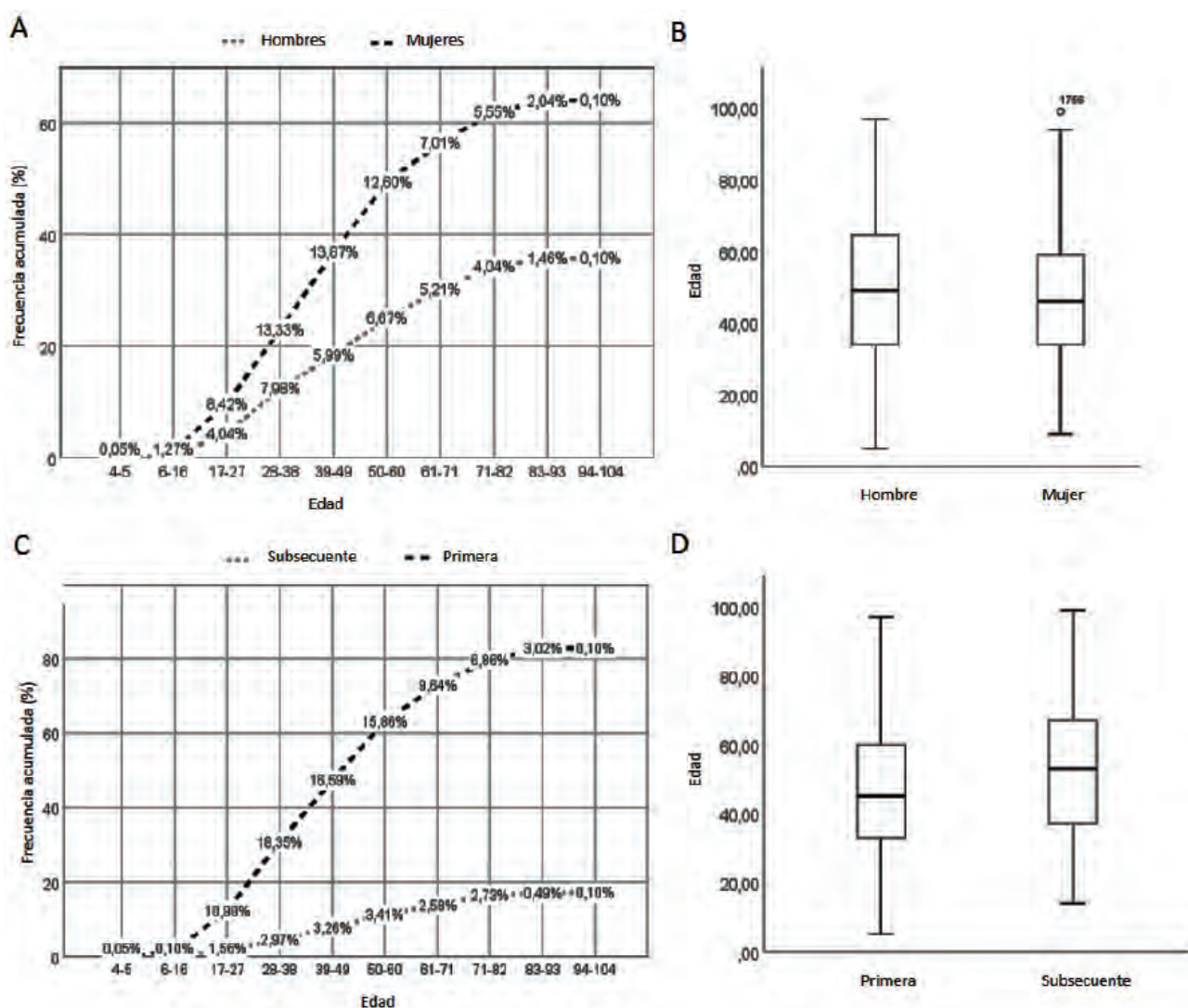


Figura 2. Distribución de las consultas por lumbalgia durante el período 2017-2020. A. Frecuencia acumulada de hombres y mujeres según grupos de edad; B. Consultas de acuerdo a sexo y edad; C. Frecuencia acumulada de consultas primeras y subsecuentes según grupos de edad; D. Consultas primeras y subsecuentes de acuerdo a edad.

cesariamente a una causa anatómico patológica subyacente. La frecuencia de lumbalgias específicas podría estar mejor representada por el porcentaje de consultas que fueron referidas al segundo nivel de atención (4,79%), ya que estas tuvieron en su mayoría una codificación diagnóstica con causas especificadas (lumbago con ciática, trastornos de disco lumbar y otros con radiculopatía, trastornos de discos intervertebrales lumbares y otros con mielopatía).

Como fortaleza del presente trabajo, se destaca su realización en un centro de atención primaria de salud, lo cual refleja los datos de los pacientes de la comunidad, a diferencia de la mayoría de las publicaciones sobre lumbalgia realizadas en hospitales o en grupos de trabajadores de un área en particular.

Entre las limitaciones, se encuentran las relacionadas al uso de una fuente de información secundaria, por lo cual no se pudieron evaluar factores de riesgo ni calcular la prevalencia de lumbalgia. Se requieren más estudios para evaluar los factores de riesgo modificables (mecánicos, comorbilidades, psicosociales) asociados a la aparición y persistencia de lumbalgia en nuestra población.

Conclusiones

Se observó un incremento en la frecuencia de consultas por lumbalgia durante el período de estudio, siendo más frecuente en mujeres, y particularmente en los grupos en edad laboral. Un bajo porcentaje fue referido al segundo nivel de atención de salud.

Contribuciones de los autores

Conceptualización, M.F. y D.G.; metodología, D.G.; software, D.G.; validación, M.F., D.G. y E.T.; análisis formal, M.F.; investigación, M.F.; recursos, E.T.; curación de datos, D.G.; redacción — preparación del borrador original, M.F.; redacción — revisión y edición, M.F. y D.G.; visualización, M.F., D.G. y E.T.; supervisión, M.F.; administración de proyectos, E.T. Todos los autores han leído y aceptado la versión publicada del manuscrito.

Conflicto de intereses

Los autores declaran no tener conflicto de intereses.

	2017		2018		2019		2020*		Total	
	n	%	n	%	n	%	n	%		
Total	338	100,00	559	100,00	753	100,00	405	100,00	2055	100,00
Sexo										
Hombre	120	35,50	191	34,17	252	33,47	173	42,72	736	35,82
Mujer	218	64,50	368	65,83	501	66,53	232	57,28	1319	64,18
Grupos de edad										
Mayor a 50 años	138	40,83	220	39,36	322	42,76	195	48,15	875	42,58
20 a 50 años	183	54,14	312	55,81	396	52,59	198	48,89	1089	52,99
Menor a 20 años	17	5,03	27	4,83	35	4,65	12	2,96	91	4,43
Etnia										
Mestizo	303	89,64	466	83,36	583	77,42	305	75,31	1657	80,63
Montubio	2	0,59	3	0,54	2	0,27	2	0,49	9	0,44
Mulato	1	0,30	1	0,18	5	0,66	5	1,23	12	0,58
Afrodescendiente	4	1,18	11	1,97	40	5,31	14	3,46	69	3,36
Blanca	2	0,59	1	0,18	0	0,00	0	0,00	3	0,15
Indígena	4	1,18	10	1,79	13	1,73	6	1,48	33	1,61
No especificada	22	6,51	67	11,99	110	14,61	72	17,78	271	13,19
Nacionalidad										
Ecuador	316	93,49	493	88,19	653	86,72	341	84,20	1803	87,74
Otros países	22	6,51	66	11,81	101	13,41	64	15,80	253	12,31
CIE-10 diagnóstico										
M545	211	62,43	400	71,56	517	68,66	269	66,42	1397	67,98
M544	120	35,50	146	26,12	220	29,22	132	32,59	618	30,07
M511	6	1,78	10	1,79	16	2,12	4	0,99	36	1,75
M510	1	0,30	3	0,54	0	0,00	0	0,00	4	0,19
Referencia a 2do nivel de atención	20	5,92	23	4,11	NR		NR		43	4,79
M545	7	2,07	6	1,07	NR		NR		13	1,45
M544	11	3,25	15	2,68	NR		NR		26	2,90
M511	2	0,59	1	0,18	NR		NR		3	0,33
M510	0	0,00	1	0,18	NR		NR		1	0,11
Número de consulta										
Primera	294	86,98	492	88,01	621	82,47	295	72,84	1702	82,82
Subsecuente	44	13,02	67	11,99	132	17,53	110	27,16	353	17,18
Número de pacientes con consultas subsecuentes	21	6,21	74	13,24	85	11,29	40	9,88	220	10,71
2 consultas subsecuentes	16	4,73	66	11,81	75	9,96	29	7,16	186	9,05
≥3 consultas subsecuentes	5	1,48	8	1,43	10	1,33	11	2,72	34	1,65

* periodo enero-noviembre. *Abreviaturas:* CSN1, Centro de Salud número 1; NR, no reportado; M544, lumbago con ciática; M545, lumbago no especificado; M511, trastornos de disco lumbar y otros con radiculopatía; M510, trastornos de discos intervertebrales lumbares y otros con mielopatía.

Tabla 1. Características de los pacientes atendidos por lumbalgia en el CSN1 durante el período 2017-2020.

Referencias bibliográficas

1. Duthey B. Update on 2004 Background Paper, 6.24 Low back pain. Geneva: World Health Organization 2013:1–29. https://www.who.int/medicines/areas/priority_medicines/BP6_24LBP.pdf (accessed August 9, 2021).
2. Wu A, March L, Zheng X, Huang J, Wang X, Zhao J, et al. Global low back pain prevalence and years lived with disability from 1990 to 2017: estimates from the Global Burden of Disease Study 2017. *Ann Transl Med* 2020;8:299. <https://doi.org/10.21037/atm.2020.02.175>.
3. Hartvigsen J, Hancock MJ, Kongsted A, Louw Q, Ferreira ML, Genevay S, et al. What low back pain is and why we need to pay attention. *Lancet* 2018;391:2356–67. [https://doi.org/10.1016/S0140-6736\(18\)30480-X](https://doi.org/10.1016/S0140-6736(18)30480-X).
4. Ministerio de Salud Pública. Dolor lumbar: Guía Práctica Clínica (GPC). 1st ed. Quito: Dirección Nacional de Normatización; 2015.
5. Fagerland MW. t-tests, non-parametric tests, and large studies—a paradox of statistical practice?. *BMC Med Res Methodol* 2012;12:78. <https://doi.org/10.1186/1471-2288-12-78>.
6. Guevara-Pacheco S, Feicán-Alvarado A, Sanín LH, Vintimilla-Ugalde J, Vintimilla-Moscoso F, Delgado-Pauta J, et al. Prevalence of musculoskeletal disorders and rheumatic diseases in Cuenca, Ecuador: a WHO-ILAR COPCORD study. *Rheumatol Int* 2016;36:1195–204. <https://doi.org/10.1007/s00296-016-3446-y>.
7. Hoy D, Bain C, Williams G, March L, Brooks P, Blyth F, et al. A systematic review of the global prevalence of low back pain. *Arthritis Rheum* 2012;64:2028–37. <https://doi.org/10.1002/ART.34347>.
8. Pérez Domínguez JA. Incidencia de lumbalgia y factores asociados en pacientes adultos que acuden al Centro de salud El Valle durante los meses de julio 2017 a febrero 2018, Cuenca. 2018.
9. Fatoye F, Gebrye T, Odeyemi I. Real-world incidence and prevalence of low back pain using routinely collected data. *Rheumatol Int* 2019;39:619–26. <https://doi.org/10.1007/S00296-019-04273-0>.
10. Abbafati C, Machado DB, Cislaghi B, Salman OM, Karanikolos M, McKee M, et al. Global burden of 369 diseases and injuries in 204 countries and territories, 1990–2019: a systematic analysis for the Global Burden of Disease Study 2019. *Lancet* 2020;396:1204–22. [https://doi.org/10.1016/S0140-6736\(20\)30925-9](https://doi.org/10.1016/S0140-6736(20)30925-9).
11. Hoy D, Brooks P, Blyth F, Buchbinder R. The Epidemiology of low back pain. *Best Pract Res Clin Rheumatol* 2010;24:769–81. <https://doi.org/10.1016/J.BERH.2010.10.002>.
12. da Silva T, Mills K, Brown BT, Herbert RD, Maher CG, Hancock MJ. Risk of Recurrence of Low Back Pain: A Systematic Review. *J Orthop Sports Phys Ther* 2017;47:305–13. <https://doi.org/10.2519/JOSPT.2017.7415>.
13. Beaudet N, Courteau J, Sarret P, Vanasse A. Prevalence of claims-based recurrent low back pain in a Canadian population: A secondary analysis of an administrative database. *BMC Musculoskelet Disord* 2013;14:1–8. <https://doi.org/10.1186/1471-2474-14-151>.
14. Bardin LD, King P, Maher CG. Diagnostic triage for low back pain: a practical approach for primary care. *Med J Aust* 2017;206:268–73. <https://doi.org/10.5694/MJA16.00828>.

ARTICLE / INVESTIGACIÓN

Study of effects Oat and Soybean on the Microbial and Sensory Analysis of Burgers (Beef, Chicken and Sheep)

Hind Mohammed Saleh¹, Firas R. Jameel^{2*}, Sara Thamer Hadi³ and Mohammed Majed Hamid³

DOI. 10.21931/RB/2022.07.01.23

¹ Food science department, college of Agriculture, Tikrit University, Tikrit, Iraq.² Department of Biotechnology, College of Applied Science, University of Fallujah, Ministry of Higher Education and Scientific Research, Republic of Iraq.³ Food Science department, College of Agriculture, University of Anbar, Al-Anbar, Iraq.Corresponding author: firasraidth1983@gmail.com

Abstract: The purpose of this study was to assess the microbiological and sensory load induced by fast-food energy reduction as an adjuvant treatment for autism, obesity, and the preparation of low-fat burgers and assess the effect of soybean and oat flour as fat substitutes. There were three treatments of the burgers consisting of (beef, chicken and sheep) for both oat and soybean and the ratio of 5,10 and 15% of each one as fundamental material used for manufacturing the model products. The burger that consists of types of meat with fillers of oats 10% and soy 10% then 5% and 15% respectively improves microbial load and sensory score. The burger that consists of types of meat with fillers of oats and soy in several concentrations Improves microbial load and sensory score.

Key words: Types of meat, Sensory analysis, Burgers, Microbial, Oats, Soybean.

Introduction

In today's trend, consumers' perceptions of food intake are mostly focused on keeping good health¹. Reduced fat in the diet, balanced protein sources, and, most crucially, the inclusion of recommended levels of dietary fiber sources in the daily diet have all grown more popular¹. The burger was first served to the United States through fast-food establishments. Burgers, sausages, hotdogs, and nuggets, among other meat items, are widely accepted and consumed in Iraq, particularly in fast-food outlets.

Recent research has focused chiefly on the development of new alternatives that, when introduced into meat products, would allow for the production of low-energy goods with an enriched content of useful components not found in meat raw material². Cereal grains, such as buckwheat and oats, have been used as alternatives for low-fat meat products². Cereal grains, such as oats and buckwheat, are high in various nutrients that are in good proportions for an organism². Furthermore, it is a primary source of important components with a wide spectrum of biological activity (for example, polyphenols), whose consumption protects against the development of civilization diseases³.

In the low-fat meat system, the combination of isolated soy protein, alginate, and carrageenan can give emulsion stability and restrict water development, which is based on stable complex formation and deformation of meat protein during the heating process⁴. The primary goal of separated soy protein is to enhance thickness, prevent water loss, and stabilize emulsion while lowering production costs.

There was a link between home hamburger preparation and the risk of contamination. A potential mechanism by which soy protein induces lowering of blood cholesterol concentrations includes thyroid status, bile acid balance and the estro-

genic effects of genistein and daidzein⁵.

The objectives of the present experiment were to evaluate the effects of adding with different proportions of oat or soya (5,10, and 15%) mixed with (Ground meat) of (cow, chicken and sheep) in fast-food on quality burgers (sensory evaluation and microbiological load).

Materials and methods

Comminuted products of the following general composition made up the material: Burgers were made with various proportions of oat or soya (5,10, and 15%) mixed with minced meat products (beef, chicken, and sheep) at a rate of 75 g in the manufacturing of burgers. 20 g fat, 5 g samoon powder (a type of famous bread in Iraq), 1.5 g sodium chloride, and 0.5 g spices; the spices are made up of a proportion of (black pepper, Kebabah, Nutmeg, Cloves and CINNAMON).

In a grinder, meat and delicate fat were minced. The amounts of oat or soya (5,10, and 15%) were mixed with minced meat products (beef, chicken, and sheep) at a rate of 75 g and stored for 24 hours under refrigeration (4 ± 10 C).

The Burger Processing Instructions

The ingredients are added to the mixture mixed for another 4 minutes. The temperature of the combination was monitored regularly to ensure that it remained between 10 and 15 degrees Celsius. The flavors and spices are then combined.

This was when the finely powdered soybean or oat was added to the mixture for samples T 1, T 2, and T3. The mixture was then beaten for a further 2 minutes. After that, each burger is weighed at 75 grams. After being molded and kept cold

Citation: Mohammed Saleh H, Jameel FR, Thamer Hadi S, Majed Hamid M. Study of effects Oat and Soybean on the Microbial and Sensory Analysis of Burgers (Beef, Chicken and Sheep). *Revis Bionatura* 2022;7(1). 23. <http://dx.doi.org/10.21931/RB/2022.07.01.23>

Received: 7 November 2021 / **Accepted:** 20 November 2021 / **Published:** 15 February 2022

Publisher's Note: Bionatura stays neutral with regard to jurisdictional claims in published maps and institutional affiliations.

Copyright: © 2022 by the authors. Submitted for possible open access publication under the terms and conditions of the Creative Commons Attribution (CC BY) license (<https://creativecommons.org/licenses/by/4.0/>).



Ingredients	Level of replacement (%)	The filling (Minced meat products)
Oat1	5%	Beef 75g
Oat2	10%	Chicken 75g
Oat3	15%	Sheep 75g
Soya	5%	
Soya	10%	
Soya	15%	
fat	20g	
Samoon powder	5 g	
NaCl	1.5	
spices	0.5g	

Table 1. Describe the components of treatment types.

at a temperature of -18°C for 1 to 2 hours, they are packed separately and kept cold for analysis purposes.

Sensory evaluation

Sensory evaluation: A well-trained group of 9 people with qualified sensory sensitivity evaluated the sensory quality of beef products, as specified by (6).

Texture, color, aroma, taste, flavor, and general acceptability were evaluated using a 7-point hedonic scale (7 like very much and 1 dislike very much). Technical staff members from the Departments of Meat Science and Technology and Poultry Science made up the sensory panel. Without any prior knowledge of the treatments, the panelists evaluated all of the features in each sample and marked the scales accordingly. The sensory evaluation sensory laboratory was used to simultaneously conduct the sensory evaluation using all of the panelists. The frozen nuggets were thawed in the refrigerator for 4 hours, then heated in a microwave oven before being served at room temperature on white porcelain plates in natural light to the panelists. The samples were assigned three-digit random numbers, and the presentation order was determined by random permutation. The sensory assessment was completed in the sensory laboratory. To ensure that each panelist made an independent decision, all required steps were taken⁷.

Coliform Counts

After incubation at 37 °C for 24 hours, Using a chromogenic E. coli/Coliform medium, Coliform Counts "TCC" (log CFU g1) were calculated (Rapid E. coli 2 Agar, Bio-Rad, Marnes La Coquette, France)⁸.

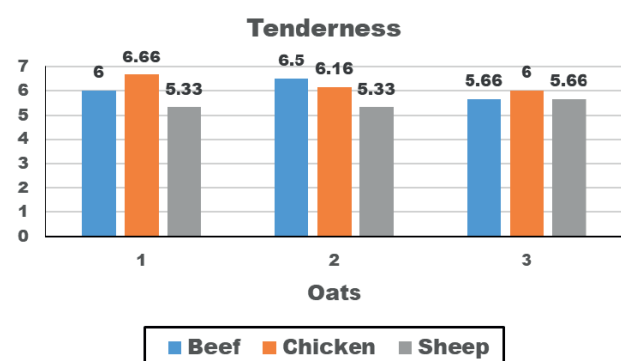


Figure 1. Experimental treatments regarding tenderness with Oats.

Statistical analysis

Three biological replicates were used in each experiment. One-way ANOVA was used to examine the statistical differences between the treatment group's means (quantitative variables), followed by repeated pairwise comparisons (Tukey's test, 0.05). SPSS version 20.0 and GraphPad Prism were used for statistical analyses and graphics. The differences between the three biological replicates were considered significant at $p < 0.05$, and the data were reported as mean SD.

Results

Regarding sensory

Concerning tenderness

The results for Oats illustrated there was no statistical significance at $p < 0.01$ in all treatments, While the sub (Chicken) of T1 (Oats5%) and the sub (Beef) of T3 (Oats15%) recorded 5.66 for each one Numerically high recorded.

While regarding soya, the results illustrated there was statistical significance at $p < 0.01$ between treatments, where all treatments recorded the highest significance statistically compared to the sub (Beef) of T1(Soya 5%) and the sub (Chicken) of T1, T3(Soya 5,15%) were recording (5.33), (5.66 and 5.00) respectively, which, in turn, showed a significant increase compared to the sub (Beef) of T3(Soya 15%)was recording the treatment lowest significance at ($p < 0.01$) (4.66).

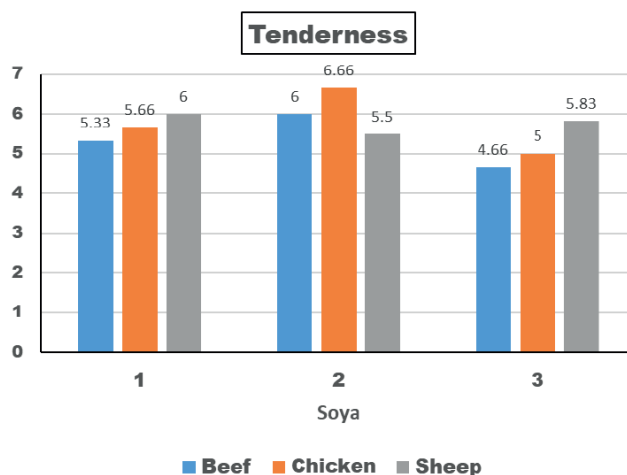


Figure 2. Experimental treatments regarding tenderness with soya.

Concerning color

The results for Oats illustrated there was no statistical significance at $p < 0.01$ between treatments, While the sub (Beef) of T2 (Oats10%) recorded 6.83 for each one Numerically high recorded.

While regarding with soya, the results illustrated there were statistical significance at $p < 0.01$ between treatments, where all treatments recorded statistical a highest significant compare to the sub (Beef) of T3 (Soya 15%) were recording lowest significant at ($p < 0.01$) (4.66).

Concerning Flavour

The results for Oats, the results illustrated there was statistical significance at $p < 0.01$ between treatments, where all treatments recorded the highest significance statistically compared to the sub (Beef) of T3 (Oats15%) and the sub (sheep) of T1 of (Oats5%) were recording lowest significant at ($p < 0.01$) (5.83), (5.00) as respectively.

The results for soya results illustrated that there was statistical significance at $p < 0.01$ between treatments, where all treatments recorded the highest effective compare statistically to the sub (Beef) of T3 (Soya 15%) were recording lowest significance at ($p < 0.01$) (4.66).

Concerning General acceptance

The results for Oats results illustrated there were statistical significance at $p < 0.01$ between treatments, where all treatments recorded a highest significant compare statistically to the sub (Beef) of T1 (Oats5%) and the sub (Chicken) of

T3 (Oats15%) were recording lowest significant at ($p < 0.01$) (5.33), (6.00) as respectively.

The results for soya results illustrated that there was statistical significance at $p < 0.01$ between treatments, where all treatments recorded a highest effective compare statistically to the sub (Beef) of T3 (Soya 15%) were recording lowest significance at ($p < 0.01$) (5.67).

Concerning juiciness

The results for Oats the results illustrated there was statistical significance at $p < 0.01$ between treatments, where all treatments recorded the highest significance statistically compared to the sub (Chicken) of T3 (Oats15%) were recording lowest significance at ($p < 0.01$) (5.66).

The results for soya results illustrated that there was statistical significance at $p < 0.01$ between treatments, where all treatments recorded the highest significance statistically compared to the sub (Beef) of T3 (Soya15%) were recording the lowest significance at ($p < 0.01$) (4.66).

Regarding with microbiology aspect

Concerning Coliform

The results for Oats the results illustrated there was statistical significance at $p < 0.05$ between treatments, the sub (T3) at 15% the sub of beef recorded best significance statistically (1.70) log CFU/g in terms of reduced microbial load compared to other treatments, especially (T3) at 15% the sub of

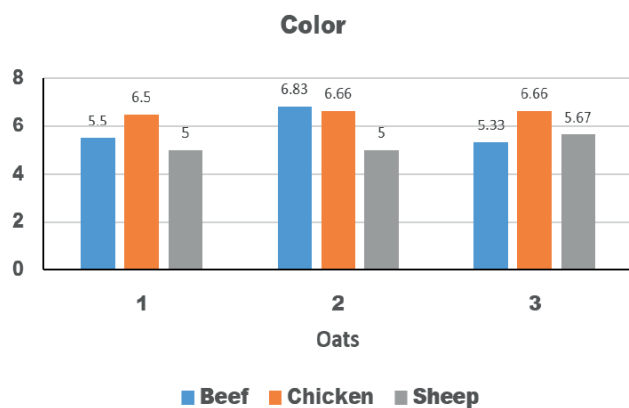


Figure 3. Experimental treatments regarding color with Oats.

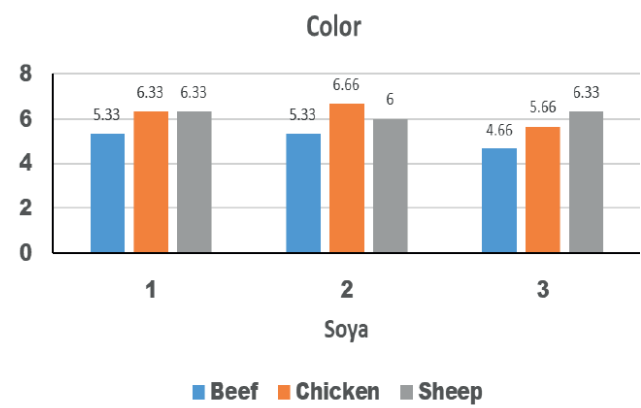


Figure 4. Experimental treatments regarding color with soya.

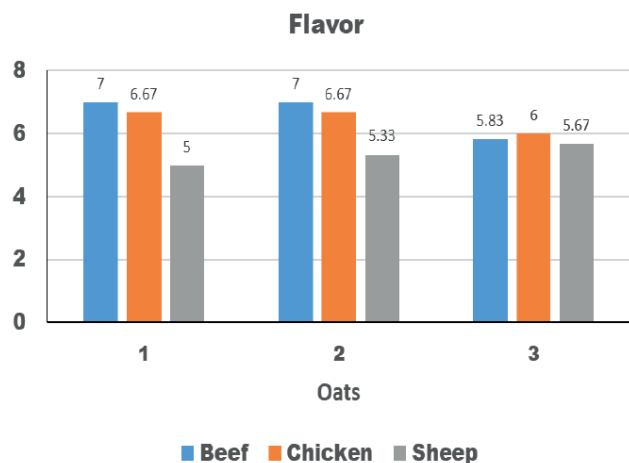


Figure 5. Experimental treatments regarding Flavour with Oats.

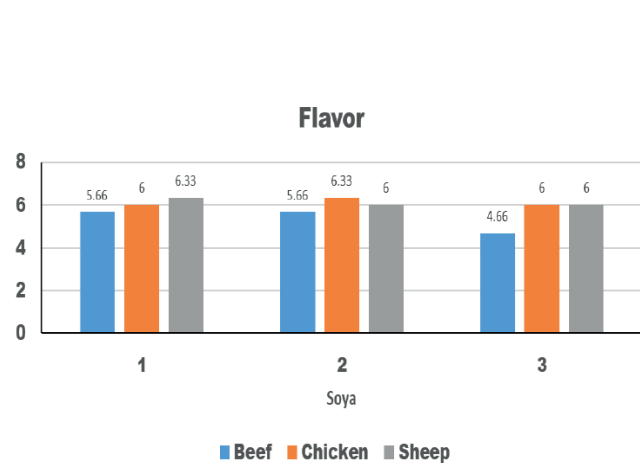


Figure 6. Experimental treatments regarding Flavour with soya.

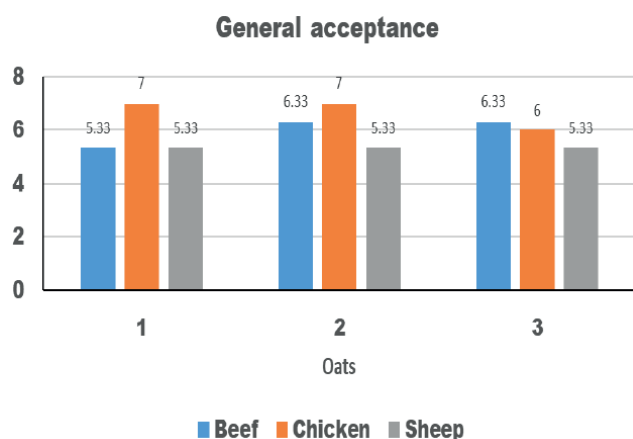


Figure 7. Experimental treatments regarding General acceptance with Oats.

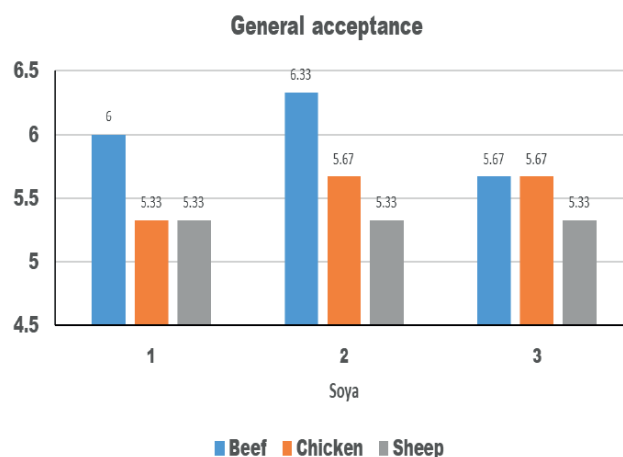


Figure 8. Experimental treatments regarding General acceptance with Soya.

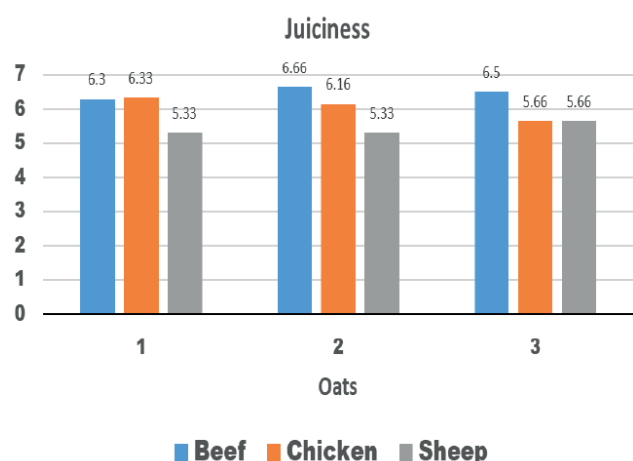


Figure 9. Experimental treatments regarding juiciness with Oats.

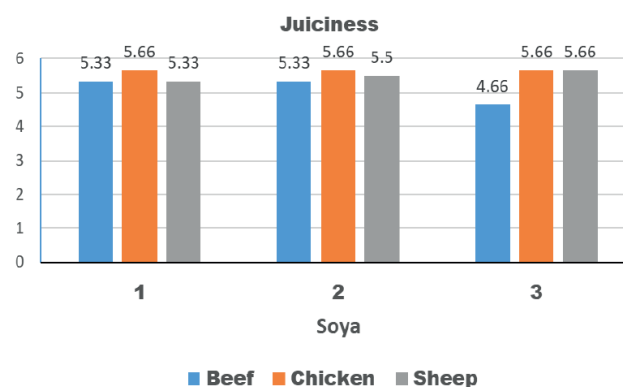


Figure 10. Experimental treatments regarding juiciness with Soya.

chicken that recorded lowest significance (95.6)log CFU/g in terms of rising microbial load.

The results for soya the results illustrated there was statistical significance at $p < 0.05$ between treatments, the sub (T3) at 15% the sub of beef recorded the lowest significance (1.3) log CFU/g in terms of rising microbial load compared to other treatments, especially Chicken and Sheep that recorded high significance (0.00)log CFU/g in terms of reducing microbial load.

Concerning Yeast & Mold

The results for Oats the results illustrated there was statistical significance at $p < 0.05$ between treatments, the sub (T1, T2) at 5%, 10% the sub of beef recorded lowest significance (1.0) log CFU/g in terms of rise microbial load compared to other treatment, especially Chicken and Sheep that recorded high significance (0.00)log CFU/g in terms of reducing microbial load.

The results for soya the results illustrated there was statistical significance at $p < 0.05$ between treatments, the sub (T3) at 15% the sub of beef recorded lowest significance (1.3) log CFU/g in terms of rise microbial load with an offer (T1, T2) at 5%, 10% recorded (1.0) log CFU/g compared to other treatment, especially Chicken and Sheep that recorded high significance (0.00) log CFU/g in terms of reducing microbial load.

Concerning Total Count Bacteria

The results for Oats the results illustrated there was statistical significance at $p < 0.05$ between treatments, the sub (T3) at 15% the sub of chicken recorded the lowest significance (2.96) log CFU/g in terms of rise microbial load compared to other treatments, especially the sub (T1) at 5% the sub of beef that recorded high significance (2.17) log CFU/g in terms of reducing microbial load.

The results for soya the results illustrated there was statistical significance at $p < 0.05$ between treatments, the sub (T3) at 15% the sub of chicken recorded the lowest significance (2.58) log CFU/g in terms of rising microbial load compared to other treatments, especially the sub (T3) at 15% the sub of Beef that recorded high significance (1.57)log CFU/g in terms of reducing microbial load.

Discussion

The findings of this investigation revealed distinct variances between all of the therapies. In general, the burgers of various types of meat with oats and soy fillers in various concentrations are finished. Improve the microbial load as well as the sensory score. It is noted that the tenderness was burgers of the chicken and sheep recorded the best significance,

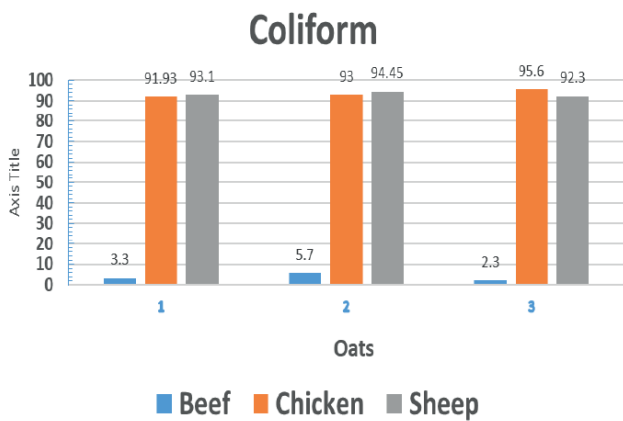


Figure 11. Experimental treatments regarding Coliform with Oats.

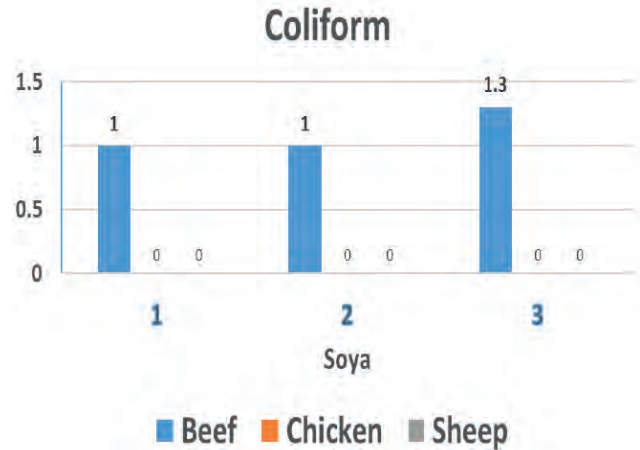


Figure 12. Experimental treatments regarding Coliform with Soya.

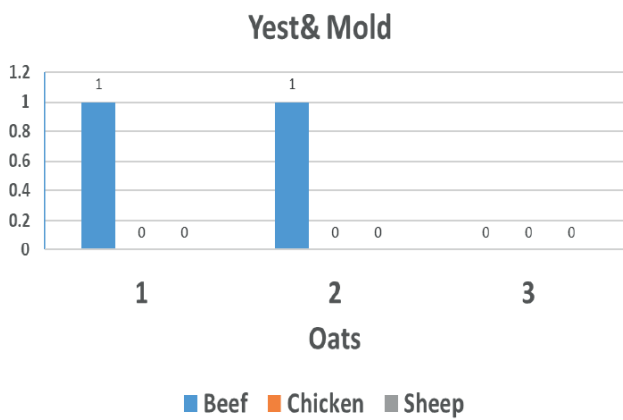


Figure 13. Experimental treatments regarding Yeast & Mold with Oats.

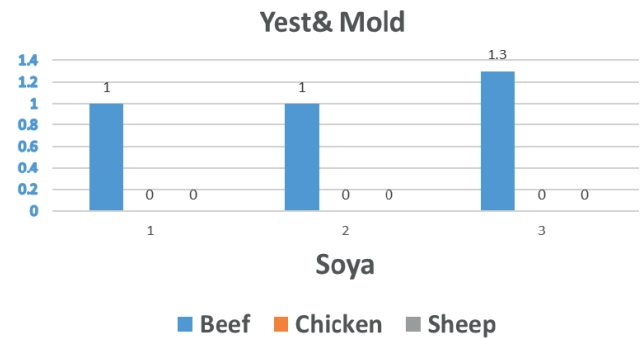


Figure 14. Experimental treatments regarding Yeast & Mold with Soya.

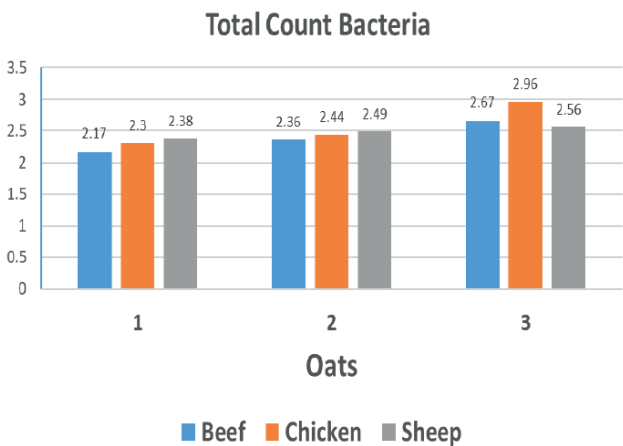


Figure 15. Experimental treatments regarding Total Count Bacteria with Oats.

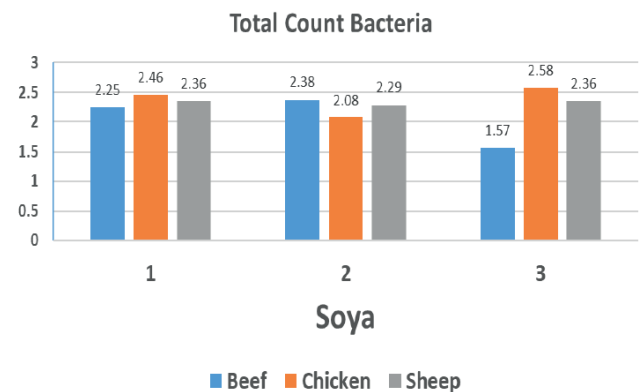


Figure 16. Experimental treatments of Soya.

for the color of chicken burger recorded the best significance, while the flavor of beef and chicken burgers recorded the best significance. While we note the recorded significance for both the general acceptance and juiciness were burgers of the beef and chicken.

Regarding the microbiology aspect, regarding Yeast & Mold were burgers chicken and sheep recorded the best significance, regarding Total Count Bacteria where burger of beef recorded the best significance. The desire to replace synthetic food antioxidants with natural ones has sparked study into ve-

getable sources and the screening of raw materials for finding antioxidants⁹. The benefits of using oat fiber include its superior capacity to retain moisture and prevent meats from drying out when cooked and its mouthfeel, which mimics fat and the ability to maintain the meat's natural flavorings⁵.

Oat fiber, it is believed, offers a comparable mouth feel too fat and retains the inherent tastes of meat¹⁰. Furthermore, it contributes extra fiber to the product¹⁰. The oat fiber also aided in water retention, producing a more juicy product¹¹. In fresh meat products, microbial deterioration and oxidation are

the leading causes of quality loss and the production of potentially harmful secondary chemicals⁹. The proliferation of disease germs can potentially compromise the safety of meat products during the time between production and consumption¹². As a result of this study, it is clear that the increment of the waste of soybean percentage will lower the percentage of cooking loss, which means that the product that has the highest percentage of soybean, the T2 sample, Due to the soybean propensity to hold fat and water, it creates more juice and weight. Generally, the T3 sample gave the lowest hardness level compared to other samples. Based on the proximate analysis performed, this could be due to a high percentage of fat, as hardness is mostly affected by the fat content of a sample, with a high fat content making the item soft and juicy¹³. The effects of chitosan and/or sulfite addition and the storage time were determined in fresh (color deterioration, lipid oxidation, pH, total viable counts, *Escherichia coli* and coliforms, *Salmonella*, appearance and odor) and cooked (appearance, odor, flavor and texture) burgers¹². Using chitosan to minimize the amount of SO₂ needed to increase the shelf life of fresh meat products in retail displays¹². The growth of *E. coli* and *Salmonella* in pork burgers was adequately inhibited by a reduction in SO₂ from 450 to 150 mg kg⁻¹, ensuring their microbial safety; however, this SO₂ reduction was less effective in reducing spoilage bacteria, the usual factor limiting the shelf life of ground meat kept under refrigeration and aerobicity¹².

Conclusions

There is little research on the quality and durability of meat products (burgers) added with fiber. The purpose of this study was to examine the influence of soybean and oat flour as fat replacers and natural antioxidants on the textural quality, microbiological, and sensory acceptability of low-fat meat burgers. Foods with health-promoting features, such as high-fiber and low-fat meat products, are higher. Consumers always have the upper hand when it comes to choosing a food that has been produced using just natural ingredients. Preschoolers, adolescents, and people of all ages should include soya and oats in their diets to increase their nutrient intake, particularly protein, calcium, phosphorus, sodium, potassium, carbohydrate, and iron. These two value-added products are also suitable for vegetarians and persons suffering from cardiovascular disease, obesity, and protein deficiency.

Author Contributions

All authors designed the experiments, who also drafted the report and approved it for publication.

Conflicts of Interest

There is no current or disclosed conflict of interest by the authors of this research or in researching this article and its findings.

Bibliographic references

1. Santhi, D. ; Kalaiannan, A. The Effect of the Addition of Oat Flour in Low-Fat Chicken Nuggets. *J. Nutr. Food Sci.* 2014. 04.
2. Karwowska, M. ; Dolatowski, Z. J. Physicochemical and Sensory Characteristics of Meat Products with Buckwheat and Oat Extrudates, Starch and Soybean Protein Addition. *Charakterystyka Fizykochemiczna I Sensoryczna Wyrobów Mięsnych z Dodatkiem Ekstraktu Gryki i Owsa, Skrobi Orz Białka Sojow.* Polish J. Nat. Sci. 2008. 23, 219–231.
3. Mattila, P., Pihlava, J. M. ; Hellström, J. Contents of phenolic acids, alkyl- and alkenylresorcinols, and avenanthramides in commercial grain products. *J. Agric. Food Chem.* 2005. 53, 8290–8295.
4. Lin, K. W; Mei, M. Y. Influences of Gums , Soy Protein Isolate , and Heating Temperatures on Reduced-Fat. *J. Food Sci.* 2000. 65, 48–52 .
5. Aisha Parveen, Alisha, M. A. ;D. R. P. D. Preparation and standardization of food product by soya chunks and oats as a substitute of meat products and nutraceuticals potential of soybean Aisha. *J. Pharmacogn. Phytochem.* 2018. 7, 1003–1008.
6. García, M. L., Dominguez, R., Galvez, M. D., Casas, C. ; Selgas, M. D. Utilization of cereal and fruit fibres in low fat dry fermented sausages. *Meat Sci.* 2002. 60, 227–236 .
7. Aminah, A. Prinsip penilaian sensori. Kuala Lumpur. Penerbit Universiti Kebangsaan Malays. 2000.
8. ISO 4831. Microbiology of food and animal feeding stuffs. Horizontal method for the detection and enumeration of coliforms. Most probable number technique, www.iso.org. 2006.
9. Moure, A., Cruz, J. M., Franco, D., Dominguez, J. M., Sineiro, J., Dominguez, H., ... ; Parajó, J. C. Natural antioxidants from residual sources. *Food Chem.* 2001. 72, 145–171 .
10. B. PRASAD, M.D. RASHMI, K. P. Y. ; V. K. M. EFFECT OF CASEIN AND OAT FLOUR ON PHYSICOCHEMICAL AND OXIDATIVE PROCESSES OF COOKED CHICKEN KOFTA. *J. Food Process. Preserv.* 2011. 35, 359–368 .
11. E. M. Desmond, D. J. T. ; D. J. B. The Effects of Tapioca Starch, Oat Fibre and Whey Protein on the Physical and Sensory Properties of Low-fat Beef Burgers. *LWT-Food Sci. Technol.* 1998. 31, 653–657.
12. Rafael Serrano, S. B. Reducing SO₂ in fresh pork burgers by adding chitosan Rafael. *Meat Sci.* 2012. 92, 651–658.
13. Baba, N. ; Bachok, S. Effects of soybean waste on the physicochemical analysis of chicken burgers. *J. Tour. Hosp. Culin. Arts* 2011.3, 49

LETTER TO EDITOR / CARTA AL EDITOR

A Single Web-Platform for Invitation or Advertisement of Online Courses and Webinars in These Covid Virus Time

Anupam Saha

DOI. 10.21931/RB/2022.07.01.24

¹M.Pharm Graduate, Pharmacology, NSHM College Of Pharmaceutical Technology, NSHM Knowledge Campus, B.L. Rd., Kolkata - 700053, WB
Corresponding author: sahaanupam05@gmail.com

Innovation is a critical phase in the pharmaceutical enterprise and the healthcare community. And advances in the healthcare era have caused significant upgrades within the greatness of healthcare, in populace fitness, and have contributed to growth in actual fitness expenditure in parallel. Its pursuit is a commercial enterprise, vital for maximum industrialized nations over the latest decades. Advances in the healthcare era have caused significant upgrades withinside the excellent healthcare and feature contributed to will increase in actual fitness expenditure in maximum industrialized nations over the latest decades.

In December 2019, adults in Wuhan, the capital town of Hubei province and a primary transportation hub of China,

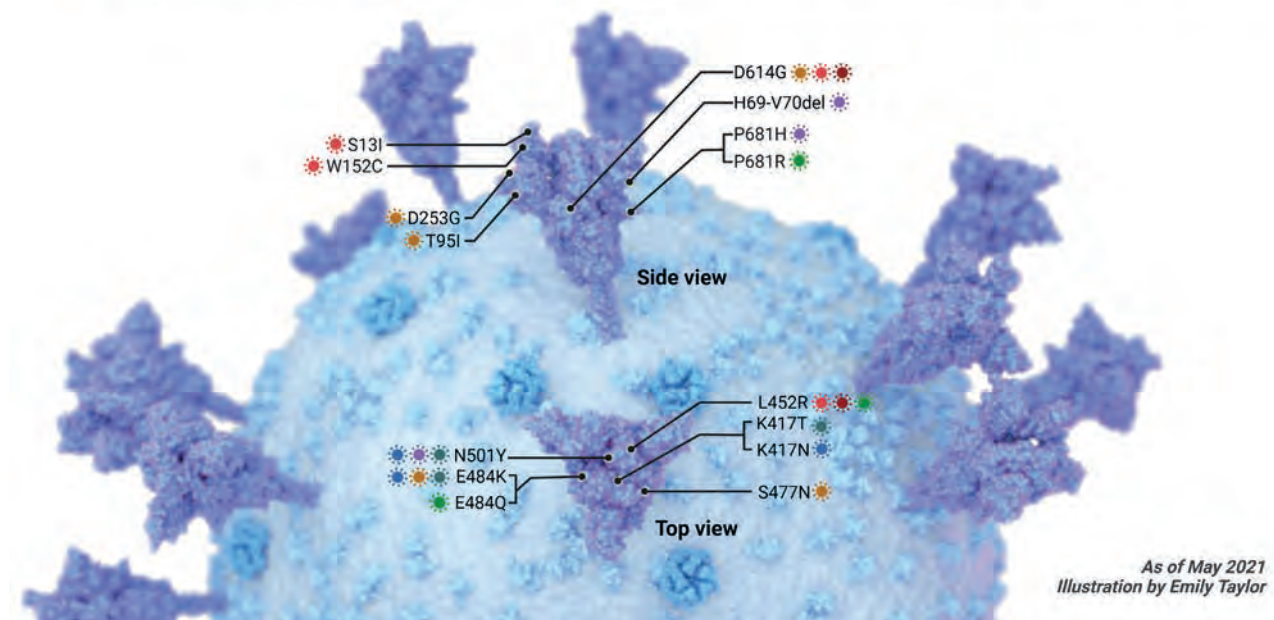
commenced providing nearby hospitals with severe pneumonia of unknown cause. Many preliminary instances had frequent publicity to the Huanan wholesale seafood market that traded stay animals. The surveillance machine (put into the area after the SARS outbreak) was activated, and the sufferers' respiratory samples were dispatched to reference labs for etiologic investigations. On December 31, 2019, China notified the outbreak to the World Health Organization^{1,2}

The Corona Virus(Covid-19) was declared a plague through the World Health Organization (WHO), has exhibited human-to-human transmissibility, and has unfolded hastily throughout nations³. The WHO spoke back shortly using coordinating diagnostics improvement and issuing help on affected

The SARS-CoV-2 Variants of Concern

Key mutations in the spike protein are shown, but mutations in other areas of the genome have been identified and are currently under investigation. Mutations occur on all spike protein subunits.

 B.1.1.7 Discovered: Dec. 14 2020	 B.1.351 Discovered: Dec. 18 2020	 P.1 Discovered: Dec. 4 2020	 B.1.526 Discovered: Nov. 2020	 B.1.427 Discovered: Dec. 2020	 B.1.429 Discovered: Nov. 2020	 B.1.617 Discovered: Oct. 2020
---	---	--	--	--	--	--



Citation: Saha A. A Single Web-Platform for Invitation or Advertisement of Online Courses and Webinars in These Covid Virus Time. *Revis Bionatura* 2022;7(1). 24. <http://dx.doi.org/10.21931/RB/2022.07.01.24>

Received: 7 June 2021 / **Accepted:** 25 November 2021 / **Published:** 15 February 2022

Publisher's Note: Bionatura stays neutral with regard to jurisdictional claims in published maps and institutional affiliations.



Copyright: © 2022 by the authors. Submitted for possible open access publication under the terms and conditions of the Creative Commons Attribution (CC BY) license (<https://creativecommons.org/licenses/by/4.0/>).

person monitoring, specimen collection, and cure and presenting time to time up to date data on the outbreak². Although the governments worldwide have taken various measures to manipulate town-to-town and character-to-person transmission and destiny, research ought to broaden elaborate fashions with an excessive spatial-temporal decision to consider technological solutions. It is the technological know-how that college students manipulate to get an acceptable education in the course of this Covid-19 state of affairs. Now no commercial enterprise assembly happens face to face⁴. Everything is online, the internet the sensation allowed these possibilities. One such inspiration or thought which can be very helpful for college students that can serene the training for college students that is a single internet portal for the commercial of webinars and online courses.

Webinars are seminars that are carried out on the World Wide Web, and they can be meetings, conferences, demonstrations, education or teaching, or activities designed to supply records both one-way or interactively. Webinars can encompass video, audio, and textual communication⁵. Any pupil searching to attend a specific subject matter may also locate a webinar session on that platform. A systematic platform appreciably scans all webinar matters on locating the described search⁶.

Various online courses and webinars occur; not every advertisement pamphlet or commercial pamphlet arrives at every student. Hence, if a single portal could be made where all the universities, all the research academies can invite college students, professionals, and researchers to attend and learn, at this time can be very enigmatic for the pupil to update and upgrade their technical skills, improve their technical abilities, research and relearn, and recognize their topics well. It's vital to acquire expertise from exclusive sources, collect resources, and gather knowledge. So if such a net portal can be generated, all the college students can get entry to and be aware of unique publications below one roof to update their skills[NSV1]. Nowadays, various organizations hold free online conferences/webinars, where many eminent scientists and researchers teach and spread awareness about COVID19 and SARS-CoV-2 variants solutions and various lectures on different topics. COVID pandemic might leave one day, but the online mode of study and online learning will stay. The future generation will benefit immensely if a platform where different organizations advertise their upcoming events on a single platform and are marketed well.

As located on the 'Bionatura' web page of your journal, this idea is encouraged to report a separate area for adaptation, as a separate section for it to be adopted by different organizations coming together to form a unity platform to avoid the missing of any critical webinar of any organization. Collectively shape a solidarity platform to keep away from missing any vital webinar of any organization. We trust that the broader adoption of this notion will notably contribute to the learner's education. To merely the activity which is the idea this letter is all about, just like there is a section in the website of the esteemed journal Bionatura "Open-Access Data and Computational Resources to Address COVID-19" if there could be another section or column to address all the upcoming online events—followed by inviting all the major universities across the globe. Each organization that wishes to advertise its event may upload the details manually, reflecting on the website.

This idea is not limited to the Bionatura journal itself; all the viewers reading this letter may reach out to their organization and use this idea to form a website or form a section. Then, reaching out to leading universities to upload their proforma or pamphlet into the portal, this lucid idea may help teachers, re-

searchers, and students immensely. More advertisements will be visible, more options will be available, and the maximum audience will capture more knowledge.

Conclusions

Technology has been the best in this generation and more to grow. The single platform could be handy for each student who uses webinars and online training to the best of their abilities. Many students from across the globe can attend web meetings and e-conferences. The organizers may also benefit not only from the students or researchers but also from professionals to get much more participants.

Acknowledgment

I want to thank Miss Moulima Das, M.Pharm from NSHM Knowledge Campus - Kolkata, for the technical help during this letter drafting and the encouragement to write this letter.

Source of Funding

Nil

Conflict of Interest

Nil

Bibliographic references

1. Singhal T. A Review of Coronavirus Disease-2019 (COVID-19). *Indian J Pediatr.* 2020;87(4):281-286. doi:10.1007/s12098-020-03263-6
2. Unhale SS, Ansar QB, Sanap S, et al. A Review On Corona Virus (Covid-19). *World J Pharm Life Sci.* 2020;6(4):109-115.
3. Sadeghian M. The Rapid Spread of COVID-19 (Corona virus) in Iran, Actions which were taken. *Biomed J Sci Tech Res.* 2020;27(4). doi:10.26717/BJSTR.2020.27.004521
4. Sri KB. World Under The Pandemic Situation: Novel Corona Virus Paralyzing World's Activities. In: *COVID-19 Pandemic Update 2020.* Royal Book Publishing; 2020:128-133. doi:10.26524/royal.37.10
5. White A. Reflections on the Use of Webinar Technology for Teaching. Published online 2019. Accessed November 21, 2020. <https://hal.archives-ouvertes.fr/hal-01976364>
6. Selcuk AA. A Guide for Systematic Reviews: PRISMA. *Turk Arch Otorhinolaryngol.* 2019;57(1):57-58. doi:10.5152/tao.2019.4058

attending the National Diabetes Center (NDC)/Mustansyriah University were enrolled in the study and compared with 40 control subjects that were defined by achieving the goals (pituitary adenoma, size regression, Insulin-like growth factor-1 and growth hormone decrement down to the recommended, predefined targets)¹². They were subdivided into subgroups according to their age, gender, lipid profile, concomitant diabetes and glycemic control in diabetic patients. Neopterin was measured using enzyme-linked immune-sorbent assay (ELISA), which is done utilizing Human Neopterin (NEOP)ELISA kit was sandwich methodology. The Micro ELISA plate provided in this kit has been pre-coated with an antibody specific to NEOP. Correlation between NEOP and other biochemical and clinical variables was studied using Pearson correlation methodology. Statistical package of social science (SPSS) _ version 27 was used to analyze the data.

Results

Eighty acromegalic patients were recruited, thirty-nine (39) are diabetics, and the other forty-one (41) are nondiabetics, while the control group includes forty (40) nondiabetic non-acromegalic healthy persons. All the recruited patients are registered in the National Diabetes Center (NDC)/ Mustansyriah University. The results of age and gender were presented in Table (1). The age was ranged from 25-78 years, and the more percentage of diabetic acromegalic patients was shown within the age group (40-49years) As they represent (46.2%) of patients. Neopterin levels are highest in diabetic acromegalic patients under 50, followed by nondiabetic acromegalic patients, and finally, the control group. Neopterin levels are higher in male diabetic acromegalic patients than in nondiabetic acromegalic patients, while the opposite is true in the control group, but this steady decline is not statistically significant. The usual range of serum neopterin is (3-100). Neopterin is high among diabetic acromegalic patients, followed by nondiabetic acromegalic patients and, finally, the control group. As revealed in table (2).

Table (3) shows that: The level of Neopterin is the lowest among the control group versus diabetic acromegalic and

nondiabetic acromegalic patients. Normalization of HDL is associated with elevation of Neopterin in diabetic acromegalic and nondiabetic acromegalic patients. Elevation of LDL is associated with high Neopterin in diabetic acromegalic, followed by nondiabetic acromegalic patients. However, the difference did not reach statistical significance. The lowest VLDL is associated with a higher neopterin in diabetic patients when compared with another study group. The highest cholesterol level was correlated with the highest neopterin level, whereas diabetic acromegalic was followed by nondiabetic acromegalic patients and the control group. Elevation of triglyceride value is associated with high Neopterin in diabetic acromegalic followed by nondiabetic acromegalic; the impact of high triglyceride on Neopterin level is true in the control groups as well. Neopterin is the highest in non-acromegalic when their HbA1C is high (does not fulfill the definition of diabetic ranging from 5.7-6.4%), the level of Neopterin drops in diabetic acromegalic subjects when their glycemic control is poor. Normalization of GH is associated with lower Neopterin levels among nondiabetic acromegalic subjects versus diabetic acromegalic subjects. The highest number of diabetic acromegalic (36) patients have an abnormal value of IGF-1 which shows a mean for neopterin in higher (89.85) than that of nondiabetic or control groups (41-78). The diabetic acromegalic patients also showed a higher neopterin level, which was associated with a highest value for IFN- γ compared with nondiabetic acromegalic patients or the control group.

Discussion

Table -1 Shows that most of the acromegalic patients are within the age group of 40-49 years at the time of diagnosis, while few patients are group 30-39, and no acromegalic subjects were registered his age is less than 30 years. The median age of acromegalic, as stated by (13) in Duhok province, was (44.9 years). The median age agrees with (14), who found that it is (49.2 \pm 8.9 years) in Bagdad province. The explanation of the results of age that acromegaly disease. Most people are diagnosed in their third or fourth decade of life. Recent studies, however, have revealed an increase in the incidence and fre-

		Diabetic Acromegaly		Nondiabetic Acromegaly		Healthy control		P-value
		No	%	No	%	No	%	
Age (years)	<30years	-	-	1	2.4	4	10.0	0.067
	30---39	3	7.7	9	22.0	7	17.5	
	40---49	18	46.2	12	29.3	16	40.0	
	50---59	10	25.6	16	39.0	9	22.5	
	=>60years	8	20.5	3	7.3	4	10.0	
Age (years)	<50years	21	53.8	22	53.7	27	67.5	0.354
	=>50years	18	46.2	19	46.3	13	32.5	
	Mean \pm SD (Range)	51.1 \pm 10.6 (30-78)		46.6 \pm 9.2 (29-67)		45.5 \pm 11.3 (25-69)		
Gender	Male	26	66.7	27	65.9	20	50.0	0.228
	Female	13	33.3	14	34.1	20	50.0	
*Significant difference between percentages using Pearson Chi-square test (χ^2 -test) at 0.05 levels.								
#Significant difference between two independent means using Students-test at 0.05 levels.								
^Significant difference among more than two independent means using ANOVA-test at 0.05 levels.								

Table 1. Demographic data of Diabetic acromegalic, nondiabetic acromegalic patients and control group (non- acromegalic nondiabetic counterparts).

		Neopterin (pg/mL)					
		Diabetic Acromegaly		Nondiabetic Acromegaly		Healthy control	
		No	Mean±SD	No	Mean±SD	No	Mean±SD
Age (years)	<30years	-	-	1	20.025±	4	30.483±18.916
	30---39	3	162.571±154.151	9	84.189±80.716	7	32.508±28.097
	40---49	18	110.488±125.313	12	56.617±44.303	16	43.710±31.496
	50---59	10	67.980±59.796	16	63.288±22.261	9	55.308±29.230
	≥60years	8	71.699±36.871	3	122.303±101.851	4	31.197±28.324
	P-value		0.417		0.268		0.444
Age (years)	<50years	21	117.928±126.779	22	66.233±61.666	27	38.846±28.843
	≥50years	18	69.633±49.561	19	72.606±45.325	13	47.889±30.072
	P-value		0.138		0.712		0.365
Gender	Male	26	113.014±118.276	27	70.571±45.285	20	37.078±28.277
	Female	13	60.888±32.328	14	66.517±70.044	20	46.492±30.018
	P-value		0.129		0.823		0.314
#Significant difference between two independent means using Students-t-test at 0.05 level.							
^Significant difference among more than two independent means using ANOVA-test at 0.05 level.							

Table 2. Neopterin concentration in Diabetic acromegalic, nondiabetic acromegalic and control group according to age, gender, duration of disease.

		Neopterin (pg/mL)					
		Diabetic Acromegaly		Nondiabetic Acromegaly		Healthy control	
		No	Mean±SD	No	Mean±SD	No	Mean±SD
HDL (mg/dL)	Low	25	90.253±110.943	17	63.412±61.999	1	4.328±
	Normal (35-70)	14	105.255±82.462	24	73.277±48.802	39	42.745±28.910
	P value		0.662		0.572		0.197
LDL (mg/dL)	Low	3	71.774±40.778	8	74.157±71.995	25	44.722±29.543
	Normal (65-170)	32	89.175±90.928	28	68.356±51.048	15	36.889±28.880
	High	4	165.244±185.981	5	65.885±50.831	-	-
	P value		0.340		0.957		0.418
VLDL (mg/dL)	Low	39	95.638±100.763	41	69.187±54.141	40	41.785±29.176
	Normal (65-170)	-	-	-	-	-	z^-
	P value		-		-		-
Cholesterol (mg/dL)	Normal (<200)	23	87.480±72.162	25	73.278±63.979	40	41.785±29.176
	High	16	107.366±133.549	16	62.794±34.582	-	-
	P value		0.551		0.552		-
Triglyceride (mg/dL)	Normal (40-140)	6	143.365±167.084	10	84.355±76.048	31	46.242±29.962
	High	33	86.961±84.795	31	64.293±45.518	9	26.432±21.003
	P value		0.211		0.314		0.072
#Significant difference between two independent means using Students-t-test at 0.05 level.							
^Significant difference among more than two independent means using ANOVA-test at 0.05 level.							

Table 3. Neopterin concentration in Diabetic acromegalic, nondiabetic acromegalic and control group according to lipid profile.

		Neopterin (pg/mL)					
		Diabetic Acromegaly		Nondiabetic Acromegaly		Healthy control	
		No	Mean±SD	No	Mean±SD	No	Mean±SD
HbA1c (%)	Normal (4.2-6.2%)	2	94.946±73.644	31	56.573±32.121	40	41.785±29.176
	High	37	95.676±102.794	10	108.287±85.685	-	-
	P value		0.992		0.007#		-
GH (ng/mL)	Low	2	77.000±20.648	2	36.957±40.549	37	44.429±28.720
	Normal (0.4-10AM; 1-14AF)	37	96.646±103.369	38	72.323±54.565	3	9.180±5.370
	High	-	-	1	14.460±	-	-
	P value		0.792		0.405		0.043#
IGF-1 (ng/mL)	Low	-	-	-	-	-	-
	Normal (200-450)	36	89.859±96.013	38	71.126±55.792	40	41.785±29.176
	High	3	164.992±154.175	3	44.620±7.940	-	-
	P value		0.219		0.421		-
Interferon-gamma (ng/mL)	Low	-	-	-	-	-	-
	Normal (1.2-80)	-	-	1	7.475±	1	43.120±
	High	39	95.638±100.763	40	70.729±53.910	39	41.751±29.557
	P value		-		0.254		0.964
#Significant difference between two independent means using Students-t-test at 0.05 level.							
^Significant difference among more than two independent means using ANOVA-test at 0.05 level.							

Table 4. Neopterin concentration in Diabetic acromegalic, non- diabetic acromegalic and control group according to HbA1C, GH, IGF-1 and Interferon – gamma.

quency of acromegaly in the elderly, most likely as a result of longer life expectancy. There is a delay in diagnosis, as there is in the younger population with acromegaly, which is exacerbated by the similarities between the aging process and some of the disease's symptoms. As one might assume, comorbidities are more common in senior people with acromegaly than in younger patients. The diagnostic criteria for older patients are the same². In the current study, males represent (66.3%) of enrolled patients while females are only (33.7%); this result is similar to other studies, the rate of Transsphenoidal- selective adenomectomy (TSA) is 89.7% and 76.5% in males and females, respectively (P, 0.001)¹⁵.

Statin use reduces the neopterin level; statin reduces the neopterin level plus the well-known cardiovascular protective effect. This may be related to the fact that neopterin is a soluble marker of monocyte activation, and monocyte activation has been linked to the pathogenesis of coronary artery disease¹⁶. In diabetic, acromegalic subjects normal HDL is associated with an increment in neopterin; some investigators pointed out to the fact that neopterin is associated with reduced HDL levels. However, it shows no association with other markers of metabolic syndrome, namely waist-hip ratio¹⁷. Poor glycaemic is associated with a decrement in neopterin level; it has been found that neopterin level is elevated in people with insulin resistance¹⁸. Neopterin is found to be high among patients with high of IGF-1, once neopterin, and IGF-1 were found to be high in elderly patients hospitalized, followed by delirium, and

it has been proposed that oxidative stress and activation of the immune system may be the cause of an increase in both biomarkers¹⁸.

Conclusions

Neopterin has the highest level among acromegalic diabetics, followed by a nondiabetic acromegalic and the control, respectively. Neopterin is higher in males with DM and acromegaly. Elevation of Triglyceride (>150 mg/dL) is associated with the high neopterin in diabetic acromegalic followed by nondiabetic acromegalic and control group. People with diabetes with poor glycaemic control have low neopterin, but the contrary is true for nondiabetic subjects where the progressive increment of HbA1c is associated with higher neopterin levels. However, those subjects did not the definition of diabetes (HbA1c<6.5%). A well designed prospective study enrolling a higher number of acromegalic subjects is highly recommended to find out the impact of neopterin on the progression of acromegaly and its mortality to find out a modal of therapy that modulates the level of this molecule fruitfully, the sometimes it may be prudent to find out if neopterin has any relation with other molecules as IGF-1 and GH and the reflection of these molecules on acromegaly and its comorbidities and mortality.

Bibliographic references

1. Sesmilo, G. et al. Changes in acromegaly treatment over four decades in Spain: Analysis of the Spanish Acromegaly Registry. *Pituitary*. (2013).16, 115–121.
2. Jallad, R.S. and Marcello, D.B. Acromegaly in the elderly patient. *Arch Endocrinol Metab*. (2019).63/6 , 638 - 645.
3. Olarescu, N. C. & Bollerslev, J. . The Impact of Adipose Tissue on Insulin Resistance in Acromegaly. *Trends in Endocrinology & Metabolism*. (2016).27, 226–237.
4. Pivonello R, Auriemma RS, Grasso LF, Pivonello C, Simeoli C, Patalano R, Galdiero M, Colao A . Complications of acromegaly: cardiovascular, respiratory and metabolic comorbidities. *Pituitary*. (2017). 20:46– 62.
5. Ferràu, F., Albani, A., Ciresi, A., Giordano, C., & Cannavò, S. Diabetes Secondary to Acromegaly: Physiopathology, Clinical Features and Effects of Treatment. *Frontiers in endocrinology*,(2018). 9, 358.
6. Pingle, Shubhangi, et al.: "Neopterin: Biomarker of cell-mediated immunity and potent usage as biomarker in silicosis and other occupational diseases." *Indian Journal of Occupational and Environmental Medicine*, (2008).vol. 12, no. 3, 2008, p. 107.
7. Grammer TB, Fuchs D, Boehm BO, Winkelmann BR, Maerz W.: Neopterin as a predictor of total and cardiovascular mortality in individuals undergoing angiography in the Ludwigshafen risk and cardiovascular health study. *Clin Chem*.(2009). 55:1135–46.
8. Sucher R, Schroecksadel K, Weiss G, Margreiter R, Fuchs D, Brandacher G.: Neopterin, a prognostic marker in human malignancies. *Cancer Lett*. (2010). 287:13– 22.
9. Oxenkrug GF.: Interferon-gamma-inducible kynurenines/pteridines inflammation cascade: implications for aging and aging-associated psychiatric and medical disorders. *J Neural Transm*. (2011).118:75–85.
10. Oxenkrug G, Tucker KL, Requintina P, Summergrad P.: Neopterin, a marker of interferon-gamma-inducible inflammation, correlates with pyridoxal-5'- phosphate, waist circumference, hdl-cholesterol, insulin resistance and mortality risk in adult boston community dwellers of Puerto Rican origin. *Am J Neuroprot Neuroreg*. (2011). 3:48–52.
11. Murr C, Widner B, Wirleitner B, Fuchs D.: Neopterin as a marker for immune system activation. *Curr Drug Metab*.(2002). 3:175–87.
12. Melmed S. Tight control of growth hormone: an attainable outcome for acromegaly treatment. *J Clin Endocrinol Metab*. (1998);83;3409-3410.
13. Qasim. B. :Duhok/IRAQ acromegaly; one year of experience. *Endocrine Abstracts* (2017) 49 EP94.
14. Hammood, S.D.: Serum Osteopontin and Osteoprotegerin levels in a sample of Iraqi patients with acromegaly and type 2 diabetes mellitus. Master thesis , Clinical Biochemistry, College of Medicine, Mustansiriyah University, Iraq.(2020).
15. Park, S.E., Cheol, R.K., Ju, H.M., Eui, H.K., Sun, H. K. and Eun, J. L.: Age- and Sex-Specific Differences as Predictors of Surgical Remission Among Patients With Acromegaly . *J ClinEndocrinol-Metab*.(2018). 103(3):909–916.
16. Ray, K. K., Morrow, D. A., Sabatine, M. S., Shui, A., Rifai, N., Cannon, C. P., & Braunwald, E.: Long-term prognostic value of neopterin: a novel marker of monocyte activation in patients with acute coronary syndrome. *Circulation*,(2016).115(24), 3071-3078.
17. Chuang, S. C., Boeing, H., Vollset, S. E., Midttun, Ø., Ueland, P. M., Bueno-de-Mesquita, B. & Aleksandrova, K. :Cellular immune activity biomarker neopterin is associated hyperlipidemia: results from a large population-based study. *Immunity & Ageing*,(2016).13(1), 1-11.
18. Gürcü, S., Girgin, G., Yorulmaz, G., Kılıçarlan, B., Efe, B., & Baydar, T. : Neopterin and biopterin levels and tryptophan degradation in patients with diabetes. *Scientific reports*,(2020).10(1), 1-8.
19. Egberts, A., Wijnbeld, E. H., Fekkes, D., Van Der Ploeg, M. A., Ziere, G., Hooijkaas, H., ... & Mattace-Raso, F. U. : Neopterin: a potential biomarker for delirium in elderly patients. *Dementia and geriatric cognitive disorders*, (2015).39(1-2), 116-124..

ARTICLE / INVESTIGACIÓN

Suitability of some well water for different human uses by studying some physicochemical properties

Israa Salman Dalas¹, Muqdad Altae² and Raghad Mukdad Mahmood³

DOI. 10.21931/RB/2022.07.01.26

¹ Department of Biology, College of Education for Pure Science, University of Tikrit, Iraq.² Ministry of Education, Salah Al-din Directorate, Iraq.

Corresponding author: muqdadaltae@yahoo.com

Abstract: The present study is carried out to identify (pH, EC, TDS, alkalinity, total hardness, calcium Ca, magnesium Mg, sulfate SO₄, chloride Cl₂) and Mpn cell / 100ml Total number of coliform bacteria of groundwater indicators in some wells within villages of Al-Dhuluiya, Al-Alam in Salahuddin and wells from Kayara (Al-Jawaana and Al-Jadaa villages). Four wells were studied for two seasons from November, December 2016 and January 2017. Results of this study showed that there was a seasonal variation in some chemical and physical factors. The groundwater was neutral because pH values were ranged (7-8.6). Electrical conductivity values were between (2543-50305) micro siemens. Total hardness values were within permissible limits (1200-2800 mg/L). Calcium and magnesium hardness between (1000-1950) mg /L, (100-1282) mg /L, respectively. Total dissolved solids were between (261-3245). Chloride ions (Cl⁻) in groundwater of studied samples were within the permissible limits for watering of animals and irrigation of plants, with values range (79-259 mg/l) and sulfate values were in range (460-1055) mg/L. The total number of coliform were between (3-240) cell/100 ml.

Key words: Groundwater, physicochemical parameters, wells, TDS, pollution.

Introduction

Groundwater can be defined as the portion of the water between two layers and the filtration of rainwater into the soil and lower ground layers. Thousands of years ago, groundwater was one of the most critical water supplies that humanity relied on, especially in dry and semi-arid regions where millions of people lived¹. It is distinguished by a high concentration of dissolved salts when compared to river water. This could be due to the slow movement of groundwater, which dissolves sections of the rocks it passes through, and the salts changed into it. The majority of these salts are calcium and magnesium. This water's mineral content separates it from other bodies of surface water. The salt ingredients vary depending on the geological nature of the place². Groundwater was employed for agricultural purposes in village settings when no other water resources were accessible. Human activities have progressively contaminated groundwater³. The quality of groundwater results from the interactions of many processes during the hydrological cycle. It is varied according to the depth, different places and nature of geological formation⁴.

Groundwater lacks suspended materials due to the infiltration process through which the water passes; therefore, deep well waters are colorless, pure, and have stable compositions, compared with less deep well waters. The depth of well waters and their isolated conditions make their temperature almost constant or change only a few degrees. This is important in the field of industry and thermodynamics⁵. Because of the low levels of the Tigris and Euphrates rivers and the recent rain drought, the demand for well water in Iraq has declined recently. Groundwater in Iraq is becoming increasingly significant for drinking and irrigation⁶. The primary goal of this study was

to assess well water quality and suitability for diverse uses by investigating some physical and chemical aspects of good samples collected.

Materials and methods

Description of the research field

Four wells were selected within villages of Al-Dhuluiya, Al-Alam in Salahuddin government and wells from Kayara (Al-Jawaana and Al-Jadaa villages). The study areas have geological formation areas and sea level characteristics.

Well 1

This well is located at a depth of 10 meters in Al-Alam, a populous region. This well is now closed and is only utilized for home purposes and irrigation.

Well 2

It is located in Al-Dhuluiya at a depth of 20 m, and it is of the open type and used for crops irrigation.

Well 3

It is located in the village of Al-Jawaana at a depth of 15 m. The well is of the closed type, which is used for crops irrigation also.

Well 4

The well is located in Al-Jadaa village at a depth of 40 m,

Citation: Salman Dalas I, Altae M, Mukdad Mahmood R. Suitability of some healthy water for different human uses by studying some physicochemical properties. *Revis Bionatura* 2022;7(1). 26. <http://dx.doi.org/10.21931/RB/2022.07.01.26>

Received: 2 December 2021 / **Accepted:** 21 January 2022 / **Published:** 15 February 2022

Publisher's Note: Bionatura stays neutral with regard to jurisdictional claims in published maps and institutional affiliations.

Copyright: © 2022 by the authors. Submitted for possible open access publication under the terms and conditions of the Creative Commons Attribution (CC BY) license (<https://creativecommons.org/licenses/by/4.0/>).



and it is of closed type and used for irrigation.

Sample Collection

Water samples were collected from different wells from November, December 2016 and January 2017. Standard methods of sample collection and laboratory analysis were followed⁷⁻⁹ by taking one sample per month during the study period. Physicochemical measurements were performed as follows: pH, Electrical Conductivity and pH were measured by using (pH-EC meter, HI 9812, Hanna instrument), TDS, Total Alkalinity: The method of correction with sulfuric acid (N 0.01) was followed by the presence of the orange instance, Total hardness and Ca hardness was measured with standard N2E-DTA (N01,0) with Erichrom Black T and Murexide as dry powder respectively^{7,8}, Calcium (Ca), Magnesium (Mg), Sulphate (SO₄), Chloride Cl⁻: was measured by correction with standard silver nitrate solution (N 0.0141) with potassium dichromate^{8,9}, and Mpn cell / 100ml (Total number of coliform bacteria).

Statistical Analysis

The computer was used through the ready-made statistical program, SPSS, (the load test of variance and the Duncan test, a test that shows us which of the categorical variables differs from the other in the occurrence of changes. The studied significance at the level of significance $p \leq 0.05$.

Results

pH

Values of pH of the present study are shown in table (1). The maximum pH value was (8.6) found in the Al-Jwaana well in November and the minimum value was 7 in wells of Salahuddin government as in table (1). Analysis of variance showed significant differences in different times and the different wells ($P \leq 0.05$).

Electrical conductivity EC

The conductivity values in the different wells ranged from 2543 $\mu\text{hs/cm}$ in January in Al-Alam well to 50305 $\mu\text{hs/cm}$ in January in Al-Jadaa well. The statistical analysis showed significant differences ($P \leq 0.05$) among the different wells. These values are shown in table (2).

Chloride

Differences were observed in the values of chloride table (3). The minimum and maximum ranges of the chloride value were (59-259)mg/L. The analysis of variance revealed considerable temporal differences ($P \leq 0.01$). During the study period, there were no geographic disparities between the wells.

Alkalinity

The alkalinity ranges of the samples during the study pe-

riod are shown in table (4). Values were from 80mg/L to 160 mg/L. Results were statistically significant ($P \leq 0.05$) spatially and non - significant temporal.

Total Hardness

The total hardness values are shown in table(5). The total hardness during the study period ranged from 1200 mg/L in November in Al-Jadaa well to 2800 mg/L in both of November and January months in Al-Jwaana well. Statistical analysis revealed that there were significant regional differences ($P \leq 0.05$) and significant temporal differences ($p \leq 0.01$).

Calcium and Magnesium hardness

The maximum value of calcium hardness was 1950mg/L, and the minimum value was 1000mg/L, and magnesium hardness was (200-1282) mg/L among the different wells. Analysis of variance showed significant spatial difference ($P \leq 0.01$). Table (6) shows these values. Table (7) shows the values of the magnesium hardness, which were (160- 2600) mg/L. Statistical analysis showed significant spatial and temporal differences ($p \leq 0.01$).

Sulfate (SO₄)

As shown in Table (8), the relative sulfate values for wells were (460-1055) mg/L. In January, a water sample taken at Al-Alam well found a low concentration of 460 mg/L, while a water sample taken at Al-Dhuluiya revealed a maximum concentration of 1055 mg/L.

Total Dissolved Solids (TDS)

Electrical conductivity (EC) and total dissolved solids (TDS): As indicated in Table (9), the TDS was obtained for four wells from different areas ranging from (261-3245) mg/L.

Drinking water coliform bacteria

In this study, as in Table (10), all wells were revealed bacteria pollution. Results were between (3-240). Maximum and only high value was in Al-Alam well in November.

Discussion

The pH of aquatic systems is an excellent indicator of water quality and contamination extent. The results of this study differed slightly from those of Ghaeeb's¹⁰ on the physical, chemical, and bacteriological properties of some wells in Tikrit city (7.49- 7.83).

EC

At 25 °C, the ability of one cm³ of water to transmit electrical current is defined. This factor is assessed by ($\mu\text{hs/cm}$) or (Mhs/cm). Conductivity depends on the soluble salts concentration and water temperature¹¹. All of the readings were close, but the Al-Alam well in January was 50305, which could

Well	Month	November	December	Jan	Mean of Wells
Al-Dhuluiya		7.1	7.4	7	7.16 A
Al-Alam		7	7.6	7.2	7.26 A
Al-Jadaa		7.6	7.5	7.8	7.63 A
Al-Jawaana		8.6	7.3	7.7	7.86 A
Mean of months		7.58 a	7.45 a	7.43 a	

* Similar symbols indicate no significant differences

Table 1. pH values during the study period.

Well	Month	November	December	Jan	Mean of Wells
Al-Dhuluiya		3503	4062	3767	3777.3 C
Al-Alam		3745	2863	2543	3050.3 D
Al-Jadaa		6651	6410	50305	21122.0 A
Al-Jawaana		4270	4431	6095	4932.0 B
Mean of months		4542.3 b	4441.5 b	15677.5 a	

* Similar symbols indicate no significant differences

Table 2. Electrical Conductivity EC ($\mu\text{S}/\text{cm}$) values during the study period.

Well	Month	November	December	Jan	Mean of Wells
Al-Dhuluiya		200	259	230	229.67 A
Al-Alam		192	150	167	169.67 B
Al-Jadaa		150	191	200	180.33 B
Al-Jawaana		79	99	81	86.33 C
Mean of months		155.25 a	174.75 a	169.5 a	

* Similar symbols indicate no significant differences

Table 3. Chloride Cl (mg/L) values during the study period.

Well	Month	November	December	Jan	Mean of Wells
Al-Dhuluiya		120	140	160	140.0 A
Al-Alam		80	115	140	111.7 B
Al-Jadaa		120	100	80	100.0 B
Al-Jawaana		160	140	120	140.0 A
Mean of months		120.0 a	123.8 a	125.0 a	

* Similar symbols indicate no significant differences

Table 4. Alkalinity (mg/L) values during the study period.

Well	Month	November	December	Jan	Mean of Wells
Al-Dhuluiya		1800	2500	2200	2166.7 B
Al-Alam		1400	1950	1400	1583.3 C
Al-Jadaa		1200	1200	1800	1400.0 D
Al-Jawaana		2800	2500	2800	2700.0 A
Mean of months		1800.0 b	2037.5 a	2050.0 a	

* Similar symbols indicate no significant differences

Table 5. Total hardness (mg/L) values during the study period.

Well	Month	November	December	Jan	Mean of Wells
Al-Dhuluiya		1000	1218	1200	1139.3 C
Al-Alam		1200	1500	1000	1233.3 B
Al-Jadaa		1000	1100	1600	1233.3 B
Al-Jawaana		1600	1450	1950	1666.7 A
Mean of months		1200.0 c	1317.0 b	1437.5 a	

* Similar symbols indicate no significant differences

Table 6. Calcium Ca (mg/L) values during the study period.

Well	Month	November	December	Jan	Mean of Wells
Al-Dhuluiya		800	1282	1000	1027.3 A
Al-Alam		200	450	400	350.0 B
Al-Jadaa		200	100	200	166.7 C
Al-Jawaana		1200	1050	850	1033.3 A
Mean of months		600.0 b	720.5 a	612.5 b	

* Similar symbols indicate no significant differences

Table 7. Magnesium Mg (mg/L) values during the study period.

Well	Month	November	December	Jan	Mean of Wells
Al-Dhuluiya		1023	1055	933	1003.67 A
Al-Alam		460	468	502	476.67 C
Al-Jadaa		835.2	625	816	758.73 B
Al-Jawaana		610.68	841.34	805	752.34 B
Mean of months		732.22 a	747.34 a	764.00 a	

* Similar symbols indicate no significant differences

Table 8. SO₄ (mg/L) values during the study period.

Well	Month	November	December	Jan	Mean of Wells
Al-Dhuluiya		261	275	446	327.33 D
Al-Alam		1171	1112	1030	1104.33 C
Al-Jadaa		2850	2563	3245	2886.00 A
Al-Jawaana		1013	1588	1232	1277.67 B
Mean of months		1323.75 c	1384.50 b	1488.25 a	

* Similar symbols indicate no significant differences

Table 9. (TDS) mg/L values during study period.

Well	Month	November	December	Jan	Mean of Wells
Al-Dhuluiya		3	9	21	11.0 C
Al-Alam		240	21	43	101.3 A
Al-Jadaa		43	75	21	46.3 B
Al-Jawaana		64	9	9	27.3 C
Mean of months		87.5 a	28.5 b	23.5 b	

* Similar symbols indicate no significant differences

Table 10. Mpn Total account of bacteria (cell/100ml) values during the study period.

be related to rainfall, which washes away salts from nearby soils. The current work's results were comparable to 1920-7675) Al-(Obaidy's hs/cm in Salahuddin Province's northwestern region¹².

Alkalinity

Most groundwater carbonate and bicarbonate ions are derived from carbon dioxide in the soil¹³. The alkalinity values ranged between 80mg/L and 160 mg/L. This could be due to the high rate of organic matter decomposition by bacteria and an increase in carbon dioxide (CO₂), which will result in the creation of bicarbonate¹⁴.

Total hardness

Show the concentration of calcium and magnesium, which can precipitate when heated and have a detrimental impact on the solubility of soap in water¹⁵. Some wells have a high value, which could be attributed to rains washing away salts from adjacent soils.

Calcium and Magnesium hardness

Calcium and magnesium ions enter the groundwater through infiltration from minerals like Calcite, Gypsum and Dolomite¹⁴. Results of this study were similar to the study of Safawi and others (2008) in their study on well water of the Shrikhand-Kubba region in Nineveh province, where they record a range of (720 -1900) mg/L¹⁶.

Sulphates

Some bacteria, such as chlorothiobacteria and rhodo-

thiobacteria, oxidize their ores and produce H₂S due to their activity. Their ions are found naturally in water and have had little or no impact on human health so far. In this study, the maximum concentration of 1055 mg/L was obtained for water sample taken at location Al-Dhuluiya, which maybe because of the sewage from the village. All values were below the WHO¹⁷ 400, 100, 250, and 200 mg/L are the maximum allowed limits, respectively. However, a buildup of sulfate in water can cause an increase in pH, resulting in acidosis¹⁸.

Total dissolved solids

Only water samples located within Al-Dhuluiya revealed average TDS values within the permissible value (500 mg/L) of the world standards. Maximum TDS is a sign of saline water, which can be caused by natural solute dissolving and weathering, and by discharge from industrial treatment plants, which causes soil contamination leaching and point-source groundwater pollution¹⁹. Implications of high TDS are organoleptic in humans and reduction in pipes, filters, and valves due to scale accumulation²⁰. The ionic concentration of a water sample, which influences its ability to conduct an electric current, is measured by EC, which is directly connected to TDS. The ionic strength of a water sample increases as the TDS content rises. The results were higher above the permitted limit of 1000 µS/cm set by international drinking water guidelines. Ionic heavy metals were dissolved during industrial activities involving heavy machinery and later found their way into groundwater through leaching of sub-soil layers²¹, and greater temperature of the location boosting mobility of ions under electrostatic potential might be blamed for the unbearable EC value²². The

main adverse effects are water corrosivity and heavy metals, which render the water unfit for consumption.

Total coliforms

Are a type of bacteria that can be found in the environment, such as soil or vegetation, as well as in humans. Although total coliform bacteria are unlikely to cause sickness, their presence signals that more dangerous microbes may contaminate your water source. *Escherichia coli* is the only member of the entire coliform bacterial genus that can only be found in the intestines of mammals, including humans. *E. coli* contamination of water implies recent fecal contamination and may indicate the presence of disease-causing microorganisms such as bacteria, viruses, and parasites. Because testing for all known pathogens is a complicated and expensive operation, total coliforms and *E. coli* are employed as indicators to determine the degree of contamination and hygienic quality of healthy water. The primary source of pathogens in drinking water is recent contamination from human or animal waste, improperly treated septic and sewage discharges, animal manure leaching, and stormwater runoff. Domesticated or wild animals Bacteria and other dangerous microbes from any source may be carried into rivers, lakes, or groundwater during and after precipitation. Poor good construction or poor maintenance can increase the risk of groundwater contamination. Bacterial contamination was discovered in all wells in this investigation. The highest and only high value was at Al-Alam in November. It could be the result of animal excrement leaching near wells, as well as poorly installed septic and sewage systems and household charges.

Conclusions

During the study period, the pH and EC levels in all wells were within the allowable range for drinking water. Also, the chloride concentration is below permissible levels, and all wells have been tested to ensure that they pose no threat when utilized for residential purposes. According to the general guidelines for hardness water categorization, most water in wells is standard.

Funding

This research was funded by self.

Acknowledgments

I would like to extend my thanks and gratitude to all who support us.

Conflicts of Interest

None

Bibliographic references

- Mahdi M J . Study groundwater in Samarra and try to improve its quality in a manner chemical deposition and ion exchange. Master Degree / college Engineering-Tikrit University. 2008.
- Mahjoub M R . Microbiology of water. Dar AL-Hikma Press Printing Press Baghdad University. 1998; 368 p.
- Mishra A and Bhatt V T . Physico-Chemical and Microbiological Analysis Under Groundwater in V. V Nagar and Nearby Pales of Anand District Guiarat, India. E-Journal of Chemistry. 2008; 5(3):487-492 p.
- Alexander P . Evaluation of groundwater quality of Mobi town in Admawa State, Nigeria . Africa Journal of Biotechnology . 2008; 7(11):1712-1715.
- Al-Obeidi M A N . Environmental study on the quality of groundwater in the district of AL-Twz and its villages, Master Thesis, college of Science, University of Tikrit. 2014.
- Jawad M A and Nassif D M . Study of the chemical and physical properties of some groundwater well sand the extent of their pollution In the city of Samarra. DIYALA JOURNAL FOR PURE SCIENCES. 2013; 11 (4) : 15-23
- Abawi S A & Hassan S M . Practical Engineering for Environment Water Testing 7. Dar AL-Hikma Directorate for Printing and Publishing Mosul. University of Mosul. 1990.
- ASTM . Annual Book of ASTM (Standards American Society for Testing and Materials). Philadelphia, USA. 1989; PP:11.
- APHA. American Public Health. Association., Standard Methods for the Examination of Water and Wastewater .20th Edition. APHA. American Water Works Association. (AWWA), and Water Pollution Control Federation, Washington, DC 1998.
- Ghaeab M G F. Ecological Study of the Physical, Chemical and Bacteriological Characteristics to Some Wells in Tikrit City. thesis of Master College of Science, University of Tikrit. 2010.
- Hem J D . Study and interpretation of the chemical characteristics of natural water, Third Edition. USGS. United State Governorate Printing Office. 1985.
- Al-Obaedy H H . Ecological study on the Quality of Groundwater North of Salahuddin province. Master of science, College of science, University of Tikrit. 2010.
- Faure G . Principles and Application of Geochemistry 2nd prentice Hall Inc ., USA. 1998; 600p.
- AL-Amar A B . The Quality of groundwater for selected area in south of Babylon governorate Iraq .(IOSR- JAGG). 2015; 2321(3):29-36.
- Bojan Antonić , Dani Dordević , Simona Jančiková , Bohuslava Tremlova and Ivan Kushkevych . Physicochemical Characterization of Home-Made Soap from Waste-Used Frying Oils. Processes journal, 2020; 8, 1219.
- Safawi, Abdel-Aziz Younes; Ali, Faeq Hassan; Kanna, Abdel Moneim Ali. Physical and chemical evaluation of some wells in the Sherikhan-Kubba area and their suitability for drinking and domestic use. Proceedings of the Sixth Periodic Scientific Conference of the Dams and Water Resources Research Center. 2008; 193-201 p.
- WHO, World Health Organization. Guidelines for Drinking-water Quality, 1st Addendum to the 3rd ed., volume 1: Recommendations, World Health Organization, Geneva, 2006515p .
- Asamoah AA, Amarin BS . Assessment of the quality of bottled sachet water in the Tarkwa-Nsuaem municipality in Ghana. Res J Appl Sci. 2011; 3(5):105-113.
- Boyd, C.E. Water Quality: An Introduction. Kluwer Academic Publishers Group, The Netherlands. 1999.
- Atekwana EA, Atekwana EA, Roweb RS, Werkema DD, Legalld FD. The relationship of total dissolved solids measurements to bulk electrical conductivity in an aquifer contaminated with hydrocarbon. J Appl Geophys. 2004; 56(4):281-294.
- Eruola AO, Adedokun NA. Analytical assessment of cadmium, lead and iron in hand dug wells of Ilaro, South Western Nigeria. Glob J Sci Front Res Chem. 2012; 12(6):23-29.
- Oguntona TS, Adedeji OO, Martins OC. Contamination of Sachet water produced within industrial area of Ikeja, Lagos Nigeria. Int J Environ Sci. 2012; 3(2):23-29.

REVIEW / ARTÍCULO DE REVISIÓN

Mejoramiento del Rendimiento de un Motor Diésel mediante la adición de nanopartículas de ZnO al diésel

Diesel Engine Performance Improvement by adding ZnO nanoparticles to diesel fuel

Carlos Segovia*, Ignacio Benavides, Jorge Melo, Víctor Montenegro

DOI. 10.21931/RB/2022.07.01.27

Universidad Técnica del Norte Av. 17 de Julio 5-21, Ibarra, 100105, Imbabura, Ecuador.
Corresponding author: cmsegovia@utn.edu.ec

Resumen: El estudio analizó el comportamiento de un MEC (Motor de encendido por compresión) cuando se adiciona nanopartículas de ZnO (Óxido de zinc), en proporciones de 144, 233 y 377 ppm. Las pruebas fueron desarrolladas usando combustible diésel con una concentración de 300 ppm de azufre con el objetivo de analizar el consumo y cómo este influye en las emisiones contaminantes y en el rendimiento del motor. Para los ensayos se utilizó un camión 2.6 ID (inyección directa) de 4 cilindros en línea, con una potencia de 85,57 HP a 4000 rpm y un torque de 167 Nm a 2200 rpm, un analizador de gases, un opacímetro y un banco dinamométrico. Las pruebas se realizaron a una altura de 2200 m s.n.m., con una presión atmosférica de 78,5 kPa. Los resultados obtenidos en cuanto al torque indican un incremento del 3,82%, mientras que en la potencia se evidencia un aumento del 3,46% con la adición de ZnO al diésel. En lo que respecta a emisiones contaminantes de CO se obtuvo una disminución del 35%. En cuanto al CO₂ los resultados mostraron una disminución del 4%. Los HC disminuyeron entre un 86% y 59%. El O₂ disminuyó un 1%. Para los NO_x, la adición de nanopartículas no evidenció mejora alguna en la mitigación de este gas. Finalmente, en la prueba de opacidad se obtuvo una disminución del 39,67%. La aplicabilidad de este estudio corrobora que la aditivación del combustible con nanopartículas mitiga las emisiones contaminantes sin sacrificar notoriamente las prestaciones de los MEC.

Palabras clave: Nanopartículas, ZnO, potencia, MEC, torque, emisiones, opacidad.

Abstract: The behavior of a CI (Compression Ignition) engine was analyzed when ZnO (Zinc Oxide) nanoparticles were added, in proportions of 144, 233 and 377 ppm. The tests were developed using diesel fuel with a concentration of 300 ppm sulfur to analyze consumption and how it influences pollutant emissions and engine performance. The tests used a 2.6 ID (direct injection) 4-cylinder in-line truck, with an output of 85.57 HP at 4000 rpm and a torque of 167 Nm at 2200 rpm, a gas analyzer, an opacimeter and a dynamometer. The tests were carried out at an altitude of 2200 m.a.s.l., with an atmospheric pressure of 78.5 kPa. Obtained results in terms of torque indicate an increase of 3.82%, while in power, an increase of 3.46% is evident with the addition of ZnO to diesel; in terms of polluting emissions of CO, a decrease of 35% was obtained. As for CO₂, the results showed a decrease of 4%. HC decreased from 86% to 59%. O₂ decreased by 1%. The addition of nanoparticles showed no improvement in the mitigation of NO_x. Finally, the opacity test shows a decrease of 39.67%. The applicability of this study corroborates that the addition of nanoparticles to diesel fuel mitigates pollutant emissions without significantly sacrificing the performance of CI engines.

Key words: Nanoparticles, ZnO, power, CI engine, torque, emissions, opacity.

Introducción

La crisis climática provocada por las emanaciones peligrosas de los motores de combustión interna^{1,2} a generado grandes preocupaciones y nuevos retos a la comunidad científica, los cuales buscan optimizar la uniformidad de la provisión de materia prima y fomentar el uso de energías sustentables³.

Los motores MEC son más eficientes que los motores MEP (motores de encendido provocado) y por ende menos contaminantes⁴, perjudicialmente un combustible diésel con altas concentraciones de azufre emana más vapores tóxicos al aire, tales como hidrocarburos, óxidos de nitrógeno y monóxido de carbono⁵, que son nocivos para el medio ambiente y la salud de las personas².

Nuevas tecnologías han establecido que mediante la adición de compuestos metálicos al combustible fósil se ha logrado reducir notablemente las emisiones contaminantes⁶. En los carburantes incompresibles la caracterización fisicoquímica de las nano partículas muestra un área superficial más determinada, debido a que ocurre con mayor facilidad la dispersión, reteniendo también una mezcla con mayor estabilidad por tiempos más prolongados. Permitiendo que la oxidación y liberación de energía sea más rápida y mayor respectivamente⁷. La adición al combustible merma las emisiones de material particulado, así como el retraso de la ignición⁸. Una de las fortalezas del ZnO es la capacidad para la retención de oxí-

Citation: Segovia C, Benavides I, Melo J, Montenegro V. Mejoramiento del Rendimiento de un Motor Diésel mediante la adición de nanopartículas de ZnO al diésel. *Revis Bionatura* 2022;7(1). 27. <http://dx.doi.org/10.21931/RB/2022.07.01.27>

Received: 2 December 2021 / **Accepted:** 21 January 2022 / **Published:** 15 february 2022

Publisher's Note: Bionatura stays neutral with regard to jurisdictional claims in published maps and institutional affiliations.



Copyright: © 2022 by the authors. Submitted for possible open access publication under the terms and conditions of the Creative Commons Attribution (CC BY) license (<https://creativecommons.org/licenses/by/4.0/>).

geno, lo que desencadenará en una oxidación concurrente de monóxido de carbono e hidrocarburos, además de la reducción de óxidos de nitrógeno y azufre, mitigando así las emisiones⁹.

Centró sus estudios en la adición de nanopartículas al diésel, empleando Al₂O₃ (óxido de aluminio) o TiO₂ (óxido de titanio) con tamaños de partícula inferiores a 45 nm en concentraciones de 25, 50, 100 y 150 ppm, mejorando la conductividad térmica, el número de cetano y viscosidad, mejorando al proceso de combustión¹⁰.

La presente investigación valora el comportamiento del motor 2.6 ID de 4 cilindros en línea, luego de mezclar ZnO al diésel, con el fin de contribuir en estudios respecto a combustibles alternativos, robusteciendo la matriz productiva del Ecuador, y a su vez mitigar las emisiones contaminantes.

El Ecuador se ha visto limitado a importar vehículos diésel con las últimas tecnologías, esto debido a la mala calidad del combustible que se comercializa. En otras latitudes el carburante diésel cumple y satisface las normativas Euro V y VI, las cuales establecen concentraciones de hasta 50 ppm de azufre; en el País, se expende un combustible con rangos superiores a las 300 partículas por millón de azufre. En consecuencia, el presente estudio pretende coadyuvar en la mejora del com-

bustible con el fin de mitigar las emisiones contaminantes sin sacrificar las prestaciones de los motores MEC.

Materiales y métodos

Caracterización Físicoquímica De Las Nanopartículas ZnO

Las nanopartículas de ZnO tienen la caracterización físicoquímica detallada en la tabla 1. Estas pueden presentar diferentes comportamientos a causa de una mayor energía y área superficial.

Microscopía Electrónica de Transmisión (TEM)

Se aprecia una repartición homogénea en la escala de 100 nm, las nanopartículas de ZnO presentan una constitución semi-hexagonal, la imagen TEM (microscopio de transmisión electrónica) ha permitido calcular el tamaño promedio, entre 10 ~ 30 nm. El círculo rojo muestra afluencia de las nanopartículas y el círculo amarillo la dispersión de las mismas^{12,13}.

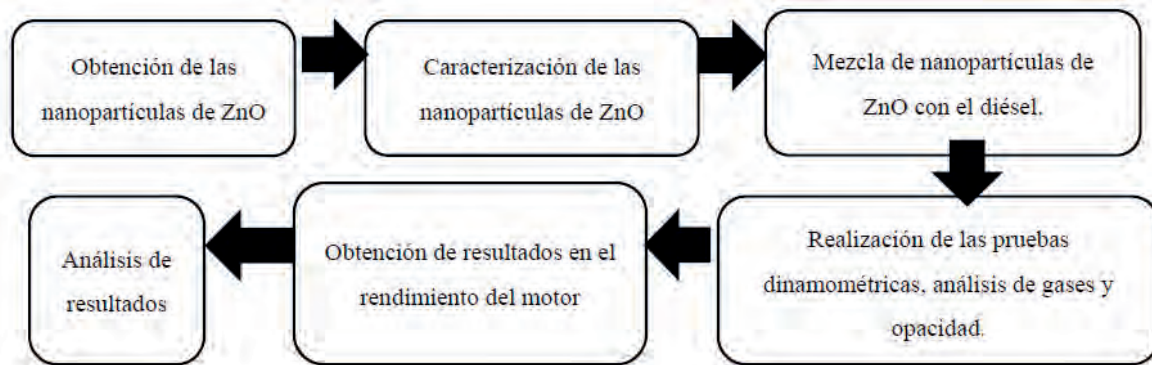


Figura 1. Proceso metodológico (secuencia metodológica seguida en el proceso de investigación).

Parámetros	Características
Forma	Polvo
Color	Blanco lechoso
Olor	Inodoro
Punto de fusión / intervalo de fusión	1975 °C
Peligro de explosión	El producto no tiene peligro de explosión.
Densidad	A 20 °C 5.606 g / cm ³
Solubilidad en / miscibilidad	Agua: Insoluble

Tabla 1. Propiedades físicoquímicas de las nanopartículas ZnO.

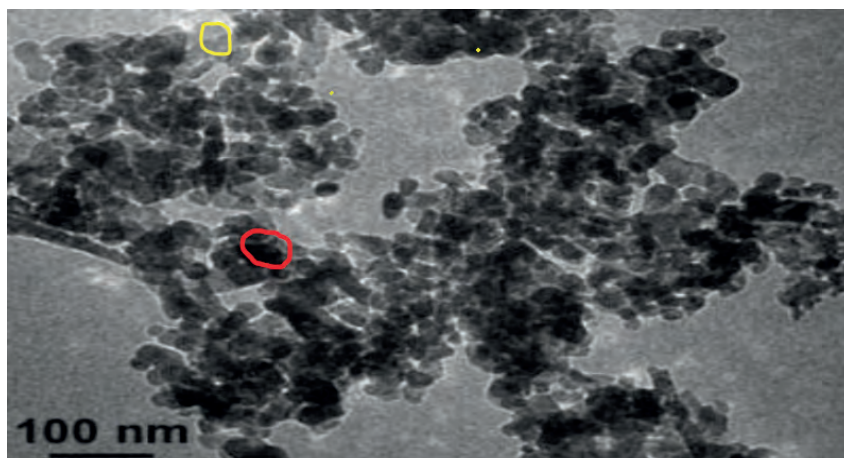


Figura 2. Imagen Microscopía Electrónica de la nanopartícula de ZnO¹¹.

Caracterización mediante microscopía electrónica de barrido (MEB)

El método de microscopía electrónica de barrido (MEB), permite analizar la morfología del material. La figura 3 indica similitud en la caracterización por MEB y TEM.

Las imágenes muestran a las nanopartículas de ZnO con un rango de tamaño desde 2400x hasta 15000x, realizadas con el equipo detector de trazas (ETD), imágenes con electrones secundarios y topografía, permitiendo una mejor nitidez.

La Figura 4 proyecta a 15000x con detector ETD, que hay aglutinados inconsistentes y porosos de partículas enlazadas entre sí, como se aprecia en la figura 3c, las figuras 3a y 3b muestran mayor esparcimiento. Al comparar morfológicamente con la figura 2, se establece un valor aproximado menor a 30 nm, según lo especificado por el proveedor¹¹.

Preparación de las mezclas

El diésel y las nanopartículas de ZnO se preparan vertiendo tres cantidades diferentes para obtener tres mezclas. Las cantidades fueron de 144, 233 y 377 ppm. Estas mezclas se obtuvieron mediante baño ultrasónico, este método mejora los fenómenos de cavitación capaces de desagregar partículas en un medio líquido⁹, las muestras de 144 ppm y 233 ppm fueron caracterizadas fisicoquímicamente.

144 ppm

1152 mg=8000 ml

$$\frac{X_1}{800 \text{ ml}} = \frac{1152 \text{ mg}}{8000 \text{ ml}} \quad (1)$$

$$X_1 = \frac{1152 \text{ mg}}{8000 \text{ ml}} * 800 \text{ ml}$$

233 ppm

1864 mg=8000 ml

$$\frac{X_2}{800 \text{ ml}} = \frac{1864 \text{ mg}}{8000 \text{ ml}} \quad (2)$$

$$X_2 = \frac{1864 \text{ mg}}{8000 \text{ ml}} * 800 \text{ ml}$$

$$X_2 = 186 \text{ mg}$$

377 ppm

3016 mg=8000 ml

$$\frac{X_3}{800 \text{ ml}} = \frac{3016 \text{ mg}}{8000 \text{ ml}} \quad (3)$$

$$X_3 = \frac{3016 \text{ mg}}{8000 \text{ ml}} * 800 \text{ ml}$$

$$X_3 = 301 \text{ mg}$$

Configuración Experimental

Después de purgar el sistema de inyección diésel, se procedió a realizar las pruebas con cada una de las mezclas (144, 233 y 377 ppm), con el fin de obtener datos de potencia, torque y cuantificar las emisiones y opacidad, dichos ensayos fueron realizados en un banco dinamométrico estático y con un analizador de gases y opacímetro, respectivamente.

Resultados

Imágenes MEB De ZnO

La Figura 5 muestra que las partículas de ZnO son homogéneas en estado aglomerado y disperso. Esta característica puede ser importante para obtener una mezcla estabilizada con diésel fósil¹¹.

Las imágenes muestran el tamaño nanométrico del material particulado. Las nanopartículas de ZnO son capaces de potenciar las propiedades físicas de diversos materiales por sus numerosas propiedades entre las que destacan su actividad fotocatalíticas, anti microbiana y de protección UV¹⁴. Las nanopartículas usadas presentan el tamaño y la caracterización apropiada para generar la actividad catalítica en el proceso de combustión de un MEC.

Pruebas Fisicoquímicas

Se determina que, de los seis ensayos realizados según normas nacionales e internacionales, con la adición de 144 y 233 ppm al diésel, dos están dentro de los estándares de calidad y cuatro están por debajo de los permitidos por dichas normas. Tal es el caso para el ensayo de destilación al 90%, el cual se encuentra por debajo del límite máximo dictaminado por las normativas mencionadas, dicho ensayo permite analizar la eficiencia del arranque y el encendido del motor a altas temperaturas de operación¹⁵. La densidad a 15°C disminuyó en un 2% respecto al límite mínimo permitido por las normas para las dos mezclas, dicha baja no ocasionó una disminución en el tiempo de inyección, es decir no afectó al proceso de combustión, ya que la potencia no disminuyó, de hecho, se incrementó ligeramente, lo mismo ocurre para las emisiones que se vieron favorecidas al menos con las dos mezclas (144 y 233 ppm). En cuanto al índice de cetano, se obtuvo un ligero aumento con la adición de 144 ppm, en el orden del 2,6 % y con 233 ppm del 2,2%, en comparación a lo establecido por las normas ASTM e INEN^{16,17}, lo que se traduciría en una reducción del ruido durante la combustión, una aceleración más amortiguada, menor tiempo entre la inyección y la combustión, permitiendo que el consumo de combustible sea más homogéneo e integral.

Mientras que, en el ensayo de corrosión de la lámina de cobre se corrobora que las mezclas con 144 y 233 ppm son combustibles aptos para el uso en MCIA (Motores de combustión interna alternativos), ya que se obtuvo una clasificación 1a¹⁸. La viscosidad cinemática a 40 °C reportó resultados inferiores a los declarados por las normas, con 144 ppm se evidenció una reducción del 14,57 % y con 233 ppm del 16% respecto al mínimo valor de 3,5 cSt requerido, repercutiendo en la inyección atomizada del combustible en el cilindro. Finalmente, con la adición de 144 y 233 ppm en el diésel el poder calorífico neto reflejó una disminución del 0,60% y del 0,59% respectivamente, lo que desencadenaría en una baja economía de combustible.

Pruebas Dinamométricas

Se empleó un dinamómetro de chasis, los ensayos se llevaron a cabo en un camión 2.6 ID (inyección directa) de 4 cilindros en línea cuyas características se evidencian en la tabla 3. Cabe recalcar que, al momento de realizar las pruebas el odómetro del vehículo registraba 320000 km de recorrido, además, las respectivas mediciones se realizaron a 2200 m s.n.m., con una presión atmosférica de 78,5 kPa y humedad relativa promedio del 56%.

Al emplear únicamente diésel se obtuvo una potencia pico

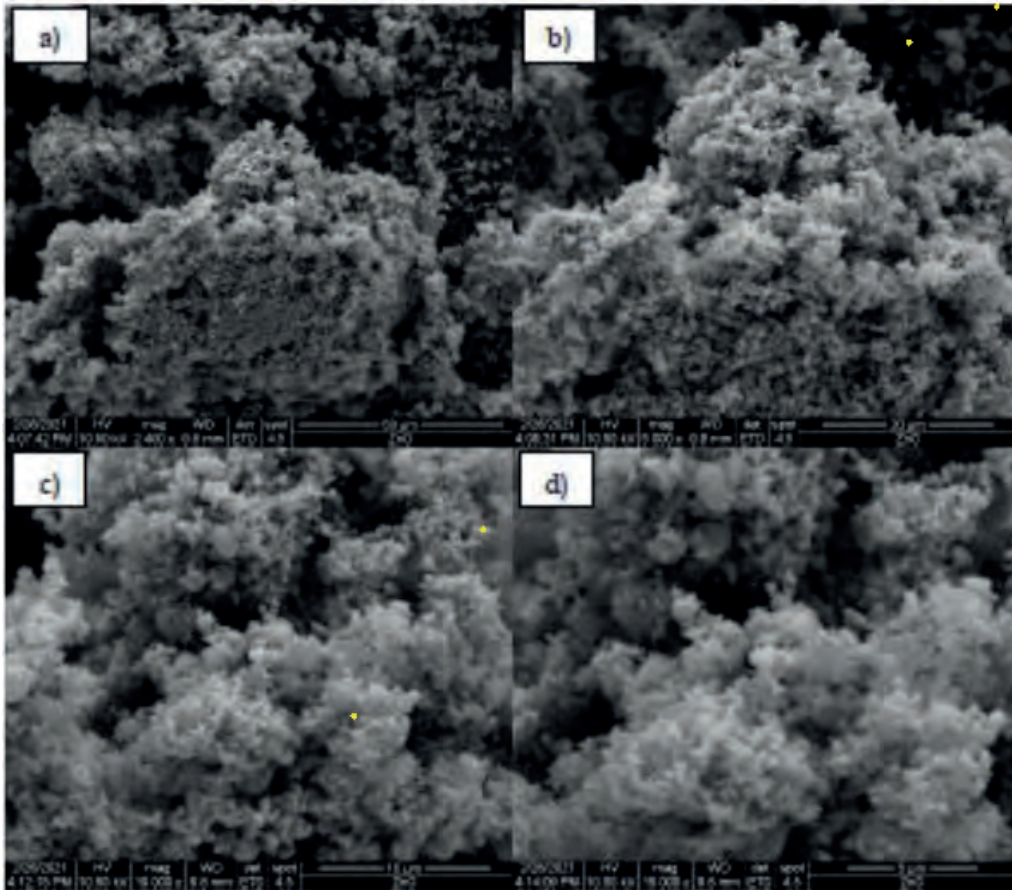


Figura 3. Imágenes a diferentes magnificaciones: a) 2400X, b) 5000X, c) 10000X y d) 15000X.

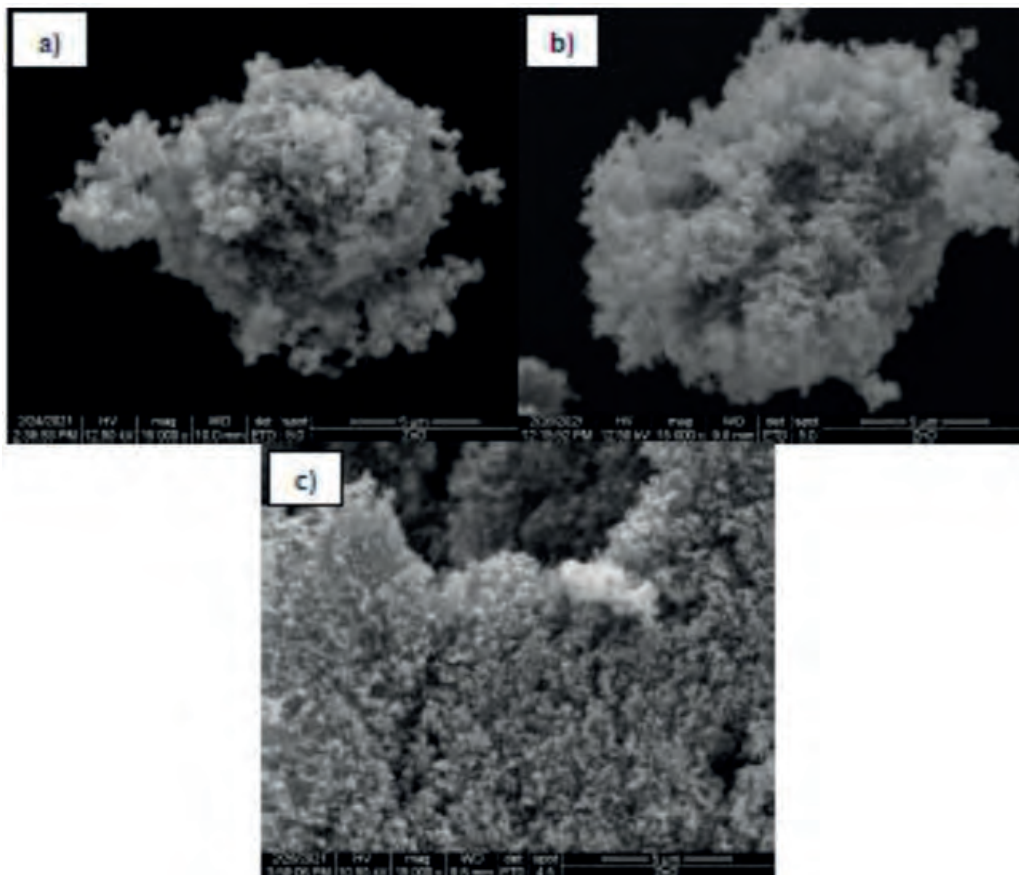


Figura 4. Imágenes de diferentes áreas a 15000X, a) y b) dispersas y c) aglomeradas.

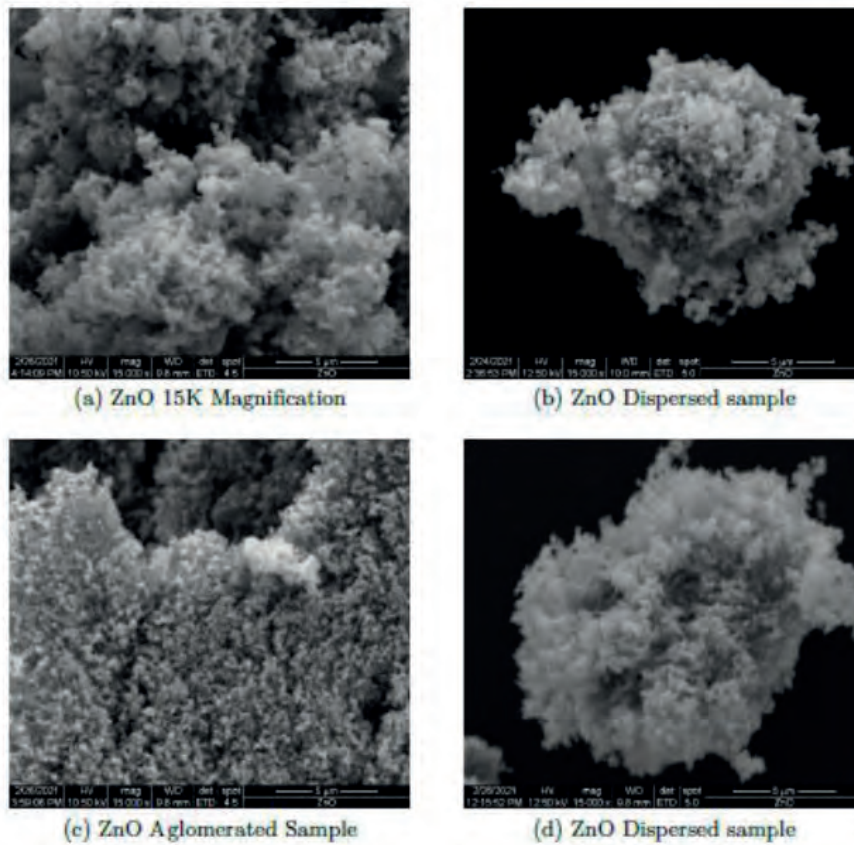


Figura 5. Imágenes de Microscopio de Barrido Electrónico. a) Aumento del ZnO; b) muestra dispersa del ZnO; c) muestra aglomerada del ZnO; d) muestra dispersa del ZnO.

Propiedad	Unidad	144 ppm	233 ppm	Norma ASTM	Norma INEN
Ensayo de Destilación al 90%	°C	342,2	343,3	Máx. 360	Máx. 360
Poder Calorífico Neto	MI/kg	42,8397	42,8444	--	Min. 43,1
Viscosidad Cinemática @ 40°C	cSt	2,99	2,94	3,5 – 5	3,5 – 5
Densidad Relativa @ 15,5 °C	Kg/m ³	842	842	860 - 900	890 - 900
Número de Cetano	–	50,03	50,01	49	49
Corrosión a Lámina de Cobre	–	1a	1a	Máx. 3	Máx. 3

Tabla 2. Caracterización fisicoquímica.

Características	Valor
Motor	Diésel 2.6iD 4 cilindros en línea- Bomba rotativa Co-vec-F
Cilindrada(cc)	2607
Diámetro x carrera(mm)	91,1 x 100
Relación de compresión	22,4:1
Potencia máxima (HP @ rpm)	85,57 @ 4000
Par de motor máximo (Nm @ rpm)	167 @ 2200
Transmisión	Manual de 5 velocidades
Tracción	Trasera

Tabla 3. Especificaciones Técnicas del vehículo¹⁹

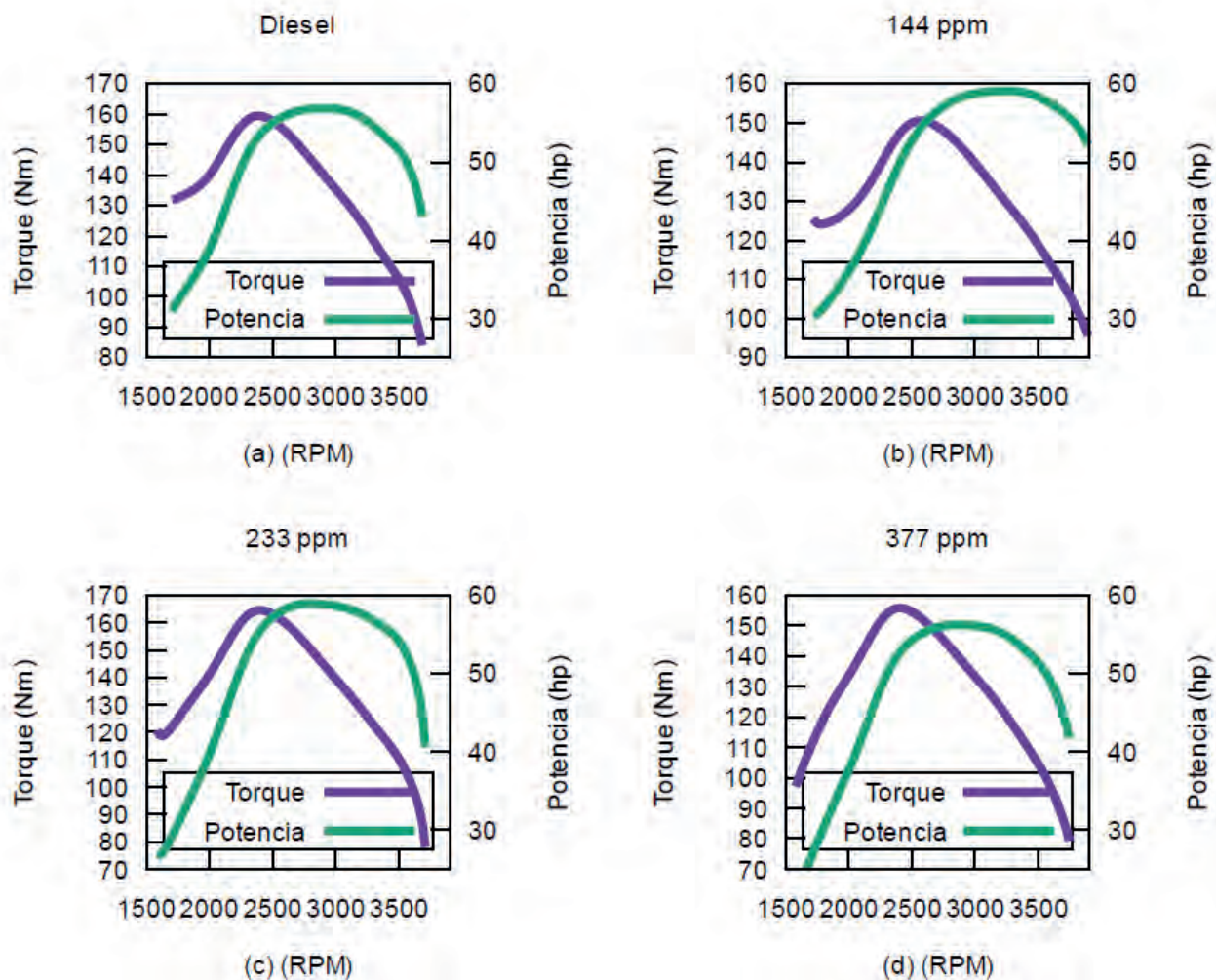


Figura 6. Curvas de par y potencia (a) con diésel, par máximo 163 Nm, potencia máxima 57,8 hp. (b) Con 144 ppm par máximo 153,4 Nm, potencia máxima 59,8 hp; (c) Con 233 ppm par máximo 168,3 Nm, potencia máxima 59,7 hp; (d) Con 377 ppm par máximo 159,9 Nm, potencia máxima 57,2 hp.

Muestra	Potencia Máxima	Torque Máximo
Diésel	57,8 hp	162 Nm
144 ppm	59,8 hp	153,4 Nm
233 ppm	59,7 hp	168,3 Nm
377 ppm	57,2 hp	163 Nm

Tabla 4. Potencia y torque máximo obtenido en cada muestra.

de 57,8 HP @ 2766 rpm; con la adición de 144 ppm al diésel las pruebas entregaron valores de 59,8 HP @ 3345 rpm, mientras que, con 233 ppm de ZnO al diésel se consiguió 59,7 HP @ 2694 rpm y con 377 ppm 57,2 HP @ 2862 rpm.

En cuanto a la medición de torque, con el uso exclusivo de diésel se obtuvo 163 Nm @ 2344 rpm, y, al añadir 144, 233 y 377 ppm de nanopartículas de ZnO al combustible de origen fósil las pruebas dinamométricas entregaron 153,4 Nm @ 2581 rpm; 168,3 Nm @ 2405 rpm y 159,9 Nm @ 2405 rpm respectivamente.

Los mejores resultados en cuanto a potencia se refieren, se obtuvieron con la adición de 144 ppm de ZnO al diésel, seguido de la mezcla de 233 ppm. En lo que respecta al torque,

únicamente la adición de 233 ppm aventajó al erogado con diésel.

Pruebas De Emisiones

Se utilizó un analizador de gases, un cuentarrevoluciones y un medidor de temperatura, las pruebas se realizaron a tres regímenes de funcionamiento del motor: 800, 1500 y 2500 rpm, para luego cuantificar las emisiones de CO, CO₂, HC, y NO_x con cada una de las mezclas de 144, 233 y 377 ppm con diésel.

Con la adición de 144 ppm de nanopartículas de ZnO al diésel, el CO disminuyó en 35% y 29% a 1500 y 2500 rpm respectivamente. Con 233 ppm a los mismos regímenes, se evi-

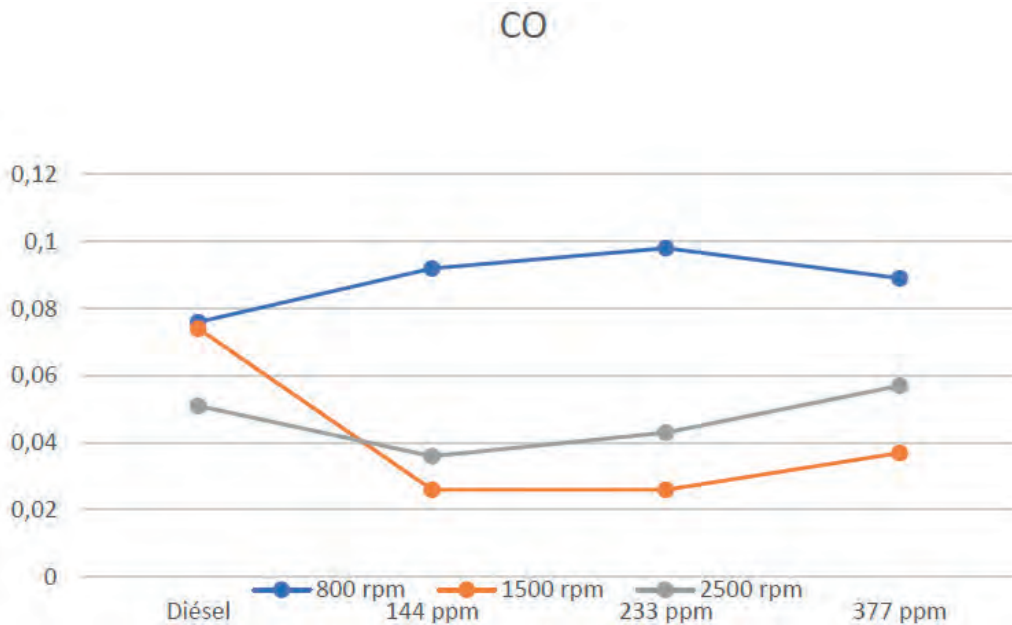


Figura 7. Comparación gráfica del CO.

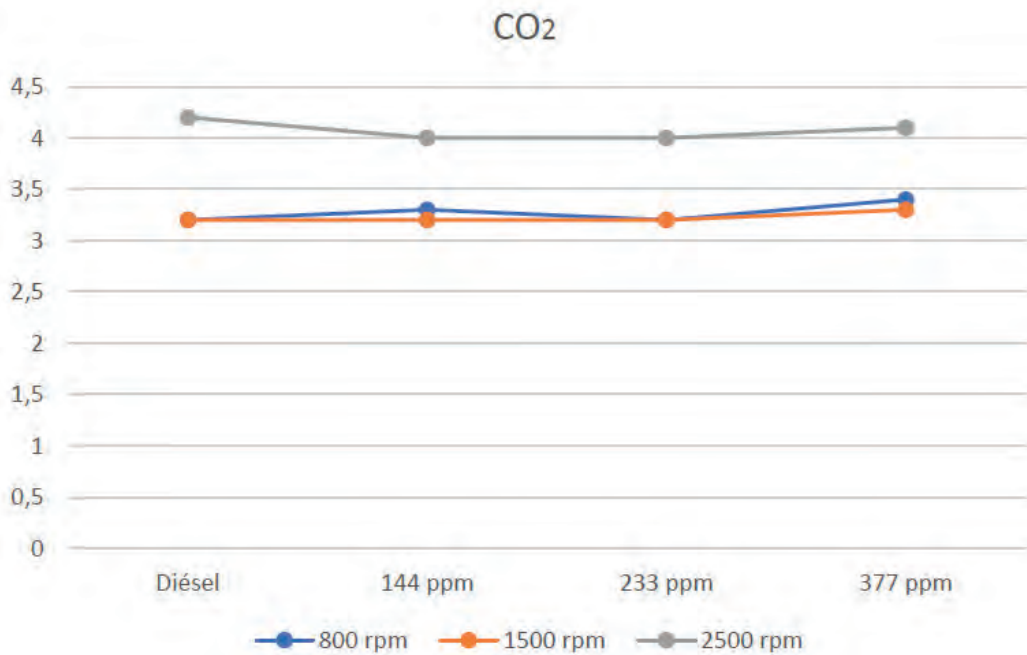


Figura 8. Comparación gráfica del CO₂.

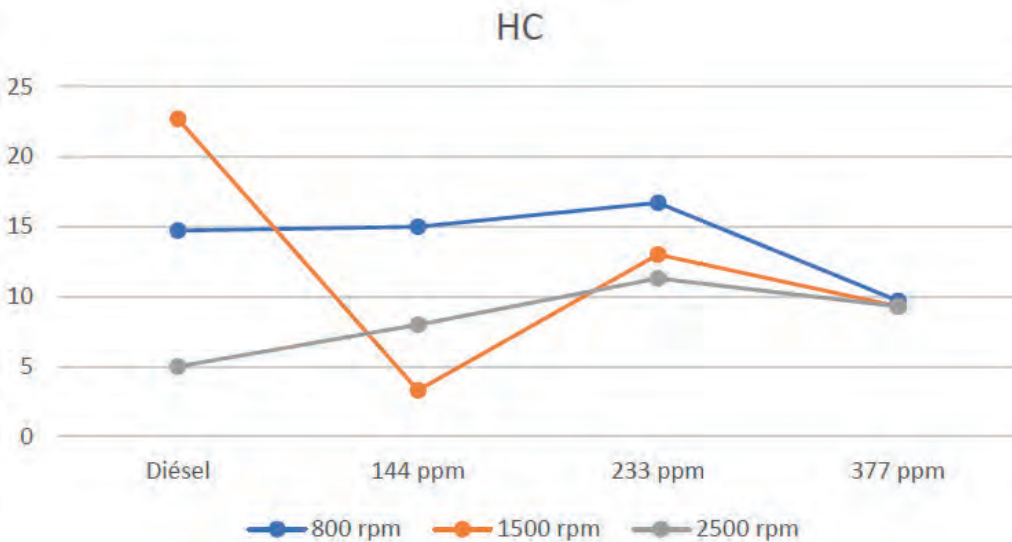


Figura 9. Comparación gráfica de HC.

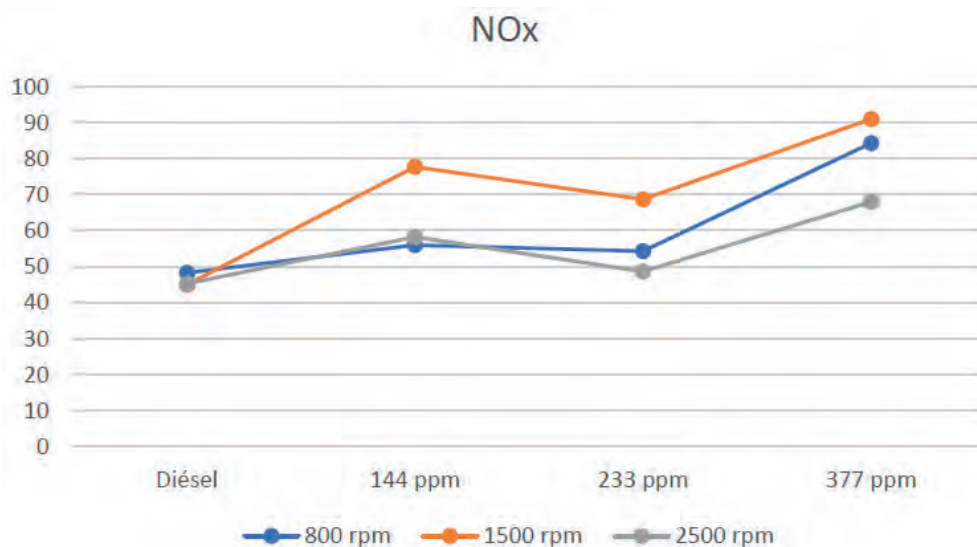


Figura 10. Comparación gráfica de NO_x.

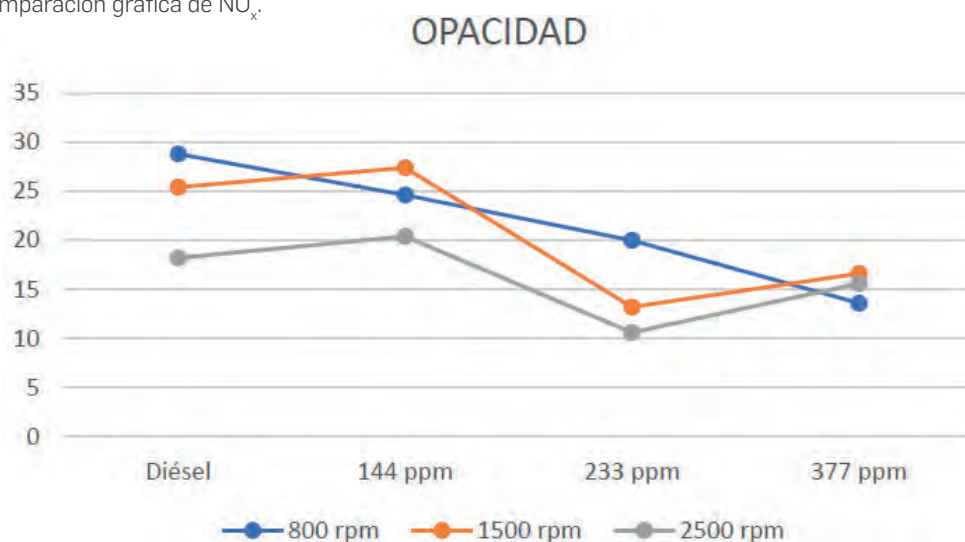


Figura 11. Comparación gráfica de los datos de las pruebas de opacidad.

Prueba	Unidad	Diésel	144 ppm	233 ppm	377 ppm
Opacidad	%	24,2	24,2	14,6	15,2

Tabla 5. Opacidad medida en el vehículo de prueba.

denció una disminución del 35% y 16%. Finalmente, con 377 ppm se obtuvo una disminución del 50% frente al uso únicamente con diésel a un régimen de 1500 rpm.

A 2500 rpm las emisiones de CO₂ se redujeron en un 5%, tanto para la proporción de 144 como para la de 233 ppm, mientras que, con el uso de 377 ppm se evidenció una reducción del 4%.

En cuanto a HC emitidos con la adición de 144 y 233 ppm se evidenció una notable mejora, disminuyendo en un 86% y 43% respectivamente a un régimen de 1500 rpm; mientras que, con 377 ppm a 800 y 1500 rpm los hidrocarburos disminuyeron en el orden del 36 y 59% respectivamente.

Los NO_x no evidenciaron disminución con ninguna de las adiciones de nanopartículas frente al uso de diésel.

Estudios previos no demuestran o no han sido llevados a cabo en ciudades de altura, como es el caso del presente trabajo, el cual se realizó a 2200 m s.n.m., con una presión de 78,5 kPa, por tal razón no se ha realizado comparación alguna.

La tecnología post-combustión de los gases de escape de los motores diésel ha ido evolucionando a lo largo de los años. Han surgido nuevos desafíos para los investigadores y los fabricantes de automóviles desde la aplicación de la norma Euro VI, en la que las emisiones de MP (MP) deben reducirse a 0.005 g/km^{20,21}.

Las tecnologías de reducción de MP que implican modificaciones en el motor de combustión interna ya no son eficientes para cumplir con los requerimientos de la legislación actual. Por lo tanto, se debe considerar a la catálisis como la opción más viable para la eliminación del MP diesel²².

Pruebas de Opacidad

Todos los valores de opacidad obtenidos cumplen con la normativa vigente NTE INEN 2202:2013 (menor al 50%)²³, el mejor valor se obtiene con la adición de 233 ppm, el cual representa un 39,67% menos que con el uso único de diésel en las pruebas de aceleración libre (régimen comprendidos entre 800 y 2500 rpm).

Conclusiones

El CO, con la adición de 144 ppm de ZnO disminuyó un 35% y 29% a regímenes de 1500 y 2500 rpm respectivamente, al igual que con la mezcla de 233 ppm el CO se redujo en un 35 y 16%, los mejores resultados se obtuvieron con la adición de 377 ppm, logrando una reducción del 50%, a 1500 rpm.

A 2500 rpm se estableció una reducción del CO₂ en el orden del 5% con las tres mezclas.

A 1500 rpm los HC se redujeron un 86% con una proporción de 144 ppm, al mismo régimen con 233 ppm disminuye un 43%, finalmente con 377 ppm a 800 y 1500 rpm los HC disminuyeron en 36 y 59% respectivamente.

Los NO_x no evidenciaron disminución alguna con la adición de nanopartículas de ZnO.

Los valores obtenidos de opacidad se encuentran dentro de los parámetros establecidos por la normativa técnica ecuatoriana, la cual establece límites inferiores al 50%, la mezcla de 233ppm proporcionó los mejores resultados, en el orden del 39,67% en la prueba de aceleración libre (regímenes comprendidos entre 800 y 2500 rpm).

La potencia aumentó 3,46% con 144 ppm y 3,28% con 233 ppm, en cuanto al torque erogado, con la adición de 233 ppm se incrementó en un 3,25% sobre el uso con diésel sin nanopartículas.

Se concluye que la adición de nanopartículas de ZnO al diésel en un Motor MEC contribuye en la mitigación de las emisiones contaminantes, sin alterar notablemente sus prestaciones.

Referencias bibliográficas

1. Achour, H. & Olabi, A. G. Driving cycle developments and their impacts on energy consumption of transportation. *J. Clean. Prod.* 112, 1778–1788 (2016).
2. Chamarravi Guerra, O. & Saavedra Calixto, G. Evaluación del impacto ambiental generado por la emisión de gases en motores que utilizan complementos lubricantes, en la ciudad de Bogotá D.C. (Universidad de Manizales, 2013).
3. Guevara, P. Impacto de los biocombustibles y desarrollo de las energías alternativas en Colombia. *Rev. Gestión y Desarro. Libr.* 1, 23–32 (2016).
4. González, F. P. & Fernández, J. M. D. Motores de combustión interna alternativos. (Universitat Politècnica de València, 2011).
5. Blumberg, K. O., Walsh, M. P. & Pera, C. Gasolina y diesel de bajo azufre: la clave para disminuir las emisiones vehiculares.
6. Gan, Y. & Qiao, L. Combustion characteristics of fuel droplets with addition of nano and micron-sized aluminum particles. *Combust. Flame* 158, 354–368 (2011).
7. David, Q. & Guayara, E. B. Escuela politécnica nacional facultad de ingeniería química y agroindustria estudio del efecto de nanoaditivos sobre la eficiencia de combustión del diésel y la eficiencia neta de una fuente fija de combustión proyecto previo a la obtención del título de .

8. Venkatesan, H., Sivamani, S., Sampath, S. & Kumar, D. M. A Comprehensive Review on the Effect of Nano Metallic Additives on Fuel Properties, Engine Performance and Emission Characteristics. vol. 7 (2017).
9. Sharma, A. K., Sharma, A., Ahmad, N. & Khan, W. Zinc Oxide Nanoparticle Fuel Additives for Improved Efficiency and Emissions of Internal Combustion Engines. *Adv. Sci. Eng. Med.* 8, 135–139 (2016).
10. Nassir, A. K. & Shahad, H. A. K. Experimental Study of a Diesel Engine Performance Fueled with Different Types of Nano-Fuel. *J. Univ. Babylon Eng. Sci.* 26, 36–57 (2018).
11. ssnano. Product_-_ZnO_Nanopowder_-_8410DL. 1 (2016).
12. Aquino, P., Osorio, A. M., Ninán, E. & Torres, F. Characterization of ZnO nanoparticles synthesized by precipitation method and its evaluation in the incorporation in enamel paints. *Rev Soc Quím Perú* vol. 84 (2018).
13. World Nuclear Association. Heat values of various fuels - World Nuclear Association. <https://world-nuclear.org/information-library/facts-and-figures/heat-values-of-various-fuels.aspx> (2016).
14. Salas, G., Rosas, N., Galeas, S., Guerrero, V. & Debut, A. Síntesis de Nanopartículas de ZnO por el Método de Pechini ZnO Nanoparticles Synthesis by Pechini Method. *Rev. Politécnica* 38, 43–47 (2016).
15. Instituto Ecuatoriano de Normalización (INEN). Nte Inen 1489:2016. Productos Derivados De Petróleo. Diésel. Requisitos. 7 (2016).
16. Standard Test Method for Distillation of Petroleum Products and Liquid Fuels at Atmospheric Pressure. <https://www.astm.org/d0086-20b.html>.
17. Instituto Ecuatoriano de Normalización. Productos De Petróleo. Determinación Del Índice De Cetano Calculado. Inen First Edit, 1–7 (2013).
18. Instituto Ecuatoriano de Normalización. Norma Técnica Ecuatoriana NTE INEN 2176 : 2013 Primera revisión. Inst. Ecuatoriano Norm. First Edit, 7–12 (2013).
19. Ficha Técnica del Hyundai H100 2.6iD, ensamblado en 2008 | TecnoAutos.com. <https://tecnoautos.com/automoviles/fichas-tecnicas/ficha-tecnica-del-hyundai-h100-2-6id-ensamblado-en-2008/>.
20. Particulate Matter (PM) Pollution | US EPA. <https://www.epa.gov/pm-pollution>.
21. EUR-Lex - 32007R0715 - EN - EUR-Lex. <https://eur-lex.europa.eu/legal-content/EN/ALL/?uri=CELEX:32007R0715>.
22. Cebada, S. Estudio de la actividad de los metales soportados del grupo ib (cu, ag y au) en la oxidación del mp de los motores diésel. *Mundo Nano. Rev. Interdiscip. en Nanociencia y Nanotecnología* 9, 7 (2017).
23. Instituto Ecuatoriano de Normalización (INEN). Norma técnica ecuatoriana NTE INEN 2202:2013 primera revisión gestión ambiental, aire, vehículos automotores. Determinación de la opacidad de emisiones de escape de motores de diesel mediante la prueba estática. Método de aceleración libre primera edición. 1–35 (2013).

ARTICLE / INVESTIGACIÓN

Purification and characterization of L-asparaginase extracted from local Iraqi green beans (*Phaseolus vulgaris*)

Nedhaal Suhail Zbar

DOI. 10.21931/RB/2022.07.01.28

Medical, Applied Biotechnology, AL-Nahrain University, Baghdad, Iraq.
Corresponding author: muqdadaltae.nedhaal@yahoo.com

Abstract: The most prevalent metabolite for the storage and transport of nitrogen used in protein production is L-asparagine; in earlier studies, L-asparaginase enzyme derived from microorganisms was utilized to treat cancer cells; therefore, this study aimed to purify and describe this enzyme derived from Iraqi green bean seeds rather than microbial sources. The enzymes were partially purified from green beans by short steps, including centrifugation of crude enzyme, dialysis by Diethylaminoethyl Sepharose Column, and equilibrated using 20 mM Tris-HCl buffer, pH 8.0, and then applied to a sephacryl S-200. Coulometric methods measured the enzymatic activity at 450 nm, and the unit of activity was calculated by comparing it to a standard curve. Purification of L-asparaginase yielded a 5 percent yield, a 2.7 fold increase in activity, and a 43 unit/ml activity. The pH of asparaginase was optimal at 8.0. After a one-day incubation period, this enzyme became more stable at pH levels ranging from 7.5 to 9.5. This enzyme had the same optimal temperature and thermal stability at 40°C, but it was more stable at temperatures ranging from 20 to 40°C, allowing it to retain its maximal activity.

Key words: Asparaginase, phaseolus vulgaris, leukemia.

Introduction

In plants, L-asparagine is the most abundant metabolite for the storage and transport of nitrogen that is utilized in protein biosynthesis. Borek¹ pointed out that there are two known routes for L-asparagine metabolism for storage and transport of nitrogen utilized in protein synthesis. The first route, catalyzed by asparaginase, involves the hydrolysis of L-asparagine to release ammonia and L-aspartate. The second route involves the transamination of L-asparagine (in the presence of an oxo-acid) to form 2-oxosuccinamic acid and appears to be important in green leaves where it may play a role in photorespiration². Lymphoblastic leukemia and non-Hodgkin's lymphoma were treated by L-asparaginase³. This enzyme catalyzes the conversion of L-asparagine into L-aspartate and ammonia, and this catalytic reaction is irreversible under physiological circumstances⁴. Asparaginase discourages protein production in cancer cells by forbidding them of the amino acid asparagine. First enzymatic hydrolysis of L-Asparagine to L-Aspartate and ammonia were reported by Lang⁵, who noticed L-Asparaginase activity in several beef tissues. L-Asparaginase has attracted much attention in both food industrial and pharmaceutical applications. In the food industry, L-Asparaginase was used to eliminate acrylamide from different processed foods using pretreatment of L-Asparaginase to degrading L-asparagine, the precursor of acrylamide, before baking⁶.

Materials and methods

Plant-Based Materials

The local Baghdad market provided mature green beans (*Phaseolus vulgaris*). Purification of Asparaginase.

Crude Extract

Asparaginase extract in its most proper form was made by homogenizing 100g of green bean in 20 mM Tris-HCl buffer, pH 8.0 (including 1 mM PMSF, 12.5 mM -mercaptoethanol, 50 mM KCl, and 10% glycerol), spin at 10,000 rpm, and the crude extract was the name given to the supernatant⁷.

Diethylaminoethyl Sepharose Column

The dialyzed crude extract was put to a 16 * 1.5 cm Diethylaminoethyl-Sepharose column that had been equilibrated before use with 20 mM Tris-HCl buffer, pH 8.0. Different concentrations of NaCl produced within a single buffer at a 1 mL/minute flow rate were used to elute the enzyme, and 3 mL fractions were collected.

Sephacryl S- 200

Choose the elutions (fractions) from the previous step's peak that have the highest activity and apply them to a sephacryl S-200 (2.6*83cm) column equilibrated with Tris-HCl at a flow rate of 0.5/minute, collecting 3.5 ml fractions.

Citation: Suhail Zbar N. Purification and characterization of L-asparaginase extracted from local Iraqi green beans (*Phaseolus vulgaris*). *Revis Bionatura* 2022;7(1). 28. <http://dx.doi.org/10.21931/RB/2022.07.01.28>

Received: 10 December 2021 / **Accepted:** 10 January 2022 / **Published:** 15 February 2022

Publisher's Note: Bionatura stays neutral with regard to jurisdictional claims in published maps and institutional affiliations.

Copyright: © 2022 by the authors. Submitted for possible open access publication under the terms and conditions of the Creative Commons Attribution (CC BY) license (<https://creativecommons.org/licenses/by/4.0/>).



Asparaginase assay

The enzyme test reaction mixture contains 0.5 milliliters of pH 8.0 Tris-HCL buffer, 0.5 ml of 100 mM L-asparaginase substrate, 0.5 milliliters of each crude enzyme, and distilled water. The reaction mixture was then incubated for 30 minutes in a water bath at 37°C. After the reaction had been incubated, point five milliliters of Trichloroacetic acid (TCA) was added to stop it. To determine nitrogen present in a sample, 0.1 ml of the reaction mixture was added to 3.7 ml of distilled water in a separate test tube, followed by 0.2 ml of Nessler reagent. The absorbance was measured at 450 nm, and the unit of activity was calculated by comparing it to a standard curve.

Characterization of asparaginase

Effect of pH

The best pH for asparaginase activity was discovered by measuring the enzyme's activity at various pH levels. The pH stability of the enzyme was assessed by incubating it in a pH range of 5.0–10.0 for 24 hours at 4°C, and the residual activity was determined under standard assay conditions.

Effect of Temperature

Asparaginase activity was measured at several temperatures to determine the optimum temperature. Heat stability was determined by incubating the enzyme alone for 1 hour at various temperatures. The enzyme solution was brought to room temperature following heat treatment, and the enduring activity was measured after adding the substrates.

Results

Table 1 was shown the findings of asparaginase purification processes from Iraqi *Phaseolus vulgaris*. Figure (1) depicted the DEAE-Sepharose column chromatography results, exhibiting three protein peaks. A Sephacryl S-200 column was used to apply peak one, which had the highest asparaginase activity. This is the last stage in the purification process and results in a single peak of the pure enzyme, as shown in Figure (2). With a specific activity of 143 units/mg protein, L-asparaginase was purified 2.7 times. After passing through the

Sephacryl S-200 column, the asparaginase was found to be pure. The optimum pH for asparaginase activity was 8, as in figure (3).

At alkaline pH, the asparaginase enzyme was found to be stable. When enhancement for 24 hours as in a frame, pH fluctuated between 7.5 and 9.5 since it used 90% of its activity (4). However, the pH optimum of L-asparaginases from a few plants was shown to be between 8.0 and 8.510. Almost L-asparaginases from bacteria have alkaline pH optimum values of 8.0 to 10¹¹.

The temperature has a significant impact on enzyme activity. The optimal temperature for asparaginase activity varies depending on the enzyme source. The optimum temperature for asparaginase was found to be 40 degrees Celsius, which was consistent with previous findings.

The enzyme activity was deliberate at several temperatures. To determine the optimum temperature for asparaginase stability, the enzyme was incubated at different temperature values, then the remaining activity was determined after assaying enzyme activity. As shown in figure (6), asparaginase was more stable at temperatures between 20 and 40°C because the enzyme gained maximal residual activity at these temperatures (100 percent). When the enzyme was incubated at temperatures higher than the optimum temperature for stability (35°C), the residual activity dropped, and around 45°C, asparaginase began to lose its activity.

Discussion

Any deviation in pH from the optimum induces ionization of R-groups of amino acids, which reduces enzyme activity; between pH 7.0 and 9.5, overmuch half of the enzyme's activity level was preserved. Even though the most significant activity at physiological pH is one of the requirements for anticancer activity in such enzymes, the revised enzyme would be feasible because 80 percent of the enzyme activity was retained at pH 8. Enzymes, like other proteins, are only stable across a narrow pH range. Changes in the charges on ionizable residues outside of this range lead to alterations to the protein's tertiary structure, which finally leads to denaturation⁹. At alkaline pH (pH 7.5–9.5), asparaginase appeared firm, as it employed 90%

Step	Total protein (mg)	Total activity (unit)	Specific activity (unit/mg protein)	Fold purification	Recovery %
Plant crude extract	11	805	73	1	100
Dialysis	5	325	65	0.89	40
DEAE-Sepharose	1.2	64	53	0.8	8
Gel filtration on Sephacryl S-200	0.3	43	143	2.7	5

Table 1. Synopsis Procedures for purifying asparaginase from Iraqi green beans.

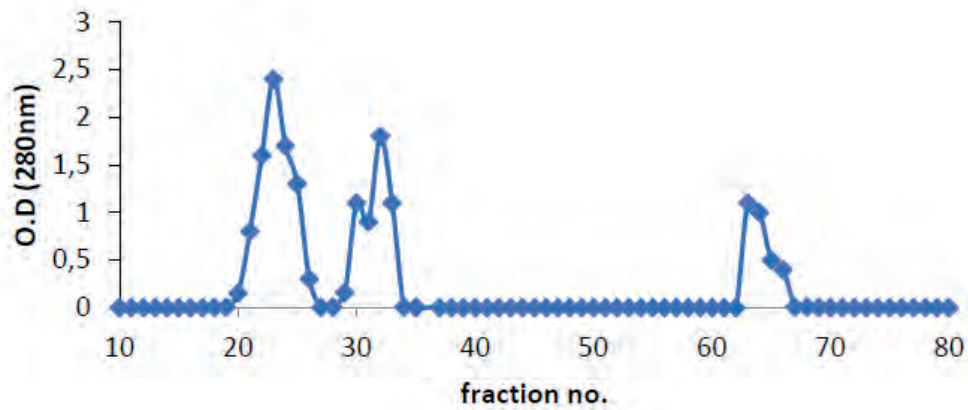


Figure 1. Chromatography of asparaginase from green beans on DEAE-Sepharose (16 × 1.5cm) already to bring to balance with 20mM Tris-HCl, pH 8.0 at a flow rate of 1ml/min. and 3mL fractions.

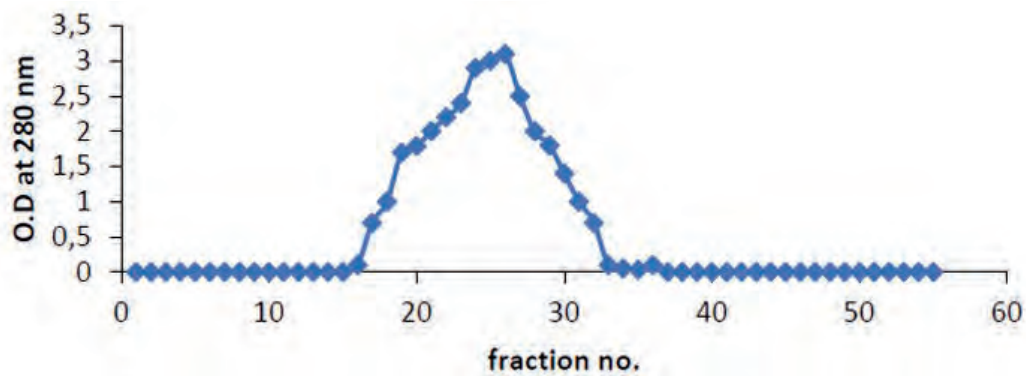


Figure 2. Size exclusion chromatography of asparaginase from anion exchanger-Sepharose fraction on Sephacryl S-200 column 2.6 x 83 cm (equilibrated with tris -HCl at flow rate 0.5/minute and 3.5 ml fraction).

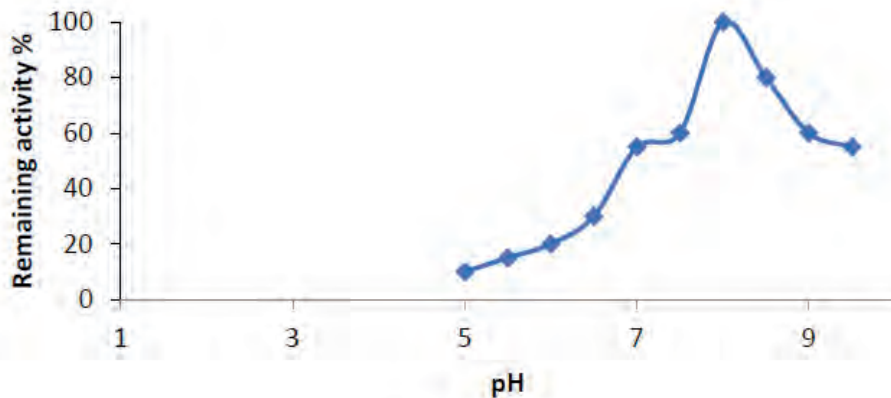


Figure 3. Optimum pH of the enzyme from green bean. Asparaginase activity was measured at different pH.

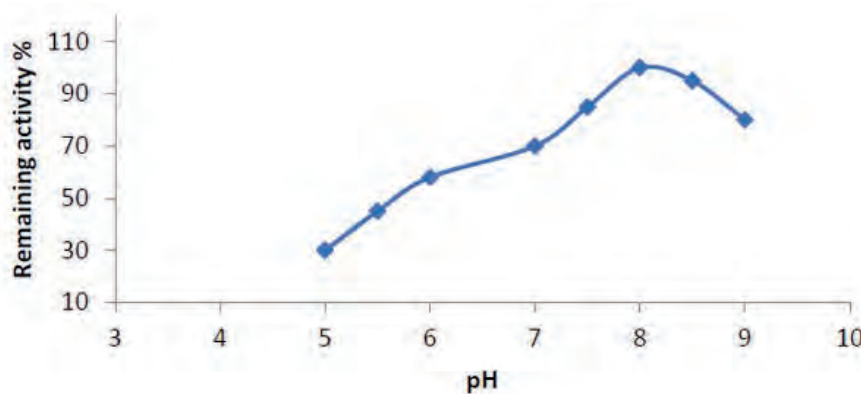


Figure 4. After a 24-hour incubation period, pH stability of asparaginase from *Phaseolus vulgaris* at various pH levels.

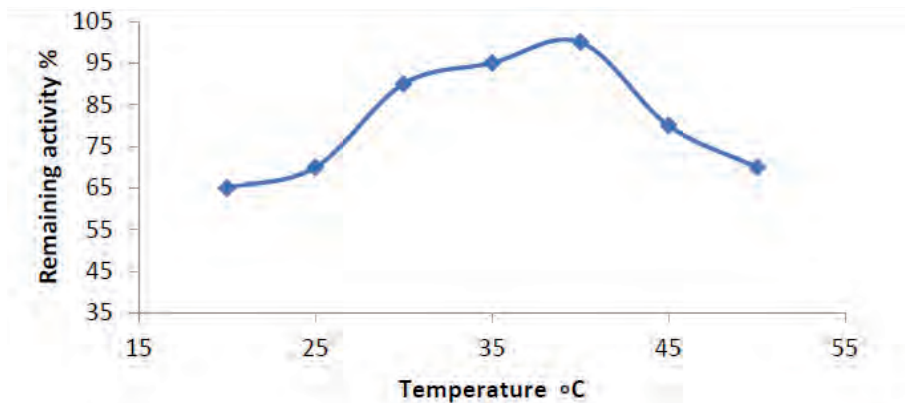


Figure 5. Optimum temperatures for purified asparaginase produced from *Phaseolus vulgaris*.

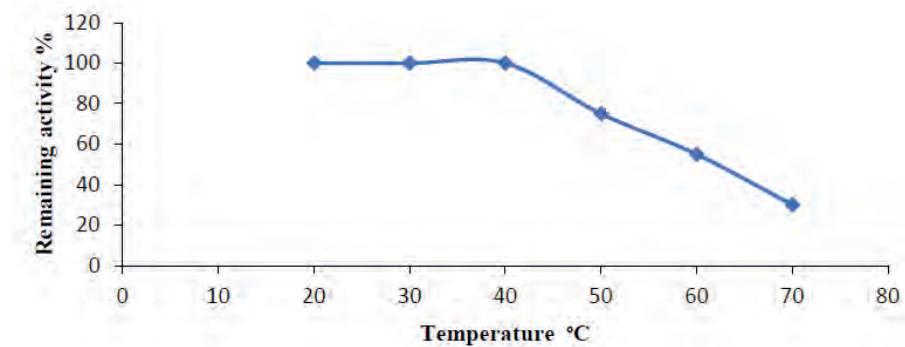


Figure 6. Stability temperature of asparaginase produced from *Phaseolus vulgaris*.

of its activity after being incubated for 24 hours, as shown in figure 4. However, the optimum pH of L-asparaginases from various plants ranged from eight to eight-point five¹⁰. Alkaline pH optima were found in nearly all L-asparaginases from bacteria, ranging from 8.0 to 10¹¹. According to Ali¹², the optimum temperature for the asparaginase enzyme produced by *Vigna unguiculata* was 40°C, and the optimum temperature for such enzyme produced by *Pseudomonas aeruginosa* was similarly 40°C, as mentioned by (13). Denaturation of the enzyme occurs when the protein's three-dimensional structure is destroyed, resulting in the creation of random polypeptide chains as the temperature rises. This produces a change in the active site, rendering the enzyme inactive at high temperatures¹⁴. *Pseudomonas acidovorans* glutaminase decreased roughly 50% of its activity after being incubated at 50°C for 10 minutes, according to Davidson¹⁵. In contrast, Koibuh¹⁶ and Daiwa¹⁷ found that glutaminase from *B. subtilis* kept all its activity after one hour of incubation at 50°C. In another bacterial enzyme, the Optimum optimal temperature for activity was 37°C, but the stability of chondroitinase was maintained 100% at 20–40°C for 30 min 18. As the temperature rises, enzyme activity may decrease, resulting in denaturation, which entails the loss of the protein's three-dimensional structure and the formation of random amino acids.

Conclusions

The enzyme L-asparaginase was isolated from Iraqi green beans so that any potential adverse effects could be ruled out if anticancer therapy is investigated. Asparaginase showed good consistency across various physiological environments, including pH and temperature. We should investigate asparaginase as cancer or leukemia treatment in the future.

Funding

This research was funded by self.

Acknowledgments

I would like to extend my thanks and gratitude to the all who support us.

Conflicts of Interest

None.

Bibliographic references

1. Borek D, Michalska K, Brzezinski K, Kisiel A, Podkowinski J, Bonthron DT, Krowarsch D, Otlewski J, Jaskolski M. Expression, purification and catalytic activity of *Lupinus luteus* asparagine amidohydrolase and its *Escherichia coli* homolog. *European journal of biochemistry*. 2004 Aug;271(15):3215-26.
2. Joy KW. Ammonia, glutamine, and asparagine: a carbon-nitrogen interface. *Canadian Journal of Botany*. 1988 Oct 1;66(10):2103-9.
3. Narta UK, Kanwar SS, Azmi W. Pharmacological and clinical evaluation of L-asparaginase in the treatment of leukemia. *Critical reviews in oncology/hematology*. 2007 Mar 1;61(3):208-21.
4. Hill JM, Roberts J, Loeb E, Khan A, MacLellan A, Hill RW. L-asparaginase therapy for leukemia and other malignant neoplasms: remission in human leukemia. *Jama*. 1967 Nov 27;202(9):882-8.
5. Lang S. Über desamidierung im Tierkörper. *Beitr chem Physiol Pathol*. 1904;5:321-45.
6. Hendriksen HV, Kornbrust BA, Østergaard PR, Stringer MA. Evaluating the potential for enzymatic acrylamide mitigation in a range of food products using an asparaginase from *Aspergillus oryzae*. *Journal of agricultural and food chemistry*. 2009 May 27;57(10):4168-76.
7. Mohamed SA, Elshal MF, Kumosani TA, Aldahlawi AM. Purification and characterization of asparaginase from *Phaseolus vulgaris* seeds. *Evidence-Based Complementary and Alternative Medicine*. 2015 Jan 1;2015.

8. Imada A, Igarasi S, Nakahama K, Isono M. Asparaginase and glutaminase activities of microorganisms. *Microbiology*. 1973 May 1;76(1):85-99.
9. Zubay, G. (1993). *Biochemistry* (3rd ed.), I. W. M. C. Bown Communications. Inc.USA.
10. Khalaf ZA, Al-Ani NK, Jasim HM. Optimum conditions for asparaginase extraction from *Pisum sativum* subspp Jof. *Iran Journal of Plant Physiology*. 2012;2:517-21.
11. Makky EA, Loh YC, Karim MR. Purification and partial characterization of a low molecular weight L-asparaginase produced from corn cob waste. *Biocatalysis and Agricultural Biotechnology*. 2014 Oct 1;3(4):265-70.
12. Ali EM. Purification and characterization of *Vigna unguiculata* cultivar asparaginase. *Journal of Biological Research-Thessaloniki*. 2009 Jan 1;11:29-36.
13. Kuwabara T, Prihanto AA, Wakayama M, Takagi K. Purification and characterization of *Pseudomonas aeruginosa* PAO1 asparaginase. *Procedia Environmental Sciences*. 2015 Jan 1;28:72-7.
14. Segal IH. *Biochemical Calculation*. John Wiley and Sons. Inc. New York. 1976.
15. Davidson LO, Brear DR, Wingard PE, Hawkins J, Kitto GB. Purification and properties of L-glutaminase-L-asparaginase from *Pseudomonas acidovorans*. *Journal of bacteriology*. 1977 Mar;129(3):1379-86.
16. Koibuchi K, Nagasaki H, Yuasa A, Kataoka J, Kitamoto K. Molecular cloning and characterization of a gene encoding glutaminase from *Aspergillus oryzae*. *Applied microbiology and biotechnology*. 2000 Jul;54(1):59-68.
17. Daiwa, K. K.; (2005). Glutaminase Daiwa C 100S. *Enzymes*. (Internet). Address: 4-19 Hie-Cho, Konan, SHIGA, 520-3203 Japan.
18. Abdul-Gani MN, Laftaah BA. Purification and characterization of chondroitinase ABC from *Proteus vulgaris*, an Iraqi clinically isolate. *Current Science*. 2017 Dec 10:2134-40.

ARTICLE / INVESTIGACIÓN

Epidemiological Molecular Analysis of *Acinetobacter baumannii* isolates using a multilocus sequencing typing and Global lineage

Heba A. Kadhom^{1*} and Munim R. Ali²

DOI. 10.21931/RB/2022.07.01.29

¹ Department of Biomedical Engineering, University of Technology, Baghdad, Iraq.² College of Science, Mustansiriyah University, Baghdad, Iraq.

Corresponding author: hkadhom@ouc.edu.iq

Abstract: The Multilocus sequence typing MLST method was used to recognize outbreaks of hospitals distinct clonal lineages of *A. baumannii*; these schemes appeared to provide largely concordant classifications that have been tools to evaluate the population structures of bacterial pathogens. One hundred fifty samples were collected from different specimens of patients within Baghdad hospitals (blood 40%, CSF 5%, urine 5%) between July 2019 to February 2020. Then identification all isolated as phenotypic detection and performed using PCR amplification of *16srRNA* and *blaOXA-51-like* as genotypic detections. According to clinical and laboratory standards institute (CLSI) guidelines, Susceptibility testing was performed. Clonally analysis was performed by global lineage ICs correlated with multilocus sequence typing (MLST) when our data showed a very high rate of antimicrobial resistance in all hospital isolates, especially against colistin (8%) which determined the PDR isolates from other types also recorded 70% of isolates standing for carbapenems antibiotics (IMI 32%, MER70% & DOR 64%). Then already clustered into four groups according to multiplex PCR for two groups of three genes (*ompA*, *csuE* & *blaOXA-51-like*) where IC II was predominant in Iraq but in our strains founding ICI (38%) more prevalence one followed by ICO (26%) then ICII and ICIII (20% & 16% respectively). MLST used for detected the common sequence types (STs) of our selected 8 *A. baumannii* strains (ICO/A11, ICI/A6,48, ICII/A33,50,19 and ICIII/A1,36) were performed by using 7 housekeeping genes than were submitted in the MLST Pasteur scheme dataset (ID 5098, 5099, 5100, 5101, 5102, 5103, 5482 & 5483) followed by statistical eBurst analysis was done to study Clonal complexes (CCs). Identified 5 new STs (8, 444, 346, 1587 & 621) within Iraq and new one ST (1830) worldwide.

Key words: *Acinetobacter baumannii*, antibiotic resistance, carbapenem, global lineage, MLST, eBURST, clonal complex, molecular typing, ST.

Introduction

The established standard for molecular typing method is multilocus sequence typing (MLST), which has been designed to study population structures of bacterial pathogens where two MLST schemes are both widely used (Oxford & Pasteur)¹. Both schemes produced largely concordant classifications with "true" phylogenetic relationships². Briefly, MLST is based on the seven housekeeping genes sequenced analysis "*gltA*, *gyrB*, *gdhB*, *recA*, *cpn60*, *gpi* and *rpoD*". All these genes must be amplified then sequenced to submit within Pub MLST database, which led to finding the allelic number and the STs were assigned to each isolate with the seven allelic profiles³. However, all datasets recorded supplementary analysis with different applications as in upon of the eBurst algorithm to describe the information of STs origins with multiple clonal complexes (CCs) and the investigation of disequilibrium linkage among alleles at the seven housekeeping genes⁴.

For the classification of worldwide clones and produced accurate results was applying widely were used designed two multiplexes PCRs selectively amplify and sequence the *ompA*, *csuE*, and *blaOXA-51-like* genes that are under selective pressure and assign *A. baumannii* strains to different sequence groups (SG), which corresponding to international clonal line-

ages upon this can be identified using other approaches, making it a useful preliminary tool for studying local epidemiology⁵⁻⁷. The rising use of monitoring of multidrug-resistant bacteria at the molecular level in the previous period of time constraints, so *A. baumannii* necessitates the search for reliable typing methods limitation in the time, labor, and costs. Global clone 1 (GC1) and global clone 2 (GC2) were two significant clones responsible for most of these outbreaks where referred to as international clones (IC) 1 and 2⁸. Within each clonal complex, the latter procedure resulted in separate lineages or sub-lineages⁹. The repeated replacement within genes further caused variations that delineate the capsule and lipooligosaccharide's outer core structure¹⁰. Hence, the heterogeneity within each close relative producing outbreaks or spreading at the local, national, or global level can be distinguished using the clonal complex and variability¹¹. Finally, these more common methods are currently used to analyze the underlying genetic differences among isolates and consider a golden standard^{12,13}. The MLST scheme provides a high level of resolution and an excellent tool for studying the population structure and long-term epidemiology of *A. baumannii*.

Citation: Kadhom HA, Ali MR. Epidemiological Molecular Analysis of *Acinetobacter baumannii* isolates using a multilocus sequencing typing and Global lineage. *Revis Bionatura* 2022;7(1). 29. <http://dx.doi.org/10.21931/RB/2022.07.01.29>

Received: 1 December 2021 / **Accepted:** 15 January 2022 / **Published:** 15 February 2022

Publisher's Note: Bionatura stays neutral with regard to jurisdictional claims in published maps and institutional affiliations.

Copyright: © 2022 by the authors. Submitted for possible open access publication under the terms and conditions of the Creative Commons Attribution (CC BY) license (<https://creativecommons.org/licenses/by/4.0/>).



Materials and methods

Clinical samples collection

For 8 months of study (from August 2019 till March 2020), 50 *A. baumannii* were isolated from patients with different infection sites attending different hospitals in Baghdad/Iraq. The *A. baumannii* isolates were obtained from blood (40), urinary tract infections (5) and CSF (5). In a nutshell, samples were distributed on MacConkey agar plates and incubated at 37°C overnight. Petri plates were submerged with bacteria species in several samples, particularly UTI samples, making isolation challenging. As a result, only isolated colonies (one per sample) exhibiting unique *A. baumannii* morphology were chosen for subsequent analysis. Traditional biochemical tests (Gram staining, oxidase, indole, urease, citrate, and methyl-red-Voges-Proskauer) and the API 20E system (BioMérieux, La Balme Les Grottes, France) were used to identify the species. Finally, the *A. baumannii* isolates were preserved at -80°C in a 15 % (V/V) glycerol brain heart infusion.

Genotyping detection for isolates

Isolates were genetically confirmed according to the existence of genus and species-specific gene (*16srRNA* & *oxa 51*, respectively). Specific two primers, "240 bp & 353bp" employed and conditions' steps listed in table 1 & 2 respectively.

Antibiotic susceptibility test

The performance standard for antimicrobial disk susceptibility testing evaluated susceptibility using the agar disk diffusion technique¹⁴. All of which were examined belonged to one of the most common antibiotic families being used to treat *A. baumannii* infections. The following antimicrobial agents have tested: amoxicillin (AMX), augmentin (AMC), piperacillin (PRL), Ticarcillin/ Clavulanic acid (TIM), Ampicillin/ sulbactam (SAM), Ticarcillin (TICER), Ceftriaxone (CRO), Cefotaxime (CTX), Cefazidime (CAZ), Meropenem (MEM), Doripenem (DOR), Imipenem (IMI), Gentamicin (GEN), Amikacin (AK) Tobramycin (TOB), Ciprofloxacin (CIP), Levofloxacin (LEV), Gatifloxacin (GATI), Tetracycline (TE), Tigecycline (TG), Doxycycline (DXT), sulfa drug (SXT), Polymyxin B (PB) finally Colisten (COL).

Identification of housekeeping genes

To retain genetic diversity during storage, isolates were kept at -70°C in 20 % (vol/vol) glycerol in LB medium and cultivated overnight on MacConkey agar at 37°C. A colony's loopful was suspended in 500 microliters of distilled water. A QIAquick PCR Purification Kit was used to recover bacterial DNA (Qiagen, USA). DNA was kept at -20°C until it was needed.

Epidemiological typing

Global lineage (GL)

Three-locus dual assay multiplex PCR (M-PCR) was used to detect the international clone (IC) lineages of *A. baumannii* isolates, which selectively amplified the outer membrane protein A (*ompA*), chaperone-subunit usher E (*csuE*), and intrinsic carbapenemase (*blaOXA-51-like*) genes. Only the *ompA* fragment was amplified in the IC II M-PCR, and only the *csuE* and *blaOXA-51-like* sequences were amplified in the IC I M-PCR, which could be referred to IC III strains. Standard *A. baumannii* IC type I, II, and III strains were being used as controls. In this experiment, strains with a double negation of IC type I, II, or III were reported as a variant (V) clonal type and labeled as ICO.

Multilocus sequence typing (MLST)

The internal portions of seven housekeeping genes were scanned via MLST: *cpn60* (60-kDa chaperonin), *fusA* (elongation factor EF-G), *gltA* (citrate synthase), *pyrG* (CTP synthase), *recA* (homologous recombination factor), *rplB* (50S ribosomal protein L2), and *rpoB* (ribosomal (RNA polymerase subunit B)). MLST website (<http://www.pasteur.fr/recherche/genopole/PF8/mlst/references-Abaumannii.html>). The housekeeping genes for the MLST scheme were selected based on their sequence availability in GenBank and in prior studies of the phylogenetic relationships for the genus *Acinetobacter* and their presence in other MLST schemes available for other bacterial species. PCR primers for amplifying the seven specified genes were chosen from prior research or particularly suited for them. All PCR amplifications were conducted with Promega's Go Taq Green Master Mix under the following conditions: 35 cycles (denaturation at 94.8C for 30 seconds, annealing at 50.8C for 30 seconds, and extension at 72 8C for 30 seconds) were followed by a 2-minute denaturation at 94 8C and a 5-minute extension at 72 8C. According to its protocol, PCR products were immediately purified from the reaction mixture through using QIAquick PCR Purification Kit (Qiagen GmbH, Hilden, Germany). Internal DNA segments of the chosen housekeeping genes, ranging in size like 297 to 633 bp, were sequenced using an ABI Prism 377 sequencer and the ABI Prism BigDye Terminator Cycle Sequencing Ready Reaction Kit v.3.1. (PE Applied Biosystems, Foster City, CA) in line with the manufacturer's instructions on both strands, PCR primers were utilized for sequencing then ClustalW was used to align the sequence data. (<http://www.ebi.ac.uk/Tools/msa/clustalw2/>).

Statically analysis

Identification of STs in our isolates due to seven housekeeping genes was selected within the pub MLST. in our search was selected 8 isolates from each ICs (IC0/A11, IC1/A6,48, ICII/A33,50,19 and ICIII/A1,36) according to global lineage Hierarchical dendrogram (Fig. 3) and their resistance patterns (most carbapenem-resistant CR) then were submitted in the MLST Pasteur scheme as in the table (1).

Results

Anti-biotypes analysis of the collection samples

Fifty isolates were detected as *A. baumannii*, then were differentiated, selective and modified media cultures accompanied by biochemical tests then confirmed by genotypic detection were collected from different hospitals samples sources.

The stander disc diffusion method (antibiotype) was conducted to determine the various resistance patterns versus all antibiotic groups. Classify all isolates according to two bases the first antibiotype to four groups dependent on resistance to carbapenem classes (IMI, MEM & DOR) (C⁰ 30%, C¹ 6%, C² 34% & C³ 30%) and second on three groups dependent on resistance to all antibiotic groups (AB R) or some of them to MDR 26% (13 isolates), XDR 66% (33 isolates) and PDR 8% (4 isolates).

Species diversity and antimicrobial susceptibility

The following steps used sensitivity test for all classes of antibiotics as for penicillin group 80% (AMX&AMC respectively), 74% (PRL), 70% (TIM, SAM & TICER respectively) secondly for cephalosporin group 98% (CRO), 88% (CTX), 74% (CAZ) thirdly for carbapenem 70% MEM, 64% (DOR, 32% (IMI)

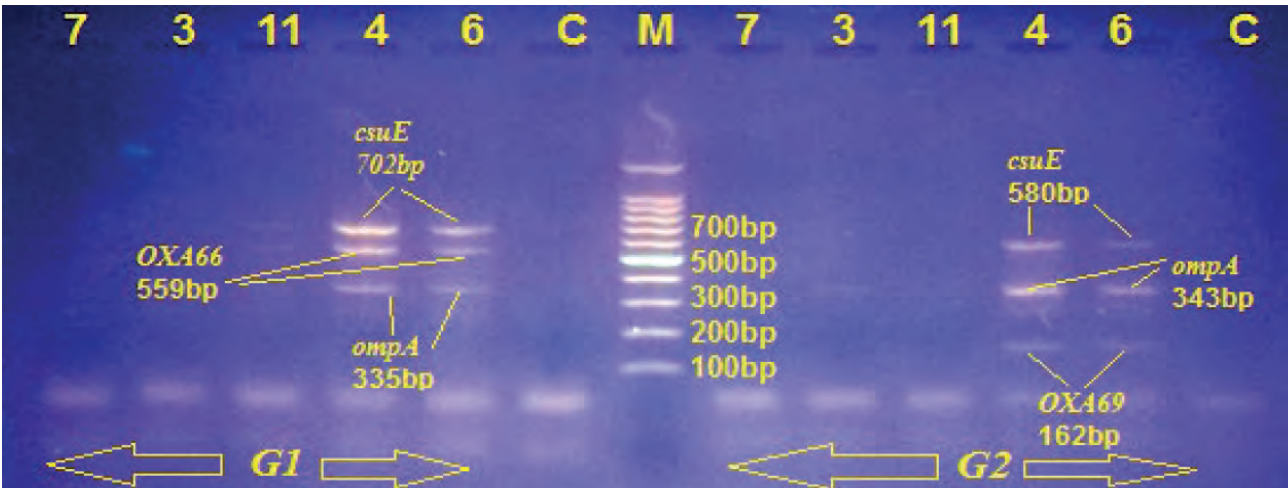


Figure 1. Genetic detection of global lineage by multiplex PCR for two listed primers G1 *ompA* (335bp), *csuE* (702bp) & *blaOXA-51-like/66* (559bp) and G2 *ompA* (343bp), *csuE* (580bp) & *blaOXA-51-like/66* (162bp). Agarose Gel Electrophoresis (1% Agarose, 7 V/Cm²) and Ethidium Bromide Staining to complete detection. In the middle lane, molecular size DNA Ladder (100bp DNA Ladder) and C refer to the negative control, isolates 4 & 6 under G1 (ICI) because harboring all G1 genes, but 11 & 7 absent any types of G1 or G2, so labeled as G0 (ICO) then isolate no. 3 under G3 (ICIII), which is positive to *ompA* in G2, absent all G1 genes.

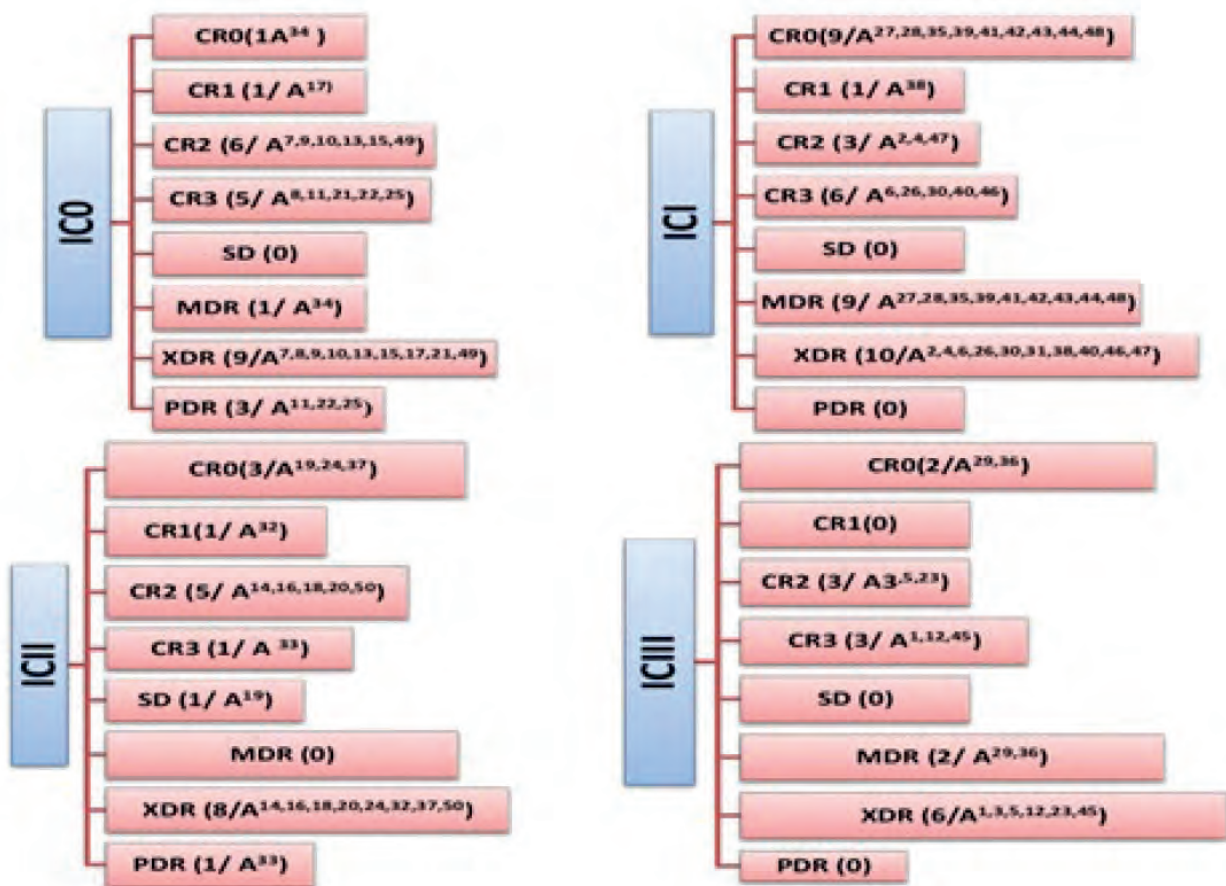


Figure 2. Dissemination of resistances patterns (AR & CR) and ICs.

then for aminoglycoside group 76% (GEN), 68% (AK & TOB respectively), for fluoroquinolone 74% (CIP), 62% (LEV), 50% (GATI), followed for glycylicycline 76% (TE), 50% (TG), 38% (DXT), and 74% (37/50) for polymyxin B, finally the sulfa drug represent 4% sensitive and 96% resistance rate. But still, all isolates gave sensitive results against colistin, except PDR isolates (A¹¹, A²², A²⁵ and A³³). Tri-locus multiplex PCR was

applied to all isolates to determine which clones belonged via two primers groups with their designated conditions¹⁵⁻¹⁷. For this purpose were targeted three intrinsic genes, "*ompA*, *csuE* & *blaOXA-51-like*" show in Fig. (1), in our strains' work, were clustered into four groups G1, G2, G3 and G0 where the all strains belonging to the G1 clonal complex yielded expressing *ompA* *csuE* and *blaOXA-51-like* alleles, so provided all three

fragments in the PCR, but none in the G2 PCR, whereas strains belonging to G2 showed the predicted opposite findings but in case of G3 clone harboring *csuE* and *blaOXA-51-like* alleles from G1 with sharing *ompA* allele as G2 or only have *ompA* allele as G2 as the report was done by Turton *et al.*¹⁷. But the finding of some outbreak strains not had any set of these genes despite positive to *blaOXA-51-like*, therefore, be readily assigned as G0 in which that not recording until now by any research. Thirty-seven (74%) different amplification patterns have been allocated to ICs, the widest dissemination of which is G1 (19/50, 38%), followed by G2 (10/50, 20%). The lower dissemination one is ICIII when reached to 16% (8/50), while IC0 reached 26% (13/50) in our study also focus on carbapenem group and other types of antibiotics resistance of isolates (ICs) with their dissemination which were summarized in Fig. (2).

Phylogenetic analysis

According to the global lineage Hierarchical dendrogram (fig. 3) and their resistance patterns (most carbapenem-resistant CR) our isolates were selected and submitted in MLST Pasteur scheme as in table (1). The relatedness between two strains in Iraq or with the entire world can then be inferred mediated by the allelic profiles varies and illustrated in the following phylogenetic trees.

MLST diagram was done to illustrate the relatedness of all isolates in this investigation locally within Iraq or entire the world as shown in Fig. (4 A & B) than were all particular strains analysis by eBURST to the clonal complex which recorded previously in Iraqi hospitals to determine the epidemiology of STs within this area and within all countries also were determined the originality of Iraqi strains as in Fig. 5, 6 (A & B) and 7 respectively.

Discussion

Reveal the fundamental process that underpins *A. baumannii* infections, including the evolution of infecting strains, resistance patterns, and genes crucial for resistance development, is essential for the development of viable infection control measures and more efficient medical interventions. Firstly, the isolates were genetically established to reduce the time and effort, according to genus and species-specific genes (16srRNA & *oxa 51* respectively). All the isolates must give positive results, indicating all were *A. baumannii*. These findings support those of other studies and are confirmed by

additional methods similar to the current study 18. The most effective antibiotic is colistin, since the percentage of resistance is 8%, four isolates within the PDR group only present this resistance (A¹¹, A²², A²⁵ and A³³). Maspi *et al.*¹⁹ reported 71% of XDR *A. baumannii* isolates from Iran which convergent with our research, while Kalal *et al.*²⁰ reached 80% isolates as XDR rather than 66% as such in the current study. And the last one identified 15/15 MDR isolates with a percentage exceeding 100%, wherein this study detected 13/50 isolates as MDR with a 26% percentage only. As mentioned before Guo *et al.*²¹, 16/67 (23.88%) and 46/67 (68.66%) isolates were defined as MDR and XDR; respectively, these results are acceptable with the current study. The current study results are comparable with the results of Shafigh *et al.*²², who identified that more affected on their isolates are colistin but, the percentage of resistance overshoot 30% while in our study does not exceed 8%. But, AL-Kadmy *et al.* recorded one isolate resist to polymyxin B. These results are more compatible with the search done by Anne *et al.*²³ for the COL (0%), MEM (83%), CRO (100%), AK (50%), GEN (84%), TE (64%), TG (48%) and SXT (100%) while incompatibles for the IMI (81%), CTX (100%), CAZ (100%), PRL (100%), TOB (87%), CIP (89%) and LEV (91%). So study revealed that the majority of isolates of *A. baumannii* tested were progressively resistant to approximately all classes of antibiotics may probably be due to the heavy selection pressure from overuse of the antibiotics within the hospital's environment, causing more spreads of these isolates to become breakouts entire the world. Although, increase this resistance may be a takeoff from the recombination by directly acquired from mobile genetic elements (Tn2006 and ISAbal, 2, 3, 4) or harboring to carbapenemase genes (OXA 23, 51, 58 etc.) which can hydrolyze carbapenems and confer resistance to virtually all β -lactam antibiotics or another mode of resistance patterns as efflux pump correlated with other secretion systems (may be QS or CDI) to confirm their persistence with verity conditions^{21,23,24}.

To better understand bacteria's epidemiology and population structure, the genotypic diversity of strains has really been uncovered using just a wide range of approaches^{25,26}. To recognize a limited origin number of clones which responsible for propagation in many countries the Strains of *A. baumannii* from geographically and genetically diverse European hospitals had been used to distinguish three primary groupings of epidemic strains, which were dubbed European international clones I, II, and clone III with their subtypes from other geno-

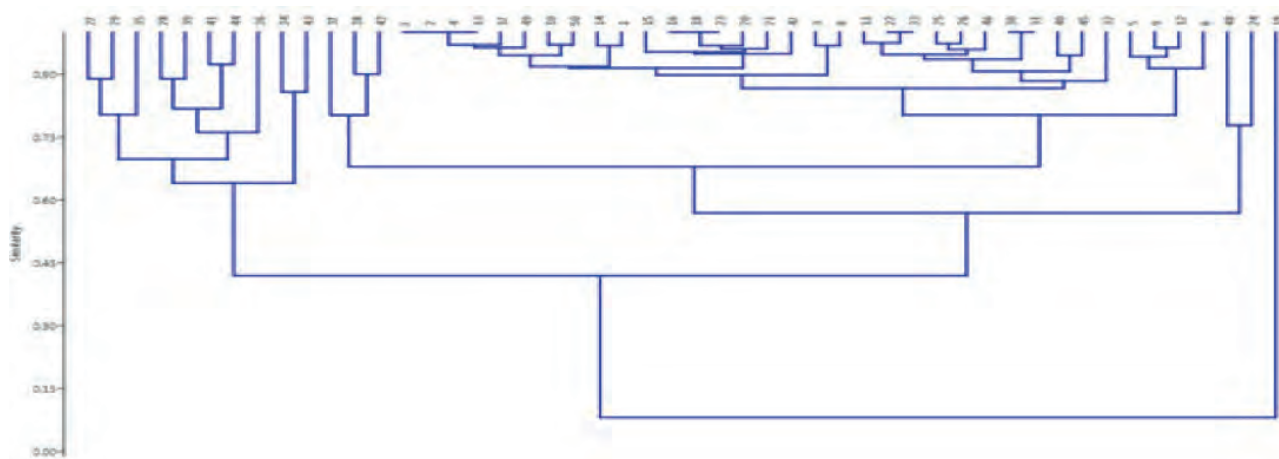


Figure 3. Global lineage Hierarchical dendrogram of all currently isolates with their seven clusters and unique A19 isolates as origin strain.

5483	5482	5103	5102	5101	5100	5099	5098	id
HA_19	HA_11	HA_50	HA_48	HA_36	HA_33	HA_06	HA_01	isolate
Iraq	Iraq	Iraq	Iraq	Iraq	Iraq	Iraq	Iraq	country
2019	2019	2019	2019	2019	2019	2019	2019	year
blood	blood	CSF	blood	blood	blood	blood	blood	source
5	5	1	39	1	1	2	3	Pas _{cpn60}
12	12	1	2	63	2	2	2	Pas _{fusA}
11	11	1	2	2	3	2	19	Pas _{gltA}
2	2	1	2	2	2	2	25	Pas _{pyrG}
228	228	1	4	9	9	2	9	Pas _{recA}
9	9	1	4	4	4	2	2	Pas _{rplB}
14	14	1	4	3	5	2	5	Pas _{rpoB}
1587	1587	8	444	621	346	2*	1830**	ST
2	2	1	1	1	1	6	0	F

Id: identification code, *: mean a dominant ST, **: mean the firstly recorder ST in the world, Pas: Pasteur scheme, ST: strain typing and F: frequency.

Table 1. Submit our isolates in MLST scheme.

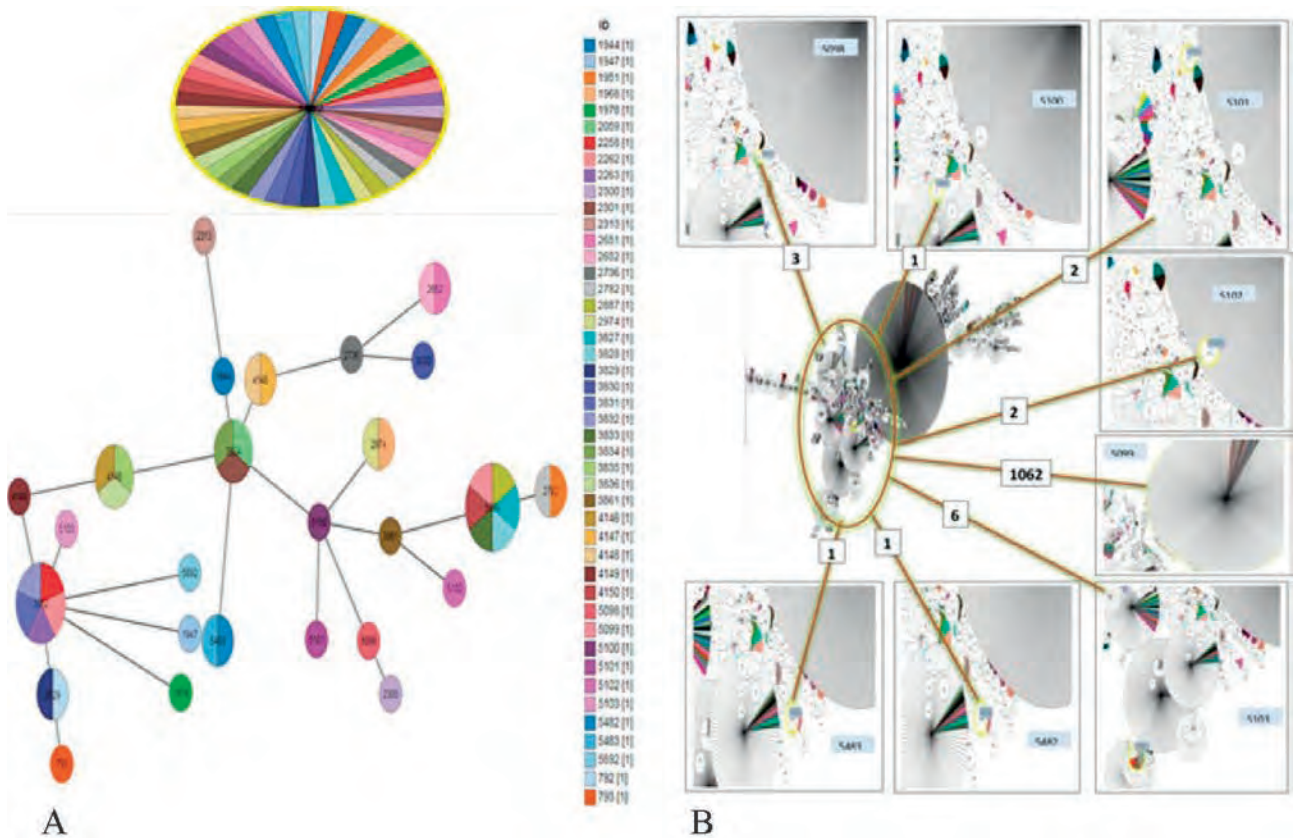


Figure 4. Phylogenetic tree. A/ MLST diagram shows the relatedness of all isolates in this investigation. STs are shown as filled circles, with the size indicating representation within the dataset. Large circles indicate the primary founder of the MLST clonal complex, small circles indicate sub-group founder within Iraqi only. B/ distribution entire the world.

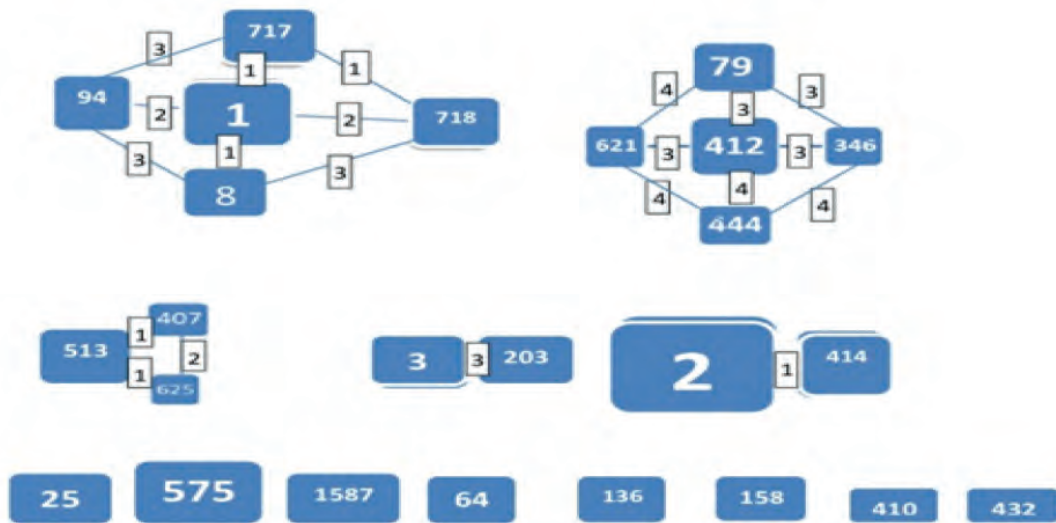


Figure 5. eBURST analysis to clonal complex (CCs). Each square signifies the sequence type and the larger size of each square corresponding to higher frequency of occurrence. Each line indicates that the connected squares share the similar alleles (SLV, DLV & TLV). In the below drawing show related less singleton squares.

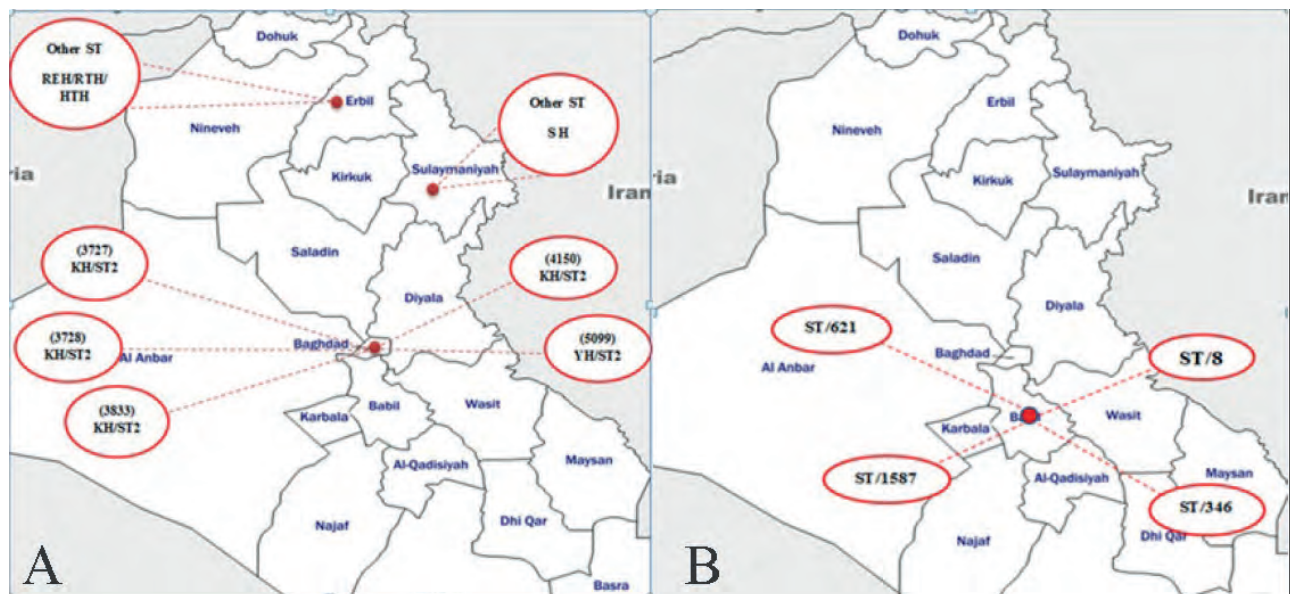


Figure 5. A, recorded returned in Iraq and B, newer recorded in Iraq only. KH: khadhmain Hospital, YH: Yarmouk Hospital, SH: Sulemani Hospital.

types remains to be established among themselves^{32,7}. Especially during recent years, hospitals in Iraq have experienced numerous outbreaks caused by widespread genotypes of nominee bacteria²⁸. Enable infection control professionals by this information is also essential for developing and balancing control strategies to reduce the spread and disease burden of *A. baumannii* in the hospital setting as in Iraq^{29,30}. The patterns of groups 0, 1, 2, and 3 identified using this method were found to pertain to IC I, IC II, and IC III, respectively, except IC0³¹ as in the report of Hamidian & Nigro³² were recording more distribution two major clones I & II on a large scale whilst these results were spaced out from results in Thailand by Khuntayaporn *et al.*³⁰ where recording ICII high prevalent rather than ICI; the reason may be due to geographical disparity or others.

In previous statistical analysis (Fig. 3) of correlation between these isolates appeared as a cluster with other PDR isolates (22 & 33); give this isolates some solitary, below Hierarchical clustering dendrogram where represented seven clusters (C) in which that A¹⁹ was considered the phylogenetic

origin of all isolates in this evolutionary tree maybe this was the reason for its being SD then will be divided to two major clusters MDR and XDR/PDR with some exceptions consequently multiple clusters with different characters where C1, C2, C3 and C4 (A²⁷&A²⁹), (A²⁸&A³⁹), (A⁴¹&A⁴⁴) and (A³⁴&A⁴³) respectively came from the one same original branch where all our isolates most MDR. C5 (A³⁸ & A⁴²) when two of them were ICI and standing to same antibiotic except two only (MEM and DXT), otherwise C6 (all other isolates except C7) in this cluster the main and only characteristic of all isolates were its considered as XDR but, exception four PDR isolates within it because its sharing other properties with other isolates in this cluster especial for A²² & A³³ as sisters, lastly for C7 (A5, A6, A9 and A12) which all of it were XDR and have resistance to 21 from 24 types of antibiotics.

We also focus on carbapenem resistance isolates, where only two from fifty isolates ICI and ICII (A³⁸ & A³²) have a MEM resistance only. However, most of ICI unable to stand against this group despite this most of them recorded MDR and XDR



Figure 7. Geographical dissemination of recorded ST entire the world. When ST2 recorded in 1062 isolates from 34 different countries, followed by ST8 were previously reported in six isolates consequently ST 444 (3), ST621 (3), ST 346 (2) and ST 1587 (3).

rather than other types on the contrary IC0 most of them standing except A³⁴ and most of them considered as PDR these results it's opposite to Zhang *et al.*³³ reports, but ICII and ICIII have variable results in these cases. ICII have only one PDR isolate A³³ and one SD isolate A¹⁹; in the thesis of Dahdouh³⁴ illustrated 37/42 under ICII and have carbapenem resistance while in our study resistance ICII isolates detected in 7/10; consequently, either PCR assays or searches of genomic data targeting the most discriminatory Global clone could simplify the analysis of the epidemiological studies of outbreaks involving multiple closely related types.

The performance of molecular typing in this study was supported by MLST analysis; this pattern has been adopted in approximately 10 researches in Iraq, as in Fig. 4 (A) in which Iraqi isolated from a variety of sources (16 wounds, 12 blood, 6 skin, 5 sputa, 2 CSF, 2 environments, 1 urine and 1 other) with the various types of MLST (Oxford/Pasteur 24 and only Pasteur 21) (<http://pubmlst.org/abaumannii/>). At the same time, the study comprised geographical dissemination of these isolates in different geographic regions worldwide (recorded 6331 isolates) as in Fig. 4 (B). Based on the phylogenetic data, ST2 recorded in 1062 isolates from 34 different countries (5 Unknown, 1 Germany, 1 South Africa, 1 Ireland, 1 Portugal, 1 Israel, 2 Poland, 2 Australia, 2 Lebanon, 2 Egypt, 2 Belarus, 3 Lithuania, 11 Thailand, 11 France, 11 Italy, 3 Taiwan, 7 Greece, 8 Japan, 5 Malaysia, 5 South Korea, 6 Iraq, 18 Singapore, 7 UK, 7 Sweden, 5 Czech Republic, 8 The Netherlands, 6 Spain, 6 Norway, 3 Denmark, 19 Croatia, 26 Saudi Arabia, 32 Turkey, 91 Russia, 348 China, 397 USA) in which that indicator to variability genome of strain type, on the contrary, the rest had very few repeaters as six Europeans for ST8 were previously reported 1, 1, 3 and 1 in the Netherland (lower respiratory tract

LRT), Italy (blood), Greece (2 LRT & 1 urine) and Turkey (blood) respectively.

For the more comprehensive analysis of the possible patterns of evolutionary descent, a set of rules were proposed and implemented in the eBURST algorithm, which allows the division of a data set into several clusters of related strains, dubbed clonal complexes (CC), by implementing a simple model of clonal expansion and diversification^{35,36}. Within each clonal complex, the rules identify which links between STs, in our study founding that isolates could cluster to more than five with Iraqi isolates as in the previously Fig. 5 and the major of isolates exhibited closely relationships in the evolution with most major clonal complex belong to CC2 were highly frequent in Iraq as MLST scheme dataset as found to be a dominant clone in all this region while our study founding only one from 8 isolates (A⁶) under ST2 and ICI. But ST1 was not among our isolates also within CC3& CC5. In 2005, only a single ST2 isolate was obtained in Iraq then increased progressively until 2016 when recorded eight isolates with six ST were recorded 3 & 2 for ST2 & ST1 respectively, and only one new ST was recorded (ST203) by Qasim *et al.*³⁷ for our time this indicating local distribution over time. Noted, the molecular characterization of the isolates by MLST identified 4 new different STs (8, 444, 346 & 621) within Iraq, indicating a high genotypic diversity and possible divergent evolution of these strains from their original clones^{37,38} in which firstly within CC1, it has four ST (1, 8*, 94, 717 and 718) and ST8 represent within IC0 follow in the CC2 (ST2* & ST414); containing as previous explain the predicted ancestor ST2 under ICI and high prevalence one in Iraq which also approved by Qasim *et al.*³⁷ reports. CC4 involve ST79, ST346*, ST412, ST444* and ST621* so in this complex, a three newer recorded types in this country with lower connected to

other STs in their CC and considered as sub-group where its A³³ST346, A³⁶ST621 and A⁴⁸ST444 isolated from Medical Center Hospital for first two types and Al-Yarmouk Hospital/Baghdad for the last one which illustrated in Fig. (6). While there, only three of our isolates were singleton (A¹ST136*, A¹¹ST1587 & A¹⁹1587). HA-1 (ST 136/ICIII) was recorded previously in Kurdistan/Iraq were isolated from different patients; most of them burns or ICU cases in their hospitals (in Erbil & Sulaimania) and clear up the successful clones to spreading among different cities and countries³⁹.

Our strain A⁵⁰ ICII was isolated from CSF source in which lower cases in the world were isolated from this source because it a more difficult to obtain its. And two strains were isolated in 2012 from urine of patients in Japan hospital which have closely relatedness to A⁴⁸ (ST444/ICI) otherwise A³⁶ (ST621/ICIII) were obtained from blood and a grouped together with France clone (unknown sources), in spite of that our study locate three clones (A^{11,19,33}/ST346 & ST1587 respectively) have only one along the universal clones firstly one isolated from Switzerland food at 2013 and the two last clone from Germany environment after our record (WWTP-AS-0520-A-V-5) that indicated some Iraqi clones originated from nonclinical samples as notably in the *A. baumannii* ST2 has been extensively isolated from humans, while some of the recent reports have also indicated the transmission of ST2 by domestic animals to human which may be served as reservoirs as in A³³ (id: 5100) which founding that only two isolates in the world as ST346 and in Switzerland the source of second isolate (id: 1856) was chicken, particularly CR, due to their selective advantage compared to the susceptible strains as in our A¹⁹ strain^{40,41}. As for the last (A^{11,19}) have a unique clone, especially A¹⁹ may be considered as a wild type when acquired their resistance by alteration or modifications due to mutation and recombination in their genome as adaptability within the varies environment to become the phylogenetic origin for the rest of the isolates branching from them.

On the other hand, could be found some types of ST entire the world correlated with antibiotic and resistance genes where ST2 in our study produce full resistance toward three major antibiotic groups (aminoglycoside/ fluoroquinolone/ carbapenem) as recorded ZQ1,2,7 in AL- khadhimai Hospital/ Baghdad/ Iraq (id/ 3827,3828 & 3833) when resistance to the same types of antibiotics give suggesting that it's maybe one of them was originally from the other or acquired its character from same exposure geographic areal conditions within the Iraqi hospitals to give this similarity. For newly ST recorder, the emergence of such strains in Iraq may predict an increase in the risk of how to deal with it and reduce it where it could be seen that in two PDR strains A³³ ST 346 & A¹¹ ST 1587 under ICII and ICO, respectively with resistance to all types of carbapenem group also A¹ST, A⁶ ST 2 & A⁵⁰ ST 8 represent a more resistance rate to antibiotic groups (XDR) except two only (polymyxin & tetracycline groups) otherwise two newer MDR strains in Iraq A³⁶ & A⁴⁸ which may be originated from France and Japan respectively. The distribution of the resistance, especially against carbapenem across multiple genetic lineages, was observed both at the national and local levels suggest an expansion of adaptations in Iraq is driven by the horizontal dissemination of resistance determinants across diverse genetic backgrounds rather than by the sole expansion of single resistant genetic clones, and that resistance to multiple antibiotics is acquired en bloc via MGEs⁴². At the local and global scale, our study identifies several high-risk clones of *A. baumannii* ST 346 & ST 1587 in Iraq by linking clonal relatedness, geographic clustering, epidemiological data with the possibility of frequent in-

ternational transmission. Finally, newer recorded ST in strain A¹ around the world indicated more modification and alteration in their genomic sequences of Iraqi isolates to become origin to other strains in other different countries.

Conclusions

In conclusion, it shows high rates of CRAB isolates and predominance of XDR and PDR under ICs in Iraqi strains compared with previous years. These findings suggest a strong correlation between resistance genes and ICs types determined on a local since different associations were detected in the different Baghdad hospitals. Also, epidemiological of Iraqi clones worldwide with newly recorded types may be more risk factors for epidemic distribution of the chronic diseases associated with these bacteria.

Acknowledgment

The authors would like to express their gratitude to Mustansiriyah University (<http://uomustansiriyah.edu.iq/>) in Baghdad, Iraq, for their assistance with this project.

Bibliographic references

1. Castillo-Ramírez, S., & Graña-Miraglia, L. Inaccurate multilocus sequence typing of *Acinetobacter baumannii*. *Emerging infectious diseases*, 2019. 25(1), 186.
2. Hu, Y. F., Hou, C. J. Y., Kuo, C. F., Wang, N. Y., Wu, A. Y. J., Leung, C. H., ... & Yeh, H. I. Emergence of carbapenem-resistant *Acinetobacter baumannii* ST787 in clinical isolates from blood in a tertiary teaching hospital in Northern Taiwan. *Journal of microbiology, immunology and infection*, 2017. 50(5), 640-645.
3. Gaiarsa, S., Batisti Biffignandi, G., Esposito, E. P., Castelli, M., Jolley, K. A., Brisse, S. et al. Comparative analysis of the two *Acinetobacter baumannii* multilocus sequence typing (MLST) schemes. *Frontiers in microbiology*, 2019. 10, 930.
4. Zhang, Y. Y., Liang, Z. X., Li, C. S., Chang, Y., Ma, X. Q., Yu, L., & Chen, L. A. Whole-Genome analysis of an extensively drug-resistant *Acinetobacter baumannii* strain XDR-BJ83: insights into the mechanisms of resistance of an ST368 strain from a Tertiary Care Hospital in China. *Microbial Drug Resistance*, 2018. 24(9), 1259-1270.
5. Redfean, D. P., Trim, G. M., Skanes, A. C., Petrellis, B., Krahn, A. D., Yee, R., & Klein, G. J. Esophageal temperature monitoring during radiofrequency ablation of atrial fibrillation. *Journal of cardiovascular electrophysiology*, 2005. 16(6), 589-593.
6. Giannouli M, Cuccurullo S, Crivaro V, Di Popolo A, Bernardo M, Tomasone et al. Molecular epidemiology of multidrug-resistant *Acinetobacter baumannii* in a tertiary care hospital in Naples, Italy, shows the emergence of a novel epidemic clone. *J. Clin. Microbiol.* 2010. 48:1223-1230. <http://dx.doi.org/10.1128/JCM.02263-09>.
7. Zarrilli R, Pournaras S, Giannouli M, Tsakris A. Global evolution of multidrug-resistant *Acinetobacter baumannii* clonal lineages. *Int. J. Antimicrob.* 2013. Agents, 41:11-19. <http://dx.doi.org/10.1016/j.ijantimicag.2012.09.008>.
8. Hamidian, M., Hawkey, J., Wick, R., Holt, K. E., & Hall, R. M. Evolution of a clade of *Acinetobacter baumannii* global clone 1, lineage 1 via acquisition of carbapenem-and aminoglycoside-resistance genes and dispersion of ISAbal. *Microbial genomics*, 2019. 5(1).
9. Schultz, M. B., Thanh, D. P., Do Hoan, N. T., Wick, R. R., Ingle, D. J., Hawkey, J. et al. Repeated local emergence of carbapenem-resistant *Acinetobacter baumannii* in a single hospital ward. *Microbial genomics*, 2016. 2(3).
10. Holt, K. E., Kenyon, J. J., Hamidian, M., Schultz, M. B., Pickard, D. J., Dougan, G., & Hall, R. M. Corrigendum: Five decades of genome evolution in the globally distributed, extensively antibiotic-resistant *Acinetobacter baumannii* global clone 1. *Microbial genomics*, 2019. 5(7).

11. Correa, A., Del Campo, R., Escandón-Vargas, K., Perenguez, M., Rodríguez-Baños, M., et al. Distinct genetic diversity of carbapenem-resistant *Acinetobacter baumannii* from Colombian hospitals. *Microbial Drug Resistance*, 2018. 24(1), 48-54.
12. Evans, B. A., & Amyes, S. G. OXA-lactamases. *Clinical microbiology reviews*, 2014. 27(2), 241-263.
13. Pearce, M. E., Chattaway, M. A., Grant, K., & Maiden, M. C. A proposed core genome scheme for analyses of the *Salmonella* genus. *Genomics*, 2020. 112(1), 371-378.
14. CLSI. M100-S25 Performance Standards for Antimicrobial Susceptibility Testing. Thirty one Informational Supplement. Clinical and Laboratory Standards Institute, 2021.
15. Woodford, N., Ellington, M. J., Coelho, J. M., Turton, J. F., Ward, M. E., Brown, S. et al. Multiplex PCR for genes encoding prevalent OXA carbapenemases in *Acinetobacter* spp. *International journal of antimicrobial agents*, 2006. 27(4), 351-353.
16. Turton, J. F., Ward, M. E., Woodford, N., Kaufmann, M. E., Pike, R., Livermore, D. M., & Pitt, T. L. The role of IS *Aba1* in expression of OXA carbapenemase genes in *Acinetobacter baumannii*. *FEMS microbiology letters*, 2006. 258(1), 72-77.
17. Turton, J. F., Gabriel, S. N., Valderrey, C., Kaufmann, M. E., & Pitt, T. L. Use of sequence based typing and multiplex PCR to identify clonal lineages of outbreak strains of *Acinetobacter baumannii*. *Clinical microbiology and infection*, 2007. 13(8), 807-815.
18. Al-Kadmy, I. M. S., Ali, A. N. M., Salman, I. M. A., & Khazaal, S. S. Molecular characterization of *Acinetobacter baumannii* isolated from Iraqi hospital environment. *New microbes and new infections*, 2018. 21, 51-57.
19. Maspi, H., Hosseini, H. M., Amin, M., & Fooladi, A. A. I. High prevalence of extensively drug-resistant and metallo beta-lactamase-producing clinical *Acinetobacter baumannii* in Iran. *Microbial pathogenesis*, 2016. 98, 155-159.
20. Kalal, B. S., Chandran, S. P., Yoganand, R., & Nagaraj, S. Molecular characterization of carbapenem-resistant *Acinetobacter baumannii* strains from a tertiary care center in South India. *Infectio*, 2020. 24(1), 27-34.
21. Guo, T., Shan, C., Li, J., Feng, H., Li, M., Zheng, W., ... & Bao, G. Correlation between antibiotic resistance and serum resistance in *Acinetobacter baumannii*. *INTERNATIONAL JOURNAL OF CLINICAL AND EXPERIMENTAL MEDICINE*, 2019. 12(8), 9804-9814.
22. Shafiqh, M., Rajabnia, R., Yahyapour, Y., Shahandashti, E. F., Khafri, S., & Namvar, A. E. Evaluation of Aminoglycoside Resistance Genes in *Acinetobacter Baumannii* Isolated from Different Parts of Babol Hospitals. *Biomed J Sci & Tech Res*. 2018. DOI: 10.26717/BJSTR.2018.08.001675. ISSN: 2574-1241.
23. Anane, Y. A., Apalata, T., Vasaikar, S., Okuthe, G. E., & Songca, S. Molecular Detection of Carbapenemase-Encoding Genes in Multidrug-Resistant *Acinetobacter baumannii* Clinical Isolates in South Africa. *International Journal of Microbiology*, 2020.
24. Botelho, J., Roberts, A. P., León-Sampedro, R., Grosso, F., & Peixe, L. Carbapenemases on the move: it's good to be on ICEs. *Mobile DNA*, 2018. 9(1), 1-11.
25. Dijkshoorn, L., Aucken, H., Gerner-Smidt, P., Janssen, P., Kaufmann, M. E., Garaizar, J., ... & Pitt, T. L. Comparison of outbreak and nonoutbreak *Acinetobacter baumannii* strains by genotypic and phenotypic methods. *Journal of clinical microbiology*, 1996. 34(6), 1519-1525.
26. Maciel, W. G., da Silva, K. E., Croda, J., Cayo, R., Ramos, A. C., de Sales, R. O., ... & Simionatto, S. Clonal spread of carbapenem-resistant *Acinetobacter baumannii* in a neonatal intensive care unit. *Journal of Hospital Infection*, 2018. 98(3), 300-304.
27. Van Dessel, H., Dijkshoorn, L., van der Reijden, T., Bakker, N., Paauw, A., van den Broek, P., ... & Brisse, S. Identification of a new geographically widespread multiresistant *Acinetobacter baumannii* clone from European hospitals. *Research in microbiology*, 2004. 155(2), 105-112.
28. Higgins, P. G., Hagen, R. M., Kreikemeyer, B., Warnke, P., Podbielski, A., Frickmann, H., & Loderstädt, U. Molecular Epidemiology of Carbapenem-Resistant *Acinetobacter baumannii* Isolates from Northern Africa and the Middle East. *Antibiotics*, 2021. 10(3), 291.
29. Tomaschek, F., Higgins, P. G., Stefanik, D., Wisplinghoff, H., and Seifert H. Head-to-Head Comparison of Two Multi-Locus Sequence Typing (MLST) Schemes for Characterization of *Acinetobacter baumannii* Outbreak and Sporadic Isolates. *PLoS One*, 2016. 11(4), e0153014.
30. Khuntayaporn, P., Kanathum, P., Houngsaitong, J., Montakantikul, P., Thirapanmethee, K., & Chomnawang, M. T. Predominance of international clone 2 multidrug-resistant *Acinetobacter baumannii* clinical isolates in Thailand: a nationwide study. *Annals of clinical microbiology and antimicrobials*, 2021. 20(1), 1-11.
31. Karah, N., Haldorsen, B., Hegstad, K., Simonsen, G. S., Sundsfjord, A., & Samuelsen, Ø. Species identification and molecular characterization of *Acinetobacter* spp. blood culture isolates from Norway. *Journal of antimicrobial chemotherapy*, 2011. 66(4), 738-744.
32. Hamidian, M., & Nigro, S. J. Emergence, molecular mechanisms and global spread of carbapenem-resistant *Acinetobacter baumannii*. *Microbial genomics*, 2019. 5(10).
33. Zhang, X., Li, F., Awan, F., Jiang, H., Zeng, Z., & Lv, W. Molecular epidemiology and clone transmission of carbapenem-resistant *Acinetobacter baumannii* in ICU rooms. *Frontiers in cellular and infection microbiology*, 2021. 11.
34. Dahdouh, E. Epidemiological and molecular analysis of virulence and antibiotic resistance in *Acinetobacter baumannii*. 2017 (Doctoral dissertation, Universidad Complutense de Madrid).
35. Feil, E. J., Li, B. C., Aanensen, D. M., Hanage, W. P., & Spratt, B. G. eBURST: inferring patterns of evolutionary descent among clusters of related bacterial genotypes from multilocus sequence typing data. *Journal of bacteriology*, 2004. 186(5), 1518-1530.
36. Francisco, A. P., Bugalho, M., Ramirez, M., & Carriço, J. A. Global optimal eBURST analysis of multilocus typing data using a graphic matroid approach. *BMC bioinformatics*, 2009. 10(1), 1-15.
37. Qasim, Z. J., Kadhim, H. S., & Abdulamir, A. S. Identification of Antibiotic Resistance Genes in Multi-Drug Resistant *Acinetobacter Baumannii* Clinical Isolates of Iraqi Patients (Zq Strains), Using Whole-Genome Sequencing. *INTERNATIONAL JOURNAL OF PHARMACEUTICAL AND CLINICAL RESEARCH*, 2019. 10(04), 670-680.
38. Ou, H. Y., Kuang, S. N., He, X., Molgora, B. M., Ewing, P. J., Deng, Z., ... & Xu, H. H. Complete genome sequence of hypervirulent and outbreak-associated *Acinetobacter baumannii* strain LAC-4: epidemiology, resistance genetic determinants and potential virulence factors. *Scientific reports*, 2015. 5(1), 1-13.
39. Ganjo, A. R., Maghdid, D. M., Mansoor, I. Y., Kok, D. J., Severin, J. A., Verbrugh, H. A., ... & Goessens, W. OXA-carbapenemases present in clinical *Acinetobacter baumannii-calcoaceticus* complex isolates from patients in Kurdistan region, Iraq. *Microbial drug resistance*, 2016. 22(8), 627-637.
40. Püntener-Simmen, S., Zurfluh, K., Schmitt, S., Stephan, R., & Nüesch-Inderbilen, M. Phenotypic and genotypic characterization of clinical isolates belonging to the *Acinetobacter calcoaceticus-Acinetobacter baumannii* (ACB) complex isolated from animals treated at a veterinary hospital in Switzerland. *Frontiers in veterinary science*, 2019. 6, 17.
41. Taj, Z., Rasool, M. H., Almatroudi, A., Saqalein, M., & Khurshid, M. Extensively drug-resistant *Acinetobacter baumannii* belonging to international clone II from a pet cat with urinary tract infection; the first report from Pakistan. *Polish journal of microbiology*, 2020. 69(2), 231.
42. Argimón, S., Masim, M. A., Gayeta, J. M., Lagrada, M. L., Macaranas, P. K., Cohen, V., ... & Carlos, C. C. Integrating whole-genome sequencing within the National Antimicrobial Resistance Surveillance Program in the Philippines. *Nature communications*, 2020. 11(1), 1-15.

ARTICLE / INVESTIGACIÓN

The influence of gamma rays and electric shock on seed germination and seedling growth in burdock plants

Mohammed Sabah Taher^{1*}, Hussein Aneed Alamrani¹, Issa Auuad Hassn², Israa Khalaf Aneed³, Batool Alaa Kadem⁴

DOI. 10.21931/RB/2022.07.01.30

¹Unit of Medical and Aromatic Plants Research, College of Agriculture Engineering Sciences, University of Baghdad, Al-Jadiriya, Baghdad, Iraq.²Karbala Agriculture Directorate, Iraq.³Department of Medical Laboratory Techniques, Iraq.⁴Department of Horticulture and Landscape Gardening, College of Agriculture Engineering Sciences, University of Baghdad, Al-Jadiriya, Baghdad, Iraq.

Corresponding author: mohammed.s@coagri.uobaghdad.edu.iq

Abstract: Burdock plant is one of the important medicinal plants, the critical part of which is the roots used to clear the body of toxins; the study aimed to stimulate burdock seed germination and seedling growth with low-cost treatments, represented by electric shock and irradiation with low doses of gamma rays on seeds. The experiment was implemented at the Medical and Aromatic Plants Research Unit, College of Agricultural Engineering Sciences, University of Baghdad, Iraq, in 2020. included 6 treatments: soaking the seeds with water for 12 hours only, an electric shock of the seeds (2 and 4 A) by soaking with water for 12 hours, irradiating the seeds (with 10, 20 or 30 Gy) and soaking in the water for 12 hours. The experiment used the design of complete randomized (CRD) with three replicates. The results indicated that the highest germination percentage was recorded under the treatment of electric shock (4 A) and water soaking seeds only (91.0 and 85.7%, respectively). On the other hand, the best germination speed was achieved when gamma rays were treated at (30 Gy) reached 5.93 days. The two treatments: seed irradiation (30 Gy) and water-soaked seeds, were distinguished in most of the seedlings' vegetative and root growth characteristics represented by the length of the seedlings, the number of leaves, and the soft, fresh and dry weight of the shoot and root systems. We conclude from the results that soaking the seeds with water before planting has a positive effect on increasing germination characteristics and seedlings, and the effect increases at treatment with gamma.

Key words: Burdock, electric shock, gamma rays, germination.

Introduction

Among the medicinal plants that have gained particular importance burdock plant (*Arctium lappa* L.) which belongs to the Asteraceae family. The critical part of the plant is the root, which contains many compounds such as Arctiin and Arctigenin, which have medical importance in the expulsion of toxic substances from the body and promoting blood circulation¹. The presence of some phenolic compounds such as Chlorogenic acid and Caffeic acid increased the importance of the plant in scavenging free radicals², which gives it importance in treating tumors resulting from inflammation. The plant extract (tea) is used to increase diuresis and reduce blood pressure and temperature, as well as the importance of the roots as antioxidants due to their content of derivatives of caffeoylquinic acid³.

Because of the role of medicinal plants in supplying drug factories and the importance of this in preserving human life, the need arose to increase the qualitative and quantitative plant production starting from germination to yield by many agricultural processes, including some low-cost physical treatments such as the treatment of seeds by a stimulus by doses from gamma rays or electric shock^{4,5}.

The effect of radiation on the plant is either stimulatory or inhibiting, or deadly. That effect depends on the radiation doses. Low doses stimulate plant growth, as exposing the seeds of some plants to low doses leads to an increase in the germination rate and the growth of the seedling. On the other hand,

some studies indicate that radioactive activation has a temporary effect. It is believed that the difference in the results of radioactive activation is due to the influence of various factors such as the biological properties of the material exposed to radiation and its physiological condition, external factors such as humidity, temperature, lighting, and storage period before and after irradiation, irradiation dose rates, soil fertility, and genotype at the level of cultivars of the same species⁶.

Radiation with gamma rays affects the plant's phenotype and its anatomical, biochemical and physiological state depending on the irradiation dose. These effects include photosynthesis, cellular composition, metabolism, antioxidant system modeling and metabolism of phenolic compounds⁷⁻¹⁰. Induction begins by increasing the effectiveness of RNA synthesis or protein production that occurs during the early stages of seed germination and improvement in respiration and the auxin hormone metabolism in germinated seeds; this effect occurs in low doses of irradiation¹⁰.

In this path, many studies were applied; it was observed that there were differences in the effect of gamma rays according to the dose, plant type, and irradiation conditions. Nassar (2004) found that the treatment of seeds of (*Chamomilla recutita* L.) with gamma rays 0, 2, 4, 6, 8 and 10 kr (kilo rad = 1000 rad) have improved the growth characteristics of plant height,

Citation: Sabah Taher M, Aneed Alamrani H, Auuad Hassn I, Khalaf Aneed I, Alaa Kadem B. The influence of gamma rays and electric shock on seed germination and seedling growth in burdock plants. *Revis Bionatura* 2022;7(1). 30. <http://dx.doi.org/10.21931/RB/2022.07.01.30>

Received: 17 July 2021 / **Accepted:** 7 November 2021 / **Published:** 15 February 2022

Publisher's Note: Bionatura stays neutral with regard to jurisdictional claims in published maps and institutional affiliations.

Copyright: © 2022 by the authors. Submitted for possible open access publication under the terms and conditions of the Creative Commons Attribution (CC BY) license (<https://creativecommons.org/licenses/by/4.0/>).



the number of branches, dry weight and fresh weight of roots compared with plants produced from untreated seeds¹¹. When exposing seeds of *Foeniculum vulgare* L. plant to different levels of gamma rays 0, 20, 40, 60, 80, and 100 Gy (Gy= 100 rad) Latif (2011) found an increase in weight of fresh and dry for vegetative growth were between the 60 and 80 Gy doses, while the 100 Gy dose inhibited growth¹². On the other hand, a gradual decrease in the chlorophyll concentration was observed at the high dose of irradiation (200 Gy), which reached 14.2 mg. Kg⁻¹ compared to 18.9 mg. Kg⁻¹ at the dose of 100 Gy in the wheat plant¹³. Melki and Marouanig (2010) studied the effect of levels from gamma rays (0, 10, 20, 30 Gy) on wheat germination and seedling growth in greenhouse conditions; they found a development in the number and length of roots by 18 and 32% respectively at dose 20 Gy¹⁴. Under laboratory conditions and field of experiment, were planted flax seeds irradiated with different doses by using⁶⁰Co (cobalt element); it was noted that doses up to 8 Kr were favorable in stimulating growth through the occurrence of significant differences in seed germination, branch length, the number of leaves and leaf area while the higher dose of 8 Kr led to a negative effect on germination¹⁵.

About electric shock, Robert (2007) indicated that electro-shocked seeds had a high germination speed and an increased yield when using stable electricity, this reduced the chance of seeds dying, but the seeds must be moist because dried seeds may be damaged¹⁶. Sidaway (2009) exposed the seeds of *Avena sativa* plant to electricity and found high speed in the plant germination and increase in growth and dry weight¹⁷. Al Taweel *et al.*(2018) showed that the best leaf area, chlorophyll content and dry weight of white and Egyptian henbane seedlings were at electric shock 2 A among three levels (2, 4, 6 A)¹⁸. Al-Mousawi (2017) showed that the electric shock treatment significantly affected vegetative and root growth indicators. The treatment of 4 A recorded the highest rates of vegetative growth indicators represented by plant height, the number of leaves, leaf area, fresh and dry weight of the *Tannacetum parthenium* L. plant⁹.

Based on the above, the study aimed to stimulate burdock seed germination and seedling growth with low-cost treatments, represented by electric shock and irradiation with low doses of gamma rays on seeds.

Materials and methods

The study was carried out to stimulate burdock seed germination and seedling growth by the effect of electric shock, gamma rays, and 12-hour soak in water. The seeds were obtained from the Medicinal and Aromatic Plants Research Unit, College of Agricultural Engineering Sciences, University of Baghdad. The seeds were divided into 18 groups according to the number of experimental units, and each group included 100 seeds. The experiment consisted of 6 treatments that included: soaking the seeds in water for 12 hours only, soaking in water for 12 hours, then shock electric of the seeds 2 and 4 A(Ampere), soaking in water for 12 hours then irradiating the seeds 10, 20 and 30 Gy (Gy=100 rad) with three replicate. The number of experimental units was 18 using the completely randomized design (CRD), and the characteristics were compared according to the LSD test at 5%¹⁹.

Each group of seeds(100 seeds) was planted in plastic pots (15 D, 25 L cm) in the plastic house on 25 / 11/2020 using the peat moss substrate. The counting of the seeds was stopped when no new germination appeared for three days. Then,

germination ratio (%) and germination speed (day) were calculated. The seedlings were separated into plastic pots (8 D, 10 L cm) for each plant in the pot (12 plants per treatment in the replicate) to make seedlings measurements. When the seedlings grew to about four true leaves, the parameters were measured: seedling length (cm), root length (cm), number of leaves, chlorophyll content (SPAD), fresh and dry weight of shoot(gm), fresh and dry root weight (gm).

Seeds were shocked in a glass container containing water (covering the seeds) with (1% NaCl). Two levels of shocking (2 and 4 amperes) were used for three minutes. Then the seeds were washed with water to remove the salt. As for irradiation treatments, the seeds were treated with gamma rays at the levels determined by using Cobalt 60.

The germination percentage was daily calculated starting for the first germination until no seed was germinated for three days.

Germination percentage = Number of germinated seeds / Total number of seeds ×100

The speed of germination was calculated according to the following formula²⁰.

$$GS = [(N1 \times D1) + (N2 \times D2) + Nn \times Dn \dots] / TG$$

GS: Germination speed.

N: Number of germinated seeds daily.

D: Number of days from planting.

TG: Total number of germinated seeds

The seedling length was measured from the surface of the substrate to the top of the seedlings. Roots were separated from the shoot and washed with water to remove the remaining substrate. The roots were dried using a piece of cloth to remove the moisture. The fresh weight was measured using a sensitive balance. All shoots and roots were put in an oven at (50 °C) for drying. A sensitive balance measured the dry weight. (The average temperature inside the plastic house is about max. 21.5± 1 and min. 11.13± 1)

Results

Figure (1.) shows a significant difference in the germination percentage due to the effect of the experimental factors. The highest germination percentage was achieved under the treatments of seeds shock (4 A) and water-soaked seeds(91.0, 85.7%, respectively). These were followed by the treatments gamma rays 20 and 30 Gy (76.0 and 75.7% respectively) compared to the lowest germination percentage under the treatment of gamma rays 10 Gy (72.0%).

In the germination speed, figure (2.) noticed that the treatment of gamma rays 30 Gy achieved the highest germination speed (5.93 days) with a significant difference from the other treatments. This was followed by the treatments gamma rays 10 and 20 Gy (6.82 and 7.08 days respectively) compared with the lowest germination speed when seeds were soaked with water only(8.05 days).

The treatments: 1 (soaking by water only) 2,3,4(irradiation 10,20,30Gy)5,6(electric shock 2,4A) respectively.

Although the highest level of chlorophyll was achieved at the treatments of shock the seeds (4 A) and gamma rays 20 Gy (49.13 and 45.8 SPAD respectively), they were not significantly different from the other treatments (Table 1).

In the number of leaves, it was noted from table 1 that the treatments of gamma-ray 30 Gy and electric shock (4 A) recorded the highest values (5.22 and 4.53 leaves. Seedlings⁻¹ respectively), followed by the treatment of water-soaked

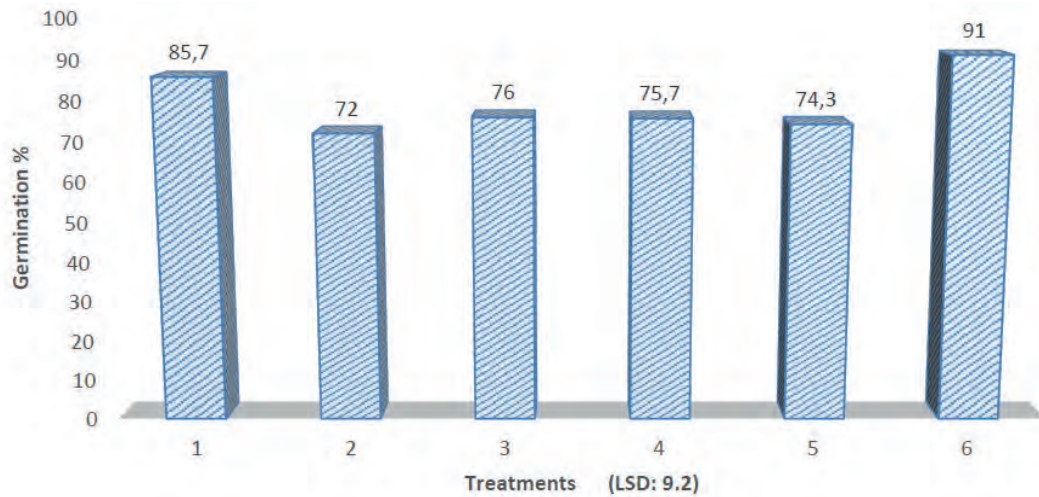


Figure 1. Effect of Gamma radiation and electric shock on germination % (GP).

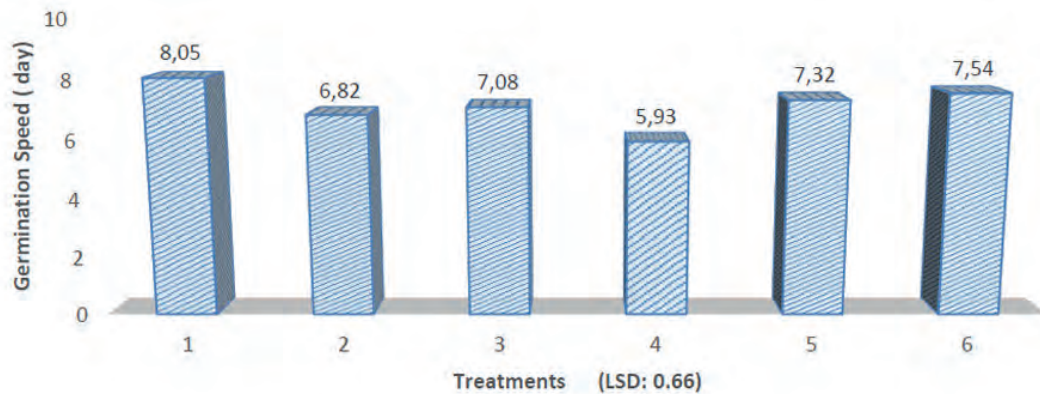


Figure 2. Effect of Gamma radiation and electric shock on germination speed (GS).

seeds (4.38 leaves. seedlings⁻¹) compared with the lowest number of leaves when treated by gamma 20 Gy (3.61 leaves. seedlings⁻¹).

From table 1, the longest seedlings and the highest dry weight resulted from the treatment of water-soaked seeds (12.0 cm, 0.440 gm respectively) and gamma rays 30 Gy (11.16 cm, 0.415 gm respectively), with a significant difference from other treatments. The shortest seedlings value was recorded under 4 A(6.00 cm) treatment. However, the shocking seeds' lowest dry weight was recorded with 2A (0.150 gm). The highest value of the fresh weight of seedling was 2.97 gm at the water-soaked treatment, followed by 2.64 gm at the treatment of gamma rays 30 Gy. Compared to the lowest value of the fresh weight, these were superior to 0.840 gm at the treatment of shocking electric 4A.

Although the root length increased at the treatments of gamma rays 30 Gy and electric shock 4A, it was not significantly different from the other treatments. The characteristics of the fresh and dry weight of roots recorded the highest values at the treatments of gamma rays 30 Gy (3.43 gm, 0.720 gm respectively) and water-soaking (3.09 gm, 0.670 gm, respectively). These values were significantly different from the other treatments (Table 2).

Discussion

It is noted from the above that most of the characteristics of the study were improved by the effect of two treatments,

water soaking and seed irradiating with 30 Gy. Soaking seeds by water before planting has a role in removing or reducing inhibitors concentration as well as softening the seed coat and increasing its permeability²¹. Therefore, it is easy to absorb water and oxygen to enter the seed embryos²², increasing the biological reactions leading to improved seedlings in the future. The characteristics' values were decreased under the rest of the treatments (10 Gy, 20 Gy, 2 A, and 4 A). This decrease may be because these treatments are not suitable for stimulation, so the opposite⁶. As for the treatment of gamma rays, 30 Gy, and water-soaking, the increase of germination speed and root characteristics may be due to the free radicals produced during the irradiation process, which may be necessary in stimulating metabolic processes it led to the germination process²³. Also, the induction begins by increasing the effectiveness of RNA or protein synthesis that occurs during the early stages of seeds germination and improvement in respiration and auxin hormone metabolic in the germinated seed and reflection on the growth of roots and leaves. This effect occurs in low doses of irradiation^{10,24}, as well as the improvement in the characteristics of vegetative growth (seedlings length, number of leaves, dry and soft weight of vegetative and root growth was reflected in the increase in the dry weight for root and vegetative characteristics).

Conclusions

The germination rate of seeds can be increased by some

Treatment	Height (cm)	Leaves No. (leaf. seedlings ⁻¹)	Chloroph SPAD	Fresh weig (gm)	Dry weigh (gm)
Soaking by water only	12.0	4.38	42.27	2.97	0.440
Gamma ray 10 Gy	6.62	3.94	43.33	0.880	0.160
Gamma ray 20 Gy	7.12	3.61	45.80	0.845	0.175
Gamma ray 30 Gy	11.16	5.22	44.0	2.64	0.415
Electric shock 2A	6.75	3.94	43.23	0.845	0.150
Electric shock 4A	6.00	4.53	49.13	0.840	0.175
L.S.D	2.07	0.78	N.S	0.590	0.121

Table 1. Effect of seed treatments on vegetative parameters of *Arictum lapa* seedlings.

Treatment	Root length	Root fresh Weight	Root Dry Weight
soaking by water only	22.50	3.09	0.670
Gamma ray 10 Gy	21.97	1.10	0.295
Gamma ray 20 Gy	22.38	1.05	0.305
Gamma ray 30 Gy	23.99	3.43	0.720
Electric shock 2A	22.69	1.40	0.350
Electric shock 4A	23.50	1.29	0.395
LSD	NS	0.40	0.169

Table 2. Effect of seeds treatments on root parameters of *Arictum lapa* seedlings.

simple treatments such as soaking with water before planting or treatment with some physical treatments (low cost) such as gamma rays and electric shock, but the appropriate dose must be determined because some doses lead to a negative effect. Our research has proven that the dose of 30 Gy was the best dose for germination and seedling characteristics of the burdock plant.

Acknowledgments

I hope thankful foe who support us to complete this re-search.

Funds

Self-funds.

Conflict of interest

Authors declare no conflicts of interest.

Bibliographic references

1. Chan Y S, Cheng L N, Wu J H, Chan E, Kwan Y W, Lee S Y, Leung G P , Yu P H, Chan S.W. A review of the pharmacological effects of Arctium lappa (burdock). *Inflammopharmacology*. 2010; 19(5): 245-54.
2. Anchena Fu, Bang An, Chau Wu , Chena Yang .The influence of different treatments on the free radical scavenging activity of burdock and variations of its active components. *Food Chemistry*. 2004; Volume 86, Issue 4 .Pages 479-484.
3. Predes F S , Ruiz A L , Carvalho J E , Foglio M A, Dolder H. Antioxidative and in vitro antiproliferative activity of Arctium lappa root extracts. *BMC Complement Altern Med*. 2011; 11: 25.
4. Al-Amrani H A H. The response of the Medicinal pumpkin to physical treatments and organic fertilizers, Ph.D. thesis, College of Agriculture, University of Baghdad. 2015; P 175.

5. Al-Mousawi Z J N. Influence of some physical and chemical factors on the production of the secondary metabolic compound from the Tanacetum parthenium L. planted field and laboratory. PhD thesis. college of Agriculture. Baghdad University. 2017; P 150.
6. Ibrahim A F, Al-Saadawi I S, Al-Janabi K K .. Applications of Nuclear Techniques in Plant Studies. Publications of the Iraqi Atomic Energy Organization. Babel Printing Press in Baghdad - Al-Saadoun. 1990; p. 524.
7. Kovács E, Keresztes A. Effect of gamma and UV- B/C radiation on plant cells. *Micron*, 2002; 33(2): 199–210.
8. Wi S G, Chung B Y , Kim J H, Baek M H, Yang D H, Lee J W, Kim J S. Ultrastructural changes of cell organelles in Arabidopsis stem after gamma irradiation. *J. Plant Biol*. 2005; 48(2):195–200.
9. Kim J H, Lee M H, Moon Y R, Kim J S, Wi S G, Kim T H, Chung B Y. Characterization of metabolic disturbances closely linked to the delayed senescence of Arabidopsis leaves after gamma-irradiation. *Environ. Exp. Bot*. 2009; 67(2): 363–371.
10. Jan S, Parween T, Siddiqi T O, Mahmooduzzafar. Effect of gamma radiation on morphological, biochemical, and physiological aspects of plants and plant products .*Environ. Rev*. 2012; 20: 17–39.
11. Nassar H A, Hashim M F, Hassan N S, Ao-Zaid H. Effect of Gamma Irradiation and Phosphorus on Growth and Oil Production of Chamomile (*Chamomilla recutita* L. Rauschert). *International.J of . Agr&Biology*. 2004; Vol. 6, No. 5.
12. Latif H H, Abdalla M A, Farag S A. Radio-stimulation of phytohormons and bioactive components of coriander seedlings *Turkish Journal of Biochemistry–Turk*. 2011; 36 (3) ; 230–236.
13. Borzouei A, Kafi M, Khazaei H, Naseriyan B , Majdabadi A. Effect gamma radiation on germination and physio- logical aspects of whwheat (*Triticum aestivum* L.) seedlings . *Pak. J. Bot*. 2010; 42(4): 2281-2290.
14. Melki M, Marouani A. Effects of gamma rays irradiation on seed germination and growth of hard wheat. *Environ Chem Lett*. 2010; 8:307–310. 3.

15. Ali H, Mumammad , Ullah R, Majeed A, Inayat N. Germination, growth and yield performance flax (*Linum usitatissimum* L.) under gamma irradiation stress .2018,, No. 2 (174) /: 17-26.
16. Robert A N. Electro Culture (The Electrical Tickle). USC. Section. 2007; 18(23):1-11.
17. Sidaway G H. Influence of Electrostatic Fields on seed Germination Department of Botony, University college. 2009; Cardiff. DOI:10.1038/211303A0.
18. Al Taweel S K, Cheyed S H, Al Amrani H A. Effect of electric shock on germination and seedling growth in henbane species. *Academia Journal of Medicinal Plants* 2018; 6(5): 071-078.
19. Al-Rawi K M , Khalaf Allah A M. Design and analysis of agricultural experiments, second edition. Books and publishing house. University of Mosul - Iraq.p 2000; 488.
20. Czabator F J. Germination value: An index combining speed and completeness of pine seed germination. *Forest Science*. 1962; 8: 386 – 395.
21. Salman M A. Horticulture propagation. Ministry of Higher Education and Scientific Research. Baghdad University. the House of Books for Printing and Publishing. University of Al Mosul. 1988; P. 552.
22. Makhoul G, Ataff W. The effect of some physical and chemical treatments on the Guava seeds germination. *Tishreen University Journal for Research and Scientific Studies - Biological Sciences Series* Vol. 2016; (38) No. (1) .
23. Amjad. M , Anjum M A. Effect of gamma radiation on onion seed viability, germination potential, seedling and orfhology. *I'ak J Agri S Vul*. 2002; 39(3).
24. Minisi F A, El-mahrouk M E, El-Din M, Rida F, Nasr M N. Effects of Gamma Radiation on Germination, Growth Characteristics and Morphological Variations of *Moluccella laevis* L. *American-Eurasian J. Agric. & Environ. Sci*. 2013; 13 (5): 696-704 .

ARTICLE / INVESTIGACIÓN

Study single nucleotide polymorphism in Promoter region of UGT1A1 Gene in Iraqi Patients with Gilbert's syndrome

Marwa A. Kubba^{1*}, Abeer Ali Marhoon² and Rafed Abbas Kadhum³

DOI. 10.21931/RB/2022.07.01.31

¹ Department of Biology, Al-Rasheed University College, Baghdad, Iraq.² Al-Rafidain University College, Baghdad, Iraq.³ Biology department Wasit University College of science. Iraq.Corresponding author: dr.marwa@alrasheedcol.edu.iq

Abstract: This study aimed to detect genetic variants of the UGT1A1 gene in patients with Gilbert's syndrome. To detect this, primers were designed; PCR and direct sequencing were done for the promoter area of the gene as a diagnostic tool for the detection of any polymorphism. Variation and polymorphism were detected within the promoter mutants of the UDP glycosyltransferase _UGT1A1 gene that causes hyperbilirubinemia in a group of Iraqi patients compared with a group of the normal healthy individual as controls. The patients with hyperbilirubinemia in this study were 30 in which the total bilirubin level was more than 12 mg/dl serum; they included 25 males and 5 females, while the control group consisted of 20 healthy individuals. This study was carried out from September 2019 till April 2021. The result displayed high occurrence of Gilbert syndrome within male patients than in females, and regarding the analyses of mutation of bilirubin UDP glycosyltransferase _UGT1A1 gene, it is clear that the genotypic distribution of variation among the hyperbilirubinemia patients included all 30 patients, while SNP was detected in 18 patients out of 30 which indicate that the UGT1A1 gene mutation was a likely risk factor for the development of hyperbilirubinemia related Gilbert syndrome in Iraq. The homozygous and heterozygous polymorphisms A/G inside the promoter region of the UGT1A1 gene were effectively identified by sequencing. Our finding suggests that TA repeats and allele of UGT1A1 polymorphism A/G are associated with Gilbert's syndrome and act as genetic markers of this disease in Iraqi patients. To analyze data and sequence variation in gene, generous software was used after amplifying the gene. All processes include DNA extraction, PCR amplification, sequencing, and assembly.

Key words: Gilbert's syndrome, UGT1A1 gene, polymorphism, hyperbilirubinemia.

Introduction

Gilbert syndrome (GS) is a disorder conspicuous by intermittent unconjugated hyperbilirubinemia and jaundice¹. Protein formed from the UGT1A1 gene, named the bilirubin uridine diphosphate glucuronosyltransferase (bilirubin-UGT) enzyme, is a hepatic enzyme in which glucuronidated bilirubin; a material formed once red blood cells are broken down. The enzyme's function changes the toxic form of bilirubin to its nontoxic form, making it capable of being thawed and detached from the body; this enzyme is required for the conversion (conjugation) and subsequent elimination of bilirubin from the body^{2,3}. Gilbert's syndrome is supposed in patients that have unconjugated hyperbilirubinemia produced by reduced activity of the UDP-glucuronosyltransferase 1A1 (UGT1A1) gene in the lack of irregular liver function and hemolysis, noticeable by unbalanced unconjugated hyperbilirubinemia, typically due to the polymorphism uridine diphosphate-glucuronosyltransferase inherited defects in uridine diphosphogluconurate glucuronosyl-transferase (UGT) that encoded by the UGT1A1 gene at chromosome 2q37.1, the reduced enzyme action are lead to hyperbilirubinemia. The variation in the UGT1A1 gene can reason for Gilbert syndrome that characterized by phases of insignificant unconjugated hyperbilirubinemia³. The main genetic variants in Gilbert's syndrome are TATA-box repeats of the

promoter region that are responsible for the manufacturing of the bilirubin-UGT enzyme and exon 1 G211A of the coding region, UGT1A1 gene mutations either decrease the affinity of UGT1A1 toward bilirubin or decrease enzyme activity. New studies presented serum bilirubin is related to a genetic variation of the UGT1A1 locus⁴. In several people, the maximum shared change cause Gilbert syndrome happens in part near the UGT1A1 gene called the promoter region. This alteration must happen in both copies of the UGT1A1 gene to cause Gilbert syndrome⁵⁻⁹.

Homozygous polymorphism is the most public UGT1A1 genotype responsible for Gilbert's syndrome when A(TA)₇TAA in the gene's promoter region; this will make a 70-80% reduction in the gene's promoter region glucuronidation activity. In contrast, the change at nucleotide 211 (G211A), which change arginine to replace with glycine at position 71 in the coding region of the UGT1A1 gene, is accountable for around 20% of Gilbert's syndrome cases in Asian people¹⁰⁻¹². Therefore this study was aimed to detect the gene variation in UGT1A1 gene in blood samples as a diagnostic tool by PCR and sequencing in patients from Iraq and determine its susceptibility to with Gilbert's syndrome.

Citation: Kubba, M. A.; Marhoon, A. A.; Kadhum, R. A. Study single nucleotide polymorphism in Promoter region of UGT1A1 Gene in Iraqi Patients with Gilbert's syndrome. *Revis Bionatura* 2022;7(1). 31. <http://dx.doi.org/10.21931/RB/2022.07.01.31>

Received: 16 October 2021 / **Accepted:** 20 November 2021 / **Published:** 15 February 2022

Publisher's Note: Bionatura stays neutral with regard to jurisdictional claims in published maps and institutional affiliations.

Copyright: © 2022 by the authors. Submitted for possible open access publication under the terms and conditions of the Creative Commons Attribution (CC BY) license (<https://creativecommons.org/licenses/by/4.0/>).



Materials and methods

This study was held from September 2019 to April 2021 at the University of Al-Rasheed / Biology Department, and the molecular study was held in the molecular laboratory of ASCo. They were a learning center in Iraq. Blood samples were collected from a population consisting of 30 subjects with Gilbert syndrome disease who complained of high bilirubin level in blood and have familial history of Gilbert syndrome with no clinical features refer to a disorder of liver functions; they were selected from those attending private Hospital in Baghdad. The age of these patients ranged from 17 - 55 years, in which 25 patients were males, and only 5 were female. The control group involved 20 healthy individuals were their ages and sex thoroughly similar to the patients and had no history of any disease.

An aliquot of 5 ml blood sample was gained from the vein of patient and control groups and divided into two parts, the first part (2 ml) was collected into an EDTA tube and kept at -20 °C for molecular analyses while serum was used for biochemical tests for liver enzyme ALT, AST, alkaline phosphatase, was recovered from the second blood part (3 ml).

Biochemical analyses of liver enzymes (ALT, AST, alkaline phosphatase) were estimated. The levels of all enzymes were examined for both the experimental and control groups.

DNA extraction

First DNA was isolated according to the procedure Relia-Prep™ Blood gDNA Miniprep System, Promega as the steps in manufacturer producer (table 1).

Polymerase Chain Reaction (PCR)

PCR was performed for 50 samples (30 patients and 20 control groups) using specific primers designed to amplify and sequence the promoter region of the UGT1A1 gene as described in table (2). PCR amplifications were performed as presented in (table 3).

DNA Standard Sequencing

To analyze the nucleotides sequences for all samples to determine the presence of single nucleotide polymorphism (SNP) and determine the genetic variation of this gene within the population, sequence analysis of the promoter area of the UGT1A1 gene was done accomplished on Gilbert syndrome patients. PCR product was directed for Sanger sequencing by ABI3730XL, automated DNA sequences, Macrogen Corporation – Korea. The obtained results were established through email and investigated by generous software.

Kits	Company/ Origin
ReliaPrep™ Blood gDNA Miniprep System, Agarose, Ethidium Bromide Solution (10mg/ml), GoTag Green Master Mix, Nuclease Free Water, TAE 40X, Quantifluor dsDNA System	Promega, USA

Table 1. Kits for DNA extraction.

Table 2. Sequences of primers used in the detection promoter region of UGT1A1 gene in this study.

primers	Sequence of primers	Annealing Temp. (°C)	PCR product size(bp)
UGT1A1-F	5'-ATAGTCGTCCTTCTCCTCTC-3'	60(°C)	892
UGT1A1-R	5'-CACTGGGTAGCCTCAAATTC-3'		

step	Temperature(C°)	Time	No. of cycles
Initial denaturation	94	4 min	1
Denaturation	94	30 sec	30
Annealing	63	30 sec	
Extension	72	30 sec	
Final extension	72	7 min	1
Stop reaction	4	10 min	

Table 3. PCR amplification program of UGT1A1 gene.

Results

Liver function test results of Gilbert syndrome patients

The patients with hyperbilirubinemia suffering from Gilbert syndrome in this study were 30 by a whole bilirubin level of more than 12 mg/dl, which comprise 25 patients were males and 5 patients were females, samples for patients and control groups have normal liver enzyme ALT, AST, alkaline phosphatase values.

Distribution of Cases According to Gender

The distribution of GS according to gender showed higher rates in males than females when the male cases were 83.33% and 16.66% for females (figure 1).

Purity and concentration of DNA extracted from

The DNA was effectively extracted from blood samples. The purity of DNA extracted from blood samples was extended from 1.8 to 2, and the concentration of DNA was extended from 70 -120 µg/ml.

Amplification of UGT1A1 gene

The molecular genetic markers related to patients with hyperbilirubinemia were examined, the segment of the UGT1A1 gene can be amplified by using the PCR, including the promoter region with a size of about 892bp shown in figure (2). The primers in this study were designed using the NCBI Primer-Design online tool to detect single nucleotide polymorphism (SNPs) that may be found in the target gene leading to hyperexpression bilirubin that leads to Gilbert syndrome.

Sequencing and Analysis of UGT1A1 gene

An investigation of any genetic variation and mutations in the UGT1A1 gene was done. The sequence analysis result for the promoter region in the UGT1A1 gene showed there were two genetic variants within the gene's promoter area. The first variant was, 8 repeats of TA copies was observed in the sequence of the gene of all patients samples; the results were directly compared with the Iraqi healthy control group in which it's clear that 7 TA repeats were detected in this region as shown in table 4; also it is compared databases at www.ncbi.nlm.nih.gov by the BLAST check-up tool and besides using Genus software program figure (3 -a,b). Also, there is the second variant in the promoter region of UGT1A1 region of the gene was de-

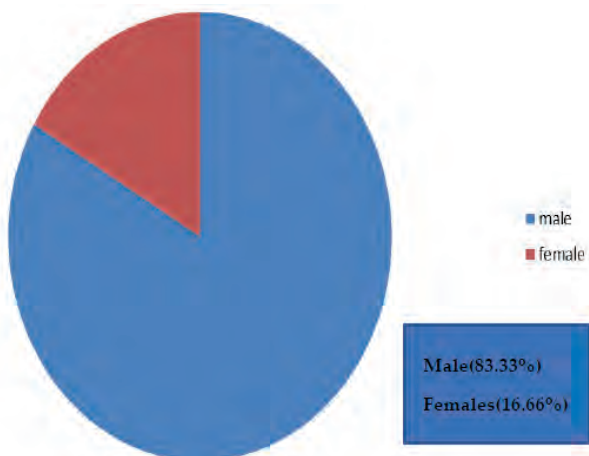


Figure 1. Distribution of Cases According to Gender.

tected in which among the thirty Gilbert Syndrome patients, there are one SNP detected in the promoter region, which is A substitution with G in site -208, as shown in table 4, and the number of patients who had this polymorphism (A instead of G) was 18 out of 30 patients (60 %) in comparison with that of healthy individuals included in this study, while the other 12 patients (40%) no variation appeared in this studied part of the gene, might have in another coding region of UGT1A1 gene, as shown in figure (4-a,b).

The outcomes of PCR analysis of UGT1A1 (-208 A/G) polymorphism subdivided GS patients into three genotypes groups: the first group is homozygous wild type (AA) in which no variation appeared when they have two identical alleles for a gene, the second group is homozygous mutant (GG), and the third group is heterozygous (AG) having two different alleles for a gene one dominant and one recessive, this is a heterozygous mutation. As a result of this observation, AG genotype may be considered as a risk factor, while GG genotype appeared only in 8 patients out of 30 patients (26.6%) when they harbored two AA/GG variations and cannot be considered as a protective factor for Gilbert syndrome in the Iraqi population examined. This observation indicated that these genotypes are associated with Gilbert's genetic predisposition. The percentage of genetic variation of the promoter region of UGT1A1 (-208 A/G) was illustrated in Table 5.

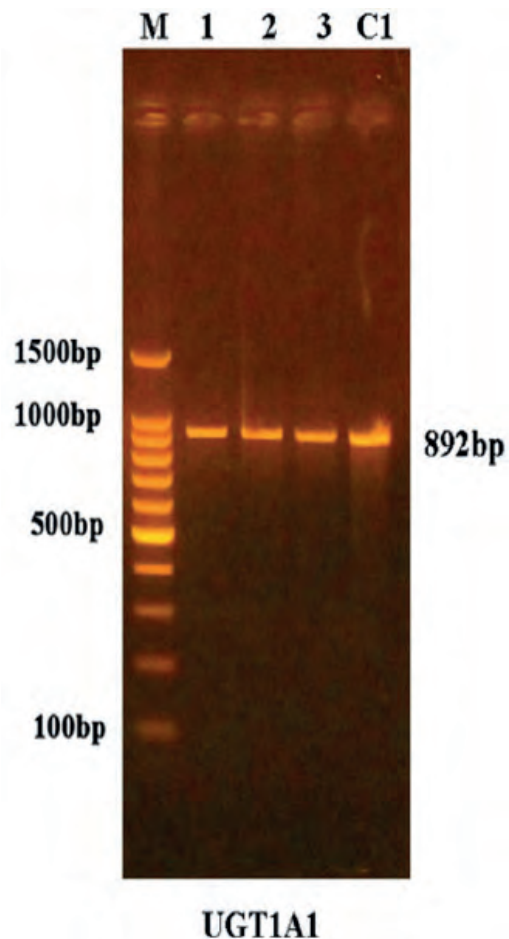


Figure 2. The amplification of UGT1A1 gene promoter region of patient M= 100bp ladder marker. Lanes 1-C1 is 892bp PCR products.

Variation Type	Position on gene	Wild type	Percentage of patients harbored this type of variation
8 repeats of TA copies	TATA box	7 repeats of TA copies	All 30 patients (100%)
A substitution with G (novel mutation)	Promoter region	G instead of A	18 out of 30 (60%)

Table 4. Genetic variation detected in the promoter area of UGT1A1 gene.

Number of samples	Samples of the patients	Wild type AA	Homozygous mutant GG	Heterozygous AG
	30	12 (out of 30) (40%)	8(out of 30) (26.6%)	10(out of 30) (33.3%)

Table 5. Genetic variation in the promoter region of UGT1A1 gene of Gilbert syndrome patients.

DISCUSSION

In this study, the distribution of patients with GS according to gender showed higher rates of infection in males (25 out of 30) (83.33%) than females (5 out of 30)(16.6%), when this results supported by the results of, Sieg A. *et al.* (1987), who found that males are more frequently affected than females, this might be clarified by the existence of a high bilirubin load per kilogram body weight in males, also may the androgen steroid inhibition of bilirubin enzymatic glucuronidation, Bosma PJ, *et al.* (1995)^{20,21}.

The promoter area of the UGT1A1 gene in Gilbert syndrome patients compared to control samples(healthy individuals) showed two types of variation; this is agreed with Canu. *et al.* 2013, showed that more than 130 variations in both regulatory and coding regions of UGT1A1 had been recognized in hereditary hyperbilirubinemia patients²². the first one was the repeats of (TA) copies in promoter region appeared in all patients in which it repeated 8 times in sequences of patients while 7 times repeated in the sequence of the control group,

Bosma *et al.*, 1995; Monaghan *et al.*, 1996; Beutler *et al.*, 1998; Biondi *et al.*, 1999; Kadakol *et al.*, 2000; Farheen *et al.*, 2006)¹⁴⁻¹⁹, who found that the determined mutual UGT1A1 genotype accountable intended for Gilbert's syndrome, in which the homozygous polymorphism A(TA)₇ TAA found within promoter area of the gene, make a 70-80% decrease in glucuronidation activity, when they repeated 7 times in a sequence of patients and 6 times in control healthy group, while in our Iraqi patients it repeats 8 times in compared with the sequence of healthy patients, it repeats only 7 times, (rs 3064744).

The second variation in the promoter area of the UGT1A1 gene show one SNP in 18 patients, A substitution with G in -308 site in the promoter region of the gene indicate that these mutations show a part in this disease in which these polymorphisms modify the expression that altered transcription factor gene binding. Genetic factors are considered as an essential factor for the disease, and it's clear that the variation in the promoter area of the gene contributes to GS disease, In which

the promoter area controls the manufacture of the bilirubin-UGT enzyme.

Results were the same in the study Xiao-xiao Mi ., 2019, which detected the association between Gilbert syndrome and UGT1A1 G/C-46 SNP (rs873478) in the proximal promoter region gene and Gilbert syndrome.

Besides, homozygous genotypes (AA/GG) in the promoter region were more frequent in the patients than in the controls. These results disagree with another study in which they found this variation in exon 1while in our study, one heterozygous SNPs were detected (AA/AG) in eight Gilbert syndrome samples.

Our finding agreed with Xiao-xiao Mi *et al.*, 2019³³, who screened many coding areas of the UGT1A1 gene in 60 Gilbert syndrome patients, who noted proximal promoter area of UGT1A1 variation in 85% of patients, but no mutations were identified (Glasow *et al.*, 2001). New genome association studies exposed that serum bilirubin is related to a genetic variation of the UGT1A1 locus⁹.

Changes in the UGT1A1 gene either decrease the affinity of UGT1A1 toward bilirubin or reduce enzyme activity¹⁰. The patients may have changes in another coding region of the UGT1A1 gene.

Single nucleotide polymorphisms (SNPs) were the most common variation in a specific gene that influences how a person responds to the environmental factor, which may alter the disease risk²³.

Conclusions

In the present study, our results indicated that variation on the promoter region of the UGT1A1 gene affects the bilirubin level; TA copies repeats were 8 times in a sequence of patients while 7 times in control healthy samples.UGT1A1 (-208 A/G) polymorphism was associated with Iraqi patients with Gilbert syndrome. However, it should also be noted that the GG and AG genotype could be considered markers of genetic predis-

a-

Homo sapiens chromosome 2, GRCh38.p13 Primary Assembly

Sequence ID: [NC_000002.12](#) Length: 242193529 Number of Matches: 1

Range 1: 233759987 to 233760788 [GenBank](#) [Graphics](#)

[Next Match](#) [Previous Match](#)

Score	Expect	Identities	Gaps	Strand
883 bits(478)	0.0	702/805(87%)	36/805(4%)	Plus/Plus

Features: [udp-glucuronosyltransferase 1a8 precursor](#)
[udp-glucuronosyltransferase 1a10 precursor](#)

Query	9	TGGTCTGTGG--ATACTAATTT-ATGGATCCTGAGGTTCTGGAAGTACTTTGCTGTGTTC	65
Sbjct	233759987	TGGTCTGTGGAATACTAATTTAATGGATCCTGAGGTTCTGGAAGTACTTTGCTGTGTTC	233760046
Query	66	ACTCAAGAATGTGATTTGAGTATGAAATTCAGCCAGTTCAACTGTTGTTGCCTATTAAG	125
Sbjct	233760047	ACTCAAGAATGTGATTTGAGTATGAAATTCAGCCAGTTCAACTGTTGTTGCCTATTAAG	233760106
Query	126	AAACCTAATAAAGCTCCACCTTCTTTATCTCTGAAAGTGAACCTCCTGCTACCTTTGTGG	185
Sbjct	233760107	AAACCTAATAAAGCTCCACCTTCTTTATCTCTGAAAGTGAACCTCCTGCTACCTTTGTGG	233760166
Query	186	ACTGACAGCTTTTTATAGTCACGTGACACAGTCAAACATTAACCTGGTGTATCGATTGGT	245
Sbjct	233760167	ACTGACAGCTTTTTATAGTCACGTGACACAGTCAAACATTAACCTGGTGTATCGATTGGT	233760226
Query	246	TTTTGCCatatatatatatataGTAGGAGAGGGCGAACCTCTGGCAGGAGCAAAGGCGC	305
Sbjct	233760227	TTTTGCCATATATATATATATAAGTAGGAGAGGGCGAACCTCTGGCAGGAGCAAAGGCGC	233760286
Query	306	CATGGCTGTGGAGTCCCAGGGCGGACGCCCACTTGTCCTGGGCCGTGCTGTGTGTGTGCT	365
Sbjct	233760287	CATGGCTGTGGAGTCCCAGGGCGGACGCCCACTTGTCCTGGGCCGTGCTGTGTGTGTGCT	233760346

b-

Homo sapiens UDP glycosyltransferase 1 family, polypeptide A1 (UGT1A1) gene

Sequence ID: [AY603772.1](#) Length: 16944 Number of Matches: 1

Range 1: 1647 to 2495 [GenBank](#) [Graphics](#)

[Next Match](#) [Previous Match](#)

Score	Expect	Identities	Gaps	Strand
1526 bits(826)	0.0	842/849(99%)	3/849(0%)	Plus/Plus

Query	10	TGGTCTGTGG--ATACTAATTTAATGGATCCTGAGGTTCTGGAAGTACTTTGCTGTGTTC	67
Sbjct	1647	TGGTCTGTGGAATACTAATTTAATGGATCCTGAGGTTCTGGAAGTACTTTGCTGTGTTC	1706
Query	68	ACTCAAGAATGTGATTTGAGTATGAAATTCAGCCAGTTCAACTGTTGTTGCCTATTAAG	127
Sbjct	1707	ACTCAAGAATGTGATTTGAGTATGAAATTCAGCCAGTTCAACTGTTGTTGCCTATTAAG	1766
Query	128	AAACCTAATAAAGCTCCACCTTCTTTATCTCTGAAAGTGAACCTCCTGCTACCTTTGTGG	187
Sbjct	1767	AAACCTAATAAAGCTCCACCTTCTTTATCTCTGAAAGTGAACCTCCTGCTACCTTTGTGG	1826
Query	188	ACTGACAGCTTTTTATAGTCACGTGACACAGTCAAACATTAACCTGGTGTATCGATTGGT	247
Sbjct	1827	ACTGACAGCTTTTTATAGTCACGTGACACAGTCAAACATTAACCTGGTGTATCGATTGGT	1886
Query	248	TTTTGCCatatatatatatataAGTAGGAGAGGGCGAACCTCTGGCAGGAGCAAAGGC	307
Sbjct	1887	TTTTGCCATATATATATATATAAGTAGGAGAGGGCGAACCTCTGGCAGGAGCAAAGGC	1946
Query	308	GCCGTGGCTGTGGAGTCCCAGGGCGGACGCCCACTTGTCCTGGGCCGTGCTGTGTGTGTG	367
Sbjct	1947	GCCATGGCTGTGGAGTCCCAGGGCGGACGCCCACTTGTCCTGGGCCGTGCTGTGTGTGTG	2006

Figure 3. A-Alignment demonstrates promoter area of UGT1A1 gene a- control, B- Gilbert syndrome using a sequencer analyzed by BLAST tool. Query number represented the present data, whereas the subject represented the reference gene sequence.

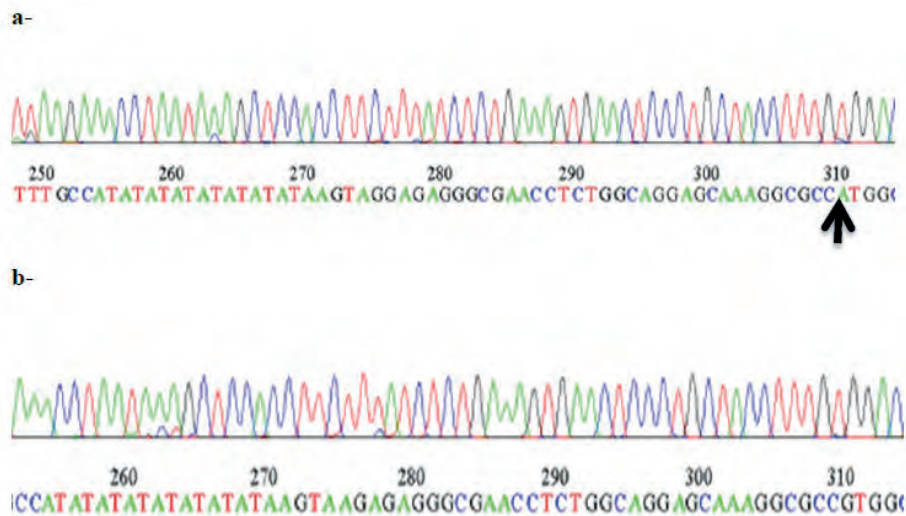


Figure 4. a,b Nucleotide sequencing profile of promoter region in UGT1A1 gene polymorphism at position -208 as recorded by ABI3730XL, automated DNA sequences.

position to higher levels of bilirubin in the Iraqi population, thereby leading to increased susceptibility to Gilbert syndrome. In conclusion, the UGT1A1 gene mutation was a possible risk factor for Gilbert syndrome in Iraq.

Author Contributions

Conceptualization, software, investigation, methodology, data duration, funding acquisition Marwa A. Kubba; validation, formal analysis, resources, visualization, Abeer Ali Marhoon; Writing—original draft preparation, writing—review and editing, Supervision, project administration, Rafed Abbas Kadhum. All authors have read and agreed to the published version of the manuscript.

Acknowledgment

I am sincerely thankful to Al-Nahrain University, College of Biotechnology for providing me with the opportunity to make paper; I am also thankful to Dr. Sahar M. Hussein for guiding us in many stages during our work.

Funding

This research received no external funding.

Ethical Clearance

The ethical research committee at scientific research by ethical approval of both environment and health and higher education and scientific research ministries in Iraq

Conflicts of Interest

The authors declare that they have no conflict of interest.

Informed Consent Statement

Informed consent was obtained from all subjects involved in the study. Written informed consent has been obtained from the patient(s) to publish this paper.

Bibliographic references

1. Bosma PJ. Inherited disorders of bilirubin metabolism. *J Hepatol* 2003; 38:107–17
2. Carpenter, S.L., Lief, S., Howard, T.A., Eggleston, B., & Ware, R.E.

- (2008). UGT1A1 promoter polymorphisms and the development of hyperbilirubinemia and gallbladder disease in children with sickle cell anemia. *Am J Hematol.* 83: 800– 803.
3. Kataoka, R., Kimata, A., Yamamoto, K., Hirosawa, N., Ueyama, J., Kondo, T., Okada, R., Kawai, S., Hishida, A., Naito, M., Morita, E., Wakai, K., & Hamajima, N. (2011). Association of UGT1A1 Gly71Arg with urine urobilinogen. *Nagoya J Med Sci.* 73(1-2):33-40
4. Johnson, A.D., Kavousi, M., Smith, A.V., Chen, M.H., Dehghan, A., Aspelund, T., Lin, J.P., Dujin, C.M., Harris, T.B., Cupples, L.A., Uitterlinden, A.G., Launer, L., Hofman, A., Rivadeneira, F., Sticker, B., Yang, Q., O'Donnell, C.J., Gudnason, V., & Witteman, J.C.(2009). Genome-wide association meta-analysis for total serum bilirubin levels. *Hum Mol Genet.* 18: 2700–2710
5. Gong QH, Cho JW, Huang T, Potter C, Gholami N, Basu NK, Kubota S, Carvalho S, PenningtonMW, Owens IS, Popescu NC. Thirteen UDPglucuronosyltransferase genes are encoded at the human UGT1 gene complex locus. *Pharmacogenetics.* 2001 Jun;11(4):357-68.
6. King CD, Rios GR, Green MD, Tephly TR. UDP-glucuronosyltransferases. *Curr Drug Metab.* 2000Sep;1(2):143-61. Review.page 4
7. Long J, Zhang S, Fang X, Luo Y, Liu J. Association of neonatal hyperbilirubinemia with uridinediphosphate-glucuronosyltransferase 1A1 gene polymorphisms: meta-analysis. *Pediatr Int.* 2011Aug;53(4):530-40. doi: 10.1111/j.1442-200X.2011.03337.x.
8. Maruo Y, Nishizawa K, Sato H, Sawa H, Shimada M. Prolonged unconjugated hyperbilirubinemia associated with breast milk and mutations of the bilirubin uridine diphosphateglucuronosyltransferase gene. *Pediatrics.* 2000 Nov;106(5):E59.
9. Owens IS, Basu NK, Banerjee R. UDP-glucuronosyltransferases: gene structures of UGT1 andUGT2 families. *Methods Enzymol.* 2005;400:1-22. Review.
10. Biondi ML, Turri O, Dilillo D, Stival G, et al. (1999). Contribution of the TATA-box genotype (Gilbert syndrome) to serum bilirubin concentrations in the Italian population. *Clin. Chem.* 45: 897-898.
11. Kadakol A, Ghosh SS, Sappal BS, Sharma G, et al. (2000). Genetic lesions of bilirubin uridine-diphosphoglucuronate glucuronosyltransferase (UGT1A1) causing Crigler-Najjar and Gilbert syndromes: correlation of genotype to phenotype. *Hum. Mutat.* 16: 297-306.
12. Farheen S, Sengupta S, Santra A, Pal S, et al. (2006). Gilbert's syndrome: High frequency of the (TA)7TAA allele in India and its interaction with a novel CAT insertion in promoter of the gene for bilirubin UDP-glucuronosyltransferase 1 gene. *World J. Gastroenterol.* 12: 2269-2275
13. Xiao-xiao Mi,1 Jian Yan,1 Xiao-jie Ma,2 Ge-li Zhu,2 Yi-dan Gao,2

- Wen-jun Yang,³ Xiao-wen Kong,² Gong-ying Chen,² Jun-ping Shi,^{1,2} and Ling Gong ², (2019). analysis of the UGT1A1 Genotype in Hyperbilirubinemia Patients: Differences in Allele Frequency and Distribution. *BioMed Research International*. Volume 2019, Article ID 6272174, 9 pages
14. Bosma PJ, Chowdhury JR, Bakker C, Gantla S, et al. (1995). The genetic basis of the reduced expression of bilirubin UDPglucuronosyltransferase 1 in Gilbert's syndrome. *N. Engl*
 15. Monaghan G, Ryan M, Seddon R, Hume R, et al. (1996). Genetic variation in bilirubin UPD-glucuronosyltransferase gene promoter and Gilbert's syndrome. *Lancet* 347: 578-581.
 16. Beutler E, Gelbart T and Demina A (1998). Racial variability in the UDP-glucuronosyltransferase 1 (UGT1A1) promoter: a balanced polymorphism for regulation of bilirubin metabolism? *Proc. Natl. Acad. Sci. U. S. A.* 95: 8170-8174.
 17. Biondi ML, Turri O, Dilillo D, Stival G, et al. (1999). Contribution of the TATA-box genotype (Gilbert syndrome) to serum bilirubin concentrations in the Italian population. *Clin. Chem.* 45: 897-898.
 18. Kadakol A, Ghosh SS, Sappal BS, Sharma G, et al. (2000). Genetic lesions of bilirubin uridine-diphosphoglucuronate glucuronosyltransferase (UGT1A1) causing Crigler-Najjar and Gilbert syndromes: correlation of genotype to phenotype. *Hum. Mutat.* 16: 297-306.
 19. Farheen S, Sengupta S, Santra A, Pal S, et al. (2006). Gilbert's syndrome: High frequency of the (TA)₇ TAA allele in India and its interaction with a novel CAT insertion in promoter of the gene for bilirubin UDP-glucuronosyltransferase 1 gene. *World J. Gastroenterol.* 12: 2269-2275.
 20. Sieg A, Arab L, Schlierf G, Stiehl A, Kommerell B. Prevalence of Gilbert's syndrome in Germany. *Dtsch Med Wochenschr* 1987.
 21. Bosma PJ, Chowdhury JR, Bakker C, Gantla S, de Boer A, Oostra BA, Lindhout D, Tytgat GN, Jansen PL, Oude Elferink RP (1995). The genetic basis of the reduced expression of bilirubin UDP-glucuronosyltransferase 1 Gilbert's syndrome. *N Eng J Med* ., 333(18):1171-5.
 22. G. Canu, A. Minucci, C. Zuppi, and E. Capoluongo, "Gilbert and crigler najjar syndromes: an update of the UDP-glucuronosyltransferase 1A1 (UGT1A1) gene mutation database," *Blood Cells, Molecules, and Diseases*, vol. 50, no. 4, pp. 273–280, 2013
 23. M. Sahar, Mohammed H. Wali, A. Marwa and H. Bushra, detection of genetic polymorphism in EGFR gene in triple negative breast cancer women from Iraq. *Biochem. Cell. Arch.* Vol. 20, No. 1, pp. 1921-1925, 2020

REVIEW / ARTÍCULO DE REVISIÓN

Recent advances on the development of a universal blood type

Esteban Guamba*, Alejandra Cevallos

DOI. 10.21931/RB/2022.07.01.32

³Yachay Tech University, School of Biological Sciences and engineering, Hda. San José s/n y Proyecto Yachay, 100119, Urcuquí, Ecuador.
Corresponding author: esteban.guamba@yachaytech.edu.ec

Abstract: Blood transfusion is the most common form of tissue transplant, and correct blood type matching is decisive for the success of this procedure. However, the availability of different blood types depends on each population, leading to a shortage of blood units from uncommon types. Then, it represents a problem for patients who need a blood transfusion because the supply for their blood type is scarce. Fortunately, researchers have been developing different techniques to engineer universal red blood cells (RBC) that could be transplanted to any human being independent of its blood type. This paper details the main features of blood transfusion and red blood cells maintenance and the two more recent procedures used to produce universal RBCs, the Enzymatically Converted Group O (ECO) and the antigen masking methods.

Key words: Blood, transfusion, red blood cells, antigen, antibody, universal RBC, immunity.

Introduction

One of the current issues in medicine is blood transfusion, it is the most common form of tissue transplant, and blood type matching is the most challenging point to achieve¹. Besides, an incorrect blood transfusion may induce a severe immune response. If the blood given during a transfusion is incompatible, the donor cells are treated as foreign, and the immune system attacks². Nowadays, several patients in hospitals are waiting for the availability of blood units. Therefore, it is essential to develop a new generation of blood transfusion systems to overcome the current issues on blood transplants. The most determinant solution is to develop a universal blood type.

Alloimmunity refers to the immune response against non-self-antigens from members of the same species. It represents an obstacle for blood transfusions because different blood types provoke immune responses in the host. Blood transfusions may induce two reactions, immunosuppression and immune activation³. To overcome this, scientists worldwide are working to develop a universal blood type to overcome the current problems on immunity. Some researchers, as Yueqi Zhao¹ *et al.*, have modified the surface of RBCs, covering them with a hydrogel framework to "hide" their antigens and therefore prevent an immune response.

One of the antigens to produce alloimmunity is the Rhesus D factor (RhD), a protein found on the erythrocyte's surface and considered one of the main immunogenic antigens on red blood cells¹. Moreover, the RhD protein is part of the Rh group, the second most important blood group system, after the ABO blood group. Consequently, the variety of blood groups leads to an unequal supply of RBCs units, which becomes worse for those uncommon blood groups as AB-. Since then, an increasing need for the positive-to-negative transition of the RhD antigen has emerged to make blood transfusions more successful.

Blood: Definition and Components

Blood accounts for about 8 to 10% of each person's body mass⁴. Throughout its path, it satisfies several functions such as: mainly transporting oxygen and nutrients, it protects the body due to the leukocytes present in it, keeping the body's water and body temperature in balance, and it also collects the residues to then be deleted^{4,5}. Blood is composed of parts, mostly the liquid part called plasma, approximately 55% of the total blood, and it is much thicker than water and has a yellowish tone. The remaining percentage is 45%, and it is distributed in different blood cells such as red blood cells, which are the most numerous in the blood. RBCs represent approximately 43%, and the other remaining part is white blood cells and platelets by 2%^{5,6}.

Blood Types

There are four blood types, and they are classified according to the antigens they possess (ABO system). But in addition to this classification, blood possesses another critical factor for determining its type, the Rh factor. The antigens are present on the surface of the RBCs, and there are two types, A and B^{4,6}. Moreover, two types of antibodies react with the proteins present on the RBCs, the Anti-A and Anti-B⁶. On the other hand, we have the Rh factor, this hereditary protein is also found on the surface of the RBCs⁵, and its classification is general; it is positive if it possesses the protein and negative if it does not have. These two types of classifications are the most common in terms of blood types, and those are the ones we will go aboard in this paper.

Type A

This group has the presence of antigen A in its red blood cells. Also, the presence of the Anti-B antibody is observed in

Citation: Guamba E, Cevallos A. Recent advances on the development of a universal blood type. *Revis Bionatura* 2022;7(1). 32. <http://dx.doi.org/10.21931/RB/2022.07.01.32>

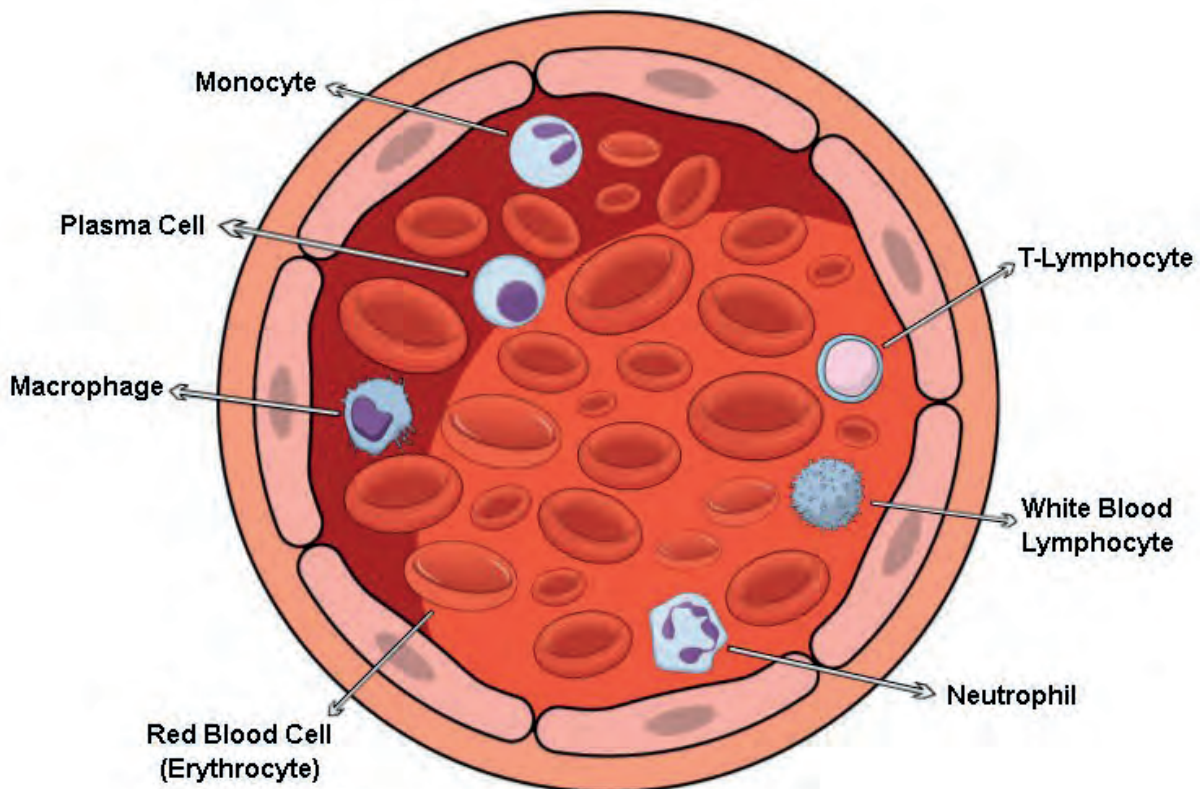
Received: 25 October 2021 / **Accepted:** 25 November 2021 / **Published:** 15 February 2022

Publisher's Note: Bionatura stays neutral with regard to jurisdictional claims in published maps and institutional affiliations.

Copyright: © 2022 by the authors. Submitted for possible open access publication under the terms and conditions of the Creative Commons Attribution (CC BY) license (<https://creativecommons.org/licenses/by/4.0/>).



BLOOD VESSEL



2

Figure 1. Blood cells composition inside a blood vessel. Inside a blood vessel, there are different types of cells such as the RBCs and immune cells like monocytes, plasma cells, macrophages, neutrophils, white blood lymphocytes, and T-Lymphocytes. In addition to some others, these different types of cells help the circulatory system avoid infections and distribute all the nutrients and molecules the body needs.

its plasma (Figure 2), which means that it cannot get the blood of any other blood type⁶. Since your blood contains marker A; it will produce B antibodies. If some problem B markers enter your body (these markers are found in the AB or B blood), your immune system will react against them and attack them. This means you can only get transfusions from people who have type A or O blood, not people with type B or AB blood⁶.

Type B

This blood group has antigen B in its red blood cells, and the presence of the Anti-A antibody is observed in its plasma (Figure 2)⁷. If your blood contains marker B, it will produce antibodies A. Therefore, as a person with type B blood, you can only receive transfusions from people who have type B or O blood (universal donor), not from people with type A or AB blood, because if another type of marker enters your body, your immune system will attack and there would be problems⁷.

Type AB

The AB group has the presence of the two antigens in their red blood cells, both A and B, and it has no antibodies in its plasma (Figure 2). This means that it can receive blood from almost all blood types⁸. In the case of blood type AB, things are a bit different. If you have both markers A and B on the surface of your red blood cells, your body won't need to fight the presence of either marker. This implies that people with AB blood can receive transfusions from A, B, AB or O blood. However, it also depended on the Rh factor of each one^{7,8}.

Type O

It is the universal donor, as its blood type is compatible with almost all other types. It is possible because they do not possess any antigens from the ABO system. However, Anti-A and Anti-B antibodies are observed in their plasma (Figure 2)^{6,8}. However, if you have O-type blood, your red blood cells do not contain A-markers or B-markers, but your body will react by making A and B antibodies when you are given A, B, or AB blood. This means that a person with blood O can only receive transfusions of the same blood type⁸.

Rh Factor

Type Rh positive

Rhesus factor, commonly known as the RH factor for its acronym, is a protein or antigen inherited from parents and occurs in the red blood cells of certain people. Rh+ are the individuals who present this protein in their erythrocytes. About 85% of people have this protein⁴. As shown in Figure 3, the illustration shows that the general population maintains an Rh+; however, a small population maintains an Rh-, so it is important to perform tests for this factor if you plan a pregnancy⁴.

Type Rh-negative

The Rh- people do not present the protein in their red blood cells; the figures are very low for this protein. Only about 15% of the world's population possesses this protein (Figure

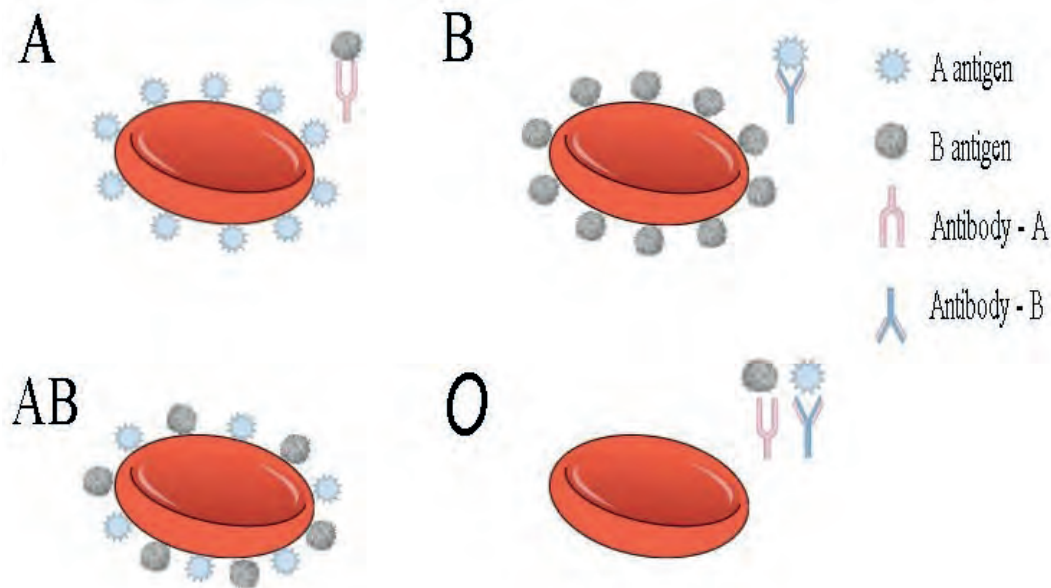


Figure 2. Illustration of the different blood groups of the ABO system. We can see the blood types A, B, AB, and O with their antigens and correspondent antibodies. In the first case, type A has a marker A, and it will produce B antibodies. In the second case, type B has a marker B, it will produce A antibodies- In the third case, type AB has markers A and B, it will not produce antibodies. And the last case, type O has no markers but will produce antigens A and B.

Rh Factor prevalence in the world

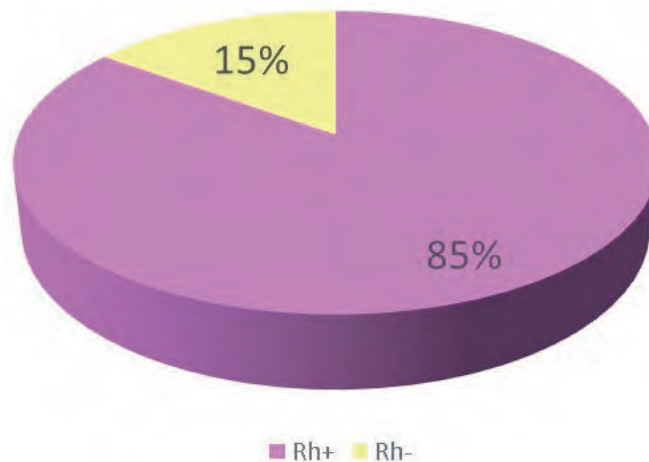


Figure 3. Rh factor, statistics. * Data obtained from OMS⁴. and Dean L⁶. In this figure, we see global statistics obtained from several studies about these factors. The illustration shows that Rh+ is the most common factor found in the world population. However, Rh- remains present in a small part of the population, and although it is not a disease, it can generate incompatibility in a pregnancy if the parents have different Rh factors.

3)⁵. However, the lack of this protein is not a disease, and it usually does not affect a person's health⁶. RH- is not a disease, but it does affect pregnancy. Pregnancy needs special care if the baby inherits the Rh factor different from that of its mother because it can be inherited from either parent. Rh incompatibility is generated if they are Rh-negative and their baby is Rh-positive, and they need special treatment⁶.

Obtaining Blood Sample

The process starts with the blood collection directly from the bloodstream to go into a well-labeled container with a pre-measured anticoagulant. Moreover, the addition of an anticoagulant avoids the agglutination of the blood and prevents the RBCs from undergoing hemolysis. There are different preservative solutions for maintaining RBC units: acid citrate dex-

trose (ACD), citrate phosphate dextrose (CPD), or CPD-adenine. Different solutions such as anticoagulants and nutrients help RBCs store and transport, enabling modern blood banking⁹. Also, between the most common anticoagulant solutions, we found Citrate-phosphate-dextrose (CPD), which is a key for blood preservation¹⁰. However, many others novel storage solutions allow the conservation of RBCs for much more time, such as SAG-Mannitol or AS-1.

The influence of ATP over the RBCs also has to be considered to keep them in efficient conditions. Since these cells do not have mitochondria, they rely on ATP from the medium as an energy source. Significantly, when ATP has been suppressed, some characteristics of the RBCs are compromised. According to research, during RBCs storage, adenosine triphosphate (ATP) decreases, modifying membrane lipid content and

Blood group worldwide

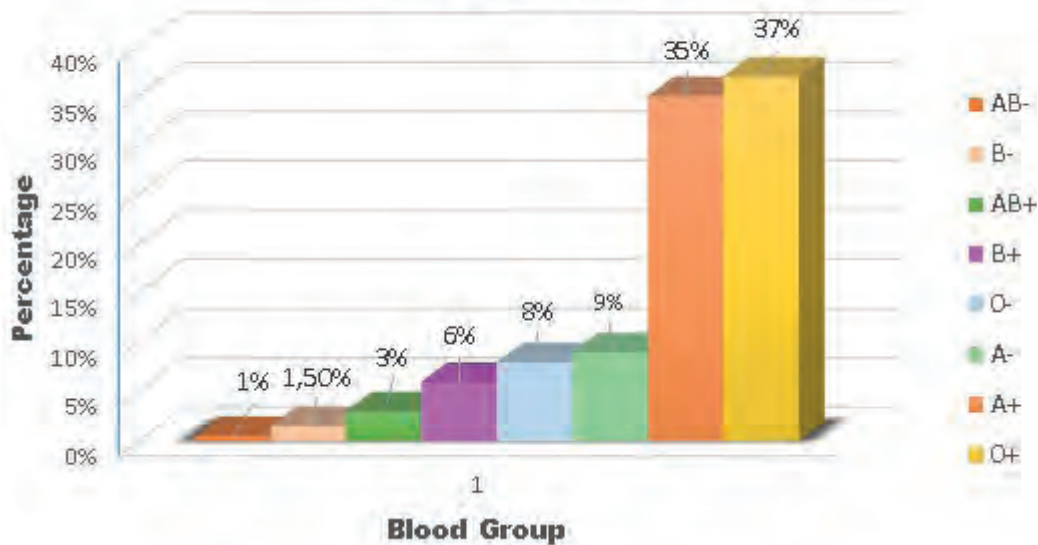


Figure 4. Blood groups statistics. * Data obtained from OMS⁴, and Dean L.⁶. We can observe that the most common blood group in the world is O+, followed by A+. Furthermore, it can be observed that the less common blood group is AB-, followed by B-. The predominance of a blood type also varies depending on the countries or continents we are located in.

cell rigidity that results in shape changes¹¹. The pH also changes during the RBCs storage, and the production of lactic acid mainly causes this due to ATP metabolism. So then, proper RBC storage relies on the correct control of the ATP levels.

RBCs Preservation

The storage and maintenance of RBCs units require precise control for some factors such as temperature, osmotic pressure, and pH. When RBCs are stored, they deteriorate, compromising their metabolic, morphologic, and membranous characteristics. The elements that are mainly altered are the hemoglobin, potassium concentration, supernatant, and a loss of discoid shape and lipid membrane vesicles¹². Moreover, RBCs units can be stored for up to 42 days. However, its ability to deliver oxygen decreases on time due to decreased 2,3-diphosphoglycerate levels¹³. Temperature, for instance, has been demonstrated to modify the live time of RBCs during storage. The best-used technique for their preservation is cryogenics. Nevertheless, even low temperatures of $4^{\circ}\text{C} \pm 2^{\circ}\text{C}$ help to the viability of RBCs and protect them from bacterial growth³.

The osmotic pressure is another crucial factor for the maintenance of RBCs. If modified, RBCs undergo hemolysis by breaking their lipid membrane because of the different gradient concentrations. To avoid that, cells have to be under isotonic conditions (0.9% NaCl) in which the outside and the inner osmotic pressure are the same. One of the leading isotonic preservative solutions used for RBCs storage is EDTA. However, using this solution for blood unit preservation produces changes in erythrocyte morphology and osmotic fragility¹⁴. Fortunately, AS-3 is another preservative solution that works better. Recent research showed that using AS-3 as the storage solution for 6 weeks allowed the recovery of 78–84% of the RBCs, and only 0.4% of hemolysis were detected⁹.

RBCs maintenance also depends on the pH concentration. Cells keep producing metabolites such as Lactate and CO₂ during blood storage, acidic molecules. The accumulation of those acidic compounds during storage results in a decrease of pH levels, and when it drops below 6.4, the deterioration of RBCs occurs faster. Moreover, the main consequences of a

low pH are the cessation of glycolysis and the change in ATP and 2,3-DPG levels¹². While according to the literature, the optimum pH for glycolysis is high (7.8–8.5) when the temperature is between 15°C and 35°C ¹⁵. Therefore, changes in pH during prolonged storage time can result in RBCs damage. Fortunately, when RBCs are stored at low temperatures, their metabolism slows down, allowing the pH to stay at optimum concentrations for a longer time.

Blood Transfusion

Blood transfusion is a medical procedure in which a patient or receptor obtains blood or any of its components from the donor's blood⁴. Blood transfusions provide the patient with the components of the blood they need, and RBCs are the most commonly used⁷. A person may need a blood transfusion for several reasons, such as surgeries, injuries, replenishing blood volume, correct serum protein levels, and improved hemoglobin and oxygen-carrying capacity¹⁶.

To start a blood transfusion, it is essential to know the type of blood the patient has (ABO system) and whether the Rh factor is positive or negative. This is because the donor's blood has to be compatible with the patient's to avoid an immune response. After checking all the data, the temperature of the blood bag is checked, and if the blood is icy, it is necessary to wait a few minutes for it to be at room temperature⁶. Transfusion in high volumes when blood is cold can cause cardiac arrest¹⁶. In most cases, it is not necessary to heat the blood to be transferred. However, suppose blood needs to be heated. In that case, it can be heated to temperatures of approximately 35 to 38°C and being careful not to exceed over 42°C ¹⁷. This is mainly because of the viability of the blood unit when blood is exposed to temperatures above 42°C hemolysis can occur¹⁰. Also, blood cannot be returned to the blood bank for reuse after some warming process. Once the temperature of the blood bag is checked, it is perforated with a blood filter, purged, and deposited in a bath. Furthermore, finally, blood is placed through the intravenous¹⁸. It is necessary to monitor the patient for a few minutes to find any problems or reactions.

Transfusions can last approximately 1 to 3 hours¹⁸, but

should not last more than 4 hours because there are dangers of bacterial proliferation¹⁰, when blood increases its temperature by staying at room temperature. According to McCullough (2017): "For routine transfusion to stable patients' rates of 2–3 mL/mn for red cells and 7–10 mL/mn for platelets and plasma are recommended"¹⁰.

Blood Transfusion Issues

Blood transfusions usually do not have adverse effects but sometimes have different effects depending on the patient (transfusion reactions). Several reactions may be due to storage, transportation, or administration of blood units. These reactions are very varied and can be fatal or straightforward. The most common are mentioned below⁸. One transfusion reaction can be incompatible blood: When the donor's blood is not compatible with the patient's. The patient's cells treat the donor's blood as foreign invaders, and the immune system attacks accordingly⁹. Another can be allergic reactions: These can cause by fever, itching, and hives¹⁹.

The most common problems in transfusions are mainly in massive transfusions. Since these transfusions replace the total volume of the patient's blood, these transfusions involve problems such as cardiac arrest¹⁰, coagulation, hypothermia¹⁹. On the other hand, another frequent problem is Transfusion-related acute lung injury (TRALI), an acute respiratory distress syndrome⁸.

Transfusion-related infections: Many protocols are now followed to prevent these infections; however, few occur. These infections can be bacterial or viral. In the case of bacterial contamination, these are often rare. For example, this can occur if an asymptomatic donor has bacterial contamination at the time of blood donation or venous puncture¹⁷. In contrast, the viral infection. They are unusual; nevertheless, if they contract, they can provoke: Hepatitis A, hepatitis B, which occurs in approximately 1 in 100 000 cases. Hepatitis C occurs in less than 1 in 1 000 000 cases¹⁶. And HIV occurs in less than 1 in 4 000 000 cases¹⁷. There are many other adverse effects, but those mentioned above are the most common.

Recent RBCs Modification Methods

The fatalities related to Blood transfusion, discarding those due to disease transmission, have been estimated to happen once in 100,000 patients. The most common reason is hemolytic reactions due to incorrect blood type matching¹⁰. As there are many immunogenic antigens on RBCs and blood transfusions that rely on the removal of these to succeed, new methods have emerged to avoid an immune response when blood transfusion is performed. The objective of these novel methods is to produce non-immunogenic RBC; therefore, these blood units can be used as a source of universal RBCs for blood transfusions. In this way, the primary goal of modified RBCs is to elicit neither an immediate nor a secondary immune response when a transfusion is accomplished²⁰. Furthermore, in clinical application, these techniques would establish an entirely new way to treat many chronic diseases with a need for a rare blood type supply. So the entire blood banking system dedicated to blood collection, distribution, and transfusion, which is focused on the ABO group, can be entirely revolutionized by the success of any RBCs modification techniques that we detail next.

Besides, it has been calculated that around 100 million units of blood are donated each year; however, the indications for RBC transfusion and the suitable time of storage before transfusion are still uncertain¹³. Blood banks have to collect

and store all blood types, even the most common ones, which spend more time saved than the uncommon ones. This can result in non-viable RBCs. However, the two main general procedures can be used to create a universal RBC; these techniques can potentially overcome the previously mentioned issues. The first way is by permanently removing the RBC antigens anchored to their surface, and the other way is by hiding their antigens so that the immune system cannot detect them²¹. These two methods have been explored over the years, and we detail these two recent and promising RBC surface modification techniques.

Enzymatically Converted Group O (Eco)

The first modification technique is then enzymatically converted group O (ECO), which removes the antigens from the RBCs surface. The main feature of this method is the use of an α -galactosidase enzyme, capable of removing the immunodominant part from the A and B antigens, which are the main characteristics of the A and B blood type respectively. For blood type A, its immunodominant monosaccharide is a terminal α 1-3 linked N-acetylgalactosamine (GalNAc), and for type B, its monosaccharide is α 1-3 linked galactose (Gal)²². As the blood group O does not have these monosaccharides on their oligosaccharide terminal chains. Therefore, the ECO technique enables A and B blood groups to be converted into O types. Although this method can produce the universal blood type donor O, it has faced some obstacles to succeed in clinical practice because of the low efficacy of the enzyme.

Nevertheless, new research shows that more efficient glycosidase enzymes present in bacteria. The first approach for the conversion of type B RBCs to O was by using an α -galactosidase enzyme, which can be extracted from coffee beans²². For this enzyme, many studies have been carried out. However, it was hard to move into the clinical application, mainly because it showed low kinetic properties. Fortunately, entirely new families of bacterial exo-glycosidases have been found, and they show better kinetic properties to remove A and B antigens from RBCs²³. Moreover, new clinical trials are now being performed to prove the efficacy of this new family of enzymes for further developing a universal blood type.

The most relevant benefit of ECO technology on transfusion medicine is eliminating hemolytic reactions due to ABO-incompatible transfusion. The technique reduces the RBC units' typing costs, avoids the unnecessary storage of common blood types, increases the availability of rare blood types units in blood banks, creates a universally compatible RBC, and saves hospital money for an inventory of blood units²³.

RBC Antigen Masking

Unlike ECO which converts different blood groups into O type, the second method attempts to camouflage or mask the antigens from the RBC surface. RBCs undergo a surface modification procedure, where these cells are treated with the polyether polymer PEG or other substances such as hydrogels and polymers. These compounds are chemically anchored to RBC surface proteins through various linking procedures. Also, this method results in stealth RBCs, which allows them to pass unseen from the immune system, disabling antigen-antibody reactions and alloimmunization to additional antigens²¹. Therefore, one of the main goals of this modification technique is to obtain healthy RBCs capable of typically performing their metabolic processes as oxygen transfer and nutrient transport.

PEG in transfusion medicine has become a key tool to

avoid immune responses, and PEGylation is the process by which PEG is linked to other molecules. This procedure improves the pharmacokinetic behavior of many substances because it avoids recognition by the cells of the immune system, allowing the introduction of several agents into the human body²⁴. Between the most used substances for the PEG-RBC linking, we found: cyanuric chloride (CN), ethylene glycol (CH₂OH)₂, propionic acid (SPA), and benzyltriazobyl carbonate (BTC)²⁵. Moreover, the research of PEGylated RBCs becomes more reliable since 4 groups of research showed that if PEG is covalently attached to the RBC surface, these cells are not capable of reacting with antigens ABO group²⁵. As a result, PEG-RBC linking is one of the most valuable procedures to stealth RBCs towards developing a universal blood type.

Nevertheless, this method may carry some complications and cell changes. For example, some biomimetic molecules such as polydopamine (PDA) can shield RBCs. However, this treatment produces noticeable changes in membrane fluidity, which leads to increased cell fragility¹. RBCs depend on their normal membrane stability to freely circulate through the bloodstream without fragmentation. Consequently, a decreased stability may lead to a breakdown even under everyday circulatory stresses²⁶. To solve the fragility problem, new methods have emerged to overcome this problem, such as polysialic acid (PSA)-tyramine hydrogel, which creates an enhanced flexible framework around RBCs that ensures their surface stability. This article's clinical trials explain the details of an experiment done with (PSA)-tyramine and rabbits.

Universal RBCs Transfusion

Different criteria must be carefully examined when modified RBCs are transfused. Some of these are similar to the analysis made on regular RBCs transfusions. However, it is more critical for the modified cells to see possible immunogenic reactions. In addition, the ECO technology is the only one that has passed into human clinical trials and with relevant success²³. This technology showed no significant changes in

the RBCs morphology and functions, so it was allowed to be used in phase 1 of clinical trials. Indeed, research have shown that during the in vitro transfusion tests, there was no noticeable increase in anti-B for the samples of type A or O. Actually, their sera remained with no indications of agglutination or hemolysis after seven weeks of the transfusion²⁵. Even though this method does not present relevant problems to the host, it is essential to take immuno-tests periodically to evaluate that the procedure has done well.

Pre-Clinical Trials

There are no clinical trials of transfusions with modified universal red blood cells yet. Nevertheless, researchers used New Zealand white rabbits in a pre-clinical study performed in vivo to evaluate immunogenicity. These rabbits were randomly divided into four groups (Table 1). Table 1 below shows the distribution of each group of rabbits, which injections they received, and the immune response for each one. The study continues with ELISAs, according to Zhao Y. *et al.* (2020), as follows: ELISA was performed to analyze the binding of both the framework and the non-framework to RhD-positive red blood cells and evaluate RhD antibody titers in vivo. Recombinant human RhD proteins were used to coat ELISA plates. At night they were incubated at 4 °C, then the plates were washed three times with PBS, and after this, for two hours, they were blocked with a blocking buffer at 37 °C. Next, the plates were washed three times, and the sera samples (100 l) were added¹. We proceeded to incubate at 37°C for one hour, then the plates were washed three times, and 100 µl of secondary antibody conjugated with HRP were added. Next, we proceeded to incubate at 37°C for 45 minutes, and afterward, the plates were washed three times, and 100 l of TMB chromogenic substrate solution was added. After 10 minutes, 50 l of H₂SO₄ 1 M were added to stop the reaction of the endpoint titers. Using a microplate reader, absorbance was measured at 450 nm¹.

It was seen that anti-RhD immunity in surface modifications could be avoided, and favorable biocompatibility was also

In vivo rabbits immunostimulation with different RBCs				
Group	First Intrapertitoneal injection	Second Intrapertitoneal injection after 3 weeks	Immune responses to RBCs	Additional Information
Rabbits in group 1	Injection of 500 ul of RhD-positive RBCs	Injection of 500 ul of RhD- positive RBCs	RhD immune response was significantly boosted at week 5 compared with that of the other three groups	Sera samples were collected every week. The humoral immune responses of human RhD-positive RBCs and engineered RBCs were evaluated using an Immunoglobulin G (IgG) enzymelinked immunosorbent assay (ELISA).
Rabbits in group 2	Injection of 500 ul of RhD-positive RBCs	Injection of 500 ul of engineered RBCs	Second injection of engineered RBCs presented a significant dampening effect on the RhD immune responses	
Rabbits in group 3	Injection of 500ul of engineered RBCs	Injection of 500 ul of engineered RBCs	Positive control group. No obvious RhD antigen-specific immune response	
Rabbits in group 4	Injection of 500 ul of RhD-Negative RBCs	Injection of 500 ul of Rh-Negative RBCs	Negative control group was observed no difference relative to the group 3	

Table 1. Process in vivo rabbits immunostimulation with different RBCs. *Data obtained from Zhao Y. *et al.*¹.

promoted. Also, there was no recognition between antigens and antibodies. Therefore, the trial worked properly as it avoided immune responses altogether, thus ensuring a successful RhD-stealth blood transfusion[†].

Conclusions

Blood units are used worldwide, and blood type matching is one of the biggest challenges in the medical field. Because there are different blood groups, and most of them have specific antigens, blood transfusion has to overcome different typing processes before being transplanted. To maintain RBCs on their normal conditions, factors such as coagulation, temperature, pH, and storage time must be controlled to prevent changes in RBCs' morphology and oxygen transport capacity. Additionally, the variety of blood types results in an unequal supply for hospitals and clinical procedures. However, there are two techniques to engineer universal red blood cells. The first is the ECO technique, which uses an α -galactosidase enzyme that removes the surface antigens from RBCs to transform them into O type. The second is antigen masking, here a framework usually made of hydrogels, or PEGs, binds to the surface of red blood cells. Hence, the host's immune system cannot recognize them after transfusion. These two methods are promising and have been extensively studied to help supply blood banks, especially for people with uncommon blood types.

Author Contributions

Conceptualization, methodology, resources and writing—original draft preparation, Esteban Guamba. Writing—review and editing, visualization, supervision, Alejandra Cevallos.

Funding

This research received no external funding.

Acknowledgments

Thanks to Ph.D. Santiago Vispo, who encouraged and tutored us to write this article.

Conflicts of Interest

The authors declare no conflict of interest.

Bibliographic references

- Zhao Y, Fan M, Chen Y, Liu Z, Shao C, Jin B, et al. Surface-anchored framework for generating RhD-epitope stealth red blood cells. *Sci Adv.* 2020;6(12):1–12.
- García-Roa M, Del Carmen Vicente-Ayuso M, Bobes AM, Pedraza AC, González-Fernández A, Martín MP, et al. Red blood cell storage time & transfusion: Current practice, concerns & future perspectives. *Blood Transfus.* 2017;15(3):222–31.
- Brunskill S, Thomas S, Whitmore E, McDonald CP, Dorée C, Hopewell S, et al. What Is the Maximum Time That a Unit of Red Blood Cells Can Be Safely Left Out of Controlled Temperature Storage? *Transfus Med Rev* [Internet]. 2012;26(3):209–223.e3. Available from: <http://dx.doi.org/10.1016/j.tmr.2011.09.005>
- OMS. Organización Mundial de la Salud [Internet]. [cited 2020 Apr 16]. Available from: <https://www.who.int/es>
- Cruz Roja Española. Grupos sanguíneos - Centro de Donación de Sangre de Cruz Roja [Internet]. [cited 2020 Apr 16]. Available from: <https://www.donarsangre.org/gruposanguineos/>
- Dean L. Blood Groups and Red Cell Antigens. ABO blood Gr [Internet]. 2005;(Md):Chapter 5. Available from: <http://www.ncbi.nlm.nih.gov/books/NBK2267>
- OMS. La Base de Datos Global de la OMS para la Seguridad Sanguínea. 1999. Organ Mund la Salud. 2001;8.
- Goodnough LT, Brecher ME, Kante M, AuBuchon J. *Transfusion Medicine.* Br J Educ Stud. 1965;13(2):208–11.
- Hess JR. An update on solutions for red cell storage. *Vox Sang.* 2006;91(1):13–9.
- McCullough J. 13 Techniques of Blood Transfusion. 2012;362–77.
- Klein HG, Spahn DR, Carson JL. Series Transfusion Medicine 1 Red blood cell transfusion in clinical practice. *Prevention.* 2007;415–26.
- Holme S. Current issues related to the quality of stored RBCs. *Transfus Apher Sci.* 2005;33(1):55–61.
- Carson JL, Guyatt G, Heddle NM, Grossman BJ, Cohn CS, Fung MK, et al. Clinical practice guidelines from the AABB: Red blood cell transfusion thresholds and storage. *JAMA - J Am Med Assoc.* 2016;316(19):2025–35.
- Antwi-Baffour S. Prolong Storage of Blood in EDTA Has an Effect on the Morphology and Osmotic Fragility of Erythrocytes. *Int J Biomed Sci Eng.* 2013;1(2):20.
- Guppy M, Attwood P V., Hansen IA, Sabaratnam R, Frisina J, Whisson ME. pH, Temperature and Lactate Production in Human Red Blood Cells: Implications for Blood Storage and Glycolytic Control. *Vox Sang.* 1992;62(2):70–5.
- Goodnough LT. Risks of blood transfusion. *Crit Care Med.* 2003;31(12 SUPPL.).
- Maxwell MJ, Wilson MJA. Complications of blood transfusion. *Contin Educ Anaesthesia, Crit Care Pain.* 2006;6(6):225–9.
- Patil V, Shetmahajan M. Massive transfusion and massive transfusion protocol. *Indian J Anaesth.* 2014;58(5):590–5.
- Eder AF, Chambers LA. Noninfectious complications of blood transfusion. *Arch Pathol Lab Med.* 2007;131(5):708–18.
- Bradley AJ, Test ST, Murad KL, Mitsuyoshi J, Scott MD. Interactions of IgM ABO antibodies and complement with methoxy-PEG-modified human RBCs. *Transfusion.* 2001;41(10):1225–33.
- Lublin DM. Universal RBCs. *Transfusion.* 2000;40(11):1285–9.
- Olsson ML, Hill CA, De La Vega H, Liu QP, Stroud MR, Valdinocci J, et al. Universal red blood cells - Enzymatic conversion of blood group A and B antigens. *Transfus Clin Biol.* 2004;11(1):33–9.
- Olsson ML, Clausen H. Modifying the red cell surface: Towards an ABO-universal blood supply. *Br J Haematol.* 2008;140(1):3–12.
- Shimizu T, Abu Lila AS, Awata M, Kubo Y, Mima Y, Hashimoto Y, et al. A Cell Assay for Detecting Anti-PEG Immune Response against PEG-Modified Therapeutics. *Pharm Res.* 2018;35(11).
- Garratty G. Progress in modulating the RBC membrane to produce transfusable universal/stealth donor RBCs. *Transfus Med Rev.* 2004;18(4):245–56.
- Chasis JA, Mohandas N. Erythrocyte Membrane Deformability and Stability : *J Cell Biol.* 1986;103(August):343–50.

REVIEW / ARTÍCULO DE REVISIÓN

Porous frameworks from Ecuadorian clays

María Calle Luzuriaga*, Edward E. Ávila, Dario Alfredo Vitoria

DOI. 10.21931/RB/2022.07.01.33

Universidad de Tecnología Experimental Yachay Tech, Escuela de Ciencias Químicas e Ingeniería, Grupo de Investigación Aplicada en Materiales y Procesos (GIAMP), Imbabura, Ecuador.
Corresponding author: maria.calle@yachaytech.edu.ec

Abstract: This research provides a literature review on several topics as a foundation to comprehend porous materials, their structure, and behavior to explore how they can be derived from clays and nanoclays. In this case, considering the several minerals present in some Ecuadorian clays, which are a potential starting material for the synthesis of porous frameworks, they constitute a solid source of metal atoms such as Silicon or Aluminum. This research presents the evaluation and characterization via XRD and AAS of clay samples collected in the southeast of Ecuador in the provinces of Azuay, Morona Santiago and Zamora Chinchipe, which present diversified soil mineralogy with many chemical and crystallographic features for suitable precursors in nanomaterials design.

Key words: Porous frameworks, clays, nanoclays, zeolites, X-ray powder diffraction, AAS.

Introduction

The greenhouse effect, global warming, and climate change have come to a state where little to nothing can be done or approached in a traditional way to mitigate or tackle their effects. Scientists have a hard job developing innovative solutions for this pollution problem. Yet, since the early 2000s, there have been advances in gases capturing and removing them from the atmosphere through chemical processes. However, these efforts are not enough, and the approach has evolved to merge these chemical processes to physical ones using nanotechnology to achieve the adsorption of different kinds of gases. The presence of acid gases in the atmosphere has had a crucial impact on the quality of life of people everywhere. Nowadays, targeting the concentration of such gases in the atmosphere is one of the biggest goals of science. One of the recent techniques is the adsorption process of such gases through porous frameworks¹.

Now, what can one understand how porous framework materials are? To answer that, one can see at these materials' nano or picoscopic scale that if the constituents are not densely stacked but form voids, the material is defined as porous material². To exemplify this better, it is easy to picture a bee panel where there are blocks formed, leaving voids to be filled with honey. In materials science, those voids are to be filled with substances such as acid gases that are chemically and structurally compatible and trapped in the frameworks. Therefore, one can say that porous frameworks materials are becoming all those with voids and a structure with framework form.

Porous frameworks synthesis can imply a wide range of processes. Materials with permanently porous structures made either entirely from organic building blocks or a combination of organic ligands and inorganic nodes have been at the forefront of chemistry for two decades³.

Decades of painstaking observational and empirical synthetic advances have made it possible to predict, with a relatively

high degree of confidence, which structures might result if certain building blocks are joined together⁴. Porous frameworks, whether they are organic or metal-organic frameworks or zeolites, have emerged as advanced materials with a wide range of applications such as chemical catalysis, gas adsorption, ion exchange, and advanced nanotechnology applications, as will be discussed later.

In the adsorption process, the molecules or ions are to be adhered to a surface rather than penetrate the framework. Particularly in nanostructured materials, the applications field for porous frameworks become a powerful tool since they present large surface areas, high stability, and small size⁵. For the adsorption process, the most remarkable feature is the large surface-volume ratio since it represents more binding sites.

In Chemistry, the applications of interest are generally removing undesired compounds, molecules, and impurities from different matrixes that may contain contaminants traces or subproducts. Therefore, the porous frameworks may act as sieves, binding layers, or regular adsorbents with an appropriate chemical reactivity, improving their efficiency when using nanostructured materials⁶.

Nowadays, nanomaterials constitute a wide range variety of materials. One of the emerging types is nanoclays, which are naturally occurring or synthetic clays treated and scaled to nanostructures⁷. Nanoclays, are of great interest since they represent an opportunity for industrial and technological applications. Nanostructures display enhanced functional features that are not found in larger dimensions materials⁸.

Consequently, the field also thrives because it has a relatively low barrier to entry: it does not generally require sophisticated apparatus or complicated synthetic techniques. This allows contributions from synthetic chemists and engineers, spectroscopists, and physicists³. All of whom are spurred by the increasing availability of these materials without necessa-

Citation: Calle Luzuriaga M, . Ávila E E, Alfredo Vitoria D. Porous frameworks from Ecuadorian clays. *Revis Bionatura* 2022;7(1). 33. <http://dx.doi.org/10.21931/RB/2022.07.01.33>

Received: 25 December 2021 / **Accepted:** 25 January 2021 / **Published:** 15 February 2022

Publisher's Note: Bionatura stays neutral with regard to jurisdictional claims in published maps and institutional affiliations.

Copyright: © 2022 by the authors. Submitted for possible open access publication under the terms and conditions of the Creative Commons Attribution (CC BY) license (<https://creativecommons.org/licenses/by/4.0/>).



rily relying on collaborators to supply samples.

The hydrothermal synthesis method of porous frameworks has become of consistent and urgent interest for material scientists due to its easy access when one refers to equipment and reagents used in the laboratory as vital factors for the manufacture of the monomers producing the framework afterward. Performing a hydrothermal method for the synthesis, there is a higher chance of successfully modifying the framework. It is well known that clays display many exciting components to produce multiple porous frameworks³ since they contain silicon, iron, and aluminum minerals.

Theoretical Background

Porous materials and frameworks

Porous material can be defined as every solid or primarily solid material that presents pores in its structure, giving certain features relative to the system's porosity, pore size, and the fraction of pore volume concerning the total volume of the material⁹. Applications of porous materials occupy a varied assortment; they are commonly used as insulators, transistors, and conductors in the electronic industry as well as sieves for the water filtration system, chemical catalysis, etc^{10,11}. Yet research in this area continues to take innovative and necessary paths.

The efforts of researchers have been reflected in the synthesis and production of materials that are being applied in processes for the elimination of polluting substances, employing the adsorption process of compounds whether they are in the liquid or gaseous phase. These materials are known as adsorbents, and these have high demand, but like any kind of material, their applications may be limited because of the precursors, specifically to the use of contaminating substances as templates, as well as due to the synthesis methods. So, the zeolites are examples of excellence since their synthesis is a greener approach.

Zeolites, silica gel, intercalated layered materials, etc., are common minerals used in such applications due to their pore dimensions⁹. These kinds of materials can be used in complex conditions given their ilk. The particularity of zeolites is that their structure is what gives such behaviors that can be utilized in several industrial applications like catalysis, gas adsorption, water purification, and treatment¹².

There is particular importance in the synthesis of the porous materials because of the specifications that they must present to be adequate and suitable for specific applications; therefore, the pore size, the porosity, the surface area, etc., must be controlled. Even in a more intricate way when the material is of nanometric scale. Engineering the design of porous material in clays is intended to change porosity, surface area¹⁴, surface content of solids, as well as thermal stability¹⁵.

Although the engineering process for the obtention of zeolites from layered silica clays has reached a high interest in the material sciences scenario, the research on three-dimensional structures (3D) from these compounds has been limited. This may be due to the limited application of pillared clay, so the effort to increase the use of coated material through pore engineering begins to transform the coating into a zeolite structure¹⁶. Now, data shows over two hundred types of zeolites based on a silica-alumina ratio¹⁷.

Clays

Clays are an extended collection of minerals, yet in chemistry, they are known as hydrous silicates¹⁸. They are found in nature from different natural sources and can be produced in their synthetic form. Their natural origin is after geological processes; whether they were physical or chemical processes, weather-dependent processes, decompositions, etc., it will determine both the composition and properties of the clays. Even though they can travel because of natural phenomena, they are generally found near their origin site. Clay minerals may be divided into four major groups, mainly in terms of the layered structure variation, as shown in Table 1. These include the kaolinite group, the smectite group, the illite group, and the chlorite group¹⁹.

The arrangement in these crystals consists of silicate layers that coordinate two tetrahedral atoms combined to edge-shared octahedral sheets²⁰. Thus, generally, clay structures are proposed in layers, and these layers are seen in sheets both tetrahedral and octahedral. This indicates that the tetrahedral layer is composed of silica-oxygen molecules sharing the corners to other tetrahedrons of the same type. Instead, the octahedral layer is structured by aluminum or magnesium in sixfold coordination, for instance, halloysite as seen in Figure 1^{18,21}, that displays this conformation in nature. The layers are then arranged by interactions such as van der Waals forces, hydrogen bonds, cationic or static forces, etc. Clay's ability for surface modification is what allows the dispersion of layered silicates into separate sheets²⁰.

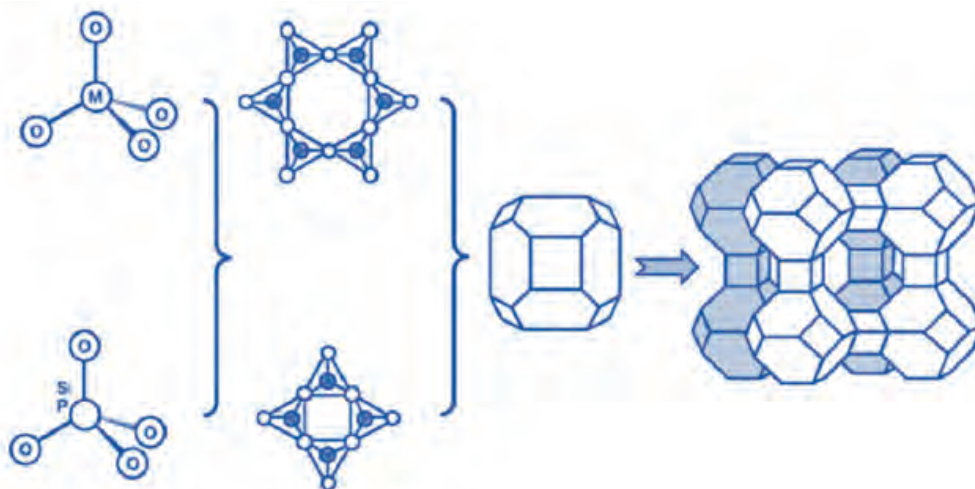


Figure 1. Formation of a zeolite, from the primary TO4 to secondary building units and further assemble to form extended zeolite¹³.

Clay particles can absorb or lose water in response to simple humidity content changes in the surrounding environment; when water is absorbed, it fills the spaces between the stacked silicate layers²².

Ecuadorian Clays

With regards to the soil mineralogy of Ecuador, there is barely any research done. Despite the large variety and existence of clays, there is still a significant lack of knowledge or information about their conformation, structure, and chemical formula.

Clays in Ecuador may have several compositions, yet they all show approximate levels of silica 60%, alumina 15%, low alkali and carbonates, and high levels of iron²³. However, the lack of information opens the door to new research being done. There is a crescent interest in using clays for nanotechnology purposes, and most Ecuadorian lands provide them. As mentioned before, the clays may be found to be of various types, as shown in Table 1, even more than the few ones already discovered. And therefore, it can be used for many applications, including the development of nanomaterials and the improvement of nano-polymers.

In the same way, there is a need to discuss strategies and their implementation in nanoscale technology to take advantage of the naturally occurring resources, such as the Ecuadorian clays that can bring new and emerging materials, tackling ecological issues also industrial and economic concerns, etc. The lack of information on Ecuadorian clays is an opportunity to research them and discover and develop many other applications.

This review considered the data from the repositories of Ecuadorian Clays by the INEDITA project at Yachay Tech University, Ecuador. Under the INEDITA project, the clays were co-

llected from Azuay, Zamora Chinchipe, and Morona Santiago provinces, located in the southeast of Ecuador, also known as the austral region of Ecuador. The total area of these provinces covers about 33000 km², yet the samples were extracted from specific points, as shown below in Figure 3.

They are labeled and enlisted in Table 2, considering the numbers used for classifying and identifying the clay series of the INEDITA-GIAMP project. The code corresponds to the origin site of the clay and the number of the sample in the set. Bouyoucos' method was used to collect the clays. Clay minerals were characterized via X-Ray Powder Diffraction. This technique is a non-destructive method that permits a collection of data about the composition of the crystallographic structure and, therefore, the physical behavior of materials²⁴. The mentioned clays were previously used in nanocomposite research.

The physical appearance of each clay sample is shown below in Figures 4 and 5, which allow seeing how they vary in color. It could be related to the content of iron oxide or iron salts, not being this the only reason for the color variance in each of the samples, as can be observed. In Table 3 as well, it is indicated the iron concentration present in them. Still, the color of the samples will derive from other factors as the different mineralogical composition, environmental factors, organic compounds, etc. It must be said that the texture of the clays was very alike between all the samples. Between clays 301, 302, and 303 there is a notorious difference in color, while there is a similarity between 303 and 306 which were collected in the same province. It could be said that 302 and 308 also look alike, although 302 is more pinkish while 308 tends to a yellowish tone.

Over 2950 phases matching the XRD data were obtained and analyzed with the software SmartLab Studio II (Rigaku Corporation, Japan), on average for all the samples. It was ne-

Group	Layer type	Species
Smectite	2:1	Montmorillonite, nontronite
Illite	2:1	Clay micas
Chlorite	2:1:1	Chamosite, nimite, sudoite
Kaolinite	1:1	Halloysite, dickite, nacrite

Table 1. Clay minerals classification¹⁹.

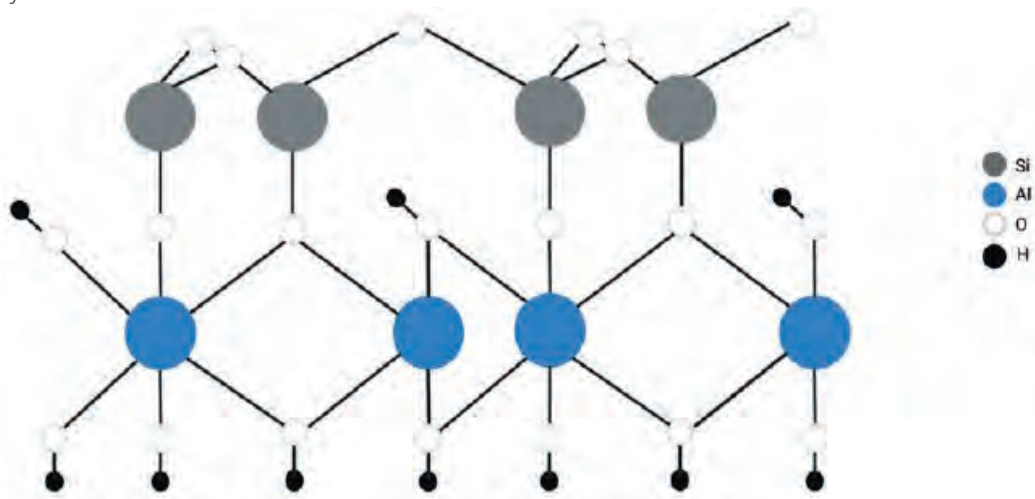


Figure 2. Chemical structure of halloysite²¹.

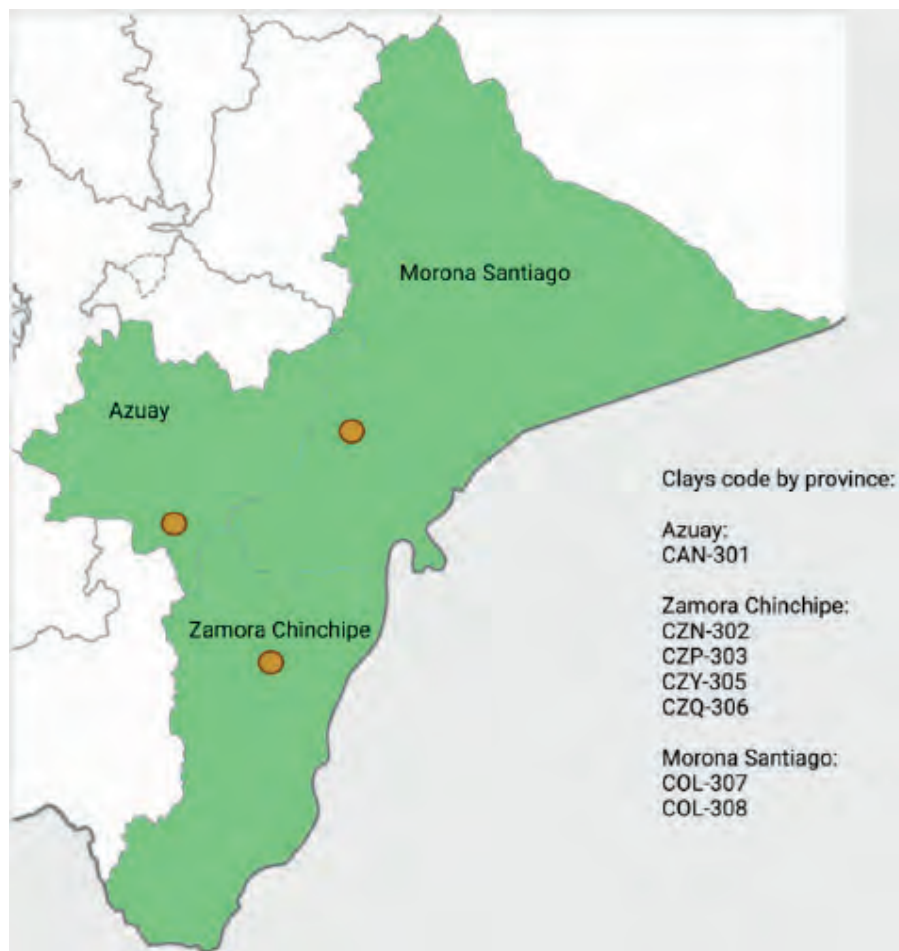


Figure 3. Map of the Ecuadorian provinces and sites where clays were collected. This sampling was performed by G.I.A.M.P (Research Group Applied in Materials and Processes).

cessary to see what compounds were present in the analyzed samples, from which it was observed that Quartz and other forms of silicon oxides appeared in all the samples in different compositions. As it is noticeable, the spectra show similarities for data sets that correspond to the exact location of provenience, and they also are alike in composition.

The most remarkable features obtained of the analyzed samples are shown in Table 2.

Besides their mineralogical composition, the samples are also composed mainly of inorganic complexes, oxides, and long carbon chains. There is a high relative abundance of Quartz in all samples except for the CAN-306 sample, composed mainly of Kaolinite.

From the characterization of clays through Atomic Absorption Spectroscopy (AAS), during the INEDITA project activities, the iron concentration data (in parts per million) was obtained for each sample. This is shown in Table 3.

The similar iron percentage in the analyzed clay samples indicates that almost all the clays share a similar element concentration. Moreover, sample CZY-305 shows a doubled concentration concerning the other clays, see Figure 6, which suggests that this sample is the most suitable precursor for porous framework synthesis designed for H₂S capture.

Nanoclays

Nanomaterials, specifically nanoclays, permit and present various chemical formulas because of their modifiable structure⁷. For example, Kaolinite or Montmorillonite which chemical formula varies depending on the environment since its structure adapts to both water and soil¹⁸. Besides, materials like clays present characteristics such as the Cation Exchange Capacity

(CEC), which allows the core of the material to create a charge imbalance that leads to a change in chemical composition. Additionally, it indicates the level of potential substitution in the core of the material, depending on which cations are used to fill the voids somewhat; thus, resulting in a promising new electronic or polymeric application. Thus, the exact theoretical formula is rarely presented in such a way in nature; rather, the material will have a certain number of waters, etc.

Research on nanoclays has made significant progress in the last years because of the urgent and rising interest in the polymer market⁷. These nanomaterials show many advantages as additives, coatings, etc. In clays, it is essential to notice that they present isomorphous substitution, which is why they tend to have a charge resulting from the exchange of Si⁴⁺ with Al³⁺ leaving a negative charge to be balanced later. This gives the matrix the space to accept positive charges, which allow the clay sheet structure to undergo modification, providing them the possibility of exciting applications as precursor material since it allows the obtention, synthesis, or manufacturing of additives for polymeric chains²⁷. Also, nanoclays are layered mineral silicate with layered nanoparticles that form a crystalline structure after stacking. After, those stacks can be dispersed in a polymeric matrix to achieve a specific new material or feature of a polymer¹⁹.

Nanoclays heavily affect the performance and behavior of nanocomposites, although research is still to be done. An extensive set of characteristics may determine the best and most optimum usage of a specific type of nanoclays but is still little and unknown. The level of intercalation and exfoliation are some of the prior mentioned features, and they could severely change the output of the nanomaterials. Nowadays, research

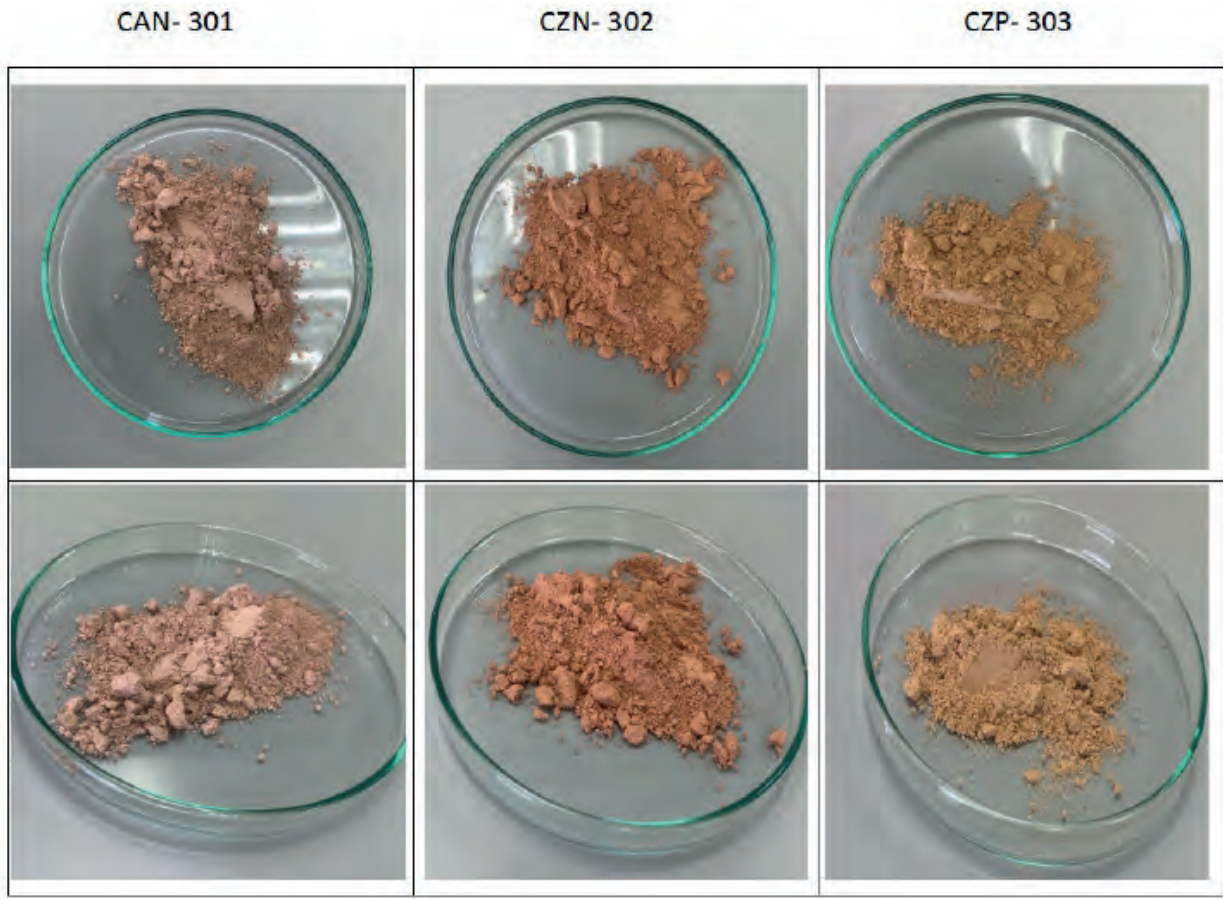


Figure 4. Samples corresponding to clays CAN-301, CZN-302 and CZP-303.

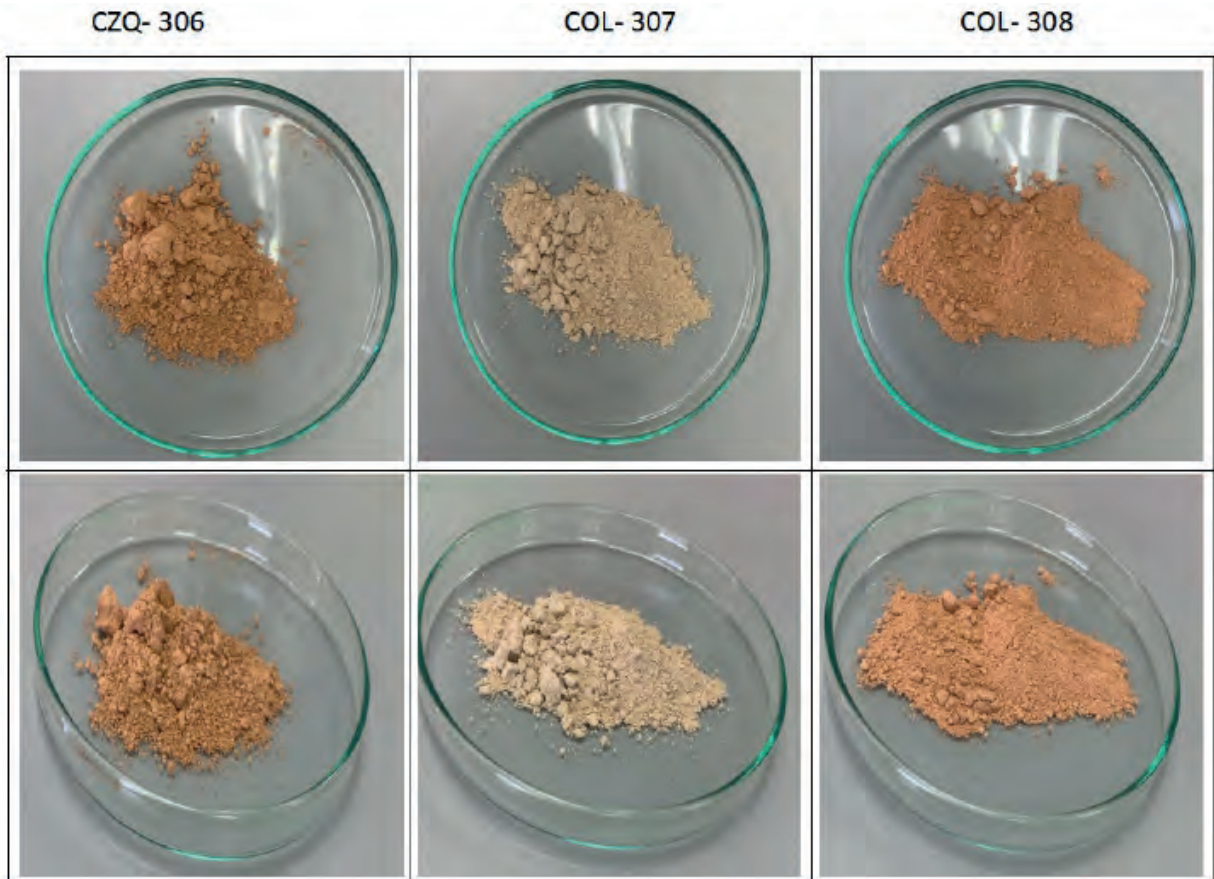


Figure 5. Samples corresponding to clays CZQ-306, COL-307 and COL-308.

Sample	Mineral Phases
CAN-301	Quartz (31.7%), Kaolinite (68.3%)
CZN-302	Quartz (27.2%), Kaolinite (70.6%), Alunite (2.2%)
CZP-303	Quartz (33.5%), Kaolinite (48.5%), Birnessite (2.0%), Titanite (14.0%)
CZY-305	Quartz (20.0%), Kaolinite (22.0%), Antigorite (19.0%), Microcline (29.6%)
CZQ-306	Quartz (9.0%), Kaolinite (63.4%), Muscovite (10.3%), Nacrite (17.3%)
COL-307	Quartz (13.8%), Kaolinite (86.2%)
COL-308	Quartz (39.1%), Kaolinite (57.6%), Dickite (3.4%)

Table 2. Data corresponding to known mineral phases of each sample analyzed by XRD and treated via QUALX2.0, the values in parenthesis correspond to relative abundance (%).

Sample	Concentration of Fe (ppm)	%Fe (+/-)
CAN-301	84	2.6
CZN-302	125	3.7
CZP-303	98	2.6
CZY-305	170	4.4
CZQ-306	103	2.7
COL-307	73	2.2
COL-308	79	2.1

Table 3. Data corresponding to Iron (Fe) concentration and percentage present in each sample²⁵.

has turned its eyes into attaining unique and functional combinations of polymer matrix and nanoclays. Some of these so desired features go from an immiscible or intercalated structure to an exfoliated structure, or even all of them together¹⁹.

Most of the research has been directing and investing its resources in flame retardancy and thermal modification, and the remaining efforts go to organophilic clays for mechanical or barrier properties¹⁸. Nonetheless, as mentioned before, extending the field of research on nanoclays features will lead to the synthesis of new materials and could even expand technology as one knows it. For example, suppose one considers the decomposition rate of certain polymers (already of commercial use) when added a more organophilic and high exfoliating nanoclay to its matrix or as a coating. In that case, it could disintegrate much more easily⁴⁸ resulting in a greener material or a vector that adsorbs toxins from the environment, etc.

Still, there is an urgency to consider the environmental impact and concerns, and the proper production of new nanoclays, as every emerging material, must be examined against

its ecological cost. In this case, the extraction of clays and the subsequent nanoclays for both nature as a whole and humans are two main factors.

Although it can be a completely clean process, the extraction represents a depletion of resources and must be carefully considered, primarily when they represent a non-renewable good, which in the long term will leave a mark on its primary source.

On the other hand, it must be considered the size of the particle and the chemical composition and its effect on both living and inert beings. Will these nanoclays be safe? For example, for living beings, if the nanomaterial has some aspects in its structure, could it enter the blood circulation system and harm it? Or could they accumulate and cause disease? And so on, many questions must be considered.

Toxicity and ecological challenges

The studies and analysis of nanoparticle toxicology focus on the capacity of nanoparticles to damage or change the function of cells, genetic code, and living environments caused

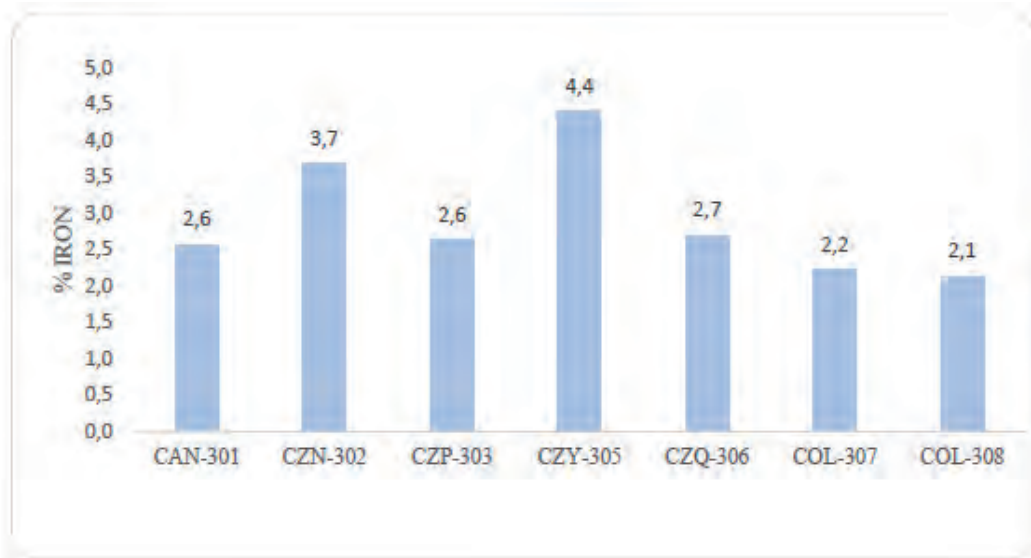


Figure 6. Percentage of iron concentration in clay samples obtained by Atomic Absorption Spectroscopy.

by shaping factors such as the very high surface area of these molecules. It aims to determine in what mechanism the damage is caused, and more importantly, it attempts to find a proper response or a bridge to change the hazardousness into a non-destructive feature.

The different modifiers and their incorporation or combination in the layered silicates can result in nanoclays very miscible in polymers but could also represent a highly dangerous when inhaled or a general direct exposure²⁸. In the same way, the factors mentioned above can lead to toxicological profiles after random scenarios as thermal degradation and chemical composition affect the nanoclays properties and their size and shape, which provokes a variation in toxicity that can be somewhat hazardous.

It was previously discussed that the modification generally occurs via ion exchange, and this process will directly impact the resulting nanocomposite²⁸. Despite the obtention of a high-quality polymer, the usage or consumption of them will certainly open the possibility of degradation and, therefore, the release of the nanoclays from the matrix²⁹, which can turn into a pool of free nanocomposites and depending on the medium or vicinity it can increase the risk of toxicity.

The obtention of naturally sourced clays for the posterior manufacture of nanoclays composites represents another ecological challenge. It is not a threatening challenge, yet it is essential to consider these factors since clays are obtained from limited resources that constitute not only the ecosystem for living beings but also the inorganic portion of a wholesome environment, and like everything in nature, it provides a balance that must be taken care of. In the obtention of clays, it is fundamental to consider the alterations in the surroundings rather than in the clays themselves.

Applications

In recent years, functionalization has been the main objective of research in nanomaterials, since it seems to be, for now, the mechanism which has shown higher effectiveness for targeting many problems, such as drug delivery, surface activity for medical and mechanical purposes, etc., and so many others³⁰.

Bioactive molecules are a new resource that has been under the loupe for many applications since it opens the possibilities of modifying both inner and outer surfaces and other types

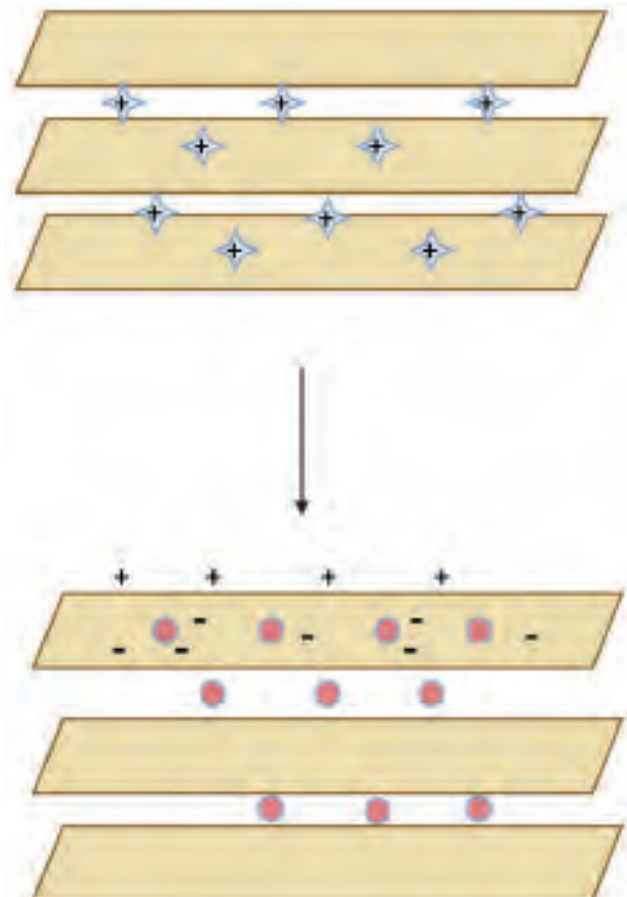


Figure 7. Adsorption of positively charged molecules on the negatively charged surface of a nanoclay²⁶.

of chemical modification³¹. For this reason, its applicability is broad. Another essential feature is that these molecules can give multifunctionality. In nanoscale chemistry, this means the opportunity to synthesize a material, a coating, or a nanoparticle formulation that can accomplish two or more objectives or target two problems at a time. This is of particular interest for material scientists who are constantly searching for new functionalities that enable the material's mechanical properties in the recipient and can adapt to the environment it is in.

One of the approaches to solve the mentioned above is supposedly the surfactant activity of the nanoparticles and, if they lack such activity, to enhance their performance by adding or assisting them via bio-templates. However, this method continues to present certain unwanted behaviors and properties, which, although not inevitable, represent a particular difficulty and hinder the exploitation of its potentials, such as the creation of micro-voids in the matrix or the existence of agglomeration³². Despite, when compared to other surface treatments, introducing a multi-scale synthesis via bio-templates is a current and promising technique to be more investigated.

There are many chemical and physical procedures to functionalize materials, as enumerated in Figure 8.

Clays and nanoclays had acquired particular interest for the applicability; they present for functionalization because of their large surface areas. Clays are characterized for their mechanical polymeric properties and one of those features is the large surface area; this remains after nano scaling them and this behavior makes them a special nanocomposite which more likely will present more necessary properties, such as favorable kinetics in adsorption terms, the desired pore size, and expected crystal arrangement, among others.

Nanoclays can provide the chance not only to be functionalized inherently but also to accept, or interact with templates, resulting in the formation of a functionalized bilayer nanomaterial. When the template comes from a naturally occurring source, such as plants, it widens the sustainability in the process of fabricating a new material, responsibly made, which tackles several green chemistry principles, some of them being:

- Prevent waste
- Less hazardous synthesis
- Design of benign chemicals
- Use of renewable feedstocks
- Reduce derivatives
- Design for degradation

From: The Twelve Green Chemistry Principles³⁴.

There are several studies in recent years corresponding to the research of functionalization of materials and their applications. This so-called functionalization takes advantage of a wide range of available resources, whether they are naturally occurring or synthetic. The branch of study they can apply is an open window to futuristic materials, devices, and medicine. An assorted list of articles is shown below on Table 4, which shows the research that has been done between 2020 and 2021 with functionalized materials.

Gas adsorption membranes

Previously, it was mentioned that nanocomposites in being widely used to revert the damage caused by the past wave of plastics mass production. Nowadays, there is a particular interest in producing new materials that are more ecological and a real option of biodegradable polymers but also in the adsorption of gases causing a greenhouse effect³⁵.

Porous frameworks can work for both liquid and gas systems since their design permit to catch of molecules depending on their size rather than any other characteristics. The benefits of a functionalized nanoclay go beyond acting as a sieve. For example, in this case, where they are placed as a gas adsorption membrane, they would trap molecules and a physisorption process. Another feature is chemical selectivity, which means that these nanoclays and their chemical makeup must also act as, in a certain way, a selector, which allows specific other molecules to pass or not³⁶.

The synthesis of nano-porous materials faces several challenges. Luckily, they are successfully overcome daily because of the increasing interest in this research field. Mao, *et al.*, designed a hierarchical membrane that can undergo volatile organic adsorption and hydrogen gas storage³⁶, demonstrating the many advantages that nanomaterials have to offer. The hierarchical nano-porous membranes in the mentioned study were synthesized from wood cellulose nanocomposites with graphene oxide and carbon spheres.

Industrial treatment for both gas separation and hydro-

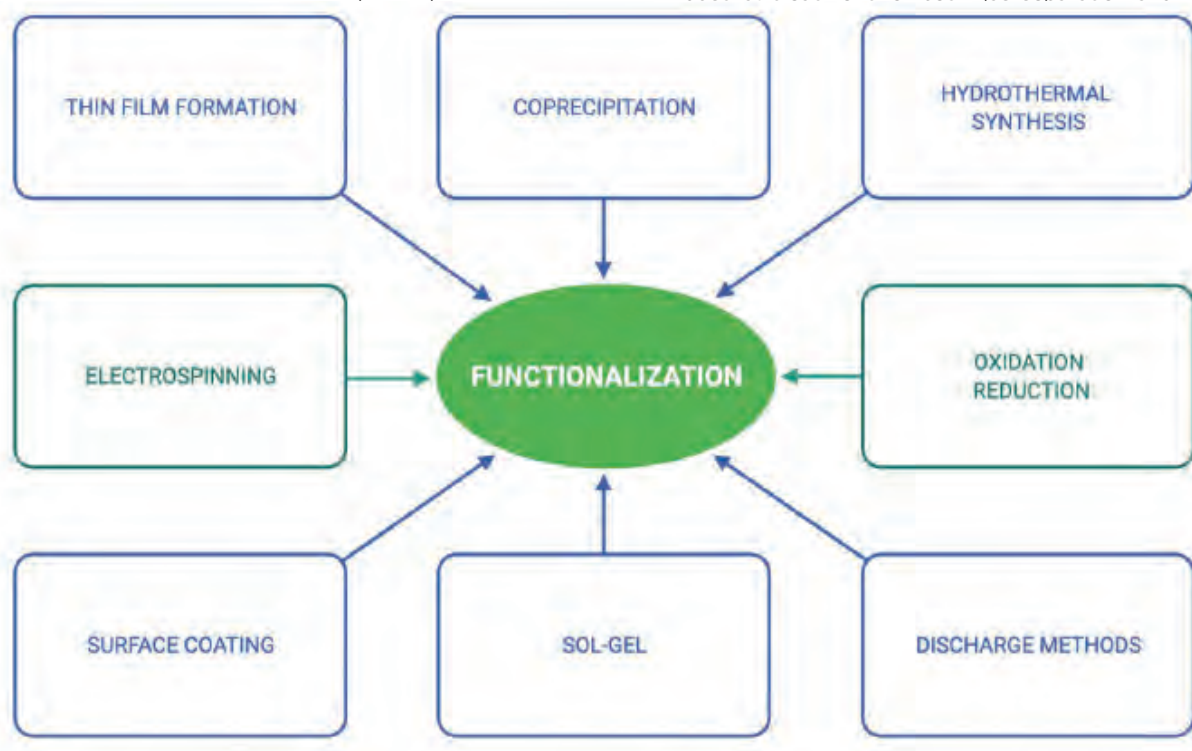


Figure 8. Common techniques used for synthesis and functionalization of nanomaterials³³.

Material functionalization	Authors	Year
Mesoporous materials for lanthanide and actinide extraction	J. Florek, S. Giret, E. Juère, D. Lari-vière, F. Kleitz	2020
Construction of C–N Bonds via Metal-Free Radical C(sp ³)–H functionalization	S. Z. Song, Y. N. Meng, Q. Li, WT Wei	2020
Magnetic nanosized materials for efficient biodiesel synthesis via acid-base/enzyme catalysis	Wang, P Sudarsanam, Y Xu, H Zhang, H Li	2020
Surface-Functionalized Graphite as Long Cycle Life Anode Materials for Li-ion batteries	Xiaohui Gong, Y. Zheng, Jiang Zheng, S. Cao, Dr. Hui, B. Lin, Y. Sun	2020
Mesoporous silica materials with amino ligands for adsorption on aromatic acids	Houmei Liu, Hui Yu, Pian Jin, Mi Jiang, G. Zhu, Yu Duan, Z. Yang, H. Qiu	2020
Rheological and antioxidant properties of chitosan/gelatin-based materials functionalized	M. R. V. Bertolo, V. C. A. Martins, M. M. Horn, L. B. Brenelli, Ana M. G. Pre-pis	2020
Proteins for engineered living materials	L. Xu, X Wang, F Sun, Y Cao, C Zhong	2021
Adsorption of chromium by functionalized metal-organic frameworks from aq. Solutions	X Xiao, Y Deng, J Xue, Y Gao	2021

Table 4. Assorted list of the recent studies on functionalized materials, corresponding to years 2020 & 2021.

gen storage have a long and robust relationship with zeolites and porous materials for the removal of volatile organic compounds^{36,37}. Still, in this era, nanotechnology offers the chance to turn those conventional techniques into brand new innovative paths to solve the same problems with a sustainable approach. Nanoclays offer large surface areas, which is of consideration when scaling membranes to industrial use. Another remarkable feature is that they are lightweight materials that improve transport, installation, replacement, etc., procedures of high cost in the industry.

Moreover, reducing the negative impact that fossil fuel footprint from the environment is always a massive triumph for green chemistry, material science, the planet, and humans. Individuals have been suffering the consequences of high concentrations of carbon dioxide in the air. By August 4, 2021, there was a 415.16 ppm presence of atmospheric CO₂ on the planet, showing a 0.31% increase concerning the same date in 2020, when the concentration was 413.88 ppm, according to co2.earth, a web page dedicated to recording daily the levels of carbon dioxide reached.

Under this perspective, it is easy to interpret that separation of carbon dioxide is a strategic and practical factor when it comes to energy storage and a wholesome ecological development³⁷. New nanomaterials, especially those functionalized, hope to ease environmental problems.

Polymeric research aims to synthesize membranes that have high flux and selectivity; however, there are many significant obstacles, such as an increased permeability when selectivity decreases or the contrary. Also, the elasticity of the

desired material may vary depending on the pore size and the permeability it presents, etc.

Development of membranes with high flux and selectivity is desirable, but one of the major problems of polymeric membranes is that as their permeability increases, their selectivity decreases significantly or vice versa. Various methods have been investigated to overcome this problem thus far; these include the synthesis of new polymers, mixing common polymers with organic and inorganic nanoparticles, etc.³⁸, which allow the formation of a membrane with high permeability, and the nanoclays should also allow a high selectivity.

Hydrogen Sulfide (H₂S) capture by porous frameworks obtained from nanoclays containing iron (Fe)

Hydrogen sulfide H₂S can represent a harmful environmental factor even at low concentration levels³⁹. It is generally the byproduct of industrial processes as it is formed after the fermentation of several organic residues. This gas is toxic and highly corrosive and deactivates catalysts, making it extremely necessary to remove it before any biogas treatment⁴⁰.

The current and most common methods for H₂S capture are wet desulfurization and dry desulfurization⁴¹. The research aims to develop new innovative and sustainable processes for the removal of H₂S increase day by day, especially considering the challenge it means to remove it while having a good sulfur recovery⁴².

The structures that are achievable with porous materials and nanoclays, provide another solution for the adsorption of toxic particles, such as H₂S. The pore size acts as a molecular

sieve at a nanometric scale, and the high surface area of these frameworks can adsorb these molecules, depending on the design of the material, such as metal-exchange zeolites and other porous materials metal-organic frameworks which are highly effective adsorbents³⁹.

Many materials scientists have already proved that there is an increased efficiency when the iron is present in zeolites, silicates, etc. Lee et al. showed that the H₂S adsorption capacity of zeolites is directly proportional to the iron concentration, under a very important condition as it is room temperature⁴³. Bentonite loaded with iron oxide was prepared via the hydrothermal method by Long and Loc, which showed to decrease the H₂S concentration after the removal processes in a fixed bed column⁴⁴.

Therefore, if clays contain iron, then they can be used as a source for the synthesis of nanoclays. This will help and enhance hydrogen sulfide removal by any porous framework derived from such starting reagents, such as the clays samples discussed previously (refer to Table 3, 4, and Figure 6).

Water Treatment

Potabilization of water

The introduction of clays for sustainable water treatment has been long researched and implemented worldwide. Commonly, most water filtration systems include at least one ceramic piece mainly composed out of clays in their structural design. Typically, ceramic filters are made with a high percentage of clays (up to 80-85%) and combustible material, which form a homogeneous mixture after a fine sieving process⁴⁵.

It is reported that polymeric Fe & Al modified clays are highly effective in heavy metals adsorption since it takes the clays' adsorbent properties and their ion exchange capacity. Clays, such as Montmorillonite and Kaolinite, had been provided suitable features for such processes because of the large surface area, which was previously discussed. It is demonstrated that these Al/Fe polymeric species are most efficient for coagulation/adsorption purposes like chemicals removal or emulsion for clean water treatment. Both natural and modified clays exhibit the potential to produce new sorbent materials⁴⁵. The combination of both organic and crystalline materials derived from clays might result in an optimum sorbent material of such properties.

In the past, an approach for achieving this has been the use of carbon in the form of charcoal¹⁰. Yet, granular-activated carbon, a microporous structure, fails to remove large molecules⁴⁶ or waste-water residues, which are generally oil and grease already emulsified. This lack of efficiency from charcoal. Large molecules plug the exposed macro-porous layer; hence the inner microporous layer becomes ineffective.

Dyes removal from water residues

It has been long studied that clays are an effective method for removing organic dyes from water residues, yet in nano dimensions, the effectiveness of these clays is still under the scientific eye⁴⁷. The applicability of these processes is of high potential. The removal of these dyes from aqueous solutions, considering three crucial conditions: temperature, pH, and ionic strength¹¹.

Nanoclays are a very innovative approach to remove some sort of residues from water samples or aqueous solutions since their large surface area provides the space to accept a larger quantity of molecules. When these nanoclays have been functionalized for improvement, they can be provoked the

process of dye removal⁴⁷. Several conditions must be studied to determine the efficacy of specific clays for these kinds of processes. One, for instance, is the pH measurements before and after, these giving the chance to track the changes in the solution while the dye is being adsorbed. Another method for determining the amount of dye is measuring the difference in dye concentrations at certain points during the experiment¹¹. A mass-balance equation must be used to obtain accurate and precise data for these. It is given below,

$$\% \text{ Adsorption} = \frac{C_0 - C_t}{C_0} \times 100,$$

with C₀ as the initial concentration and C_t as the concentration different from the initial. Any C_t can be considered, yet is highly recommended to consider the final time to have a wider window of a full adsorption process. Under the same considerations, the above equation can also be used to study gas adsorption; however, many factors would change because gas molecules' behavior is much different from liquids.

Handling and treatment of nanoclays: suggestions on their toxicity

The nanoscale size of nanoclays allows them to play an innovative role in new biological and environmental functions. Yet, they can also become a significant problem since they also can interfere with cellular processes⁸. The complexity of nanoclays effects and behavior requires putting up very detailed and systematic handling and precautions to reduce the risks of exposure.

Despite the several useful biological and environmental applications of nanoclays, their nanoscale size enables them to penetrate the cell membranes and interfere with cellular processes. Given the complex and uncertain effects of nanoclays on biological environments, systemic management, analysis, and precautions are required to assess and minimize the exposures during their use, handling, and discarding.

More research advances in this specific topic are required to comprehend the dynamics and behavior of nanoclays in living environments and assess the possible damages and side effects caused by the toxicity of the mentioned molecules. It is of primary importance to achieve a safe production of nanocomposites and nanomaterials as they represent and play a fundamental role in the next significant generation of polymers and their application.

Nowadays, there is no clear nor solid explanation of the exact mechanism of how these molecules can be prevented to cause adverse effects on cells, yet the most researched motive seems to be its large and augmented surface area, which also is what gives such excellent properties they present also allowing the surface functionalization, becoming a double edge sword.

Conclusions

Porous frameworks are a suitable approach to tackle contamination in many forms. Therefore, they provide the door to chemical modification and the opportunity to create novel materials from a wide range of precursors, as clays since they constitute a primary and naturally occurring source of starting materials such as Silicon or Aluminum. The soil mineralogy of Ecuador allows the obtention of such nanoclays, that can lead to the synthesis of nano-porous materials. This idea derived the characterization of Ecuadorian clays from the

INEDITA project as a plus contribution to a repository and research compendium of the soils they came from. This review also displays the usefulness and possible applications such as adsorption of the greenhouse effect, water cleaning, and purification, dyes removal, etc., as a starting point of what can be achieved with nanoclays and porous frameworks resulting from the proposed synthesis while considering late and new research on the topic.

Acknowledgments

The INEDITA project and the Research Group Applied in Materials and Processes' GIAMP' are deeply acknowledged for supporting this research, providing data and materials. In the same way, Yachay Tech University for the materials used for the characterization of clays.

Conflicts of Interest

The authors declare no conflict of interest.

Bibliographic references

- Jeon, M. Y., Kim, D., Kumar, P., Lee, P. S., Rangnekar, N., Bai, P., Shete, M., Elyassi, B., Lee, H. S., Narasimharao, K., Basahel, S. N., Al-Thabaiti, S., Xu, W., Cho, H. J., Fetisov, E. O., Thyagarajan, R., DeJaco, R. F., Fan, W., Mkhoyan, K. A., ... Tsapatsis, M. (2017). Ultra-selective high-flux membranes from directly synthesized zeolite nanosheets. *Nature*, 543(7647), 690–694. <https://doi.org/10.1038/nature21421>
- Chen, Y., Wang, N., Ola, O., Xia, Y., & Zhu, Y. (2021). Porous ceramics: Light in weight but heavy in energy and Environment Technologies. *Materials Science and Engineering: R: Reports*, 143, 100589. <https://doi.org/10.1016/j.mser.2020.100589>
- Dincă, M., & Long, J. R. (2020). Introduction: Porous framework chemistry. *Chemical Reviews*, 120(16), 8037–8038. <https://doi.org/10.1021/acs.chemrev.0c00836>
- Rosi, N. L., Kim, J., Eddaoudi, M., Chen, B., O'Keeffe, M., & Yaghi, O. M. (2005). Rod Packings and metal–organic frameworks constructed from rod-shaped secondary building units. *Journal of the American Chemical Society*, 127(5), 1504–1518. <https://doi.org/10.1021/ja045123o>
- Kecili, R., & Hussain, C. M. (2018). Mechanism of adsorption on nanomaterials. *Nanomaterials in Chromatography*, 89–115. <https://doi.org/10.1016/b978-0-12-812792-6.00004-2>
- Azodi-Deilami, S., Najafabadi, A. H., Asadi, E., Abdouss, M., & Kordestani, D. (2014). Magnetic molecularly imprinted polymer nanoparticles for the solid-phase extraction of paracetamol from plasma samples, followed its determination by HPLC. *Microchimica Acta*, 181(15-16), 1823–1832. <https://doi.org/10.1007/s00604-014-1230-9>
- Huczko, A. (2000). Template-based synthesis of nanomaterials. *Applied Physics A: Materials Science & Processing*, 70(4), 365–376. <https://doi.org/10.1007/s003390051050>
- Zanjani, J. S., Oğuz, O., Okan, B. S., Yildiz, M., & Menciloğlu, Y. Z. (2019). Polymer composites containing functionalized nanoparticles and the environment. *Polymer Composites with Functionalized Nanoparticles*, 437–466. <https://doi.org/10.1016/b978-0-12-814064-2.00014-7>
- Ishizaki, K., Komarneni, S., & Nanko, M. (1998). Porous materials. *Materials Technology Series*. <https://doi.org/10.1007/978-1-4615-5811-8>
- Beall, G. (2003). The use of organo-clays in water treatment. *Applied Clay Science*, 24(1-2), 11–20. <https://doi.org/10.1016/j.clay.2003.07.006>
- Salam, M. A., Kosa, S. A., & Al-Beladi, A. A. (2017). Application of nanoclay for the adsorptive removal of Orange G dye from aqueous solution. *Journal of Molecular Liquids*, 241, 469–477. <https://doi.org/10.1016/j.molliq.2017.06.055>
- Sabarish, R., & Unnikrishnan, G. (2019). Synthesis, characterization and evaluations of micro/mesoporous ZSM-5 zeolite using starch as Bio Template. *SN Applied Sciences*, 1(9). <https://doi.org/10.1007/s42452-019-1036-9>
- Zhu, G., & Ren, H. (2015). Porous organic frameworks design, synthesis and their advanced applications. Springer Berlin Heidelberg.
- Aguado, S., Bergeret, G., Daniel, C., & Farrusseng, D. (2012). Absolute molecular sieve separation of ethylene/ethane mixtures with silver zeolite a. *Journal of the American Chemical Society*, 134(36), 14635–14637. <https://doi.org/10.1021/ja305663k>
- Greer, H. F., Zhou, W., Zhang, G., & Ménard, H. (2017). Nancone decorated zno microspheres exposing the (0001) plane and enhanced photocatalytic properties. *Advanced Materials Interfaces*, 4(13), 1601238. <https://doi.org/10.1002/admi.201601238>
- Rahman, A., Purwanto, A., Endah, A., Handoko, E., Kusri, E., & Prasetyanto, E. A. (2019). Synthesis and characterization of LTA zeolite from Kaolin Bangka. *Journal of Physics: Conference Series*, 1402, 055057. <https://doi.org/10.1088/1742-6596/1402/5/055057>
- Khaleque, A., Alam, M. M., Hoque, M., Mondal, S., Haider, J. B., Xu, B., Johir, M. A. H., Karmakar, A. K., Zhou, J. L., Ahmed, M. B., & Moni, M. A. (2020). Zeolite synthesis from low-cost materials and environmental applications: A Review. *Environmental Advances*, 2, 100019. <https://doi.org/10.1016/j.envadv.2020.100019>
- Uddin, F. (2008). Clays, nanoclays, and Montmorillonite Minerals. *Metallurgical and Materials Transactions A*, 39(12), 2804–2814. <https://doi.org/10.1007/s11661-008-9603-5>
- Guo, F., Aryana, S., Han, Y., & Jiao, Y. (2018). A review of the synthesis and applications of polymer–nanoclay composites. *Applied Sciences*, 8(9), 1696. <https://doi.org/10.3390/app8091696>
- Rajeswari, A., Jackcina Stobel Christy, E., Gopi, S., Jayaraj, K., & Pius, A. (2020). Characterization studies of polymer-based composites related to functionalized filler–matrix interface. *Interfaces in Particle and Fibre Reinforced Composites*, 219–250. <https://doi.org/10.1016/b978-0-08-102665-6.00009-1>
- Na Nazir, M.S., Kassim, M.H., Mohapatra, L., Gilani, M.A., Raza, M.R., & Majeed, K. (2016). Characteristic Properties of Nanoclays and Characterization of Nanoparticulates and Nanocomposites.
- The Clay Mineral Group. THE CLAY GROUP. (n.d.) from http://www.galleries.com/Clays_Group
- Cárdenas, J.L., Paredes, C.A., Pacheco, J., 2003. La industria cerámica en el Ecuador. *Rev. Tecnol.* 16, 19–23.
- Sima, F., Ristoscu, C., Duta, L., Gallet, O., Anselme, K., & Mihailescu, I. N. (2016). Laser thin films deposition and characterization for biomedical applications. *Laser Surface Modification of Biomaterials*, 77–125. <https://doi.org/10.1016/b978-0-08-100883-6.00003-4>
- Vera, D. (2020). Characterization of Ecuadorian Ferruginous and Titaniferous Sands for Hydrogen Sulfide Capture (thesis).
- Hosseini, F., Hosseini, F., Jafari, S. M., & Taheri, A. (2018). Bentonite nanoclay-based drug-delivery systems for treating melanoma. *Clay Minerals*, 53(01), 53–63. doi:10.1180/clm.2018.4
- Wagner, A., White, A. P., Stueckle, T. A., Banerjee, D., Sierros, K. A., Rojanasakul, Y., Agarwal, S., Gupta, R. K., & Dinu, C. Z. (2017). Early assessment and correlations of Nanoclay's toxicity to their physical and chemical properties. *ACS Applied Materials & Interfaces*, 9(37), 32323–32335. <https://doi.org/10.1021/acsmi.7b06657>
- Saleh Alghamdi, S., John, S., Roy Choudhury, N., & Dutta, N. K. (2021). Additive Manufacturing of Polymer Materials: Progress, promise and challenges. *Polymers*, 13(5), 753. <https://doi.org/10.3390/polym13050753>
- Roes, L., Patel, M. K., Worrell, E., & Ludwig, C. (2012). Preliminary evaluation of risks related to waste incineration of polymer nanocomposites. *Science of The Total Environment*, 417–418, 76–86. <https://doi.org/10.1016/j.scitotenv.2011.12.030>
- Araújo, F., das Neves, J., Martins, J. P., Granja, P. L., Santos, H. A., & Sarmento, B. (2017). Functionalized materials for multistage platforms in the oral delivery of biopharmaceuticals. *Progress in Materials Science*, 89, 306–344. <https://doi.org/10.1016/j.pmatsci.2017.05.001>

31. Patra, J. K., Das, G., Fraceto, L. F., Campos, E. V., Rodríguez-Torres, M. del, Acosta-Torres, L. S., Díaz-Torres, L. A., Grillo, R., Swamy, M. K., Sharma, S., Habtemariam, S., & Shin, H.-S. (2018). Nano based drug delivery systems: Recent developments and future prospects. *Journal of Nanobiotechnology*, 16(1). <https://doi.org/10.1186/s12951-018-0392-8>
32. Blasco, E., Sims, M. B., Goldmann, A. S., Sumerlin, B. S., & Barner-Kowollik, C. (2017). 50th anniversary perspective: Polymer functionalization. *Macromolecules*, 50(14), 5215–5252. <https://doi.org/10.1021/acs.macromol.7b00465>
33. Ozkantar, N., Yilmaz, E., Soylak, M., & Tuzen, M. (2020). Pyrocatechol violet impregnated magnetic graphene oxide for magnetic solid phase microextraction of copper in water, black tea and diet supplements. *Food Chemistry*, 321, 126737. <https://doi.org/10.1016/j.foodchem.2020.126737>
34. American Chemical Society. (n.d.). Retrieved February 3, 2022, from <https://www.acs.org/content/acs/en.html>
35. Khajeh, M., & Ghaemi, A. (2020). Exploiting response surface methodology for experimental modeling and optimization of CO₂ adsorption onto NaOH-modified Nanoclay Montmorillonite. *Journal of Environmental Chemical Engineering*, 8(2), 103663. <https://doi.org/10.1016/j.jece.2020.103663>
36. Mao, H., Tang, J., Chen, J., Wan, J., Hou, K., Peng, Y., Halat, D. M., Xiao, L., Zhang, R., Lv, X., Yang, A., Cui, Y., & Reimer, J. A. (2020). Designing hierarchical nanoporous membranes for highly efficient gas adsorption and storage. *Science Advances*, 6(41). <https://doi.org/10.1126/sciadv.abb0694>
37. Amini, Z., & Asghari, M. (2018). Preparation and characterization of ultra-thin poly ether block amide/nanoclay nanocomposite membrane for gas separation. *Applied Clay Science*, 166, 230–241. <https://doi.org/10.1016/j.clay.2018.09.025>
38. Dehghani Kiadehi, A., Rahimpour, A., Jahanshahi, M., & Ghoreyshi, A. A. (2015). Novel carbon nano-fibers (cnf)/polysulfone (PSF) mixed matrix membranes for gas separation. *Journal of Industrial and Engineering Chemistry*, 22, 199–207. <https://doi.org/10.1016/j.jiec.2014.07.011>
39. Khabazipour, M., & Anbia, M. (2019). Removal of hydrogen sulfide from gas streams using porous materials: A Review. *Industrial & Engineering Chemistry Research*, 58(49), 22133–22164. <https://doi.org/10.1021/acs.iecr.9b03800>
40. Liu, D., Li, B., Wu, J., & Liu, Y. (2019). Sorbents for hydrogen sulfide capture from biogas at low temperature: A Review. *Environmental Chemistry Letters*, 18(1), 113–128. <https://doi.org/10.1007/s10311-019-00925-6>
41. Wang, F., Zhong, H.-H., Chen, W.-K., Liu, Q.-P., Li, C.-Y., Zheng, Y.-F., & Peng, G.-P. (2016). Potential hypoglycaemic activity phenolic glycosides from moringa oleifera seeds. *Natural Product Research*, 31(16), 1869–1874. <https://doi.org/10.1080/14786419.2016.1263846>
42. Chiappe C., Pomelli C.S. (2017) Hydrogen Sulfide and Ionic Liquids: Absorption, Separation, and Oxidation. In: Kirchner B., Pert E. (eds) Ionic Liquids II. Topics in Current Chemistry Collections. Springer, Cham. https://doi.org/10.1007/978-3-319-89794-3_10
43. Lee, E. Y., & Suh, M. P. (2004). A robust porous material constructed of linear coordination polymer chains: Reversible single-crystal to single-crystal transformations upon dehydration and rehydration. *Angewandte Chemie International Edition*, 43(21), 2798–2801. <https://doi.org/10.1002/anie.200353494>
44. Long, N.Q., Loc, T.X. Experimental and modeling study on room-temperature removal of hydrogen sulfide using a low-cost extruded Fe₂O₃-based adsorbent. *Adsorption* 22, 397–408 (2016). <https://doi.org/10.1007/s10450-016-9790-0>
45. Zereffa, E. A., & Bekalo, T. B. (2017). Clay ceramic filter for water treatment. *Materials Science and Applied Chemistry*, 34(1). <https://doi.org/10.1515/msac-2017-0011>
46. Jjagwe, J., Olupot, P. W., Menya, E., & Kalibbala, H. M. (2021). Synthesis and application of granular activated carbon from biomass waste materials for water treatment: A Review. *Journal of Biore-sources and Bioproducts*, 6(4), 292–322. <https://doi.org/10.1016/j.jobab.2021.03.003>
47. Stagnaro, S. M., Volzone, C., & Huck, L. (2015). Nanoclay as adsorbent: Evaluation for removing dyes used in the textile industry. *Procedia Materials Science*, 8, 586–591. <https://doi.org/10.1016/j.mspro.2015.04.112>
48. Fu, X., & Qutubuddin, S. (2000, September 28). Clay nanocomposites: Exfoliation of organophilic montmorillonite nanolayers in polystyrene. *Polymer*. Retrieved February 3, 2022, from <https://www.sciencedirect.com/science/article/abs/pii/S0032386100003852>

ARTICLE / INVESTIGACIÓN

A16974C polymorphism of the IL-12 p40 gene in Cuban patients having recovered from COVID-19

Estela Morales Peralta¹, Yaíma Zúñiga Rosales², Teresa Collazo Mesa², Elvia Nelemi Santos González², Yadira Hernández Pérez², María de los Angeles González Torres², Hilda Roblejo Balbuena², Beatriz Marcheco Teruel²

DOI. 10.21931/RB/2022.07.01.34

¹10 de Octubre University Hospital. Havana, Cuba.

²National Medical Genetics Center. Havana, Cuba.

Corresponding author: foraris@infomed.sld.cu

Abstract: COVID-19 has had severe consequences worldwide. It has been estimated that the contribution of genetic factors to the disease is about 50%. The A16974C polymorphism of the IL-12 p40 gene has been described as being related to resistance or susceptibility to other infectious diseases; therefore, it is likely that it can also be related to COVID-19. The objective of this study was to describe the relationship between the A16974C polymorphism of the IL12 p40 gene with clinical forms of COVID-19 in Cuban patients. The genotypes of the A16974C polymorphism of gene IL-12 p40 were determined through PCR in 102 persons with a COVID-19 epidemiologic discharge from the hospital. In this research, the CC genotype of this polymorphism was found only in symptomatic cases of this disease; since there are signs of relationship between the A16974C polymorphism of the IL12 p40 gene with clinical forms of COVID-19 in the studied Cuban patients, the variations of this polymorphism may be a predisposing risk factor in the development of COVID-19.

Key words: COVID-19, genetic polymorphism, genetic predisposition to disease, genetic susceptibility, human genetic variants, Cuba, alleles.

Introduction

Infectious diseases are produced by the interaction between the agent's characteristics, the environment and the host. Human variations or polymorphisms have been identified among the latter, which are related to the clinical course of the disease. This occurs with the c.554_585del mutation of the CCR5 gene, linked to the resistance to the progression of the acquired immunodeficiency syndrome and the c.1521_1523delCTT of gene CFTR –the cause of cystic fibrosis– that confers susceptibility to infection by *Pseudomonas aeruginosa*, to give two examples¹.

COVID-19 (the acronym of COronaVirus Disease and the year 2019), produced by the SARS-CoV-2 virus (from severe acute respiratory syndrome coronavirus 2), has had severe consequences worldwide².

Studies in twins demonstrated that the concordance of the clinical severity of COVID-19 is greater among monozygotic twins, estimating that the contribution of genetic factors to this disease is approximately 50%³. Therefore, there is evidence that the genetic constitution, with its variations, contributes to the predisposition or resistance to this disease⁴.

In relation to the pathophysiology of COVID-19, a group of genes may possibly participate in the risk of contracting the disease or its more severe forms. These include genes coding for the virus receptors, those related to inflammation and immune response, as well as those involved in clotting and the acute res-

piratory distress syndrome. Those related to inflammation and immune response comprise genes coding for pro-inflammatory cytokines, including interleukins 1, 6, 12 (IL-1, IL-6, IL-12)^{1,4}.

Interleukin 12 (IL-12) promotes cell immunity. It plays an essential role in the differentiation of lymphocytes T towards the T helper 1 (Th1) pattern and the increase in the cytotoxic activity of the Natural Killer (NK) cells against viral infections and other intracellular pathogens⁵. It also participates in the induction of an increase in the synthesis and secretion of other cytokines, such as IL-1, IL-6, IFN- γ , and TNF- α , producing the "cytokine storm"⁶, which is a sign of a poor prognosis of COVID-19 (Figure 1)⁷. Therefore, variants of the genes coding for the synthesis of the IL-12, such as A16974C polymorphism, may also be related to an increase in the susceptibility to SARS-CoV-2^{8,9}.

By identifying the genetic variants of the Cuban population that have a predisposition to developing COVID-19, and even in its most severe clinical forms, we can design prevention strategies that range from vaccination to therapeutic measures. This may help generate a clinical guide for the management and advances in genomic medicine applied to COVID-19 management.

The objective of this study was to describe the relationship between the A16974C polymorphism of the IL12 p40 gene with clinical forms of COVID-19 in Cuban patients.

Citation: Morales Peralta E, Zúñiga Rosales Y, Collazo Mesa T, Santos González E, Hernández Pérez Y, González Torres M, Roblejo Balbuena H, Marcheco Teruel B. A16974C polymorphism of the IL-12 p40 gene in Cuban patients having recovered from COVID-19. *Revis Bionatura* 2022;7(1):34. <http://dx.doi.org/10.21931/RB/2022.07.01.34>

Received: 20 October 2021 / **Accepted:** 13 December 2021 / **Published:** 15 February 2022

Publisher's Note: Bionatura stays neutral with regard to jurisdictional claims in published maps and institutional affiliations.

Copyright: © 2022 by the authors. Submitted for possible open access publication under the terms and conditions of the Creative Commons Attribution (CC BY) license (<https://creativecommons.org/licenses/by/4.0/>).



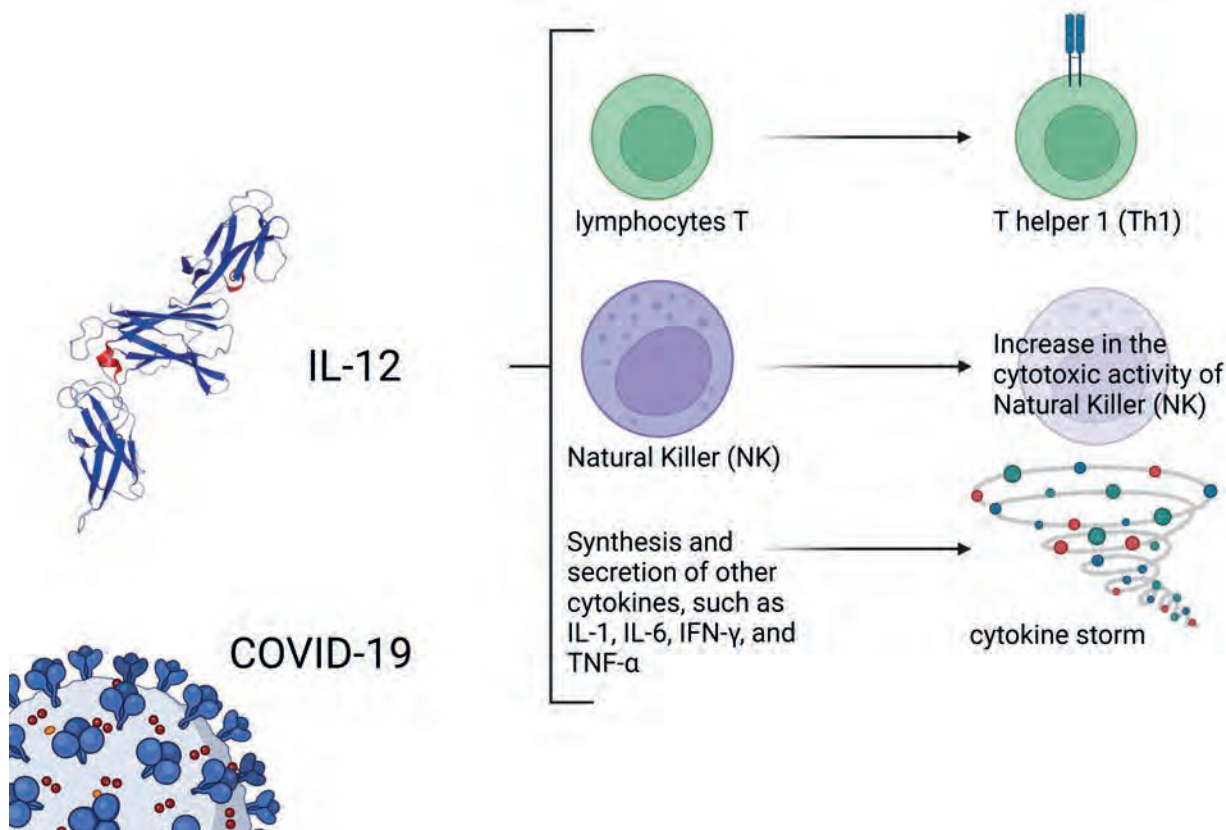


Figure 1. The immunopathological mechanisms of COVID-CS. SARS-CoV-2 infects the epithelial cells or immune cells, causing tissue damage and release of inflammatory cytokines (e.g., IL-1, IL-6, IL-12, and TNF α) by epithelial cells and immune cells. These inflammatory cytokines then recruit innate immune cells (monocytes, macrophages, neutrophils, DCs, and NK cells) and activate adaptive immune cells (CD4⁺ T cells and CD8⁺ T cells) to induce the occurrence of myelopoiesis and emergency granulopoiesis, as well as the production of sustained and excessive circulating cytokines.

Materials and methods

Subjects /patients

A sample of 102 patients was randomly taken from all Cuban patients over one year of age, who initially tested positive for Sars-CoV-2 by RT-PCR (Reverse transcription-polymerase chain reaction) and tested negative twice as of June 11, 2020, for SARS-CoV-2 by RT-PCR, in 14 days after being discharged from the hospital.

Demographic variables

EDemographic variables included age in years, skin color (according to the patient's self-perception) and sex. These were taken from a survey designed for the project: "Genetic risk factors associated to the clinical severity of COVID-19 in Cuban patients and their first-degree relatives", in which this study was included.

The persons studied were classified according to the clinical forms of the disease (considering whether they had symptoms or not) as symptomatic and asymptomatic, respectively.

Molecular studies

The DNA was obtained from 4 mL of peripheral blood collected in a Vacutainer with EDTA (K3E 7.2mg). QIA Symphony DNA kits were used following the manufacturer's instructions¹⁰.

To identify the alleles of the A16974C polymorphism, we used the polymerase chain reaction (PCR) described by See-

gers et al. We designated alleles A and C from this polymorphism, as defined by the above authors⁹.

The sequences of the primers used were

Forward: 5'-ATT-TGG-AGG-AAA-AGT-GGA-AGA-3'

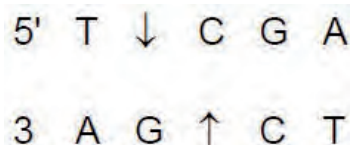
Reverse: 5'-AAT-TTC-ATG-TCC-TTA-GCC-ATA-3'

The amplifications were made in an MJ Research thermocycler in the following way: primary denaturalization (10 min at 94 °C), followed by 30 cycles of: denaturalization (30 s at 94 °C), hybridization (30 s at 65 °C) and elongation:

30 s at 72 °C, with the final extension at 72 °C for 10 minutes.

To verify each amplification, we carried out an electrophoretic run in 2% agarose gel stained with ethidium bromide, with a molecular weight marker of 100bp, at a fixed voltage of 250 V. The amplification was verified when we identified that the fragment obtained was 1046 base pairs (bp).

The amplified product was digested with the Taq I restriction enzyme because of its recognition sequence and enzymatic digestions:



This procedure was made under the manufacturer's conditions, which recommends the use of 10 μ l of the product of the PCR, 2 μ l (20U) of the Taq I enzyme, 3.5 μ l of buffer B, and 19.5 μ l of H₂O. The incubation was performed at 65 °C overnight.

The processed product was then submitted to a run in 2% agarose gel for 30 minutes at 250 V, with a molecular weight marker of 100bp. The genotypes related to the polymorphisms that were obtained were: an entire fragment of 1046 bp, corresponding to the homozygous genotype for allele A; for the homozygous genotype of allele C, we obtained two fragments, one of 906 bp and the other of 140 bp, and the three fragments (1046, 906 and 140 bp) for the heterozygote.

Processing, analysis, summary and presentation of the information:

The data obtained were processed with the IBM SPSS Statistics software version 22.0. The absolute and relative frequencies were calculated (percentage).

Bioethical issues

This research was part of the project named "Genetic risk factors associated to the clinical severity of COVID-19 in Cuban patients and their first-degree relatives", approved by the Research Ethics Committee of the National Medical Genetics Center. Throughout its implementation, we supervised the compliance to the ethical principles for human medical research, including in the Helsinki Declaration¹¹. All participants in this research signed written consent for their participation, and in the case of children under 16 years of age, they were represented by their parents or tutors.

Results

Demographic characteristics of the patients infected with SARS-CoV-2 are shown in table 1; they included age, sex and

skin color, according to the clinical forms of the malady considered in this investigation (asymptomatic or symptomatic).

The average age of the patients was 52 years old (95% CI 48-55), ranging from 4 to 96 years of age. The mean age was more significant in symptomatic patients than asymptomatic patients (55 compared to 39), increasing the proportion of symptomatic patients with age. More females were included in the study, and they were predominant in both clinical forms. The number of individuals with white skin color was more remarkable in both clinical categories.

Table 2 shows the number of patients studied according to their genotype for the A16974C polymorphism of the IL12p40 gene and their clinical forms. Genotype CC was not present in those showing asymptomatic forms.

The alleles A and C frequency were 0.75% and 0.25%; 0.83% and 0.17% for symptomatic and asymptomatic patients, respectively.

Discussion

The SARS-CoV-2 infection and the development of clinical forms of COVID-19 could be influenced by several factors, of which the immunological genotype-phenotype relationship is of particular interest. It is essential to identify the persons with the highest risks for applying preventive measures so that their care can be personalized as much as possible.

It was found that the average age was higher in symptomatic cases. Similar results were described in the literature¹². The factors explaining this finding include the alteration of the innate and adaptive immune response with a decreased capacity for responding specifically to new antigens (immuno-

Characteristics	Groups according to the clinical form of the disease. No. (%)	
	Asymptomatic (n=20)	Symptomatic (n=82)
Age (years)		
<20	4 (20%)	3 (3.7%)
20-39	7 (35%)	13 (15.8%)
40-59	6 (30%)	36 (44%)
≥60	3 (15%)	30 (36.5%)
Median (IQR)	38 (25-51)	55 (43-67)
Mean (95% CI minimum;maximum)	39 (31;47)	55 (51;59)
Sex		
Male	8 (40.0%)	35 (42.7%)
Female	12 (60.0%)	47 (57.3%)
Skin color*		
White	12 (60.0%)	54 (66.7%)
Mestizo	5 (25.0%)	22 (27.1%)
Black	3 (15.0%)	5 (6.2%)
IQR: Interquartile range *A symptomatic case with missing information on skin color		

Table 1. Distribution of the patients infected with SARS-CoV-2 in the study, according to age, sex, and skin color, depends on the disease's clinical forms.

CHARACTERISTICS	GENOTYPES		
	AA	AC	CC
Clinical forms			
Symptomatic (n=82)	43 (52.43%)	37 (45.12%)	2 (2.43%)
Asymptomatic (n=20)	13 (65%)	7 (35%)	0

Table 2. Clinical forms in patients infected by SARS-CoV-2 according to the polymorphic genotypes of A16974C of the IL12p40 gene.

senescence), the trend towards mainly pro-inflammatory response (low degree inflammation or "inflamm-aging")¹³, and the increase of the probability of having comorbidities^{14,15}.

This study's comparatively higher incidence of affected women may be because it was carried out through home visits to recovered patients who had resumed their usual occupations. For this reason, the voluntary collaboration of women was more significant. The highest proportion of the recruited individuals was of white skin, agreeing with the results of other studies made in the same population¹⁶. The proportion observed for this skin color agrees with the Cuban population census of the year 2012¹⁷.

COVID-19 is related to a series of pathophysiological mechanisms mobilizing many biomolecules. In the more severe cases, the prognoses may be markedly worsened by the hyperproduction of cytokines (frequently called the cytokine storm), leading to vascular damage, the activation of other immune response mechanisms and the worsening of clinical results¹⁸. The cytokines include IL-12⁹, coding for a gene located at 5q33.3 of which several polymorphisms have been described¹⁹. The one explored here was identified through the Taq I enzyme, and it is found at the untranslatable 3' region of the gene, at position 16974, which enables the identification of alleles A and C, given by the presence of adenine or cytosine, and corresponding to the absence or presence of the cut at the Taq I enzyme. It is considered that allele A is the wild type and that C affects the secretion of IL-12 in vitro⁹. Genotype CC, and of course, allele C, had the lowest frequency in all populations, including the normal Cuban population²⁰, and it has been associated with the predisposition to several diseases²¹. In fact, this genotype was not found in the asymptomatic cases included in this study. These results could prove that the clinical form may be related to the genotypes studied. The variants evaluated here can be used for prognosis purposes, including those related to a higher probability of presenting complications or more severe clinical conditions. This can be important in the personalized care of the patients, and above all, in terms of disease prevention.

All results observed can be explained by the small sample size of this study, which was a significant limitation of this research; the results of this type of research are applicable to the population where it was carried out.

Studies, such as the one shown here will help identify the genetic variants or polymorphisms related to diseases that do not show Mendelian inheritance, including infectious diseases²². More in-depth studies on this topic are required in the future.

Conclusions

Since there are signs of relationship between the A16974C polymorphism of the IL12 p40 gene with clinical forms of COVID-19 in the studied Cuban patients, the variations of this polymorphism may be a predisposing risk factor in the development of COVID-19.

Ethics approval and consent to participate

This study is part of a research project that the Ethics Committee approved of the National Center for Medical Genetics and conducted by this institution in all the municipalities and provinces of Cuba.

Consent for publication

Not applicable

Availability of data and material

The datasets used and/or analyzed during the current study are available from the corresponding author on reasonable request.

Competing interests

The authors declare that there are no competing interests.

Funding

Not applicable because this research did not receive any external funding.

Authors contributions

EMP: did conceptualization, data selection, formal analysis, methodological design, software application, visualization, was a major contributor in writing the manuscript. YZR: did research, methodological design. TCM: did research, attention to resources. ENSG and YHP: performed the molecular procedures. MAGT: did formal analysis, software application. HRB: did attention to resources, visualization. BMT: did project administration, revision and editing. All authors read and approved the final manuscript.

Acknowledgements

The authors would like to thank Miriam Ribas Hermelo for her advice and the translation of this paper.

Bibliographic references

- Murray MF, Kenny EE, Ritchie MD, Rader DJ, Bale AE, Giovanni MA, et al. COVID-19 outcomes and the human genome. *Genet Med* 2020;22:1175–7. <https://doi.org/10.1038/s41436-020-0832-3>.
- Pasrija R, Naime M. The deregulated immune reaction and cytokines release storm (CRS) in COVID-19 disease. *Int Immunopharmacol* 2021;90:107225. <https://doi.org/10.1016/j.intimp.2020.107225>.
- Williams FM, Freydin M, Mangino M, Couvreur S, Visconti A, Bowyer RC, et al. Self-reported symptoms of covid-19 including symptoms most predictive of SARS-CoV-2 infection, are heritable 2020. <https://doi.org/10.1101/2020.04.22.20072124>.
- Yousefzadegan S, Rezaei N. Case Report: Death due to COVID-19 in Three Brothers. *Am J Trop Med Hyg* 2020;102:1203–4. <https://doi.org/10.4269/ajtmh.20-0240>.
- Kenney AD, Dowdle JA, Bozzacco L, McMichael TM, St Gelais C, Panfil AR, et al. Human Genetic Determinants of Viral Diseases. *Annu Rev Genet* 2017;51:241–63. <https://doi.org/10.1146/annurev-genet-120116-023425>.

6. Öztürk R, Taşova Y, Ayaz A. COVID-19: pathogenesis, genetic polymorphism, clinical features and laboratory findings. *Turk J Med Sci.* 2020 Apr 21;50(SI-1):638–57.
7. Costela-Ruiz VJ, Illescas-Montes R, Puerta-Puerta JM, Ruiz C, Melguizo-Rodríguez L. SARS-CoV-2 infection: The role of cytokines in COVID-19 disease. *Cytokine Growth Factor Rev* 2020;54:62–75. <https://doi.org/10.1016/j.cytogfr.2020.06.001>.
8. Trinchieri G. Interleukin-12: a pro-inflammatory cytokine with immunoregulatory functions that bridge innate resistance and antigen-specific adaptive immunity. *Annu Rev Immunol* 1995;13:251–76. <https://doi.org/10.1146/annurev.iy.13.040195.001343>.
9. Seegers D, Zwiers A, Strober W, Peña AS, Bouma G. A TaqI polymorphism in the 3'UTR of the IL-12 p40 gene correlates with increased IL-12 secretion. *Genes Immun* 2002;3:419–23. <https://doi.org/10.1038/sj.gene.6363919>.
10. QIAGEN. QIASymphony® DSP DNA Instructions for Use (Handbook) 2015.
11. World Medical Association Declaration of Helsinki: ethical principles for medical research involving human subjects. *J Am Coll Dent* 2014;81:14–8.
12. Garibaldi BT, Fiksel J, Muschelli J, Robinson ML, Rouhizadeh M, Perin J, et al. Patient Trajectories Among Persons Hospitalized for COVID-19: A Cohort Study. *Ann Intern Med* 2021;174:33–41. <https://doi.org/10.7326/M20-3905>.
13. Saavedra Hernández D, García Verdecia B. Inmunosenescencia: efectos de la edad sobre el sistema inmune. *Rev Cuba Hematol Inmunol Hemoter* Vol 30 No 4 2014 Oct - DICIEMBRE 2014.
14. Plasencia-Urizarri TM, Aguilera-Rodríguez R, Almaguer Mederos LE. Comorbilidades y gravedad clínica de la COVID-19: revisión sistemática y meta-análisis. *Rev Habanera Cienc Médicas* Vol 19 Supl Temático COVID-19 2020.
15. Pérez Rodríguez N de las M, Remond Noa R, Torres Reyes A, Veranes Miranda A, Fernández Lorenzo JM, Oviedo Álvarez V, et al. Distribución de la población vulnerable a la enfermedad COVID-19 en La Habana, Cuba. *Rev Cuba Hig Epidemiol* Vol 57 2020 Enero - Diciembre 2020.
16. Marcheco-Teruel B, Parra EJ, Fuentes-Smith E, Salas A, Buttenschøn HN, Demontis D, et al. Cuba: exploring the history of admixture and the genetic basis of pigmentation using autosomal and uniparental markers. *PLoS Genet* 2014;10:e1004488. <https://doi.org/10.1371/journal.pgen.1004488>.
17. Oficina Nacional de Estadística e Información de la República de Cuba. El color de la piel según el censo de población y viviendas de 2012. La Habana: 2016.
18. Mangalmurti N, Hunter CA. Cytokine Storms: Understanding COVID-19. *Immunity* 2020;53:19–25. <https://doi.org/10.1016/j.immuni.2020.06.017>.
19. Online Mendelian Inheritance in Man, OMIM®. Johns Hopkins University, Baltimore, MD. MIM Number: 161561 2021. <https://omim.org> (accessed June 16, 2021).
20. Morales Peralta E, Hernández Pérez Y, Peñalver Morales K, Lamas Torres Y, Rumbaut Castillo R, Collazo Mesa T. Asociación de los polimorfismos T352C y A16974C con la lepra lepromatosa en pacientes cubanos. *Rev Haban Cienc Méd* 2017;16:10.
21. Sánchez de la Rosa R, Sánchez de la Rosa E, Rodríguez Hernández N. Interleucina-12 VS: Enfermedades infecciosas. *Rev Cuba Med* 2001;40:118–21.
22. Hashemi SMA, Thijssen M, Hosseini SY, Tabarraei A, Pourkarim MR, Sarvari J. Human gene polymorphisms and their possible impact on the clinical outcome of. *Arch Virol.* 2021 Aug;166(8):2089–108.

ARTICLE / INVESTIGACIÓN

Temporal progress of web blight in three common bean genotypes on the central coast of Ecuador

Walter R. Chávez-García¹, Fiorella N. Mera-Vera¹, Diego Portalanza², and Felipe R. Garcés-Fiallos^{1*} DOI. 10.21931/RB/2022.07.01.35¹ Technical University of Manabí, Faculty of Agronomic Engineering, Experimental Campus La Teodomira, Km 13.5, Santa Ana, Manabí, Ecuador.² Federal University of Santa Maria, Department of Physics, Climate Research Group, Av. Roraima, 1000, Santa Maria (RS), Brazil.

Corresponding author: felipe.garces@utm.edu.ec

Abstract: Web blight caused by *Rhizoctonia solani* Kuhn is one of the main common beans (*Phaseolus vulgaris* L.) diseases of the Ecuadorian central coast. Thus, the present study aimed to evaluate the progress of web blight incidence using nonlinear models in promising genotypes SER 03 and SER 08, using the commercial cultivar INIAP 473 as a control. This study was carried out between the 2010 and 2012 seasons in Quevedo, Ecuador. Epidemiological parameters such as initial disease (y_0), disease progress rate (r), final incidence and the area under the disease progress curve were estimated using the Exponential, Logistic, and Gompertz models. In general, progress curves, epidemiological parameters and other evaluated plant health variables were lower in the INIAP 473 cultivar than the other genotypes in 2011 and 2012, especially in the last season when higher y_0 and r were observed in the commercial cultivar. It seems that soil and seeds inoculum and temperature play an important role in standard bean crop disease progress. While the response of genotypes and each location conditions influenced the epidemic modeling, the Logistic model better described the web blight progress under these conditions.

Key words: *Phaseolus vulgaris* L., *Rhizoctonia solani* Kuhn, initial disease, disease progression rate, final incidence.

Introduction

Common bean (*Phaseolus vulgaris* L.) is a socially important crop in Ecuador and an important legume in the Ecuadorian diet. Currently, the bean area is estimated at 25253 ha with a mean yield¹ of 0.61 t ha⁻¹, highlighting the provinces of Los Ríos, Imbabura, and Azuay, which have the largest planted area for this crop². On the central Ecuadorian coast, farmers use native and introduced cultivars³, which are generally susceptible to different biotic-based diseases.

Several diseases affect bean crops on the central Ecuadorian coast, i.e., rust (*Uromyces appendiculatus* Pers.: Pers.), web blight (*Rhizoctonia solani* Kuhn), virus infections, and root rot (*Fusarium* spp., *R. solani* and *Macrophomina phaseolina* Tassi)⁴. Among these diseases, the one that most predominates over the rest is the web blight, both in monoculture and association systems^{5,6}. In general, the disease may be observed affecting bean crops established each year in the north of Los Ríos province, reaching a severity of 88% in susceptible genotypes⁷. Web blight considerably reduces the number of nodes, pods, and grains per plant and the grain yield^{4,7}. Another predominant factor is the association between web blight and root rot, caused by *R. solani*³. Diseases management in commercial cultivars and landrace bean genotypes established in this part of Ecuador is usually through fungicides³.

Although there is currently valuable information about the web blight intensity in promising bean genotypes, obtained from different experiments established on the central Ecuadorian coast during some years, no epidemiological studies have been carried out in this pathosystem. From an epidemiological

point of view, an epidemic may or may not generate sufficient levels of damage to cause economic loss in an agro-productive system⁸. Different linear and nonlinear mathematical models can be used to describe the development of epidemics, i.e., Exponential, Monomolecular, and Logistic, with polycyclic diseases being able to be described using the Logistic model and monocyclic diseases using the Monomolecular model⁹.

The parameters used are the initial disease, the apparent disease increase rate, and the maximum disease level¹⁰. In any case, not all disease progress curves are well or quickly described using a growth curve model, and alternative methods such as the Area Under the Disease Progress Curve (AUDPC) can also be used, which allow quantitative resistance to disease assessment¹¹. Mathematical growth models can summarize, in the form of relatively simple mathematical expressions, the relationship between disease and time, having practical importance, or simply contributing to a better understanding of the disease's infectious progression¹².

A web blight epidemiological study under natural conditions in different bean genotypes and seasons in a row can expose valuable information that will help select efficient disease management strategies for this legume. Therefore, in the present work, epidemiological parameters of web blight such as the quantity of initial inoculum and the progress rate were compared, using the Exponential, Logistic and Gompertz models, in the promising genotypes SER 03 and SER 08, using the commercial cultivar INIAP 473 as a control between 2010 and 2012, in Quevedo, Los Ríos province, Ecuador.

Citation: Chávez-García, W.R.; Mera-Vera, F.N.; Portalanza, D.; Garcés-Fiallos FR, Temporal progress of web blight in three common bean genotypes on the central coast of Ecuador. *Revis Bionatura* 2022;7(1). 35. <http://dx.doi.org/10.21931/RB/2022.07.01.35>

Received: 26 November 2021 / **Accepted:** 13 January 2022 / **Published:** 15 February 2022

Publisher's Note: Bionatura stays neutral with regard to jurisdictional claims in published maps and institutional affiliations.

Copyright: © 2022 by the authors. Submitted for possible open access publication under the terms and conditions of the Creative Commons Attribution (CC BY) license (<https://creativecommons.org/licenses/by/4.0/>).



Materials and methods

Study Area

Field experiment was carried out at La María Experimental Farm (79° 30' 08" W and 0° 00' 35" S) between 2010 and 2011 (Experiments 1 and 2), and at Hacienda Florencia (79° 50' 86" W and 01° 06' 84" S) in 2012 (Experiment 3). Both locations are in Quevedo, Los Ríos province, Ecuador, characterized by having conditions of humid tropical forest (bh-T), with uniform topography, clay loam type *Inceptisol* soil, and pH 5.7. The mean air temperature and rain precipitation of these experiments are shown in Figure 1. Meteorological data from Client for 'NASA' 'POWER' global meteorology, surface solar energy and climatology data' API. 'POWER' (Prediction Of Worldwide Energy Resource) freely available for download with a spatial resolution of 0.5 x 0.625 degree latitude and longitude for meteorology were used as observed data.

Genetic material

Three Ecuadorian common bean genotypes, two promising lines, and a commercial cultivar were used to control (Table 1).

Field experiments

Tor 2010-2011 the experiment was established in a successive bean crop season area. The soil was mechanically prepared three days before sowing. The seeds were treated before being sown with carbendazim fungicide (200 mL per 100 kg seeds⁻¹). Using a conventional sowing system, two seeds per site were sown, spaced 0.20 m between plants and 0.50 m between rows, resulting in an approximate density of 100000 plants ha⁻¹. Each plot was comprised of four 7.5 m² plant rows totaling 65 m². Fertilization consisted of applications of N, P, K in 100 kg ha⁻¹ doses, at 13 and 27 days after sowing (DAS). A foliar biostimulant (containing macro and microelements, phytohormones, humic acids, and vitamins) was also applied at 68 DAS (1.5 L ha⁻¹). The weeds were controlled with glyphosate and pendimethalin with 2 L ha⁻¹ doses each and manual weeding during crop establishment. For insect pests, lambda-cyhalothrin (0.2 L ha⁻¹), methomyl (0.5 kg ha⁻¹), and pyrethroid (0.5 L ha⁻¹) were applied on three occasions. To compensate for crop water needs, several sprinkler irrigations were carried out. No fungicides were used.

In the 2012 season, the experiment was established in a previous banana crop field. All experiments were the same as the 2010-2011 experimental management, except for plant

density. Two seeds per hole were sown in a 0.20 m between plants x 0.60 m between rows scheme, resulting in a planting density of approximately 90000 plants ha⁻¹. Each plot was composed of four rows of plants and 9 m², totaling 96 m². All cultural management according to the previous seasons was developed.

Disease assessment

Web blight incidence (%) was measured during five (2011 and 2012) and six (2010) consecutive weeks, from the phenological stage R6 (full flowering). Central leaflets were taken from the lower, middle, and upper canopy strata from four plants located in the two rows outside the proper plot (two central rows) in each treatment (genotype), totaling 12 leaflets. Leaflets with lesions larger than 2 mm were classified as diseased. The plant material was analyzed in a stereomicroscope with a 2X optical magnification binocular lens during the first two weeks. The diseased leaflets percentage defined this variable.

To verify the presence of the causal agent, some infected leaflets were placed for a few days in a humid chamber with a photoperiod of 12 h at room temperature. Subsequently, different samples were prepared to observe morphological characteristics (mycelium) of the microorganism associated with web blight symptoms.

Experimental design and statistical analysis

A randomized complete block design (RCBD) was used in each experiment, with four blocks for each treatment (genotypes). All the values obtained in the experiments were integrated as the area under the disease progress curve (AUDPC).

For the analysis of disease progress, the disease progress rate (r) was calculated using the Logistic model equation¹⁰ (Eq. 1); $y = 1 / (1 + \exp(-a + rt))$ (1), where y = disease proportion (0 < y < 1), a = logit (y₀), r = rate, and t = time; the Gompertz model equation¹⁰ (Eq. 2); $y = \exp(-B \cdot \exp(-kt))$ (2), where B is a position parameter, k = rate, and t = time, and the exponential model equation (Eq. 3); $y = y_0 \exp(rt)$ (3) where y₀ is the initial value, r is the rate and t the time.

AUDPC, model curve calculation, and residuals were estimated using the epifitter package¹³ for Rstudio¹⁴. All figures were plotted using GGPlot¹⁵.

After verifying the homogeneity of the variance of the data sets, the data were subjected to analysis of variance. Tukey (P ≤ 0.05) test was used to make the comparisons. Pearson correlation between mean meteorological variables and disease progression was performed (P ≤ 0.05).

Genotype	Growth type	Origin
SER 03	Indeterminate growth habit type IIb	ITAV ¹
SER 08		
INIAP 473	Determined Growth habit type Ia	INIAP ²

¹ ITAV: Instituto Tecnológico Agropecuario de Vinces

² INIAP: Instituto Nacional de Investigaciones Agropecuarias

Table 1. Genotype, growth type, and origin of the common bean genotypes used in the research. Quevedo, Los Ríos, Ecuador.

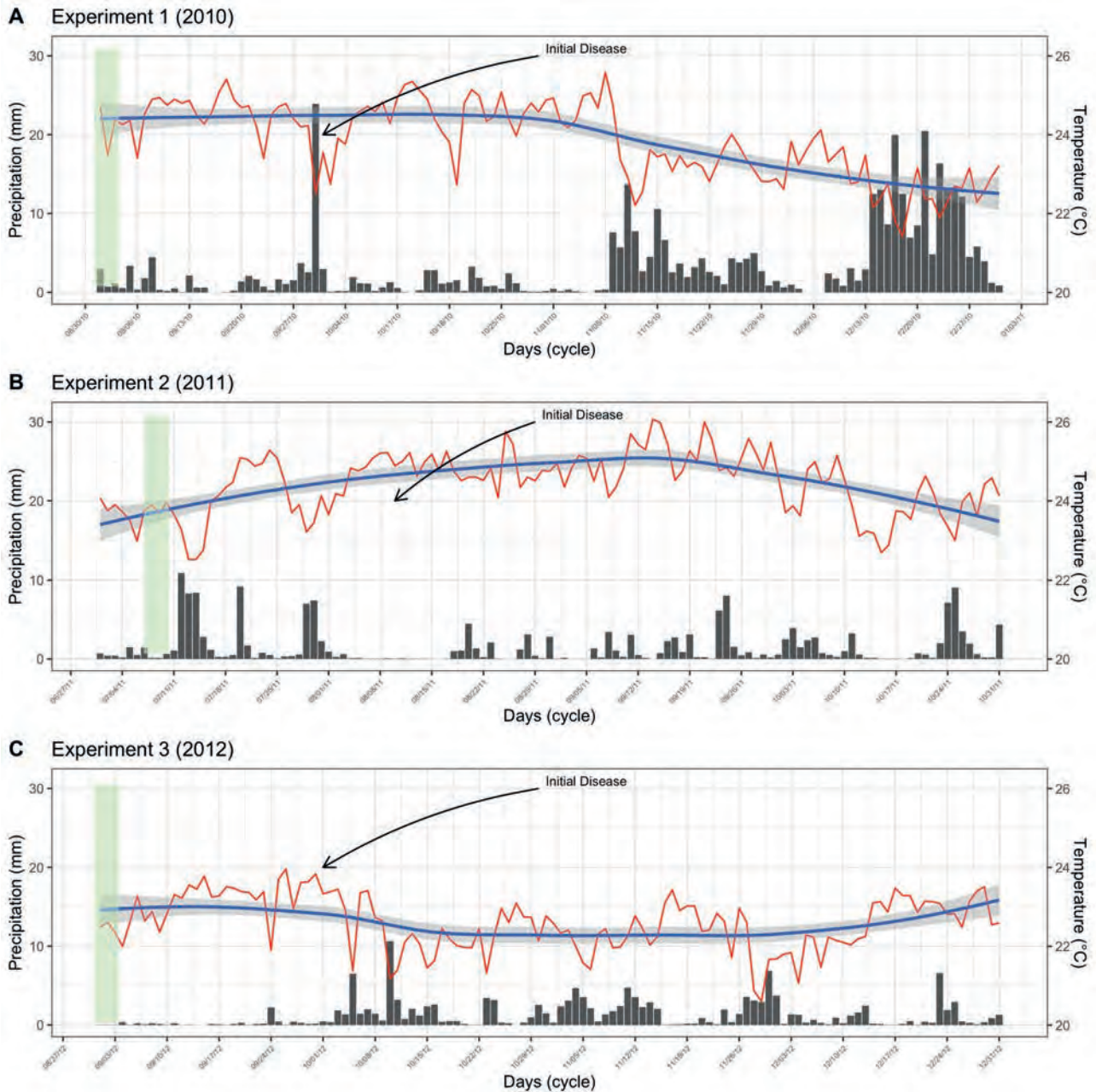


Figure 1. Daily variation of meteorological variables throughout the experimental crop cycle. Mean air temperature ($^{\circ}\text{C}$, red lines), and pluvial precipitation (mm, black bars) for experiments 1 (A), 2 (B), and 3 (C). The blue lines represent the smoothed tendency of air temperature, and the light gray represents the confidence interval of the data.

Results

The average temperature was 24.2, 25.1, and 23.3 $^{\circ}\text{C}$, and growing season precipitation was 390, 179, and 149 mm, respectively, in 2010, 2011, and 2012. The relationship between mean meteorological variables used in this study and disease progression was not found (data not shown).

Hyphal branching varied from 45 to 90 $^{\circ}$ (spores were not found) was observed (Figure 2A) when mounting specimens in the microscope from samples in symptomatic leaf tissue previously placed in a humid chamber. Regarding symptoms, the lesions began as necrotic spots with a yellowish halo (Figure 2B) that increased over with time until they became brown and dark-bordered, covering the leaflet area forming a cobweb (Figure 2C).

The progress of the web blight varied between genotypes

and years (Figure 3). In 2010, disease incidence was practically similar in the three evaluated genotypes (Figure 3A). Although in 2011 (Figure 3B) and 2012 (Figure 3B), the incidence was higher in the commercial INIAP 473 variety, the disease began a little earlier, only in the first year.

In general, the amount of initial disease (y_0) and progress rate (r) obtained from web blight incidence varied between genotypes only in some years using the Exponential, Gompertz, and Logistic, nonlinear models (Table 2). Curve analyses were significant ($P \leq 0.05$) in all genotypes and models in 2010 and 2012, and 2011 but only for the Exponential model.

When both epidemiological parameters were compared, no significant difference was observed between genotypes in any model for 2010. Using the exponential model, y_0 was higher in the INIAP 473 variety (three times on average) and in the SER 03 (four times on average) in 2011 and 2012, respecti-

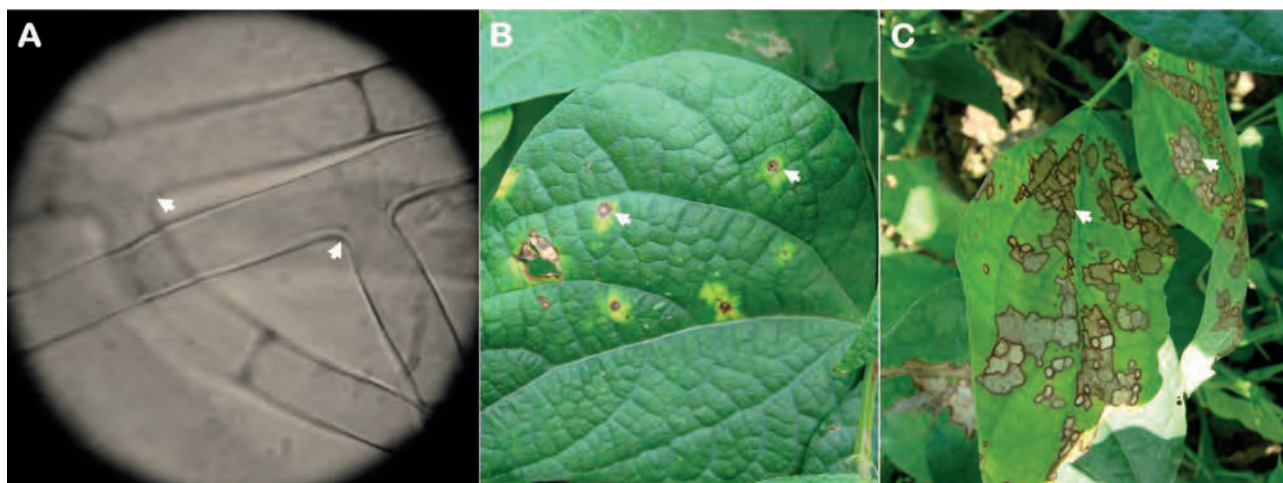


Figure 2. *Rhizoctonia solani* mycelium (A) and web blight symptoms (B and C) observed on common bean leaflets. The arrows indicate the angle of 45 and 90 ° of the mycelium and the disease lesions.

vely, compared to the other genotypes. Using the same model in 2011, the r was higher in the SER 03 and SER 08 genotypes (three times on average) compared to the commercial variety. Regarding the Gompertz model, in 2012, the INIAP 473 and SER 08 genotypes (twice on average) presented the highest y_0 compared to the SER 03, while the r was higher only for INIAP 473 (six times in average), compared to the other two genotypes. Finally, only y_0 was higher in the INIAP 473 genotype (three times on average) than SER 03 and SER 08 in 2012 for the logistic model approach.

The lowest mean square of residuals (MSR) was obtained in the INIAP 473 and SER 03 genotypes with the Logistic, Gompertz, and Exponential models in 2010, 2011, and 2012, respectively (Table 3). Although this pattern (models and years) was recurrent in the SER 08, lower MSRs were also observed using the Gompertz and Exponential models in 2011 and 2012, respectively.

The residuals of the progress curves (Figure 4) varied considerably between genotypes and epidemiological models only in 2011 and 2012, having a similar pattern between the factors analyzed in 2010. Although in 2011 and 2012 the points were located closer to the central axis, this was more evident in the last year. In fact, in 2012 the residuals were lower in the SER 03 and SER 08 lines using all nonlinear models, compared to the INIAP 473 in the same year, and with the other factors analyzed in 2010 and 2011.

The final incidence (%) and the AUDPC of web blight (Figure 5) were similar in plants of all genotypes analyzed (17% and 2 units on average) in 2010 (Figures 5A and 5B). Instead, plants of commercial variety INIAP 307 presented a final incidence and AUDPC between two (Figures 5C and 5D) and five (Figures 5E and 5F) times higher in 2011 and 2012, respectively, when compared to those of the SER 03 and SER 08. Concerning the amount of disease in each of the three years evaluated, the highest final incidence and AUDPC were observed in 2011 (50% and 10 units in the INIAP 473 variety), followed by 2010 (17% and 2 units on average) and 2012 (12% and 0.8 units in the INIAP 473 variety).

Discussion

Web blight is one of the main diseases that negatively affect grain yield, both in monoculture and in association with others, on the central coast of the Ecuadorian coast⁴⁻⁶.

For the first time in Ecuador, in three common bean genotypes with a differentiated response to web blight, using the incidence, the epidemic was modeled using the nonlinear Exponential, Logistic, and Gompertz models, obtaining even epidemiological parameters such as y_0 and r , for three consecutive years.

The mycelium characteristic (branching from 45 to 90°) and the observed symptoms in advanced stages (web shape) of the disease suggest that the causal agent is *R. solani*. Furthermore, these results are similar to those observed⁴, who found similar morphological characteristics in the vegetative tissues of this phytopathogenic fungus, but in common bean seedlings with damping-off symptoms. Even in Ecuador or other countries, *R. solani* has been found in both underground and aerial organs³.

The progress curves obtained from the proportion of the incidence of web blight in common bean plants were different in each genotype and year. Although in 2010 the incidence was similar in the three genotypes evaluated, in the following years, it was higher only in the commercial variety INIAP 473. In part, this result was similar to that of the epidemiological parameters, especially in 2010, where there were no differences between genotypes. However, both the amount y_0 and r varied between genotypes in a differentiated way in 2011 and 2012, generally observing the sanitary inferiority of the INIAP variety 473.

Web blight may be influenced by environmental conditions, being more intense in lowland areas with hot and humid conditions¹⁶, especially between 25 and 100% humidity¹⁷. These conditions are similar to those of the study areas. Although the pluvial precipitation was higher in 2010, the disease incidence was higher in 2011. This suggests that temperature was the only environmental factor that affected the amount of disease in bean plants. The optimum temperature for mycelial growth in the soil is between 20 and 25 °C, regardless of the anastomosis group¹⁸. It seems that the pathogen increased its aggressiveness in temperatures above 25 °C, as in 2011. Some strains are highly virulent at higher temperatures¹⁹.

It must be considered that y_0 is of particular interest as an epidemic component for root diseases caused by soil-borne pathogens¹⁰, such as *R. solani*. In order, r may be negatively affected by the nature of the host's resistance, consequently, the model to be used must be well fitted²⁰. In the nonlinear models used, the Exponential can be used for the initial phases of an epidemic, when disease intensity does not exceed

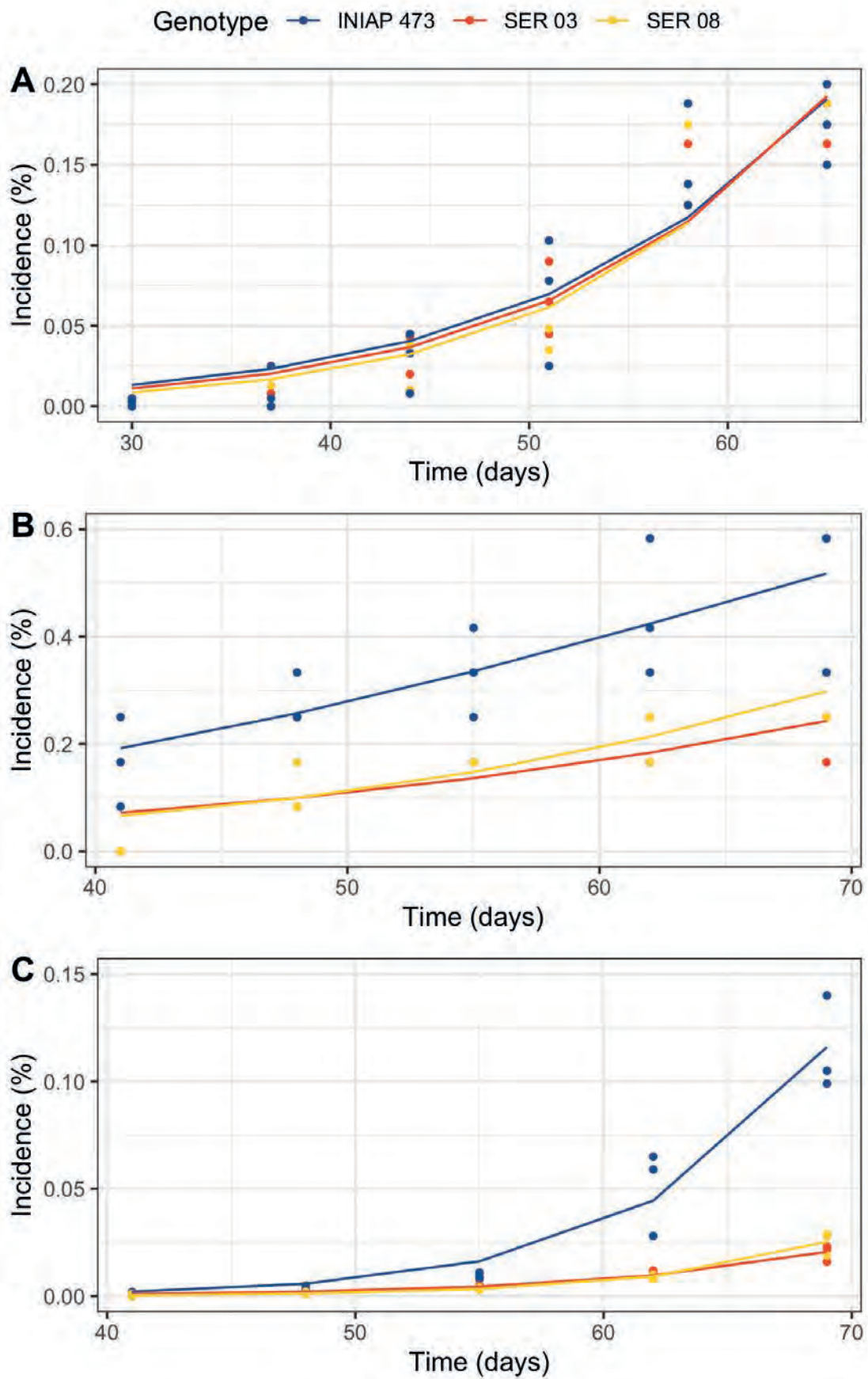


Figure 3. Web blight progress from incidence proportion in INIAP 473, SER 03, and SER 08 common bean genotypes, established in 2010 (A), 2011 (B), and 2012 (C), Quevedo, Los Ríos, Ecuador.

Genotypes	y_0			r			R_2			P-value		
	2010	2011	2012	2010	2011	2012	2010	2011	2012	2010	2011	2012
Exponential												
INIAP 473	0.053 * [‡]	0.338 a [‡]	0.019 b [‡]	0.168	0.065 b	0.261	0.89	0.49	0.86	0.001	0.007	0.001
SER 03	0.051	0.107 b	0.082 a	0.170	0.095 a	0.134	0.90	0.52	0.90	0.001	0.007	0.001
SER 08	0.044	0.109 b	0.002 c	0.180	0.106 a	0.302	0.87	0.61	0.96	0.001	0.003	0.001
Gompertz												
INIAP 473	1.161	0.871	0.927 a	0.257	0.215	0.593 a	0.95	0.57	0.94	0.004	0.222	0.020
SER 03	1.118	0.386	0.403 b	0.274	0.308	0.143 b	0.98	0.61	0.90	0.001	0.173	0.043
SER 08	1.076	0.456	0.826 a	0.364	0.344	0.070 c	0.96	0.76	0.97	0.001	0.079	0.020
Logistic												
INIAP 473	0.983	0.838	0.884 a	0.507	0.304	0.348	0.95	0.57	0.94	0.001	0.149	0.003
SER 03	0.971	0.381	0.217 b	0.523	0.411	0.392	0.98	0.60	0.89	0.001	0.144	0.017
SER 08	0.984	0.437	0.403 b	0.643	0.530	0.443	0.97	0.75	0.97	0.001	0.056	0.001

* An analysis of variance with its respective comparison of averages was performed only when the probability values for all genotypes in each year were significant ($P \leq 0.05$).

[‡] Not significant

[‡] Letters in the column indicate the difference between averages by Tukey's test ($P \leq 0.05$).

Table 2. Initial disease (y_0), and progress rate (r) using Exponential, Gompertz, and Logistic nonlinear models, from web blight incidence in INIAP 473, SER 03, and SER 08 genotypes, established in 2010, 2011, and 2012, Quevedo, Los Ríos, Ecuador. Coefficient of determination (R_2), and probability value (P-value) statistical parameters.

Genotypes	2010	2011	2012
INIAP 473			
Exponential	0.288	0.036	0.016
Gompertz	0.053	0.033	0.061
Logistic	0.008	0.036	0.007
SER 03			
Exponential	0.274	0.097	0.007
Gompertz	0.050	0.010	0.001
Logistic	0.002	0.012	0.000
SER 08			
Exponential	0.018	0.014	0.000
Gompertz	0.063	0.010	0.003
Logistic	0.005	0.010	0.000

Table 3. Mean squares of residuals obtained using Exponential, Gompertz, and Logistic nonlinear models, from web blight incidence in INIAP 473, SER 03, and SER 08 genotypes, established in 2010, 2011, and 2012, Quevedo, Los Ríos, Ecuador. Coefficient of determination (R_2), and probability value (P-value) statistical parameters.

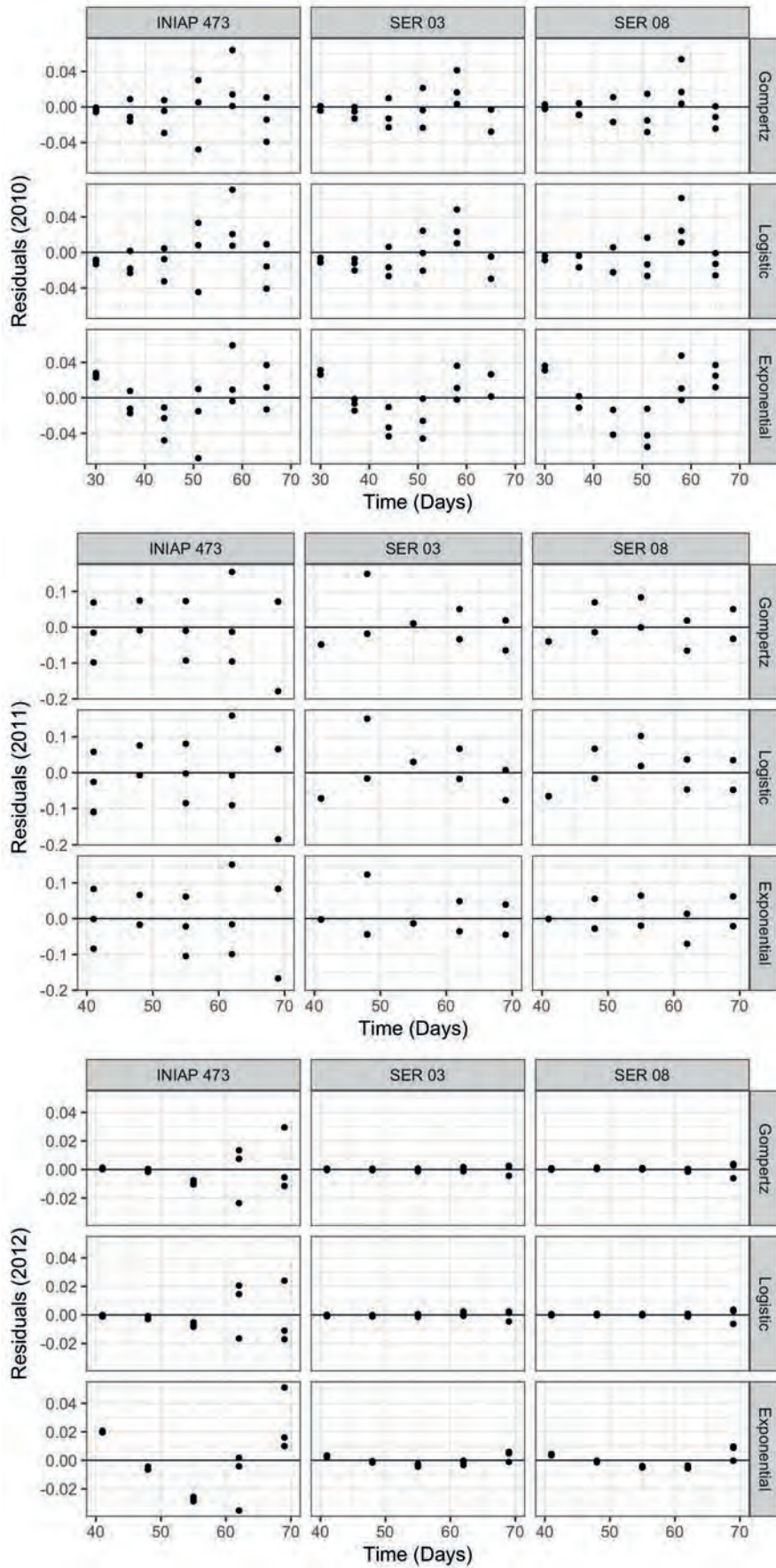


Figure 4. Progress curve residuals obtained using the Exponential, Gompertz, and Logistic nonlinear models, from web blight incidence in INIAP 473, SER 03, and SER 08 genotypes, established in 2010, 2011, and 2012, Quevedo, Los Ríos, Ecuador.

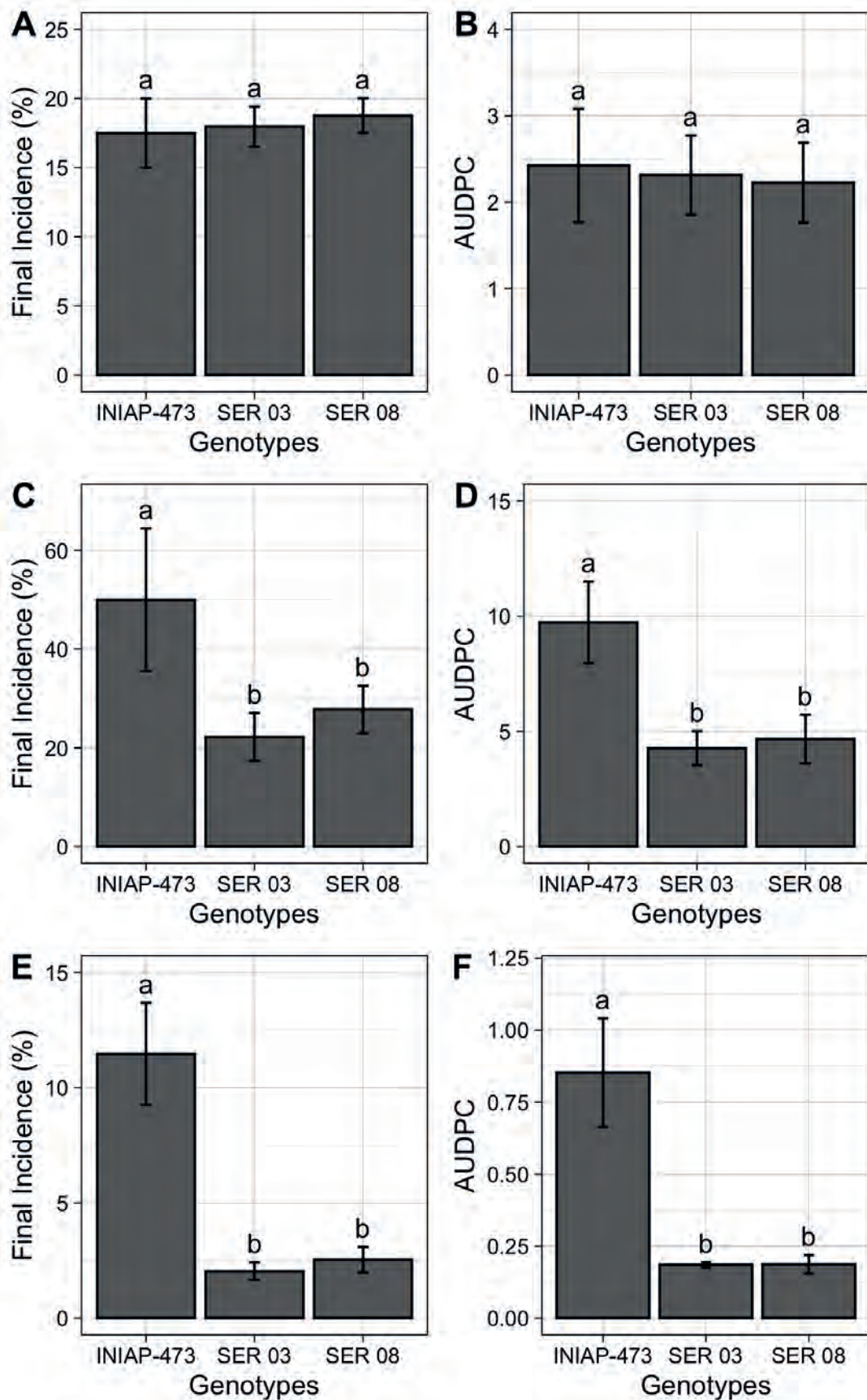


Figure 5. Final incidence (%), and area Under the Disease Progress Curve (AUDPC) of web blight in the INIAP 473, SER 03 and SER genotypes of common beans, established in 2010 (A and B), 2011 (C and D) and 2012 (E and F), Quevedo, Los Ríos, Ecuador. Letters indicate similarity or statistical difference ($P < 0.01$) among genotypes in each year by Tukey test. Bars represent the standard deviations of mean.

5%¹². Therefore, to compare the epidemiological parameters between genotypes, the Gompertz, and Logistic models can be used. A higher y_0 was obtained in INIAP 473 plants using both models, while a higher r was observed in plants of the same genotype in 2012. If it is considered that in 2010, the experiment was established in a different place than the others, and having previously been occupied by a banana crop, possibly the only source of inoculum was found in the seed. Thus, this y_0 also caused a significant increase in r in INIAP 473 plants.

Although high determination coefficients (R_2) were obtained in different genotypes and years from each of the epidemiological methods used, this cannot serve as a standard²¹. On the contrary, smaller MSR and residuals obtained from epidemiological models may be used to choose the model that best explains the disease^{5,22}. Under the conditions under which the experiments were carried out, both decision variables differed on the year and genotype studied. Generally, in other crops, the Logistic and Gompertz models can satisfactorily explain the progress of some diseases, while Gompertz can better model diseases such as rusts⁷.

Even on some occasions, the use of epidemiological models can help determine the etiology of the disease¹². The response of the genotypes and temporal conditions of each locality possibly influenced the epidemic modeling. Anyhow, taking the lowest MSR as a parameter to choose the best model, we can mention the Logistic model that better describes the epidemic caused by web blight in common beans.

The final incidence and AUDPC of web blight were higher in INIAP 473 in 2011 and 2012. On the one hand, the differentiated response to web blight or another disease caused by *R. solani* has already been reported in common beans^{3,5} and other crops²³. Concerning the superiority of the SER 03 and SER 08 genotypes, as they present a lower incidence and AUDPC, this is similar to that others' work reported^{3,5}, in the same experimental conditions, finding a lower disease intensity in foliar and root tissues of both common bean lineages. Although the mechanisms used by these advanced common bean lines to defend against *R. solani* are unidentified, they could be associated with physical²⁴ and molecular factors²⁵. To date, no common bean genotypes with complete resistance against *R. solani* have been found in Ecuador, as happens in other beans, where late colonization materials may be an option for this disease management²⁴.

In 2011, a higher final incidence and AUDPC were observed in plants of the three genotypes studied, compared to 2010 and 2012. Two suggestions can be raised to explain this comportment: the source soil inoculum and the *R. solani* seed dissemination. The source of pathogen inoculum found in the soil due to 2010 beans establishment, and even in years before this, seems to have caused a considerable increase in 2011 plants disease^{26,27}. However, the low amount of the disease observed in 2012 was because the only source of inoculum was found in the seed, and the pathogen could have spread through the seed^{27,28}. The experiment established in this last year was in a different place than in the other years, having previously been occupied by a banana crop. This implies that carbendazim seed treatment did not show efficacy, despite the fact that this fungicide is used to control *R. solani*²⁹.

Conclusions

Under the conditions of these experiments, all the web blight evaluated parameters the progress curves, epidemiological parameters, and other evaluated plant-health variables

were lower in the INIAP 473 variety than the other genotypes in 2011 and 2012. Soil and seeds inoculum and temperature play an important role in expected bean crop web blight increase. The Logistic model better described the progress of the web blight in the conditions of the central coast of Ecuador.

Author Contributions

Analyzed and interpreted the data, and wrote the manuscript Chávez-García WR, Mera-Vera FN, and Portalanza D. Designed, performed, and supervised the experiments, interpreted the data, and wrote the manuscript Garcés-Fiallos, FR. All authors of this paper have read and approved the final version of submitted manuscript.

Funding

This research was funded by the project "Rendimiento de líneas arbustivas y volubles de fréjol procedentes del CIAT, Colombia", at State Technical University of Quevedo (UTEQ).

Conflicts of Interest

The authors declare no conflict of interest.

Bibliographic references

1. Sistema de Información Pública Agropecuaria (SIPA). Available online: <http://sipa.agricultura.gob.ec/index.php/cifras-agroproductivas> (accessed on 15 september 2021).
2. SINAGAP. Fréjol Tierno y Seco, Sistema Nacional del Ministerio de Agricultura: Quito, Ecuador, 2018; pp. 12-143.
3. Garcés-Fiallos, F.R.; Gamarra, H.V.; Garcés-Estrella, R.E. Doenças e produtividade de genótipos promissores de feijão comum em Quevedo, Equador. *Rev. Bras. Cienc. Agrar.* 2015, 10, 128-133. <https://doi.org/10.5039/agraria.v10i1a5254>
4. Garcés-Fiallos, F.R. Cuantificación de enfermedades en líneas promisorias y variedades de fréjol en Quevedo, Ecuador. *Rev. Bio. Agro.* 2013, 11, 196-207.
5. Garcés-Fiallos, F.R.; Vera, F.D. Progreso de enfermedades foliares en el cultivo de trigo en Passo Fundo, RS, Brasil. *Sci. Agropecu.* 2011, 2, 255-259. <https://doi.org/10.17268/sci.agropecu.2011.04.07>
6. Godoy-Montiel, L.; González-Osorio, B.; Defaz-Defaz, E.; Díaz-Coronel, T.G.; Vásconez-Montúfar, G.H. Evaluación de dos variedades de fréjol durante tres épocas de siembra bajo sistema de cultivo asociado con maíz. *Cienc. Tecnol.* 2011, 4, 5-11. <https://doi.org/10.18779/cyt.v4i1.98>
7. Garcés-Fiallos, F.R. Modelo de ponto crítico para estimar danos causados pela mela na cultura do feijoeiro. *Cienc. Tecnol.* 2011, 4, 1-4. <https://doi.org/10.18779/cyt.v4i1.99>
8. Savary, A.; Nelson, A.D.; Djurle, A.; Esker, P.D.; Sparks, A.; Amorim, L.; Bergamin Filho, A.; Caffi, T.; Castilla, N.P.; Garrett, K.A.; McRoberts, N.; Rossi, V.; Yuen, J.E.; Willocquet, L. Concepts, approaches, and avenues for modeling crop losses. *Eur. J. Agron.* 2018, 100, 132-141. <https://doi.org/10.1016/j.eja.2018.04.003>
9. Van der Plank, J. E. Analysis of epidemics. In *Plant Pathology. An Advanced Treatise, The Diseased Population. Epidemics and Control*, 1st ed.; Horsfall, J.G.; Dimond, A.E., Academic Press: New York, United States of America, 1960; Volume 3, pp. 229-289.
10. Campbell, C.L.; Madden, L.V. *Introduction to Plant Disease Epidemiology*, 1st ed.; John Wiley & Sons: United States of America, 1990. pp. 1-532.
11. Van Maanen, V.; Xu, X.M. Modelling plant disease epidemics. *Eur. J. Plant Pathol.* 2003, 109, 670-682. <https://doi.org/10.1023/A:1026018005613>
12. Bergamin Filho, A. Análise temporal de epidemias. In *Manual de Fituopatologia. Princípios e Conceitos*, 5th ed.; Amorim, L.; Rezende, J.A.M.; Bergamin Filho, A.; Agrônômica Ceres: Ouro Preto, Brasil, 2018; Volume I, pp. 519-530.

13. Alves, K.S.; Del Ponte, E.M. Analysis and simulation of plant disease progress curves in R: introducing the epifitter package. *Phytopathol. Res.* 2021, 3, 22. <https://doi.org/10.1186/s42483-021-00098-7>
14. RStudio Team. RStudio. Available online: <http://www.rstudio.com/> (accessed on 14 August 2021).
15. Wickham, H. Package "ggplot2" Title Create Elegant Data, 1st ed.; Springer: New York, United States of American, 2009; p. 213. <https://doi.org/10.1007/978-0-387-98141-3>
16. Cuenca-Tinoco, A.C.; Castro-Delgado, N.I.; Cargua-Chávez, J.E.; Cedeño-García, G.A.; Cedeño-Zambrano, J.L. Effectivity of amendments on growth and yield of common beans in an acidic andisol soil. *Temas Agrarios*, 2020, 25, 54-65. <https://doi.org/10.21897/rta.v25i1.2236>
17. Bolton J, Brown. Photosynthesis of grass species differing in carbon dioxide fixation pathways: V. Response of *Panicum maximum*, *Panicum milioides*, and Tall fescue (*Festuca arundinacea*) to nitrogen nutrition. *Plant Physiol.* 1980, 66, 97-100. <https://doi.org/10.1104/pp.66.1.97>
18. Ritchie, F.; Bain, R.A.; McQuilken, M.P. Effects of nutrient status, temperature and pH on mycelial growth, sclerotial production and germination of *Rhizoctonia solani* from potato. *J. Plant Pathol.* 2009, 91, 589-596. <http://dx.doi.org/10.4454/jpp.v91i3.550>
19. Schultz, F.A.; Bateman, D.F. Temperature response of seeds during the early phases of germination and its relation to injury by *Rhizoctonia solani*. *Phytopathology* 1969, 59, 352-355.
20. Shtienberg, D. Modelling: the basis for rational disease management. *Crop Prot.* 2000, 19, 747-752. [https://doi.org/10.1016/S0261-2194\(00\)00099-5](https://doi.org/10.1016/S0261-2194(00)00099-5)
21. Jeger MJ. Asymptotic behaviour and threshold criteria in model plant disease epidemics. *Plant Pathol.*, 1986. 35. 355-361. <https://doi.org/10.1111/j.1365-3059.1986.tb02026.x>
22. Bergamin Filho, A.; Amorim, L.; Laranjeira, F.F.; Berger, R.D.; Hau, B. Análise temporal do amarelecimento fatal do dendezeiro como ferramenta para elucidar sua etiologia. *Fitopatol. Bras.* 1998, 23, 391-396.
23. Prabhu, A.S.; Filippi, M.C.; da Silva, G.B.; de Santos, G.R. Resistência de cultivares de arroz a *Rhizoctonia solani* e *Rhizoctonia oryzae*. *Pesqui. Agropecu. Bras.* 1983, 37, 1323-1332. <https://doi.org/10.1590/S0100-204X2002000500003>
24. Bashyal, B.M.; Kharayat, B.S.; Kumar, J.S.; Dubey, S.C.; Aggarwal, R. Histopathological studies of *Rhizoctonia solani* infection process in different cultivars of mungbean: *Vigna radiata* (L.) Wilczek. *Natl. Acad. Sci. Lett.* 2018, 41, 269-273. <https://doi.org/10.1007/s40009-018-0669-3>
25. Oladzad, A.; Zitnick-Anderson, K.; Jain, S.; Simons, K.; Osorno, J.M.; McClean, P.E.; Pasche, J.S. Genotypes and genomic regions associated with *Rhizoctonia solani* resistance in common bean. *Front. Plant Sci.* 2019, 10, 956. <https://doi.org/10.3389/fpls.2019.00956>
26. Andrade, D.E.G.T.; Silva, C.F.B.; Silva, L.G.C.; Michereff, S.J.; Sales Júnior, R.; Assis, T.C. Influência da densidade de inóculo e de isolados de *Rhizoctonia solani* na severidade da rizoctoniose do meloeiro. *Caatinga* 2005, 18, 164-168.
27. Garcés-Fiallos, F.R.; TayHing-Cajas, C.C.; Sánchez-Mora, F.D.; Gamarra-Yáñez, H.V. Modelos integral e de ponto crítico para estimar danos no rendimento e seus componentes pela mela na cultura do feijoeiro. *Cienc. Tecnol.* 2013, 6, 17-22. <https://doi.org/10.18779/cyt.v6i1.127>
28. Oliveira, J.A.; de Andrade, M.J.B.; Fraga, A.C. Eficiência de fungicidas no tratamento de sementes de feijão (*Phaseolus vulgaris* L.) para o controle da podridão radicular causada por *Rhizoctonia solani* Kuhn. *Rev. Bras. Sementes* 1997, 19, 91-95.
29. Cheng, X.; Man, X.; Wang, Z.; Liang, L.; Zhang, F.; Wang, Z.; Liu, P.; Lei, B.; Hao, J.; Liu, X. Fungicide SYP-14288 Inducing multidrug resistance in *Rhizoctonia solani*. *Plant Dis.* 2020, 104, 2563-2570. <https://doi.org/10.1094/PDIS-01-20-0048>

REVIEW / ARTÍCULO DE REVISIÓN

T and B Cells Immune Response and the importance of vaccines Against SARS-CoV-2

Ronny Ordoñez*, Dulexy Solano, and Gustavo Granizo

DOI. 10.21931/RB/2022.07.01.36

School of Biological Science and Engineering, Yachay Tech University, Hacienda San José s/n, San Miguel de Urququí 100119, Ecuador.
Corresponding author: ronny.ordonez@yachaytech.edu.ec

Abstract: SARS-CoV-2 has become a global pandemic because it is a severe respiratory syndrome that attacks many people worldwide and can lead to death depending on the severity. In recent years, the study of the acquired immune response (T cells) and innate (B cells) has increased to better treat the disease from the quantitative cell count. A picture has begun to emerge revealing that CD4+ T cells, CD8+ T cells, and neutralizing antibodies contribute to the control of SARS-CoV-2 in COVID-19 cases. This work studies the three fundamental components of the adaptive immune system: B cells (the source of antibodies), CD4+T cells, and CD8+T cells and their function against SARS-CoV2. The importance of vaccines and the different types of existing vaccines are discussed. Implications of covid-19 variants on Immunity and vaccine types are also analyzed to understand how the action of the immune system will help treat the disease.

Key words: Vaccine, B cells, CD4+, CD8+, SARS-CoV-2.

Introduction

Coronaviruses have been present within the human population for generations. Severe acute respiratory syndrome coronavirus 2 (SARS-CoV-2) is now the third of Betacoronavirus genus transferred to humans in the last twenty years. It has reported the highest contagiousness but the lowest mortality rate¹. It emerged in China in December 2019. From that point on, it would mark the beginning of a pandemic that would affect millions of people worldwide due to its high transmissibility².

Covid-19, resulting disease from SARS-CoV-2, presents common clinical manifestations for most patients, which are fever, cough, and a grave "flu" that can evolve into respiratory distress (ARDS), pneumonia, renal failure, and death³. It has also been demonstrated that it can present post-Covid-19 complications, such as myocardial inflammation, arrhythmia, pneumothorax, and pleural effusion⁴. The meta-analysis carried out in January 2021 has shown that SARS-CoV-2 is most contagious when symptoms appear, but this contagiousness decreases to almost zero after ten days in mild-moderately ill patients. The same study suggests that it has a mean incubation period of 6.38 days, a time that can be considered relatively short if we take into account that the adaptive response takes between 15 and 21 days⁵. Once the virus enters the body and the innate immune response fails, the second line of defense, the adaptive immune system, is put into action thanks to the dendritic cells, which carry the virus antigen to the CD4+ T cells (helper T cells)⁶. These cells are responsible for triggering the humoral and cellular responses. This first response is in charge of defending the extracellular space through the action of antibodies produced by B cells⁷. The second one is focused on killing the virus in the intracellular space through

the activity of CD8+ T cells (cytotoxic T cells). These cells are of particular interest in this review because after people get infected with SARS-CoV-2, they tend to generate CD8+ T cells that can target more than 15 distinct fragments of coronavirus proteins inside the infected cells giving them more protection to new variants. In contrast to B cells antibodies, which target the spike protein on the virus's surface, a protein that is susceptible to mutating⁸.

T Cells Response

Knowing about the adaptive response to certain diseases is essential for creating vaccines; in this case, it is necessary to understand how this response works against SARS-Cov-2. The first step for such an understanding is quantifying the virus-specific CD4+ and CD8+ T cells⁹. T cells primarily react to the spike protein on the coronavirus to initiate antiviral immunity¹⁰. In addition, depending on the patient and the severity of SARS-Cov-2, the immune response of T cells can range from optimal to suboptimal. Over the years, the population of naïve T cells has declined. Still, conversely, antigen-experienced memory T cells become an essential part of the T cell population due to their memory system^{11,12}. The older the person, the better the immune response to previously exposed pathogens.

On the contrary, T cells are easier to educate against new pathogens in children. For this reason, it has been observed that children who become infected are not significantly affected by the disease¹¹. Furthermore, CD4+T cells stimulate B cells to produce viral-specific antibodies and cytotoxic CD8+T cells to target virus-infected cells¹⁰. In addition, activated CD4+ and CD8+ T cells have been found to help both clearances of the acute infection caused by the disease and protective

Citation: Ordoñez R , Solano D , Granizo G. T and B Cells Immune Response and the importance of vaccines Against SARS-CoV-2. *Revis Bionatura* 2022;7(1). 36. <http://dx.doi.org/10.21931/RB/2022.07.01.36>

Received: 2 January 2021 / **Accepted:** 13 February 2022 / **Published:** 15 February 2022

Publisher's Note: Bionatura stays neutral with regard to jurisdictional claims in published maps and institutional affiliations.

Copyright: © 2022 by the authors. Submitted for possible open access publication under the terms and conditions of the Creative Commons Attribution (CC BY) license (<https://creativecommons.org/licenses/by/4.0/>).



immunity against reinfection by establishing immunological memory against the pathogen¹³.

CD4+ T

CD4+ T cells are central organizers of antiviral immune responses. Furthermore, some of the functions of CD4+ T cells in SARS-CoV-2 infection are their ability to differentiate into various helper and effector cell types. This serves different actions: it helps CD8+ T cells, instructs B cells, recruits innate cells, has direct antiviral activities, and facilitates tissue repair¹⁴ (Figure 1). In situations of uncontrolled immune or inflammatory responses, CD4+ T cells can cause pathology¹⁵. Different studies have made it possible to find CD4+ T cells that are reactive against SARS-CoV-2 in patients who have not suffered from the disease, which is suggested according to Bacher. P., *et al* (2020) arise in response to infection by the common cold coronavirus (CCCoV)¹⁶. In addition, a correlation between the reappearance of CD4+ T cells and the patient's recovery has been observed when the patient has a severe SARS-CoV-2 infection¹⁷. This suggests that the patient's cells have already acquired some immunity against SARS-CoV-2 and give them protection against the disease, which causes them to recover.

CD8+ T

Through the literature, it can be known that CD8+ T cells have an essential role in eliminating viral infections. Activated CD8+ T cells have been found to display a wide range of cytotoxic molecules, which appear in the blood of infected patients before they recover from the disease¹⁸. In SARS-CoV-2 infections, the presence of virus-specific CD8+T cells has been associated with better Covid-19 outcomes¹⁹. This is because immunodominance is one of the main characteristics of the responses of CD8+ T cells in viral infections. According to Peng, they knew how CD8 T cells could better attack the disease of interest. Y *et al.* 2021, knowing this characteristic will be essential for the design of vaccines to obtain optimal responses from CD8+ T cells²⁰. Overall, circulating SARS-CoV-2-specific CD8+T cells are less consistently observed than CD4+T cells²¹.

Furthermore, Activated T cells directed toward spike (S), nucleocapsid (N), membrane (M), and other types of open reading frames can be detected in approximately 70% of acute and convalescent Covid-19 patients⁹. This is possible observed utilizing human leukocyte antigen (HLA) class I and II predicted peptide "mega pools" to stimulate peripheral blood mononuclear cells (PBMCs) of the patient²² (Figure 2)

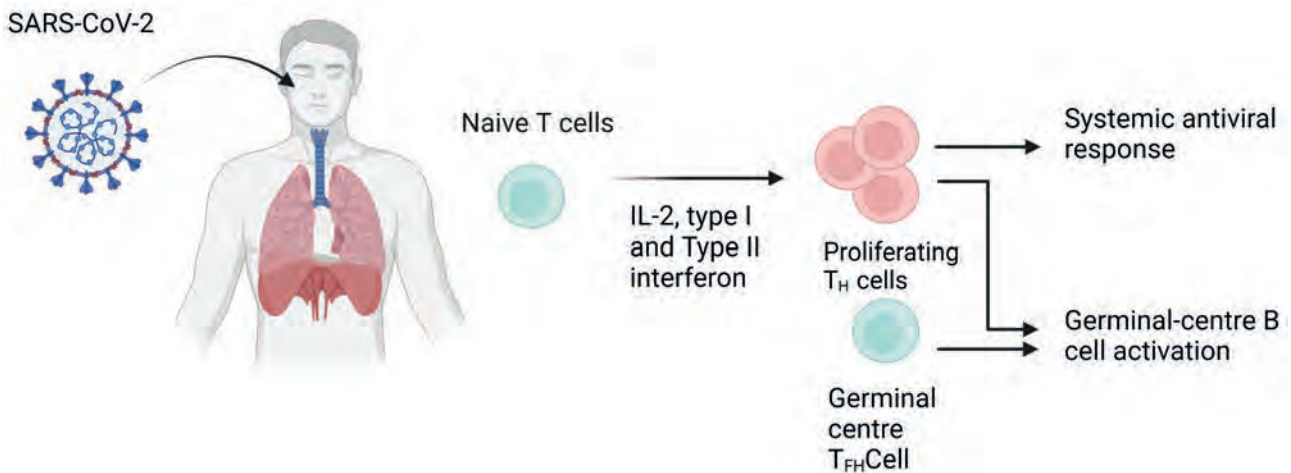


Figure 1. CD4+ T cell response during Covid-19. We can see how the virus enters the organism, which can happen differently. Later we can see how a naive T cell acts, the cell has contact with the interferon type I and types II, after the contact, we can see that there is a proliferation of T_{DH} cells which can activate the antiviral response system, or they can join Germinal Centre T cells, to generate the activation of Germinal-center B cells. BioRender (<https://biorender.com/>).

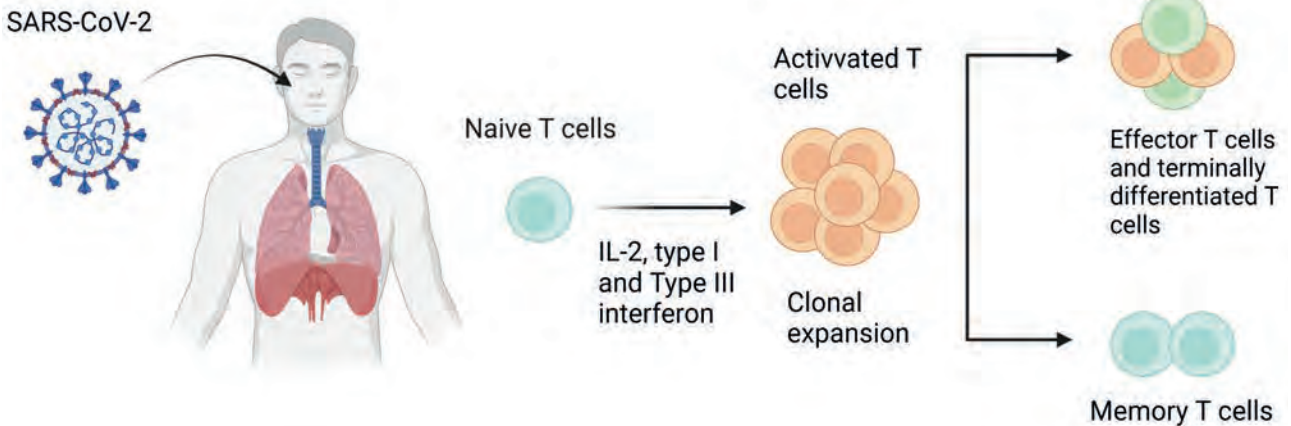


Figure 2. CD8+ T cell response during Covid-19; We can see how the virus enters the organism, which can happen differently. Later we can see how a Naive T cell acts, the cell has contact with type I and Type III interferon, after the contact, we can see that there is an activation of T cells, which can produce effector T cells and terminally differentiated T cells or they can produce memory T cells to attack the virus. BioRender (<https://biorender.com/>).

B cells

The Immune system has numerous ways to detect and avoid the return of infectious pathogens. It selects B cells to produce antibodies that bind to the virus. It also extracts a store of memory B cells that jumps into action if the virus attacks again²³. B cells are just as crucial as T cells within the immune system because they produce antibodies that trap specific invading viruses. These pathogen-specific B cells are induced to differentiate and secrete their antigen receptors into the blood in the form of antibodies²⁴. These antibodies circulate throughout the body and bind to the pathogen that triggers the response wherever it occurs²⁵. Thus, B cells play a critical role in the innate immune response against bacterial and viral diseases^{26,27}. All would-be invaders have their compatible pre-existing B and T cells ready to respond when needed during the immune response. This is because each B cell and T cell expresses on its surface an antigen receptor that is different from all the others²⁸.

It is essential to highlight that one of the immune system's most effective protection methods is the secretion of high-affinity antibodies. As the infection progresses in our body, the antibodies improve their affinity for the antigen, and the isotope class changes (immunoglobulin [Ig]M, IgG, IgA, IgE)²⁵. This process allows for the neutralization of pathogens and a better binding of antibodies²⁹. The isotype is the part of the antibody that does not bind antigen directly but triggers other immune effector functionalities, such as activating the complement cascade or binding to receptors on immune cells to guide responses to pathogens^{30,31}. Persistent antibody evolution occurs in germinal centers. This process requires that B cells are exposed to antigens trapped in immune complexes on follicular dendritic cells³². Improvements in B-cell affinity occur in germinal centers (GCs), which develop in secondary lymphoid organs, for example, lymph nodes and the spleen. GCs are developed after the immune challenge and are essential for immunological memory production³³ (Figure 3).

Spike and nucleocapsid are the primary antigens tested for seroconversion³⁴. In Covid-19 cases, the Spike protein tar-

gets >90% of neutralizing antibodies, some of them targeting the N-terminus^{35,36}. The study developed by Gaebler et al. demonstrates that during the first six months after infection, the anti-SARS-CoV-2 memory B cell response evolves. This process occurs with the accumulation of somatic Ig mutations and the production of antibodies with greater amplitude and neutralizing power²⁴.

The neutralizing antibodies are produced by B cells and are developing rapidly in most SARS-CoV-2- infected people, on the same time frame as seroconversion³⁶. Understanding the conditions under which an antibody neutralizes SARS-CoV-2 is necessary to predict immunity after infection or vaccination. When SARS-CoV-2 infection is severe, GC formation is impaired, affecting affinity maturation and memory quality and quantity, but it is unclear whether this occurs in mild or asymptomatic infections³⁵. However, the antibody structure required to neutralize SARS-CoV-2 may not be particularly complex, as some of the reported neutralizing antibodies contain few mutations and embryos in a relatively short time. Therefore, it is suggested that they can be generated in GC relatively quickly^{37,38}.

Studies suggest that various monoclonal antibodies with exquisite virus-neutralizing activity are promising candidates for development as modalities to treat or prevent SARS-CoV-2 infection (Figure 4)^{39,40}. In addition, the use of monoclonal antibodies against the respiratory syncytial virus (RSV)⁴¹ and for Ebola^{42,43} has been registered.

Implications of Variants on Immunity and Vaccines

Variants occur through naturally produced nucleotide changes in the viral genome during replication, and these changes develop faster in RNA viruses than in DNA viruses⁴⁴. Coronaviruses, however, make fewer mutations than most RNA viruses because they encode an enzyme that corrects some of the errors made during replication⁴⁵. SARS-CoV-2 variants of concern (VOC) pose a threat: divergent strains with an accumulation of mutations in the different S domains can evade infection or vaccination-induced neutralizing antibodies⁴⁶.

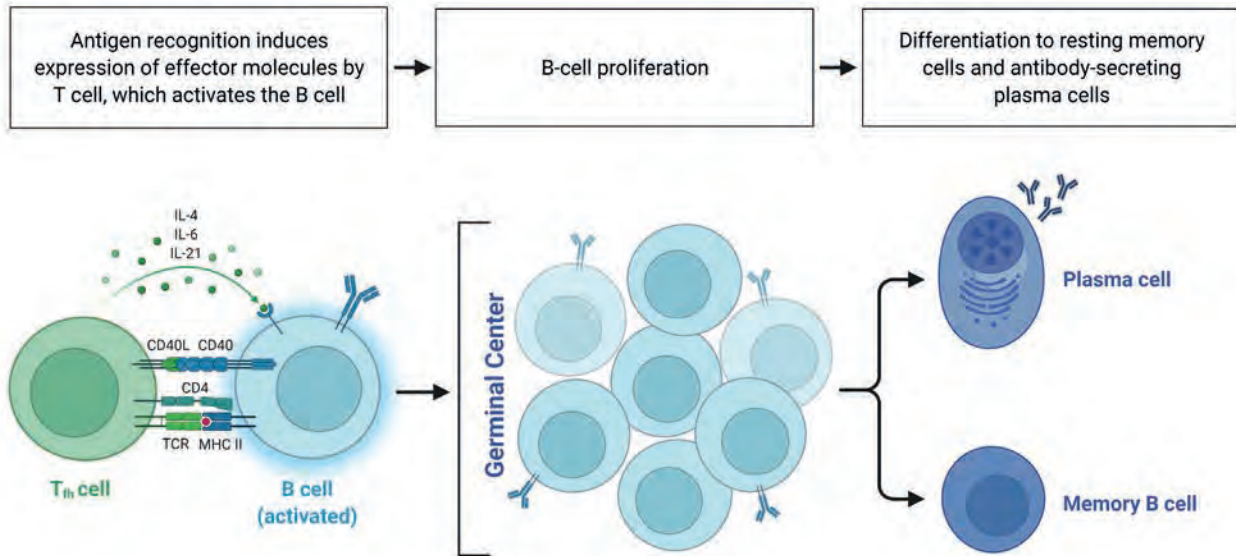


Figure 3. The germinal center reaction. The B cells proliferate faster once the GC response is initiated in a secondary lymphoid organ. In addition, some cells will change from immune response cells to pre-GC memory B cells. The remaining B cells initiate and participate in the GC reaction where iterative cycles of proliferation, mutation, and selection increase the average antigen-binding strength of the B cell receptors (affinity maturation). Some B cells will differentiate throughout the response into short-lived plasmablasts (secreting the now affinity-matured Abs), long-lived plasmablasts, and memory b cells. Image created using BioRender (<https://biorender.com/>)

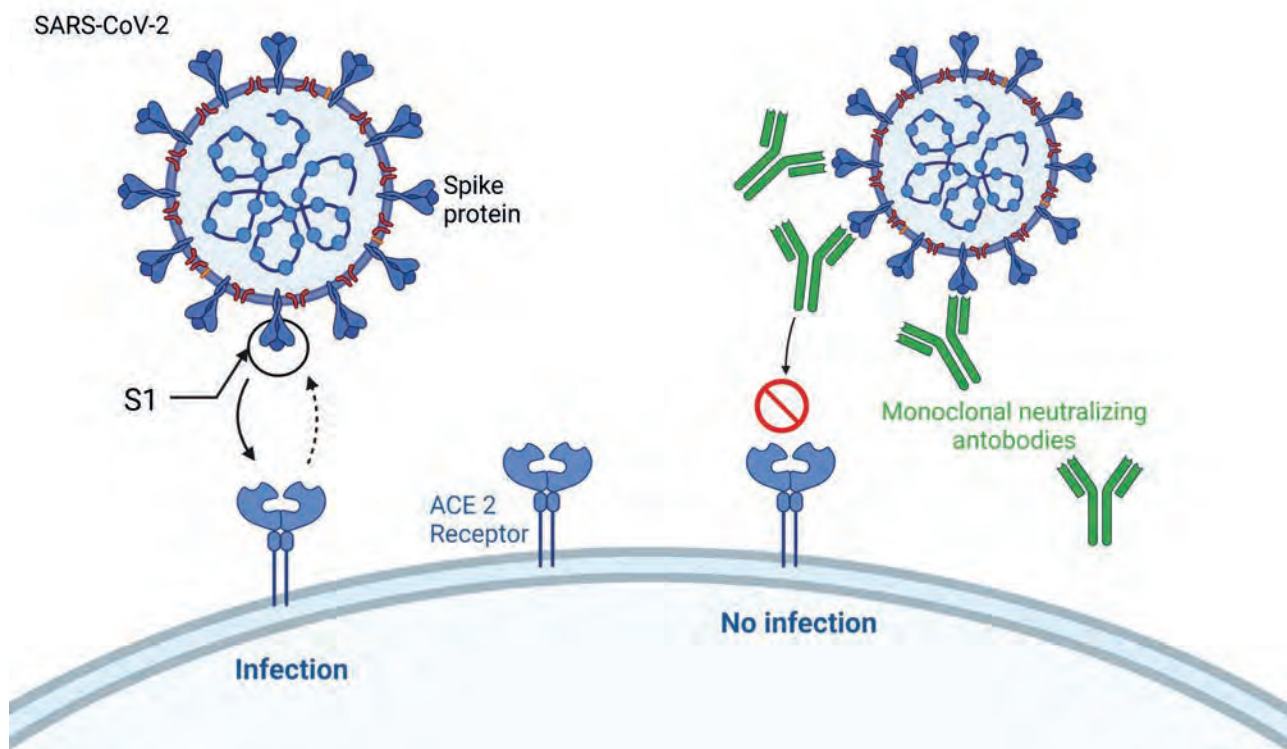


Figure 4. Monoclonal neutralizing antibodies. A functioning system of monoclonal antibodies binds to the virus's spike protein. These neutralizing antibodies prevent SARS-CoV-2 from binding to angiotensin-converting enzyme 2 (ACE2), resulting in decreased effectiveness of the virus. Image created using BioRender (<https://biorender.com/>).

These VOC include the Alpha Variant (B.1.1.7) lineage initially detected in the United Kingdom and spread worldwide⁴⁷. Beta Variant (B.1.351) and Gamma Variant (P.1) lineages were detected in South Africa and Brazil, respectively⁴⁸. These variants have several mutations and deletions compared to previously circulating viruses located in the receptor-binding domain (RBD). In December 2020, the Delta variant (B.1.617.2) was detected⁴⁵. This variant caused many infections in the United States⁴⁹ and India's second wave of infections^{50,51}. In November 2021, the Omicron variant (B.1.1.529) was detected, causing multiple infections around the world⁵² (Figure 5).

Genomic surveillance of SARS-CoV-2 variants has primarily focused on mutations in the spike glycoprotein, which mediates attachment to cells and targets neutralizing antibodies because the spike is the major viral antigen in the current vaccines. It is hoped that adequate protection may still occur despite a few changes at antigenic sites in SARS-CoV-2 variants because current vaccines provoke an immune response to the entire spike protein⁵³. The generation of powerful and long-lasting antibodies through the induction of long-lived memory B cells and plasma cells is the key to a vaccine's effectiveness. The antibody response provides a continuous supply of high-affinity antibodies that circulate and test our bloodstream and mucosal surface⁵⁴.

A recent study identified a new monoclonal antibody (S2X259) with broadly neutralizing effects targeting a highly conserved RBD region called antigenic site II⁵⁵. This region is usually inaccessible because of the RBD conformation, and therefore a low fraction of antibodies generally target this site in infected individuals. S2X259 reacted with 29 of 30 S proteins of arboviruses, including SARS-CoV-2 and its new variants. The study demonstrated its broad applicability as a broadly neutralizing antibody because it showed the cross-reactivity of S2X259 with bat arboviruses. Alterations did not hinder the

binding of this antibody in the RBD, which are present in the Alpha, Beta, and Gamma variants. The antibody binds to the epitope is conserved in all circulating SARS-CoV-2 variants. In addition, it does not target the 417 or 484 residues in new variants and, therefore, might explain its potency against different variants.

Importance of vaccines

For some time now, vaccines have become a preventive, routine, and effective measure to reduce the eradication rate or near eradication of certain viral diseases⁵⁶. Furthermore, vaccines help in the creation of acquired immunity. Because a viral vector containing the information of the virus to be treated entered in the vaccine. If the virus enters the body, the immune system can attack it early. Also, vaccines prevent disease among vaccinated people. In addition, vaccines reduce infections even among people who are not vaccinated through herd immunity. Herd immunity happens if a sufficient proportion of the population is immunized or is immune to the virus⁵⁷. Pharmaceuticals can use the knowledge obtained in the realization of vaccines against SARS-CoV to develop and obtain vaccines for SARS-CoV-2. Since it has been observed that SARS-CoV-2 and SARS-CoV have significant similarities in their genomic sequences because they come from the same family and share a common cell receptor (ACE2)^{58,59}, SARS-CoV-2 spike mRNA vaccines have been shown to mediate protection against severe disease, which can occur as early as ten days after the first vaccination when neutralizing antibodies are barely detectable^{60,61}. Therefore, vaccine-induced CD8+ T cells may be the primary protection mediators at this early stage⁶¹.

The first two members of the Betacoronavirus genus, MERS and SARS, left us with experience and specific knowledge when designing vaccines to combat this type of virus. This facilitated the rapid response from scientists to start the de-

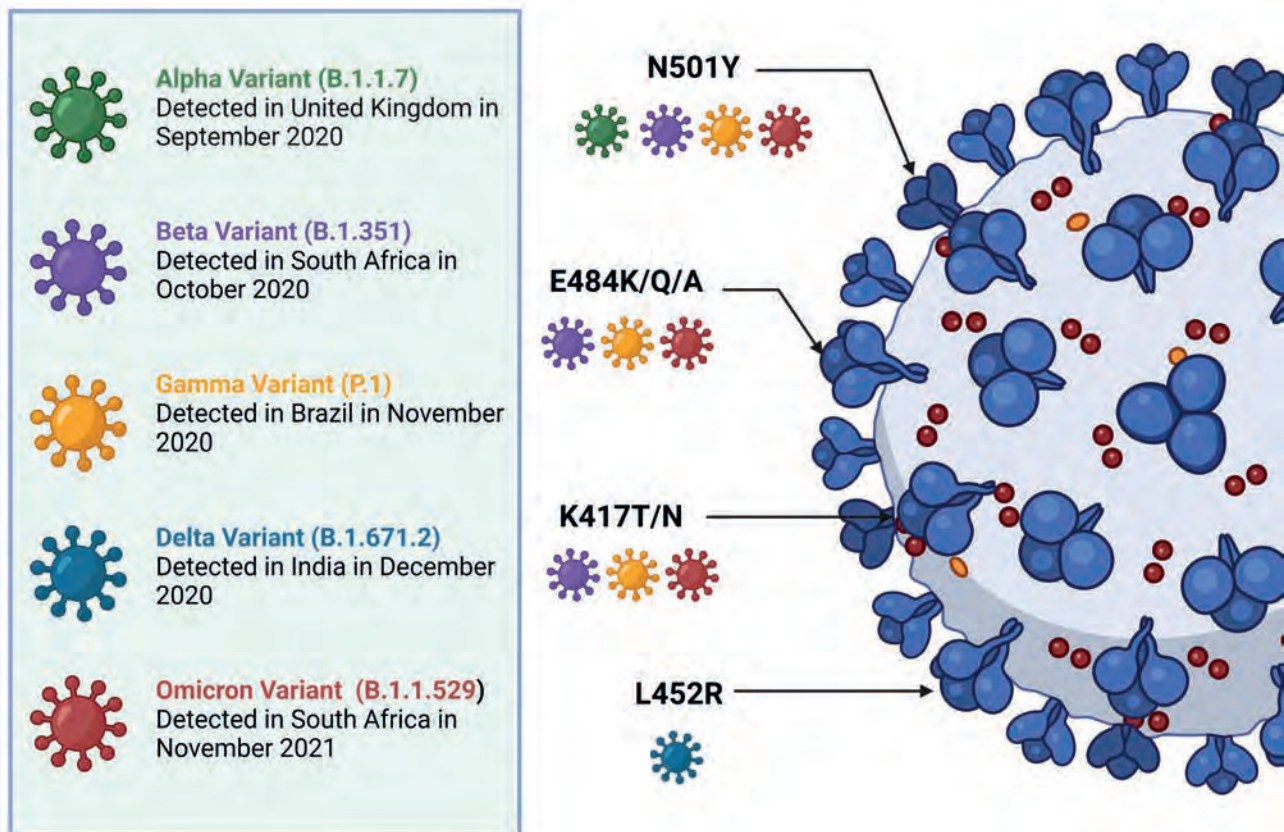


Figure 5. They are currently circulating SARS-CoV-2 variants of concern, and their receptor-binding domain (RBD) amino acid substitutions to virulence and immune evasion are relevant. The N501Y substitution is common to the Alpha, Beta, Gamma, and Omicron variant strains. The E484K/Q/A and K417T/N substitutions are present in the Beta, Gamma, and Omicron strains, while the L452R substitution is unique to the Delta variant. Image created using BioRender (<https://biorender.com/>).

velopment of the SARS-CoV-2 vaccines⁶². As we can observe in Table 1, scientists were based on 5 different leading platforms: RNA, DNA, Non-Replicant Viral Vector, Inactivated Viral Products, and Recombinant to develop the vaccines Protein Subunit. However, not all types of vaccines trigger the same immune responses in the body. Such is the case of LNP encapsulated mRNA and Inactivated vaccines, capable only of triggering the humoral immune response, representing a clear disadvantage if antibodies fail to detect emerging variants⁸.

Multidose importance

Almost all the Covid-19 vaccines approved to circulate worldwide were designed to require two doses to reach full efficacy⁶⁹. The first clinical trials revealed that a pretty weak immune response was found after only one dose of the vaccine. Although it offers little protection against the virus, it can potentially lead to partial immunity, which drastically increases the risk that vaccine-resistant variants of SARS-CoV-2 emerge⁷⁰. On the other hand, the immune responses are more robust after completing the two-dose vaccine series and have shown sustained protection against new variants. One of the last documented examples is the delta variant, which has been reported a 33% protection after a single shot of a two-dose Covid-19 vaccine, while individuals who completed the two-dose vaccine series reported a 90% protection against this variant⁶⁹.

Lately, researchers have opted for a new strategy known as heterologous prime and boost. It gives a third dose (booster shot) of a different Covid-19 vaccine after 5-6 months of the second dose⁷¹. Studies have shown that persons over fifty years of age who took the booster shot had a 90% lower mor-

tality rate from Covid-19 than those who did not⁷². The reason behind this is that the neutralizing antibody responses were enhanced to such a level that they exceeded the estimated levels necessary to protect us from the virus. What remains uncertain is if this third dose will be enough to lengthen the protection gap or if this booster will become a standard measure to control population immunity⁷³.

Discussion

An idea that has taken root in the population during the pandemic is that only by forming antibodies (humoral response) against SARS-CoV-2 will we be able to overcome the virus and the social consequences it has brought, but this is not entirely true. It is evident according to the literature data collected that, although at first, the researchers wanted to give a solution to Covid-19 by stimulating the generation of B antibodies through vaccines, with the arrival of new variants in increasingly shorter periods, they had to shift their focus to the cellular immune response⁷⁰. This decision is because the B antibodies bind like a lock-and-key to spike proteins on the surface of the virus. However, these spikes are very susceptible to mutations; consequently, the B antibodies could become obsolete⁶⁹, unlike what happened with the CD8+ T cells, which can target more than 15 distinct fragments of coronavirus proteins inside the infected cells. In this way, the next generation of Covid-19 vaccines will be dedicated to stimulating the cellular response more effectively provide more robust protection against emerging variants⁸.

Platform	Type of Vaccine	Immune Reaction	Immune Cells	Developer	Reference
RNA	LNP encapsulated mRNA	Humoral response	Th1 CD4+ T cells	Moderna/NIAID	63
	3 LNP-mRNAs	Humoral and cellular responses	CD4+ T cells, CD8+ T cells	Pfizer/BioNTech/Fosun Pharma	63
	mRNA	Humoral and cellular responses	CD4+ T cells, CD8+ T cells	CureVac/Bayer	63
Non-Replicant Viral Vector	ChAdOx1-S	Humoral and cellular responses	CD4+ T cells, CD8+ T cells	University of Oxford/Astra Zeneca	62
	Adenovirus Type 5 Vector	Humoral and cellular responses	CD4+ T cells, CD8+ T cells	CanSino BiologicalInc/ Beijing Institute of Biotechnology	64
Inactivated Viral Products	Inactivated+ alum	Humoral response	CD4+ T cells	Sinovac	65
	Inactivated	Humoral response	CD4+ T cells	Wuhan Institute of Biological Products/Sinopharm	65
	Inactivated	Humoral response	CD4+ T cells	Beijing Institute of Biological Products/Sinopharm	65
DNA	DNA plasmid vaccine with electroporation	Humoral and cellular responses	CD4+ T cells, CD8+ T cells	Inovio Pharmaceuticals/International Vaccine Institute	66
	DNA plasmid vaccine	Humoral and cellular responses	CD4+ T cells, CD8+ T cells	Cadila Healthcare Limited	67
Recombinant Protein Subunit	Full length recombinant SARS-CoV-2 glycoprotein nanoparticle Vaccine adjuvanted with Matrix M	Humoral and cellular responses	Th1 cells, CD4+ T cells, CD8+ T cells	Novavax	68

Table 1. Immune response according to each type of vaccine.

Conclusions


The SARS-CoV-2 virus population is constantly evolving and will likely remain a part of our lives for many years to come. This virus has revolutionized the world economically and socially. This virus has revolutionized the world economically and socially. In addition, the development of vaccines against Covid-19 is related to immunological memory. To prevent Covid-19 disease and avoid transmission, the vaccine must elicit high titers of neutralizing antibodies. Memory T cells can fight infection if they have a high amount of neutralizing antibodies. Almost all vaccines against Covid-19 attack the spike protein. Older people have a poor T-cell response, so they risk severe Covid-19. Therefore, the elderly should be vaccinated so that the immunization provided by the vaccine occurs long before the infection, which allows the response, expansion, and maturation of the adaptive immune system.

Although the characteristics and functions of the virus have been deciphered during the last two years, there is still to investigate the relationships of SARS-CoV-2 with the severity of the disease, immunological memory, protection, and vaccines. However, studies of antigen-specific CD4+T cells, CD8+T cells, B cells, and antibodies together in larger cohorts of acute patients, representing a range of disease severity, are needed to understand protective adaptive immune responses mechanisms Covid-19 further. In addition, the scientific community must continue to improve surveillance and monitoring strategies to prevent these occurrences from having such damaging effects in the future.

Bibliographic references

- Liang Y, Wang M-L, Chien C-S, Yarmishyn AA, Yang Y-P, Lai W-Y, et al. Highlight of Immune Pathogenic Response and Hematopathologic Effect in SARS-CoV, MERS-CoV, and SARS-CoV-2 Infection. *Frontiers in Immunology*. 2020 May 12;11.
- Poland GA, Ovsyannikova IG, Kennedy RB. SARS-CoV-2 immunity: review and applications to phase 3 vaccine candidates. *The Lancet*. 2020 Nov;396(10262):1595–606.
- Harrison AG, Lin T, Wang P. Mechanisms of SARS-CoV-2 Transmission and Pathogenesis. *Trends in Immunology*. 2020 Dec;41(12):1100–15.
- Suvvari TK, Kutikuppala LVS, Tsagkaris C, Corriero AC, Kandi V. Post COVID 19 complications: Multisystemic approach. *Journal of Medical Virology*. 2021 Dec 28;93(12):6451–5.
- Elias C, Sekri A, Leblanc P, Cucherat M, Vanhems P. The incubation period of COVID-19: A meta-analysis. *International Journal of Infectious Diseases*. 2021 Mar;104:708–10.
- Domínguez N, Galocha A. Así es la lucha entre el sistema inmune y el coronavirus. EL PAÍS [Internet]. 2020 Apr 21 [cited 2022 Feb 5]; Available from: https://elpais.com/elpais/2020/04/20/ciencia/1587379836_984471.html
- Janeway C, Travers P, Walport M, Shlomchik M. *Immunobiology: The Immune System in Health and Disease*. 5th ed. Vol. 9. New York: Garland Science; 2001. 401–454 p.
- Ledford H. 'KILLER' CELLS COULD BOOST COVID IMMUNITY AMID NEW VARIANTS. *Nature*. 2021 Feb 18;590(7846):374–5.
- Grifoni A, Weiskopf D, Ramirez SI, Mateus J, Dan JM, Moderbacher CR, et al. Targets of T Cell Responses to SARS-CoV-2 Coronavirus in Humans with COVID-19 Disease and Unexposed Individuals. *Cell*. 2020 Jun 25;181(7):1489–1501.e15.
- Toor SM, Saleh R, Sasidharan Nair V, Taha RZ, Elkord E. T-cell responses and therapies against SARS-CoV-2 infection. Vol. 162, *Immunology*. Blackwell Publishing Ltd; 2021. p. 30–43.
- Ahmadpoor P, Rostaing L. Why the immune system fails to mount an adaptive immune response to a COVID-19 infection. Vol. 33, *Transplant International*. Blackwell Publishing Ltd; 2020. p. 824–5.
- Onder G, Rezza G, Brusaferro S. Case-Fatality Rate and Characteristics of Patients Dying in Relation to COVID-19 in Italy. Vol. 323, *JAMA - Journal of the American Medical Association*. American Medical Association; 2020. p. 1775–6.
- Zelba H, Worbs D, Harter J, Pieper N, Kyzirakos-Feger C, Kayser S, et al. A Highly Specific Assay for the Detection of SARS-CoV-2-Reactive CD4 + and CD8 + T Cells in COVID-19 Patients. *The Journal of Immunology*. 2021 Feb 1;206(3):580–7.
- Sette A, Crotty S. Adaptive immunity to SARS-CoV-2 and COVID-19. Vol. 184, *Cell*. Elsevier B.V.; 2021. p. 861–80.
- Chen Z, John Wherry E. T cell responses in patients with COVID-19. *Nature Reviews Immunology*. 2020 Sep 1;20(9):529–36.
- Bacher P, Rosati E, Esser D, Martini GR, Saggau C, Schiminsky E, et al. Low-Avidity CD4+ T Cell Responses to SARS-CoV-2 in Unexposed Individuals and Humans with Severe COVID-19. *Immunity*. 2020 Dec 15;53(6):1258–1271.e5.
- Wang D, Hu B, Hu C, Zhu F, Liu X, Zhang J, et al. Clinical Characteristics of 138 Hospitalized Patients with 2019 Novel Coronavirus-Infected Pneumonia in Wuhan, China. *JAMA - Journal of the American Medical Association*. 2020 Mar 17;323(11):1061–9.
- Koutsakos M, Rowntree LC, Hensen L, Chua BY, van de Sandt CE, Habel JR, et al. Integrated immune dynamics define correlates of COVID-19 severity and antibody responses. *Cell Reports Medicine*. 2021 Mar 16;2(3).
- Sette A, Crotty S. Adaptive immunity to SARS-CoV-2 and COVID-19. Vol. 184, *Cell*. Elsevier B.V.; 2021. p. 861–80.
- Peng Y, Felce SL, Dong D, Penkava F, Mentzer AJ, Yao X, et al. An immunodominant NP105–113-B*07:02 cytotoxic T cell response controls viral replication and is associated with less severe COVID-19 disease. *Nature Immunology* [Internet]. 2022 Jan 1;23(1):50–61. Available from: <https://www.nature.com/articles/s41590-021-01084-z>
- Peng Y, Mentzer AJ, Liu G, Yao X, Yin Z, Dong D, et al. Broad and strong memory CD4+ and CD8+ T cells induced by SARS-CoV-2 in UK convalescent individuals following COVID-19. *Nature Immunology*. 2020 Nov 1;21(11):1336–45.
- Nguyen THO, Rowntree LC, Petersen J, Chua BY, Hensen L, Kedzierski L, et al. CD8+ T cells specific for an immunodominant SARS-CoV-2 nucleocapsid epitope display high naive precursor frequency and TCR promiscuity. *Immunity*. 2021 May 11;54(5):1066–1082.e5.
- Pal N, Mavi AK, Kumar S, Kumar U, Joshi MD, Saluja R. Current updates on adaptive immune response by B cell and T cell stimulation and therapeutic strategies for novel coronavirus disease 2019 (COVID-19) treatment. *Heliyon*. 2021 Apr;7(4):e06894.
- Gaebler C, Wang Z, C Lorenzi JC, Muecksch F, Finkin S, Tokuyama M, et al. Evolution of Antibody Immunity to SARS-CoV-2 1 2.
- Quast I, Tarlinton D. B cell memory: understanding COVID-19. Vol. 54, *Immunity*. Cell Press; 2021. p. 205–10.
- Aziz M, Brenner M, Wang P. Therapeutic Potential of B-1a Cells in COVID-19. Vol. 54, *Shock (Augusta, Ga.)*. NLM (Medline); 2020. p. 586–94.
- Aziz M, Holodick NE, Thomas •, Rothstein L, Wang • Ping. The role of B-1 cells in inflammation. *Immunologic Research*. 2026;63.
- Akkaya M, Kwak K, Pierce SK. B cell memory: building two walls of protection against pathogens. Vol. 20, *Nature Reviews Immunology*. Nature Research; 2020. p. 229–38.
- Zhang LX, Miao SY, Qin ZH, Wu JP, Chen HY, Sun HB, et al. Preliminary Analysis of B- and T-Cell Responses to SARS-CoV-2. *Molecular Diagnosis and Therapy*. 2020 Oct 1;24(5):601–9.
- Rombauts A, Stadlbauer D, Aslam S, Abelenda-Alonso G, Escalera A, Amanat F, et al. Antibody Immunological Imprinting on COVID-19 Patients.
- Baumgarth N, Nikolich-Zugich J, Lee FE-H, Bhattacharya D. Antibody Responses to SARS-CoV-2: Let's Stick to Known Knowns. *The Journal of Immunology*. 2020 Nov 1;205(9):2342–50.
- Victoria GD, Nussenzweig MC. Germinal centers. Vol. 30, *Annual Review of Immunology*. 2012. p. 429–57.
- Wajnberg A, Amanat F, Firpo A, Altman DR, Bailey MJ, Mansour M, et al. Robust neutralizing antibodies to SARS-CoV-2 infection persist for months. *Science*. 2020 Dec 4;370(6521):1227–30.
- Piccoli L, Park YJ, Tortorici MA, Czudnochowski N, Walls AC, Beltramello M, et al. Mapping Neutralizing and Immunodominant Sites on the SARS-CoV-2 Spike Receptor-Binding Domain by Structure-Guided High-Resolution Serology. *Cell*. 2020 Nov 12;183(4):1024–1042.e21.
- Robbiani DF, Gaebler C, Muecksch F, C Lorenzi JC, Wang Z, Cho A, et al. Convergent antibody responses to SARS-CoV-2 in convalescent individuals. *Nature*. 2020;584:437.
- Rogers TF, Zhao F, Huang D, Beutler N, Burns A, He W, et al. Isolation of potent SARS-CoV-2 neutralizing antibodies and protection from disease in a small animal model.
- Jiang S, Hillyer C, Du L. Neutralizing Antibodies against SARS-CoV-2 and Other Human Coronaviruses.
- Putcharoen OI, Wacharapluesadee S, Ni Chia W, Paitoonpong L, Wah Tan C, Suwanpimolkul G, et al. 2 Thai Red Cross Emerging Infectious Diseases Health Science Centre World Health Organization Collaborating Centre for Research and Training on Viral Zoonoses. 2021;
- Suthar MS, Zimmerman MG, Kauffman RC, Mantus G, Linderman SL, Hudson WH, et al. Rapid Generation of Neutralizing Antibody Responses in COVID-19 Patients. *Cell Reports Medicine*. 2020 Jun 23;1(3).
- Liu L, Wang P, Nair MS, Yu J, Rapp M, Wang Q, et al. Potent Neutralizing Antibodies Directed to Multiple Epitopes on SARS-CoV-2 Spike 1 2.
- Andabaka T, Nickerson JW, Rojas-Reyes MX, Rueda JD, Bacic Vrca V, Barsic B. Monoclonal antibody for reducing the risk of respiratory syncytial virus infection in children. Vol. 2013, *Cochrane Database of Systematic Reviews*. John Wiley and Sons Ltd; 2013.
- Mulangu S, E L, T R. A Randomized, Controlled Trial of Ebola Virus Disease Therapeutics. *The new england journal of medicine*. 2019 Dec;381:2293–303.

43. Levine MM. Editorials Monoclonal Antibody Therapy for Ebola Virus Disease. 2019;
44. Medical Association A. Genetic Variants of SARS-CoV-2-What Do They Mean? 2021;
45. Mistry P, Barmania F, Mellet J, Peta K, le Strydom A, Viljoen IM, et al. SARS-CoV-2 Variants, Vaccines, and Host Immunity. 2019;
46. Prévost J, Finzi A. The great escape? SARS-CoV-2 variants evading neutralizing responses. *Cell Host and Microbe*. 2021 Mar 10;29(3):322–4.
47. Andrew Rambaut, Nick Loman, Oliver Pybus, Wendy Barclay. Preliminary genomic characterisation of an emergent SARS-CoV-2 lineage in the UK defined by a novel set of spike mutations. *virological.org*. 2020 Dec;
48. Tegally H, Wilkinson E, Giovanetti M, Iranzadeh A, Fonseca V, Giandhari J, et al. Detection of a SARS-CoV-2 variant of concern in South Africa. *Nature*. 2021 Apr 15;592(7854):438–43.
49. Brown CM, Vostok J, Johnson H, Burns M, Gharpure R, Sami S, et al. Morbidity and Mortality Weekly Report Outbreak of SARS-CoV-2 Infections, Including COVID-19 Vaccine Breakthrough Infections, Associated with Large Public Gatherings-Barnstable County, Massachusetts, July 2021.
50. Mlcochova P, Kemp S, Shanker Dhar M, Papa G, Meng B, Mishra S, et al. SARS-CoV-2 B.1.617.2 Delta variant replication, sensitivity to neutralising antibodies 1 and vaccine breakthrough 2 3.
51. Cherian S, Potdar V, Jadhav S, Yadav P, Gupta N, Das M, et al. microorganisms SARS-CoV-2 Spike Mutations, L452R, T478K, E484Q and P681R, in the Second Wave of COVID-19 in Maharashtra, India. 2021;
52. WHO. Classification of Omicron (B.1.1.529): SARS-CoV-2 Variant of Concern. 2021.
53. Grubaugh ND, Petrone ME, Holmes EC. We shouldn't worry when a virus mutates during disease outbreaks.
54. Ecdc. Detection of new SARS-CoV-2 variants related to mink. 2020.
55. Alejandra Tortorici M, Czudnochowski N, Starr TN, Marzi R, Walls AC, Zatta F, et al. Broad sarbecovirus neutralization by a human monoclonal antibody. *Nature*. 2021;597:103.
56. Hajj Hussein I, Chams N, Chams S, el Sayegh S, Badran R, Raad M, et al. Vaccines Through Centuries: Major Cornerstones of Global Health. Vol. 3, *Frontiers in Public Health*. Frontiers Media S.A.; 2015.
57. Fisher KA, Bloomstone SJ, Walder J, Crawford S, Fouayzi H, Mazor KM. Attitudes toward a potential SARS-CoV-2 vaccine: A survey of U.S. adults. Vol. 173, *Annals of Internal Medicine*. American College of Physicians; 2020. p. 964–73.
58. Ma C, Su S, Wang J, Wei L, Du L, Jiang S. From SARS-CoV to SARS-CoV-2: safety and broad-spectrum are important for coronavirus vaccine development. *Microbes and Infection*. 2020 Jul 1;22(6–7):245–53.
59. Zhou R, To KKW, Wong YC, Liu L, Zhou B, Li X, et al. Acute SARS-CoV-2 Infection Impairs Dendritic Cell and T Cell Responses. *Immunity*. 2020 Oct 13;53(4):864–877.e5.
60. Polack FP, Thomas SJ, Kitchin N, Absalon J, Gurtman A, Lockhart S, et al. Safety and Efficacy of the BNT162b2 mRNA Covid-19 Vaccine. *New England Journal of Medicine*. 2020 Dec 31;383(27):2603–15.
61. Oberhardt V, Luxenburger H, Kemming J, Schulien I, Ciminski K, Giese S, et al. Rapid and stable mobilization of CD8+ T cells by SARS-CoV-2 mRNA vaccine. *Nature*. 2021 Sep 9;597(7875):268–73.
62. Zandi M, Rashid S, Nasimzade S, Pourhossein B, Fazeli M. A Snapshot Of Different Types Of Under Research Vaccines A Gainst Covid 1 9: A Review. *ARCHIVES OF MEDICAL LABORATORY SCIENCES*. 2020;6(1).
63. Park JW, Lagniton PNP, Liu Y, Xu R-H. mRNA vaccines for COVID-19: what, why and how. *International Journal of Biological Sciences*. 2021;17(6):1446–60.
64. Zhu F-C, Li Y-H, Guan X-H, Hou L-H, Wang W-J, Li J-X, et al. Safety, tolerability, and immunogenicity of a recombinant adenovirus type-5 vectored COVID-19 vaccine: a dose-escalation, open-label, non-randomised, first-in-human trial. *The Lancet*. 2020 Jun;395(10240):1845–54.
65. Jantarabenjakul W, Chantasrisawad N, Puthanakit T, Wacharapluesadee S, Hirankarn N, Ruenjaiman V, et al. Short-term immune response after inactivated SARS-CoV-2 (CoronaVac®, Sinovac) and ChAdOx1 nCoV-19 (Vaxzevria®, Oxford-AstraZeneca) vaccinations in health care workers. *Asian Pacific Journal of Allergy and Immunology*. 2023;
66. Andrade VM, Christensen-Quick A, Agnes J, Tur J, Reed C, Kalia R, et al. INO-4800 DNA vaccine induces neutralizing antibodies and T cell activity against global SARS-CoV-2 variants. *npj Vaccines*. 2021 Dec 14;6(1):121.
67. Momin T, Kansagra K, Patel H, Sharma S, Sharma B, Patel J, et al. Safety and Immunogenicity of a DNA SARS-CoV-2 vaccine (ZyCoV-D): Results of an open-label, non-randomized phase I part of phase I/II clinical study by intradermal route in healthy subjects in India. *EClinicalMedicine*. 2021 Aug;38:101020.
68. Keech C, Albert G, Cho I, Robertson A, Reed P, Neal S, et al. Phase 1–2 Trial of a SARS-CoV-2 Recombinant Spike Protein Nanoparticle Vaccine. *New England Journal of Medicine*. 2020 Dec 10;383(24):2320–32.
69. Crutcher M, Seidler PM. Maximizing Completion of the Two-Dose COVID-19 Vaccine Series with Aid from Infographics. *Vaccines*. 2021 Oct 22;9(11):1229.
70. Livingston EH. Necessity of 2 Doses of the Pfizer and Moderna COVID-19 Vaccines. *JAMA*. 2021 Mar 2;325(9):898.
71. Callaway E. MIXING COVID VACCINES TRIGGERS POTENT IMMUNE RESPONSE. *Nature* [Internet]. 2021 May 27 [cited 2022 Feb 7];593:491–491. Available from: http://myvax.com.s3.amazonaws.com/uploads/my_vax_article/article/d41586-021-01359-3.pdf
72. Arbel R, Hammerman A, Sergienko R, Friger M, Peretz A, Netzer D, et al. BNT162b2 Vaccine Booster and Mortality Due to Covid-19. *New England Journal of Medicine*. 2021 Dec 23;385(26):2413–20.
73. Juno JA, Wheatley AK. Boosting immunity to COVID-19 vaccines. *Nature Medicine*. 2021 Nov 11;27(11):1874–5.



SOMOS LA PRIMERA UNIVERSIDAD
DEL ECUADOR
CON MAYOR RELEVANCIA EN

**PUBLICACIONES
CIENTÍFICAS**

Docencia, investigación,
extensión y proyección
social al servicio del territorio



Fortalezas institucionales

- > Biotecnología
- > Limnología
- > Derechos Humanos – Posconflicto
- > Internacionalización
- > Inclusión Social
 - SER – Servicio Educativo Rural
 - Educación de Alfabetización
- > MII S – Instituto de formación para el trabajo y el desarrollo humano
- > Formación humanística “Ruta Humanística en el currículo - Cátedra abierta Maestra de la Sabiduría”
- > Investigación y desarrollo tecnológico
- > Comprometida con la calidad
- > Centro de Estudios Territoriales
- > Biodiversidad
 - Herbario
 - Ictiología
 - Fitoteca

Áreas del conocimiento

- Ciencias Agropecuarias
 - Ciencias de la Educación
 - Ciencias de la Salud
 - Ciencias Económicas y Administrativas
 - Ciencias Sociales
 - Derecho
 - Ingenierías
 - Teología y Humanidades
- > 26 programas de pregrado
 - > 16 programas de posgrado
 - 1 doctorado
 - 8 maestrías
 - 7 especializaciones

www.uco.edu.co  Universidad Católica de Oriente  @uconio



“Servicio educativo con calidad en
Personas, procesos y servicios”

Contacto institucional Universidad Católica de Oriente
Sector 3, Cra. 46 No. 40B 50 - PBX: +(57)(4) 569 90 90. Ext. 604
Fax: +(57)(4) 501 09 72 - Email: uco@uco.edu.co

